

ADO 781804

AFFDL-TR-73-50
Volume I

**ADVANCED METALLIC STRUCTURES:
AIR SUPERIORITY FIGHTER WING
DESIGN FOR IMPROVED COST,
WEIGHT AND INTEGRITY**

VOLUME I PROGRAM OVERVIEW

D. F. Davis, et al.

**GENERAL DYNAMICS
Convair Aerospace Division
Fort Worth Operation**

**Technical Report AFFDL-TR-73-50, Volume I
July 1973**

Approved for public release;
distribution unlimited.

**Air Force Flight Dynamics Laboratory
Air Force Systems Command
Wright Patterson Air Force Base, Ohio**

20080818 040

NOTICE

When Government drawings, specifications, or other data are used for any purpose other than in connection with a definitely related Government procurement operation, the United States Government thereby incurs no responsibility nor any obligation whatsoever; and the fact that the government may have formulated, furnished, or in any way supplied the said drawings, specifications, or other data, is not to be regarded by implication or otherwise as in any manner licensing the holder or any other person or corporation, or conveying any rights or permission to manufacture, use, or sell any patented invention that may in any way be related thereto.

Copies of this report should not be returned unless return is required by security considerations, contractual obligations, or notice on a specific document.

ADVANCED METALLIC STRUCTURES:
AIR SUPERIORITY FIGHTER WING
DESIGN FOR IMPROVED COST,
WEIGHT AND INTEGRITY

Volume I Program Overview

D. F. Davis, et al.
GENERAL DYNAMICS
Convair Aerospace Division
Fort Worth Operation

Approved for public release;
distribution unlimited.

AD781806

FOREWORD

The efforts reported herein were sponsored by the Air Force Flight Dynamics Laboratory (AFFDL) under the joint management and technical direction of AFFDL and the Air Force Materials Laboratory, WPAFB, Ohio, 45433. The work was performed under Contract F33615-72-C-2149, Flight Dynamics Laboratory Project Number 486U, "Advanced Metallic Structures: Air Superiority Fighter Wing Design for Improved Cost, Weight and Integrity." Mr. Lawrence R. Phillips of AFFDL is the Air Force Project Engineer.

These studies were performed by the Structural Design Group, Convair Aerospace Division of General Dynamics, Fort Worth Operation with D. F. Davis as the Program Manager. Other principal participants in the program are as follows: R. W. McAnally, Structural Design; E. W. Gomez, Stress Analysis; J. W. Morrow, Fatigue and Fracture Analysis; J. M. Shults, Materials Engineering; T. E. Henderson, Mass Properties; J. D. Jackson, Value Engineering; J. L. McDaniel, Manufacturing Engineering; B. G. W. Yee, Nondestructive Inspection; D. Duncan, Quality Assurance; H. E. Bratton, Information Transfer; and R. L. Jones, Engineering Test Laboratory.

The work was performed from June 1972 to June 1973 and was released for publication June 1973.

This report has been reviewed and is approved.



JOHN C. FRISHETT, Major, USAF
Program Manager, AMS Program Office
Structures Division
Air Force Flight Dynamics Laboratory

A B S T R A C T

This report describes the preliminary design and analysis for an Advanced Air Superiority Fighter Stores Loaded, Wet Wing Structure. The wing box of the F-111F airplane designed by the Convair Aerospace Division of General Dynamics was used as the baseline vehicle.

A unique design methodology was followed to arrive at three configurations which offer an optimum balance between structural efficiency and technological advancement. This methodology consists of compiling element concepts; integrating them into cross-section drawings; optimizing them in analytical assemblies; and finally preparing full wing box designs. Each step was followed with a detailed evaluation and ranking step which utilized a formal merit rating system. This system permitted the evaluation of numerous concepts and insured that each technical discipline participated in the design selection.

A subsequent program is proposed to evaluate the capability of the selected design to meet the overall program goals of advancing technology without significantly affecting costs. The subsequent program involves additional preliminary design, a development test program, detail design, manufacture, and tests; including static, fatigue, and damage tolerance testing. Information generated during this effort will be disseminated to the Air Force and industry in general through an intensive information transfer effort.

T A B L E O F C O N T E N T S

<u>Section</u>		<u>Page</u>
I	INTRODUCTION	1
II	PROGRAM SUMMARY	15
	2.1 Objectives and Approach	15
	2.2 General Program Results	15
	2.3 Specific Program Results	19
	2.4 Potential Technology Advances	24
III	BASELINE SELECTION AND DEFINITION	25
	3.1 Baseline Selection Rationale	25
	3.1.1 Cost-Effective Aspects of Selected Baseline Component	25
	3.1.2 F-111 Wing Structural Integrity Verification Program	27
	3.2 Baseline Component Description	34
	3.3 Baseline Requirements	37
	3.3.1 Static Load Requirements	37
	3.3.2 F-111 Fatigue Requirements	37
	3.4 Baseline Materials	42
	3.5 Updated Baseline	43
	3.5.1 Fatigue Analysis Update	43
	3.5.2 Damage Tolerance Assessment of Baseline	46
	3.5.3 Effect of Usage Variation	46
IV	STRUCTURAL DESIGN	61
	4.1 Design Approach and Evaluation System	61
	4.1.1 Design Effort at the Element Concept Level	61
	4.1.2 Design Effort at the "Wing Cross- Section Concept" Level	63
	4.1.3 Design Effort at the Analytical Assembly Level	70

TABLE OF CONTENTS (Continued)

<u>Section</u>	<u>Page</u>
4.1.4 Preliminary Designs	73
4.1.5 Final Iterative Phase, Wing Box Preliminary Design	73
4.1.6 Design Assessment	73
 V STRESS ANALYSIS	 115
5.1 Design Loads	115
5.2 Analysis Techniques	117
5.2.1 Concept Screening	117
5.2.2 Cross-Section Sizing and Study	117
5.2.3 Analytical Assembly Technique	118
5.2.4 Preliminary Design Analysis Technique	119
5.3 Structural Integrity and Reliability Evaluation Technique	133
 VI FATIGUE ANALYSIS	 137
6.1 Fatigue Analysis Criteria and Procedures	137
6.2 Concept Analysis and Evaluation	139
6.2.1 Fatigue Design Data	139
6.2.2 Fatigue Data for Analysis	141
6.2.3 Fatigue Quality Guidelines	162
6.3 Preliminary Design Analysis	165
6.4 Reliability Analysis	172
 VII FRACTURE ANALYSIS	 177
7.1 Fracture Control Summary	177
7.2 Damage Tolerance Criteria	178
7.2.1 Design Service Loads Spectrum	178
7.2.2 Design Environment Definition	182
7.3 Concept Analysis and Evaluation	184
7.3.1 Fracture Design Data	185

TABLE OF CONTENTS (Continued)

<u>Section</u>	<u>Page</u>
7.3.2 Analysis Assumptions and Procedures	191
7.3.3 Fracture Data Assumed for Analysis	199
7.4 Preliminary Design Analysis	211
7.4.1 Preliminary Design 610RW003 - Laminated Lower Skin, Corrugated Spar Webs, Aluminum	213
7.4.2 Preliminary Design 610RW002 - Multi-Wet Cell, Planked Lower Skin, Titanium	220
7.4.3 Preliminary Wing Design 610RW004 - Adhesive Bonded Honeycomb Skin Panels, Upper and Lower, Aluminum	223
7.5 Risk Assessments	227
7.5.1 Assessment Method	227
7.5.2 Assessment Results	229
VIII MATERIALS ENGINEERING	235
8.1 Material Selection Criteria	235
8.2 Candidate Materials	239
8.2.1 Baseline Materials	239
8.2.2 Candidate Aluminum Alloys	239
8.2.3 Candidate Titanium Alloys	240
8.2.4 Candidate Steel Alloys	241
8.3 Test Program	241
8.3.1 Test Plan	241
8.3.2 Test Specimens	242
8.3.3 Material Tested	242
8.3.4 Test Procedures	245
8.3.5 Discussion of Test Results	256
8.4 Selected Materials	265

TABLE OF CONTENTS (Continued)

<u>Section</u>		<u>Page</u>
IX	VALUE ENGINEERING	267
	9.1 Cost Estimating Procedures	267
	9.1.1 Detail Estimates	267
	9.1.2 Example of Detail Estimating Procedures	268 268
	9.2 Baseline Costs	278
	9.3 Cross-Section Concepts	279
	9.3.1 Early Cost Estimating Problems	279
	9.3.2 Cross-Section Data	279
	9.4 Analytical Assembly Concepts	279
	9.5 Full Wing Box Preliminary Design Concepts	280
	9.5.1 Splices	280
	9.6 Optimized Full Wing Box Concepts	281
	9.6.1 Final Cost Comparisons	281
	9.6.2 Comparison of Estimating Tech- niques	284 284
	9.7 Engineering Support Activities	286
	9.7.1 Support Benefits	286
X	MANUFACTURING	289
	10.1 Influence of Manufacturing on Design	289
	10.1.1 Basic Metal Processing Programs	289
	10.1.2 Secondary Metal Processing	293
	10.2 New Manufacturing Methods and Their Ap- plications to Design Concepts	294 294
	10.2.1 Basic Metal Processing Applications	295 295
	10.2.2 Secondary Metal Processing	300

TABLE OF CONTENTS (Continued)

<u>Section</u>	<u>Page</u>
10.3 Concept Evaluation and Rating	314
10.3.1 Merit Rating System for Manufacturing	314
10.3.2 Rating of Element Concept Drawings	322
10.3.3 Rating of Cross-Section Drawings	322
10.3.4 Rating of Analytical Assembly Drawings	326
10.3.5 Rating of Preliminary Design Drawings	326
10.4 Preliminary Manufacturing Planning	329
10.4.1 Preliminary Manufacturing Plan for 610RW003	329
10.4.2 Preliminary Manufacturing Plan for 610RW004	337
10.4.3 Preliminary Manufacturing Plan for 610RW002	351
XI QUALITY ASSURANCE AND NDI	369
11.1 Inspection Capabilities	369
11.2 Concept Evaluations	375
11.2.1 Element Concepts	376
11.2.2 Cross Sections and Analytical Assemblies	377
11.2.3 Preliminary Designs	377
11.3 Quality Assurance Planning	381
XII POTENTIAL TECHNOLOGY ADVANCES	387
12.1 Elimination of Fasteners Thru Tension Members	387
12.2 Thin Skin Laminates in Tension Members	387
12.3 Low Temperature Brazing of High Heat Treat Titanium Alloys	388

TABLE OF CONTENTS (Continued)

<u>Section</u>		<u>Page</u>
XIII	SUMMARY OF FOLLOW-ON PROGRAM	389
	13.1 Program Discussion	390
	REFERENCES	393

Contents of Volumes II, III, and IV are as follows:

Volume II

APPENDIX I	ELEMENT CONCEPT SKETCHES
APPENDIX II	CROSS SECTION DRAWINGS
APPENDIX III	ANALYTICAL ASSEMBLY DRAWINGS
APPENDIX IV	PRELIMINARY DESIGN DRAWINGS

Volume III

APPENDIX V	STRESS ANALYSIS
APPENDIX VI	FATIGUE AND FRACTURE ANALYSIS
APPENDIX VII	COST DATA
APPENDIX VIII	MATERIAL TEST PROGRAM DATA

Volume IV

APPENDIX IX	BASELINE DAMAGE TOLERANCE EVALUATION AND FOLLOW-ON PLAN
-------------	--

L I S T O F I L L U S T R A T I O N S

<u>Figure</u>		<u>Page</u>
1	Main Objective of ADP's	2
2	Technology Vs. Air Superiority	3
3	Exploitation Areas to Achieve Objectives	5
4	Technology Advancement Vs. Program Risks	7
5	Common Design Goals	9
6	Advanced Fighter Wing - ADP	10
7	F-111 Wing Box	12
8	Fighter Wing ADP Baseline	13
9	Program Design Goals	14
10	Fighter Wing ADP Design Approach	17
11	Summary of Symmetric Maneuver Conditions	32
12	Overview of Various Conditions That Con- figure F-111 Wing Box	33
13	F-111 Wing Structural Arrangement	35
14	Baseline Wing Box	36
15	Limit Maneuver Load Factors - F-111F Airplane	38
16	Mission Analysis Approach	41
17	Control Points/F-111 Preliminary Fatigue Analysis	45
18	Summary of Usage Effects - C.S.S. 140 Base- line Fatigue and Fracture Allowables	49
19	Center Spar Station 140 - F-111 Baseline Fatigue Design Allowable Curve Phase I and II Training Spectrum	52

LIST OF ILLUSTRATIONS (Continued)

<u>Figure</u>		<u>Page</u>
20	Center Spar Station 140 - F-111 Baseline Fatigue Design Allowable Curve Air Superiority Spectrum	53
21	Center Spar Station 140 - F-111 Baseline Fatigue Design Allowable Curve Flight Recorder Spectrum	54
22	Center Spar Station 140 - F-111 Baseline Design Allowable Curve Surface Flaw in $t = 0.611$ Skin, Mid-Point K_{IC} & da/dN Phase I and II Training Spectrum	55
23	Center Spar Station 140 - F-111 Baseline Frac- ture Design Allowable Curve Surface Flaw in $t = 0.611$ Skin, Mid-Point K_{IC} & da/dN Air Superiority Spectrum	56
24	Center Spar Station 140 - F-111 Baseline Frac- ture Design Allowable Curve Surface Flaw in $t = 0.611$ Skin, Mid-Point K_{IC} & da/dN Flight Recorder Spectrum	57
25	Center Spar Station 140 - Baseline Fracture Design Allowable Curve Through Flaw in 5/16 Hole, Mid-Point K_{IC} & da/dN Phase I and II Training Spectrum	58
26	Center Spar Station 140 - F-111 Baseline Frac- ture Design Allowable Curve Through Flaw 5/16 Hole, Mid-Point K_{IC} & da/dN Air Superiority Spectrum	59
27	Center Spar Station 140 - F-111 Baseline Fracture Design Allowable Curve Through Flaw in 5/16 Hole, Mid-Point K_{IC} & da/dN Flight Recorder Spectrum	60
28	Fighter Wing ADP Design Approach	62
29	Rating System for the Analytical Assembly	64
30	Baseline Wing Box	75

LIST OF ILLUSTRATIONS (Continued)

<u>Figure</u>		<u>Page</u>
31	Sandwich Upper Skin, Laminated Lower With Tension Straps Outboard	77
32	Multi-Wet Cell Construction	79
33	Corrugated Spar - Laminated Al Lower Skin Construction	81
34	Adhesive Bonded Aluminum Honeycomb Panels	83
35	Adhesive Bonded Titanium Honeycomb Panels	85
36	Brazed Titanium Space Truss	87
37	Wing Box - Bonded Aluminum Laminated Lower Panel; Hat Stiffened Upper Panel	89
38	Bonded Aluminum Laminated Lower Panel; Hat Stiffener Upper Panel with Close Tip	91
39	Laminated Lower Skin/Plate Upper Spliced to Multi-Spar Bonded Aluminum	93
40	Wing Box - Multi-Cell Construction	95
41	Wing Box Laminated Lower Skin with Stepped Spar Caps, Plate Upper Skin, Corrugated Spar Webs	99
42	Wing Body - Adhesive Bonded Honeycomb Panel Upper and Lower	103
43	Wing Box - Brazed Titanium Space Truss Structure	107
44	Fatigue Allowable Approach	140
45	C.S.S. 140 Lower Surface ADP Wing Preliminary Fatigue Design Allowable Curves Based on Phase IA Tested S/N Data (6.125 Sht.) Applicable to 7475-T761 Sheet Alloy	142

LIST OF ILLUSTRATIONS (Continued)

<u>Figure</u>		<u>Page</u>
46	C.S.S. 140 Lower Surface ADP Wing Preliminary Fatigue Design Allowable Curves Based on Phase IA Tested S/N Data Applicable to 7475-T7351 Aluminum Alloy Plate (1-1/2")	143
47	C.S.S. 140 Lower Surface ADP Wing Preliminary Fatigue Design Allowable Curves Based on Phase IA Tested S/N Data (0.0625 Sht.) Applicable to 7050-T76 Sheet Alloy	144
48	C.S.S. 140 Lower Surface ADP Wing Preliminary Fatigue Design Allowable Curves Based on Phase IA Tested S/N Data (3-In. Plate) Applicable to X7050-T73651 Plate Alloy	145
49	C.S.S. 140 ADP Wing Preliminary Fatigue Design Allowable Curves Based on Phase IA Tested S/N Data Applicable to 8-8-2-3 Titanium Sheet	146
50	C.S.S. 140 ADP Wing Preliminary Fatigue Design Allowable Curves for Use in Concept Screening Applicable to 8-8-2-3 Titanium Plate S/N Data Tested in Phase IA	147
51	S-N Curves 7475-T61, T761 Aluminum Sheet	149
52	S-N Curves 7475-T61, T761 Aluminum Sheet	150
53	S-N Curves 7475-T735 Aluminum 1-1/2-Inch Plate	151
54	S-N Curves 7457-T7351 Aluminum 1-1/2-Inch Plate	152
55	S-N Curves 7050-T76 Aluminum Alloy Sheet Longitudinal	153
56	S-N Curves 7050-T76 Aluminum Alloy Sheet Longitudinal	154
57	S-N Curves X7050-T73651 Aluminum 3-Inch Plate	155

LIST OF ILLUSTRATIONS (Continued)

<u>Figure</u>		<u>Page</u>
58	S-N Curves X7050-T73651 Aluminum 3-Inch Plate	156
59	S-N Curves 8-8-2-3 Titanium 1/16-Inch Sheet Longitudinal	157
60	S-N Curves 8-8-2-3 Titanium 1/16-Inch Sheet Longitudinal	158
61	S-N Curves 8-8-2-3 Titanium 1-Inch Plate Longitudinal Grain - Sta.	159
62	S-N Curves 8-8-2-3 Titanium 1-Inch Plate Longitudinal Grain - Sta.	160
63	S-N Curves 6Al-4V Titanium Sta. Sheet	161
64	Stress Concentration Factors	164
65	Corrugated Spar - Laminated Aluminum Lower Skin Fatigue Control Points, Configuration 610RW003	167
66	Adhesive Bonded Aluminum Honeycomb Panels Fatigue Control Points, Configuration 610RW004	168
67	Brazed Titanium Space Truss Fatigue Control Points, Configuration 610RW006	169
68	Multi-Wet Cell Construction Fatigue Control Points, Configuration 610RW002	170
69	Bonded Aluminum Laminated Lower Panel: Hat Stiffened Upper Panel Fatigue Control Points, Configuration 610RW007	171
70	Block Spectrum Vs. Flight by Flight Spectrum for Flaw Growth Analysis	183
71	Crack Growth Allowable Approach	186
72	Fracture Design Data, C.S.S. 140 Lower Surface 8-8-2-3 Titanium Alloy	187

LIST OF ILLUSTRATIONS (Continued)

<u>Figure</u>		<u>Page</u>
73	Phase IA Fracture Design Allowables 7050 Aluminum Alloy Plate, Part Through Surface Crack	188
74	Phase IA Fracture Design Allowables, Part Through Surface Flaw	189
75	Phase IA Design Allowable Curves Surface Flaw	190
76	Metals Fracture Analysis Summary	192
77	Analytic Flaw Growth Model	193
78	Residual Strength with Cracks	195
79	Crack Growth Rate Data for 7050-T3651 Aluminum Plate	203
80	Crack Growth Data for 7050-T76 Aluminum Sheet	204
81	Crack Growth Rate Data for 8-8-2-3 Ti Plate	205
82	Ti-6Al-4V, 0.625 Inch Sta Plate, CT Specimens, L-T Direction	206
83	Preliminary da/dN Data, 6Al-4V Titanium Recrystallized Annealed Plate	207
84	610RW003 Wing Box Laminated Lower Skin, Cor- rugated Spar Webs, Aluminum Phase IA Fracture Analysis	217
85	610RW003 Wing Box Laminated Lower Skin, Cor- rugated Spar Webs, Aluminum Phase IA Fracture Analysis	218
86	610RW003 Wing Box Laminated Lower Skin, Cor- rugated Spar Webs, Aluminum Phase IA Fracture Analysis	219
87	610RW003 Wing Box Laminated Lower Skin, Cor- rugated Spar Webs, Aluminum Phase IA Fracture Analysis	221

LIST OF ILLUSTRATIONS (Continued)

<u>Figure</u>		<u>Page</u>
88	610RW002 Wing Box Multi-Wet Cell, Planked Lower Skin Phase IA Fracture Analysis	222
89	610RW004 Wing Box Adhesive Bonded Honeycomb Panel, Upper and Lower Phase IA Fracture Analysis	224
90	610RW004 Wing Box Adhesive Bonded Honeycomb Panel, Upper and Lower Phase IA Fracture Analysis	226
91	Initial Flaw Length-Inches Flaw Fracture Risk Assessment, 610RW003 Flaw Size Distribution Lower Skin Outer Ply	228
92	Determination of No Failure Probability	230
93	Probability of No Failure Vs. Flight Time	232
94	Materials Selection Process	235
95	Surface Flawed Crack Growth Rate Specimens in Test	250
96	Electronic Control Equipment for Crack Growth Rate Testing	251
97	Titanium Surface Flawed Crack Growth Rate Specimens in Test in CGS Electrohydraulic Fatigue Machine	254
98	Analytical Assembly - Laminated Lower Skin With Stepped Spar Caps	269
99	Rating System for the Analytical Assembly Drawings, Advanced Air Superiority Fighter Wing Structures Program	283
100	Advanced Basic Manufacturing Techniques	291
101	Advanced Secondary Manufacturing Techniques	292

LIST OF ILLUSTRATIONS (Continued)

<u>Figure</u>		<u>Page</u>
102	Advanced Manufacturing Technology Concept Rating Schedule, Titanium Alloys	317
103	Advanced Manufacturing Technology Concept Rating Schedule, Aluminum Alloys	318
104	Manufacturability Concept Rating Schedule, Titanium Alloys	320
105	Manufacturability Concept Rating Schedule, Aluminum Alloys	321
106	Wing Section - Laminated Lower Skins With Stepped Spar Caps: Plate Upper Skin: Corrugated Spar Webs	323
107	Compression Skins Concept Rating	324
108	Tension Skins Concept Ratings	325
109	Concept Rating Cross-Section Concepts at C.S.S. 140	327
110	Concept Rating Cross-Section Concepts at C.S.S. 340	328
111	Basic Manufacturing - Front Spar	330
112	Basic Manufacturing Corrugated Spar Details	331
113	Basic Manufacturing Lower Skin Laminates	333
114	Basic Manufacturing Upper Skin	334
115	Basic Manufacturing Bulkheads, Ribs, and Pylon Fittings	335
116	Secondary Manufacturing Rear Spar Assembly Weldbond Spar Webs and Caps	336
117	Secondary Manufacturing Surface Laminated Skin Panel Adhesive Bonded Assembly	338

LIST OF ILLUSTRATIONS (Continued)

<u>Figure</u>		<u>Page</u>
118	Secondary Manufacturing Weldbond Spar Webs and Caps	339
119	Secondary Manufacturing Final Bond Assembly and Weldbond Cure Lower Surface Laminated Skins and Corrugated Spars	340
120	Secondary Manufacturing Final Assembly Upper Skin and Understructure	341
121	Basic Manufacturing Spar Details Front and Rear Spars	343
122	Basic Manufacturing Spar Details Auxiliary Spars	344
123	Basic Manufacturing Skin Panel Details	345
124	Secondary Manufacturing Front and Rear Spars Adhesive Bonded Assembly	346
125	Secondary Manufacturing Lower Skin Panel Assembly	347
126	Secondary Manufacturing Assembly of Lower Skin Panel and Auxiliary Spars	348
127	Secondary Manufacturing Upper Skin Panel Assembly	349
128	Secondary Manufacture Final Assembly of Wing Box Structure	350
129	Basic Manufacture Spar Details Front and Rear Spars	352
130	Basic Manufacture Wing Skin Details	353
131	Basic Manufacturing Pylon Fittings	354
132	Basic Manufacturing Fabrication of Core Cell Details	355

LIST OF ILLUSTRATIONS (Continued)

<u>Figure</u>		<u>Page</u>
133	Secondary Manufacturing Core Cell Fabrication	357
134	Rear Spar and Pylon Fitting Joining	358
135	Welding of Rear Spar Web and Caps	359
136	Welding of Front Spar Assembly	360
137	Installation of End Bulkheads and Fittings	361
138	Machining of First Stage Multi-Wet Cell Core	363
139	Machining of Second Stage Multi-Wet Core	364
140	Installation of First Stage Multi-Wet Cell Core	365
141	Installation of Second Stage Multi-Wet Cell Core	366
142	Final Braze Operation Large Area Brazing	367
143	Logic for Estimating Inspection Capabilities	371
144	NDI Engineering Task Flow Diagram for the Follow-On Program	380
145	Example of Quality Assurance Plan Prior to Fabrication	384
146	Example of Fabrication Inspection Outline	385

L I S T O F T A B L E S

<u>Table</u>		<u>Page</u>
I	Summary of Results	16
II	Reasons for Weight Savings and Cost Differences in Final Preliminary Designs	21
III	Candidate Baseline Aircraft Characteristics	26
IV	Critical Wing Test Conditions	28
V	F-111 Wing Fatigue Test Spectrum Summary	30
VI	F-111F Gross Weight - Load Factor Summary	39
VII	F-111 Fatigue Damage Summary/Preliminary Fatigue Analysis	44
VIII	Fatigue Spectrum Mission Segment Distribution	48
IX	Effects of Usage Variation on Fatigue Allowables	50
X	Effects of Usage Variation on Fracture Allowables Mid-Point K_{IC} and da/dN Data	51
XI	Cross-Section Concepts, C.S.S. 140, Evalua- tion Summary	65
XII	Cross-Section Concepts, C.S.S. 340, Evalua- tion Summary	68
XIII	Analytical Assembly Concepts, C.S.S. 140, Evaluation Summary	71
XIV	Analytical Assembly Concepts, C.S.S. 340, Evaluation Summary	72
XV	Preliminary Design Concepts - Evaluation Summary	74
XVI	Final Iterative Phase Wing Box Evaluation Summary	111

LIST OF TABLES (Continued)

<u>Table</u>	<u>Page</u>
XVII Stress Data Summary Sheet for Wing Box Design Concept No. 610RW000	121
XVIII Stress Data Summary Sheet for Wing Box Design Concept No. 610RW001	122
XIX Stress Data Summary Sheet for Wing Box Design Concept No. 610RW002	123
XX Stress Data Summary Sheet for Wing Box Design Concept No. 610RW003	124
XXI Stress Data Summary Sheet for Wing Box Design Concept No. 610RW004	125
XXII Stress Data Summary Sheet for Wing Box Design Concept No. 610RW005	126
XXIII Stress Data Summary Sheet for Wing Box Design Concept No. 610RW006	127
XXIV Stress Data Summary Sheet for Wing Box Design Concept No. 610RW007	128
XXV Stress Data Summary Sheet for Wing Box Design Concept No. 610RW008	129
XXVI Stress Data Summary Sheet for Wing Box Design Concept No. 610RW009	130
XXVII Distribution of Weight in Preliminary Design Wings	131
XXVIII Comparison of Preliminary Design Stiffness to F-111F Baseline	132
XXIX Advanced Air Superiority Fighter Preliminary Wing Designs Fatigue Damage Summary	166
XXX Fatigue Reliability Predictions for 506 Vehicle Fleet	173

LIST OF TABLES (Continued)

<u>Table</u>		<u>Page</u>
XXXI	Proposed Damage Tolerance Requirements	179
XXXII	Flaw Growth Data Used for Preliminary Design Analysis	202
XXXIII	Summary of Material Screening Tests	209
XXXIV	Residual Strength Summary for Lower Surface of Preliminary Wing Box Designs	214
XXXV	Preliminary Wing Designs Lower Surface Structure/Assumed Stress State	215
XXXVI	Flaw Fracture Risk Assessment 610RW003 Failure, 506 Aircraft Fleet	233
XXXVII	Candidate Materials - Aluminum Alloys	236
XXXVIII	Candidate Materials - Titanium	237
XXXIX	Candidate Materials - Steel	238
XL	ADP Wing/Phase IA	253
XLI	Summary of Mechanical Properties of Alloys	257
XLII	Advanced Air Superiority Fighter Full Wing Box Costs - Unit #506 - 20 A/C Per Month	282
XLIII	Estimating Methodologies Comparisons for 610RW004"A"	285
XLIV	Titanium Castings	295
XLV	Diffusion Molding	295
XLVI	Precision Forging	296
XLVII	Isothermal Forgings	296
XLVIII	Integral Panel Extrusions	297

LIST OF TABLES (Continued)

<u>Table</u>		<u>Page</u>
XLIX	Precision Titanium Extrusions	298
L	Integral Formed Panel	299
LI	Tapered Rolled Shapes	299
LII	Diffusion Bonding	300
LIII	Continuous Seam Diffusion Bonding (CSDB)	301
LIV	Roll Diffusion Bonding	302
LV	Diffusion Bond Riveting	303
LVI	T-Burn Through Welding	304
LVII	Gas Tungsten Arc Welding (Pulsed)	305
LVIII	Electron Beam Welding	306
LIX	High Frequency Resistance Welding	306
LX	Low Temperature Brazing	307
LXI	Adhesive Bonded Laminates	309
LXII	Rivet Bonding	310
LXIII	Weldbonding	312
LXIV	Composite Reinforced Structure (Boron or Graphite)	314
LXV	Merit Rating System for Concept Designs	315
LXVI	Material Parameters That Affect NDI Sensitivities	372
LXVII	Estimated NDI Capabilities	373
LXVIII	Examples of Cross Section Inspectability Ratings	378

LIST OF TABLES (Continued)

<u>Table</u>		<u>Page</u>
LXIX	Example of Analytical Inspectability Rating Sheet	379
LXX	Inspectability Rating Traceability for Preliminary Design 610RW003	382

SECTION I

INTRODUCTION

The main thrust of the Advanced Development Programs is aimed at ensuring USAF air superiority in the 1980's (reference Figure 1).

The measure of superiority or the degree to which USAF vehicles will dominate the air in the 1980's will depend on the ingenuity, diversity, significance and direct applicability of the aero-technology advancements that are made in the immediate future (reference Figure 2).

Technology is advancing in the fields of weaponry, electronics, aerodynamics and propulsion. In order that airframe characteristics not penalize the overall capability of the integrated weapons system of the future, Aero-Structures Technology must keep pace with other advancing technologies in the areas of:

- o Minimum Weight/Performance
- o Production/Operational Cost
- o Strength/Safety
- o Vehicle Life/Durability
- o Maintainability/Inspectability
- o Operational Dependability/Reliability

Achieving significant improvements in these design parameters requires that significant technological advancements be made in:

- o The Inception of New and Innovative Concepts in Structural Design
- o Fracture Mechanics
- o Stress Analysis Methods
- o Fatigue Analysis Methods.

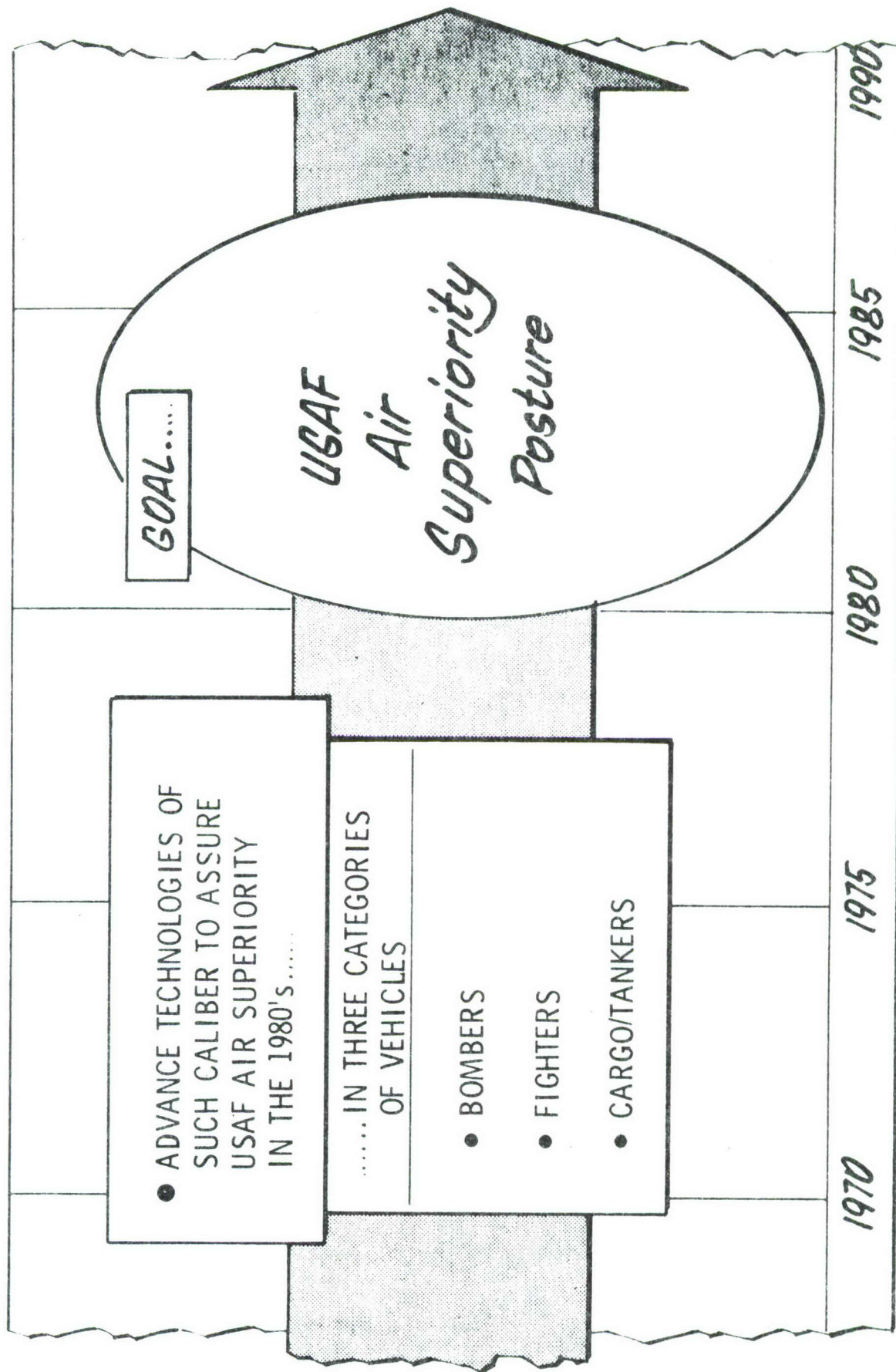


Figure 1 Main Objective of ADP's

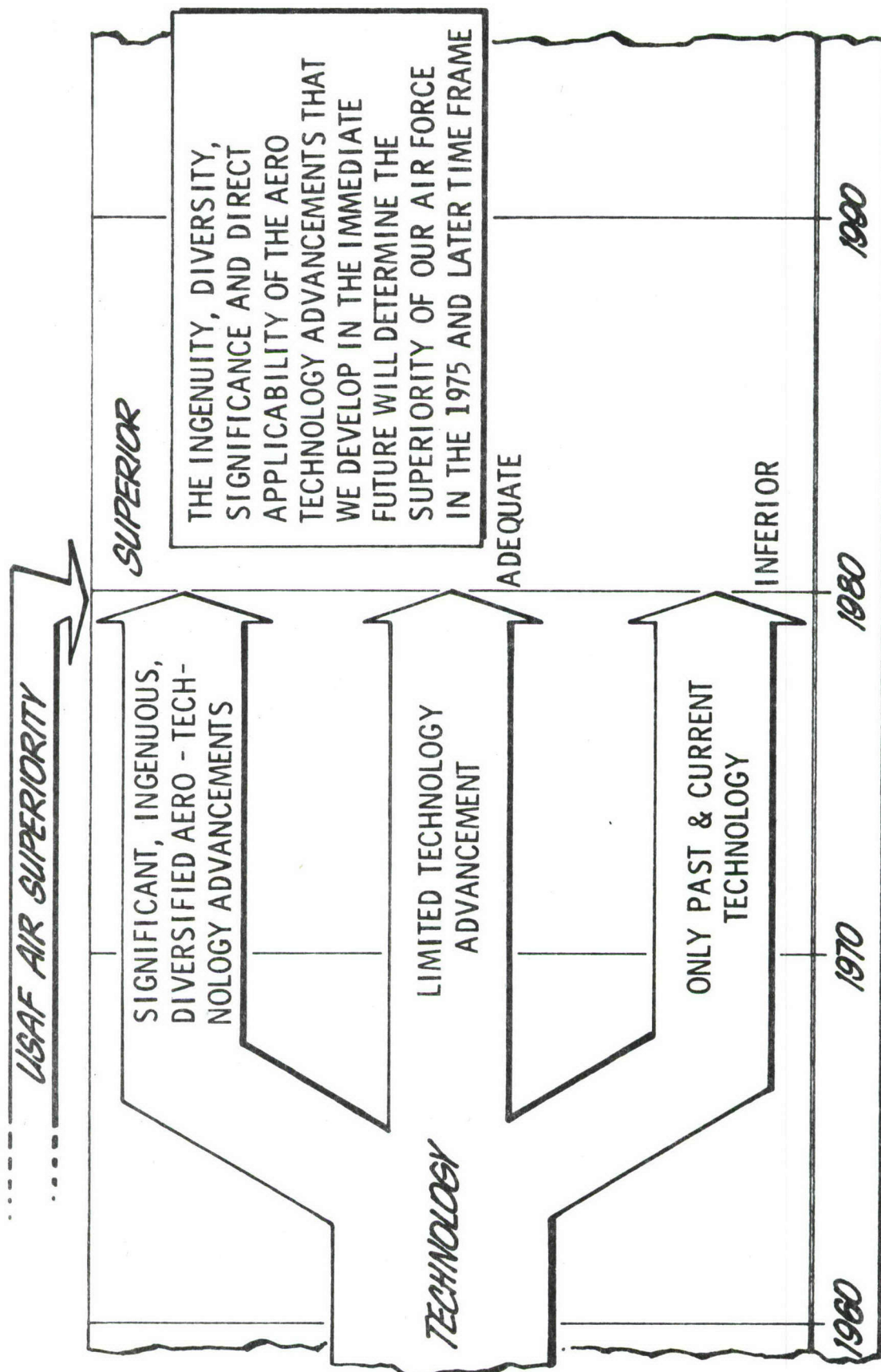


Figure 2 Technology vs Air Superiority

- o New Materials and Definition of Their Structural Capabilities
- o Manufacturing Methods
- o Non-Destructive Inspection Techniques
- o Weight/Strength and Cost Optimization Procedures
- o The Overall Engineering Methodology and Management Approach to Integrate These Technology Advancements Into a Superior Airframe Structural Design/Operational Vehicle
- o Dissemination of Technical Information to the Concerned Agencies of the Government and the Aircraft Industry.

These areas are displayed schematically in Figure 3.

Historically, airframe technological advancement and development of new structural concepts and materials have been a part of major hardware procurement programs. This approach to airframe technological advancement has resulted in a high degree of risk being associated with achieving program goals such as:

- o Schedule
- o Overall Program Costs
- o Vehicle Weight/Performance Goals
- o Airframe Fatigue Life Requirements
- o Vehicle Maintenance & Operational Costs

Examples where technological advancement during major programs was costly are:

- o The use of 7079 AL alloy in some B-52 models, B-58, and many other vehicles before the stress corrosion cracking characteristics of the material were determined.

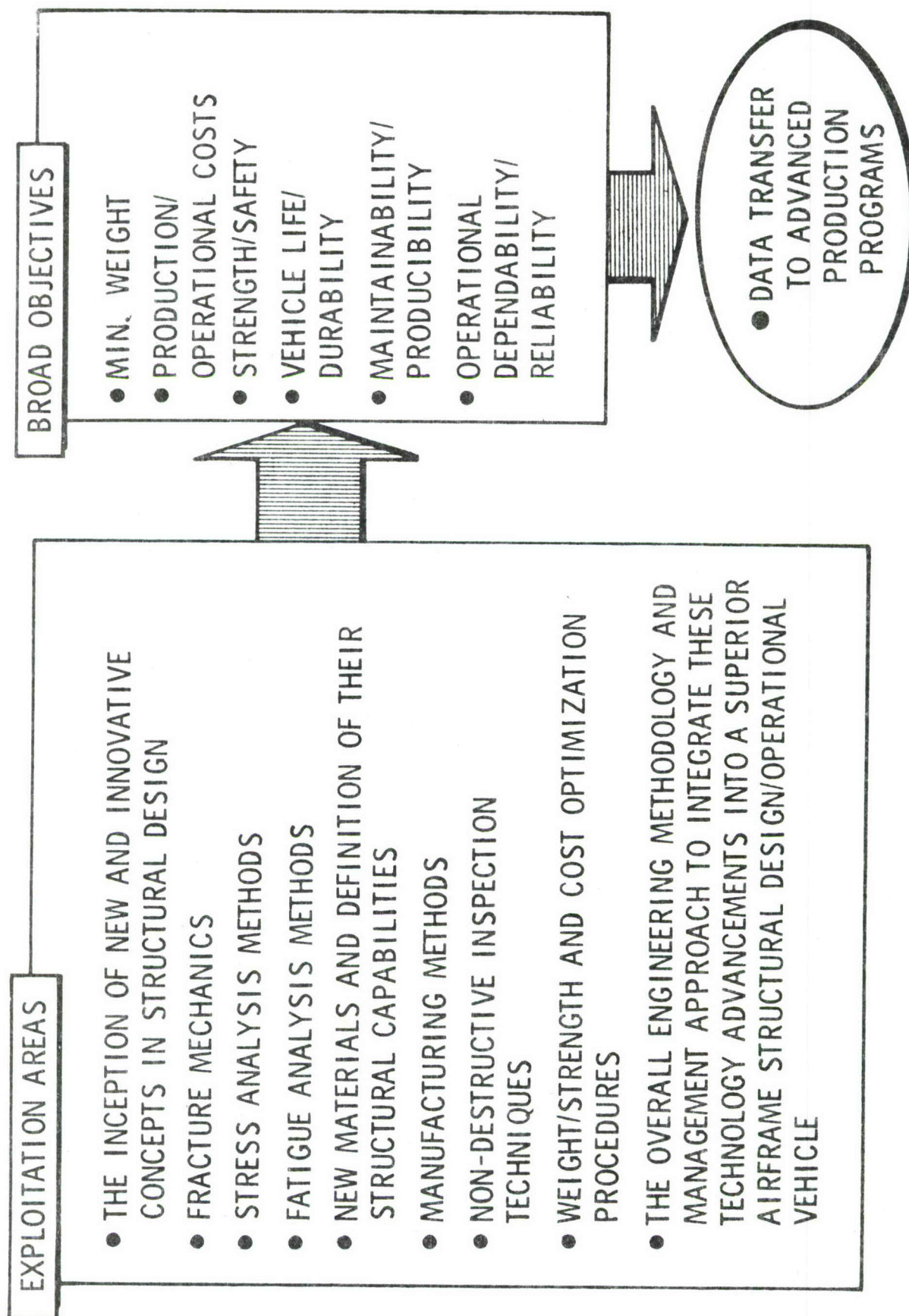


Figure 3 Exploitation Areas to Achieve Objectives

- o Brazing and weld joining of stainless steel wing panels during the B-70 program.
- o Certain applications of D6AC steel in the F-111 before damage tolerance characteristics were determined for the new alloy.

Where the risk of program success is reduced by utilizing only past technology - the result is a vehicle with little improvement in capability or performance over existing vehicles of the USAF or other air powers (reference Figure 4).

The successful Flight Dynamics Laboratory execution of the current ADP program will:

- o Provide improved structural technology consistent with requirements of future superior vehicles.
- o Provide technology advancements to future fleets at a small fraction of the cost required to make the advancements during a production program.
- o Provide the technology in advance of future planned programs so as not to incur high risks and costs in those programs.
- o Further define the tensile, fatigue, stress corrosion cracking and crack growth characteristics of new aircraft materials, such as 7050 & 7475 aluminum, 8-8-2-3 titanium, and 10 NI-2CR-MO-8CO steel.
- o Determine the feasibility, applicability, limitations, advantages and problems of using these materials in advanced aircraft structures.
- o Select applications for and continue development of advanced manufacturing methods for aircraft structures in areas such as welding, brazing, adhesive bonding, diffusion bonding, other joining techniques, machining, diffusion molding, creep forming, taper rolling, taper and integral stiffened panel extruding, and isothermal and precision forging.

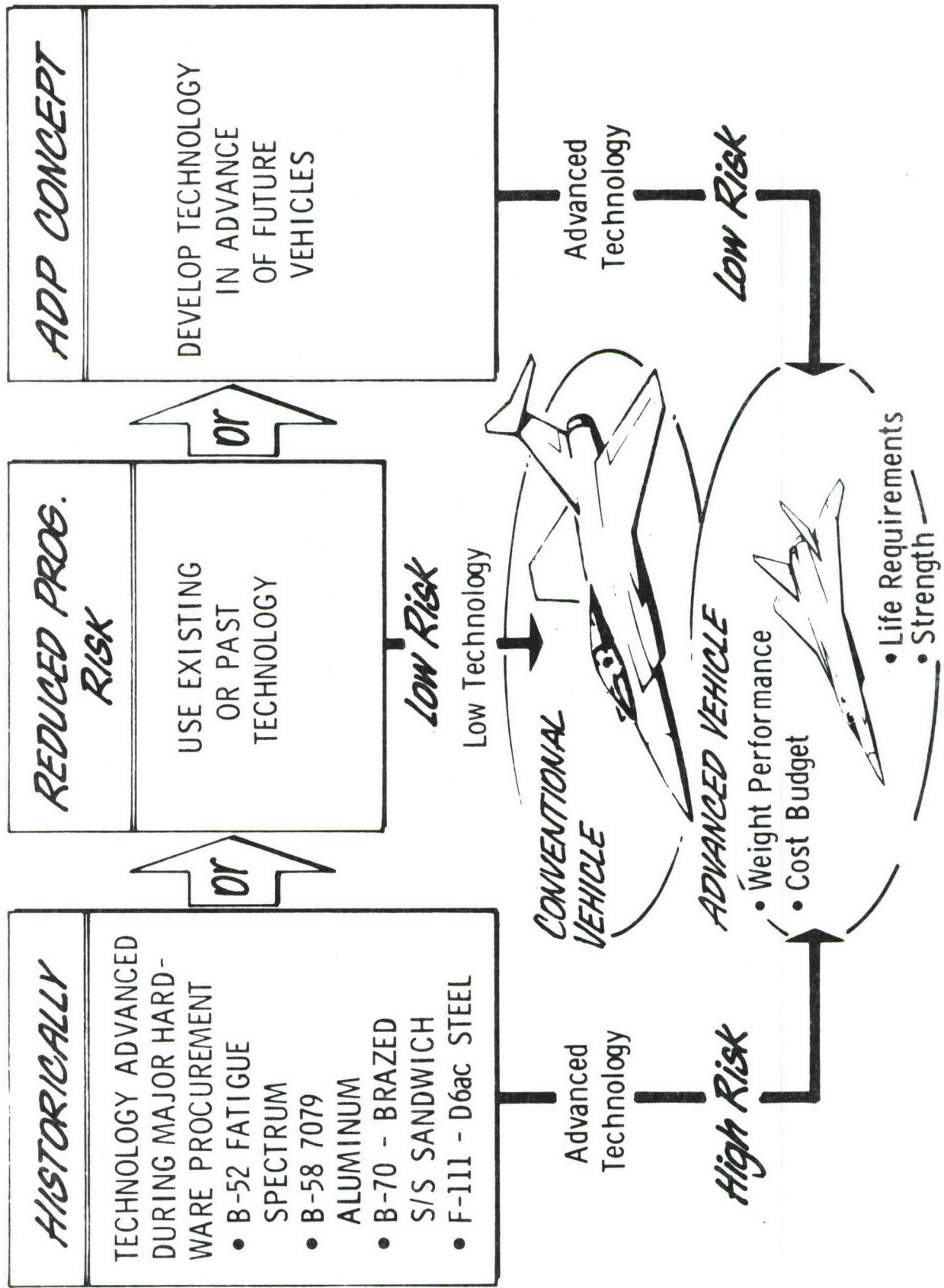


Figure 4 Technology Advancement vs Program Risks

- o The applicability of advanced NDI methods is being determined. The areas requiring further development of NDI methods will be defined.
- o Advanced stress analysis and fatigue analysis methods and criteria are being employed and perfected.
- o Advanced fracture mechanics analysis methods are being utilized and integrated into the design at the preliminary design phase of the program.
- o Realistic service life criteria for an advanced air superiority fighter are being developed that will assure safe, reliable structure with a negligible effect on weight and cost.
- o Advanced costing techniques are being exercised and developed. Projected costs for airframe production quantities will be determined for the 1975-1985 time frame.
- o New and innovative concepts in aircraft structures are being conceived, defined, and evaluated. Over 100 concepts have been defined and evaluated.

The Advanced Fighter Wing ADP Program goal is:

Apply innovative effort and new technology to develop an Advanced Metallic Wing Structure that will afford a significant reduction in weight while maintaining cost approximately equivalent to the base line article.

The relationship between this goal and the other ADP programs is demonstrated by Figure 5.

During pursuit of the program goals, various areas of structures technology were exploited and advancements resulted. These areas were: the creation of new and innovative concepts in structural design, fracture mechanics, stress analysis methods, fatigue analysis methods, new materials and definition of their structural capabilities, manufacturing methods, non-destructive inspection techniques, weight/strength and cost optimization procedures (reference Figure 6).

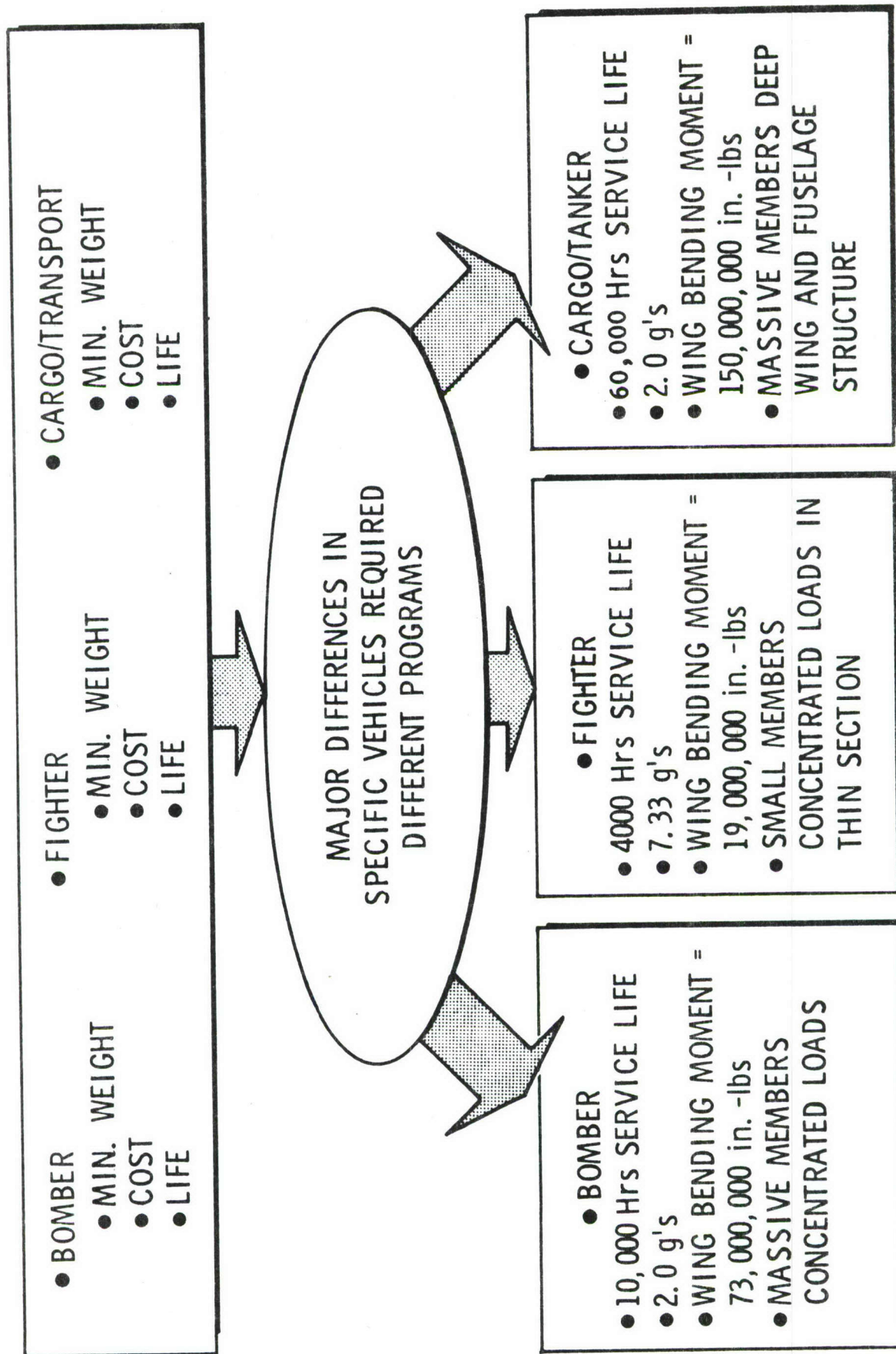


Figure 5 Common Design Goals

ADVANCED FIGHTER WING - ADP

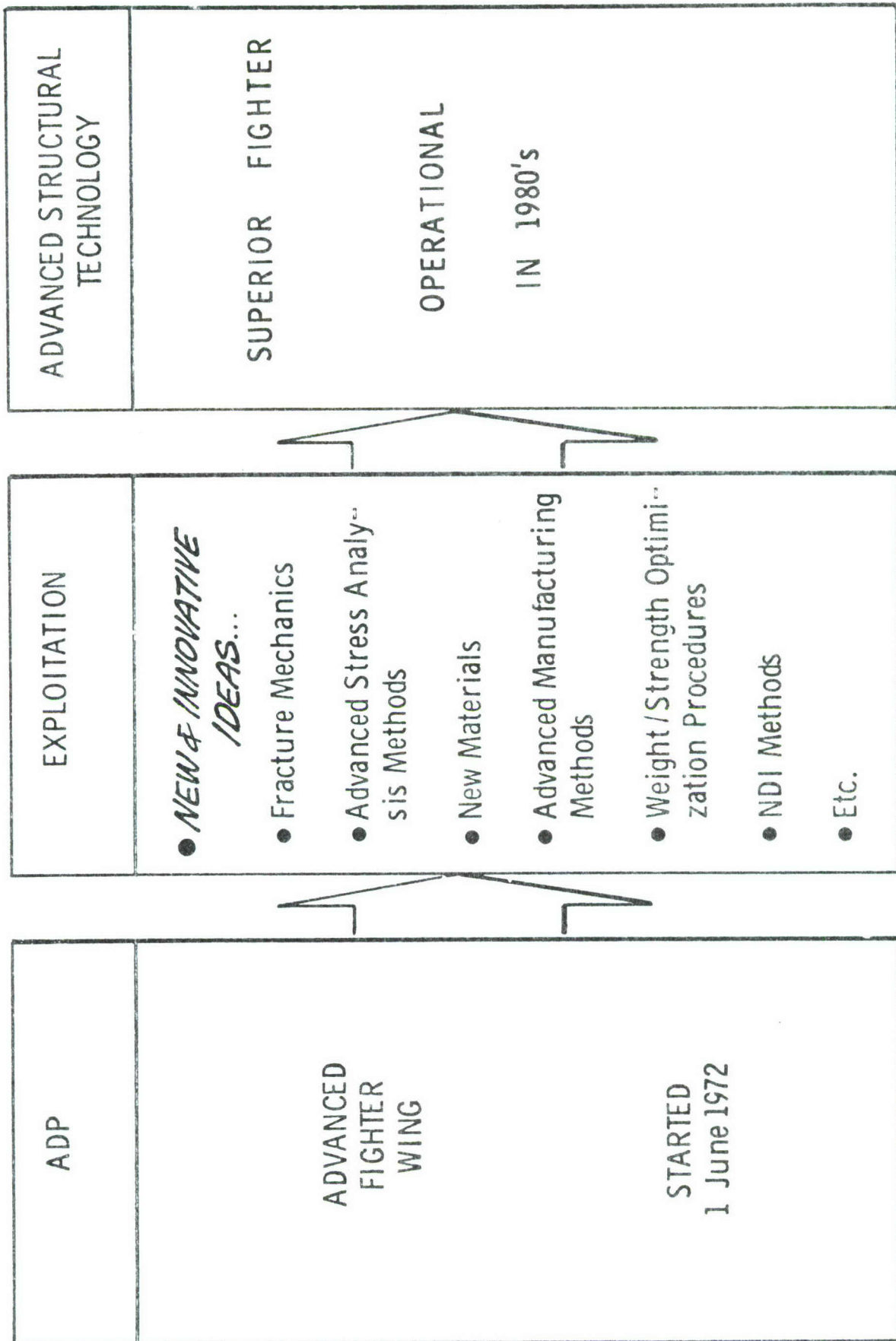


Figure 6 Advanced Fighter Wing - ADP

The F-111F aircraft was chosen as the baseline for the program because it represents current state-of-the-art in structures technology. Its flight envelope and range exceed that of all other USAF operational fighters from Sea Level altitude to the stratosphere. The F-111 wing box, shown in Figure 7 is the baseline component for this program.

The F-111F airframe has been designed and tested to the requirements of the MIL-A-8860 series specifications, and the entire F-111F program effort has been conducted in accordance with the intent of the ASIP as described in TR66-57. Extensive service experience data, reflecting over 150,000 flight hours, are available on the F-111.

The F-111F is a long-range fighter with the capability of Mach 1.2 flight at low level and Mach 2.5 at high altitude. It should be emphasized that the F-111F wing is highly representative of current structures technology (reference Figure 8).

Nine designs have been developed during the program to meet the goals shown in Figure 9. At least one of these designs provides a weight reduction of 15% while maintaining cost equal to or below the baseline; at least one design provides a 15% cost reduction over the baseline at Airplane #506 while maintaining weight equal to or below the baseline; and, the other configurations developed show savings between these two goals.

Perhaps the most important result of this program has been the development of an overall engineering methodology and management approach to integrate technology advancements into a superior airframe structure for a future aircraft.

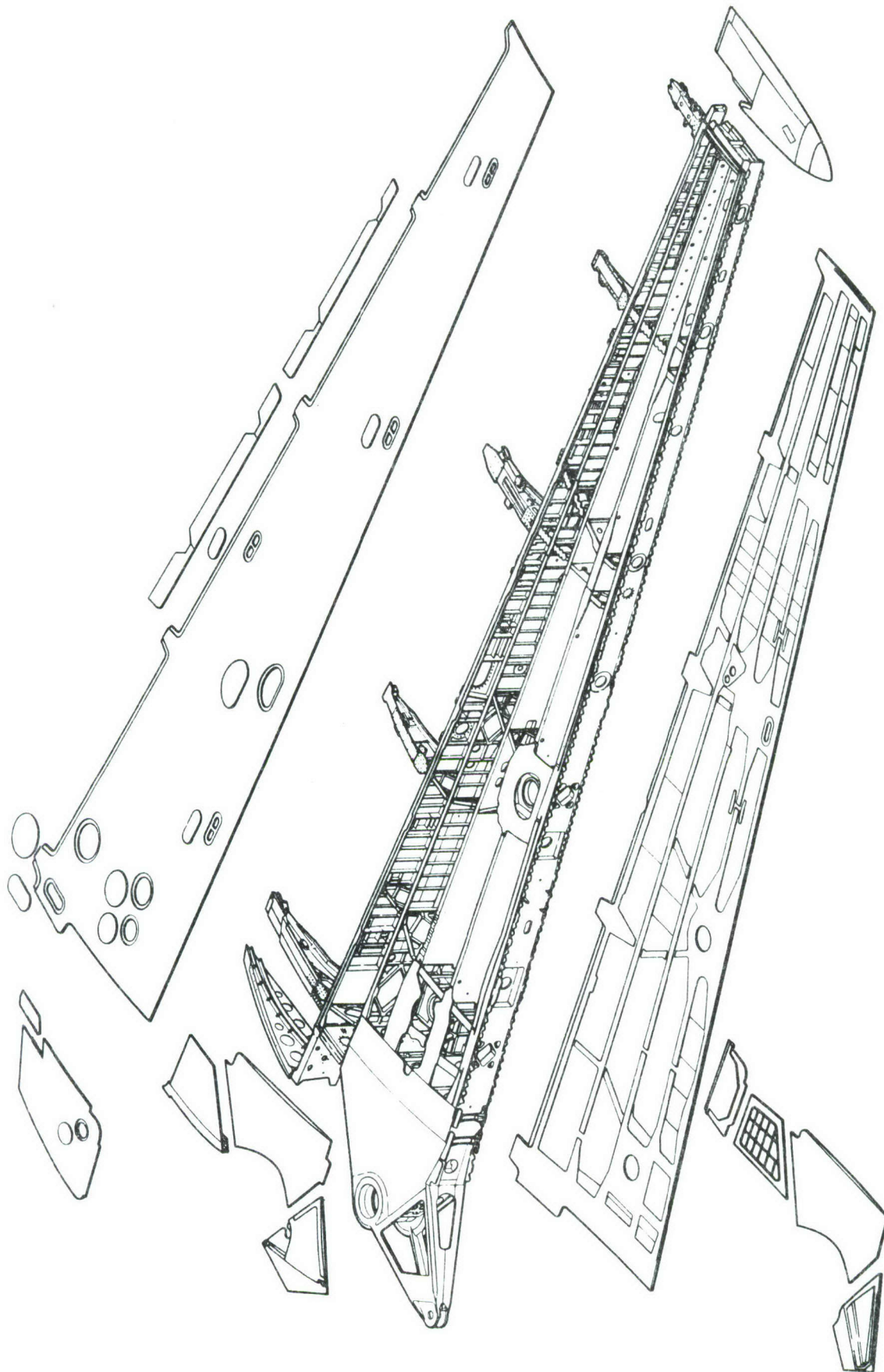
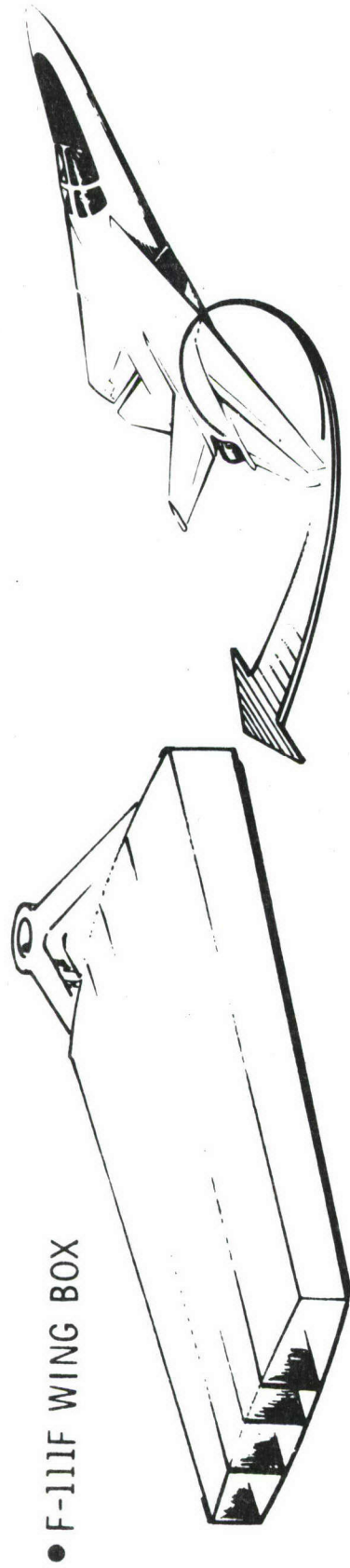


Figure 7 F-111 Wing Box



- THE F-111 WING BOX BASELINE FOR THIS PROGRAM UTILIZES LATEST STATE-OF-THE-ART MATERIALS AND MANUFACTURING PROCESSES
- THE F-111F FLIGHT ENVELOPE EXCEEDS THAT OF ALL OTHER OPERATIONAL FIGHTERS AT LOW AND HIGH ALTITUDE
- THE WING IS A VARIABLE SWEEP CONFIGURATION, CONTAINS FUEL, SUPPORTS A LARGE ARRAY OF CONVENTIONAL AND NUCLEAR WEAPONS OR EXTERNAL FUEL TANKS AT EIGHT WING HARDPOINTS
- THE BASELINE DESIGN HAS BEEN TEST VERIFIED TO MEET THE LATEST MIL-A-8860 SERIES SPECIFICATIONS
- IT WILL SERVE AS THE MEASURING STICK FOR DETERMINATION OF THE REAL IMPROVEMENTS MADE DURING THE PROGRAM

Figure 8 Fighter Wing ADP Baseline

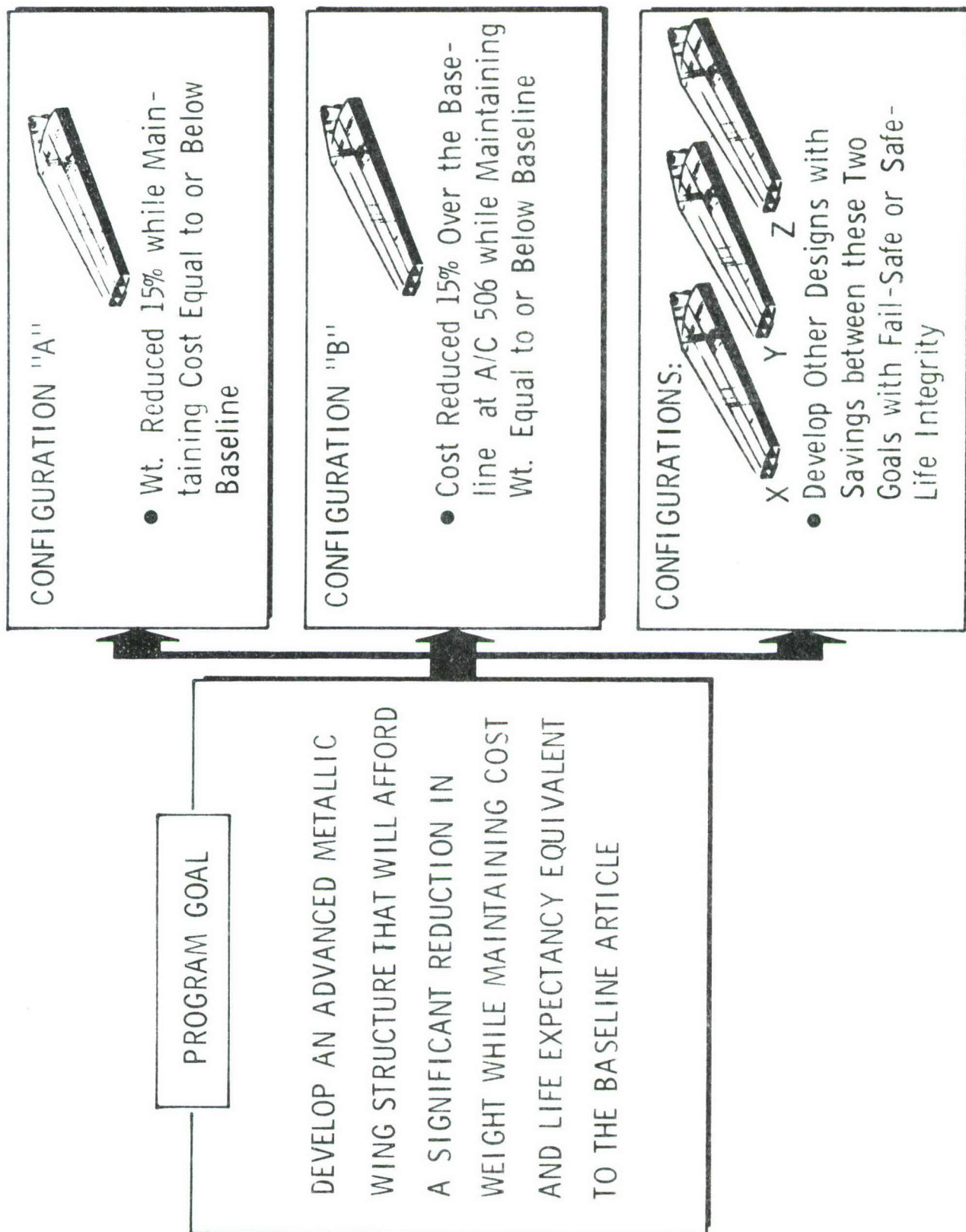


Figure 9 Program Design Goals

SECTION II

PROGRAM SUMMARY

The objectives set for this program have been met successfully through utilization of systematic and innovative techniques.

2.1 OBJECTIVES AND APPROACH

The objective of this program is to develop and demonstrate new and/or improved manufacturing, materials, and structures technologies that meet the requirements of future Air Force fighter system.

The specific objective of Phase IA of the program has been to develop advanced metallic structural concepts that will afford a reduction in the weight of fighter wings while maintaining cost and life expectancy approximately equivalent to the baseline article.

More specifically, goals of 15% weight reduction on at least one design and 15% cost reduction on at least one design were established. These goals have been met as described in the body of the report and as summarized in Table I.

The highly innovative and successful approach to meeting these goals is described fully in the body of the report and is summarized schematically in Figure 10.

2.2 GENERAL PROGRAM RESULTS

Several wing box configurations were defined in advanced aluminum alloys that save weight and reduce cost when compared to the baseline structure.

One aluminum design saves 24.0% weight and reduces the cost by 13.8%. Another aluminum design with an 18.9% weight savings, reduced costs by 15.7%.

Table I SUMMARY OF RESULTS

GOALS	PERFORMANCE
WEIGHT REDUCTION OF 15% WHILE MAINTAINING COST EQUAL TO OR BELOW BASELINE	61ORW002 - 38.8% WEIGHT SAVINGS
COST REDUCTION OF 15% @ A/C 506 WHILE MAINTAINING WEIGHT EQUAL TO OR BELOW BASELINE	61ORW004 - 15.7% COST SAVING
ADDITIONAL DESIGNS THAT ARE BELOW BASELINE IN BOTH WEIGHT AND COST	61ORW003 - 24.2% WEIGHT SAVING - 13.8% COST SAVING
ALL DESIGNS MUST MEET THE SERVICE LIFE CRITERIA	ALL DESIGNS MEET THE SERVICE LIFE CRITERIA

● A NEW, SYSTEMATIC STRUCTURAL DESIGN PROCEDURE HAS EVOLVED THAT CAN BE UTILIZED TO SYNTHESIZE AN INTEGRATED, BALANCED, OPTIMUM DESIGN FOR ANY DESIRED APPLICATION. THIS SYSTEM IS DEPICTED ON THE CHART BELOW:

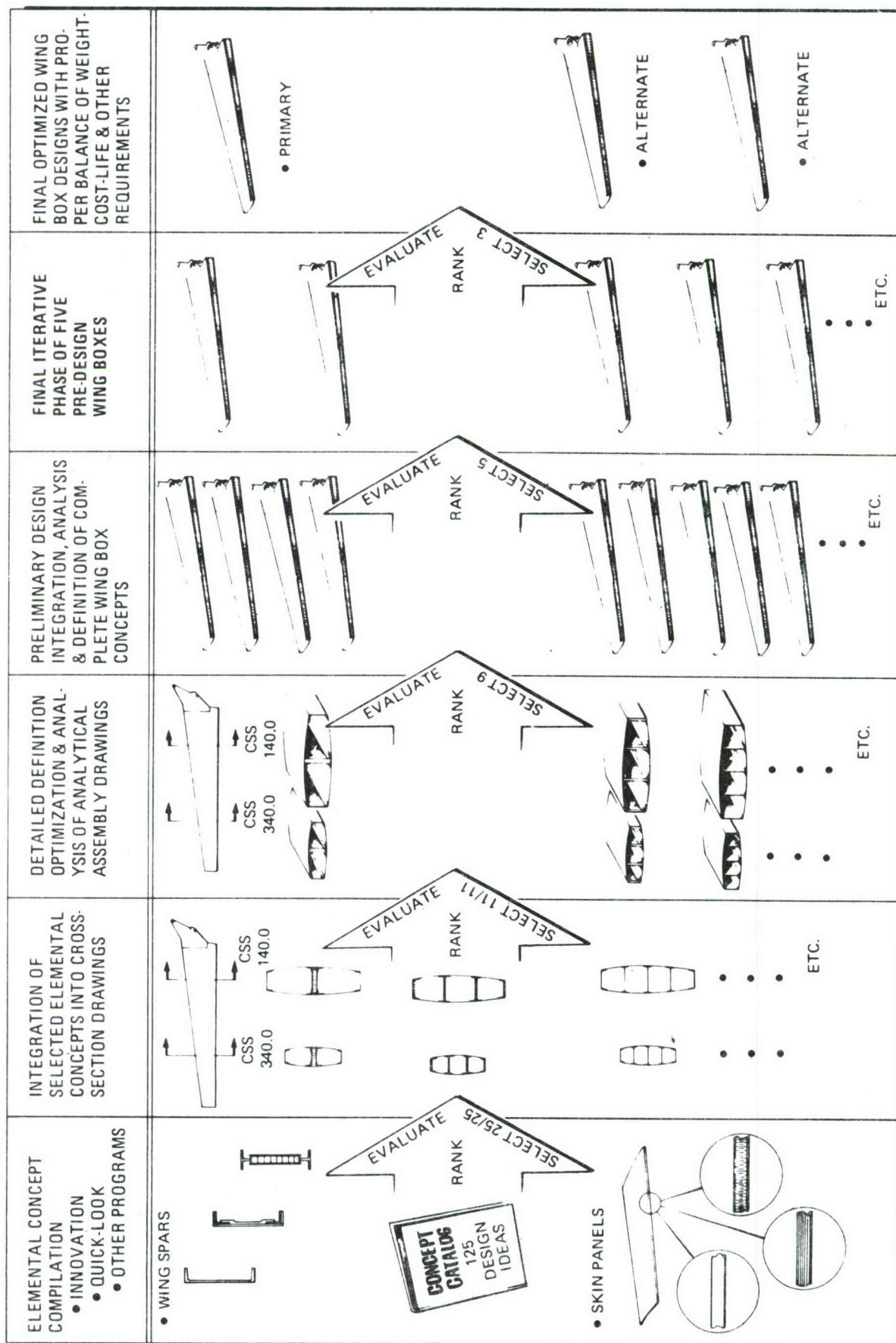


Figure 10 Fighter Wing ADP Design Approach

Three wing box configurations were defined in high strength titanium alloy, titanium designs showed greater weight savings than aluminum designs but an increase in cost resulted on all titanium designs. For example, the highest ranking titanium design saved 38.8% weight with a cost increase of 31.0%. It should be noted, however, that the weight savings potential of advanced titanium configurations are of a sufficient magnitude to allow reducing the size of an aircraft during its preliminary design phase when designed to fixed mission requirements. Aircraft cost savings as a result of reduction in aircraft size will offset the increase in airframe cost as a result of configuring of advanced titanium in lieu of aluminum.

The careful screening and evaluation that has been conducted indicates that weight savings can be attained even though severe fracture control is imposed. The weight savings have been achieved largely by elimination of fastener holes through the lower surface in order to attain maximum utilization of the latest metallic material tension properties. Calculations in paragraph V.7, Appendix V, illustrate this point.

The successful results of this program are to a large extent attributable to the systematic design approach employed during the program. Figure 10 depicts the design approach employed during the program.

Analytical compliance with the most recent Air Force fatigue and damage tolerance requirements has been emphasized throughout a unique and systematic preliminary design process directed toward the development of Advanced Air Superiority Fighter wing concepts. The products of this effort are a substantial number of highly efficient full wing designs utilizing materials and fabrication techniques not yet fully proven but having unlimited potential. The risks associated with these technology advancements have been identified, and the feasibility of demonstrating their compliance with fatigue and damage tolerance requirements has been planned for implementation in subsequent phases of this program.

2.3 SPECIFIC PROGRAM RESULTS

A very useful method for preliminary structural analysis has evolved from the various analysis - evaluation steps followed in this program. This method can be followed, with the aid of examples, in Section V.

Several highly innovative structural concepts have been analyzed and evaluated using flight measured loadings and using the latest available techniques for fracture control. These concepts include:

- . Elimination of traditional lower surface fasteners for reduced stress concentration.
- . Planked, laminated lower skin panels for multiple load paths, crack arrest and reduction in crack growth rate.
- . Wide, corrugated, spars to reduce panel unsupported width and to increase panel edge restraint.
- . Scalloped skin/spar shear tabs for skin attachment without holes through outer surface.
- . Spanwise fuel flow holes to reduce stress concentrations which would be more pronounced with chordwise fuel transfer holes.

The improvement in fatigue quality and damage tolerance characteristics resulting from elimination of fastener systems in primary wing structure has permitted use of higher stresses and thereby reduced weight. These weight reductions have been analytically demonstrated during this program.

An extensive evaluation of the detailed damage tolerance requirements being proposed by the Air Force as a revision to MIL-A-8866A has been made in Phase IA. The requirements for slow crack growth structure were exercised on the baseline structure using sensitivity studies to lend visibility to the impact of variation in the many parameters influencing damage tolerance assessment. The requirements for fail safe structure were applied to the Phase IA preliminary wing designs to achieve minimum weight structure and structural integrity as a reasonable cost. These goals are often incompatible.

In its present form, the damage tolerance criteria is technically feasible but often awkward to interpret and apply. This is primarily true of the requirements for fail safe structure which are presently separated with respect to multiple load path and crack arrest. Many of the requirements specified for these two classifications overlap and are difficult to apply to design concepts utilizing both damage tolerance features. The criteria is also directed toward traditional sheet/stringer construction with regards to damage assumptions following primary load path failure, crack arrest, or inservice inspections. Application of these damage requirements, as well as those for assumed damage in intact new structure, is very ambiguous for thin sheet laminated structure. The assumption made for analysis of laminated structure in this report (paragraph 7.4) was that each ply constituted a load path and that complete failure of the laminate involved failure of successive plies.

It is also felt that specific attention should be given to requiring that basic fracture data for laminates be obtained when they are used rather than data for only the ply material comprising the laminate.

Additional interpretation is needed regarding assumed initial flaws, particularly in thin sheet structure, to alleviate the present contractor responsibility (at added cost to the Air Force) of defining the worst flaw shape and size.

The words, "experimentally verified," should be added to the requirements in connection with spectrum retardation effects, due to its dependence on spectrum shape and content (and possibly type of material).

The criteria itself would be easier to use if, after classifying a structure fail safe or monolithic, the requirements for that classification were a separate entity without cross referencing.

Cost and weight differences between the baseline and the various concepts are summarized in Table II to document sources of savings. Specific numerical comparisons with the baseline are shown.

Table II REASONS FOR WEIGHT SAVINGS AND COST DIFFERENCES IN
FINAL PRELIMINARY DESIGNS

Configuration No.	Configuration Name	Weight and % Savings	Cost and % Change	Reasons for Weight Savings	Reasons for Cost Change
610RW000	F111F Baseline	16650.0	\$64,283.00		
610RW002	Multi-Wet Cell Brazed Titanium	1019.6 -38.8% savings	\$84,163.00 +31 % increase	<ul style="list-style-type: none"> o No fastener penetrations or other severe stress raisers in lower tension skin o Lower skin laminated and planked for a fail safe and crack growth arrest/reduced growth rate resulting in high fracture allowable stress. o High strength alloy use is permitted by laminated structure and elimination of stress raisers in tension members. No weight penalty is paid to meet static strength requirement. 	<ul style="list-style-type: none"> o Titanium material results in a matl. cost increase over aluminum. o Tooling for titanium brazing is more costly than aluminum designs. o This titanium design is more economical than some aluminum or other titanium designs where a large percent of matl is wasted by machining spars, fittings and ribs in lieu of built-up sheet metal design.
				<ul style="list-style-type: none"> o Multi-wet cell core efficiently reacts internal pressure loads and stabilizes upper panel for compression stresses equal to yield strength of upper panel material. 	

Table II (Contd)

Configuration No.	Configuration Name	Weight and % Savings	Cost and % Change	Reasons for Weight Savings	Reasons for Cost Change
610RW003	Laminated lower skin with stepped spar caps, Plate Upper skin, corrugated Spar Webs (A1)	1261.4 -24.2% Savings	\$55,377.00 -13.8 % Savings	<ul style="list-style-type: none"> o Elimination of fasteners and other stress raisers in lower tension panel bending material permits operating to higher stress level. o Laminated lower skin of tough alloy results in reduced crack growth rate and high fracture allowable stress. o Wide cap, corrugated spars stabilize upper panel to yield strength of matl. o Corrugated spars are lighter than machined spars. o Upper panel rivets are lighter than bolts. 	<ul style="list-style-type: none"> Reasons for cost savings: <ul style="list-style-type: none"> o Built-up spar designs are more economical than machined designs because of material savings. o Elimination of fasteners on lower surface reduces cost. o Using rivets in lieu of bolts on upper panel reduces cost. o Simplicity of plate upper panel reduces costs. o Weights savings in built-up sheet metal equates to a cost savings in materials.
		1351.15 -18.9% Savings	\$54,211.00 -15.7% Savings	<ul style="list-style-type: none"> o No fastener penetrations and other severe stress raisers in lower tension panel bending material. o Upper sandwich panel stable in compression up to yield strength of upper panel matl. o Sandwich spar webs lighter than machined webs. 	<ul style="list-style-type: none"> Reasons for cost savings: <ul style="list-style-type: none"> o Built up sandwich spars more economical than machined spars. o Constant thickness skins on constant thickness slugs results in an economical sandwich panel. o Using rivets in lieu of bolts in upper surface achieves cost savings.
610RW004	Adhesive Bonded Aluminum Honeycomb Panels				

Table II (Contd)

Configuration No.	Configuration Name	Weight and % Savings	Cost and % Change	Reasons for Weight Savings	Reasons for Cost Change
610RW004 (Cont'd)					<ul style="list-style-type: none"> o Elimination of fasteners through lower surface (taper-loks) is a significant cost savings. o Weight savings effects a cost savings in materials.
610RW006	Space Truss, Brazed Titanium	1109.0 -33.4% Savings	\$122,120.00 +90% Increase	<ul style="list-style-type: none"> o Elimination of fasteners and other stress raisers in lower tension panel bending material. o Planking and laminating of lower skin provides fail safe and crack arrest capabilities in lower skin permitting design to higher operating stress than allowed with monolithic structure. o Trussed spar webs of tubular design are highly efficient. o Close spar spacing stabilizes upper panel to a compression buckling allowable stress to near yield strength of the material. 	<ul style="list-style-type: none"> Reasons for cost increase. o High titanium raw matl. cost. o Brazed titanium spars require different high cost braze tool for each spar.

2.4 POTENTIAL TECHNOLOGY ADVANCES

Several Preliminary Design Drawings in Appendix IV utilize the concept of laminating and planking for fail-safe characteristics and to reduce crack growth rate and the likelihood of crack growth through the skin thickness.

This concept, if tests verify these desired characteristics, offers versatility in design by allowing selective placement of load paths to be coordinated with options for fabrication. Additionally, the Bi-metallic concept of 610-123 and 610-130 (in Appendix I) offers potential in reducing tensile stresses on the outer surfaces of skins.

The integration of the following four factors into brazed or bonded design concepts for primary wing box structure has the potential of achieving significant weight reductions while still meeting stringent fatigue and damage tolerance criteria:

- (1) All fasteners through the lower surface are eliminated by the use of bonded or brazed joints.
- (2) Reduced crack growth rates are achieved in high strength 8-8-2-3 titanium and 6AL-4V STA alloys by utilizing brazed laminated sheet.
- (3) Reduced crack growth rates are achieved in aluminum alloys by utilizing bonded laminated sheet.
- (4) The high strength of the STA titanium is retained by use of a low temperature brazing alloy, as yet undeveloped but very feasible.

Brazing has been exploited in the Preliminary Designs of Appendix IV. Existing technology relies on furnace heating with possible use of inert gas ambient, 610RW002 and 610RW006 rely on this process and a low temperature (approximately 1100°F) brazing alloy. The potential exists for brazing by applying heat internally by a recirculating inert fluid and using fixtures and insulators externally.

SECTION III
BASELINE SELECTION AND
DEFINITION

The F-111F was selected as the baseline aircraft for the Phase IA Convair Aerospace effort. The F-111F is a deep-interdiction, all-weather, day or night fighter with close support capability. It is the most advanced operational fighter in the TAC Inventory. The flight envelopes of all other operational U.S. tactical fighters fall inside the F-111F operational envelope. A summary of the most promising baseline candidates and their characteristics is presented in Table III.

3.1 BASELINE SELECTION RATIONALE

The F-111F wing box was used as the baseline component for this program. The ready availability of existing data, equipment, and facilities associated with the F-111 will result in a program of maximum cost effectiveness. Further, a comparative evaluation of other baseline candidates (including the F-4, F-5, F-100, F-104, F-105, F-106, and F-15) indicates that the F-111 wing is the only available component that meets all of the requirements stated in the RFQ.

The F-111F airframe has been designed and tested to the requirements of the MIL-A-8860 series specifications, and the entire F-111F program effort has been conducted in accordance with the intent of the ASIP as described in ASD-TR-66-57. Extensive service experience data, reflecting over 150,000 flight hours, are available on the F-111.

The F-111F is a long-range fighter with the capability of Mach 1.2 flight at low level and Mach 2.5 at high altitude. It should be emphasized that the F-111F wing is highly representative of current structures technology.

3.1.1 Cost-Effective Aspects of
Selected Baseline Component

As previously mentioned, the availability of existing F-111 assets will significantly reduce program costs, both for the initial phase and for the follow-on phases. A comprehensive library

Table III CANDIDATE BASELINE AIRCRAFT CHARACTERISTICS

Comparison* Parameter									Future Fighter System
	F-111	F-106	F-4	F-15	F-105	F-104	F-5	F-100	
Design Mach High Alt Low Alt	2.5 1.2	2.1 1.0	2.0 1.16	2.4 1.2	2.08 1.1	2.0 1.15	1.4 1.0	1.38 0.96	2.5-3.0 1.2-1.6
Gross Weight Flt Design	73,000	34,700	37,500	40,000	35,000	16,400	11,550	29,390	60,000
Max Load Factor Max q @ V _L	7.33 2780	7.33 2000	6.5 1980	7.33 2800	8.6 2000	7.33 1950	6.5 1700	7.33 1680	8.00 3000--4000
Wing Area Ft ²	525	698	530	608	385	196.0	170	400	Undetermined
External Skin Temp	350°F	260°F	250°F	350°F	250°F	250°F	200°F	200°F	Above 350°F

of analytical and test data covering the many phases of structural integrity substantiation is available. For example, a detailed definition of the usage spectrum and the corresponding service loads spectra are available for use in computer analyses. In addition, tooling is available, and static and fatigue test setups are in existence. Thus, the F-111F wing constitutes a highly cost-effective baseline component for demonstrating advancements in structures technology.

3.1.2 F-111 Wing Structural Integrity Verification Program

Structural integrity of the F-111F wing has been verified by a comprehensive program of tests and analyses. Tests include laboratory static and fatigue, flight loads, inflight dynamic response, flight flutter, and vibration.

3.1.2.1 F-111F Wing Static Test Summary

The F-111 wing has been subjected to an extensive structural qualification static test program. Test conditions were applied for positive and negative load factors as well as stowed and extended high-lift surface positions. The critical test conditions for the production wing component are summarized in Table IV. In all cases, test loads met or exceeded 150 percent of limit load.

3.1.2.2 Baseline Fatigue Strength

The fatigue life of the F-111 wing has been established as greater than 10,000 hours (or 25 years) in terms of the current design service load spectra which include a scatter factor of 4.0. The excellent fatigue strength has been developed through an extensive program of design development testing, fatigue analysis, and full-scale verification fatigue tests. The program was developed in accordance with the Air Force Structural Integrity Program and includes

1. Fatigue design criteria and loads spectra
2. Design development test program
3. Preliminary (design) fatigue analysis
4. Full-scale wing fatigue test

5. Revised fatigue analysis
6. Fleet service load monitoring
7. Fatigue damage monitoring of the fleet.

The first four elements of the program have been completed; fatigue analyses are being updated to reflect the full-scale fatigue test results, and service load/fatigue damage monitoring of the F-111 fleet has begun. The F-111 wing development program encompassed a sizable number of fatigue development tests, in which variable amplitude testing was emphasized. The wing fatigue development test program is summarized below:

Element Tests. Multiple tests (~150) were run to develop the upper and lower skin and spar design detail.

Preproduction Design Verification Tests. More than 31 lower-surface wing-splice tests were conducted in addition to tests of the upper-surface splice and pylon-cutout detail in the lower surface. Eight two-spar box beams were also tested to failure under the original design load spectra.

Table IV CRITICAL WING TEST CONDITIONS

Condition	Maneuver ⁽³⁾	Mach No.	Alt	Weight	Sweep	n _z	Temp °F	Test Load Lmt Load
B-9(1)	BS	1.4	26K	50,000	50°	6.5	167	161.5%
C-14	BPO	0.96	25K	70,000	35°	-3.0	85	155%
P-101	BSPU	0.50	S.L.	80,000	16°	4.0	130	150%
P-503	BSPU	1.05	S.L.	70,000	50°	7.33	212	151%
FBW-17 ⁽²⁾	NSPU	0.44	S.L.	122,900	16°	1.86	-	150%
FBW-19 ⁽²⁾	NSPU	0.50	S.L.	109,852	16°	2.00	-	150%

- NOTES: (1) Navy condition
 (2) FB-111A conditions tested as Test Condition FBW-19/17
 (3) Maneuvers: BS - Balanced Symmetric; BPO - Balanced Push-Over; BSPU - Balanced Symmetric Pullup; and NSPU - Normal Symmetrical Pullup.

3.1.2.3 Full-Scale Wing Fatigue Tests

Fatigue analyses of 10 points in the wing were prepared on the basis of the Mission Analysis Composite (MAC) spectrum to provide an initial service life evaluation and for use in development of the full-scale fatigue test spectra. The initial minimum-life estimate was calculated to be essentially 16,000 hours with the critical point estimated to be in the steel wing-pivot fitting that forms the most inboard section of the wing.

Two full-scale wings have been fatigue tested to failure as part of the F-111 Fatigue Test Program. These tests were conducted at the Convair Aerospace Test Laboratories in San Diego, California. The pivoting wing design provided a unique opportunity for running the wing tests separately from the fuselage tests with no compromise to test load reactions and boundary conditions. The test spectrum was developed to be equivalent to the MAC design service spectrum and was applied in 400-hour blocks. The spectrum is summarized in Table V. The results of the two wing fatigue tests were as follows:

Right-Hand Wing. Failure occurred during application of loading block No. 31 through the lower plate of the D6ac steel wing pivot fitting. Fatigue initiated at a fuel cross-flow hole in an integral stiffener which attaches to a center spar web. Disassembly and detailed inspection of other areas in the wing revealed no fatigue damage.

Left-Hand Wing. Failure occurred after the application of 100 loading blocks plus 10,151 cycles of the most severe loading condition in the fatigue spectrum (Condition T-1, Layer 5, of Table V). Limit proof loads (positive and negative) were applied to the test article after Block No. 2 consistent with the proof testing conducted on the F-111 fleet. Following Block No. 10, a boron-epoxy composite reinforcement was added to the lower surface of the steel wing-pivot fitting. This reinforcement was consistent with planned fleet action. The reinforcement was developed after failure of the right-hand fatigue test article and promised significant improvements in the fatigue strength of the pivot fitting by reducing the stress levels. Fatigue failure of the left-hand wing initiated in the aluminum lower wing skin at the most outboard bolt row of the splice connecting the skin to the steel pivot-fitting lower plate. The test article is being shipped to the Air Force Sacramento Air Materiel Center for disassembly and thorough inspection.

Table V F-111 WING FATIGUE TEST SPECTRUM SUMMARY

Test Condition	Layer	Max Load	Min Load	Cycles Per 400 Hr. Block	Load Factors
T-1 Δ L.E. = 26° BM = 19.87x10 ⁶ @ 100%	1	% of T-1 34.4	% of T-1 5.0	256	2.14
	2	43.0	5.0	196	3.01
	3	51.3	14.5	29	5.50
	4	61.5	14.5	5	4.03
	5	75.3	14.5	1	7.33
M = 0.6 @ S.L.					
T-2 Δ L.E. = 26° BM = -11.48x10 ⁶ @ 100%	1	% of T-2 20.9	% of T-1 14.5	5	-0.90
	2	31.3	14.5	1	-1.50
M = 0.75 @ S.L.					
T-3 Δ L.E. = 50° BM = 23.07x10 ⁶ @ 100%	1	% of T-3 29.9	% of T-3 2.5	1045	2.48
	2	36.8	2.5	321	3.10
	3	43.7	12.1	267	4.03
	4	48.6	12.1	46	6.23
	5	56.3	12.1	1	8.12
M = 0.75 @ S.L.					
T-13 Δ L.E. = 50° BM @ 100% Same as T-2	1	% of T-3 12.1	% of T-2 13.1	6	-0.60
	2	12.1	26.7	1	-1.20
M = 0.75 @ S.L.					
T-5 Δ L.E. = 72.5° BM = 20.27x10 ⁶ @ 100%	1	% of T-5 27.1	% of T-5 3.2	143	3.01
	2	39.3	7.8	34	4.03
	3	48.7	7.8	15	4.90
	4	58.3	7.8	5	5.75
	5	73.5	7.8	2	7.70
M = 0.90 @ S.L.					
TOTAL			$\Sigma =$	2379	

3.1.2.4 Final Fatigue Analysis

Final fatigue analyses of the wing structure are being prepared to reflect the full-scale test results. Preliminary results based on the left-hand wing failure show the MAC service life to be in excess of 10,000 hours with a scatter factor of 4.0. The final analysis will constitute a detailed evaluation of the fatigue strength of the baseline wing design and will also provide the necessary fatigue damage equations for use in monitoring the fatigue life in the fleet.

3.1.2.5 Fleet Service Load/Fatigue Damage Monitoring

Data from in-flight recorders in the F-111 fleets are being accumulated and processed for analysis. This data will soon be available in sufficient quantity to afford development of wing loading spectra reflecting service operations. Consequently, valid comparisons between the design MAC usage and service usage can be made.

3.1.2.6 Flight Test Wing Loads

The F-111A has undergone and is continuing to undergo an extensive flight test loads measurements and demonstration program. Because of the F-111A's large flight envelope, both the analytical and flight test efforts to isolate critical conditions for demonstration and to validate these choices has been unusually comprehensive. From the standpoint of wing design loads, the symmetric maneuvers in the basic configuration (slats and flaps retracted) and takeoff and landing configurations are the most significant. A summary of symmetric maneuver conditions for the F-111A is shown in Figure 11.

Flap-track loads at the wing box rear spar and slat-track loads at the wing box front spar are shown in Figure 12. These data were obtained by extrapolation and refinement of flight test data at 26 degrees and 16 degrees in the landing approach and takeoff configuration.

3.1.2.7 Dynamic Response

The F-111 aircraft has been subjected to a comprehensive dynamic response program of analysis and flight test which has included response to landing, taxi, gust, buffet, store ejection, and abrupt maneuver conditions.

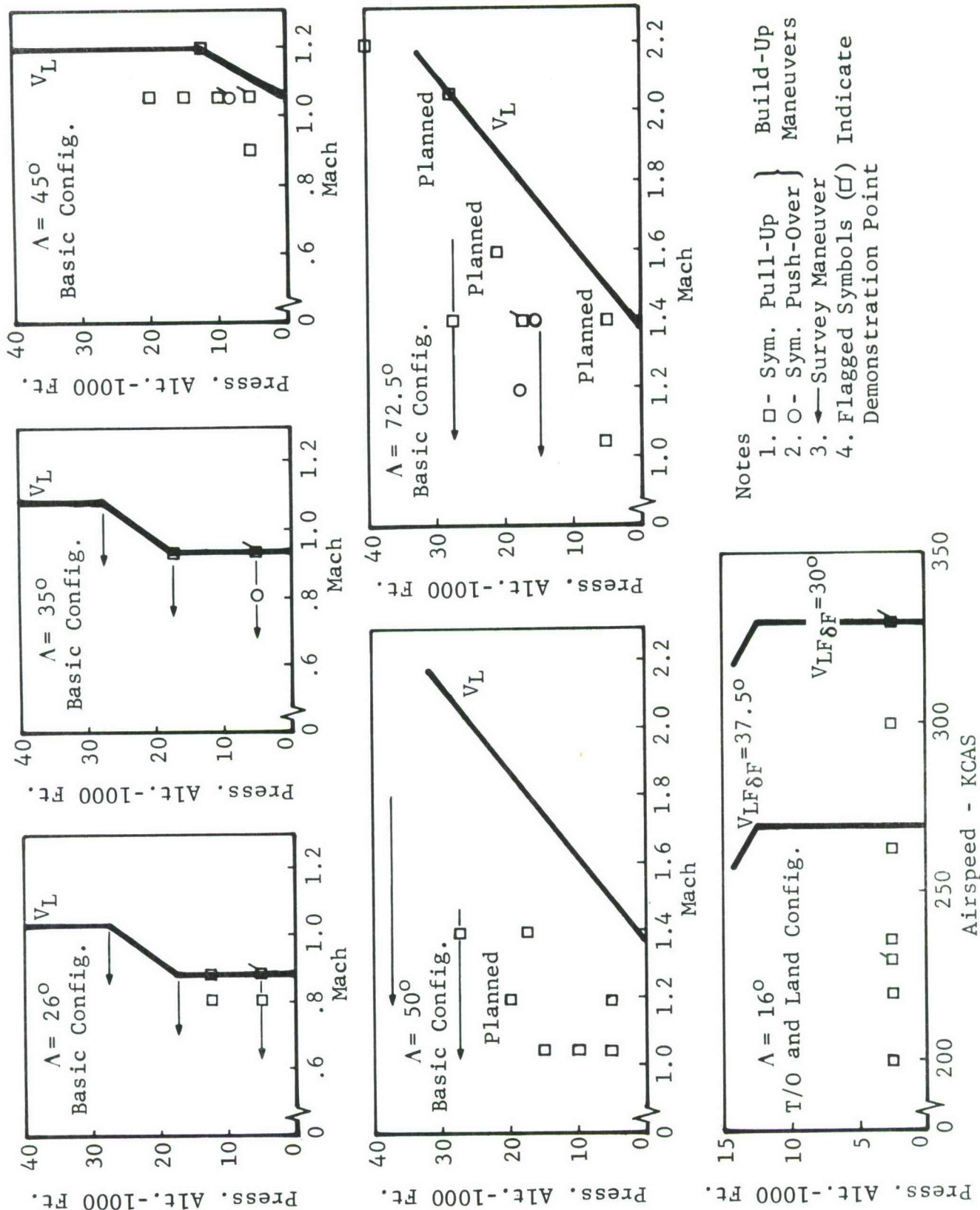


Figure 11 Summary of Symmetric Maneuver Conditions

3.1.2.8 Wing Flutter Prevention

The F-111A flutter program has been completed. The flutter prevention task was characterized by an integrated analytical, model test, ground vibration test, and flight test approach to fulfill the requirements of MIL-A-8870 as expeditiously as possible. The wing has been demonstrated to be free from flutter without wing-mounted store loadings throughout the design flight envelope. With store loadings equal to 3000 pounds or less per pylon, the airplane is cleared to fly to the design flight envelope or store limit, whichever is lower. Loadings greater than 3000 pounds per pylon have been cleared to high subsonic speeds.

F-111 ground vibration test results have been used for validation of analytical modes and flutter model vibration results and as a basis for final flutter analyses of the airplane.

3.2 BASELINE COMPONENT DESCRIPTION

The F-111F wing box is a low-cost, minimum-weight structure, which reflects state-of-the-art structures technology for an advanced operational fighter and is consistent with a safe-life design philosophy.

The wing box is defined as the primary wing structure outboard of the wing pivot fitting. It consists of five spars, upper and lower one-piece skins, and eight primary bulkheads. Additional short bulkheads provide framing for the four pylon hard points. The wing box is spliced to the wing pivot fitting between center spar stations 97.7 and 106.8. All wing box loads are transferred to the pivot fitting through this connection. The wing structural arrangement is shown in Figure 13. An exploded view of the wing box structure is shown in Figure 14.

The design of the primary wing structure and support structure for the high-lift systems is based almost exclusively on structural parts machined from high-strength aluminum and steel plate, forged billets, and die forgings. To offset costs, a large percentage of these parts were programmed for numerical control machining.

A minimum weight design was achieved by utilizing tapered and etched, unspliced skins from root to tip. The spars and bulkheads are designed as integrally stiffened machined members.

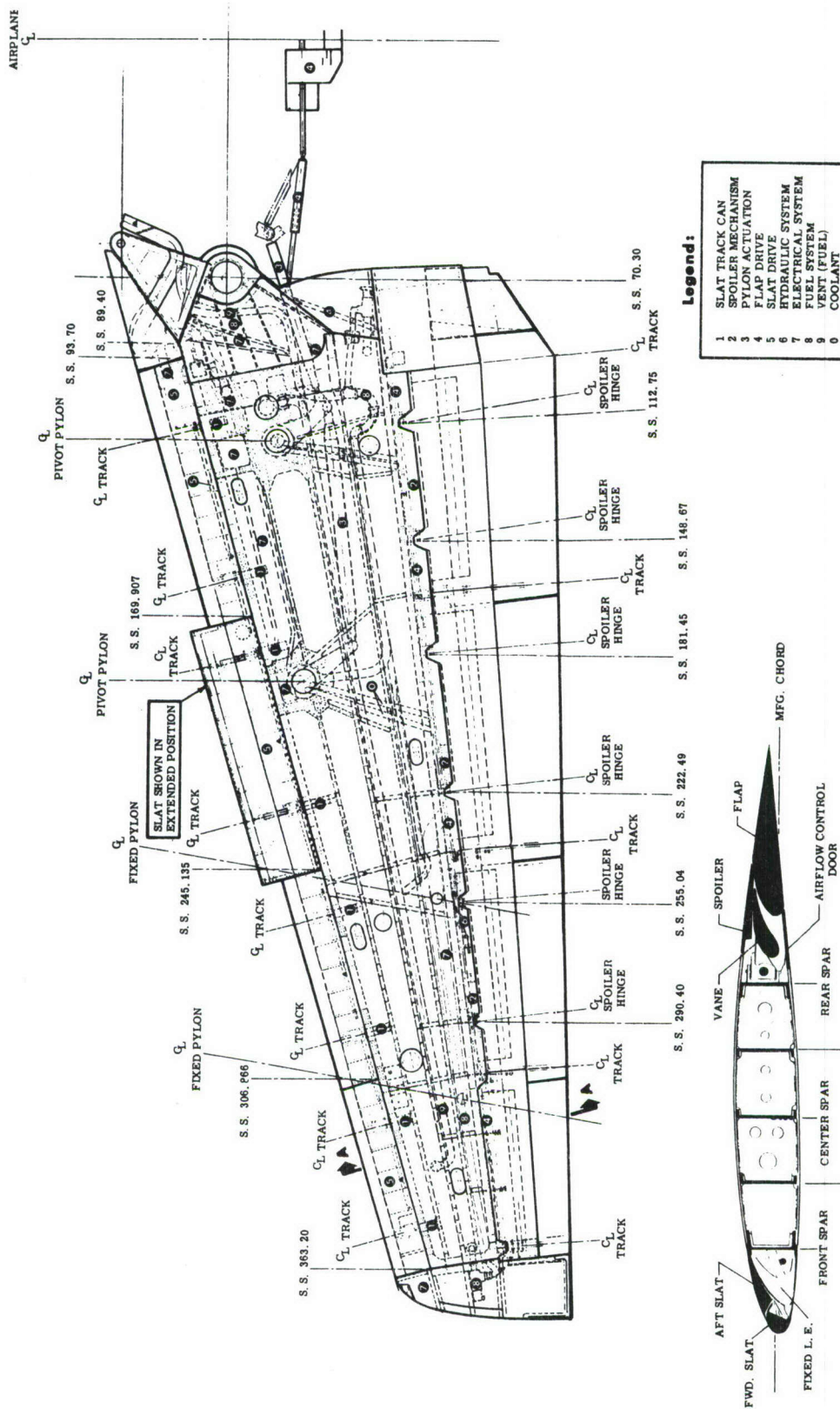


Figure 13 F-111 Wing Structural Arrangement

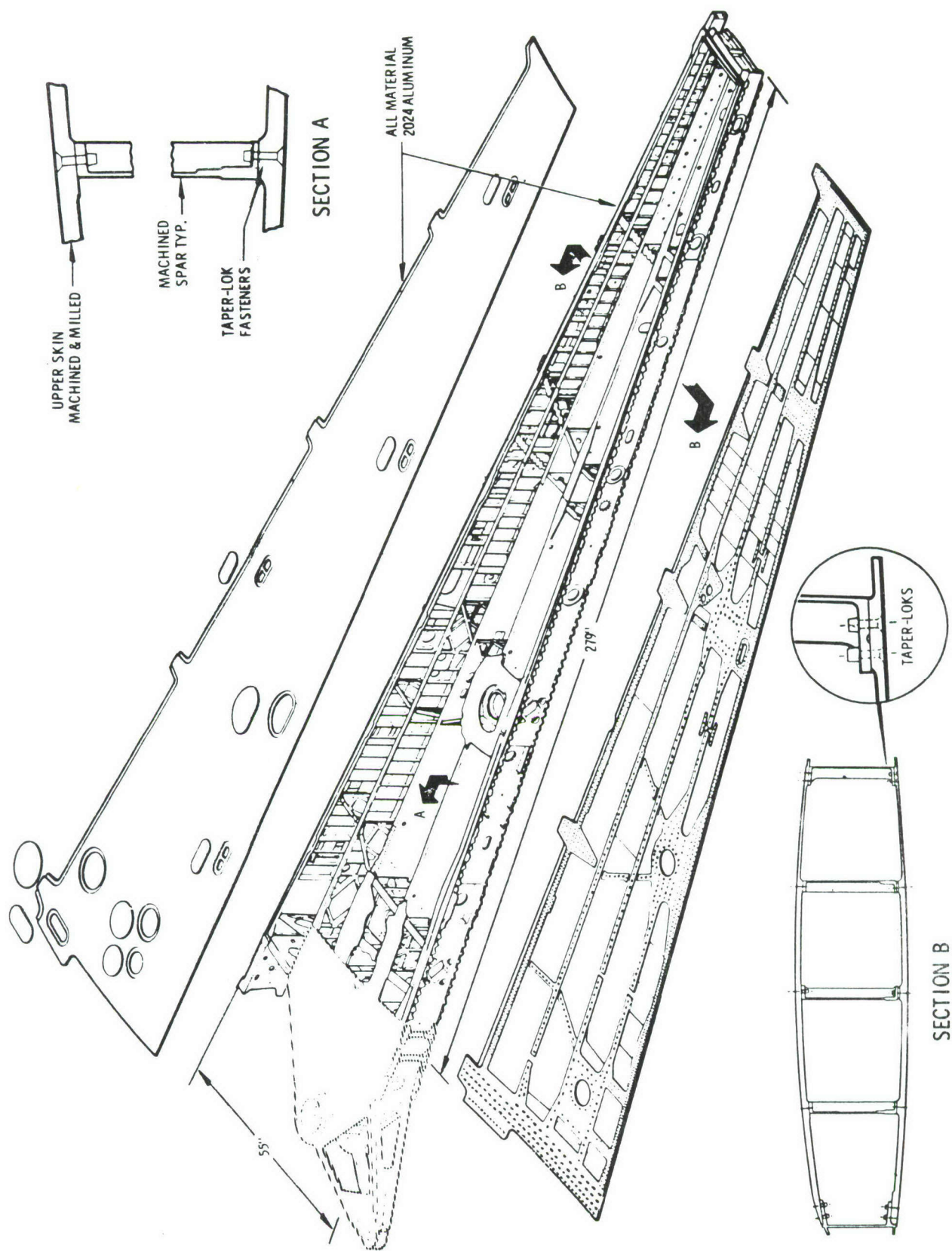


Figure 14 Baseline Wing Box

The wing box also serves as an integral fuel tank.

The critical design considerations for the wing upper and lower surfaces are indicated in Figure 12.

3.3 BASELINE REQUIREMENTS

The F-111F structure was designed to the criteria summarized in FZS-12-12002, "F-111F Structural Design Criteria," dated October 1969. Gross weight and load factor summaries are shown in Figure 15 and Table VI. Associated supporting documents are listed below:

- o MIL-A-8860 series specifications defining airplane strength and rigidity requirements
- o FZM-12-12071, "F-111F Air Vehicle Specification"
- o FZM-12-104A, "Environmental Criteria Specification"
- o ASD-TR-66-57, "Air Force Structural Integrity Program Requirements"
- o FZS-12-005D, "F-111A/E/D/F Fatigue Criteria"

3.3.1 Static Load Requirements

The static loads for the F-111F, derived in accordance with FZS-12-12002, are given in FZS-12-8165, Addendum II, "Magnitude and Distributions of Design Loads for F-111F." Discussions and results of the balanced symmetric, unbalanced symmetric and lateral maneuver conditions are included. In addition, the loads generated by extended high-lift devices and external stores are presented with particular reference to wing hard points.

3.3.2 F-111 Fatigue Requirements

The F-111 fatigue requirements reflect an evolutionary process beginning with the initial selection of usage profiles in 1961 and culminating in the wing test loads spectra shown in Table V.

A - Symmetric maneuver load factor,
basic and high drag configurations.

B - Asymmetric maneuver load factor,
basic and high drag configurations.

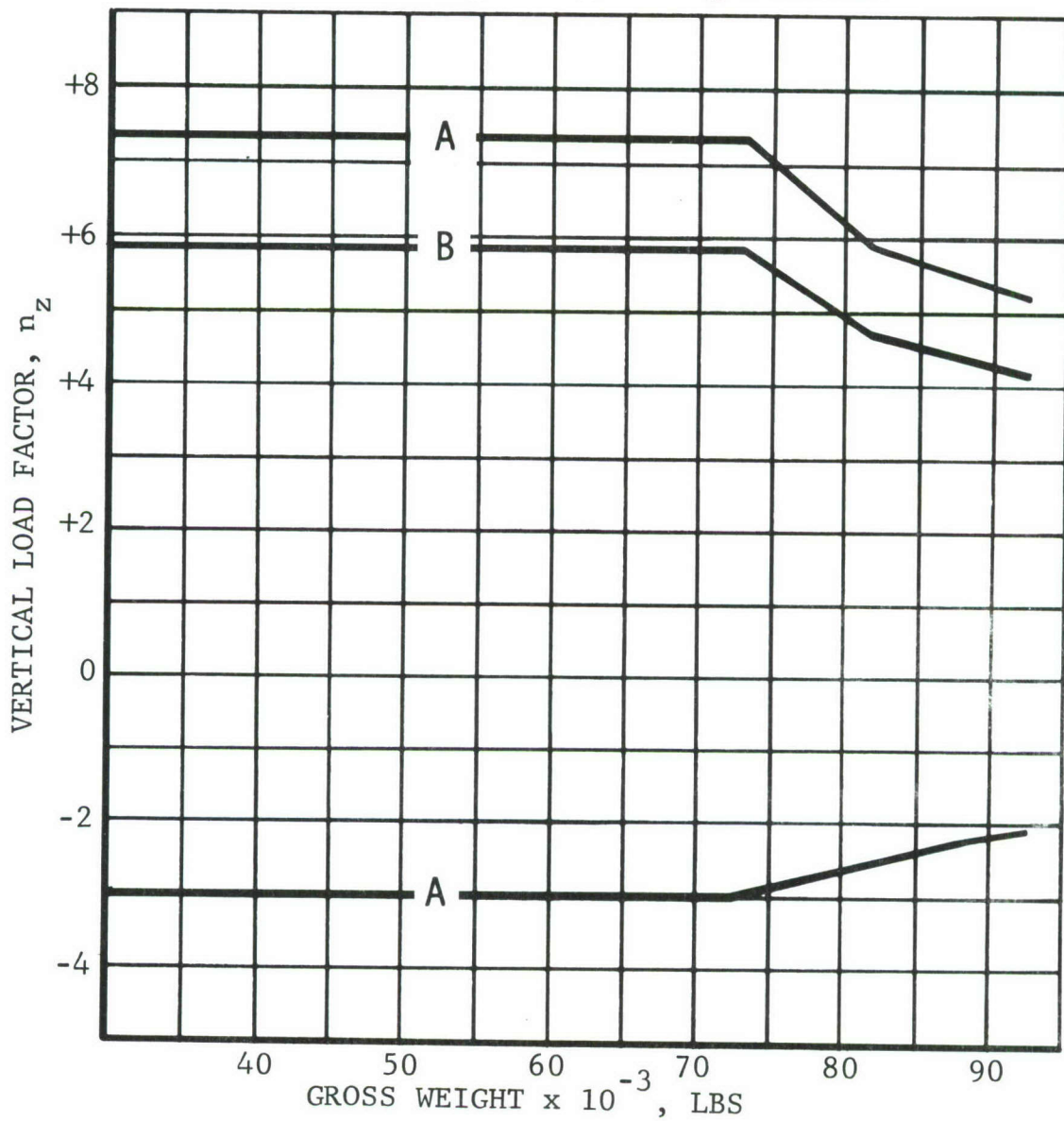


Figure 15 Limit Maneuver Load Factors
F-111F Airplane

Table VI F-111F GROSS WEIGHT - LOAD FACTOR SUMMARY

(Airplane with No External Stores and
With External Stores on Pivoting Pylons)

Condition	Gross Weight	Limit Load Factor	
		Maneuver	Gust
Maximum Design G.W.	92,500 lbs.	+5.2,-2.0	+3.84,-1.84
Basic Flight Design G.W.	73,000 lbs.	+7.33,-3.0	+4.54,-2.54
* Maximum Taxi and Takeoff G.W.	92,500 lbs.	+3.1,-0.0	+2.16,-0.16
* Maximum Landing Design G.W.	82,500 lbs.	+3.6,-0.0	+2.30,-0.30
* Landplane Landing Design G.W.	73,000 lbs.	-4.0,-0.0	+2.47,-0.47

*Takeoff or Landing Approach Configuration

3.3.2.1 Original Fatigue Design Criteria/Load Spectra

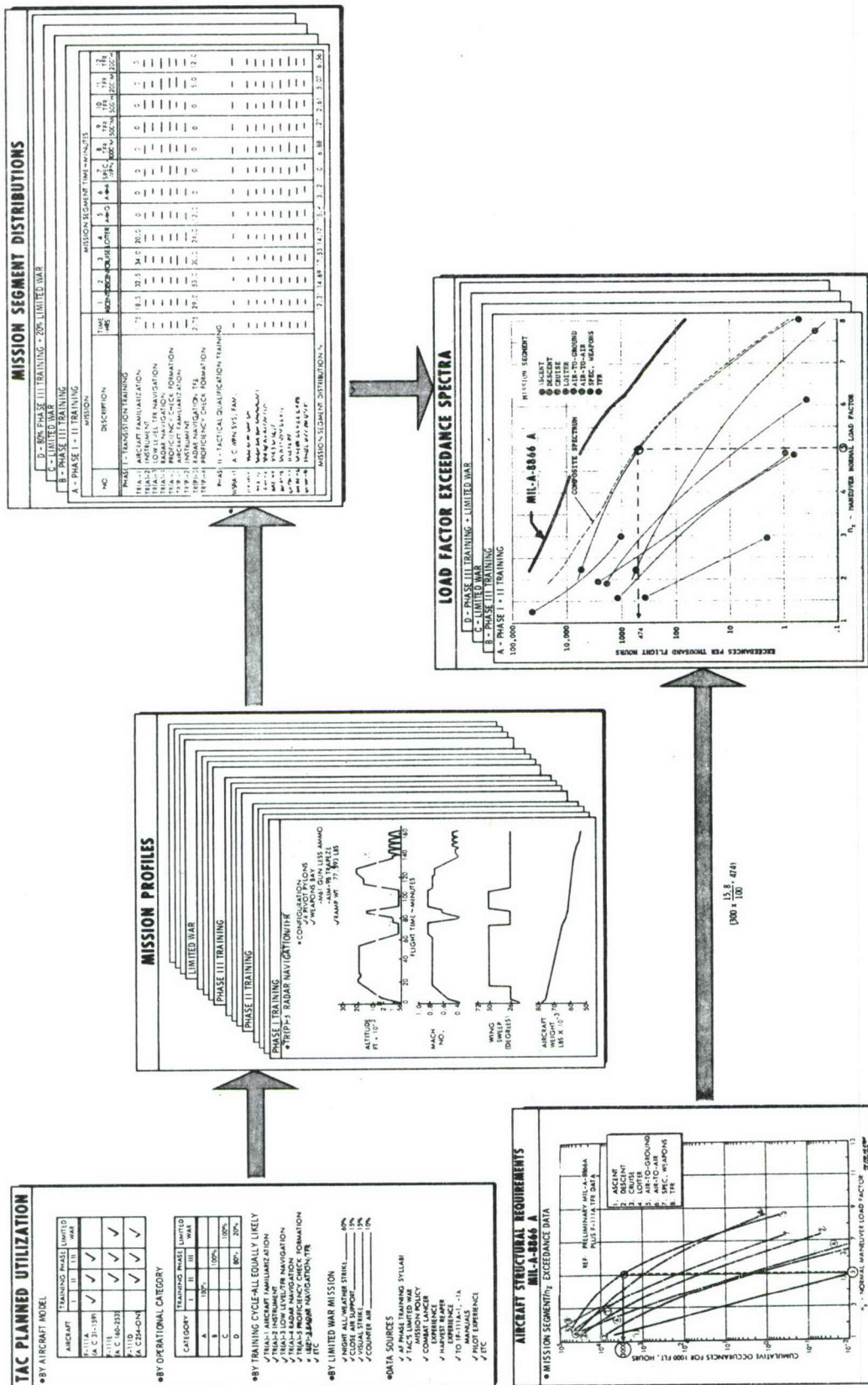
The required design service life for the F-111 was 4000 flight hours and 4000 landings. A design fatigue-scatter factor of 4.0 was applied to load occurrence to account for service and fatigue strength variations in the fleet. Applicable documentation included specification MIL-A-8866 (ASG), dated 18 May 1960, and ASD TN61-141. The design service loads spectrum was developed to define the expected number of load cycles according to load magnitude for each significant loading source. Load sources and magnitudes were established on the basis of 10 preliminary mission profiles defined by the Tactical Air Command (TAC) in 1961. The wing load spectra were defined for positive and negative symmetric maneuvers, asymmetric maneuvers, gusts, ground-air-ground transitions, and ground operations. Exceedance data and the atmospheric turbulence model specified in MIL-A-8866 were used.

3.3.2.2 Revised Fatigue Design Criteria and Load Spectra

Prior to conducting the full-scale fatigue test program on the wing, the fatigue criteria and design load spectra were revised as directed by the F-111 Systems Program Office. The revisions reflected updated TAC usage and Air Force-planned revisions to MIL-A-8866. The revised criteria include

- o Twenty-nine mission profiles describing Phase I and II training. Operations analysis shows this usage to be more severe than a combination of training and limited war
- o Twenty-three usage blocks developed from the mission profiles in terms of Mach number, altitude, and time spent by mission segment (e.g., air-to-ground, air-to-air, cruise, etc.)
- o Exceedances per mission segment as specified by an initial revision to MIL-A-8866 made available to Convair Aerospace in early 1969
- o Use of the basic flight design gross weight (71,000 pounds) for all fatigue flight conditions except high-lift configurations where take-off and landing gross weights are used
- o Loading sources (maneuvers, gusts, etc.) identical to those used in the original design spectrum except that terrain-following radar (TFR) operations were added. TFR is a significant fatigue load source and required development of exceedance criteria.

The revised fatigue design spectrum is referred to as the Mission Analysis Composite (MAC) spectrum and is currently applicable to the F-111 wing. Load data were derived from the F-111A Flight Loads Program and these data were supplemented by wind tunnel data as required. The approach used in the development of the MAC spectrum is illustrated in Figure 16. The original design exceedance data, based on the 1960 MIL-A-8866 requirements, are shown for comparison. The current fatigue criteria and MAC spectra are described in detail in Convair Aerospace documents FZS-12-005D, "F-111A/E/D/F Fatigue Criteria," dated 1 May 1970, and FZS-12-168A, "F-111A/E/D/F Design Loads Spectra," to be published.



3.4 BASELINE MATERIALS

The F-111 wing utilizes 2024 aluminum for upper and lower skins, spars and ribs in an efficient form, as numerically controlled machined plate with spars spaced to achieve a high buckling strength and a high degree of material utilization. This is an economically produced and structurally efficient wing with a demonstrated high structural reliability. As a baseline, it presents a major challenge for weight and cost reduction and for increased fatigue life.

The F-111 wing and the spars under three inches in plate thickness are of conventional 2024-T851. This has proven to be a good material for that program. For plate thicknesses above three inches, the procurement specification required that control of short transverse ductility be achieved. Thus, the heavier spars have been procured to this requirement. A later specification which required short transverse control from 1.5 to 3.0 inches of plate thickness was released. Suppliers were compelled to provide a higher purity 2024-T851, identified now as 2124-T851, to meet the short transverse requirements in the new specifications. This alloy has excellent exfoliation and stress corrosion resistance, adequate fracture toughness, and remains a competitive candidate, along with the newer 7000 series alloys and tempers, principally because of its superior performance at elevated temperatures.

3.5 UPDATED BASELINE

The fatigue life of the current F-111 wing has been established as greater than 10,000 hours (or 25 years) in terms of the current design service load spectra which include a scatter factor of 4.0. The excellent fatigue strength has been developed through an extensive program of design development testing, fatigue analysis, and full scale proof of compliance tests. A more detailed summary of this program is given in paragraph 3.1.

Two requirements connected with Phase IA made it necessary to recalculate the fatigue strength of the baseline:

1. The more severe exceedance and ground-air-ground transition requirements of the March 1971 version of MIL-A-8866A.
2. Damage tolerance assessment of baseline.

In addition to recalculating the baseline fatigue strength as affected by the above requirements, an evaluation of the impact of usage variation (alternate mission segment mixes) on the updated baseline was performed.

A summary of the baseline update activity is given below.

3.5.1 Fatigue Analysis Update

The design service loads spectrum used for Phase IA analysis is identical to the baseline fatigue spectrum with one exception. The exception is: The number of occurrences were revised to reflect the more severe exceedance data and ground-air-ground transition requirements included in MIL-A-8866A (USAF), dated 31 March 1971. (The exceedance data used in developing the current F-111 spectrum was that data included in a preliminary version of the MIL-A-8866A series which became available to the contractor in early 1969. See paragraph 3.3.2.2 for additional discussion of the revised F-111 criteria and spectra.)

The results of recalculating the fatigue damage for six selected control points in the current baseline wing box are given in Table VII. The damage calculated for the current baseline spectrum is shown in the table for comparison. Locations of the control points are shown in Figure 17. The updated service loads spectra does increase the calculated

Table VII

F-111 FATIGUE DAMAGE SUMMARY/PRELIMINARY FATIGUE ANALYSIS

- BASED ON PHASE I AND II UNRESTRICTED USAGE
- SCATTER FACTOR = 4.0 INCLUDED

CONTROL POINT DESCRIPTION	K _T	FATIGUE DAMAGE ($\Sigma n/N$)	
		Current F-111 Spectrum	Modified Spectrum
① WING LOWER SKIN-TO-PIVOT FITTING SPLICE	3.13*	0.2380	0.8480
② CENTER SPAR LOWER CAP BOLT HOLE AT C.S.S. 173.08	2.7	0.0252	0.1684
③ WING SKIN BOLT HOLE AT C.S.S. 205.28	2.5	0.0164	0.0536
④ WING CENTER SPAR FUEL HOLE AT C.S.S. 140.50	3.2	0.0760	0.2976
⑤ WING LOWER SKIN INBOARD PIVOTING PYLON CUTOUT	2.7	0.0088	0.0752
⑥ WING UPPER SKIN-TO-PIVOT FITTING SPLICE	2.5	0.0004	0.0195

*K_f Established from A/4 L/H Wing Test Results

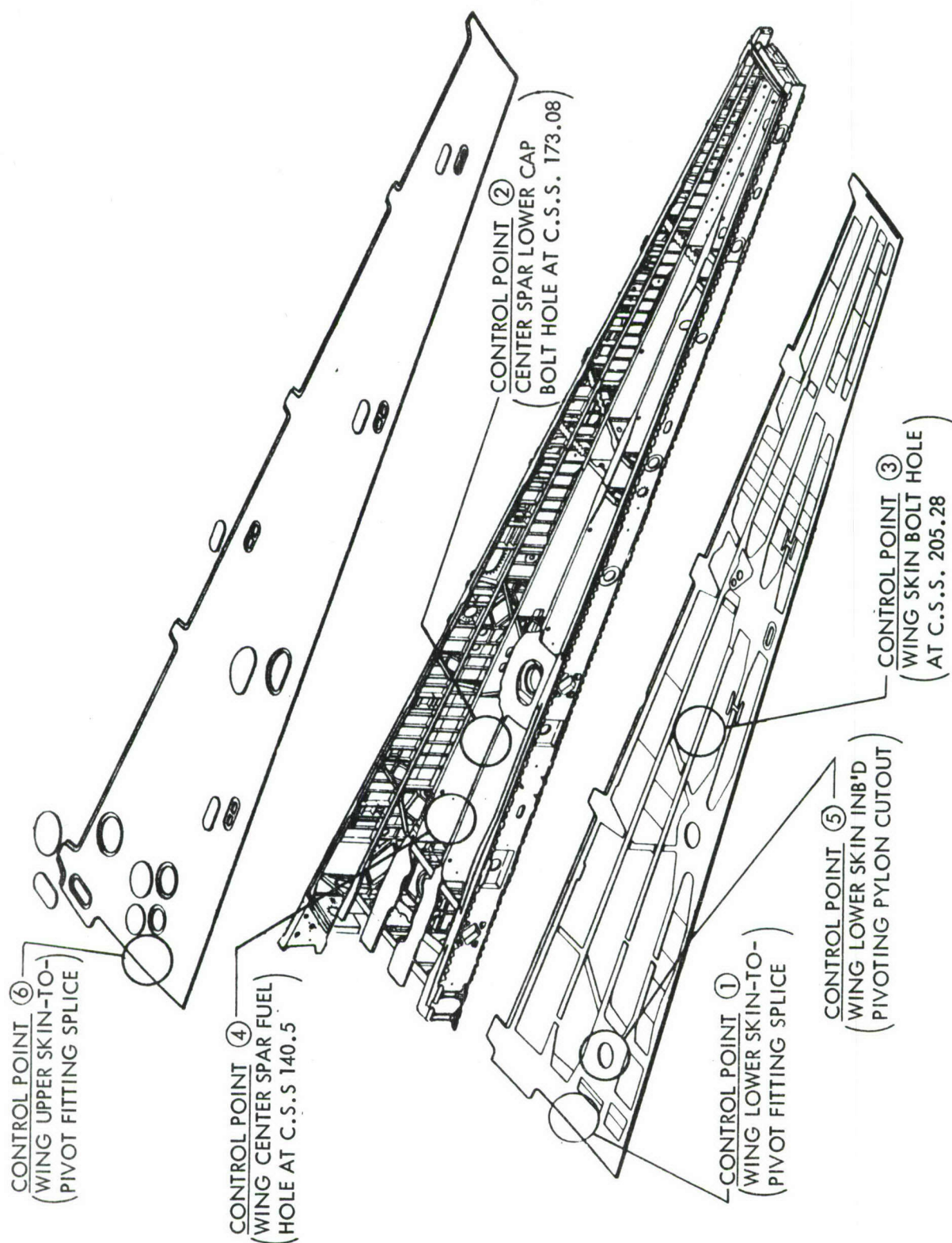


Figure 17 Control Points/F-111 Preliminary Fatigue Analysis
(Ref. FZS-12-174)

damage at all points, but the fatigue requirement is still easily met. The results shown in the table for control point No. 1 (lower wing-to-pivot fitting splice) are for information only since the splice is not defined as part of the baseline in Phase IA. The final splice configuration and analysis will be addressed in Phase IB.

The reader is referred to the baseline document, FZM-6100, dated 12 April 1973 for a more detailed discussion of the F-111 fatigue integrity program.

3.5.2 Damage Tolerance Assessment of Baseline

The principles of linear fracture mechanics have been used successfully to establish inspection intervals for D6ac steel parts in the F-111 airframe during the F-111 Recovery Program. However, there is no F-111 criteria requiring damage tolerance assessment. In addition, while the advanced fighter wing designs evolving from Phase IA must meet detail damage tolerance requirements, no such analysis was required for the baseline wing box by the original Phase IA contract.

After Phase IA work was underway, an addendum to the original contract was accepted to update the baseline as required to meet damage tolerance requirements. This was accomplished by increasing the thickness of the lower wing skin to reduce current stress levels. The complete details of the baseline damage tolerance assessment, including extensive criteria sensitivity studies, are given in Appendix IX.

The reduction of lower surface stress levels in the baseline resulted in the calculated fatigue damage becoming zero for the control points previously discussed in paragraph 3.5.1. The lower splice area was also considered "nonbaseline" for the damage tolerance assessment with the final configuration and analysis (including fracture) of the wing root splice intended to be a part of Phase IB.

3.5.3 Effect of Usage Variation

As stated in paragraph 4.2.2.1 of the proposal document, FZP-1402, the effects of alternate baseline fatigue spectra have been investigated. The evaluation was made on the basis of a comparison of fatigue and fracture design data (allowables) curves. Design curves are shown based on fatigue spectra

developed for three usages, Primary (Phase I and Phase II training), Alternate "A" (air superiority), and Alternate "B" (flight recorder). Table VIII lists the time distribution of mission segments for each spectrum. The "primary" spectrum distribution is based on planned usage by the Tactical Air Command. The "air superiority" spectrum is similar, with an increase in air-to-air time and a decrease in air-to-ground time. Development of the "flight recorder" spectrum is based on 500 hours of recorder data representing actual TAC F-111 usage. A summary of wing pivot bending moment exceedances for the three spectra is shown in Figure 18 along with a pictorial summary of the effects of the spectra on allowable stress for fatigue and two types of flaws. Tables IX and X list these effects in tabular form.

3.5.3.1 Effects on Fatigue Allowables

Figures 19 , 20 , and 21 show the maximum allowable spectrum stress as a function of stress concentration, K_T . These curves are for one lifetime (4000 hours) and include a scatter factor of 4.0. Details of how the fatigue design data curves are generated may be found in paragraph 6.2.1.

3.5.3.2 Effects on Fracture Allowables

As noted above, usage effects were investigated for two flaw types, a surface flaw in $t = 0.611$ in. lower skin and a through crack radiating from a lower skin 5/16 in. diameter bolt hole. For both flaw types, mid-point K_{IC} and da/dN data were used. For each spectrum, allowable stresses were determined for a range of initial flaw sizes for 800, 2000, 4000, and 8000 flight hours (various degrees of inspectability). Curves for each of the flight times are shown in Figures 22 , 23 , and 24 for the surface flaw and Figures 25 , 26 and 27 for the hole flaw. In the summary in Figure 18, only the 8000 hour curves are shown.

A discussion of how fracture design data sheets are generated in general is given in paragraph 7.3.1. The details and assumptions used in performing the flaw propagation analyses (flaw models, spectrum retardation, fracture data, etc.) necessary to evaluate the impact of usage on the baseline are given in Appendix XI on baseline damage tolerance assessment for the primary and alternate B" usage spectra. The work performed for the alternate "A" usage spectra was accomplished in an identical manner and the resulting design curves reported only in this paragraph.

Table VIII FATIGUE SPECTRUM MISSION SEGMENT DISTRIBUTION

Mission Segment	Distribution		
	Phase I & II Training	Air Superiority	Flight Recorder
Ascent	12.3	12.3	12.3
Descent	14.7	14.7	14.7
Cruise	17.5	17.5	27.9
Loiter	14.2	14.2	22.7
Air-to-Ground	15.8	3.9	0
Air-to-Air	3.1	15.0	0
TFR	22.4	22.4	22.4

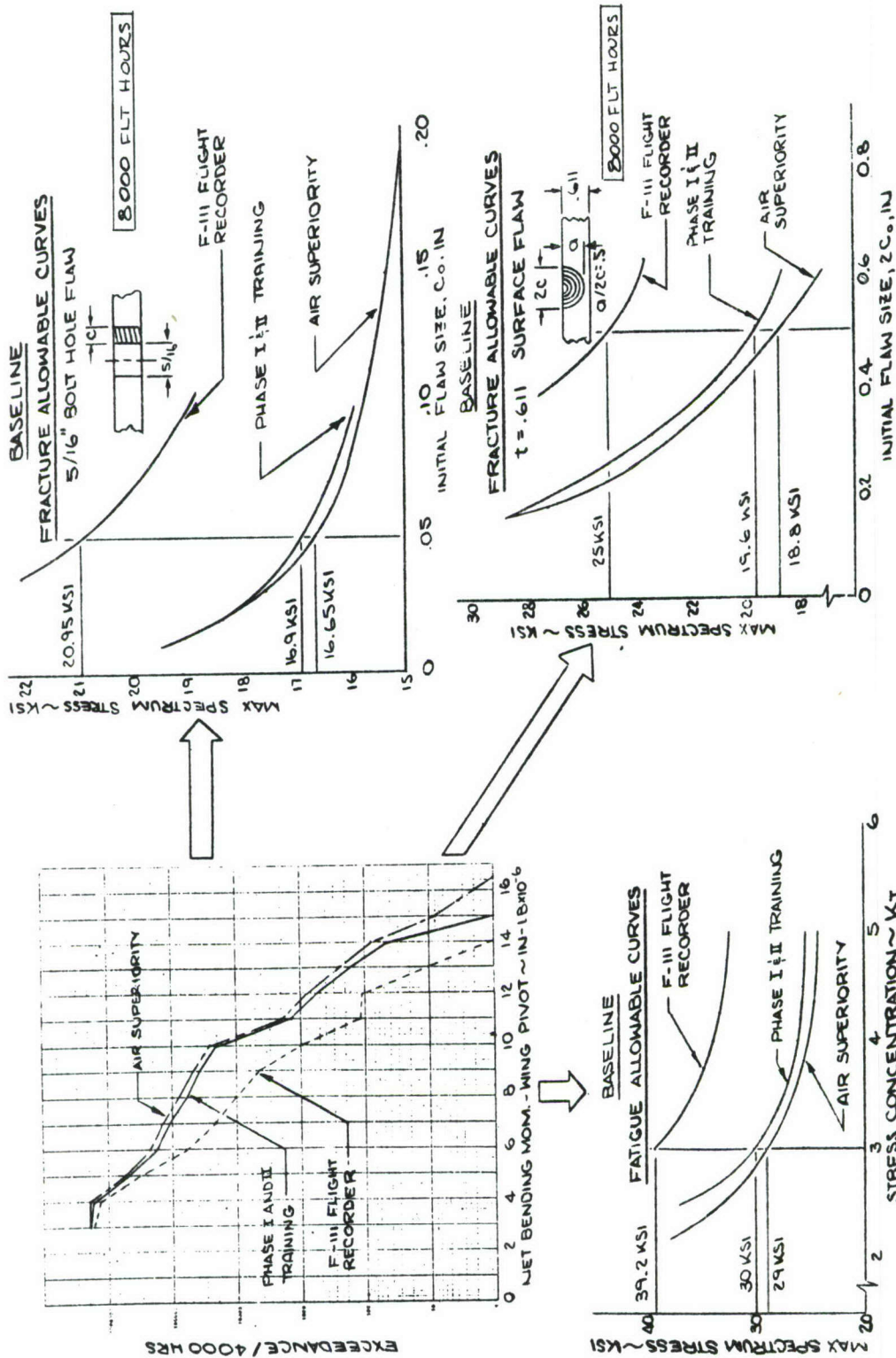


Figure 18 Summary of Usage Effects--C.S.S. 140
Baseline Fatigue and Fracture Allowables

Table IX EFFECTS OF USAGE VARIATION ON FATIGUE ALLOWABLES
ONE LIFETIME = 4000 HOURS
SCATTER FACTOR = 4.0 INCLUDED

Fatigue Spectrum	Allowable Stress, KSI		
	$K_T = 3.0$	$K_T = 4.0$	$K_T = 5.0$
Phase I and II Training	30.2	26.1	25.3
Air Superiority	29.0	25.1	24.1
Flight Recorder	39.2	33.9	32.4

Table X EFFECTS OF USAGE VARIATION ON FRACTURE ALLOWABLES
MID-POINT K_{IC} AND da/dN DATA

	Allowable Stress, KSI							
	*Surface Flaw in $t = 0.611$ Skin				**Through Flaw at a 5/16 Hole			
	800 Hrs	2000 Hrs	4000 Hrs	8000 Hrs	800 Hrs	2000 Hrs	4000 Hrs	8000 Hrs
Fatigue Spectrum								
Phase I and II Training	26.7	24.4	21.9	19.7	21.5	20.3	18.6	16.9
Air Superiority	26.1	23.6	21.2	18.7	21.3	19.9	18.3	16.6
Flight Recorder	28.5	27.6	26.5	24.9	23.8	22.9	22.1	20.9

* $a/Q = 0.1$, $a_0 = 0.246$ in.

** $a/Q = 0.1$, $a_0 = 0.050$ in.

Initial flaw size assumptions consistent with criteria requirements.

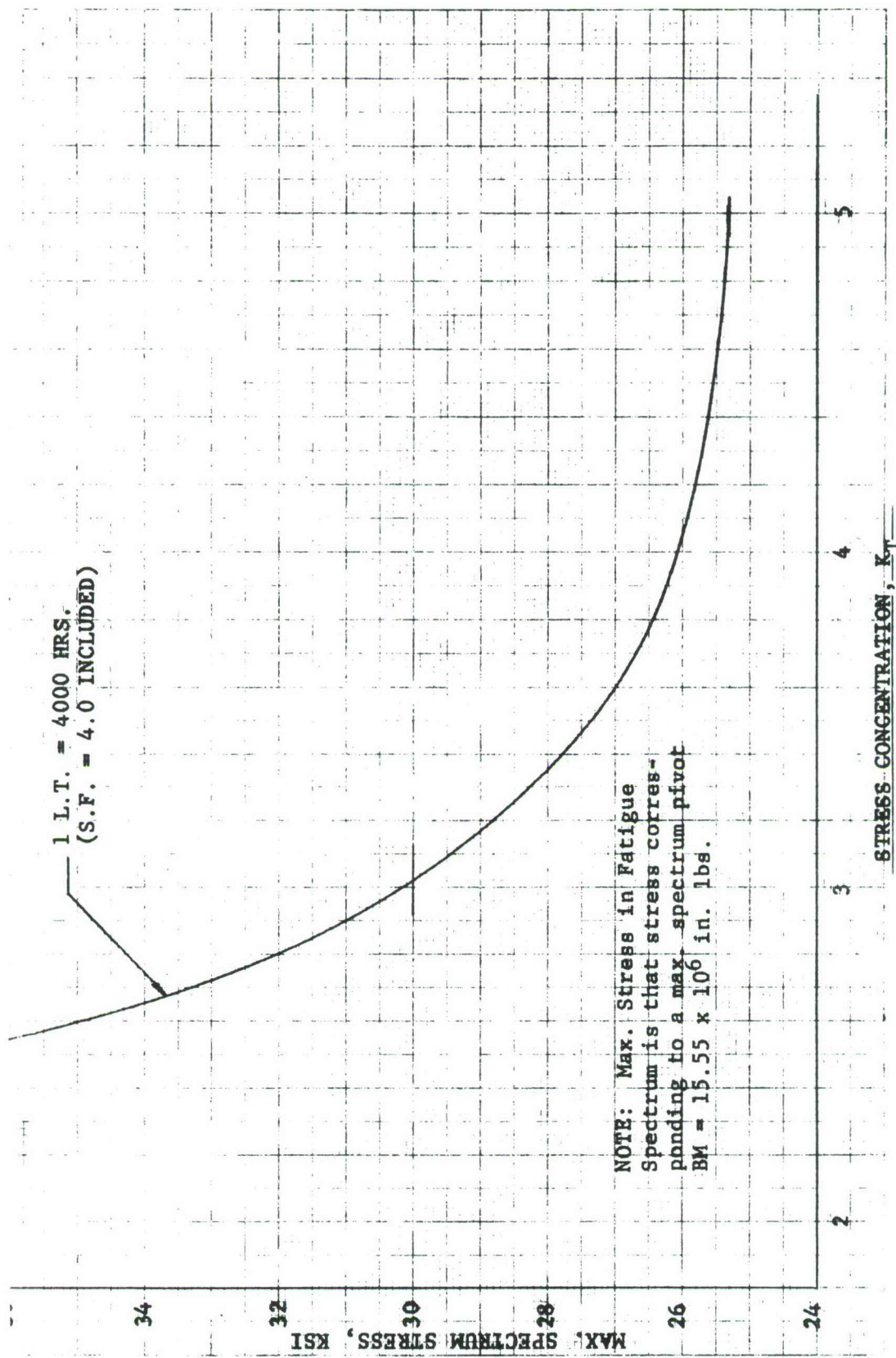


Figure 19 Center Spar Station 140 - F-111 Baseline Fatigue Design Allowable Curve Phase I and II Training Spectrum

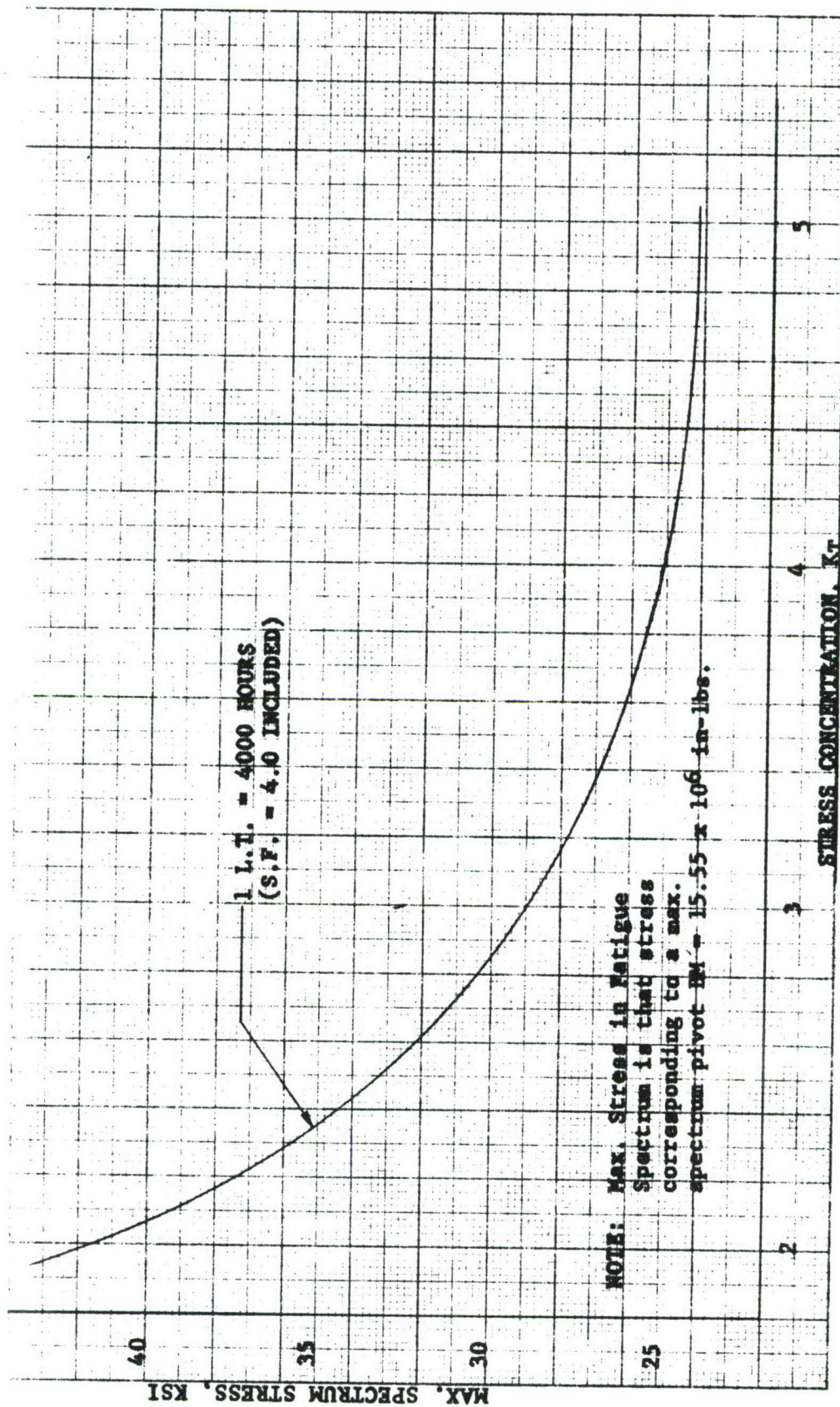


Figure 20 Center Spar Station 140 - F-111 Baseline Fatigue Design Allowable Curve Air Superiority Spectrum

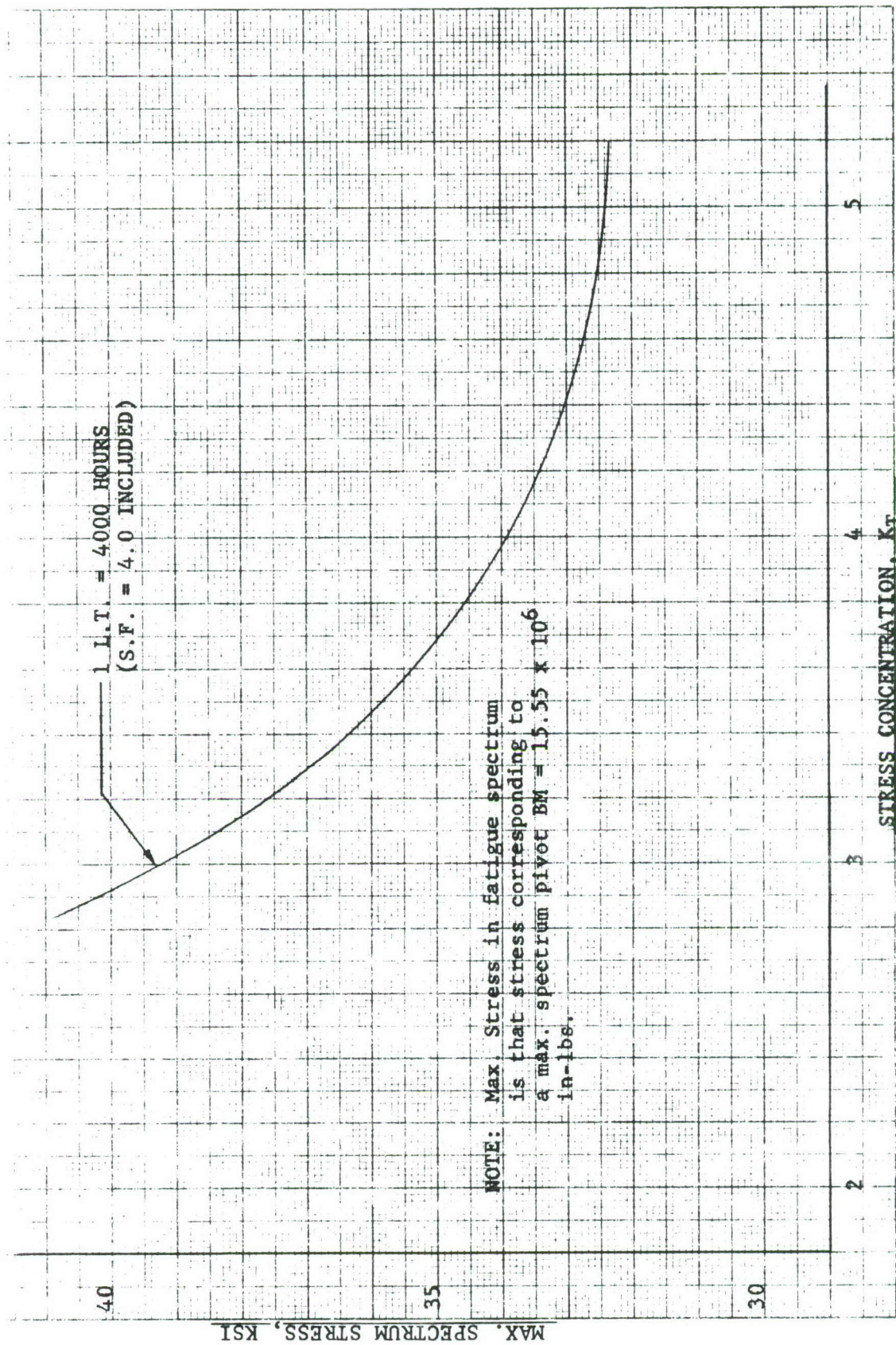


Figure 21 Center Spar Station 140 - F-111 Baseline Fatigue Design
Allowable Curve Flight Recorder Spectrum

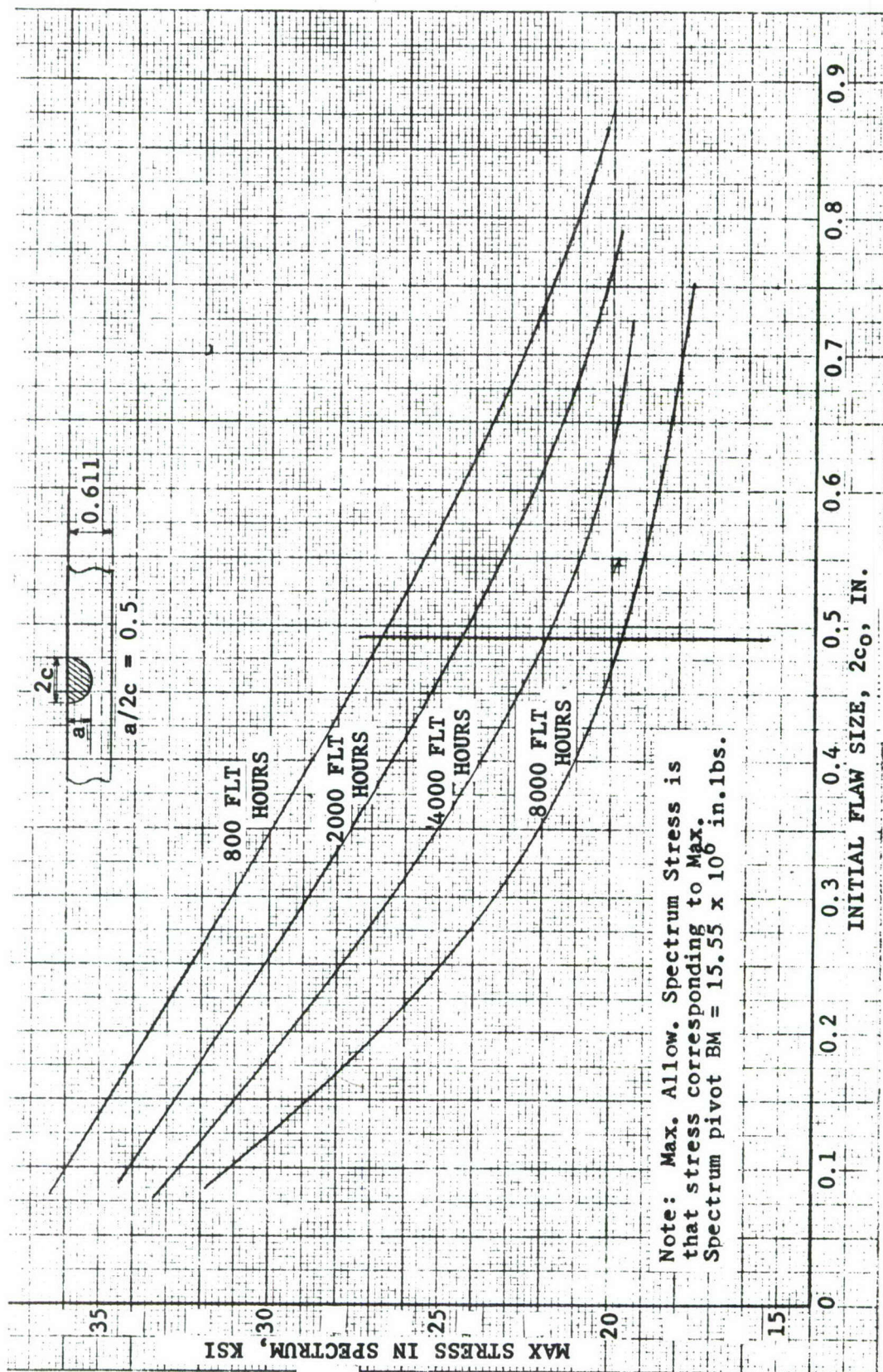


Figure 22 Center Spar Station 140 - F-111 Baseline Fracture Design Allowable Curve Surface Flaw in $t = 0.611$ Skin, Mid-Point KIC & da/dN Phase I and II Training Spectrum

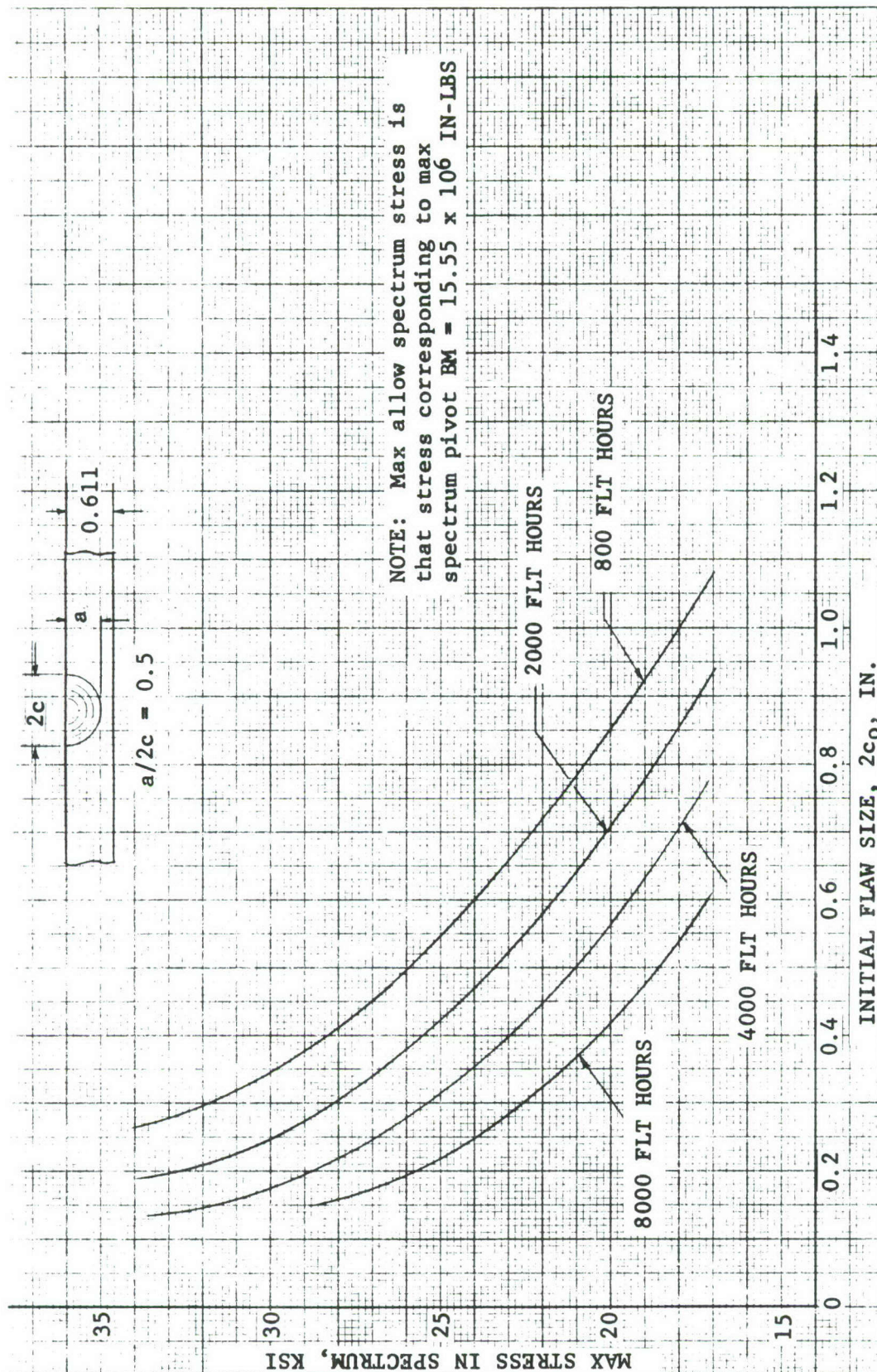


Figure 23 Center Spar Station 140 - F-111 Baseline Fracture Design Allowable Curve Surface Flaw in $t = 0.611$ Skin, Mid-Point KIC & da/dN Air Superiority Spectrum

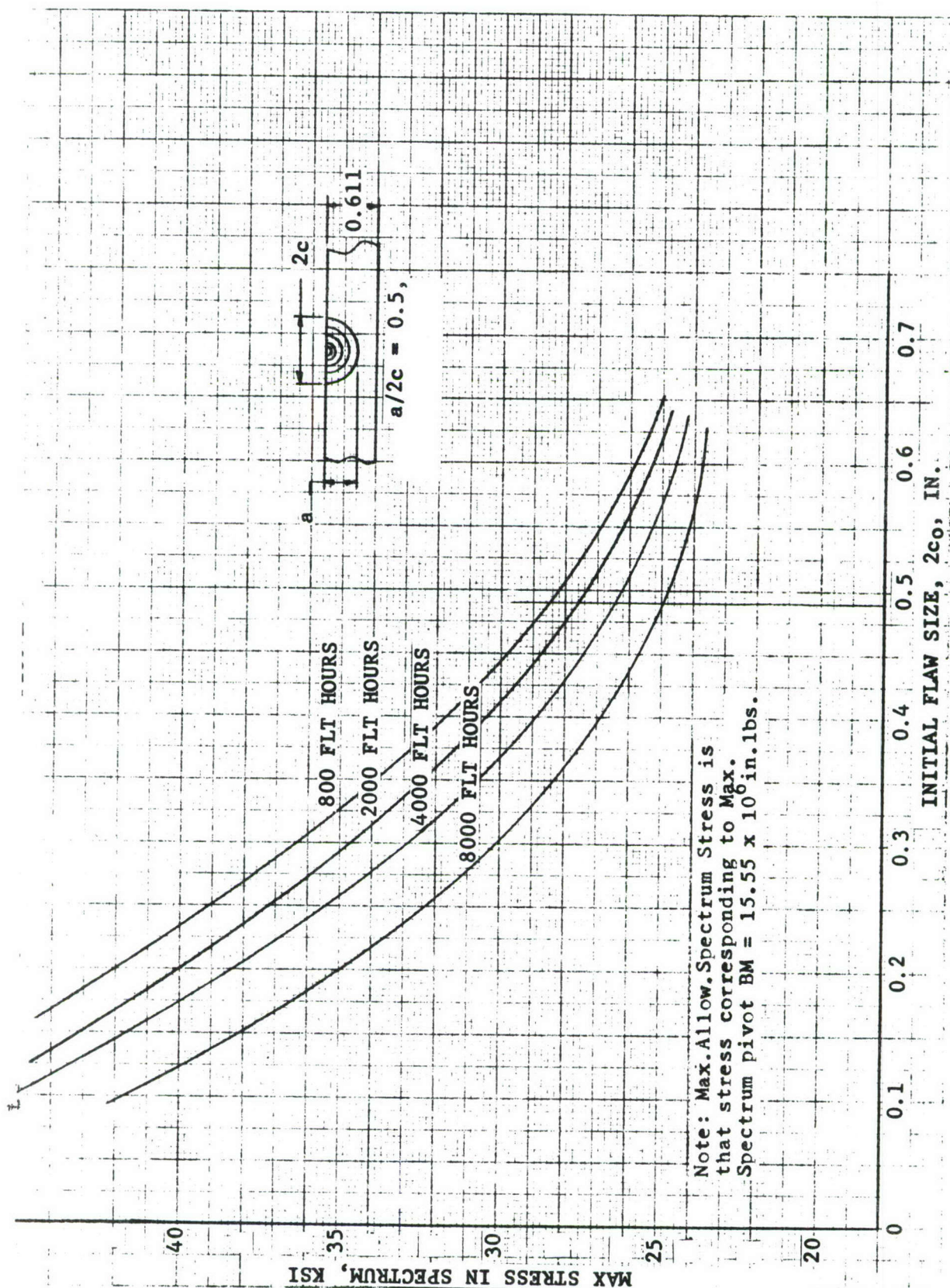


Figure 24 Center Spar Station 140 - F-111 Baseline Fracture Design
Allowable Curve Surface Flaw in $t = 0.611$ Skin, Mid-Point
KIC & da/dN Flight Recorder Spectrum

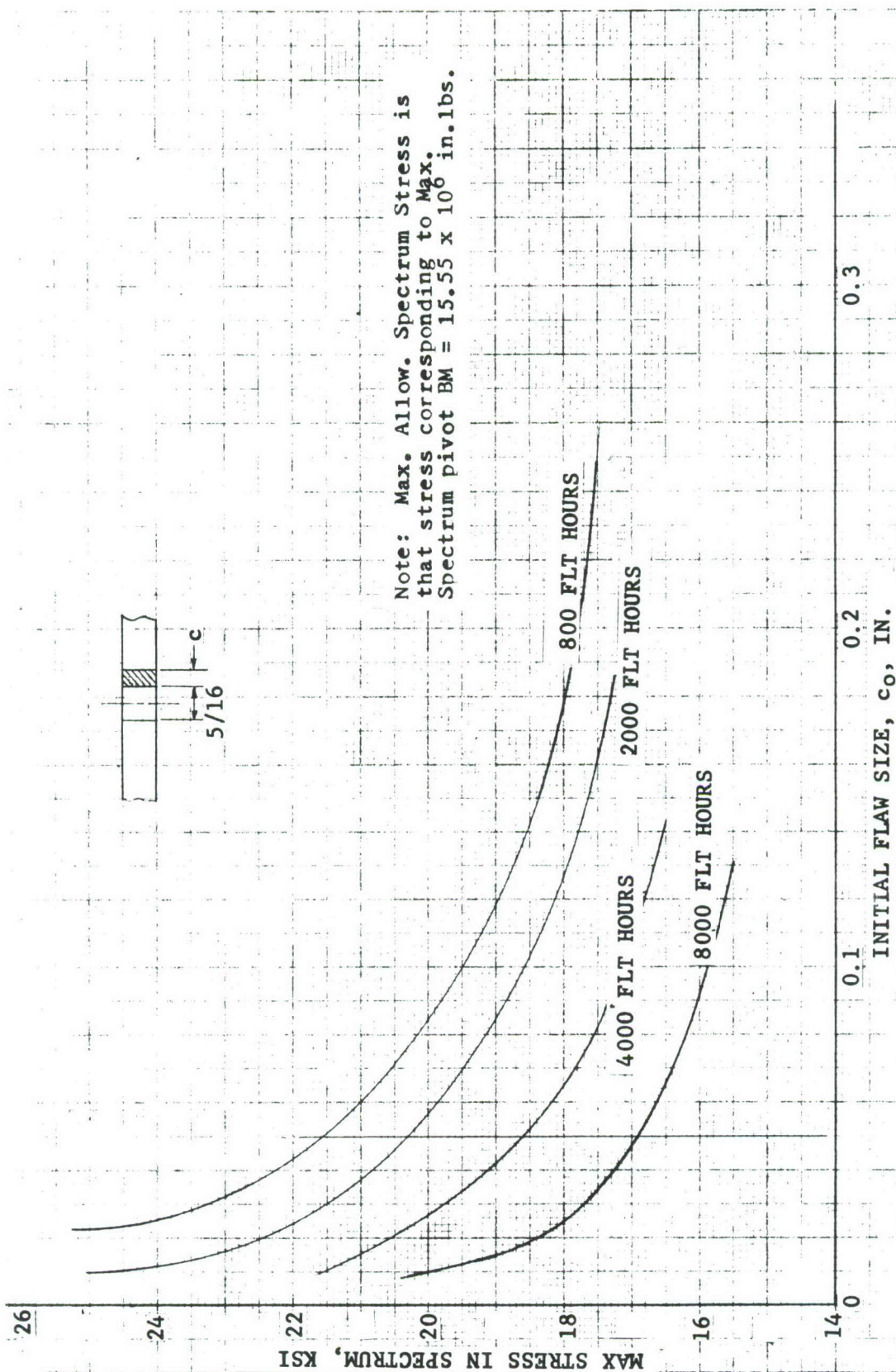


Figure 25 Center Spar Station 140 - F-111 Baseline Fracture Design Allowable Curve Through Flaw in 5/16 Hole, Mid-Point KIC & da/dN Phase I and II Training Spectrum

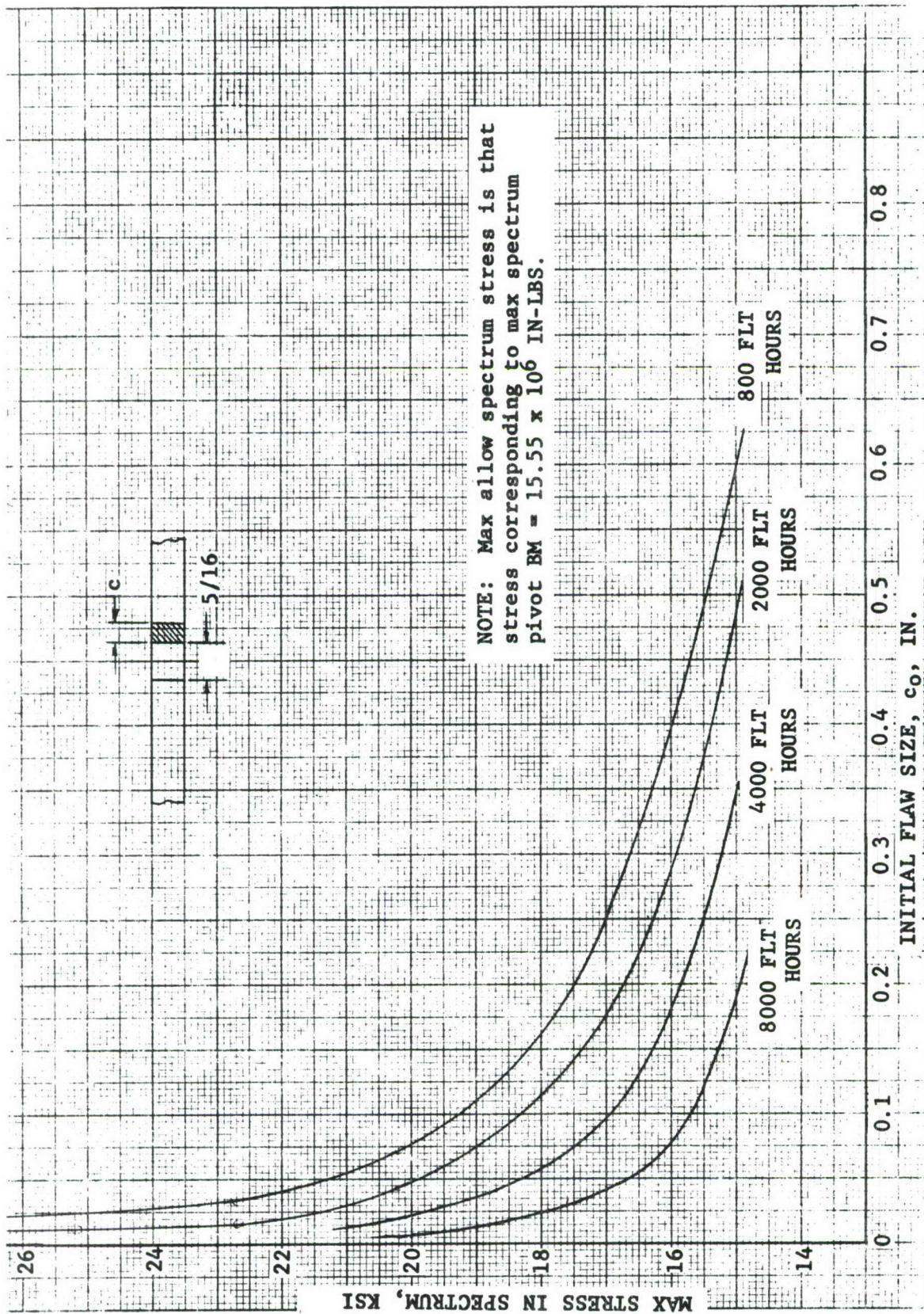


Figure 26 Center Spar Station 140 - F-111 Baseline Fracture Design Allowable Curve Through Flaw in 5/16 Hole, Mid-Point K_{IC} & da/dN Air Superiority Spectrum

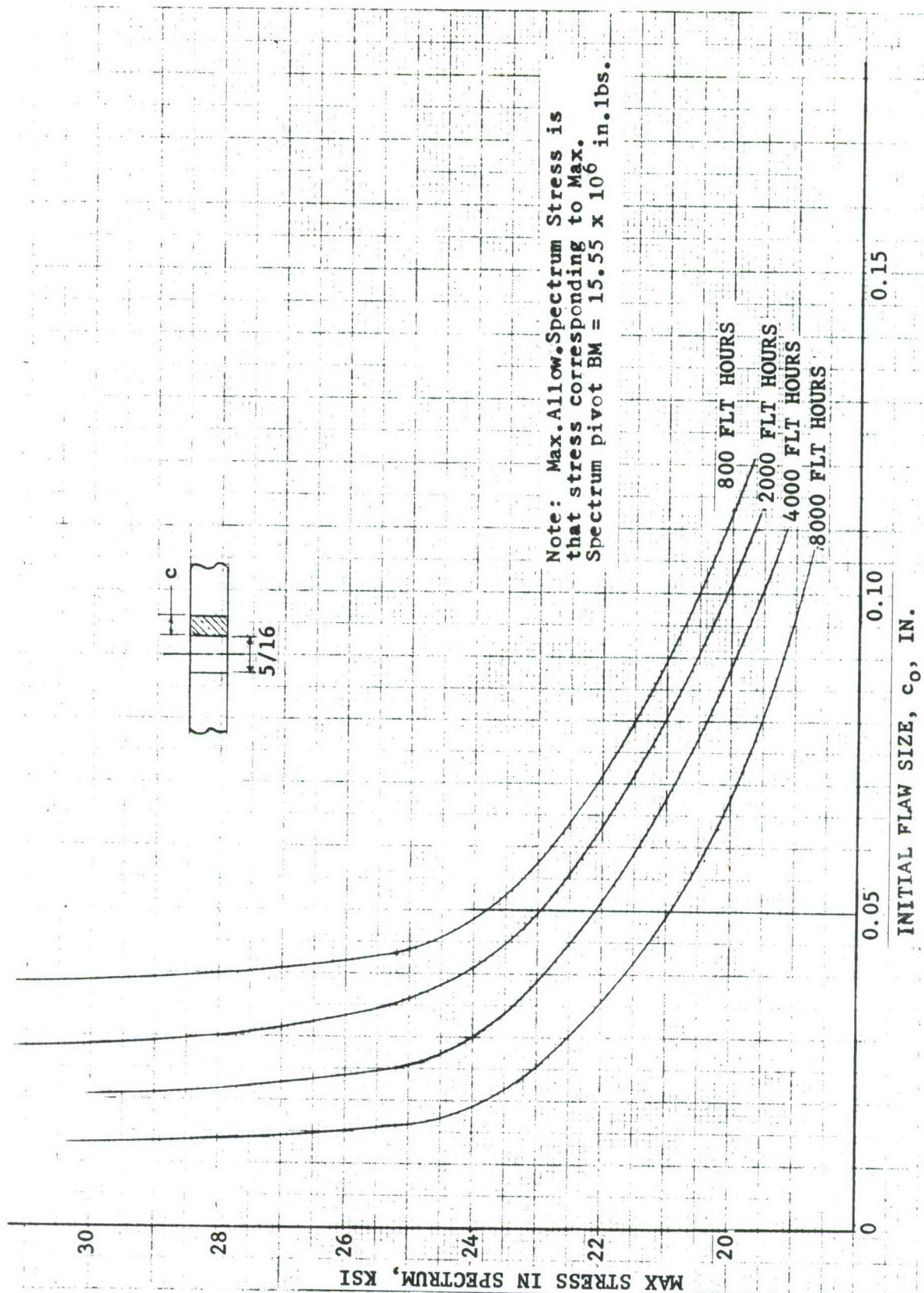


Figure 27 Center Spar Station 140 - F-111 Baseline Fracture Design Allowable Curve Through Flaw in 5/16 Hole, Mid-Point KIC & da/dN Flight Recorder Spectrum

S E C T I O N I V

S T R U C T U R A L D E S I G N

A new, in depth, systematic design approach was employed during Phase 1A of the program to achieve the design goals. This five step approach resulted in the innovation of several advanced design concepts which were selectively integrated and optimized to produce a preliminary design definition of a prime wing box configuration and two alternate configurations that potentially represent significant advancements in fighter structures technology.

4.1 DESIGN APPROACH AND EVALUATION SYSTEM

An overview of the five step approach is depicted by Figure 28.

4.1.1 Design Effort at the Element Concept Level

The initial step of the design effort was the innovation of new applicable concepts and the collection of existing advanced concepts. Element concepts are single structural element ideas, such as (a) laminated, planked, adhesive bonded lower skin without fastener penetrations or (b) bonded sandwich spar webs, etc.

The objective of this step of the design approach is to establish a broad base or large number of applicable structural concepts from which optimum wing designs can be built.

Innovative efforts were most fruitful during the period before detailed analysis or evaluation commenced; that is, new ideas emerged most freely in an atmosphere where attention to numerical details was omitted and where criticism of ideas was disallowed.

A total of 119 element concepts were defined on pre-printed formats entitled "Structural Concepts". The element concepts were evaluated and 56 feasible, promising concepts selected for incorporation into cross-section sketches. Selection of element concepts for further design study was on the basis of weight savings potential, life characteristics, technology advancement, feasibility to manufacture and inspect after development during the follow-on program time frame. See Appendix I Element Concepts.

● A NEW, SYSTEMATIC STRUCTURAL DESIGN PROCEDURE HAS EVOLVED THAT CAN BE UTILIZED TO SYNTHESIZE AN INTEGRATED, BALANCED, OPTIMUM DESIGN FOR ANY DESIRED APPLICATION. THIS SYSTEM IS DEPICTED ON THE CHART BELOW:

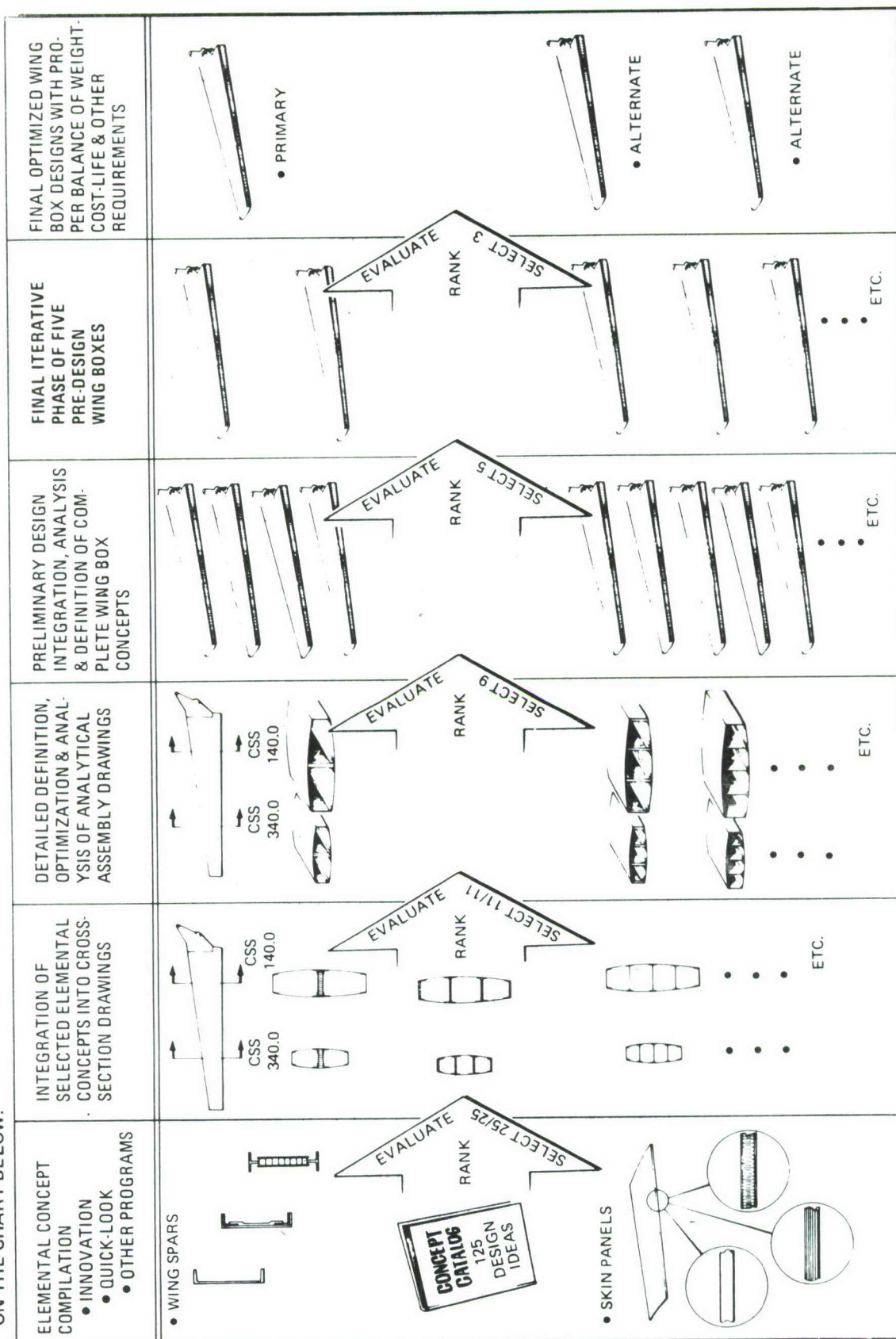


Figure 28 Fighter Wing ADP Design Approach

4.1.2 Design Effort at the "Wing Cross-Section Concept" Level

Cross-sections were cut at F111F wing center spar stations 140.0 and 340.0 and the cross section lines at these stations superimposed on preprinted drawing formats entitled "Cross-Section Concept". The 56 element concepts were re-iterated, integrated and defined on 31 cross-section drawings at CSS 140.0 and 20 cross-section drawings at CSS 340.0. The baseline configuration was also defined on cross-section drawings at CSS 140.0 and 340.0. The cross-section concepts were configured and sized to satisfy static loads plus fatigue and fracture criteria.

Weights and costs were computed for 1.0 inches of cross-section length for each concept drawn at CSS 140.0 and 340.0. In addition, each cross-section concept drawn was evaluated and scored to weighted parameters specified by the Air Force Flight Dynamics Laboratory shown in Figure 29.

Table XI and XII summarize the results of the cross-section concept effort. Thirteen concepts at CSS 140.0 and 10 concepts at CSS 340.0 were selected from the cross-section sketches for input into the "Analytical Assembly" phase.

The cross-section drawing provides a work sheet and a valuable iterative step for integrating element concepts into workable wing cross section designs. The simplicity of the cross-section drawings allows a large number of design concepts to be economically weighed, costed and evaluated. By configuring all concepts at a specific wing station to identical external lines and static loads plus identical fatigue and fracture criteria, an equitable and meaningful evaluation has resulted.

For a comprehensive description of design and evaluation of the cross-section concepts see Appendix II Phase Summary, Cross-Section drawings.

STRUCTURAL EFFICIENCY = 0.3	TECHNOLOGY ADVANCEMENT = 0.3	INTEGRITY AND RELIABILITY = 0.3	ABILITIES = 0.1
Cost = 0.5	Concepts = 0.3	Static = 0.1	Inspectability = 0.5
Weight = 0.5	Manufacturing = 0.3	Fatigue = 0.3 *	Manufacturability = 0.2
	Materials = 0.3	Safecrack = 0.3	Maintainability = 0.1
	Fracture = 0.1	Fail Safe = 0.3	Repairability = 0.1
			Predictability = 0.1

* Service Life maintained at 4000 flight hours. Any design not maintaining this life will be considered unacceptable.

** Revised rating system Jan 1973.

Figure 29 Rating System** for the Analytical Assembly

Table XI
CROSS-SECTION CONCEPTS C.S.S. 140.0
EVALUATION SUMMARY (REVISED RATING SYSTEM 11-10-72)

CONFIG NUMBER	CONFIGURATION DESCRIPTION	STRUCTURAL EFF.		TECHNOLOGY ADVANCE (.30)	STRUCTURAL INTEGRITY (.30)	ABILITIES (.10)	TOTAL SCORE	RANK	REMARKS
		WEIGHT (.15)	COST IN \$/IN (.15)						
610R000	F-111F WING BOX CROSS-SECTION CUT @ C.S.S. 140.0 (BASELINE)	(7.14) S.C. .074	\$50.29 .096	.027	.111	.094	.402	30	BASELINE
610R001	WING SECTION WELDED SPARS, CONSTANT DEPTH SAND UPPER SKIN - LAMINATED LOWER SKIN (140.0)	OBSOLETE		REITERATED UPPER SKIN ON 610R028 & LOWER SKIN ON 610R013A					
610R002	WING SECTION INTEGRALLY FORMED SPARS, STIFFENED UPPER SKIN, LAM. LOWER SKIN WITH HAT STIFFENERS	(3.962) F.S. .149	164.95 .079	.239	.217	.060	.694	3	COMBINE WITH 610R022 -1
610R003	WING SECTION WELDED SPARS, SQ. TUBE UPPER SKIN PLANK LOWER SKIN	(7.09) F.S. .083	141.92 .034	.144	.168	.069	.498	24	OUT
610R004	WING SECTION SANDWICH SPARS SIMPL. SAND UPPER SKIN, LAMINATED STIFFENED LOWER PANEL	F.S.	OBSOLETE REITERATED UPPER SKIN ON 610R028 & LOWER SKIN ON 610R013A						
610R005	WING SECTION LAMINATED SPARS, WELDED UPPER SKIN, ADH. BOND. SAND. LOWER SKIN	F.S.	OBSOLETE REITERATED UPPER SKIN ON 610R017A & LOWER SKIN ON 610R027						
610R006	WING SECTION BRAZED LOWER SKIN WITH CRACK STOPPERS - ADH. BONDED UPPER SKIN	F.S.	OBSOLETE REITERATED UPPER SKIN ON 610R019 & LOWER SKIN ON 610R018 - (MANUFACTURABILITY PCOR)						
610R007	WING SECTION FULL DEPTH LARGE CELL CORE BRAZED TO UPPER & LOWER SKIN	(4.740) S.C. .104	211.96 .023	.217	.140	.026	.510	22	OUT
610R008	WING SECTION WELDED UPPER SKIN, PLAIN LOWER SKIN, WELD'D TRUSSES (ALL TI)	OBSOLETE REITERATED UPPER SKIN ON 610R021 & LOWER SKIN ON 610R018. SPAR DESIGN RETAINED ON 610R015A							
610R009	WING SECTION BONDED BULB STIFFENED UPPER SKIN, MACHINED/BRAZED SAND LOWER SKIN	(4.374) F.S. .135	240.15 .020	.239	.202	.047	.643	9	OUT - EXCES- SIVE COST
610R010	WING SECTION ADH. BONDED TI SANDWICH SKINS, LOWER SKIN WITH COMPOSITE SLUGS	(4.72) F.S. .125	204.89 .024	.189	.144	.053	.535	20	OUT
610R011	WING SECTION ADHESIVE BONDED SANDWICH UPPER/LOWER SKINS & INTERNAL SPARS	(4.27) F.S. .139	129.82 .037	.141	.175	.068	.560	17	OUT
610R012	WING SECTION ADH. BONDED UPPER PANEL, BRAZED LOWER PANEL WITH PRESS. WRAPPED INNER SKINS	DISCONTINUED REASON: SKIN DESIGN NOT EFFICIENT FOR REACTING INTERNAL PRESSURE							

Table XI (CONT'D)
CROSS-SECTION CONCEPTS C.S.S. 140.0
EVALUATION SUMMARY (REVISED RATING SYSTEM 11-10-72)

CONFIG NUMBER	CONFIGURATION DESCRIPTION	STRUCTURAL EFF.		TECHNOLOGY ADVANCE (.30)	STRUCTURAL INTEGRITY (.30)	ABILITIES (.10)	TOTAL SCORE	RANK	REMARKS
		WEIGHT (.15)	COST IN \$/IN (.15)						
610R013"A"	WING SECTION LAMINATED LOWER SKIN, STEPPED SPAR CAPS - HAT STIFF. UPPER SKIN	(5.48) 5.48 F.S. .108	54.45 .088	.167	.250	.072	.685	4	A/A
610R014	WING SECTION FULL DEPTH SAND WITH HEX. CELL CORE; FOUR SIDES CORRUGATED	(4.016) 4.016 F.S. .147	233.69 .021	.276	.175	.031	.650	8	A/A
610R015"A"	WING SECTION WELDED SPACE TRUSS SUB-STRUCT - BRAZE ON SKINS	(3.99) 4.31 F.S. .137	118.29 .041	.138	.211	.034	.561	15	A/A LOW COST LOW WT 6AL-4V ANN TI
610R016	WING SECT. ALUM. INTEGRALLY STIFFENED SKIN PANELS MACHINED	(5.61) 5.69 S.C. .104	39.83 .124	.092	.148	.088	.556	18	A/A - LOW COST DES.
610R017	WING SECT. RECTANGULAR TUBE TRUSS CORE SAND PANEL, WELDED (6AL-4V TI) LOWER	(4.484) 4.91 S.C. .120	192.70 .025	.138	.155	.054	.492	26	OUT
610R018	WING SECT. WELDED Y-TEE STIFFENED SKINS	(4.044) 5.154 S.C. .114	195.11 .025	.135	.136	.057	.467		OUT
610R019-1	WING SECT. INTEGRAL FORMED BULBED TEE	(4.030) 4.030 F.S. .146	126.35 .038	.183	.175	.048	.590	13	A/A
610R020	WING SECTION SANDWICH WITH TRUSS MEMBER CORE	(4.264) 4.80 S.C. .123	157.58 .031	.146	.156	.056	.512	21	OUT
610R021 -1	WING SECTION DIFFUSION BONDED/TEE STIFFENED PANELS	(4.024) 5.13 S.C. .115	159.43 .030	.130	.138	.060	.473	28	OUT
610R022 -1	WING SECT. ADH. BOND. LAM. SKINS WITH HAT STIFFENERS	(4.624) 4.624 F.S. .128	115.83 .042	.147	.236	.063	.616	11	COMBINE WITH 022-2
610R023 -1	WING SECT. MONOLITHIC/WELDED STIFF'R, INTEGRAL SPAR CAPS (6AL 4V ANN)	(4.65) 5.08 S.C. .116	95.58 .050	.117	.156	.063	.502	23	A/A LOW COST TI DES.
-2	(6AL-4V STA & 8.8.2.3 TI)	(4.17) 5.27 S.C. .112	96.06 .050	.126	.136	.063	.487	27	OUT
610R024	WING SECTION BRAZED SANDWICH SKINS WITH TRUSS MEMBER CORE	(3.94) 3.94 F.S. .150	150.12 .032	.278	.185	.060	.705	2	A/A

Table XI (CONT'D)

CROSS-SECTION CONCEPTS C.S.S. 140.0
EVALUATION SUMMARY (REVISED RATING SYSTEM 11-10-72)

CONFIG NUMBER	CONFIGURATION DESCRIPTION	STRUCTURAL EFF.		TECHNOLOGY ADVANCE (.30)	STRUCTURAL INTEGRITY (.30)	ABILITIES (.10)	TOTAL SCORE	RANK	REMARKS
		WEIGHT (.15)	COST IN \$/IN (.15)						
610R019 -2	WING SECTION INTEGRAL FORMED BULBED TEE (7050 AL)	(5.89) F.S.	5.89 .100	68.44 .070	.150	.170	.050	.540	19 OUT
610R021 -2	WING SECTION DIFFUSION BONDED TEE STIFFENED PANEL	(4.644) S.C.	5.17 .114	156.38 .031	.130	.159	.060	.494	25 OUT
610R022 -2	WING SECT ADH. BONDED LAM. SKINS WITH HAT STIFFENERS	(4.04) F.S.	4.04 .146	115.74 .042	.183	.217	.063	.651	7 A/A-
610R025	WING SECTION ADH. BONDED HAT STIFFENERS (7050 AL)	(5.66) F.S.	5.66 .104	32.15 .150	.135	.212	.076	.677	5 A/A
610R026	WING SECTION MODIFIED TRIANGLE CORE (7050 AL)	(5.70) F.S.	5.70 .104	38.25 .126	.137	.196	.062	.625	10 A/A
610R027	WING SECTION HONEYCOMB SANDWICH PANEL - SPARS INTGR'L WITH LOWER PANEL (TI)	(4.25) F.S.	4.25 .139	109.54 .044	.146	.191	.069	.589	14 A/A
610R028	WING SECTION AL HONEYCOMB PANEL UPPER & LOWER - INT. SPAR CAPS ADH. BONDED	(5.64) F.S.	5.64 .105	59.84 .081	.158	.184	.070	.598	12 A/A
610R029	WING SECTION LAMINATED LOWER SKIN WITH STEPPED SPAR CAPS; PLATE UPPER SKIN, CORRUGATED SPAR CAPS	(5.84) F.S.	5.84 .101	44.82 .108	.179	.250	.070	.768	1 A/A
610R030	WING SECTION ADH. BONDED CORRUGATED STIFFENER INNER SKIN C.S.S. 140.0	(5.86) F.S.	5.86 .101	49.45 .098	.138	.172	.065	.574	15 OUT
610R031	WING SECT. AL HONEYCOMB SAND. UPPER PANEL - TI, BLADE STIFFENED PLANK LOWER	(4.82) F.S.	4.82 .123	91.96 .052	.227	.191	.058	.651	6 A/A

Table XII
CROSS-SECTION CONCEPTS - C.S.S. 340.0
EVALUATION SUMMARY (REVISED RATING SYSTEM 11/10/72)

CONFIG. NUMBER	CONFIGURATION DESCRIPTION	STRUCTURAL EFF. COST IN		TECHNOLOGY ADVANCE (.30)	STRUCTURAL INTEGRITY (.30)	ABILITIES (.10)	TOTAL SCORE	RANK	REMARKS
		WEIGHT (.15)	\$/IN. (.15)						
610R104	F-111F WING BOX CROSS SECT. CUT @ C.S.S. 340.0 (BASELINE)	1.295 .058	34.72 .099	.053	.221	.095	.526	11	BASELINE
610R100	WING SECTION ADHESIVE BONDED SAND. LOWER SKIN & SPARS - TRUSS CORE SAND. UPPER SKIN	1.105 .068	44.14 .078	.153	.098	.054	.451	21	OUT
610R101"B"	WING SECTION FULL DEPTH LARGE CELL CORE BRAZED TO UPPER & LOWER SKINS (C.S.S. 340.0)	.580 .129	106.75 .032	.246	.092	.022	.521	12	OUT
610R102	WING SECTION ADH. BONDED CLOSE SPAR SPACING	.624 .120	41.74 .083	.182	.168	.026	.579	3	A/A
610R103	WING SECTION BONDED TI SAND. UPPER PANEL BOND. TI SAND. LOWER PANEL	1.059 .071	81.83 .042	.212	.138	.038	.501	16	OUT
610R105	WING SECTION ADH. BOND. LOWER SKINS PRESS. REACTED	.990 .076	51.97 .066	.177	.142	.055	.516	14	OUT
610R106	WING SECTION BRAZED TI SAND LOWER SKIN/WAFFLE GRID AL UPPER SKIN								OUT
610R107	WING SECTION TI SAND SKINS WITH "RIBBON CANDY" FUEL FLOW PROVS.	1.119 .067	73.70 .047	.249	.123	.047	.553	8	RETAIN FUEL FLOW FEATURE ONLY
610R108	WING SECTION FULL DEPTH SANDWICH WITH HEX. CELL CORE, FOUR SIDE COR - (C.S.S. 340.0)	.706 .106	90.46 .038	.241	.144	.029	.558	5	A/A
610R109	WING SECTION MULTIPLE TENSION STRAP WELDED STIFFENER PRESS. CARRYING STRUCT.	.882 .085	54.50 .063	.107	.200	.077	.532	10	A/A
610R110	WING SECTION WELDED/ADH. BONDED TRUSS CORE PANELS	.815 .092	96.12 .036	.097	.240	.052	.517	13	OUT
610R111	WING SECTION RECT. TUBE PANELS INTEGRAL SPAR CAPS	.71 .105	87.62 .039	.148	.188	.052	.532	9	A/A
610R112	WING SECTION INTEGRAL BLADE STIFFENED ALUMINUM (C.S.S. 340.0)	.658 .114	23.43 .146	.064	.077	.090	.491	17	OUT
610R113	WING SECTION WELDED BLADE STIFFENED TITANIUM (C.S.S. 340.0)	.717 .104	63.60 .054	.091	.151	.068	.468	20	OUT
610R114	WING SECTION BRAZED TITANIUM TRUSS CORE PANELS INTEGRAL SPAR CAPS	.855 .098	63.72 .054	.190	.089	.053	.484	18	OUT

Table XII (CONT'D)
CROSS-SECTION CONCEPTS - C.S.S. 340.0
EVALUATION SUMMARY (REVISED RATING SYSTEM 11/10/72)

CONFIG. NUMBER	CONFIGURATION DESCRIPTION	STRUCTURAL EFF.		TECHNOLOGY ADVANCE (.30)	STRUCTURAL INTEGRITY (.30)	ABILITIES (.10)	TOTAL SCORE	RANK	REMARKS
		WEIGHT (.15)	COST IN \$/IN. (.15)						
61OR115 -1	WING SECTION INTEGRAL TEE STIFFENED SKINS (C.S.S. 340.0) (ALUMINUM)	.524 .143	47.12 .073	.107	.083	.077	.483	19	OUT
61OR115 -2	WING SECTION INTEGRAL TEE STIFFENED SKINS (C.S.S. 340.0)	.652 .115	148.11 .023	.115	.182	.067	.502	15	OUT
61OR116	WING SECTION ADH. BONDED, CORRUGATED STIFFENER INNER SKIN (C.S.S. 340.0)	.636 .118	28.43 .021	.121	.103	.070	.533	7	A/A
61OR117	WING SECTION SANDWICH SKIN PANELS INTEGRAL LOWER SPAR CAPS	.498 .150	34.69 .099	.158	.123	.062	.592	2	A/A
61OR118	WING SECTION MODIFIED TRIANGULAR CORE - ADH. BONDED AL.	.820 .091	28.26 .122	.155	.120	.059	.547	6	A/A
61OR119	WING SECTION ADH. BONDED HAT STIFFENER; 7050 AL	.65 .115	22.87 .150	.151	.164	.081	.661	1	A/A
61OR120	WING SECTION INTEGRAL FORMED BULB TEE	.66 .113	49.49 .070	.164	.162	.062	.571	4	A/A

4.1.3 Design Effort at the Analytical Assembly Level

From the cross section concepts, 13 concepts at CSS 140.0 and 10 concepts at CSS 340.0 were selected for re-iteration, detailed analysis and definition on Analytical Assembly Drawings. Analytical Assembly Drawings were also prepared for the baseline at the two stations.

The Analytical Assembly Drawings for CSS 140.0 and 340.0 are 48 inch long wing segments of constant cross section which were designed to the geometry, the static loads and the fatigue and fracture criteria that occur at each of these two wing stations. Weights and costs were computed and weighted score values established for each concept. The other design parameters as specified by AFFDL were also quantitatively evaluated and scored for each concept at each of the two stations.

The results of the design effort at the Analytical Assembly level is summarized in Tables XIII for CSS 140 and Table XIV for CSS 340.

The Analytical Assembly has proven to be a valuable preliminary design tool. It provides on a single drawing a definition of configuration and the critical numerical values that measure weight, cost, strength/stress levels, fatigue quality, damage tolerance and overall desirability of a design concept. When worked in conjunction with the evaluation format, it serves as an instrument to bring together and coordinate the technical efforts of the various disciplines necessary to optimize and produce a complex design concept. The concept data block on each Analytical Assembly Drawing provides detailed evaluative data on each wing part, i.e., upper skin, lower skin, front spar, etc. which permits optimizing additional designs by combining the best features of several Analytical Assembly concepts. In addition to providing an additional iterative step in the design process, the Analytical Assembly drawing provides valid data for evaluating a number of design concepts to specified parameters on a completely uniform, equitable basis.

Refer to Appendix III Phase Summary, Analytical Assembly Drawings for a comprehensive report of the 13/10 design concepts studied and evaluated during this phase of the program.

Table XIII
ANALYTICAL ASSY. CONCEPTS CSS 140.0
EVALUATION SUMMARY

CONFIG. NO.	DESCRIPTION	STRUCT. EFFICIEN.		TECHNOLOGY ADVANCEMENT				STRUCT. INTEGRITY RELIABILITY				ABILITIES				TOTAL SCORES	RANK			
		COST (.15) See Note 1	WEIGHT (.15)	CONCEPT TECH (.09)	MFG G TECH (.09)	MAT'L'S TECH (.09)	FRACT TECH (.03)	STATIC (.03)	FATIGUE QUALITY (.09)	SAFE CRACK (.09)	FAIL (.09)	INSPECT (.05)	MFG (.02)	MAIN- TAIN (.01)	REPAIR (.01)			PREDICT (.01)		
610RA000	FLIP BASELINE			\$2985.68	384.89 lbs .146	.009	0	0	.012	.029	.041	.039	0	.050	.02	.010	.010	.0039	.4459	14
610RA001	WING-MULTI-WET CELL CONSTR. (TI)			7215.31	195.00 .060	.090	.0824	.072	.024	.017	.087	.073	.025	.0344	.0122	.0071	.0056	.0061	.7458	4
610RA002	BRAZED SANDWICH TRUSS CORE SKINS (TI)			11,035.44	219.78 .0390	.050	.0900	.036	.024	.017	.085	.073	.057	.0375	.0116	.0098	.0097	.0036	.6762	8
610RA003	LAMINATED LOWER SKIN STEP'D CAPS SAND. UPR. (AL)			4554.84	283.90 .096	.063	.0354	.036	.024	.017	.088	.088	.090	.039	.0124	.0084	.009	.0058	.7150	5
610RA004	AL HONEYCOMB UPR SKIN, TI BLADE STIFF - LWR SRN			9576.07	249.94 .045	.058	.0584	.09	.024	.017	.089	.073	.025	.037	.0124	.0071	.0076	.0051	.6431	11
610RA005	ADH BOND - HAT STIFF. UPR (AL)			3018.58	300.88 .144	.054	.0348	.054	.024	.017	.090	.088	.090	.031	.0132	.0097	.009	.0029	.7586	2
610RA006	LAMINATED LWR SKIN - PLATE UPR - (AL)			3343.74	296.94 .130	.086	.0231	.054	.024	.017	.088	.088	.090	.0375	.0160	.0097	.009	.0061	.7774	1
610RA007	ADH. BOND LAM. SKINS HAT STIFF. (TI)			9476.66	246.17 .046	.072	.0328	.090	.024	.017	.089	.073	.041	.039	.0102	.0089	.0083	.0038	.6240	10
610RA008	BRAZED SPACE TRUSS WING (TI)			14,967.16	200.94 .029	.086	.0748	.054	.024	.017	.085	.073	.041	.0355	.0128	.0073	.0070	.0076	.7000	6
610RA009	MODIFIED TRIAG. CORE-ADH. BOND AL			4777.44	300.00 .091	.054	.0260	.036	.024	.017	.086	.088	.082	.0360	.0135	.0097	.0090	.0046	.6748	9
610RA010	AL HONEYCOMB SKINS INTEG. SPAR CAPS			2902.10	293.06 .150	.081	.0167	.054	.030	.017	.088	.088	.049	.0398	.0145	.0092	.010	.0017	.7489	3
610RA011	INTEGRAL FORMED BULB-TEE STIFF(TI)			8346.75	239.70 .0321	.054	.0492	.054	.024	.017	.087	.073	.041	.03225	.0110	.0091	.0063	.0057	.6376	12
610RA012	SAND SKINS- INTEGRAL SPARS(TI)			7043.06	239.92 .0618	.072	.0246	.072	.030	.017	.089	.073	.041	.0413	.0124	.0095	.0097	.010	.6831	7
610RA013	AL HONEYCOMB UPR SKIN - 6-4 TI ANNEALED BLADE LWR			6761.02	267.36 .064	.058	.0368	.054	.024	.030	.049	.090	.025	.0365	.0128	.0071	.0076	.0051	.6031	13

Note 1. Cost figures are for evaluation purposes only and do not include General and Administrative, Engineering, Material burden, allocations, etc.

Table XIV
ANALYTICAL ASSY CONCEPTS CSS 340.0
EVALUATION SUMMARY

CONFIG. NO.	DESCRIPTION	STRUCT. EFFICIENCY		TECHNOLOGY ADVANCEMENT		STRUCT. INTEGRITY-RELIABILITY				ABILITIES		PREDICT	TOTAL SCORE	RANK
		COST (.15) See Note 2	WEIGHT (.15)	CONCEPT TECH (.09)	MAT'L'S TECH (.09)	STATIC (.03)	FATIGUE QUALITY (.09)	SAFE CRACK (.09)	FAILSAFE (.09)	INSPECT (.05)	MFG. (.02)	MAIN- TAIN (.01)	REPAIR (.01)	
610RA100	FILLIF BASELINE @ CSS 340.0	\$1846.01 .133	69.17 lbs .0538	.011	0.0	.012	.058	.032	0	.050	.0165	.010	.0051	4.084
610RA101	ADH BONDED-HAT STIFF SKINS (AL)	2146.90 .114	51.12 .0728	.045	.0326	.030	.020	.021	0	.0325	.0175	.0084	.0083	4.841
610RA102	SAND SKIN PANELS INT LWR SPAR CAPS (AL)	2713.00 .0905	39.84 .0935	.045	.0218	.030	.024	.037	.045	.0455	.0177	.0079	.0090	5.480
610RA103	ADH BONDED CLOSE SPAR SPACE (AL)	2032.01 .1193	24.81 .150	.09	.0457	.024	.027	.043	.090	.029	.020	.0051	.0057	7.102
610RA104	INTEGRAL FORMED BULB TEE (AL)	2622.89 .0936	40.75 .0913	.067	.047	.030	.020	.017	0.0	.0205	.0142	.0072	.0057	5.195
610RA105	WING-MULTI-WET CELL CONSTR. (TI)	3805.64 .0646	33.97 .110	.09	.090	.023	.072	.028	0.0	.0345	.0145	.0058	.0057	5.945
610RA106	MODIFIED TRIANGLE CORE (AL)	1631.24 .1500	60.27 .0618	.0562	.0174	.045	.086	.090	0.0	.0295	.0189	.0092	.010	6.391
610RA107	ADH BOND-CORRUPT'D INNER SKINS (AL)	2172.61 .1128	48.72 .0764	.0338	.01622	.045	.013	.014	0.0	.0325	.0173	.0083	.0077	4.270
610RA108	RECTANG. TUBE PANELS INT. S. CAPS (TI)	See Note 1	41.59 .0852	.0450	See Note 1	.018	.024	.031	0.0	.0380	See Note 1	.0062	.0077	See Note 1
610RA109	MULTIPLE TEN. STRAP WELD'D STIFF (TI)	2661.74 .0922	48.39 .0768	.023	.060	.018	.036	.040	0.0	.0365	.0146	.0069	.0077	4.328
610RA110	DIAG. TENSION WIRE SYSTEM	2047.16 .1194	39.34 .0948	.045	.013	.045	.029	.035	0.0	.0415	.0123	.0060	.0063	4.923

Note 1. Not economically feasible to manufacture

Note 2. Cost figures are for evaluation purposes only and do not include General and Administrative, Engineering, Material burden, allocations, etc.

4.1.4 Preliminary Design

The seven highest ranking Analytical Assemblies at CSS 140.0 were layed out as full size wing box designs. Four splice layouts were made that joined combinations of the two highest ranking Analytical Assembly concepts at CSS 140.0 with the two highest ranking Analytical Assembly concepts at CSS 340.0. Two additional wing box layouts were made utilizing the #1 and #2 ranking analytical assemblies at CSS 140.0 with the #1 ranking analytical assembly concept at CSS 340.0

The nine wing box designs were costed and weighed by utilizing data from the Analytical Assembly data blocks. The other design parameters were evaluated by working with the nine wing box layouts.

The results of this evaluation are summarized in Table XV . The nine wing box drawings and the baseline wing box are shown in Appendix IV Phase Summary, Preliminary Design.

Figures 30 thru 39 depict the 9 configurations and the baseline. Sheet 2 of Figures 30 thru 39 shows highlights of these designs.

4.1.5 Final Iterative Phase, Wing Box Preliminary Design

From the preliminary design considerations of nine wing boxes, four top ranking designs were chosen for optimization and further study. Figures 40 , 41 , 42 and 43 are the preliminary design drawings of these configurations. It should be noted that weight and costs for these four designs were re-computed in detail after optimization and the values recorded on each drawing.

4.1.6 Design Assessment

The four designs were re-evaluated in detail. The results of this evaluation is shown in Table XVI. Each design is discussed in the paragraphs below. 610RW001 was not included in the final iteration because of its likeness to 610RW003.

Table XV

PRELIMINARY DESIGN CONCEPTS—EVALUATION SUMMARY

CONFIG. NO.	DESCRIPTION	STRUCT. EFFICIENCY		TECHNOLOGY ADVANCEMENT			STRUCT. INTEGRITY-RELIABILITY				ABILITIES					TOTAL SCORE	RANK	
		COST (.15)	WEIGHT (.15)	CONCEPT TECH (.09)	MFG. TECH (.09)	MAT'L'S TECH. (.09)	FRACT. TECH. (.03)	STATIC (.03)	FATIGUE QUALITY (.09)	SAFE CRACK (.09)	FAIL SAFE (.09)	INSPECT (.05)	MFG. (.02)	MAIN-TAIN (.01)	REPAIR (.01)			PREDICT (.01)
610RW000	F-111F BASELINE (MODIFIED)	64,283 .140	1665.0 .092	.009	0	0	.012	.030	.041	.041	0	.050	.020	.010	.010	.0039	.4589	10
610RW001	SANDWICH UPR. SKIN, LAM LWR SKIN WITH TENSION STRAPS OUTBD (ALUM)	98,774 .091	1385.0 .110	.063	.0387	.045	.024	.017	.088	.090	.090	.039	.0124	.0084	.009	.0058	.7313	6
610RW002	MULTI-WET CELL, BRAZED TITANIUM	140,069 .064	1019.6 .150	.090	.090	.090	.024	.017	.087	.075	.025	.0344	.0122	.0071	.0056	.0061	.7774	4
610RW003	LAM. LWR. SKIN W/STEP-FED SPAR CAPS: PLATE UPR, CORR. SPAR WEBS AL.	70,965 .1269	1261.4 .121	.086	.0252	.0675	.024	.017	.088	.090	.090	.0375	.0160	.0097	.009	.0061	.8139	1
610RW004	ADHESIVE BONDED AL. HONEYCOMB PANELS	60,027 .150	1351.15 .113	.081	.0182	.0675	.030	.017	.088	.090	.049	.0398	.0145	.0092	.010	.0017	.7789	3
610RW005	ADHESIVE BONDED TI. HONEYCOMB PANELS	130,294 .0691	1178.6 .1297	.072	.0269	.09	.030	.017	.089	.075	.041	.039	.0124	.0084	.009	.0058	.7143	9
610RW006	SPACE TRUSS, BRAZED TITANIUM	176,431 .0512	1109.0 .1379	.086	.0817	.0675	.024	.017	.085	.075	.041	.0355	.0128	.0073	.007	.0076	.7370	5
610RW007	LAM. LWR SKIN, HAT STIFFENED UPR. SKIN (ALUMINUM)	64,712 .1391	1347.0 .1135	.054	.038	.0675	.024	.017	.090	.090	.090	.031	.0132	.0097	.009	.0029	.7596	2
610RW008	LAM. LWR. HAT UPR/ SPliced TO MULTI-SPAR BONDED ALUMINUM	64,828 .1389	1282.0 .1193	.087	.0454	.0675	.022	.017	.076	.090	0	.031	.0149	.0097	.009	.0029	.7596	7
610RW009	LAM. LWR. PLATE UPR/ SPlice TO MULTI-SPAR BONDED ALUMINUM	71,019 .1268	1207.0 .1266	.088	.0303	.0675	.022	.017	.075	.090	0	.0375	.0154	.0097	.009	.0061	.7209	8

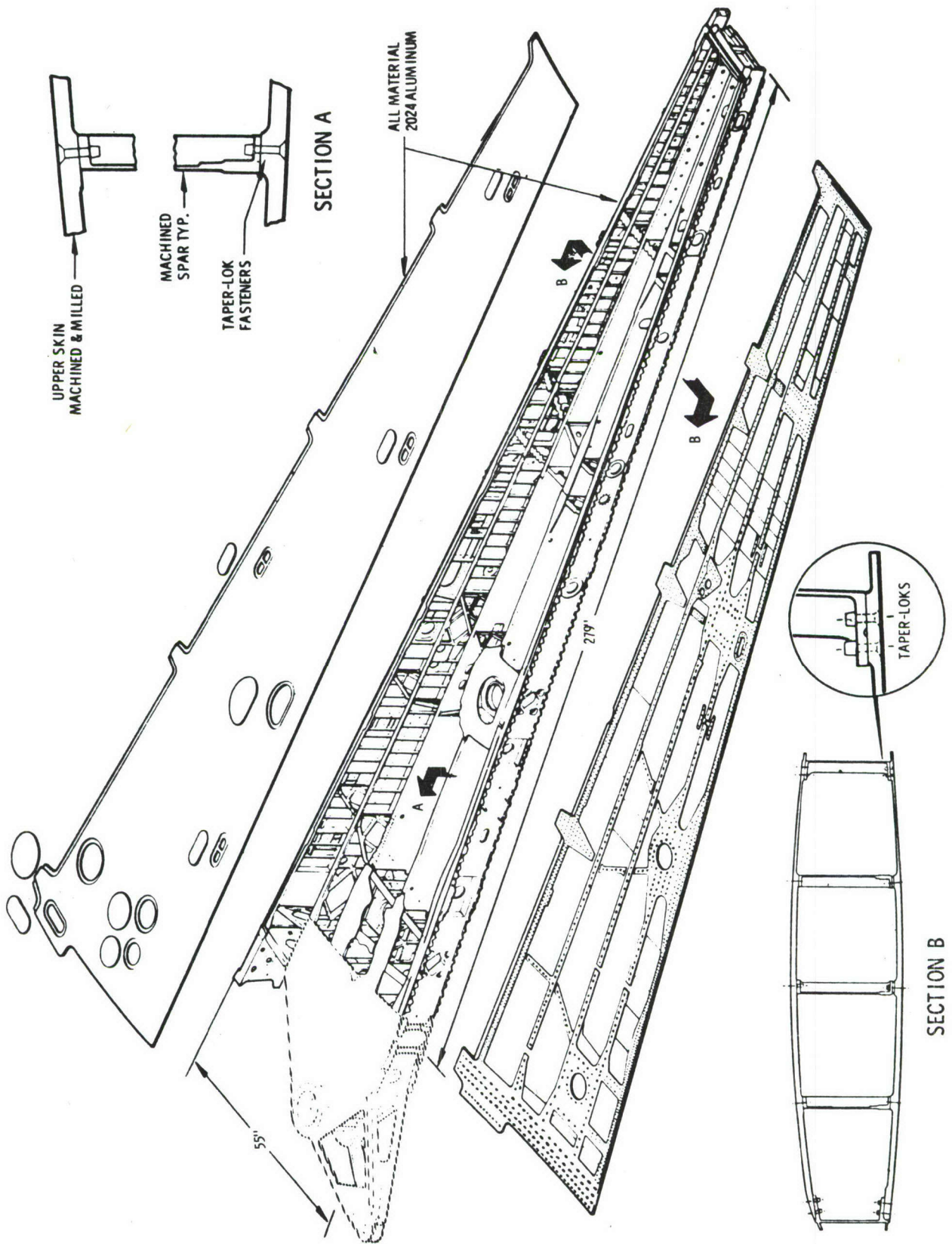
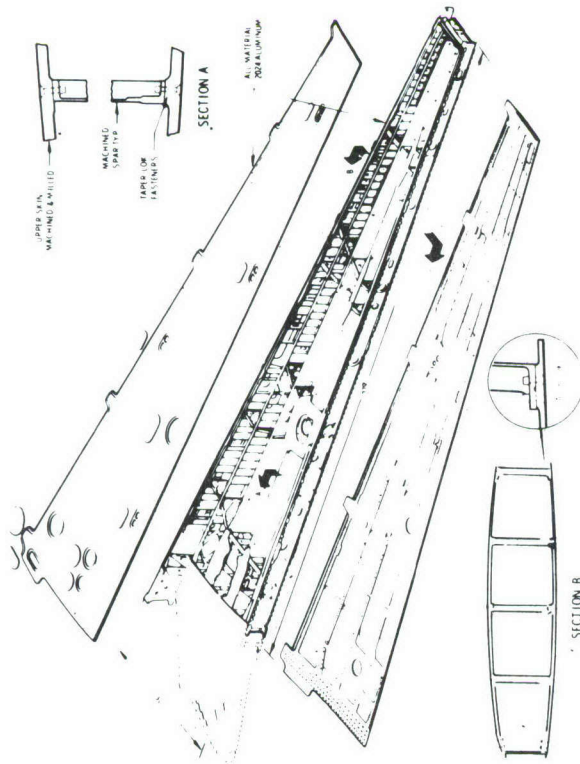


Figure 30 Baseline Wing Box (Sheet 1)



BASELINE WEIGHT	1665 LBS
BASELINE RECURRING COST	\$64,283

- EFFICIENT USE OF PROVEN METALS WITH RESPECT TO COST AND WEIGHT
- PROVEN FATIGUE AND STRENGTH PERFORMANCE
- HIGH PRODUCIBILITY
- HIGHLY RELIABLE INTEGRAL FUEL TANK DESIGN AND CORROSION PROTECTION
- DEMONSTRATED MAINTAINABILITY AND RELIABILITY
- UPPER PANEL REMOVABLE FOR COMPLETE ACCESSIBILITY
- INTERFACE FIT TAPERED FASTENERS IN LOWER SURFACE BENDING MATERIAL TO IMPROVE FATIGUE LIFE

Figure 30 (Sheet 2)

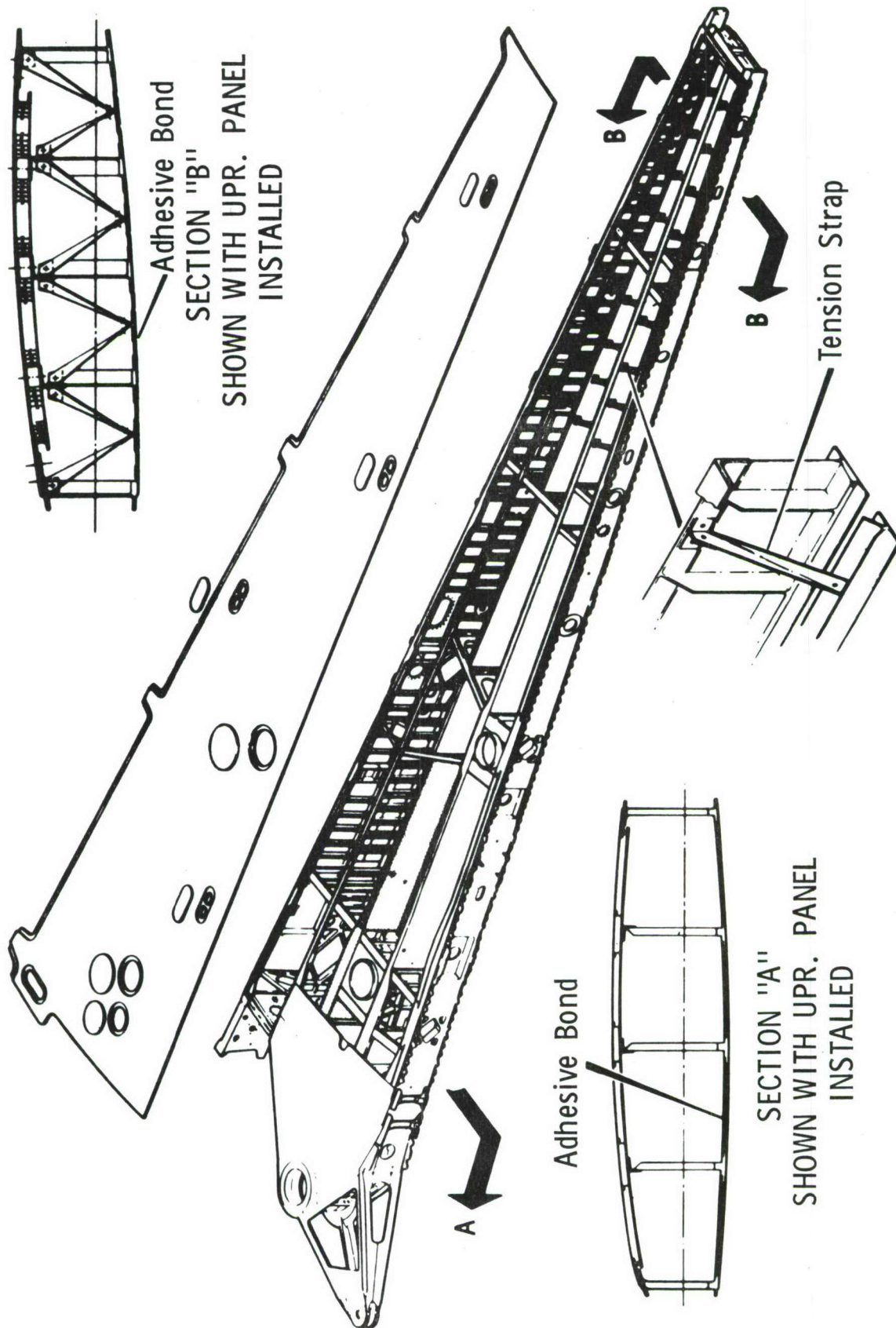


Figure 31 Sandwich Upper Skin, Laminated Lower With Tension Straps Outboard (Sheet 1)

CONFIGURATION 610RW001

TOTAL WING BOX WEIGHT	1385.0
% SAVINGS FROM B/L	20.7%

- LOWER PANEL LAMINATED AND PLANKED TO PROVIDE FAIL SAFE STRUCTURE
- LOW KT IN TENSION MEMBERS BY ELIMINATING ALL FASTENERS THRU LOWER SURFACE
- UPPER PANEL REMOVABLE FOR COMPLETE ACCESSIBILITY

Ref A/A 610RA003

Figure 31 (Sheet 2)

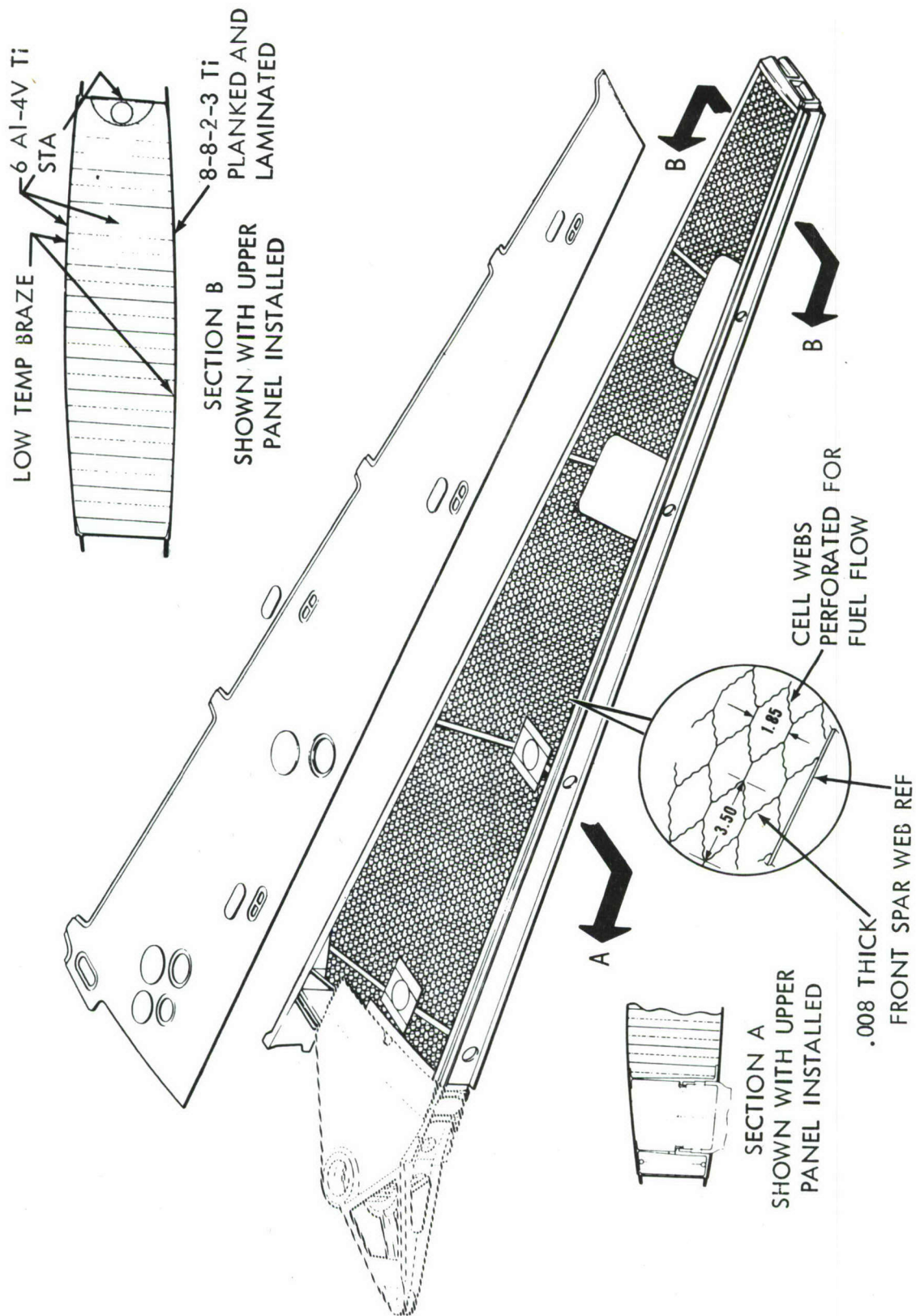
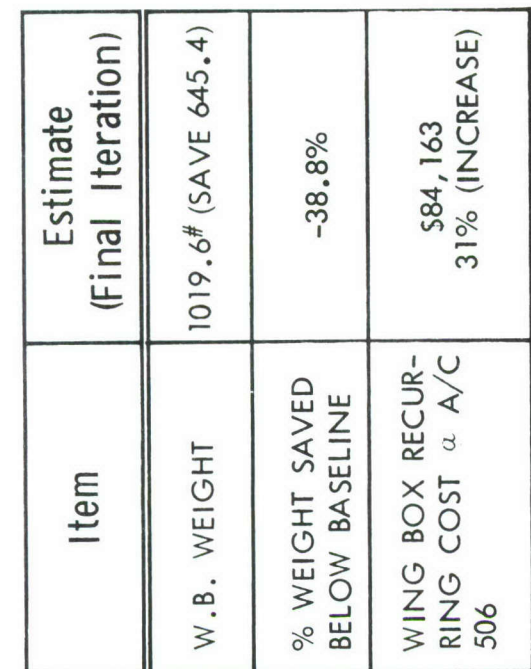


Figure 32 Multi-Wet Cell Construction (Sheet 1)



- Figure 32 (Sheet 2)

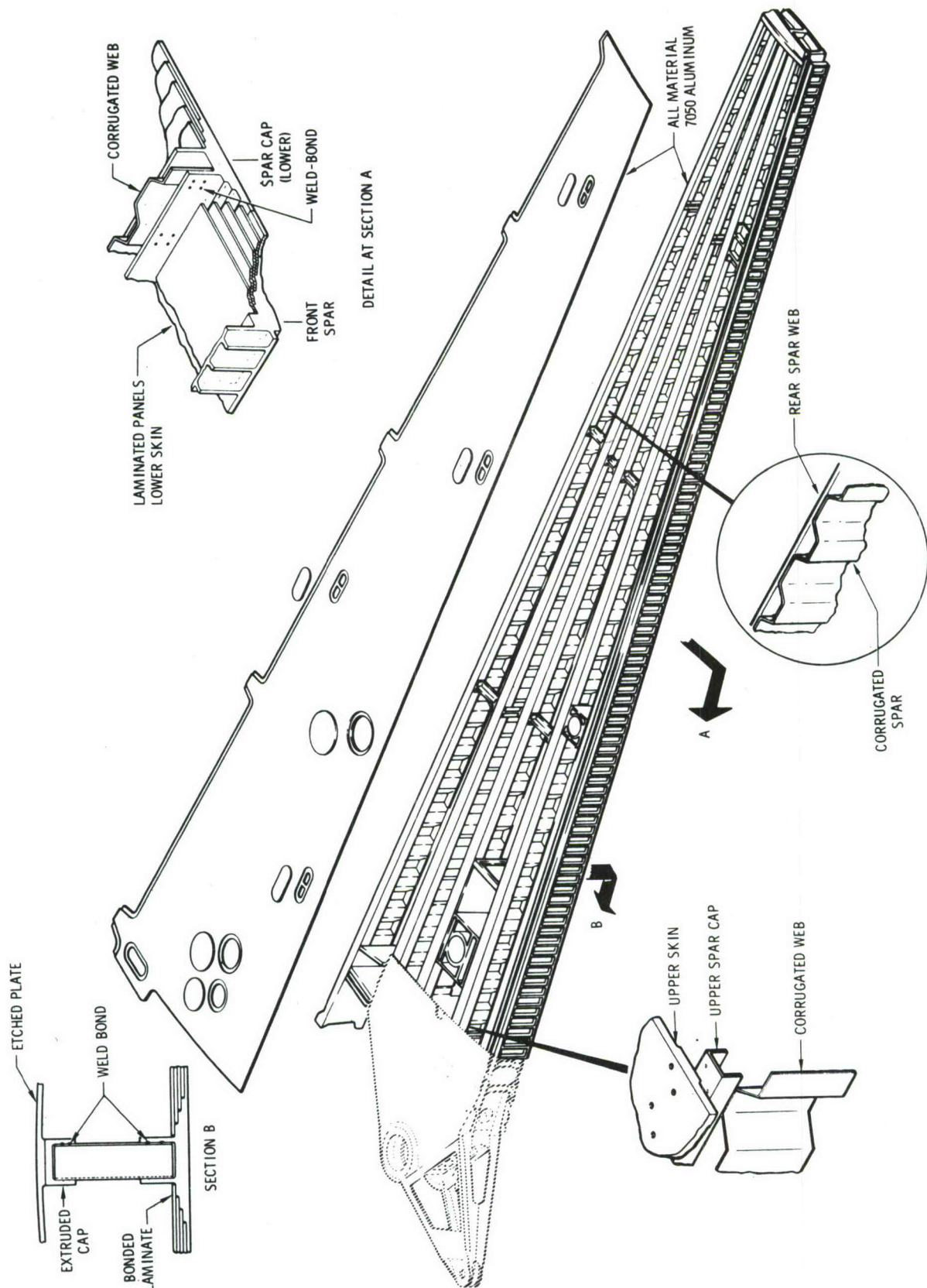
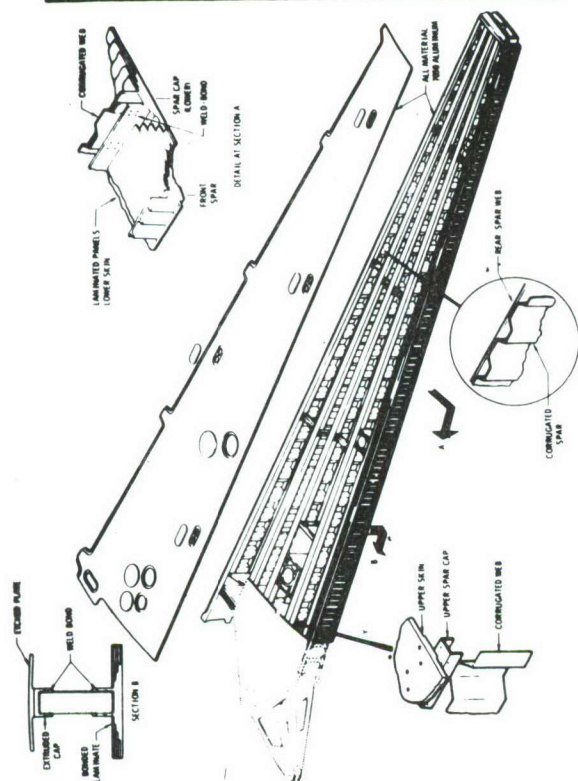


Figure 33 Corrugated Spar - Laminated Al Lower Skin Construction
(Sheet 1)



Item	Estimate (Final Iteration)
W.B. WEIGHT	1261.4 (SAVED 403.6)
% BELOW BASELINE	-24.2%
WING BOX RECUR- RING COST @ A/C 506 (20/MONTH)	\$55,377 (-13.8% SAVINGS)

- LOWER PANEL LAMINATED AND PLANKED TO PROVIDE FAIL SAFE STRUCTURE & DECREASE CRACK GROWTH RATE
- LOW KT IN LOWER SURFACE BY ELIMINATING ALL FASTENERS THROUGH THE LOWER SURFACE BENDING MATERIAL
- WIDE SPAR CAPS STABILIZE THE SKINS TO REDUCE SKIN THICKNESS
- SKIN THICKNESS READILY TAILORED TO LOCAL LOAD REQUIREMENTS
- LOWER SPAR CAPS VISIBLE FROM EXTERIOR FOR INSPECTION
- UPPER PANEL REMOVABLE FOR COMPLETE ACCESSIBILITY

Figure 33. (Sheet 2)

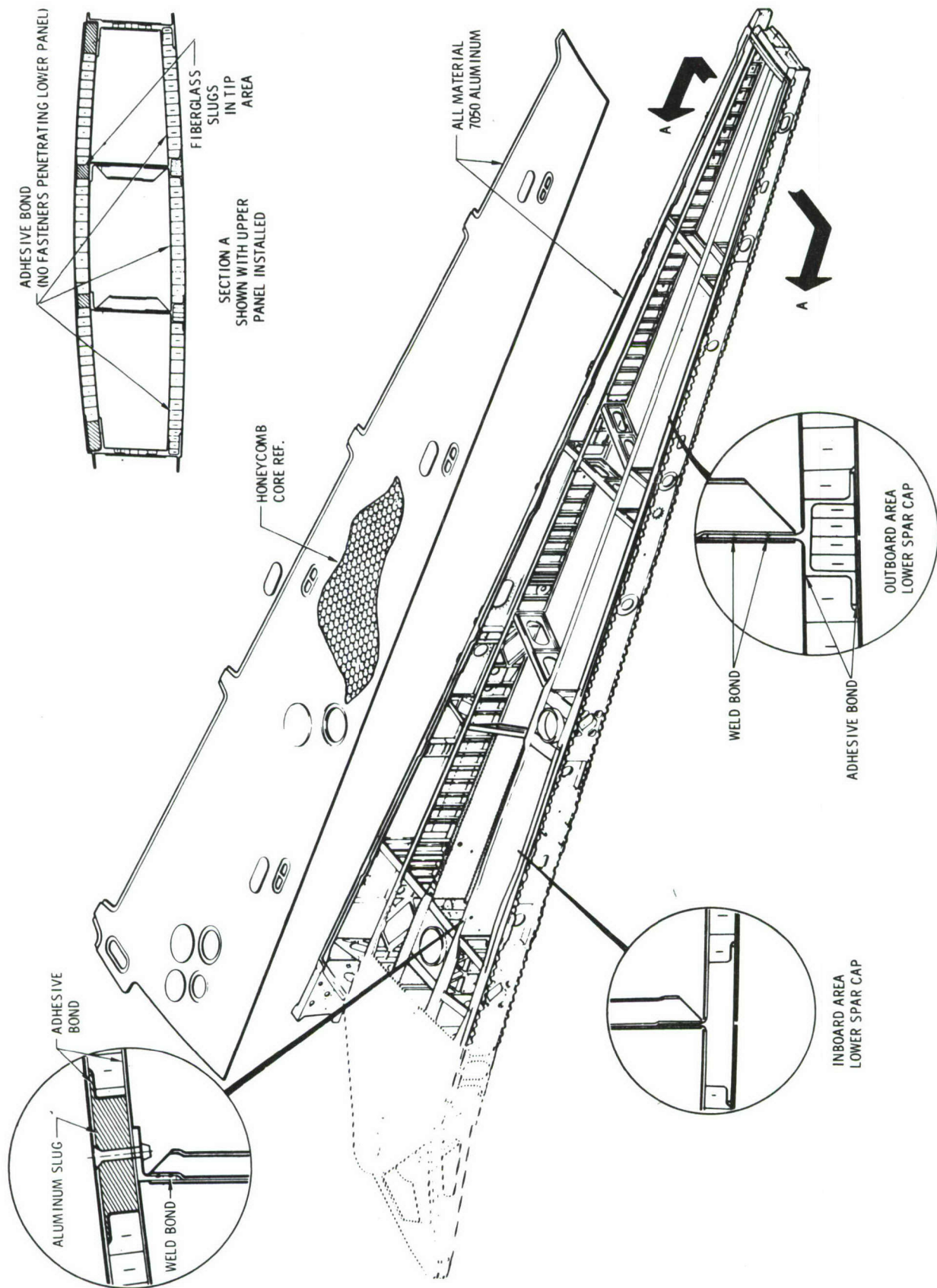
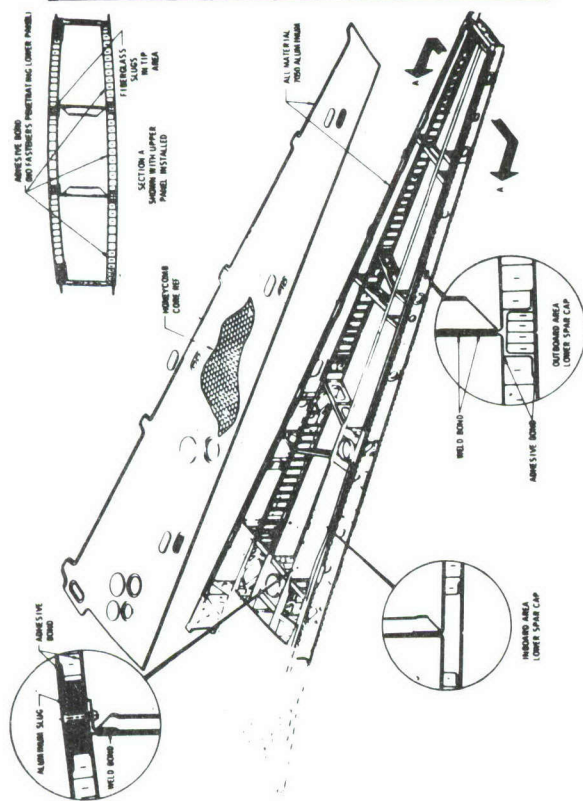


Figure 34 Adhesive Bonded Aluminum Honeycomb Panels (Sheet 1)



Item	Estimate (Final Iteration)
W.B. WEIGHT	1349.6# (SAVED 315.4)
% WEIGHT SAVED BELOW BASELINE	-18.9%
WING BOX RECUR- RING COST @ A/C 506	\$54,211 (DECREASE -15.7%)

- LOWER PANEL DESIGNED WITH MULTIPLE LOAD PATHS TO ACHIEVE A FAIL SAFE DESIGN
- LOW K_T IN LOWER SURFACE BY ELIMINATING ALL FASTENERS THROUGH THE LOWER SURFACE BENDING MATERIAL
- FRONT AND REAR SPARS ARE OF BONDED HONEYCOMB CONSTRUCTION, THEREBY REDUCING MATERIAL AND FABRICATION COSTS
- INTERMEDIATE SPARS ARE BUILT-UP, RATHER THAN MACHINED, THEREBY REDUCING MATERIAL AND FABRICATION COSTS

Figure 34 (Sheet 2)

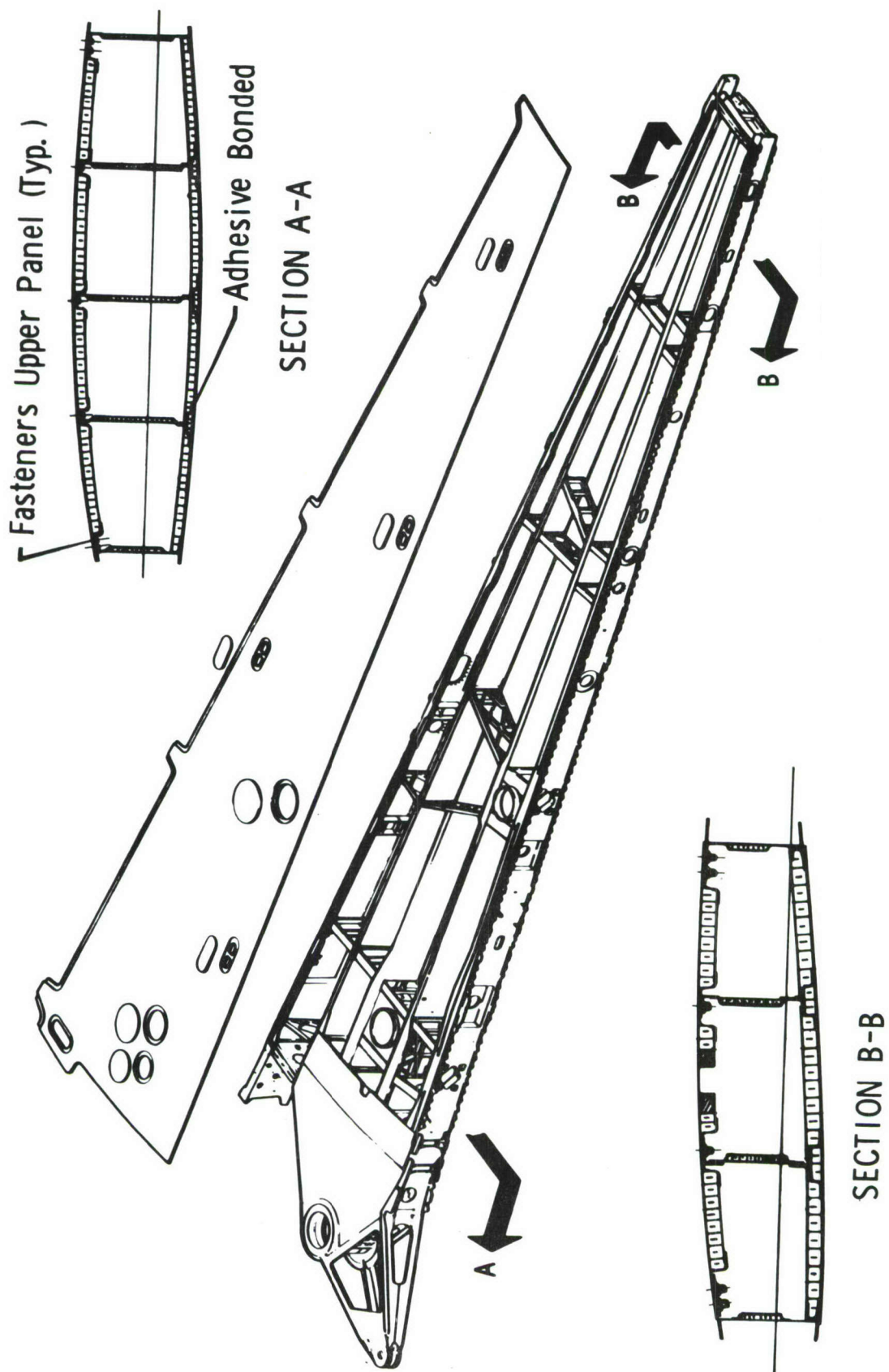


Figure 35 Adhesive Bonded Titanium Honeycomb Panels (Sheet 1)

TOTAL WING BOX WEIGHT	1196 LBS
% SAVINGS FROM B/L	29.0%

LOWER PANEL/SPAR CONFIGURATION PROVIDES MULTIPLE
LOAD PATHS

LOW KT IN TENSION MEMBERS BY ELIMINATING ALL
FASTENERS THRU LOWER SURFACE

UPPER SURFACE IS REMOVABLE FOR COMPLETE ACCESSIBILITY

Ref A/A 610RA012

Figure 35 (Sheet 2)

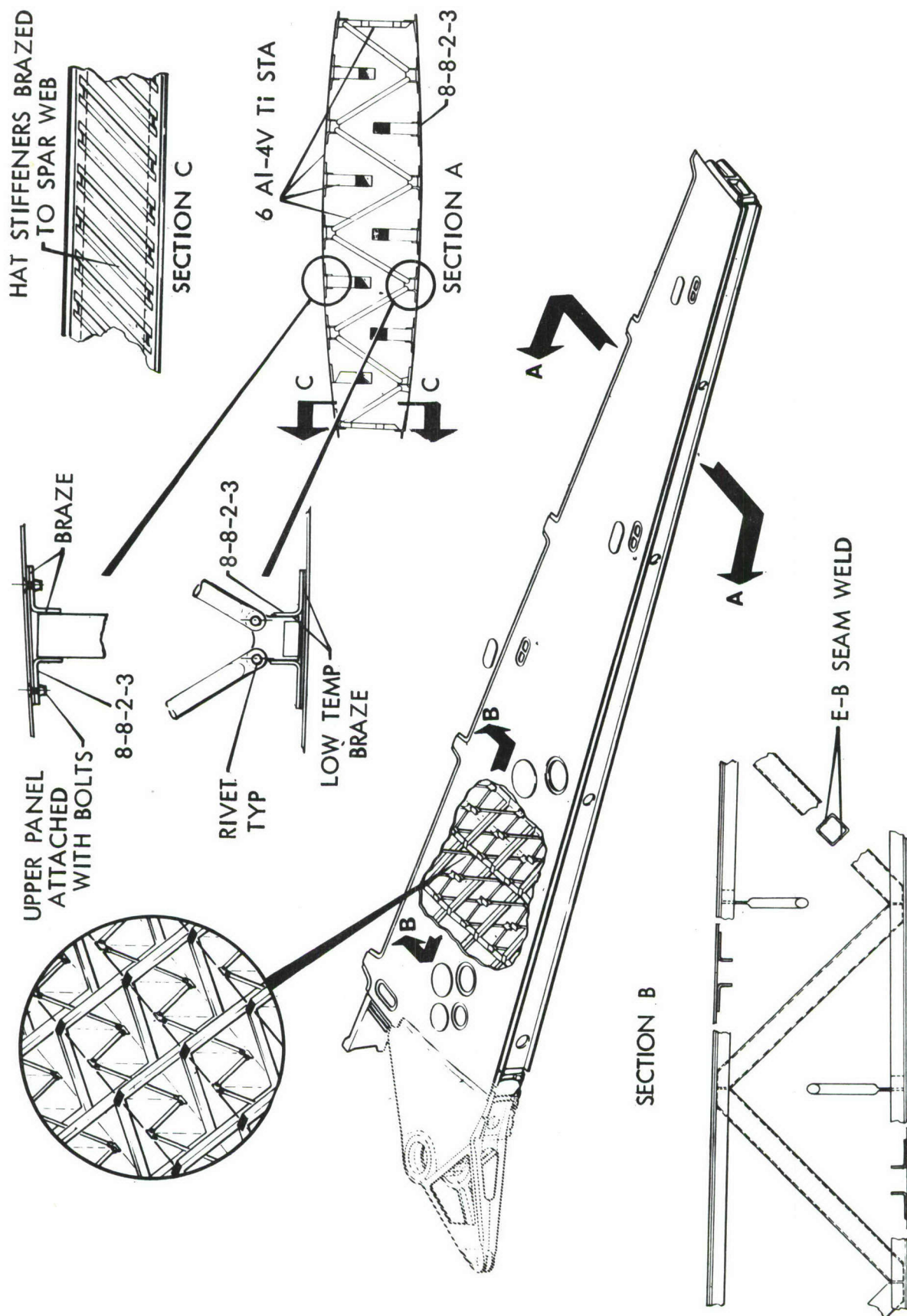
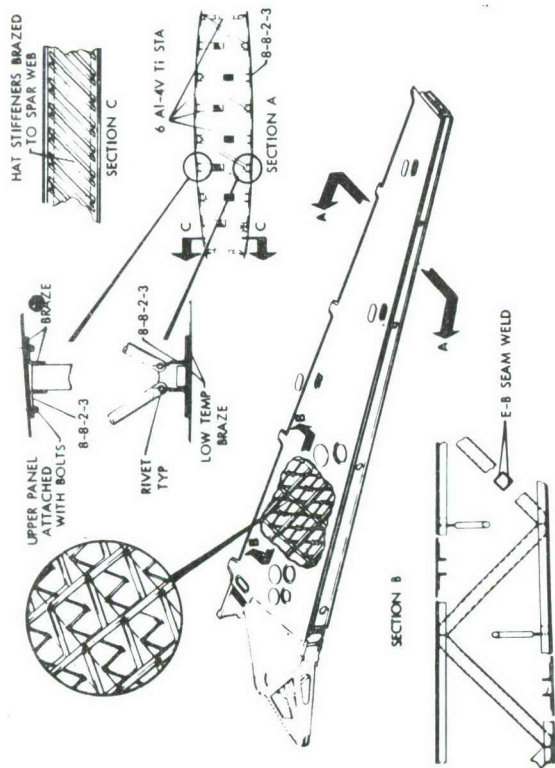


Figure 36 Brazed Titanium Space Truss (Sheet 1)



Item	Estimate (Final Iteration)
W.B. WEIGHT	1109.0# (SAVED 556)
% WEIGHT BELOW BASELINE	-33.4%
WING BOX RECUR- RING COST @ A/C 506 (20/MONTH)	\$122,120 +90% (INCREASE)

- LOWER SKIN PLANKS BRAZED TO MULTIPLE LOWER SPAR CAPS PROVIDES MULTIPLE LOAD PATHS FOR A FAIL SAFE STRUCTURE
- LOW K_T IN LOWER SURFACE BY ELIMINATING ALL FASTENERS THROUGH THE LOWER SURFACE BENDING MATERIAL
- STRUCTURE IS HIGHLY TOLERANT TO STRUCTURAL DAMAGE
- CONCEPT HAS HIGH TEMPERATURE RESISTANCE WITH POTENTIAL APPLICATION ON ULTRA HIGH PERFORMANCE AIRCRAFT
- UPPER PANEL REMOVABLE FOR COMPLETE ACCESSIBILITY
- DESIGN CAN READILY BE TAILORED TO DEVELOP THE STRENGTH AND RIGIDITY REQUIRED IN VARIOUS DIRECTIONS
- DESIGN PROVIDES AMPLE SPACE FOR INTERNAL ROUTING

Figure 36 (Sheet 2)

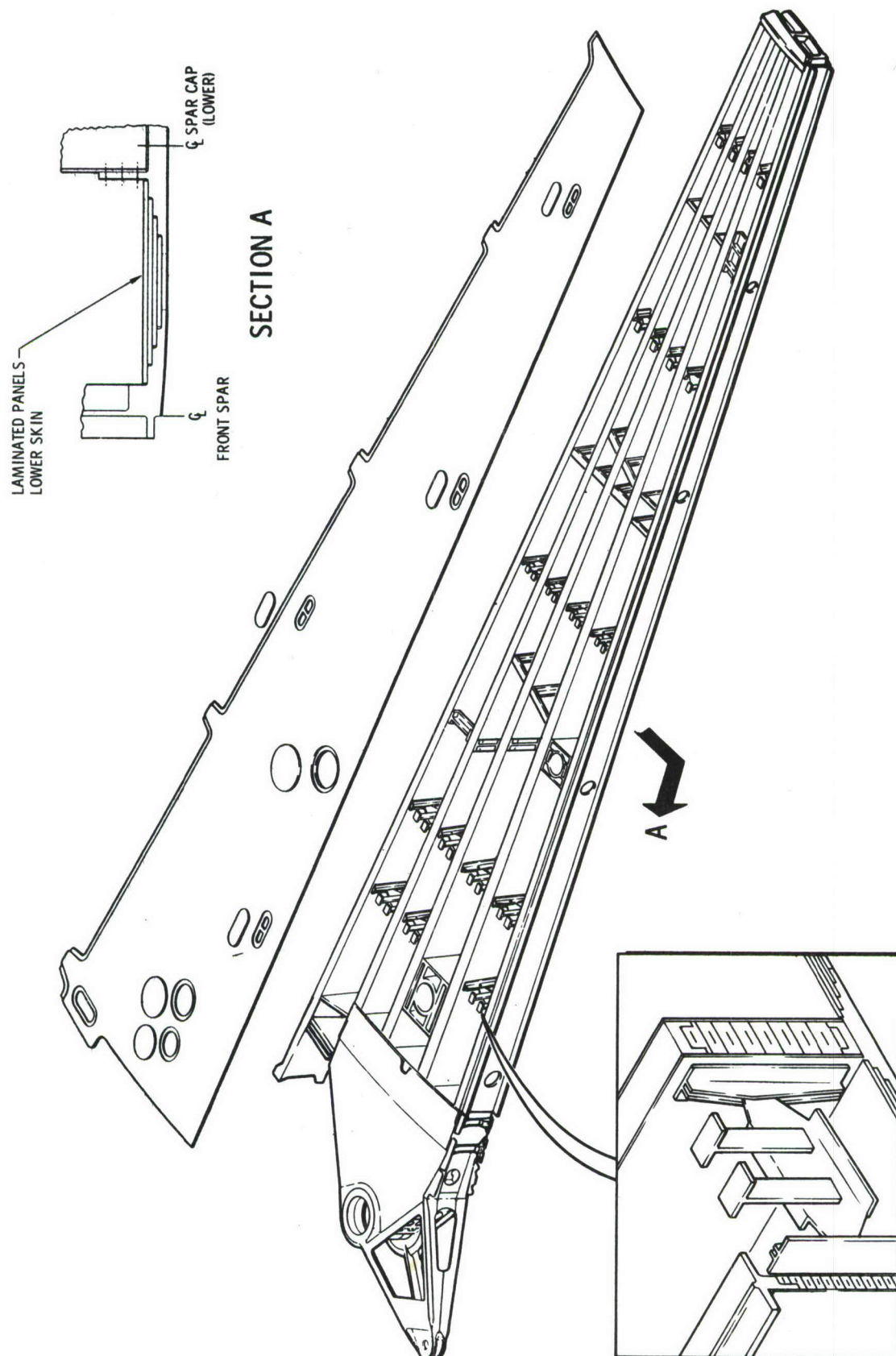


Figure 37 Wing Box - Bonded Aluminum Laminated Lower Panel;
Hat Stiffener Upper Panel (Sheet 1)

TOTAL WING BOX WEIGHT	1375 LBS
% SAVINGS FROM B/L	18.3%

LOWER PANEL LAMINATED AND PLANKED TO ACHIEVE FAIL SAFE FEATURE

LOW KT IN TENSION MEMBERS BY ELIMINATING ALL FASTENERS THRU LOWER SURFACE

UPPER SURFACE IS REMOVABLE FOR COMPLETE ACCESSIBILITY

REDESIGN PROVIDES HIGH INTERNAL FUEL VOLUME

Ref 610RA005

Figure 37 (Sheet 2)

610RW008

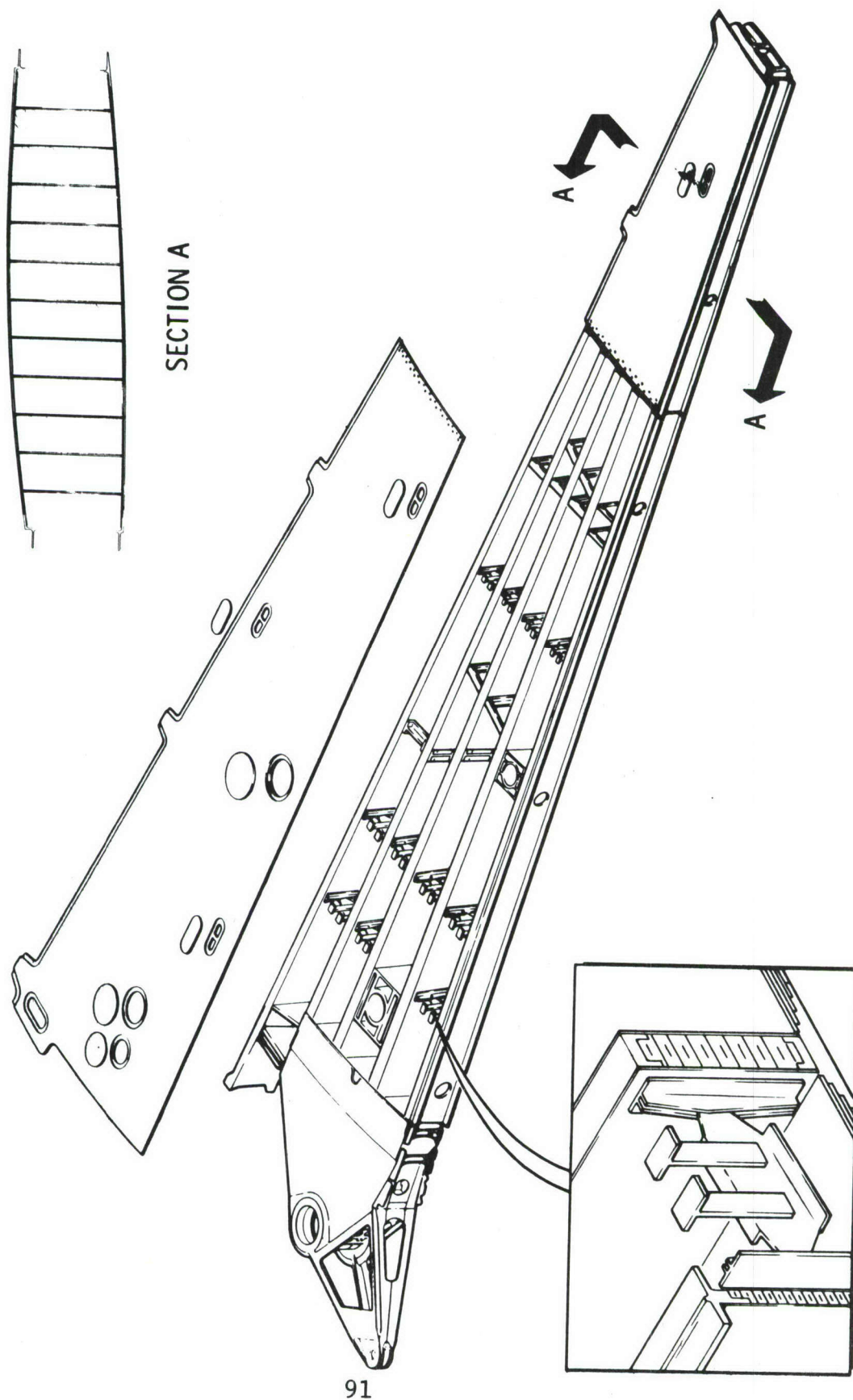


Figure 38 Bonded Aluminum Laminated Lower Panel; Hat Stiffener
Upper Panel With Close Tip (Sheet 1)

TOTAL WING BOX WEIGHT	1291
% SAVINGS FROM B/L	23.3%

LOWER PANEL LAMINATED AND PLANKED TO ACHIEVE FAIL SAFE FEATURE

DESIGN PROVIDES HIGH INTERNAL FUEL VOLUME

FASTENERS THRU LOWER SURFACE ARE OMITTED WHERE HIGH CYCLIC TENSION LOADS OCCUR.

Ref A/A's 610RA005
610RA103

Figure 38 (Sheet 2)

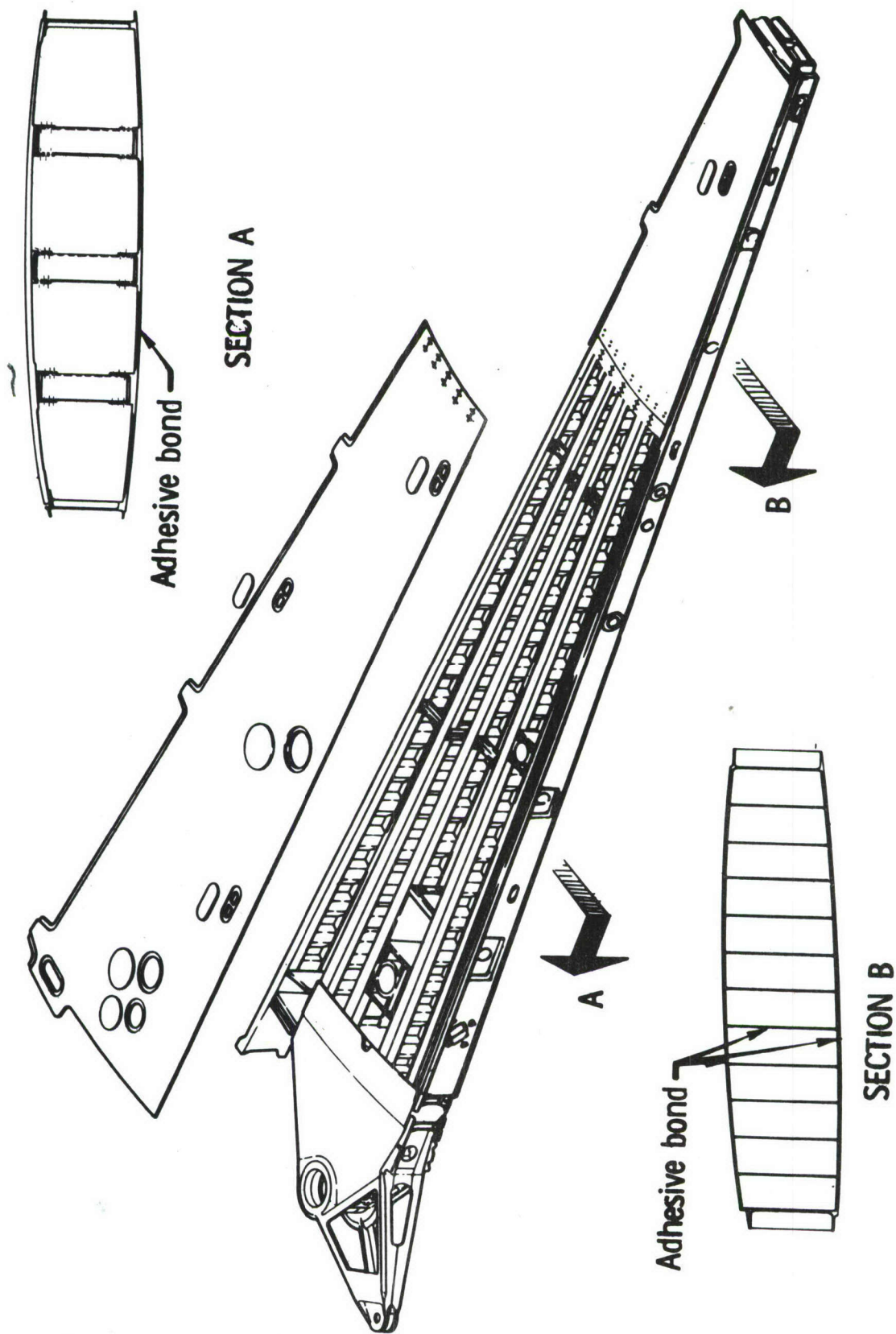


Figure 39 Laminated Lwr Skin/Plate Upper Spliced to Multi-Spar Bonded Aluminum (Sheet 1)

TOTAL WING BOX WEIGHT	1300 LBS
% SAVINGS FROM B/L	22.8%

LOWER PANEL LAMINATED AND PLANKED TO ACHIEVE FAIL SAFE FEATURE

DESIGN PROVIDES HIGH INTERNAL FUEL VOLUME

FASTENERS THRU LOWER SURFACE ARE OMITTED WHERE HIGH CYCLIC TENSION LOADS OCCUR

Figure 39 (Sheet 2)

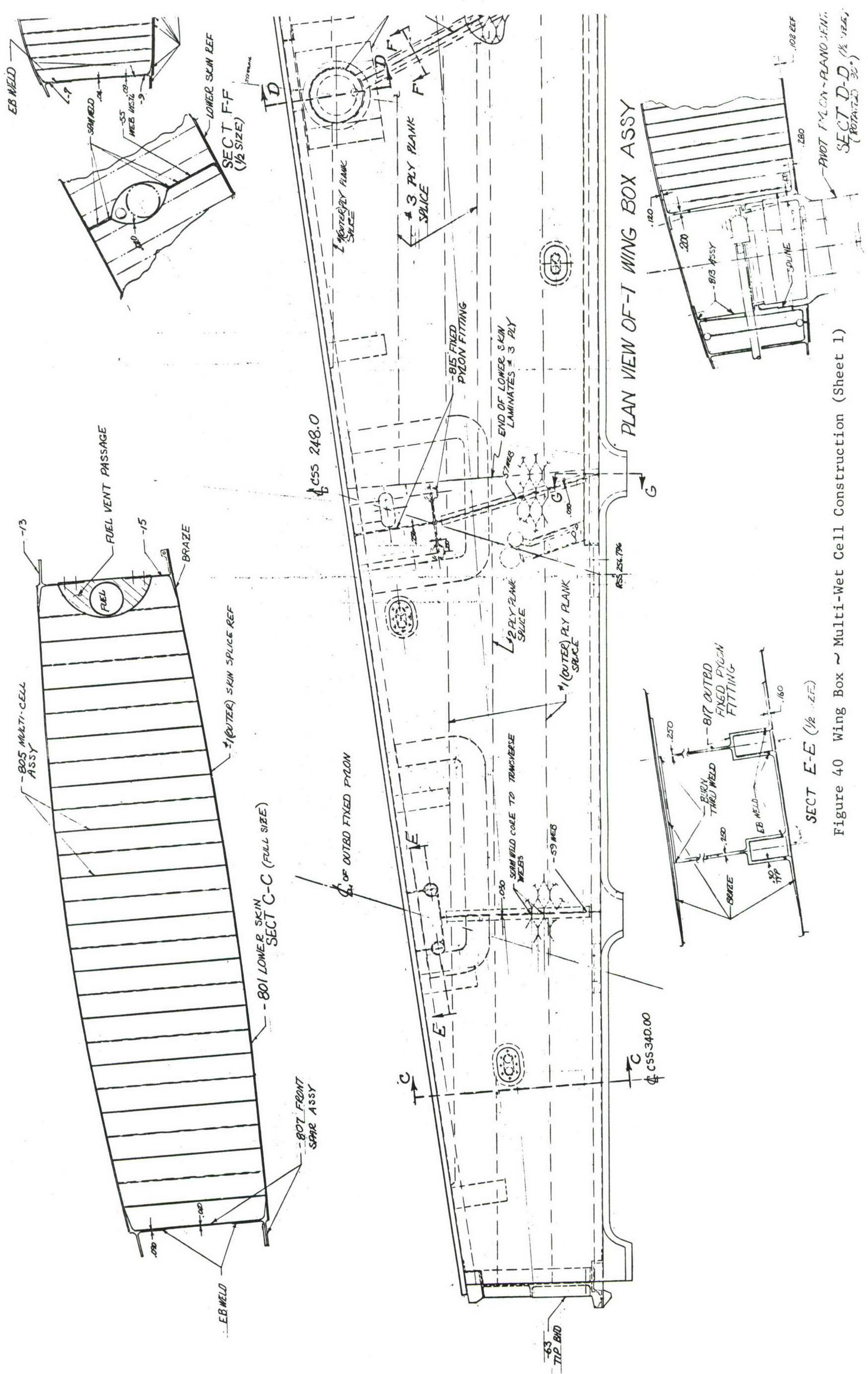
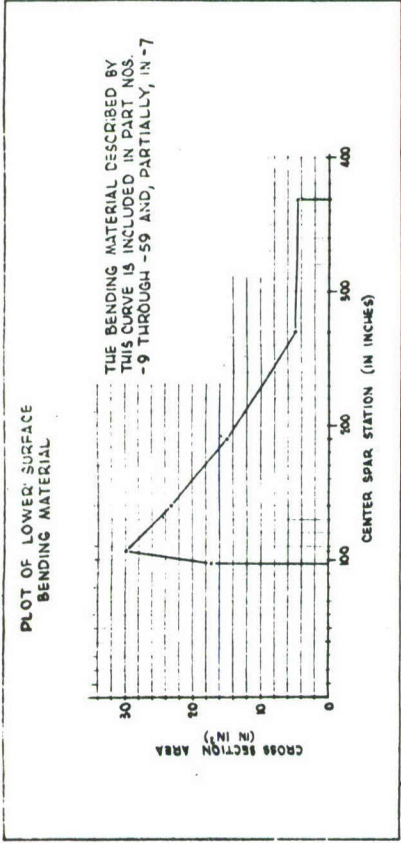
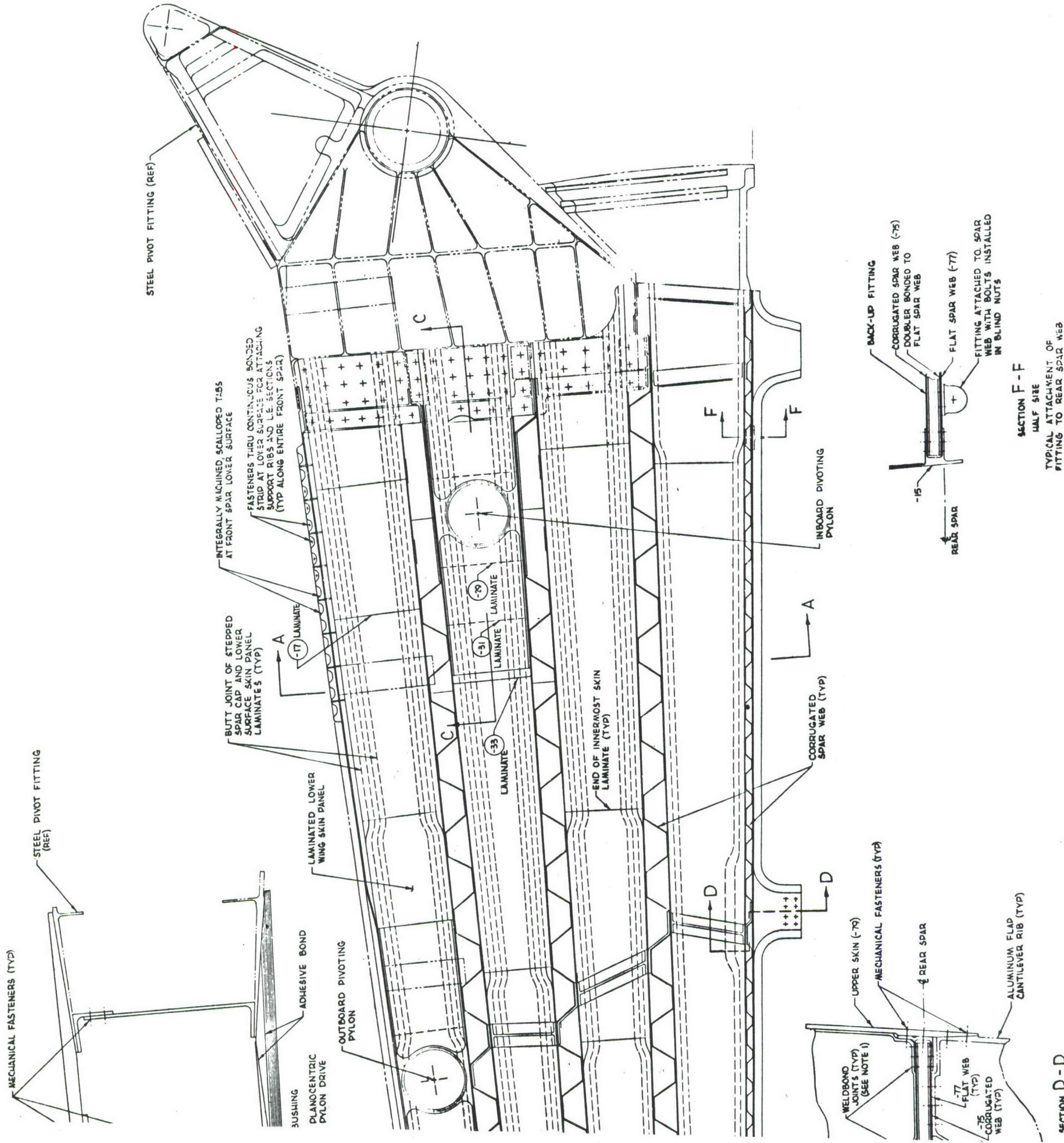
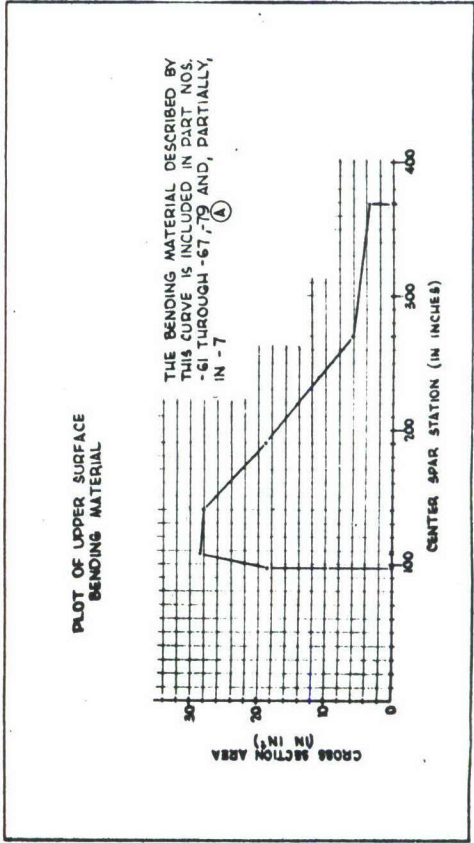


Figure 40 Wing Box ~ Multi-Wet Cell Construction (Sheet 1)



DASH NO.	PART NO. NAME	NO. REQ.	DESCRIPTION	MATERIAL	RAW STOCK SIZE	RAW WEIGHT (LB)	FINISHED WEIGHT (LB)	COST
-9	LWR FAS SPAR CAP	1	MACHINE FROM EXTRUSION	7050-T7651 AL ALLOY	EXTRU*276 (1.5 IN)	347.5		
-11	LWR CS SPAR CAP	1			EXTRU*276 (1.1 IN)	314.1		
-13	LWR AAS SPAR CAP	1			EXTRU*276 (10.2 IN)	283.6		
-15	LWR RS SPAR CAP	1	MACHINE FROM EXTRUSION	7050-T7651 AL ALLOY	EXTRU*282 (9.4 IN)	265.1		
-17	LWR FAS SPAR CAP	1	PROFILE, CHEM. ETCH A CONSTANT 10 PERCENT OF THE TOTAL ROLL FORM CONTOUR PRIOR TO BONDING	7050-T7651 AL ALLOY	EXTRU*276 (1.5 IN)	347.5		
-19	LWR CS SPAR CAP	1			EXTRU*276 (1.1 IN)	314.1		
-21	LWR AAS SPAR CAP	1			EXTRU*276 (10.2 IN)	283.6		
-23	LWR RS SPAR CAP	1			EXTRU*282 (9.4 IN)	265.1		
-25	LWR FAS SPAR CAP	1			EXTRU*276 (1.5 IN)	347.5		
-27	LWR CS SPAR CAP	1			EXTRU*276 (1.1 IN)	314.1		
-29	LWR AAS SPAR CAP	1			EXTRU*276 (10.2 IN)	283.6		
-31	LWR RS SPAR CAP	1			EXTRU*282 (9.4 IN)	265.1		
-33	LWR FAS SPAR CAP	1			EXTRU*276 (1.5 IN)	347.5		
-35	LWR CS SPAR CAP	1			EXTRU*276 (1.1 IN)	314.1		
-37	LWR AAS SPAR CAP	1			EXTRU*276 (10.2 IN)	283.6		
-39	LWR RS SPAR CAP	1			EXTRU*282 (9.4 IN)	265.1		
-41	LWR FAS SPAR CAP	1			EXTRU*276 (1.5 IN)	347.5		
-43	LWR CS SPAR CAP	1			EXTRU*276 (1.1 IN)	314.1		
-45	LWR AAS SPAR CAP	1			EXTRU*276 (10.2 IN)	283.6		
-47	LWR RS SPAR CAP	1			EXTRU*282 (9.4 IN)	265.1		
-49	LWR FAS SPAR CAP	1			EXTRU*276 (1.5 IN)	347.5		
-51	LWR CS SPAR CAP	1			EXTRU*276 (1.1 IN)	314.1		
-53	LWR AAS SPAR CAP	1			EXTRU*276 (10.2 IN)	283.6		
-55	LWR RS SPAR CAP	1			EXTRU*282 (9.4 IN)	265.1		
-57	LWR FAS SPAR CAP	1			EXTRU*276 (1.5 IN)	347.5		
-59	LWR CS SPAR CAP	1			EXTRU*276 (1.1 IN)	314.1		
-7	FRONT SPAR	1	INTEGRALLY STIFFENED MEMBER	7050-T7651 AL ALLOY	50-9.5-268	1730	648.8	

*264 LB OF THIS WEIGHT IS INCLUDED IN THE LOWER SURFACE BENDING MATERIAL CURVE AND 16.8 LB. IS INCLUDED IN THE UPPER SURFACE BENDING MATERIAL CURVE



DASH NO.	PART NO. NAME	NO. REQ.	DESCRIPTION	MATERIAL	RAW STOCK SIZE	RAW WEIGHT (LB)	FINISHED WEIGHT (LB)	COST
-61	UPR FAS SPAR CAP	1	MACHINE FROM EXTRUSION	7050-T7651 AL ALLOY	EXTRU*276 (1.4 IN)	34.6		
-63	UPR CS SPAR CAP	1			EXTRU*263 (1.3 IN)	34.2		
-65	UPR AAS SPAR CAP	1			EXTRU*263 (1.3 IN)	34.2		
-67	UPR RS SPAR CAP	1	MACHINE FROM EXTRUSION	7050-T7651 AL ALLOY	EXTRU*277 (1.2 IN)	32.4		
-79	UPR SURF SKIN	1	PROFILE, FORM, MACHINE AND CHEM. ETCH (USED SIMILAR TO BASELINE WING UPPER SURFACE SKIN)	7050-T7651 AL ALLOY	10-60-780	1680.0	332.2	
-69	FAS CORR. SPAR WEB	1	44 CORN. ETCH AND POLISH (1.0 IN)	7050-T7651 AL ALLOY	0.71-11.3-552	28.2	15.8	
-71	CS CORR. SPAR WEB	1	50 CORN. ETCH AND POLISH (1.0 IN)	7050-T7651 AL ALLOY	0.71-11.3-552	35.7	18.4	
-73	AAS CORR. SPAR WEB	1	44 CORN. ETCH AND POLISH (1.0 IN)	7050-T7651 AL ALLOY	0.63-11.25-552	21.7	11.5	
-75	RS CORR. SPAR WEB	1	44 CORN. ETCH AND POLISH (1.0 IN)	7050-T7651 AL ALLOY	0.63-11.25-552	15.4	8.9	
-77	FLAT CORR. SPAR WEB	1	44 CORN. ETCH AND POLISH (1.0 IN)	7050-T7651 AL ALLOY	0.40-11.5-271	12.4	7.8	

*LENGTH FACTOR FOR FORMING CORRUGATIONS IN -69,-71 AND -73 IS 1.32
*LENGTH FACTOR FOR FORMING CORRUGATIONS IN -75 IS 1.24

FASTENERS (BLIND)	FOR WEIGHT AND COST, ASSUME NAS171-100B-08 FOR UPR SURF ATTACH	MONEL		
	FITTINGS, BULKHEADS, BUSHINGS, SEALANT AND GASKETS			17.6
	SEE NOTES 1 AND 2	AF 66 AF 143		355.0
	ADDITIONAL MATERIAL REQUIRED TO ACCOMPLISH ROOT SPLICE			19.5
				35.5
			TOTALS	1261.4 555.3720

- THE FAYING SURFACES FORMED BY THE -79 UPPER SURFACE SKIN AT THE FRONT AND THE -77 FLAT REAR SPAR WEB ARE JOINED TO THE UPPER AND LOWER SPAR CAPS BY THE ADHESIVE BONDING. IN THIS PROCESS, APPLY AF 66 ADHESIVE (3M COMPANY) IN THE FAYING SURFACES OF THE PARTS BEFORE SPOTWELDING. (DESIGN AND PROCESS CONTINGENT UPON TEST.)
- APPLY AF 143 ADHESIVE (3M COMPANY) BETWEEN ALL LOWER SURFACE SKIN LAMINATES THE ADJACENT STEPPED LOWER FLANGE OF -7 FRONT SPAR, AND ADJACENT STEPPED FLANGES OF THE FOUR LOWER SPAR WEBS (-9 THRU -15).
- THE UPPER AND LOWER SPAR CAPS BY THE ADHESIVE BONDING. IN THIS PROCESS, APPLY AF 66 ADHESIVE (3M COMPANY) IN THE FAYING SURFACES OF THE PARTS BEFORE SPOTWELDING. (DESIGN AND PROCESS CONTINGENT UPON TEST.)

NOTES:

PRELIMINARY DESIGN DRAWING
WING BOX - LAMINATED LWR SKIN WITH STEPPED SPAR CAPS; PLATE UPPER SKIN; CORRUGATED SPAR WEBS; ALUMINUM FLAP CANTILEVER RIB (TYP)
GENERAL DYNAMICS CORPORATION
GENERAL DYNAMICS CORPORATION
General Aerospace Division
P.O. Box 1000
Grand Rapids, Michigan 49503
101/102

Figure 41 Wing Box Laminated Lower Skin With Stepped Spar Caps, Plate Upper Skin, Corrugated Spar Webs (Sheet 2)





DESIGN PART NO.	PART NAME	REMARKS	MATERIAL	STATION	WING STATION
-7	UPPER SKIN EXCLUSIVE OF ALL DOUBLERS	PROFILE, FORM & CHEM. ETCH APPROX. AND IN OF VARI-ABLE THICK. 50 IN. OF 120 IN. OF CONST. THICK.	6-4 T STA	128.51	
-9	LOWER SKIN EXCLUSIVE OF ALL DOUBLERS	PROFILE, FORM & CHEM. ETCH APPROX. AND IN OF VARI-ABLE THICK. 50 IN. OF 120 IN. OF CONST. THICK.	B-8-23 STA	128.04	
-11	FORMED ANGLES	PROFILE, FORM & CHEM. ETCH APPROX. AND IN OF VARI-ABLE THICK. 50 IN. OF 120 IN. OF CONST. THICK.	B-8-23 STA	128.04	
-13	UPPER SURFACE SPAR DOUBLER	PROFILE, FORM & CHEM. ETCH APPROX. AND IN OF VARI-ABLE THICK. 50 IN. OF 120 IN. OF CONST. THICK.	6-4 T STA	128.27	
-15	UPPER SURFACE SKIN DOUBLER	PROFILE, FORM & CHEM. ETCH APPROX. AND IN OF VARI-ABLE THICK. 50 IN. OF 120 IN. OF CONST. THICK.	6-4 T STA	43.25	
-17	LOWER SURFACE DOUBLER	PROFILE, FORM & CHEM. ETCH APPROX. AND IN OF VARI-ABLE THICK. 50 IN. OF 120 IN. OF CONST. THICK.	B-8-23 STA	39.99	
-19	SQUARE TUBE	PROFILE, FORM & CHEM. ETCH APPROX. AND IN OF VARI-ABLE THICK. 50 IN. OF 120 IN. OF CONST. THICK.	6-4 T STA	41.53	
-21	ROUND TUBE	PROFILE, FORM & CHEM. ETCH APPROX. AND IN OF VARI-ABLE THICK. 50 IN. OF 120 IN. OF CONST. THICK.	6-4 T STA	18.68	
-23	STIFFENER	PROFILE, FORM & CHEM. ETCH APPROX. AND IN OF VARI-ABLE THICK. 50 IN. OF 120 IN. OF CONST. THICK.	6-4 T STA	10.32	
-25	FRONT SPAR	PROFILE, FORM & CHEM. ETCH APPROX. AND IN OF VARI-ABLE THICK. 50 IN. OF 120 IN. OF CONST. THICK.	6-4 T STA	41.46	
-27	REAR SPAR	PROFILE, FORM & CHEM. ETCH APPROX. AND IN OF VARI-ABLE THICK. 50 IN. OF 120 IN. OF CONST. THICK.	6-4 T STA	42.73	
-29	CLIP	PROFILE, FORM & CHEM. ETCH APPROX. AND IN OF VARI-ABLE THICK. 50 IN. OF 120 IN. OF CONST. THICK.	6-4 T STA	23.42	
-31	FASTENERS	PROFILE, FORM & CHEM. ETCH APPROX. AND IN OF VARI-ABLE THICK. 50 IN. OF 120 IN. OF CONST. THICK.	6-4 T STA	34.43	
-33	PIVOTING Pylon	PROFILE, FORM & CHEM. ETCH APPROX. AND IN OF VARI-ABLE THICK. 50 IN. OF 120 IN. OF CONST. THICK.	6-4 T STA	19.81	
-35	FIXED Pylon	PROFILE, FORM & CHEM. ETCH APPROX. AND IN OF VARI-ABLE THICK. 50 IN. OF 120 IN. OF CONST. THICK.	6-4 T STA	51.07	
-37	UPPER SURFACE-6-4 T STA; LOWER SURFACE-B-8-23 T STA	PROFILE, FORM & CHEM. ETCH APPROX. AND IN OF VARI-ABLE THICK. 50 IN. OF 120 IN. OF CONST. THICK.	6-4 T STA	44.53	
-39	UPPER SURFACE-6-4 T STA; LOWER SURFACE-B-8-23 T STA	PROFILE, FORM & CHEM. ETCH APPROX. AND IN OF VARI-ABLE THICK. 50 IN. OF 120 IN. OF CONST. THICK.	6-4 T STA	5.57	
-41	UPPER SURFACE-6-4 T STA; LOWER SURFACE-B-8-23 T STA	PROFILE, FORM & CHEM. ETCH APPROX. AND IN OF VARI-ABLE THICK. 50 IN. OF 120 IN. OF CONST. THICK.	6-4 T STA	23.42	
-43	BLADEHEAD	PROFILE, FORM & CHEM. ETCH APPROX. AND IN OF VARI-ABLE THICK. 50 IN. OF 120 IN. OF CONST. THICK.	6-4 T STA	4.5	
TOTALS				109	122.120

NOTES:

- THE EXISTING FULL LEADING EDGE SLAT DRIVE SYSTEM (i.e. TRACK-POLLS-3) CAN BE PROTRUDING INTO THE WING BOX. IT IS NOT CONSIDERED A PROBLEM. IT IS THEREFORE ASSUMED THAT A POWER-HOUSE SYSTEM WILL BE EMPLOYED FOR THE SLAT DRIVE.
- ALTERNATE UPPER-SURFACE-SKIN DESIGN CONCEPT: APPLY CHEM. ETCH-AS PROCESS TO INTEGRALLY FORM THE -15, -37, -39, & -41 DOUBLERS WITH THE -7 SKIN.

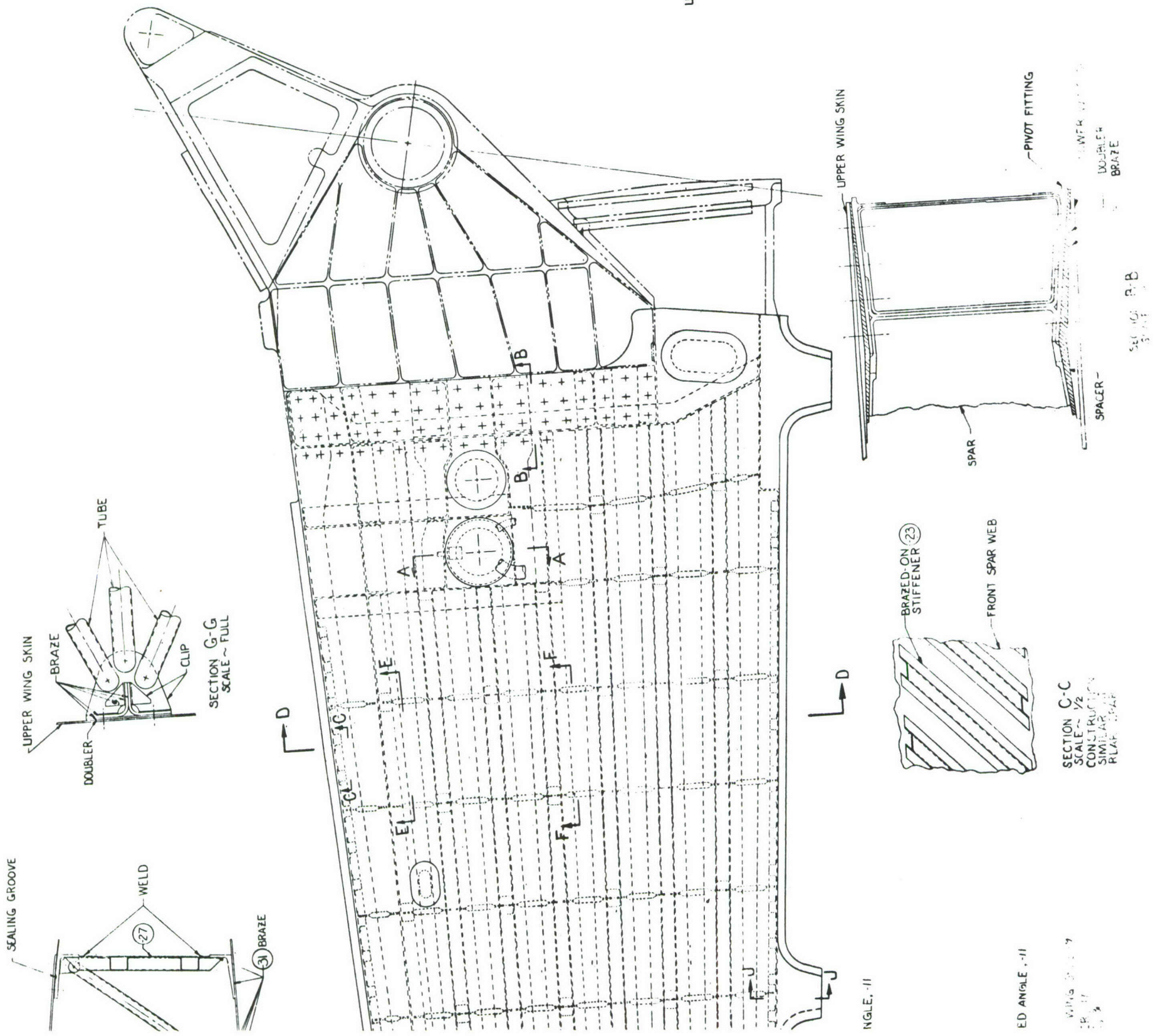


Figure 43 Wing Box ~ Brazed Titanium Space - Truss Structure (Sheet 2)

PRELIMINARY DESIGN DRAWING

WING BOX ~ BRAZED TITANIUM SPACE

GENERAL NOTES

1. ALL DIMENSIONS ARE IN INCHES UNLESS OTHERWISE SPECIFIED.

2. ALL DIMENSIONS ARE TO CENTER UNLESS OTHERWISE SPECIFIED.

3. ALL DIMENSIONS ARE TO CENTER UNLESS OTHERWISE SPECIFIED.

4. ALL DIMENSIONS ARE TO CENTER UNLESS OTHERWISE SPECIFIED.

5. ALL DIMENSIONS ARE TO CENTER UNLESS OTHERWISE SPECIFIED.

6. ALL DIMENSIONS ARE TO CENTER UNLESS OTHERWISE SPECIFIED.

7. ALL DIMENSIONS ARE TO CENTER UNLESS OTHERWISE SPECIFIED.

8. ALL DIMENSIONS ARE TO CENTER UNLESS OTHERWISE SPECIFIED.

9. ALL DIMENSIONS ARE TO CENTER UNLESS OTHERWISE SPECIFIED.

10. ALL DIMENSIONS ARE TO CENTER UNLESS OTHERWISE SPECIFIED.

Table XVI

FINAL ITERATIVE PHASE WING BOX EVALUATION SUMMARY

CONFIG NO.	DESCRIPTION	STRUCT. EFFICIENCY		TECHNOLOGY ADVANCEMENT				STRUCT INTEGRITY-RELIABILITY				ABILITIES					TOTAL SCORE	RANK
		COST (.15)	WEIGHT (.15)	CONCEPT TECH (.09)	MFG TECH (.09)	MATL's TECH (.09)	FRACT TECH (.03)	STATIC (.03)	FATIGUE QUALITY (.09)	SAFE CRACK (.09)	FAIL SAFE (.09)	INSPECT. (.05)	MFG (.02)	MAIN-TAIN (.01)	REPAIR (.01)	PREDICT (.01)		
610RW000	F-111F BASELINE (MODIFIED)	64,283 .126	1665.0 .092	.009	0	0	.012	.030	.041	.041	0	.050	.020	.010	.010	.004	.445	5
610RW002	MULTI-WET CELL, BRAZED TITANIUM	84,163 .0967	1019.6 .150	.09	.09	.09	.024	.017	.087	.075	.025	.0344	.0122	.0071	.0056	.006	.810	2
610RW003	LAM. LWR SKIN W/STEP SPAR CAPS; PLATE UPR, CORR. SPAR WEBS, AL.	55,377 .147	1261.4 .121	.086	.0252	.0675	.024	.017	.088	.090	.090	.0375	.0160	.0097	.009	.006	.834	1
610RW004	ADHESIVE BONDED AL. HONEYCOMB PANELS	54,211 .150	1351.15 .113	.081	.0182	.0675	.030	.017	.088	.090	.049	.0398	.0145	.0092	.010	.002	.779	3
610RW006	SPACE TRUSS, BRAZED TITANIUM	122,120 .0666	1109.0 .138	.086	.0817	.0675	.024	.017	.085	.075	.041	.0355	.0128	.0073	.007	.008	.752	4

4.1.6.1 610RW002 Multi-Wet Cell Construction

This titanium configuration is the integration of several advanced design features, namely:

- (a) No fastener penetrations through the lower skin bending material resulting in very low stress concentration (K_T) permitting sizing to an operating stress of 92,500 psi.
- (b) Laminated and planked lower skin with laminates joined by low temp brazing for a multi-load path, fail safe tension member with reduced crack growth rate characteristics.
- (c) Upper and lower skins of high strength titanium alloys 8-8-2-3 (175,000 psi FTU) 6AL-4V-STA (160,000 psi FTU) joined by low temperature brazing alloy with braze temperature that corresponds to the aging temperature of the titanium alloy. Configuring with high strength alloys avoids paying a weight penalty when sizing to meet the static strength requirement of the wing box structure.
- (d) Multi-Wet Cell wing beam shear material. Each cell wall is perforated for fuel flow and corrugated for shear stability. In addition to serving as the wing beam shear webs, the cells react internal fuel pressure loads and stabilize upper and lower skins to a compression buckling stress allowable in the vicinity of compression yield.

The integration of the above advanced design features resulted in the lowest weight design of all design concepts considered. Although more expensive per pound to fabricate than aluminum designs, the "Multi-Wet Cell" design is a promising concept for advanced, high performance fighter aircraft where airframe weight is critical and skin operating temperatures exceed the capability of aluminum.

4.1.6.2 610RW003

The 610R003 wing box design integrates several advanced design features that result in an optimum, balanced configuration in aluminum alloy. It is low cost and low weight. The structural concepts that enhance this design are:

- (a) The elimination of fasteners through the lower surface bending material with resulting low KT. This permits sizing the lower skin to an operating stress level of 37,100 psi instead of 17,000 psi as in conventional aluminum structure with mechanical fastener penetrations through the lower skin.
- (b) Laminated and planked lower skin for improved crack growth characteristics and multiple load paths.
- (c) Corrugated wide spar concept for stabilizing upper skin to a compression buckling allowable stress in the vicinity of compression yield.
- (d) The entire assy is of 7050 aluminum alloy with improved tensile strength and fracture toughness properties.

4.1.6.3 610RW004

The 610RW004 is the most economical of the wing box designs studied. Cost savings with respect to the "Baseline" wing box is 15.7%. The savings are primarily in the area of: (1) material and machine time saved in using built up sheet metal spars vs. machined spars, (2) utilizing more economical joining systems and, (3) overall reduction in weight resulted in a reduction in material cost.

Although considerable attention was directed toward cost savings, a significant decrease in weight with respect to the baseline was achieved. Weight savings was 18.9%. The weight savings were achieved by the following design features:

- (a) Elimination of fasteners through the lower skin.
- (b) Sandwich panel upper panel with compressive allowables in the vicinity of compression yield.
- (c) Improved allowables of 7050 aluminum alloy.

4.1.6.4 610RW006

The space truss concept is the 2nd lightest design but most expensive of all designs considered. It has certain advantages over the 610R002 Multi-Wet Cell configuration as follows:

- (a) The upper panel is removable for complete accessibility to the inside of the wing box.
- (b) The space truss design can be easily coated with a corrosion protective coating such as polyurathane.
- (c) It readily accommodates equipment routing.

The advanced concepts integrated into the design that provide structural advantages are as follows:

- (a) The lower skin is configured of Ti planks and laminates joined by low temperature brazing alloy for crack arrest, reduced crack growth rate and multiple load paths.
- (b) The lower panel skin and spar caps are configured so as to eliminate all fastener penetrations through the lower panel bending material.
- (c) The closely spaced truss configured spars and ribs provide good local stability for working skins to high compressive and shear stresses. The sub-structure also efficiently reacts internal pressure loads.
- (d) High strength 8-8-2-3 and 6AL-4V-STA titanium alloys are employed to contribute to a low weight design.

SECTION V

STRESS ANALYSIS

Design Loads, Analysis Techniques and the Structural Integrity and Reliability Evaluation Technique are discussed in this section with reference to data and sample calculations in Appendix V.

5.1 DESIGN LOADS

Design loads have been obtained from FZM-6100, "Baseline Document for Advanced Air Superiority Fighter Wing Structures," and all are available for reference in Appendix VI.

Typical external loadings were selected for maximum positive bending (condition F400A), maximum negative bending (condition F401A), maximum torsion (condition F101A) and for torsion associated with negative bending (condition F702A).

Fuel pressure loads used for design represent the effects of combinations of vertical and lateral inertia, maximum roll rates and vent pressure.

The external store pylon loadings used for design represent the test-demonstrated hardpoint strength, for the fixed pylons, and the most severe loadings applicable to the F-111 wing for the pivoting pylon hardpoints.

Assumptions made for application of loadings.

- o The four maneuver loadings were considered to act equally on all the designs without aeroelastic or inertia difference effects from the baseline loads.

- o Pressure loadings were assumed to act independently of the four maneuver design conditions because the maneuvers do not involve high roll rates, and pressure loadings are due principally to high roll rates.

- o External store pylon loadings were assumed to design only in the vicinity of the load introduction.

Description of methods for obtaining internal loadings:

- o The baseline wing was simulated using Procedure TR4 (a variation of Convair-developed Procedure TL7). Material quantities and properties were simulated using constant stress bars, triangles and quadrilaterals. The program computes nodal displacements, element stresses and unit loadings and node point forces for both linear and non-linear stress/strain situations. Samples of printed and graphic output are shown in Figures 35 to 39 of Appendix V.

Load cases 1, 2, 3 and 4 represent conditions F101A, F400A, F401A and F702A respectively.

The results at CSS 140 and 340 were used to prepare Figure 40 and Table XX of Appendix V. These loads were used to analyze cross-section drawings and analytical assemblies at these two stations.

The finite element program results were also used to prepare tables of spanwise loading for the maximum bending condition (F400A) by multiplying stresses at spanwise locations by the appropriate areas. These distributions are shown in Table XXI and XXII of Appendix V.

- o Pivoting pylon loadings were resolved internally into horizontal couples acting in the local planes of the upper and lower skins and vertical forces acting on wing vertical shear material.

- o Fixed pylon pitching moments were resolved into a vertical couple of forces acting at two forward attachment bolts and at a hook fitting at the Rear Spar. Fixed pylon rolling moment was resolved into a horizontal couple of forces acting in the local planes of the upper and lower skins. Vertical loads were applied directly to wing vertical shear material.

- o Flap loadings were resolved into a horizontal couple of forces acting on 11.5 inches of upper and lower skin at the Rear Spar and a vertical force applied to the

Rear Spar.

o Math models were made to aid in sizing the lower skin at pylon cutouts. Lower skin attachment of flap tracks was made outside the wing bending stress zone using a model. Samples can be seen in Appendix V, section V.6.

5.2 ANALYSIS TECHNIQUES

The stress analysis techniques used during this program have evolved into a very useful Method for preliminary design of wings. The method is described in the following paragraphs (5.2.1 thru 5.2.4) and is illustrated with sample calculations in Appendix V.

5.2.1 Concept Screening

The element concepts contained in the series 610-XXX drawings of Appendix I were screened for structural efficiency using the screening procedure described and illustrated fully in Appendix V. Loadings and wing cross-section geometry at Center Spar Station (CSS) 140 were used for this purpose, assuming a constant cross section. The programmed computations resulted in material being placed in the most advantageous way to meet the load-carrying and stability requirements. The program also computed the weight of structural material.

Some manual calculations were required to supplement the automatic procedure, but the bulk of the screening was performed automatically.

Element Concept 610-132 will be traced from screening through the finished Preliminary Design Drawing to illustrate the method.

5.2.2 Cross-Section Sizing and Study

The sized element concepts were incorporated into the series 610R Cross Section Drawings shown in Appendix II.

Element Concept 610-132 was incorporated into 610R-013 and 610R-029.

The boltless, fail-safe laminated construction of the lower surface was expected to score high in structural integrity. The cost of the upper surface was reviewed for possible cost reduction by considering a sandwich skin and a monolithic plate skin in cross sections 610R-013 and 610R-029 respectively.

Wide, corrugated, spars were developed to provide increased buckling resistance of the monolithic plate and also to provide reduction in the bay sizes for better fuel pressure resistance.

The Cross Section Drawings were rated and ranked as described in Section 5.3.

Cross Section Drawings 610R-013B and 610R-029 ranked fourth and first, respectively.

5.2.3 Analytical Assembly Technique

The analytical assembly technique is a low-cost procedure for obtaining detailed definition of competing concepts and for making orderly and uniform concept comparisons. This is accomplished by expanding cross-section drawings at two wing stations into 48-inch long boxes identified as "analytical assemblies". The two wing stations were carefully selected to represent the extremes in the various structural requirements. Wing station 140 is highly loaded and is typical of structure designed by wing bending loads. Wing station 340 is typical of structure with low wing bending loads, high fuel pressure loads and a considerable amount of minimum gage material.

Detail structural analyses have been performed at each analytical assembly location taking into account fuel sealing requirements, manufacturing constraints, minimum gage limitations and differences in effective section depths.

Structural stability analyses of upper surface panels reflect non-linear material stress-strain behavior. Lower surface allowable tension stress levels have been selected consistent with fatigue and crack growth allowables.

The Analytical Assembly Technique enables estimating of finished wing structural weights based on the accurate structural sizing at two (or more) sections. Appendix V contains an example of the use of this technique.

Our example element concept (610-132) appears in Analytical Assemblies 610RA-003 and 610RA006 (Appendix III) by virtue of ranking fifth and first, respectively, in the evaluation of cross section Drawings (610R-013B and 610R-029, Appendix II).

Sample calculations are shown in Appendix V.

All the Analytical Assembly drawings were ranked for Structural Integrity by the method described in Section 5.3. Overall ranking placed 610RA006 first.

5.2.4 Preliminary Design Analysis Technique

The technique for analysis of complete wing Preliminary Designs depends largely on data obtained in Analytical Assembly analyses. It is an expansion of these data since accurate sizing was done there at representative sections.

Sizing was done along the entire span of the wing in proportion to loadings and checking for local stability while keeping the structural arrangement of the Analytical Assemblies.

Skins, caps and webs were checked and sized individually to permit spanwise description of material quantities and thereby simplify weight and cost calculations.

Pylon hardpoints, flap and slat track attachments were analyzed for structural integrity but their weights were considered a part of 355 lbs of recurring baseline weight. A part of this weight could be decreased due to advancement in material properties and in design technology.

The 355-lb recurring weight was maintained in order to give the best visibility to the improvements in the structural wing box proper.

The example element concept (610-132) has evolved into Preliminary Design Drawing 610RW003 by virtue of ranking first in the Analytical Assembly evaluation. It was mentioned earlier that elimination of fasteners thru the lower surface was necessary to realize the maximum mechanical properties from advancements in materials. This is evident when one traces concepts through the analysis and evaluation procedure.

A summary of analysis data has been prepared for each of the nine Preliminary Designs and is shown in Tables XVII thru XXVI. Sample calculations are shown in Appendix V. The weight distribution for each design is tabulated in Table XXVII.

All the preliminary designs achieved weight savings and therefore also reduced the torsion and bending stiffness. The effect of stiffness reduction is considered using the data and procedure given for this purpose in Appendix V. A comparison between the baseline stiffness and the stiffness of each concept is shown in Table XXVIII.

It can be seen there that stiffness reductions up to 50% do not require further consideration for the clean wing. Also, stiffness reductions beyond 21% may involve reduction of present operating limits when carrying certain stores.

The stiffness reduction in the case of 610RW003 is slightly less than 21% so no further checks need be made at this time.

The stiffness reduction in the case of 610RW006 is approximately 40%. This case will be used to demonstrate the use of the data in Appendix V as follows: from Figure 45 it is seen that with 20% stiffness margin available (for store group 7-9 in Table XXVII), the available flutter speed margin is 34%. Entering Figure 46 at 34% speed margin and 40% stiffness reduction it is seen that a 13.5% reduction in operating envelope would be required. The current operating envelope, from Table XXVIII for store group 7-9 (B-43), is the clean airplane envelope.

Table XVII STRESS DATA SUMMARY SHEET FOR WING BOX DESIGN CONCEPT NO. 610RW000

REPRESENTATIVE LOWER SURFACE DATA INBOARD OF CSS 290 :

COMPONENT	MATERIAL	STRUCTURAL DESCRIPTION	DESIGN CONDITIONS	APPLIED STRESSES		ALLOWABLE OPERATING STRESSES			CRITICAL SIZING CRITERIA
				OPERATING	ULTIMATE	FATIGUE	CRACK GROWTH	STATIC	
FRONT AUX SPAR LWR CAP	2024-T851 PLATE $F_{70} = 66 \text{ KSI}$	MACHINED SHEAR RESISTANT, INTER- GRANULAR STIFFENED	POSITIVE AND NEGATIVE BENDING	14.0 KSI	26.4 KSI	27.7 KSI	14.4 KSI	35.0 KSI	SURFACE FLAW GROWTH, $260 =$ $.492 A/Q =$
LOWER SKIN	2024-T851 PLATE $F_{70} = 66 \text{ KSI}$	ETCHED, BOLTED PLATE 8000 HR NON-INSP. SLOW CRACK GROWTH	POSITIVE AND NEGATIVE BENDING	19.6 KSI	36.9 KSI	27.7 KSI	19.6 KSI	35.0 KSI	8000HR. NON INSP. SCG.

REPRESENTATIVE UPPER SURFACE DATA @ CSS 140 :

COMPONENT	MATERIAL	STRUCTURAL DESCRIPTION	DESIGN CONDITIONS	APPLIED STRESSES		ALLOWABLE ULTIMATE STRESS	CRITICAL SIZING CRITERIA
				OPERATING	ULTIMATE		
UPPER SKIN	2024-T851	ETCHED MONOLITHIC PLATE	POSITIVE BENDING	-28.9 KSI	-54.50 KSI	-54.50 KSI	PLATE BUCKLING

REPRESENTATIVE DATA OUTBOARD OF CSS 290 :

COMPONENT	MATERIAL	STRUCTURAL DESCRIPTION	DESIGN CONDITIONS	APPLIED STRESSES		ALLOWABLE ULTIMATE STRESS	CRITICAL SIZING CRITERIA
				OPERATING	ULTIMATE		
UPPER SKIN	2024-T851	ETCHED PLATE	FUEL PRESSURE	38.6 KSI	57.9 KSI	66.0 KSI	BENDING AND MEMBRANE TENSION
LOWER SKIN	2024-T851	ETCHED PLATE	FUEL PRESSURE	38.6 KSI	57.9 KSI	66.0 KSI	BENDING AND MEMBRANE TENSION

Table XVIII STRESS DATA SUMMARY SHEET FOR WING BOX DESIGN CONCEPT NO. 610RW001

REPRESENTATIVE LOWER SURFACE DATA INBOARD OF CSS 250 _____:

COMPONENT	MATERIAL	STRUCTURAL DESCRIPTION	DESIGN CONDITIONS	APPLIED STRESSES		ALLOWABLE OPERATING STRESSES			CRITICAL SIZING CRITERIA
				OPERATING	ULTIMATE	FATIGUE	CRACK GROWTH	STATIC	
LOWER SKIN PANELS	ALUM. SHT. 7050-T76 $F_t = 70000$	LAMINATED PLATE $K_t = 1.0$ $2 C_o = .06"$ FAIL-SAFE	POSITIVE & NEGATIVE BENDING	370 KSI	700 KSI	403 KSI	395 KSI	370 KSI	STATIC LOADS

REPRESENTATIVE UPPER SURFACE DATA @ CSS 140 _____:

COMPONENT	MATERIAL	STRUCTURAL DESCRIPTION	DESIGN CONDITIONS	APPLIED STRESSES		ALLOWABLE ULTIMATE STRESS	CRITICAL SIZING CRITERIA
UPPER SKIN PANEL	ALUM. SHT. 7050-T76	HONEYCOMB SANDWICH	POSITIVE BENDING	-350 KSI	-660 KSI	-660 KSI	PLATE BUCKLING

$F_{ty} = 62500$

REPRESENTATIVE DATA OUTBOARD OF CSS 292 _____:

COMPONENT	MATERIAL	STRUCTURAL DESCRIPTION	DESIGN CONDITIONS	APPLIED STRESSES		ALLOWABLE ULTIMATE STRESS	CRITICAL SIZING CRITERIA
UPPER SKIN PANEL	ALUM. 7050-T76 $F_{cy} = 62500$	HONEYCOMB PANELS $t_f = .016$	FUEL PRESSURE	-260 KSI	-390 KSI	625 KSI	MINIMUM SKIN GAGE
LOWER SKIN PANEL	ALUM 7050-T76 $F_{cy} = 62500$	THIN PLATE	FUEL PRESSURE & NEGATIVE	620 KSI		625 KSI	DEFORMATION LIMIT PRESSURE

Table XIX STRESS DATA SUMMARY SHEET FOR WING BOX DESIGN CONCEPT NO. 610RW002

REPRESENTATIVE LOWER SURFACE DATA INBOARD OF CSS 300 :

COMPONENT	MATERIAL	STRUCTURAL DESCRIPTION	DESIGN CONDITIONS	APPLIED STRESSES		ALLOWABLE OPERATING STRESSES			CRITICAL SIZING CRITERIA
				OPERATING	ULTIMATE	FATIGUE	CRACK GROWTH	STATIC	
LOWER SKIN	8-8-2-3(STA) SHEET $F_{TU}=175\text{KSI}$	PLANKED, BRAZED LAMINATION, $K_T=1$ $2C_0 = .06$	POSITIVE BENDING	92.58 KSI	175.0 KSI	145.0 KSI	102.5 KSI	92.6 KSI	STATIC STRENGTH
		SUPPORTED BY CELLULAR SHEAR MATERIAL							

REPRESENTATIVE UPPER SURFACE DATA @ CSS 180 :

COMPONENT	MATERIAL	STRUCTURAL DESCRIPTION	DESIGN CONDITIONS	APPLIED STRESSES		ALLOWABLE ULTIMATE STRESS	CRITICAL SIZING CRITERIA
UPPER SKIN, MID-CORD	6-4 (STA) PLATE	MONOLITHIC, ETCHED PLATE	POSITIVE BENDING	81.8 KSI	154.1 KSI	155.0 KSI	INTRA CELL DIMPLING

REPRESENTATIVE DATA OUTBOARD OF CSS 300 :

COMPONENT	MATERIAL	STRUCTURAL DESCRIPTION	DESIGN CONDITIONS	APPLIED STRESSES		ALLOWABLE ULTIMATE STRESS	CRITICAL SIZING CRITERIA
UPPER SKIN	6-4 (STA) PLATE	ETCHED PLATE, MULTI-CELL	FUEL PRESSURE $P=83\text{PSI (ULT)}$	46.3 KSI	69.5 KSI	154.0 KSI	BENDING STRESS LIMITED TO FCY
LOWER SKIN		LAMINATED PLATE, MULTI-CELL	FUEL PRESSURE $P=83\text{PSI (ULT)}$	46.3 KSI	69.5 KSI	164.0 KSI	BENDING STRESS LIMITED TO FCY

Table XX STRESS DATA SUMMARY SHEET FOR WING BOX DESIGN CONCEPT NO. 610RW003

REPRESENTATIVE LOWER SURFACE DATA INBOARD OF CSS 320 _____ :

COMPONENT	MATERIAL	STRUCTURAL DESCRIPTION	DESIGN CONDITIONS	APPLIED STRESSES		ALLOWABLE OPERATING STRESSES			CRITICAL SIZING CRITERIA
				OPERATING	ULTIMATE	FATIGUE	CRACK GROWTH	STATIC	
FRONT AUX.SPAC	7050-T73	STEPPED BONDED	POSITIVE &	37.15	70.00	37.15	45.00	37.15	FATIGUE AND
LWR CAP	EXTRUSION	CAP, $K_T = 2.0$	NEGATIVE	KSI	KSI	KSI	KSI	KSI	STATIC STRENGTH
	$F_{TU}=70\text{KSI}$	2 Co=.148	BENDING						
LOWER SKIN	7050-T76	LAMINATED BONDED	POSITIVE &	37.15	70.00	40.40	39.50	37.15	STATIC
	SHEET	SHEET, $K_T=1.0$	NEGATIVE	KSI	KSI	KSI	KSI	KSI	STRENGTH
		$2G=.06$							

REPRESENTATIVE UPPER SURFACE DATA @ CSS 140 _____ :

COMPONENT	MATERIAL	STRUCTURAL DESCRIPTION	DESIGN CONDITIONS	APPLIED STRESSES		ALLOWABLE ULTIMATE STRESS	CRITICAL SIZING CRITERIA
				OPERATING	ULTIMATE		
UPPER SKIN, BETWEEN CS & FAS	7050-T76	ETCH SCULPTURED	POSITIVE	-31.31	-59.00	-59.00	PLATE BUCKLING
	PLATE	MONOLITHIC PLATE	BENDING	KSI	KSI	KSI	

REPRESENTATIVE DATA OUTBOARD OF CSS 320 _____ :

COMPONENT	MATERIAL	STRUCTURAL DESCRIPTION	DESIGN CONDITIONS	APPLIED STRESSES		ALLOWABLE ULTIMATE STRESS	CRITICAL SIZING CRITERIA
				OPERATING	ULTIMATE		
UPPER SKIN PANEL	7050-T76	ETCH SCULPTURED	FUEL PRESSURE	46.67	70.00	70.00	PLATE BENDING
	PLATE	MONOLITHIC PLATE	P=83PSI(ULT)	KSI	KSI	KSI	
LOWER SKIN PANEL	7050-T76	LAMINATED BONDED SHEET	FUEL PRESSURE	22.00	32.50	70.00	PLATE BENDING AND MINIMUM GAGES
	SHEET		P=83PSI(ULT)	KSI	KSI	KSI	

Table XXI STRESS DATA SUMMARY SHEET FOR WING BOX DESIGN CONCEPT NO. 610RW004

REPRESENTATIVE LOWER SURFACE DATA INBOARD OF CSS 268 :

COMPONENT	MATERIAL	STRUCTURAL DESCRIPTION	DESIGN CONDITIONS	APPLIED STRESSES		ALLOWABLE OPERATING STRESSES			CRITICAL SIZING CRITERIA
				OPERATING	ULTIMATE	FATIGUE	CRACK GROWTH	STATIC	
SKIN/SPAR JOINT	ALUM. EXTR. 7050-T736511 $F_t = 70,000$	BOLTED, SCALLOPED SHEAR TABS $K_T = 2.5$ 2Co=.02"	POSITIVE & NEGATIVE BENDING	27.5 KSI	52.0 KSI	30.0 KSI	30.2 KSI	27.5 KSI	STATIC STRENGTH
LOWER SKIN	ALUM. SHT. 7050-T76 $F_t = 70,000$	SANDWICH PANEL FACINGS $K_T = 1.0$ 2Co=.06"	POSITIVE & NEGATIVE BENDING	37.0 KSI	70.0 KSI	37.3 KSI	39.7 KSI	37.0 KSI	STATIC STRENGTH

REPRESENTATIVE UPPER SURFACE DATA @ CSS 193 :

COMPONENT	MATERIAL	STRUCTURAL DESCRIPTION	DESIGN CONDITIONS	APPLIED STRESSES		ALLOWABLE ULTIMATE STRESS	CRITICAL SIZING CRITERIA
CENTER SKIN PANEL	ALUM. SHT 7050-T76 $F_{cy} = 62,500$	HONEYCOMB PANELS	POSITIVE BENDING	-31.6 KSI	-62.0 KSI	-65.0 KSI	PLATE BUCKLING

REPRESENTATIVE DATA OUTBOARD OF CSS 314 :

COMPONENT	MATERIAL	STRUCTURAL DESCRIPTION	DESIGN CONDITIONS	APPLIED STRESSES		ALLOWABLE ULTIMATE STRESS	CRITICAL SIZING CRITERIA
UPPER SKIN PANEL	ALUM. SHT. 7050-T76	HONEYCOMB PANEL $t_f = .016"$	FUEL PRESSURE	26.0 KSI	39.0 KSI	62.5 KSI	MINIMUM SKIN GAGE
LOWER SKIN PANEL	ALUM. SHT. 7050-T76	HONEYCOMB PANEL $t_f = .016"$	FUEL PRESSURE	26.0 KSI	39.0 KSI	62.5 KSI	MINIMUM SKIN GAGE

Table XXII STRESS DATA SUMMARY SHEET FOR WING BOX DESIGN CONCEPT NO. 610RW005

REPRESENTATIVE LOWER SURFACE DATA INBOARD OF CSS 268 :

COMPONENT	MATERIAL	STRUCTURAL DESCRIPTION	DESIGN CONDITIONS	APPLIED STRESSES		ALLOWABLE OPERATING STRESSES			CRITICAL SIZING CRITERIA
				OPERATING	ULTIMATE	FATIGUE	CRACK GROWTH	STATIC	
SKIN/SPAR JOINT	TITANIUM 8-8-2-3 $F_t = 175000$	WELD BOND $K_T = 2.5$ $2 C_G = .06$	POSITIVE BENDING	715 KSI	1350 KSI	750 KSI	1025 KSI	715 KSI	STATIC STRENGTH
OUTER SKIN	TITANIUM 8-8-2-3 $F_t = 175000$	ADHESIVE BONDED HONEYCOMB SANDWICH $K_t = 1.0$ $2 C_G = .06$	POSITIVE BENDING	925 KSI	1750 KSI	1420 KSI	1025 KSI	925 KSI	STATIC STRENGTH

FAIL SAFE

REPRESENTATIVE UPPER SURFACE DATA @ CSS 193 :

COMPONENT	MATERIAL	STRUCTURAL DESCRIPTION	DESIGN CONDITIONS	APPLIED STRESSES		ALLOWABLE ULTIMATE STRESS	CRITICAL SIZING CRITERIA
UPPER SKIN PANEL	TITANIUM 6A1-4V STA $F_y = 154000$	HONEYCOMB SANDWICH	POSITIVE BENDING	-750 KSI	-1420 KSI	-1420 KSI	PLATE BUCKLING

REPRESENTATIVE DATA OUTBOARD OF CSS 292 :

COMPONENT	MATERIAL	STRUCTURAL DESCRIPTION	DESIGN CONDITIONS	APPLIED STRESSES		ALLOWABLE ULTIMATE STRESS	CRITICAL SIZING CRITERIA
UPPER SKIN PANEL	TITANIUM 6A1-4V STA	HONEYCOMB SANDWICH	FUEL PRESSURE	380 KSI	570 KSI	1540 KSI	MINIMUM GAGE
LOWER SKIN PANEL	TITANIUM 8-8-2-3	HONEYCOMB SANDWICH	FUEL PRESSURE	255 KSI	380 KSI	1620 KSI	MINIMUM GAGE

Table XXIII STRESS DATA SUMMARY SHEET FOR WING BOX DESIGN CONCEPT NO. 610RW006

REPRESENTATIVE LOWER SURFACE DATA INBOARD OF CSS 250 :

COMPONENT	MATERIAL	STRUCTURAL DESCRIPTION	DESIGN CONDITIONS	APPLIED STRESSES		ALLOWABLE OPERATING STRESSES			CRITICAL SIZING CRITERIA
				OPERATING	ULTIMATE	FATIGUE	CRACK GROWTH	STATIC	
LOWER SKIN	8-8-2-3 (Sta) SHEET $F_{TU}=175\text{KSI}$	PLANKED, BRAZED SHEET, $K_T = 1$ $2 C_o = .06$	POSITIVE BENDING	92.58 KSI	175.00 KSI	145.00 KSI	102.50 KSI	92.58 KSI	STATIC STRENGTH
DIAGONAL TUBE SPAR MEMBER	6-4 STA $F_{CY}=154\text{KSI}$	FORMED WELDED SHEET	SPAR SHEAR DUE TO POSITIVE BENDING	64.22 KSI	+121.00 KSI	87.00 KSI	65.50 KSI	125.00 KSI	BUCKLING

REPRESENTATIVE UPPER SURFACE DATA @ CSS 140 :

COMPONENT	MATERIAL	STRUCTURAL DESCRIPTION	DESIGN CONDITIONS	APPLIED STRESSES		ALLOWABLE ULTIMATE STRESS	CRITICAL SIZING CRITERIA
				OPERATING	ULTIMATE		
UPPER SKIN	6-4 (STA) SHEET	ETCHED WITH BRAZED DOUBLERS	POSITIVE BENDING	79.61 KSI	150.00 KSI	150 KSI	SKIN BUCKLING BETWEEN DOUBLERS

REPRESENTATIVE DATA OUTBOARD OF CSS 250 :

COMPONENT	MATERIAL	STRUCTURAL DESCRIPTION	DESIGN CONDITIONS	APPLIED STRESSES		ALLOWABLE ULTIMATE STRESS	CRITICAL SIZING CRITERIA
				OPERATING	ULTIMATE		
LOWER SKIN	8-8-2-3 (STA) SHEET	PLANKED, BRAZED SHEET	FUEL PRESSURE	78.0 KSI	117.00 KSI	160.00 KSI	BENDING STRESS LIMITED TO F_{TY}
UPPER SKIN	6-4 (STA)	ETCHED WITH BRAZED DOUBLERS	FUEL PRESSURE	78.0 KSI	117.00 KSI	162.50 KSI	BENDING STRESS LIMITED TO F_{CY}

Table XXIV STRESS DATA SUMMARY SHEET FOR WING BOX DESIGN CONCEPT NO. 610RW007

REPRESENTATIVE LOWER SURFACE DATA INBOARD OF CSS 250 _____:

COMPONENT	MATERIAL	STRUCTURAL DESCRIPTION	DESIGN CONDITIONS	APPLIED STRESSES		ALLOWABLE OPERATING STRESSES			CRITICAL SIZING CRITERIA
				OPERATING	ULTIMATE	FATIGUE	CRACK GROWTH	STATIC	
LOWER SKIN	ALUM SHT. 7050-T76 $F_{tu} = 70000$	LAMINATED PLATE $K_T = 1.0 \quad 2 \quad C = .06$ FAIL SAFE	POSITIVE & NEGATIVE BENDING	37.0 KSI	70.0 KSI	40.0 KSI	39.0 KSI	37.0 KSI	STATIC LOAD

REPRESENTATIVE UPPER SURFACE DATA @ CSS 140 _____:

COMPONENT	MATERIAL	STRUCTURAL DESCRIPTION	DESIGN CONDITIONS	APPLIED STRESSES		ALLOWABLE ULTIMATE STRESS	CRITICAL SIZING CRITERIA
UPPER SKIN PANELS	ALUM SHT 7050-T76 $F_{cy} = 62500$	HAT-STIFFENED SKINS	POSITIVE BENDING	-32.4 KSI	-61.3 KSI	61.3 KSI	COLUMN BUCKLING

REPRESENTATIVE DATA OUTBOARD OF CSS 250 _____:

COMPONENT	MATERIAL	STRUCTURAL DESCRIPTION	DESIGN CONDITIONS	APPLIED STRESSES		ALLOWABLE ULTIMATE STRESS	CRITICAL SIZING CRITERIA
UPPER SKIN PANELS	7050-T76 ALUM SHT.	HAT STIFFENED SKIN	POSITIVE BENDING	-9.2 KSI	-17.4 KSI	20.7 KSI	SKIN CRIPPLING
LOWER SKIN PANELS	7050-T76 ALUM. SHT.	BONDED SHEETS	FUEL PRESSURE & REVERSE BENDING		62.0 KSI	62.5 KSI	DEFORMATION @ LIMIT PRESSURE

Table XXV STRESS DATA SUMMARY SHEET FOR WING BOX DESIGN CONCEPT NO. 610RW008

REPRESENTATIVE LOWER SURFACE DATA INBOARD OF CSS 250 _____:

COMPONENT	MATERIAL	STRUCTURAL DESCRIPTION	DESIGN CONDITIONS	APPLIED STRESSES		ALLOWABLE OPERATING STRESSES			CRITICAL SIZING CRITERIA
				OPERATING	ULTIMATE	FATIGUE	CRACK GROWTH	STATIC	
LOWER SKIN	ALUM SHT. 7050-T76 $F_{tu} = 70000$	LAMINATED PLATE $K_T = 1.0$ $2 C_o = .06"$	POSITIVE & NEGATIVE BENDING	37.0 KSI	70.0 KSI	40.3 KSI	39.7 KSI	37.0 KSI	STATIC STRENGTH
	PSI	FAIL SAFE							

REPRESENTATIVE UPPER SURFACE DATA @ CSS 140 _____:

COMPONENT	MATERIAL	STRUCTURAL DESCRIPTION	DESIGN CONDITIONS	APPLIED STRESSES		ALLOWABLE ULTIMATE STRESS	CRITICAL SIZING CRITERIA
UPPER SKIN PANEL	ALUM SHT. 7050-T76 $F_{ey} = 62500$	HAT-STIFFENED SKINS	POSITIVE BENDING	-32.4 KSI	-61.3 KSI	61.3 KSI	COLUMN BUCKLING

REPRESENTATIVE DATA OUTBOARD OF CSS 268 _____:

COMPONENT	MATERIAL	STRUCTURAL DESCRIPTION	DESIGN CONDITIONS	APPLIED STRESSES		ALLOWABLE ULTIMATE STRESS	CRITICAL SIZING CRITERIA
UPPER SKIN	ALUM.SHT. 7050-T76	SHEET LAMINATE	FUEL PRESSURE & POSITIVE BENDING	45.7 KSI	68.5 KSI	70.0 KSI	PLATE BENDING
LOWER SKIN	ALUM.SHT. 7050-T76	SHEET LAMINATES	FUEL PRESSURE & NEGATIVE BENDING	45.7 KSI	68.5 KSI	70.0 KSI	PLATE BENDING

Table XXVI STRESS DATA SUMMARY SHEET FOR WING BOX DESIGN CONCEPT NO. 610RW009

REPRESENTATIVE LOWER SURFACE DATA INBOARD OF CSS 280 _____ :

COMPONENT	MATERIAL	STRUCTURAL DESCRIPTION	DESIGN CONDITIONS	APPLIED STRESSES		ALLOWABLE OPERATING STRESSES			CRITICAL SIZING CRITERIA
				OPERATING	ULTIMATE	FATIGUE	CRACK GROWTH	STATIC	
FRONT AUX SPAR LWR CAP	7050-T EXTRUSION $F_{tu} = 70$ KSI	STEPPED BONDED CAP, $K_t = 2.0$ $2 C_o = .148$	POSITIVE & NEGATIVE BENDING	37.15 KSI	70.00 KSI	37.15 KSI	45.00 KSI	37.15 KSI	FATIGUE AND STATIC STRENGTH
LOWER SKIN	7050-T76 SHEET	LAMINATED BONDED SHEET, $K_t = 1.0$ $2 C_o = .06$	"	37.15 KSI	70.00 KSI	40.40 KSI	39.50 KSI	37.15 KSI	STATIC STRENGTH

FAIL SAFE

REPRESENTATIVE UPPER SURFACE DATA @ CSS 140 _____ :

COMPONENT	MATERIAL	STRUCTURAL DESCRIPTION	DESIGN CONDITIONS	APPLIED STRESSES		ALLOWABLE ULTIMATE STRESS	CRITICAL SIZING CRITERIA
UPPER SKIN BETWEEN CS & FAS	7050-T76 PLATE	ETCH SCULPTURED MONOLITHIC PLATE	POSITIVE BENDING	-31.31 KSI	-59.00 KSI	-59.00 KSI	PLATE BUCKLING

REPRESENTATIVE DATA OUTBOARD OF CSS 280 _____ :

COMPONENT	MATERIAL	STRUCTURAL DESCRIPTION	DESIGN CONDITIONS	APPLIED STRESSES		ALLOWABLE ULTIMATE STRESS	CRITICAL SIZING CRITERIA
UPPER SKIN	7050-T76 SHEET	BONDED BUILT-UP SHEET	FUEL PRESSURE & POSITIVE BENDING	4570 KSI	6850 KSI	7000 KSI	PLATE BENDING
LOWER SKIN	"	"	FUEL PRESSURE & NEGATIVE BENDING	4570 KSI	6850 KSI	7000 KSI	PLATE BENDING

Table XXVII

DISTRIBUTION OF WEIGHT IN PRELIMINARY DESIGN WINGS

	610RW000 Lbs	610RW001 Lbs	610RW002 Lbs	610RW003 Lbs	610RW004 Lbs	610RW005 Lbs	610RW006 Lbs	610RW007 Lbs	610RW008 Lbs	610RW009 Lbs
TENSION	525.1	321.0	208.1	320.6	381.0	245.0	234.3	347.4	302.7	302.5
COMPRESSION	394.7	357.0	216.0	386.0	356.5	268.0	279.6	417.3	385.9	358.5
SHEER	349.4	220.0	162.0	127.2	150.4	178.7	166.5	81.4	111.6	103.1
RIBS, BULKHEAD	41.2	61.7	58.6	45.0	45.0	45.0	23.5	45.0	80.0	56.0
FASTENERS	92.1	37.0	.5	17.6	36.9	40.0	19.8	43.6	33.8	13.7
SECONDARY STRUCT.	242.3	330.3	345.9	310.0	313.0	310.0	192.6	310.2	296.1	309.9
MISCELLANEOUS	20.2	58.0	28.0	55.0	58.2	91.9	192.7	102.1	71.9	63.9
TOTAL WT. IN. LBS.	1665	1385.0	1019.1	1261.4	1341.0	1178.6	1109.0	1347.0	1282.0	1207.6
REDUC. FROM BASE- LINE	0	280.0	645.0	403.6	324.0	486.4	556.0	318.0	384.0	457.4
% REDUC. FROM BASELINE	0	16.8%	38.8%	24.2%	19.4%	29.2%	33.4%	19.1%	23.0%	27.5%
REML. OF FASTNRS, ETC.	0	4.3%	10.6%	6.5%	3.3%	7.2%	9.8%	2.8%	3.4%	7.4%
MTL., CHG, LAM.	0	2.4%	17.2%	3.8%	1.9%	13.1%	14.6%	1.6%	1.9%	4.3%
STABILITY IMPROV.	0	10.1%	11.0%	13.9%	14.2%	8.9%	9.0%	14.7%	17.7%	15.8%

Table XXVIII COMPARISON OF PRELIMINARY DESIGN WING STIFFNESSES TO
F-111F BASELINE

	<u>BENDING STIFFNESS</u> (TYPICAL % OF BASELINE)	<u>TORSIONAL STIFFNESS</u> (TYPICAL % OF BASELINE)
F-111F BASELINE	100	100
61ORW001	73.5	44.5
61ORW002	65.5	61.0
61ORW003	81.0	81.5
61ORW004	91.9	40.6
61ORW005	79.2	52.7
61ORW006	76.5	47.1
61ORW007	94.9	75.9
61ORW008	94.9	75.9
61ORW009	81.0	81.5

5.3 STRUCTURAL INTEGRITY AND RELIABILITY EVALUATION TECHNIQUE

The structural characteristics to be assessed in the "integrity and reliability", evaluation have been categorized as "static, fatigue, safe crack and multiple load path." The approach employed to perform this evaluation is described below.

The term "static" is based on static margin. Thus, a structure that is sized by fatigue or crack propagation criteria will have excess static strength. The degree of excess static strength is the ratio of static strength available to static strength required. If the structure is critical for static loads this ratio is unity. In comparing the many candidate concepts the first step is to calculate the static strength ratio for each concept. The next step is to normalize all values based on that concept which shows the highest static strength ratio. A final weighted value is then determined for each concept by multiplying its normalized static strength ratio by .03 (since $.30 \times .10 = .03$).

To compare the fatigue quality characteristics of the various design concepts the ratio, C_F , is the first calculated for each concept where:

$$C_F = \frac{\sqrt{F}}{\sqrt{S}}$$

\sqrt{F} = maximum allowable stress based on fatigue considerations

\sqrt{S} = maximum static stress in the wing cross-section

The allowable fatigue stress reflects the F-111F service loads spectrum, the type of material and the maximum stress concentration factor, K_T .

The C_F ratios are then divided by the maximum such ratio to convert all values to a unit scale $C'_F = \frac{C_F}{\text{Max } C_F}$

The preceeding paragraph describes the manner in which the stress concentration (K_T) in each design concept has been accounted for in the fatigue quality comparisons.

However, in addition to the apparent stress concentrations certain designs have sources of potential stress concentrations which might very well exceed the existing K_T values. For example, lower surface holes with a readily assignable $K_T = 3.4$ (for carefully prepared tapered fasteners) were considered to be sources of potential additional stress concentration because of possible sharp scratches during bolt installation. In addition, chordwise changes of thickness were considered to be potential sources of stress concentration due to machining defects that might occur. Spanwise welds were also considered in a similar fashion. A count of all such sources of potential K_T increases was conducted for each design concept and a two percent reduction in C_F was taken for each possible source of trouble. The relative fatigue rating for each concept is then expressed as follows:

$$R = C_F - .02n \text{ Where: } n = \text{number of potential defects.}$$

The final weighted value of fatigue quality for each concept was then obtained by multiplying R by .09 (.30 x .30).

"Safe crack" is interpreted as referring to the maximum stress in the fatigue stress spectrum consistent with stable crack growth. Each design concept is analyzed for cracks starting at both surface flaws and at holes (unless the concept is free of holes). There are four damage tolerance categories:

FS = fail-safe, hole-free structure

FSH = fail safe structure with holes

SCG = slow crack growth (not fail-safe) structure

SCGH = slow crack growth structure with holes

The maximum allowable crack growth stress in the loading spectrum, σ_{CG} , is controlled by the damage tolerance category and the type of material in accordance with Revision D of the proposed USAF Damage Tolerance Criteria, dated 18 August 1972. The maximum allowable ultimate stress based on crack growth considerations only is:

$$F_{cr} = \left(\frac{29.3}{15.5} \right) \sqrt{\sigma_{CG}}$$

Then the ratio of the equivalent ultimate crack growth stress to the maximum static tension stress is:

$$K_{CG} = \frac{F_{cr}}{\sqrt{S}}$$

Where: \sqrt{S} = maximum operating stress based on static considerations.

These ratios are then divided by the maximum such ratio and multiplied by .09 to obtain the final weighted values:

$$.09 R_{CG} = .09 \frac{K_{CG}}{\text{Max } K_{CG}}$$

The "Multiple Load Path" category is considered synonymous with fail safe capability. For each cross-section design concept, a count has been made of the maximum number of individual structural elements that could be failed without impairing limit load capability. By dividing all such counts by the maximum all values are converted to a unit scale. The weighted values are then obtained by multiplying the normalized counts by .09 (.3 x .3).

Final weighted values of structural integrity and reliability are obtained by summing the values for fatigue quality, safe crack growth, fail safe characteristics and static strength for each concept.

SECTION VI

FATIGUE ANALYSIS

Fatigue Analyses have been performed to demonstrate potential compliance of the selected preliminary wing designs with the specified fatigue requirements. The following discussions provide a summary of fatigue analysis results and procedures used in Phase IA.

6.1 FATIGUE ANALYSIS CRITERIA AND PROCEDURES

The fatigue requirements used for the design of proposed advanced fighter wing structure are identical to those of the baseline component. These requirements are summarized below and more fully discussed in paragraph 3.3.

1. The total service life shall be 4000 flight hours and 4000 landings.
2. Repeated load occurrences shall be increased to include a scatter factor = 4.0.
3. Fatigue loads spectra shall include the discrete repeated loads specified in MIL-A-8866 as interpreted for the F-111.
4. Typical service life usage shall be as represented by TAC Phase I and II Training Mission Profiles.

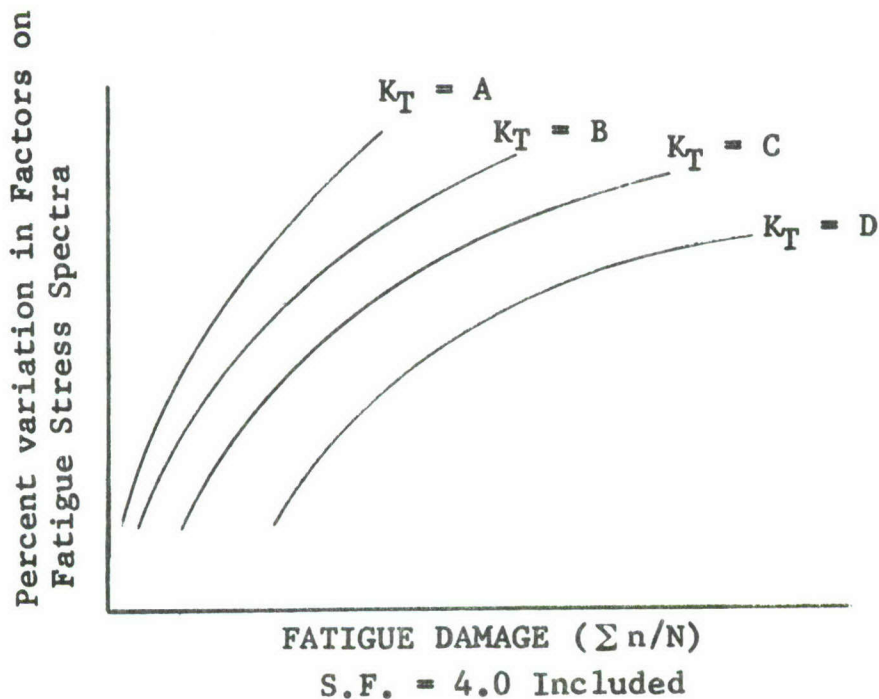
Safe-life was used as the primary means of satisfying the fatigue life requirements. The primary objective for each new wing design was the ability to withstand a minimum of four structural service lifetimes without fatigue cracking. Proof of compliance by full scale testing is reserved for the follow-on program.

The design service loads spectrum was identical to the baseline fatigue spectrum with one exception. The exception is: The number of occurrences were revised to reflect the more severe exceedance data and ground-air-ground transition requirements included in MIL-A-8866A (USAF) dated 31 March 1971. (The exceedance data used in developing the current baseline spectrum was that data included in a preliminary version of the MIL-A-8866A series which became available to the contractor in early 1969.)

Following development of fatigue loads spectra, the procedure for performing fatigue analyses was generally as follows:

1. Fatigue control points were selected.
2. Control point unit stresses (stress per unit of load) were established.
3. Fatigue test (S-N) data was selected for each control point which reflects appropriate stress concentrations (K_T).
4. Fatigue stress spectra were established for each control point by combining the repeated loads and occurrences with the unit stress data. Stress spectra were also adjusted for compatibility with selected S-N data and environment.
5. Fatigue damage calculations were made for the stress spectra of (4) using the S-N data selected in (3) and Miner's cumulative damage rule ($\sum n/N = 1.0$ at failure).

Flexibility and rapid determination of fatigue damage was accomplished for this program by expanding the above procedure on a parametric basis as shown schematically below.



Using the parametric approach, fatigue damage curves reflecting variation in factors on fatigue stress spectra and variation in stress concentration were generated for each material selected as applicable to Phase IA. These curves were updated as additional S-N data became available from the Phase IA test program.

The above fatigue damage "catalog" was also utilized to construct fatigue design data sheets, or allowable curves, to support the actual design effort as required. These data sheets are discussed and presented in paragraph 6.2.1.

6.2 CONCEPT ANALYSIS AND EVALUATION

Fatigue prevention requires that fatigue analysis begin in the earliest stages of the design phase. Fatigue analyses were continually fed into the design process, reflecting revisions as more appropriate fatigue test data became available.

The design effort in Phase IA progressed systematically from cross sections to analytical assemblies, to preliminary wing designs culminating in the final three wing selections summarized in Section II. Fatigue design data sheets were developed to insure that fatigue strength requirements would be reflected in design formulation and trade studies.

Based on the allowables dictated by preliminary fatigue design data sheets, an early conclusion was reached to reduce potential stress concentrations (e.g., bolt holes) in the lower surface by using bonded, brazed, or welded construction. This decision practically eliminated significant weight penalties due to fatigue.

6.2.1 Fatigue Design Data

Fatigue design data sheets (allowable curves) essentially indicate the interacting relationships between stress, stress concentration factor, and fatigue life. These curves were developed for each of the materials being evaluated for use in the lower surface. Figure 44 depicts the general development procedure for design data sheets. Additional details of this procedure are given in Appendix VI.

The allowable stresses determined from the data sheets are representative of stresses at the lower surface at center spar station (C.S.S) 140. Review of the baseline math model stress analyses for selected design conditions indicated this

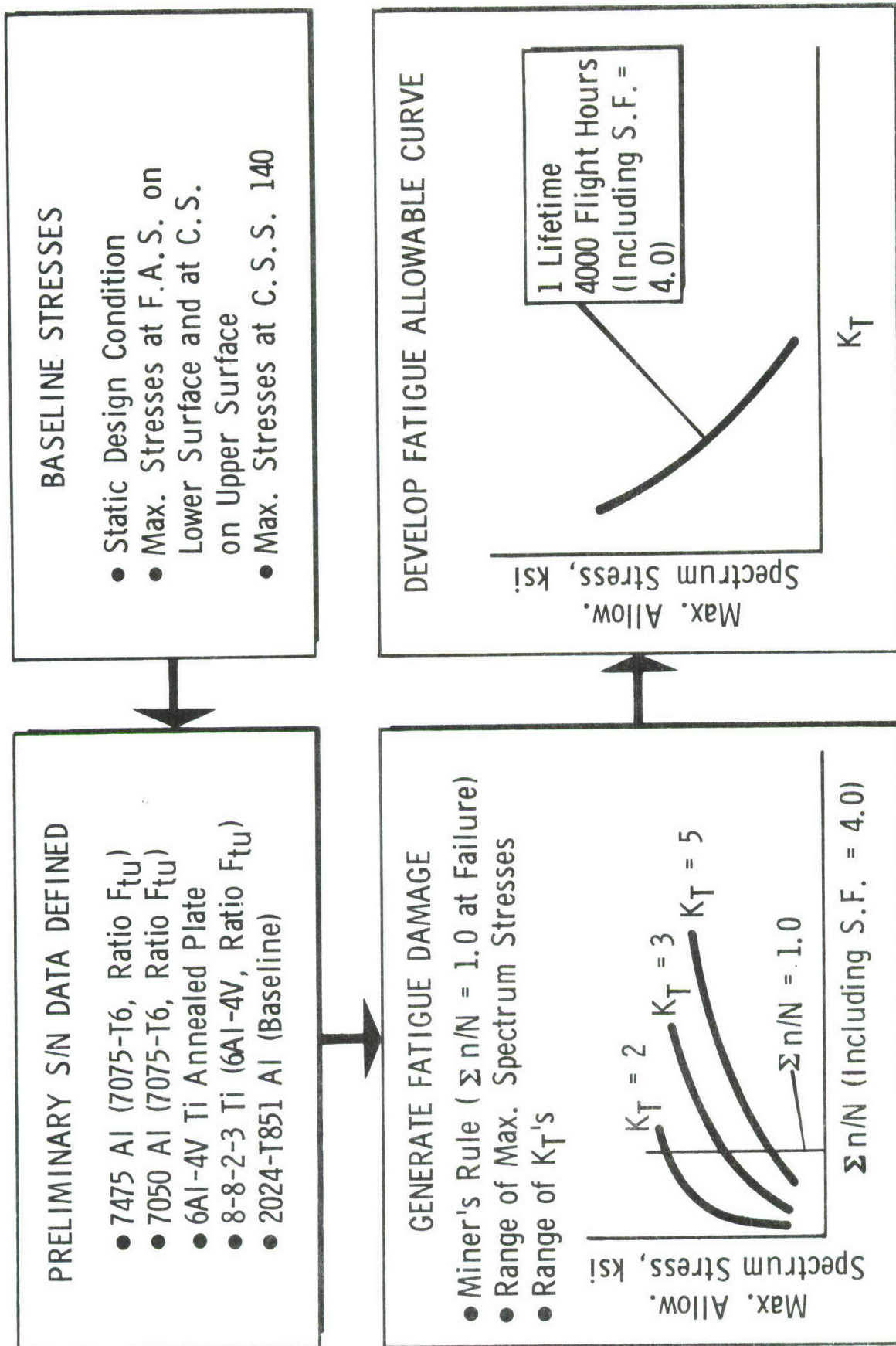


Figure 44 Fatigue Allowable Approach

area of the baseline lower surface experiences the highest stresses. Experience gained from the F-111 fatigue test program also indicated that upper surface control points experience no significant fatigue damage primarily because the upper surface is sized for compression buckling and the baseline spectrum contains very little negative maneuver time. This lack of calculable damage is also the case for the out-board portion of the wing box (typically C.S.S. 340) where design pressure and stiffness govern size of the structure.

Because fatigue S-N data was not yet available for the newer materials being considered, preliminary S-N data thought to be representative of the actual data required was utilized to generate the initial design data sheets. As test data became available from the Phase IA test program, the data sheets were updated. The final design data sheets developed from test data are given in Figures 45 through 50. See paragraph 6.2.2 for further discussion of fatigue test S-N data used in Phase IA.

The fatigue quality index or stress concentration factor (K_T) is a function primarily of design concept and detail. As previously stated, every effort was made to eliminate stress concentrations in the lower surface. Additional discussion of guidelines for fatigue quality in design is given in paragraph 6.2.3.

6.2.2 Fatigue Data for Analysis

Because fatigue S-N data was not initially available from the Phase IA test program for the newer materials being considered, the early procedure was to assemble data which was available and which is representative of the actual data required. The preparation of initial preliminary fatigue design data sheets was accomplished using this representative data.

The preliminary S-N data assumed early in Phase IA is discussed in Appendix VI.

Limited fatigue test data was subsequently generated for the new materials during the course of Phase IA and is reported in Section VIII of this report. This test data was generated for each material using only one "R" value (minimum load/maximum load) and two stress concentration factors. Additional definition of S-N data will be required in Phase IB, particularly in the various sheet forms.

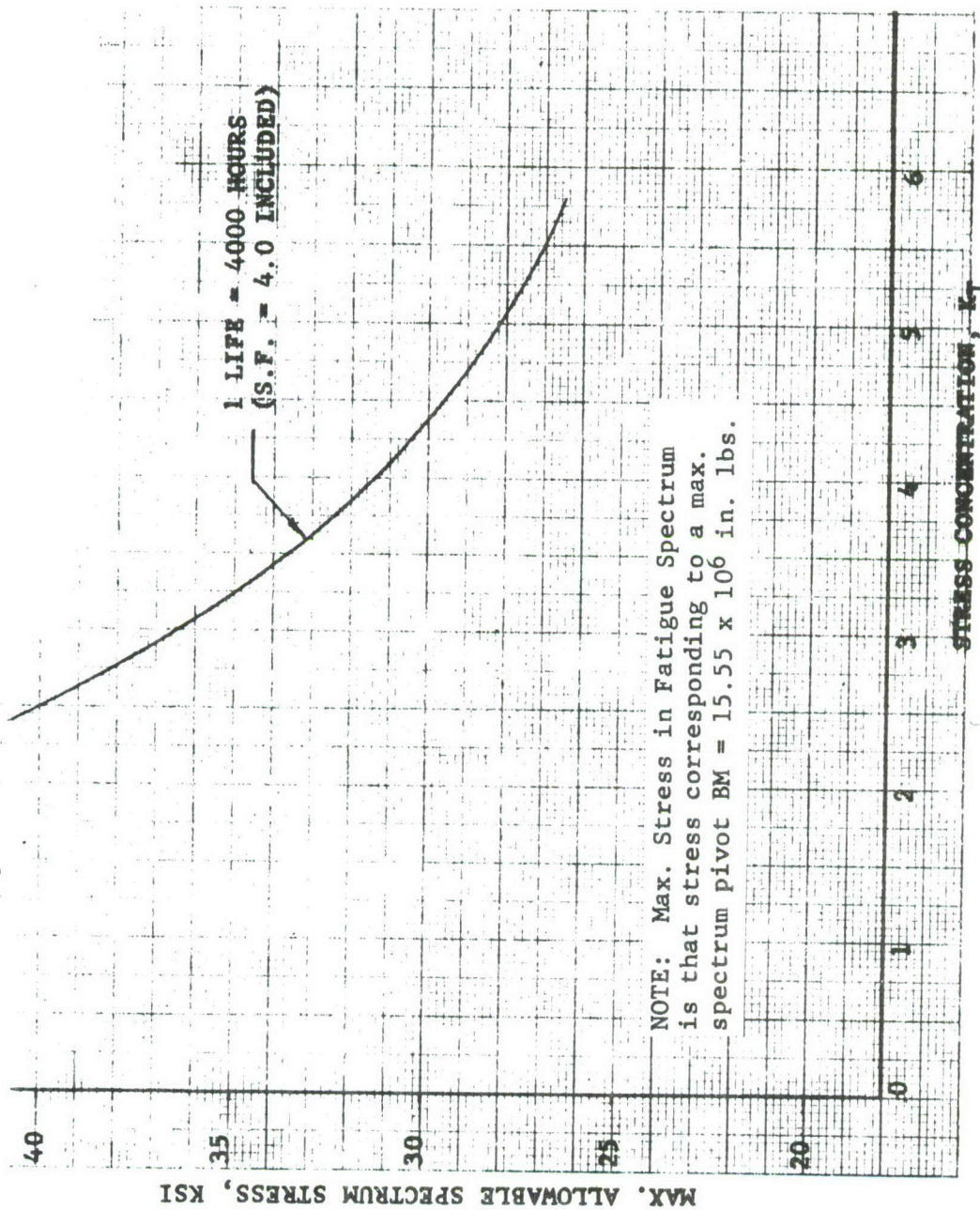


Figure 45 C.S.S. 140 Lower Surface ADP Wing Preliminary Fatigue Design Allow. Curves Based on Phase IA Tested S/N Data (0.125 Sht.) Applicable to 7475-T761 Sht. Alloy

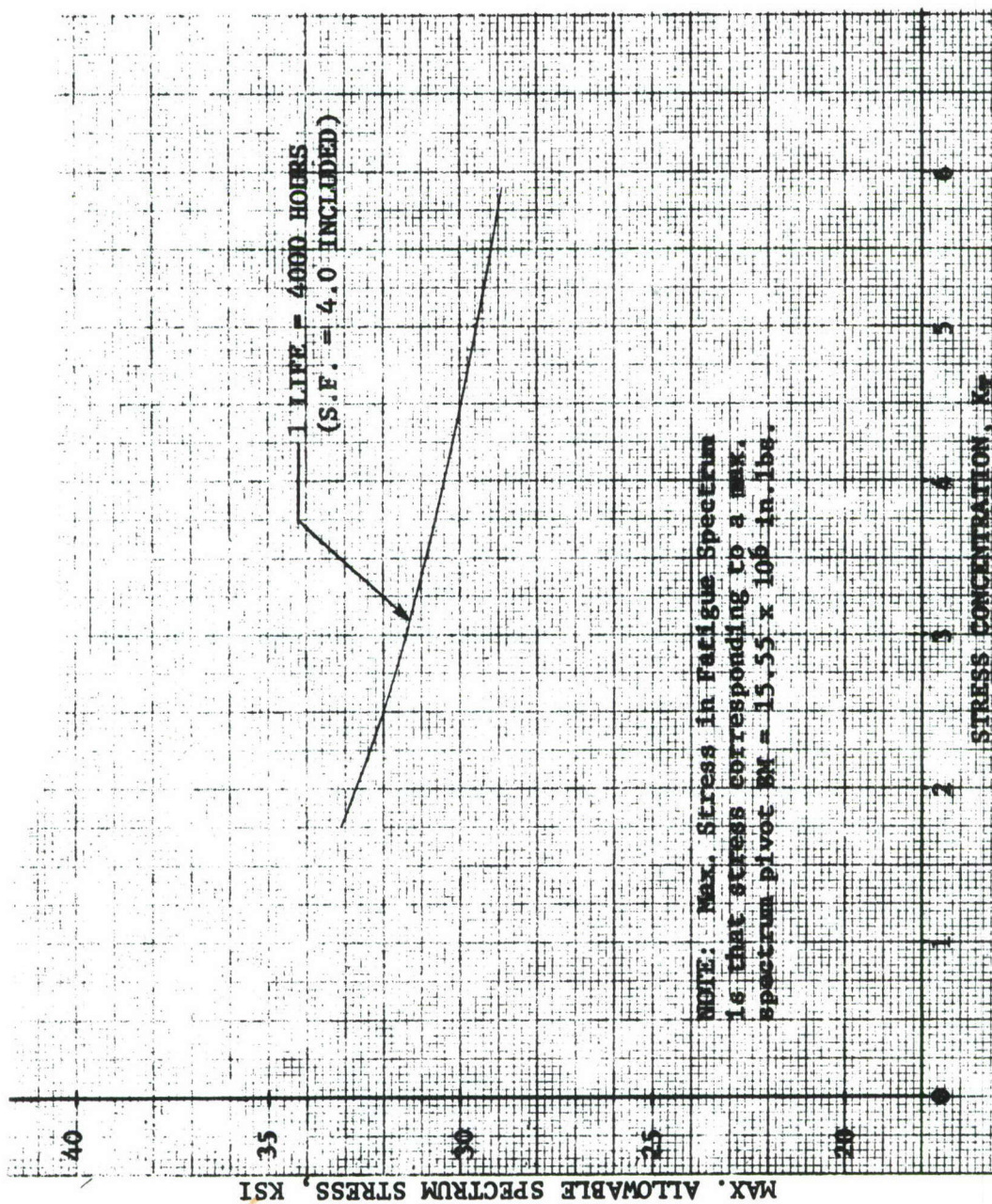


Figure 46 C.S.S. 140 Lower Surface ADP Wing Preliminary Fatigue Design Allow. Curves Based on Phase IA Tested S/N Data Applicable to 7475-T7351 Al. Alloy Plate (1-1/2")

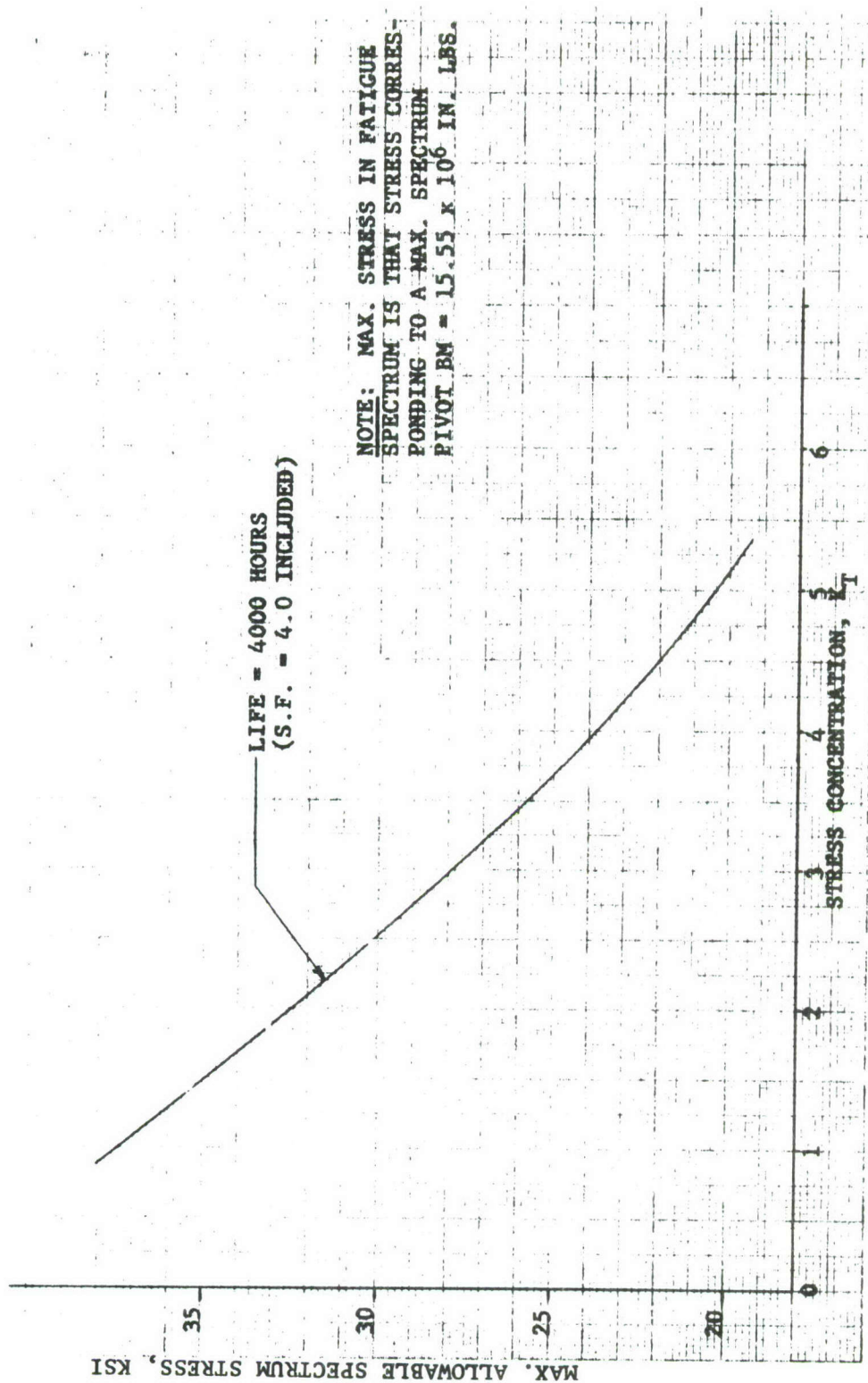


Figure 47 C.S.S. 140 Lower Surface ADP Wing Preliminary Fatigue Design Allow. Curves Based on Phase IA Tested S/N Data (0.0625 Sht.) Applicable to 7050-T76 Sht. Alloy

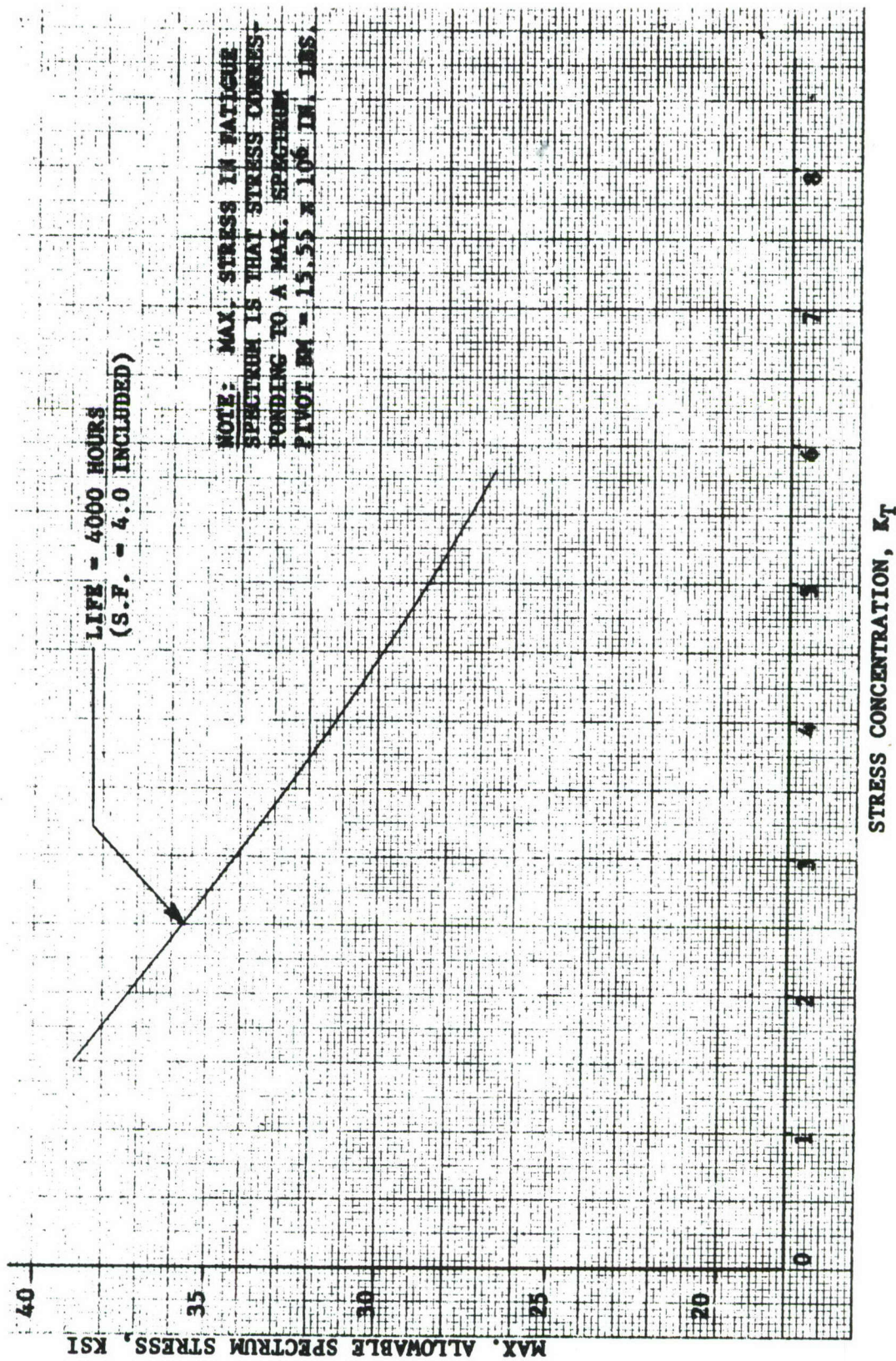


Figure 48 C.S.S. 140 Lower Surface ADP Wing Preliminary Fatigue Design Allowable Curves Based on Phase IA Tested S/N Data (3-In. Plate) Applicable to X7050-T73651 Pl. Alloy

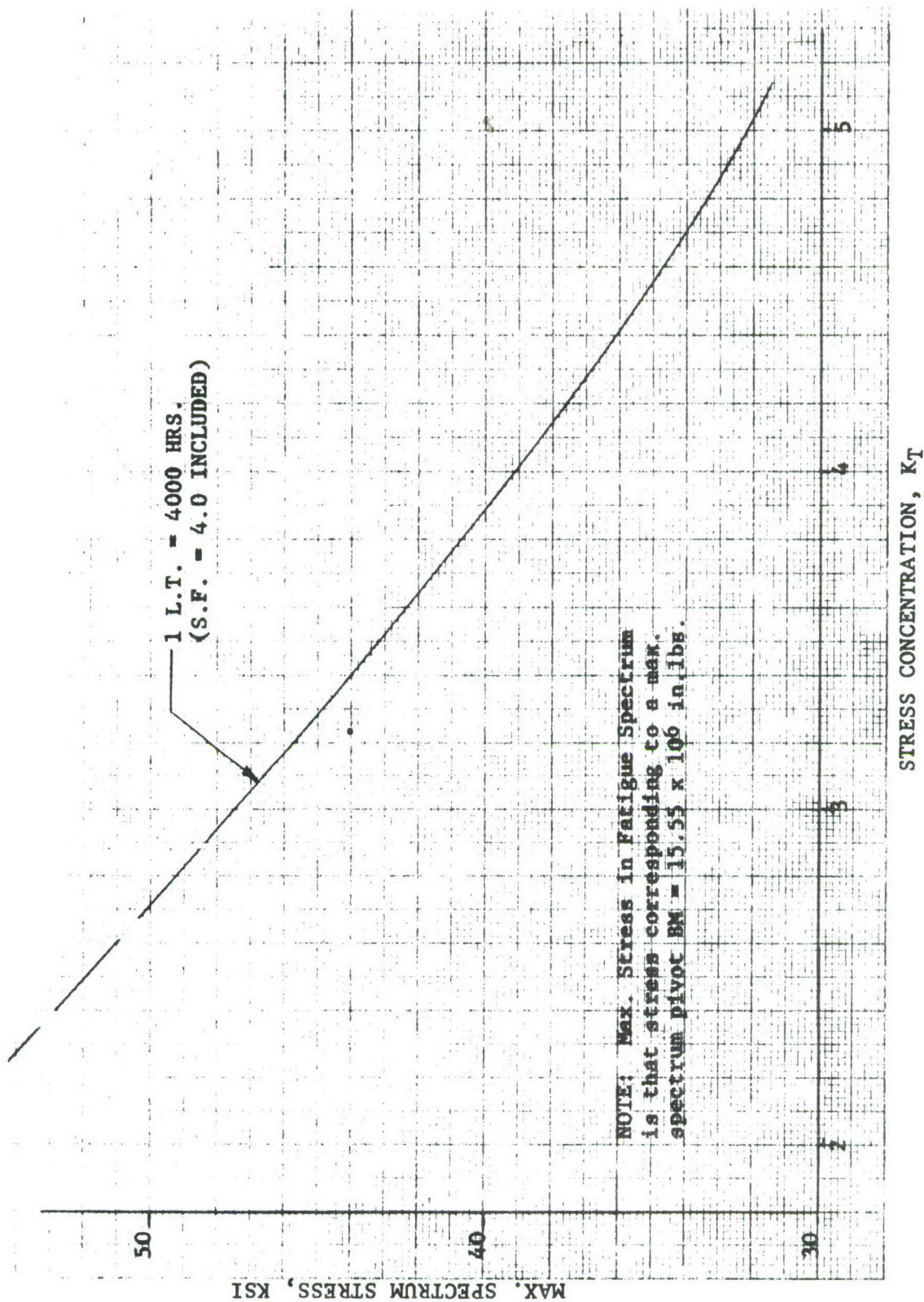


Figure 49 C.S.S. 140 ADP Wing Preliminary Fatigue Design Allow.
Curves Based on Phase IA Tested S/N Data Applicable to
8-8-2-3 Titanium Sheet

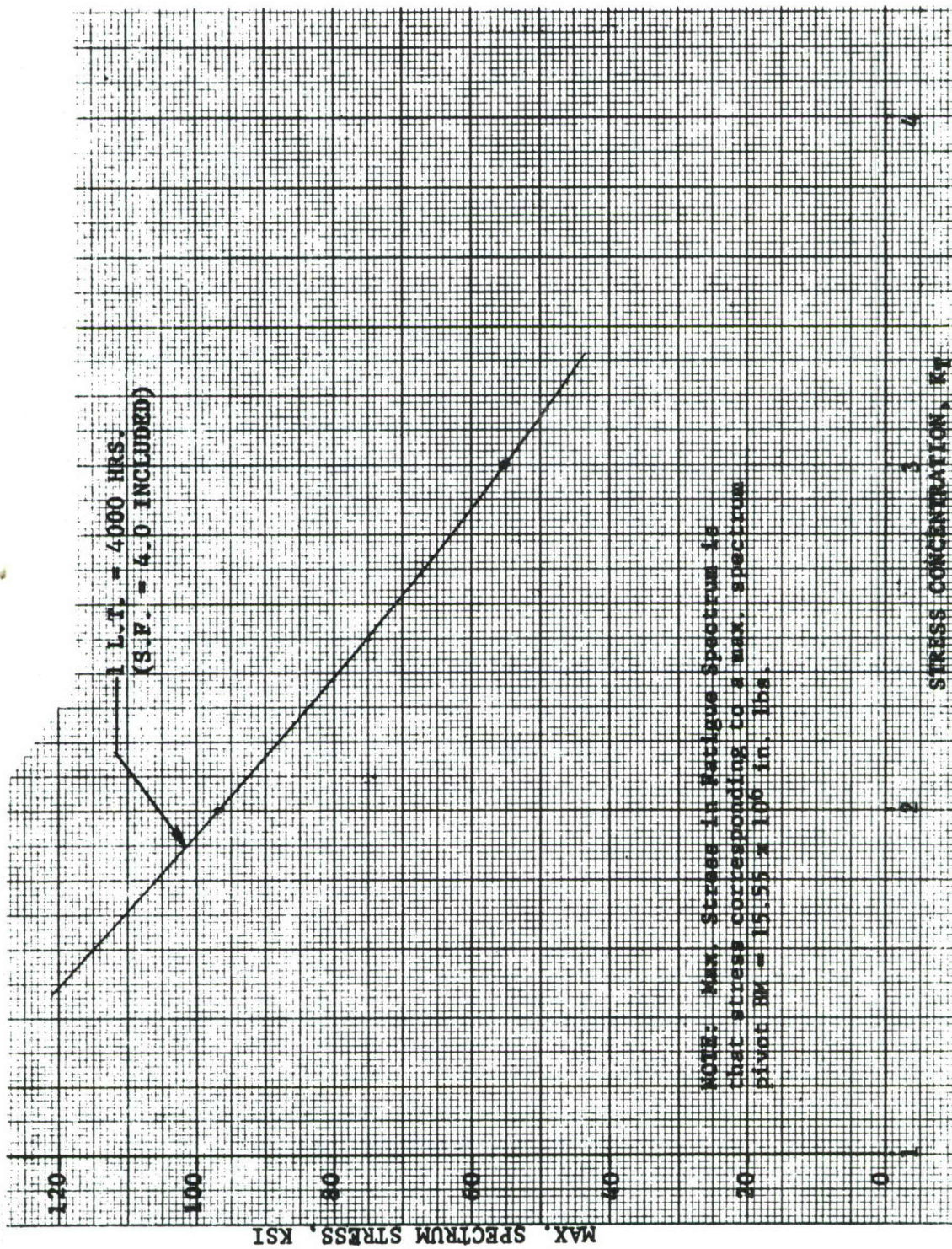


Figure 50 C.S.S. 140 ADP Wing Preliminary Fatigue Design Allow.
Curves for Use in Concept Screening Applicable to
8-8-2-3 Ti Plate S/N Data Tested in Phase IA

Since the baseline fatigue spectrum contains multiple "R" values, the test data was plotted in the form of a modified Goodman diagram. From the diagrams a family of S-N curves for fatigue analysis was developed. These curves were developed in terms of alternating and mean cyclic stresses which eliminate the need to directly consider a single "R" value. The S-N curves generated by this procedure are given in Figures 51 through 63.

The fatigue test data ($K_T = 3$ and 5) obtained for the 8-8-2-3 titanium sheet material seems relatively low. It was discovered that grinding the notches in the sheet specimens had resulted in some burning of the material. Subsequent data obtained using 8-8-2-3 titanium plate specimens ($K_T = 2$ and 3) was considerably better than the sheet data at a comparable $K_T = 3.0$, and the plate specimen notches had been machined instead of ground. It was therefore concluded that the sheet data was questionable, and this data was not used for any further analysis purposes, the plate data being used instead. Additional sheet data for 8-8-2-3 titanium will be obtained in Phase IB to verify or contradict this decision.

In addition to the apparent problems with 8-8-2-3 titanium in sheet form, fatigue test data generated for 7050-T76 sheet ($K_T = 3$ and 5) was also somewhat on the low side compared with data generated for 7475-T761 sheet, 7475-T7351 plate, and 7050-T73651 plate. An extensive review, including requested advice from ALCOA, has failed to provide an explanation for the 7050-T76 sheet data being low. ALCOA data for $K_T = 3$ in 7050-T76 sheet also substantiates that the Convair test data is low. In fact, the ALCOA data agrees well with the Convair-tested 7050-T73651 plate data at a $K_T = 3.0$. Therefore, Convair test data for 7050-T76 was considered questionable, and no further analyses were performed with it. ALCOA states that more 7050-T76 fatigue test data will soon evolve from NASC Contract No. N00019-72-C-0512. The sheet form of 7050 will also receive additional attention in the Phase IB test program. Meantime, subsequent fatigue analyses in Phase IA were performed using the 7050-T73651 plate data.

Additional discussion of the problems encountered with the fatigue test data may be found in Section VIII on Materials Engineering.

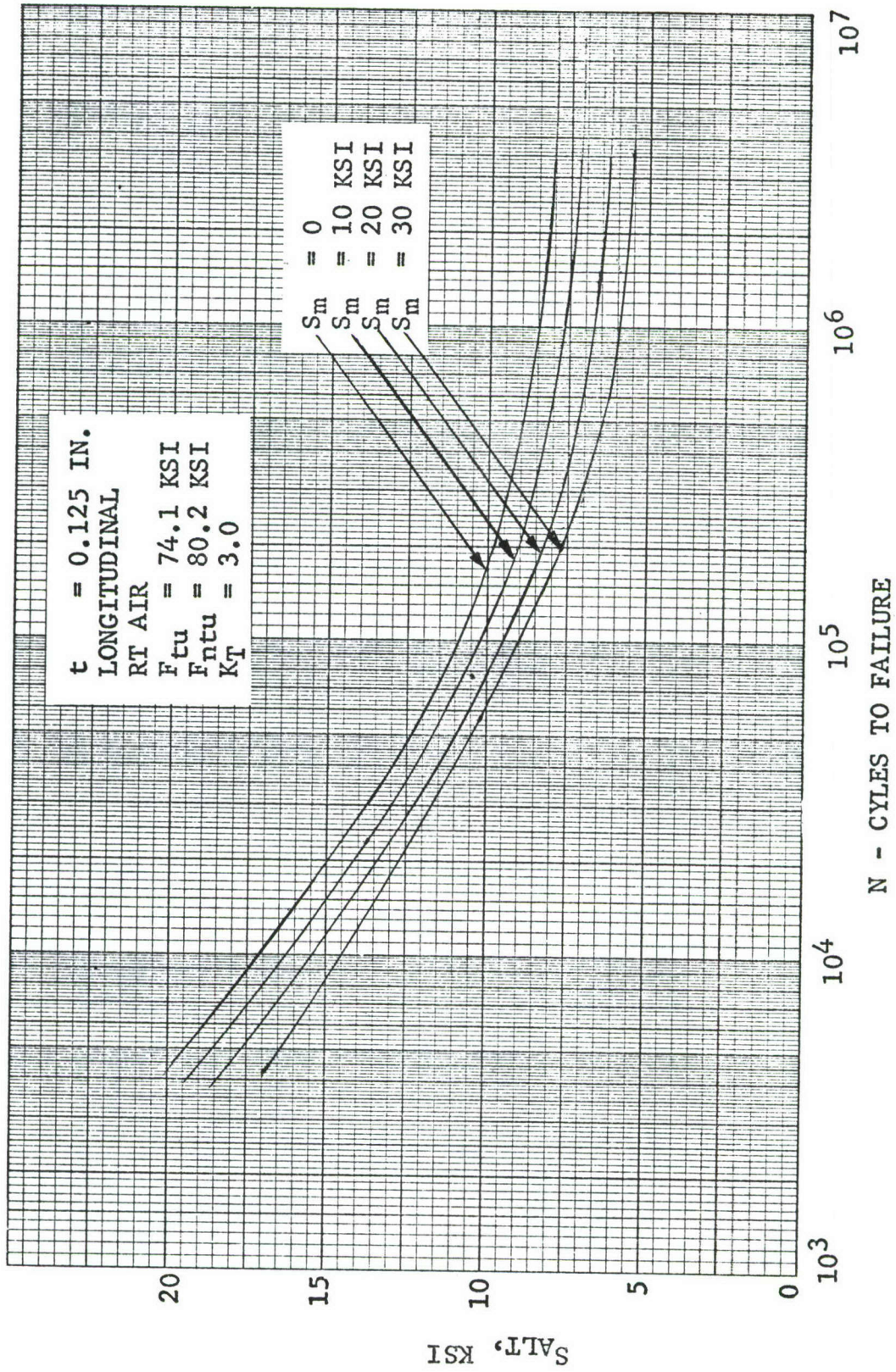


Figure 51 S-N Curves 7475-T61, T761 Aluminum Sheet

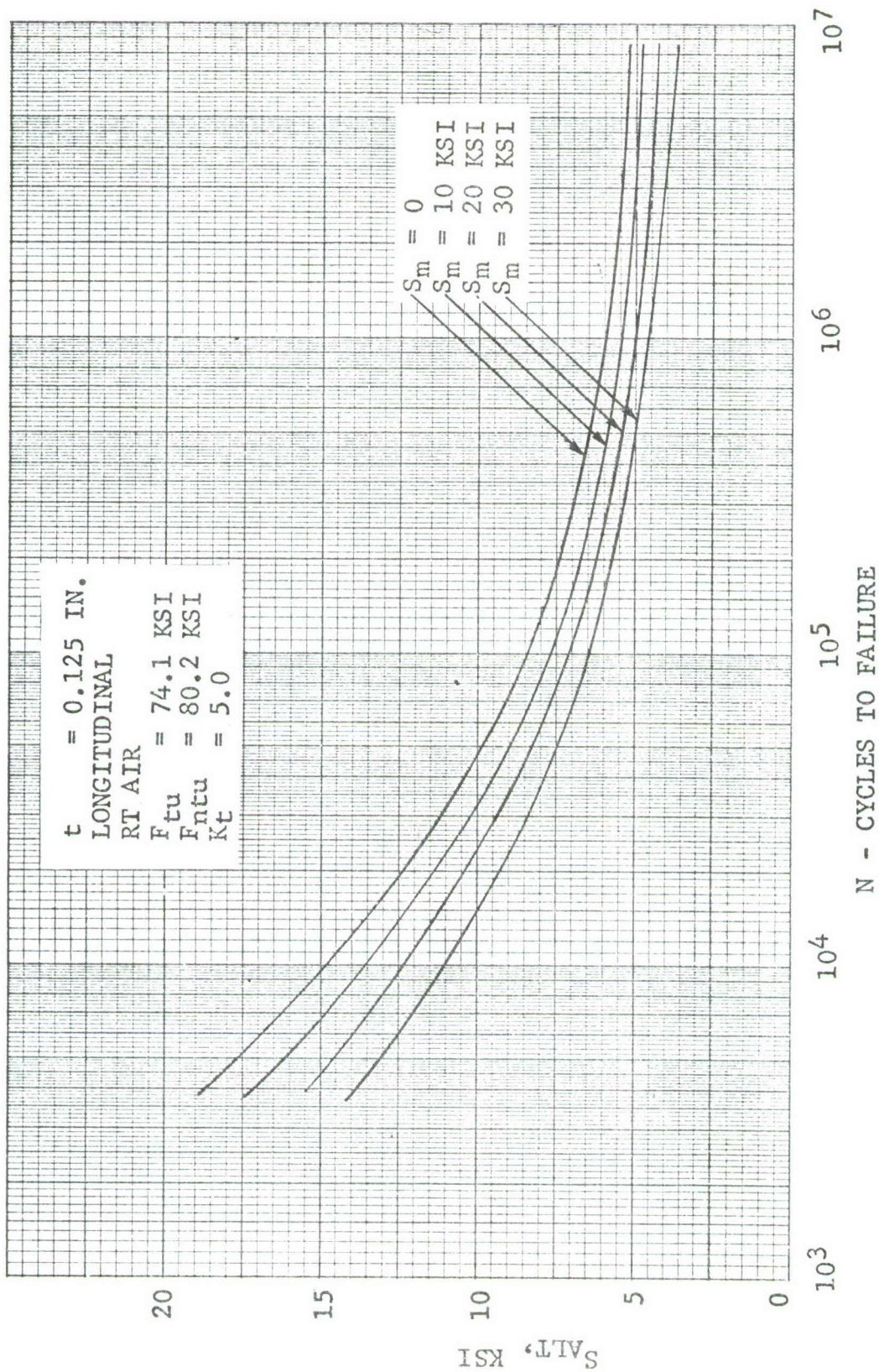


Figure 52 S-N Curves 7475-T61, T761 Aluminum Sheet

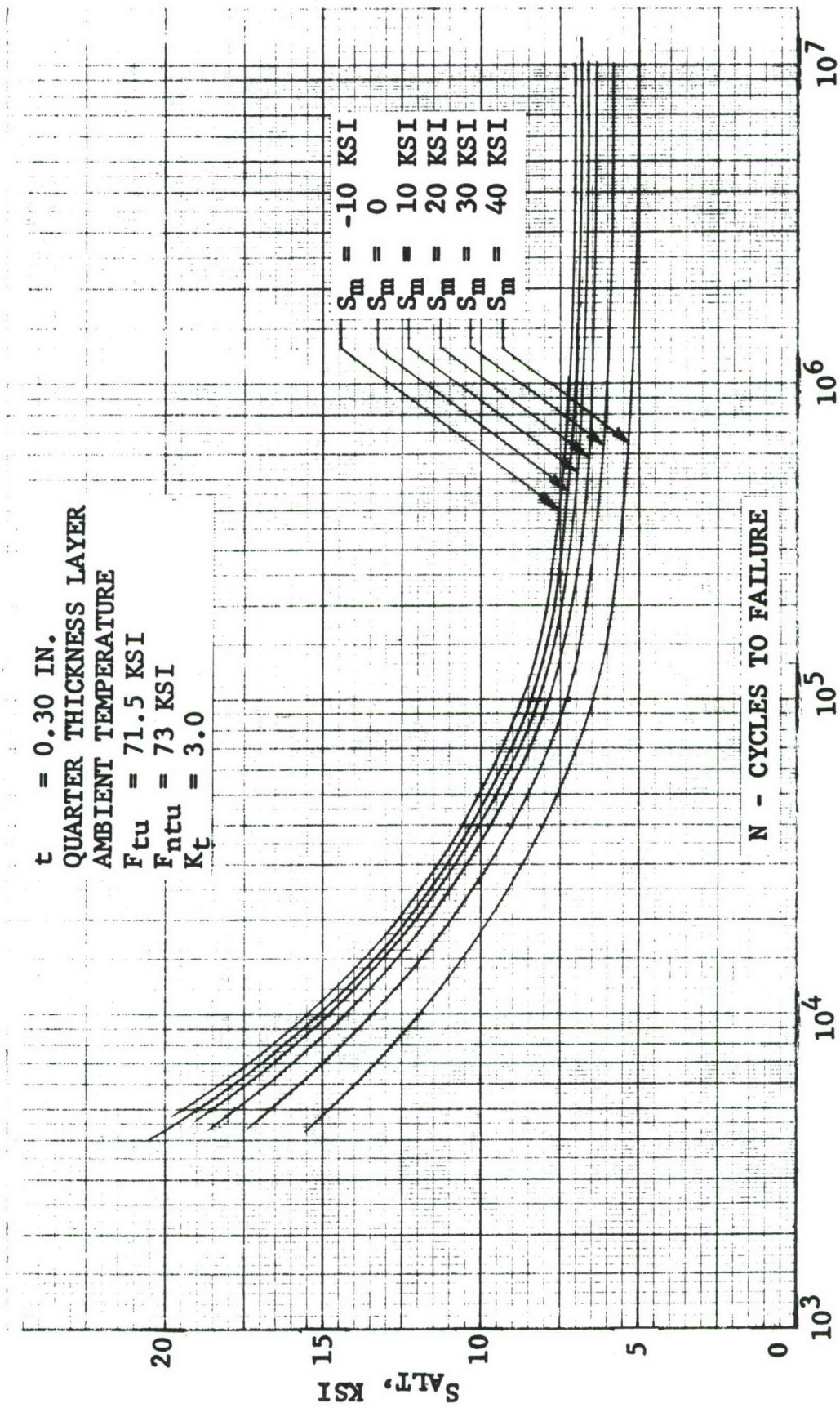


Figure 53 S-N Curves 7475-T735 Aluminum $1\frac{1}{2}$ -inch Plate

$t = 0.30$ IN.
 QUARTER THICKNESS LAYER
 AMBIENT TEMPERATURE
 $K_{tu} = 71.5$ KSI
 $F_{ntu} = 73$ KSI
 $K_t = 5.0$

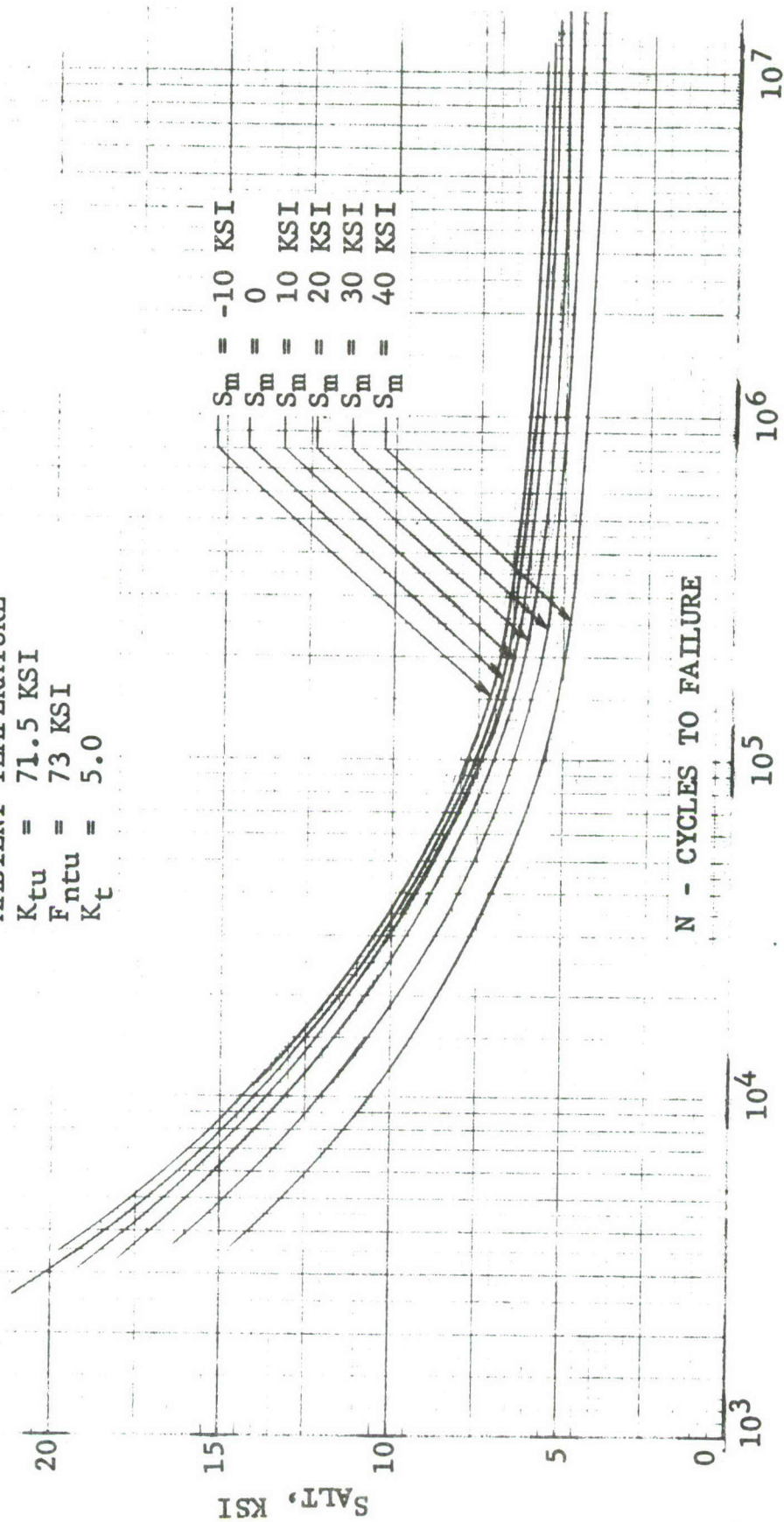


Figure 54 S-N Curves 7475-T7351 Aluminum $1\frac{1}{2}$ -inch Plate

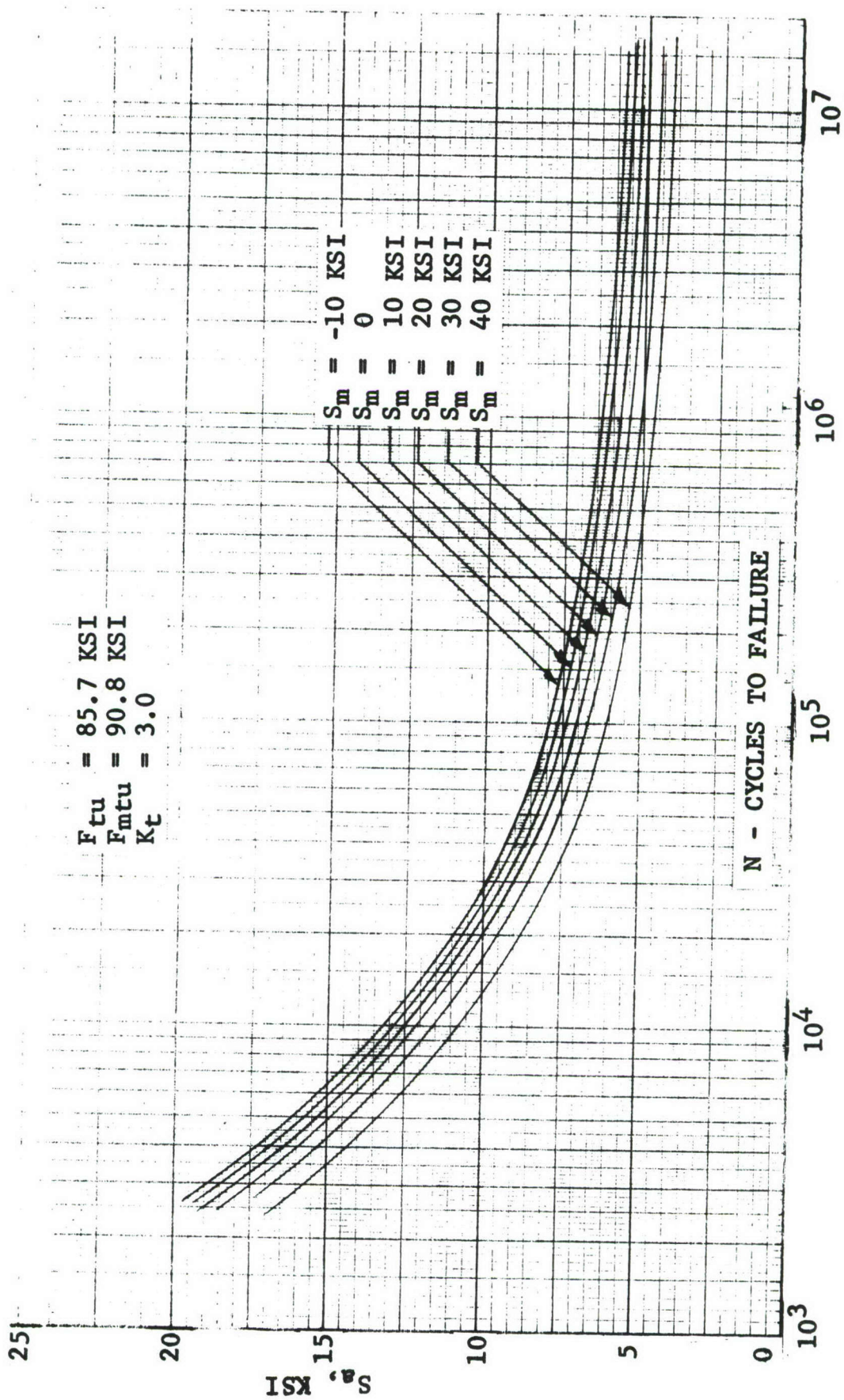


Figure 55 S-N Curves 7050-T76 Aluminum Alloy Sheet Longitudinal

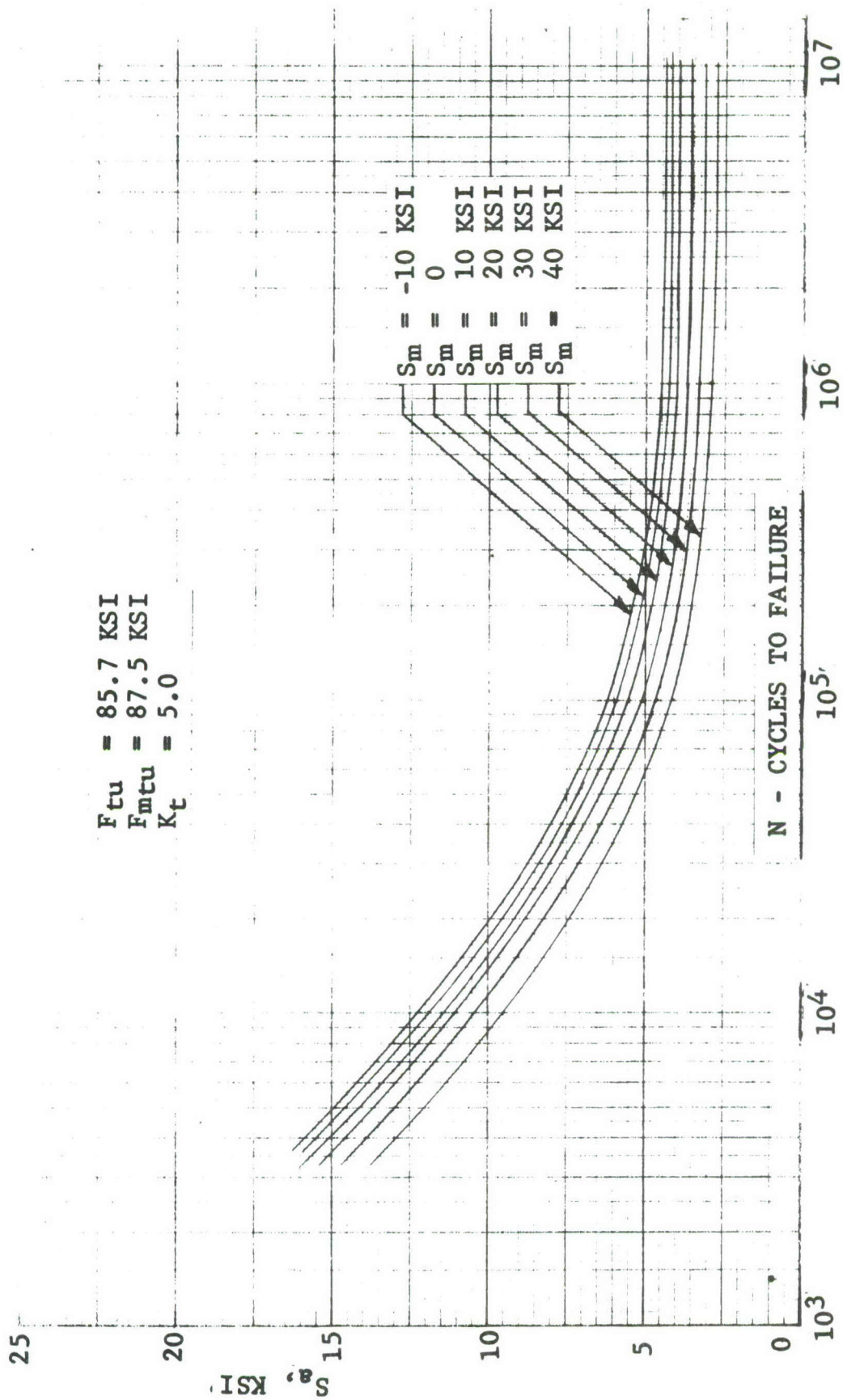


Figure 56 S-N Curves 7050-T76 Aluminum Alloy Sheet Longitudinal

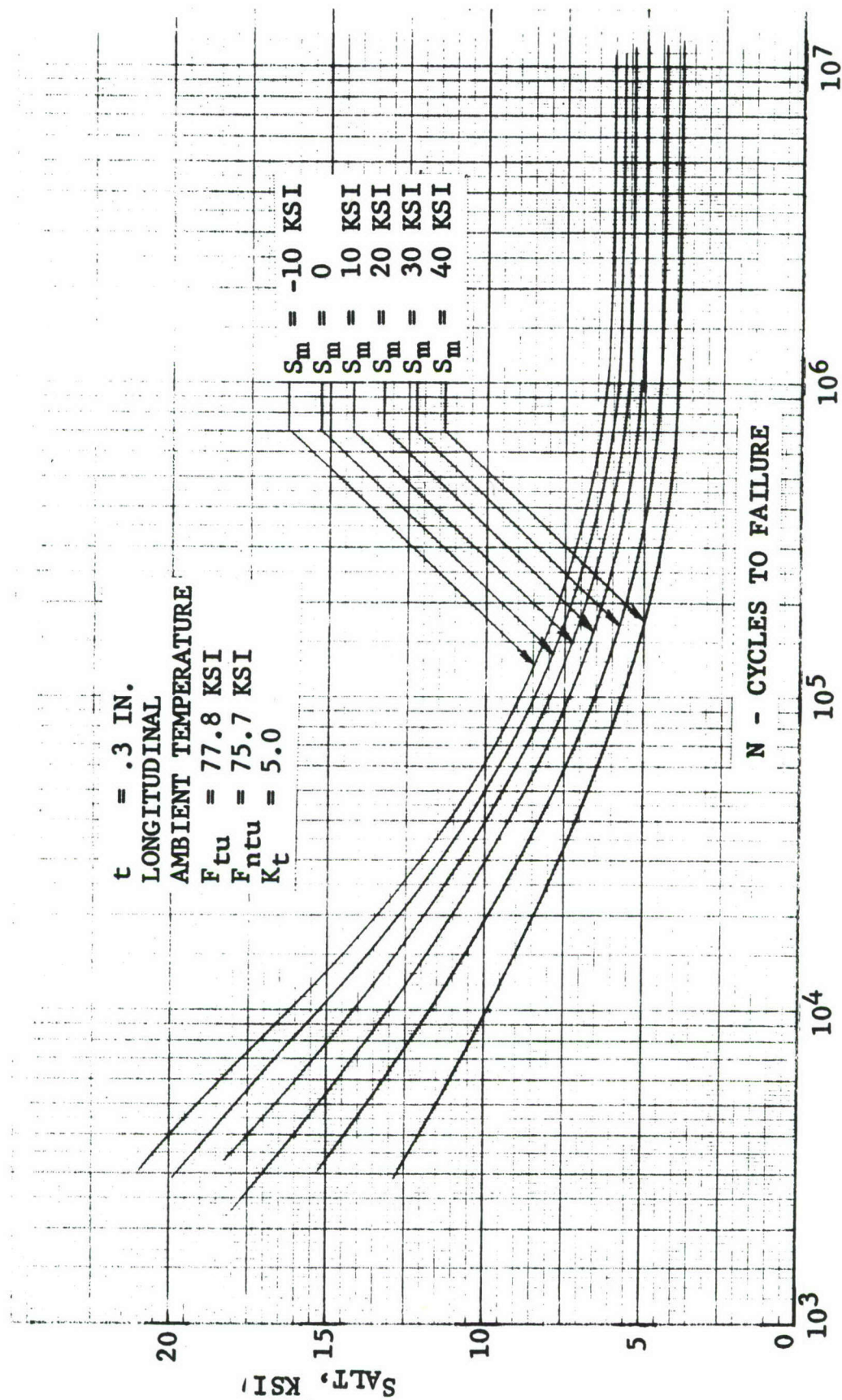


Figure 57 S-N Curves X7050-T73651 Aluminum 3-inch Plate

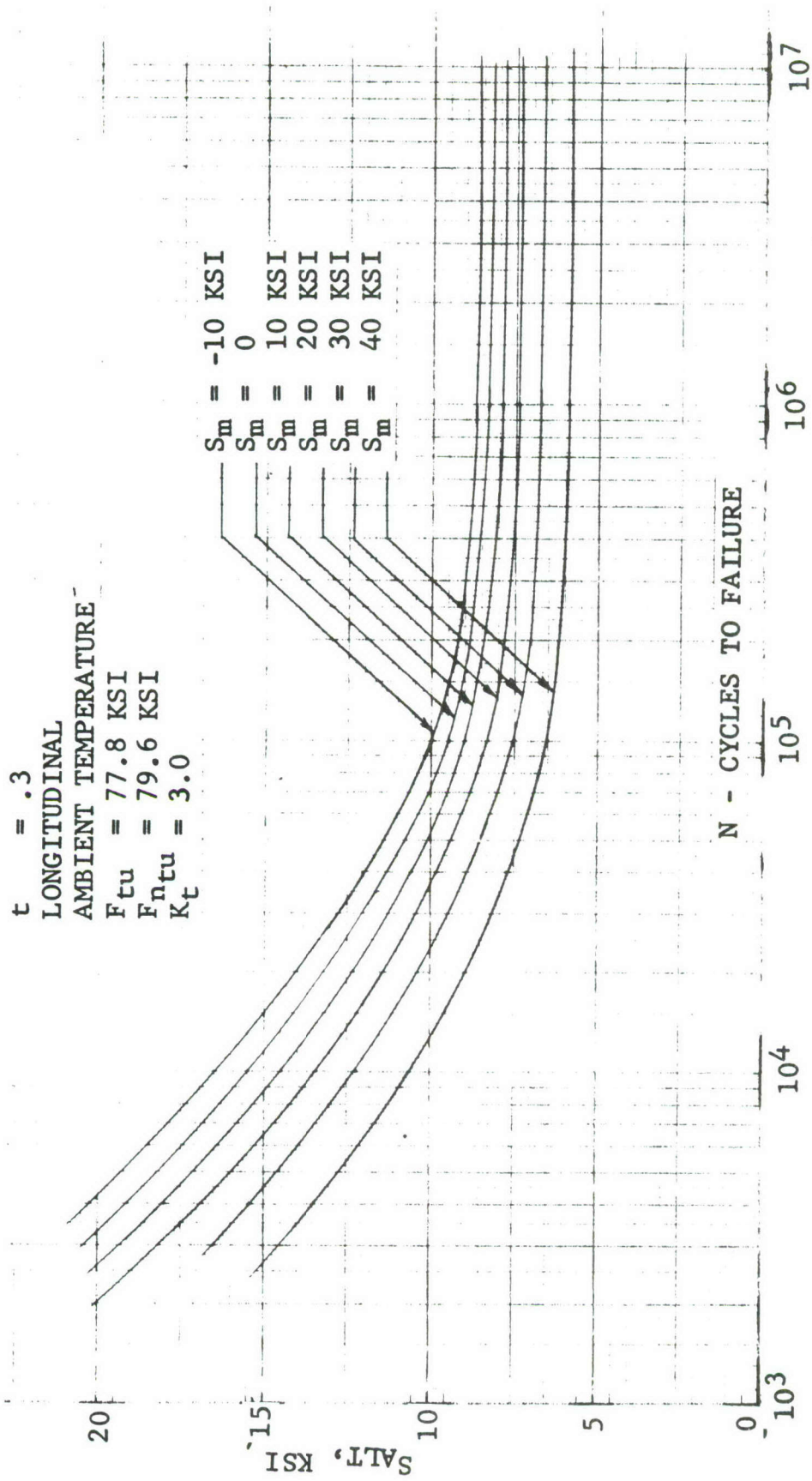


Figure 58 S-N Curves X7050-T73651 Aluminum 3-inch Plate

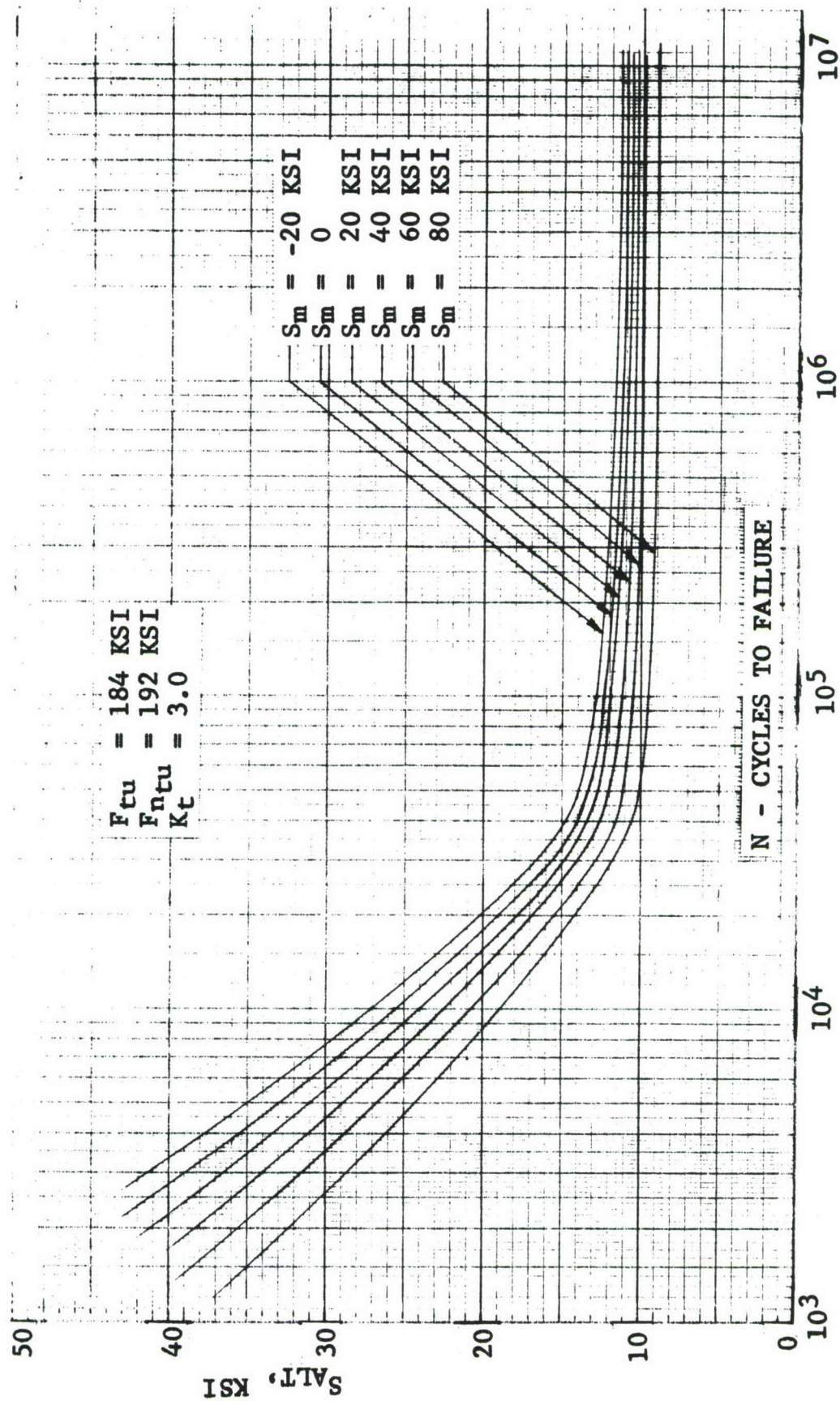


Figure 59 S-N Curves 8-8-2-3 Titanium 1/16-inch Sheet Longitudinal

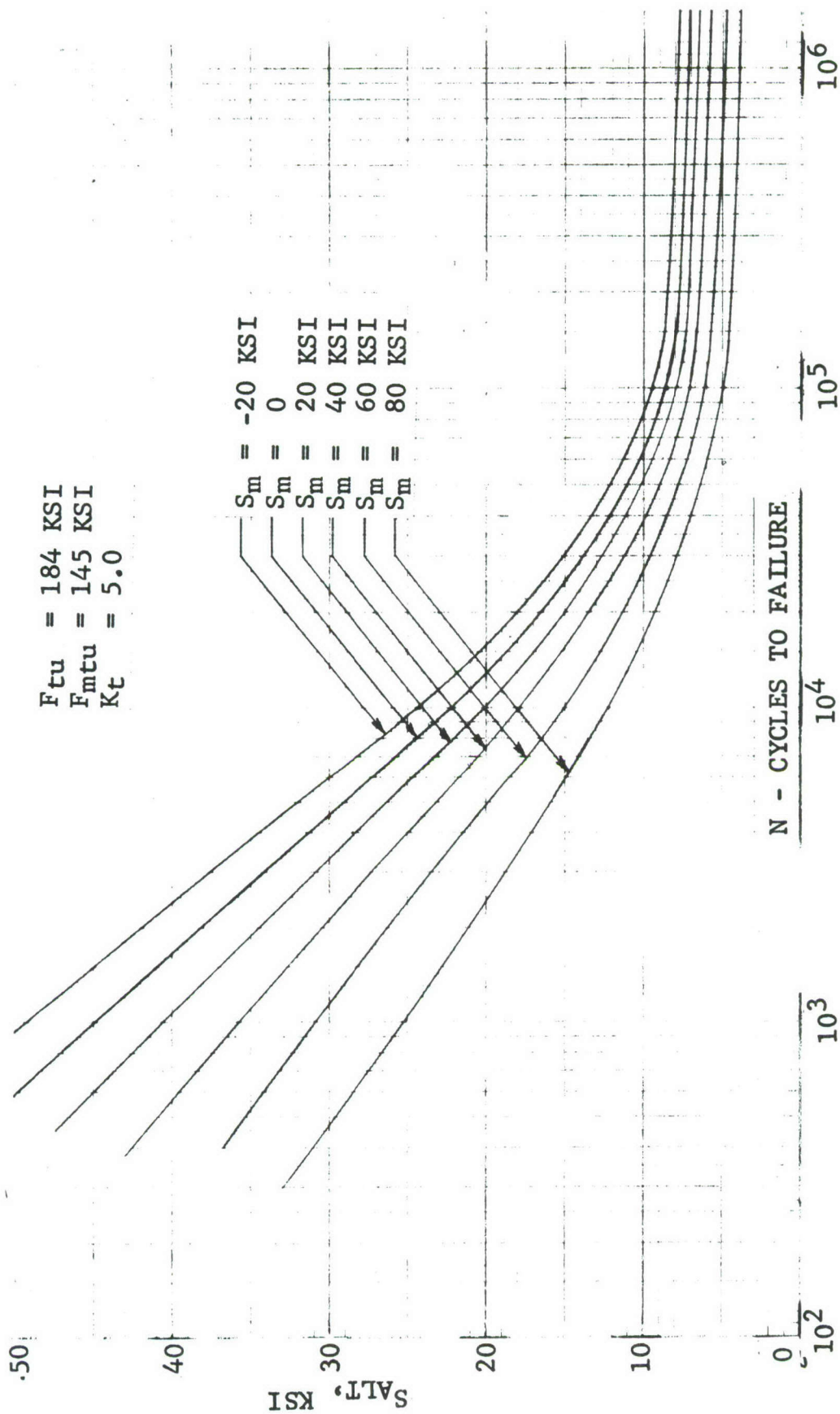


Figure 60 S-N Curves 8-8-2-3 Titanium 1/16-inch Sheet Longitudinal

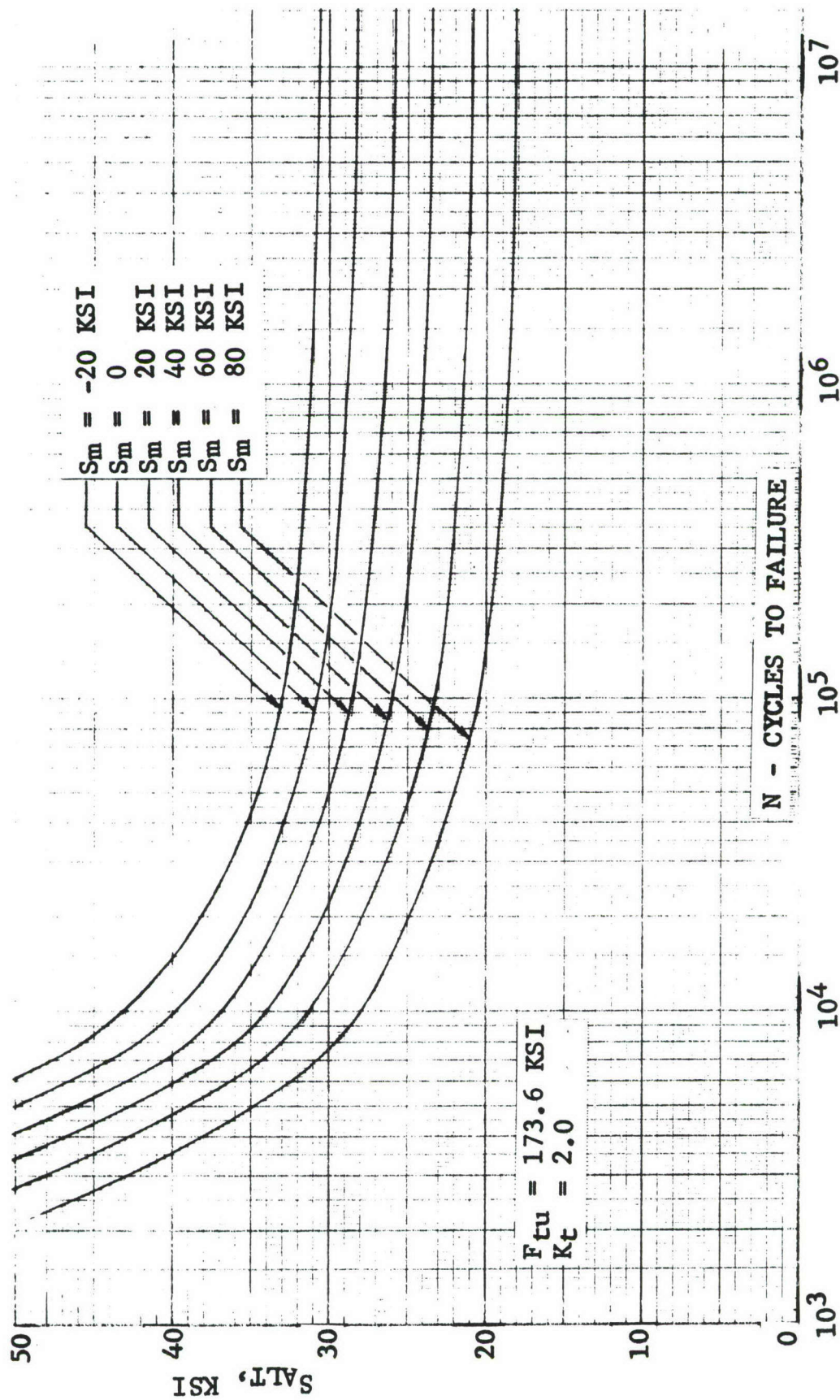


Figure 61 S-N Curves 8-8-2-3 Titanium 1-inch Plate Longitudinal Grain-Station

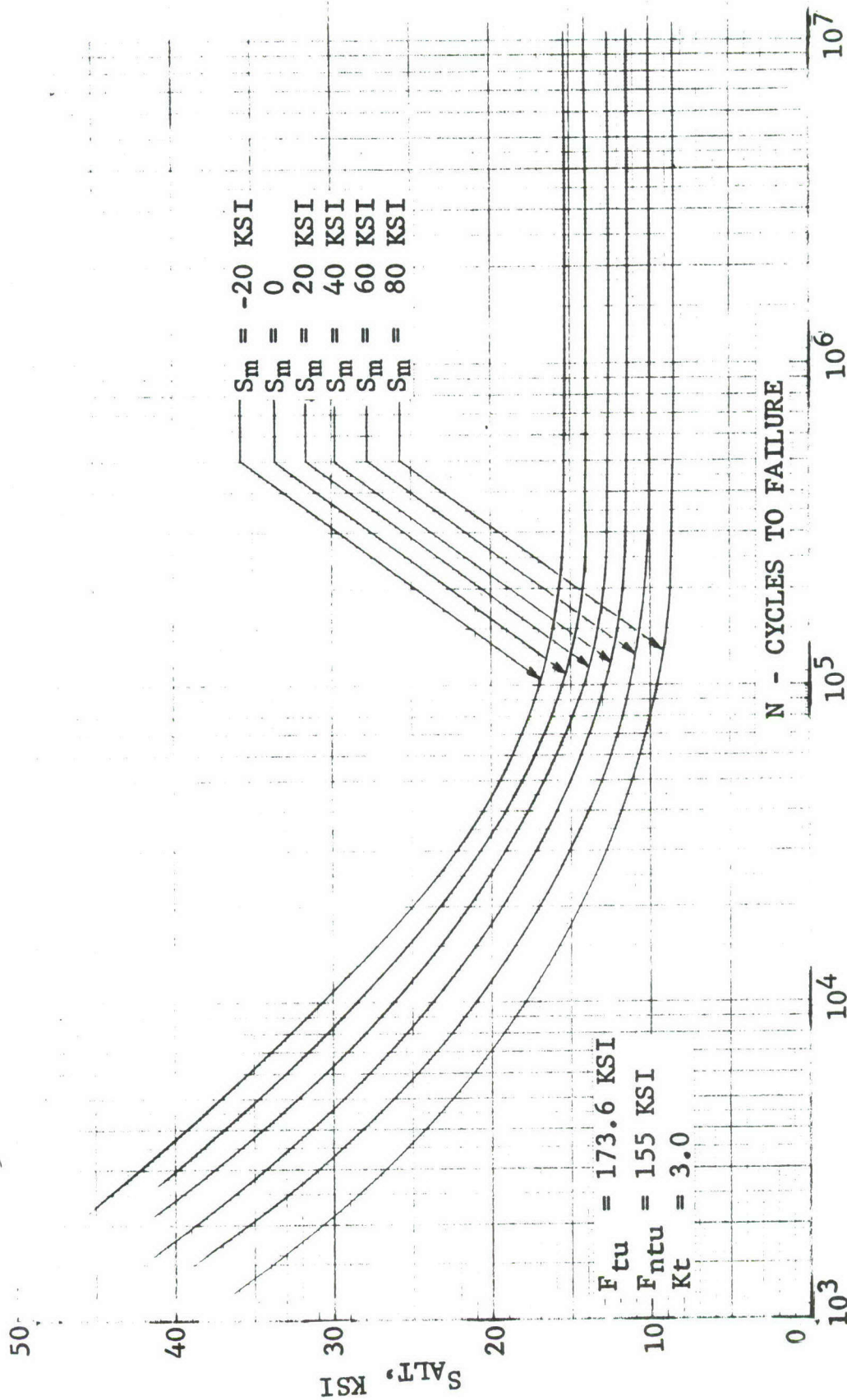


Figure 62 S-N Curves 8-8-2-3 Titanium 1-inch Plate Longitudinal Grain - Sta

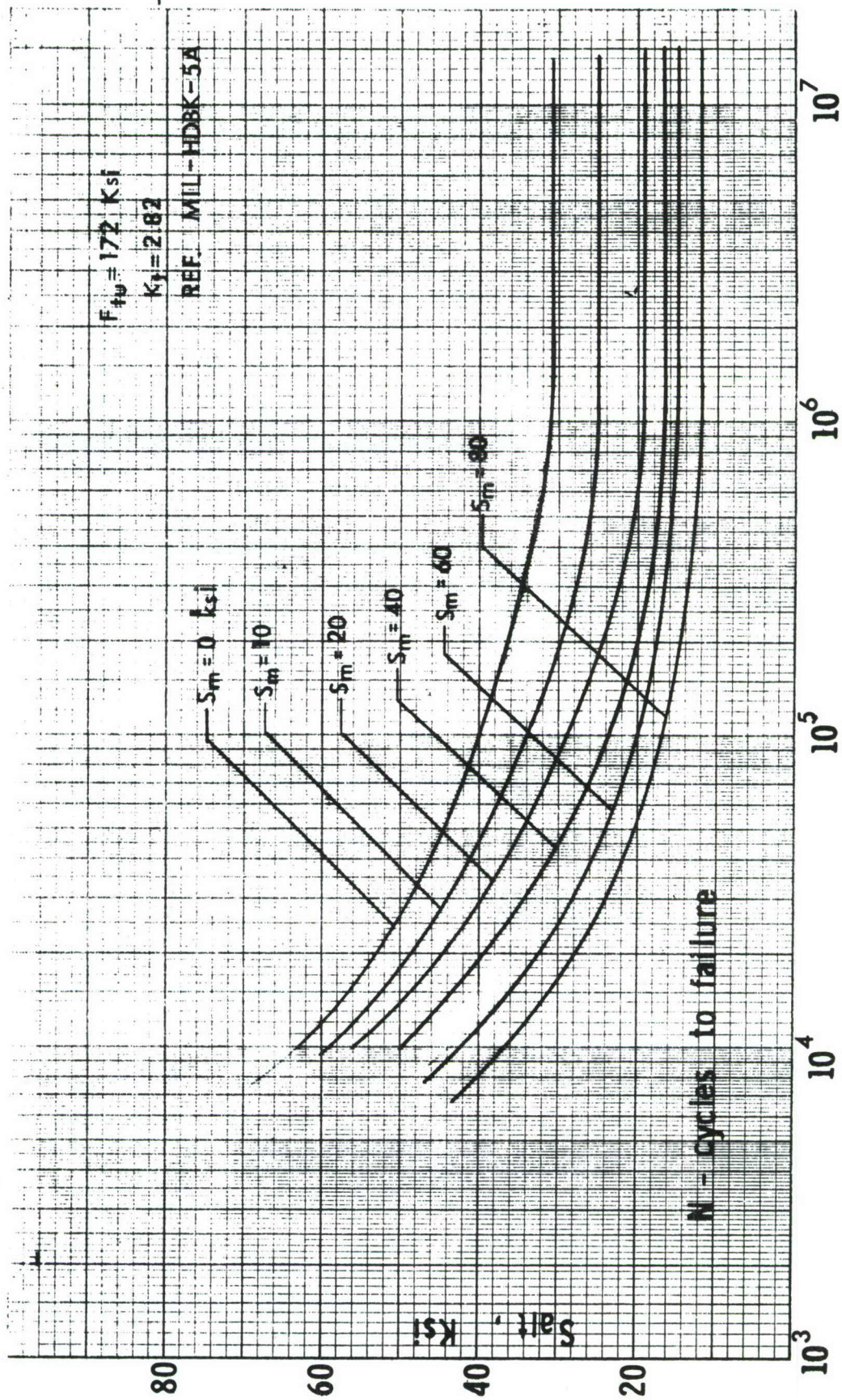


Figure 63 S-N Curves 6Al-4V Titanium Sta Sheet

6.2.3 Fatigue Quality Guidelines

The fatigue quality index is basically the stress concentration factor with certain limits on its application. It is a function primarily of design concept and detail. The index varies with the load spectrum and has more meaning when established by tests conducted on aircraft components whereby it is usually denoted as K_f . The upper limit fatigue quality index (K_f) for the baseline F-111F wing box lower surface is about 3.13 as determined from a full scale wing component tests. (See Section 3.3 for a discussion of F-111 wing component tests.) While no statistical significance can be attached to the baseline index of 3.13, this value was the basis for establishing an upper limit index of 3.0 as a goal for achieving good design detail at the lower surface of Phase IA designs. Accomplishing this goal contributed to extensive use of bonding and brazing techniques at the lower surface so that fastening systems could be eliminated. The use of bonding and brazing for the lower surface is judged to yield an index limit closer to 2.0 than 3.0. Substantiation of this will be an important part of the Phase IB test program where K_f values will be established using spectrum loaded tests of bonded and brazed components. Welds (including spot welds) and weld-bonding were assumed to have an index somewhere between 2.0 and 3.0; consequently, use of these techniques has been restricted to areas above the lower surface where stresses are significantly less. Again, substantiation will be required through fatigue testing.

The only holes present in the lower surface of the final Phase IA designs are those cutouts necessary for accommodating baseline pylons, access, etc. Special attention was given these areas by carefully providing local reinforcement to reduce stress levels. The fatigue quality index, or K_f , assumed for the worst case inboard pivot pylon location, was 2.5. This is based on a K_f value of 2.7 established from baseline development testing of lower skin panels with 6.5 inch diameter cutouts. Phase IA designs utilize an improved pivoting pylon arrangement requiring a larger 9.0 inch cutout. The $K_f = 2.5$ is simply $K_f = 2.7$ adjusted for the difference in cutout diameters.

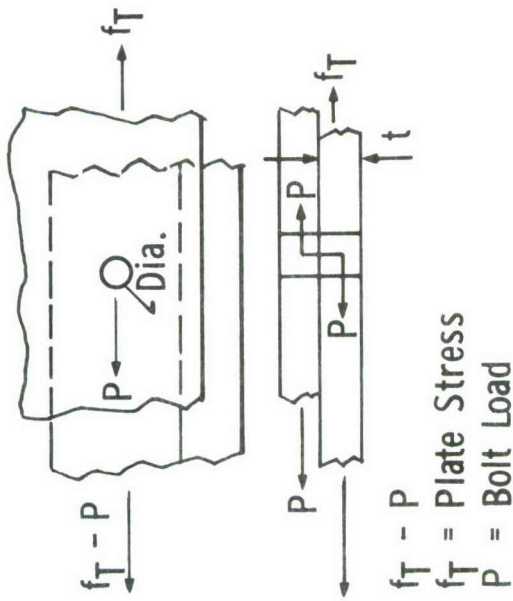
As stated in paragraph 6.2.1, the baseline spectrum does not produce significant tension in the upper wing surface to produce calculable fatigue damage since the upper surface is sized primarily for compression buckling; however, the upper surfaces of Phase IA designs utilize fasteners to provide for upper skin removal and access to the interior for inspection and repair. Stress concentration factors for upper surface

bolt holes are calculated using a procedure taken from Metal Fatigue by Sines and Waisman. This procedure accounts for the ΔK_T resulting from loaded fasteners as shown in Figure 64.

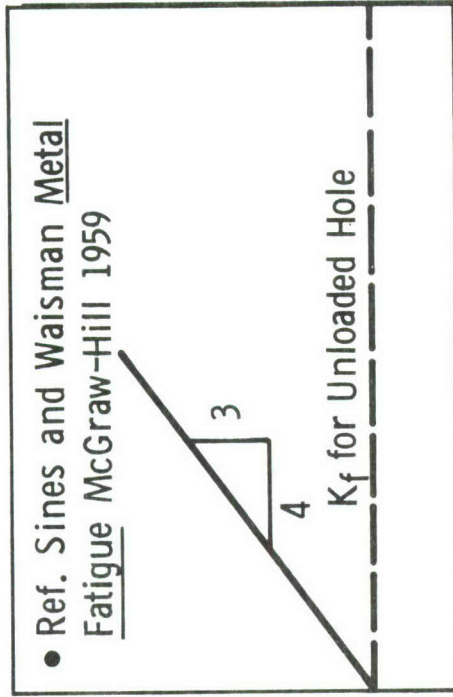
Fatigue analysis results, including assumed $K_{T,s}$ are summarized for selected fatigue control points in each of the top five Phase IA designs in paragraph 6.3 on preliminary design analysis.

STRESS CONCENTRATION FACTORS

• SINGLE SHEAR BOLT LOADS



Total K_T



$$\frac{\text{Bearing Stress}}{\text{Tension Stress}}$$

• TOTAL $K_T = K_T$ FOR UNLOADED HOLE + ΔK_T FOR LOADED HOLE EFFECT

$$\text{WHERE } \Delta K_T = .75 \left(\frac{\text{Bearing Stress}}{\text{Net Tension Stress}} \right) = .75 \left(\frac{\text{Bolt Load/Bolt Dia.} \times \text{Plate Thickness}}{f_T, \text{ Net Section}} \right)$$

• K_T Unloaded Holes

- Interference Fit Fasteners - $K_T = 1.9$ (BASED ON F-111 FATIGUE DEVELOPMENT TESTS)
- Non-Interference Fit Fasteners - $K_T = 3.0$ (OPEN HOLE)

Figure 64 Stress Concentration Factors

6.3 PRELIMINARY DESIGN ANALYSIS

Final Phase IA preliminary fatigue analyses have been prepared for selected control points in the five top rated wing designs and summarized in Table XXIX. The table also indicates the stress concentration factor (K_T) and the maximum operating tensile stress experienced at each control point. Maximum operating stress corresponds to the maximum load in the baseline fatigue spectrum, i.e., 15.6×10^6 in-lbs of net pivot bending moment. Selected control points are primarily located at the lower surface inboard areas of each design. Analyses were performed for an upper surface bolt hole control point on two designs to typically illustrate that fatigue damage at these points is zero. Control point locations are shown in Figures 65 through 69.

The selection of control points was based on a review of stresses and a review of drawings to locate areas of known or potential stress concentration. An example of potential stress concentration is the machined steps in the lower spar cap extrusions utilized by designs 610RW003 and 610RW007. While the step geometry is oriented parallel to the primary loading, the potential of having an inadvertant notch due to machining was accounted for.

Values of K_T were assigned using the guidelines discussed in paragraph 6.2.3. Phase IB fatigue development testing will establish K_f values for each of these areas in addition to possible other critical areas that may be determined in the detail design effort. It is anticipated that the preliminary values used for K_T in Table XXIX will prove to be conservative.

The fatigue damage calculated for each control point is less than 1.0. As previously stated, Miner's Rule was used for fatigue analysis ($\sum n/N = 1.0$ at failure). Therefore, each of the designs meet the fatigue requirements summarized in paragraph 6.1. The fatigue analysis results were also used as an input into the reliability analysis effort discussed in the following paragraph 6.4.

The three full wing designs finally recommended for further evaluation in the follow-on are 610RW003, 610RW002, and 610RW004. However, the fatigue analysis results for 610RW006 and 610RW007 were retained in Table XXIX for information.

Table XXIX ADVANCED AIR SUPERIORITY FIGHTER PRELIMINARY WING DESIGNS
FATIGUE DAMAGE SUMMARY

- o Baseline Phase I and Phase II Training Unrestricted Usage
- o Scatter Factor = 4.0 Included

WING CONFIGURATION (DWG. NO.) AND CONTROL POINTS	K _T	MAX. OPERATING TENSILE STRESS KSI	FATIGUE DAMAGE ($\sum n/N$)
7050 PL. TOP/LAM. LWR SKIN/CORR. SPARS (610RW003)			
o INBD PYLON CUTOUT	2.5	24.1	0
o MACHINE STEP AT F.A.S. [Inadv. Notch]	2.0	37.1	0.90
o WELD BOND AT F.A.S.	3.0	24.4	0.07
o UPPER SURFACE BOLT HOLE AT C.S.	3.4	6.9	0
7050 SANDWICH TOP AND BOTTOM (610RW004)			
o INBD PYLON CUTOUT	2.5	35.0	0.80
o WELD BOND AT F.A.S.	3.0	29.4	0.23
BRAZED SPACE TRUSS/8-8-2-3 LWR SKIN (610RW006)			
o INBD PYLON CUTOUT	2.5	58.5	0.80
o WELD AT F.S. WEB (6A1-4V STA TI)*	2.0	71.6	0.116
o WELD AT PYLON CUTOUT	2.0	41.2	0
o LWR SKIN-TO-DOUBLER BRAZE AT F.A.S.	2.0	92.2	0.63
o UPPER SURFACE BOLT HOLE AT C.S.	3.1	17.4	0
MULTI WET CELL 8-8-2-3 LWR SKIN AND SPARS (610RW002)			
o INBD PYLON CUTOUT	2.5	58.5	0.80
o WELD AT F.S. WEB (6A1-4V STA TI)*	2.0	47.0	0
o WELD AT PYLON CUTOUT	2.0	41.5	0
7050 HAT TOP/LAM. LWR SKIN (610RW007)			
o INBD PYLON CUTOUT	2.5	24.1	0
o MACHINE STEP AT F.A.S. [Inadv. Notch]	2.0	37.1	0.90

* Available S-N data for 6A1-4V STA was for K_T = 2.82. Therefore, calculated damage should be conservative.

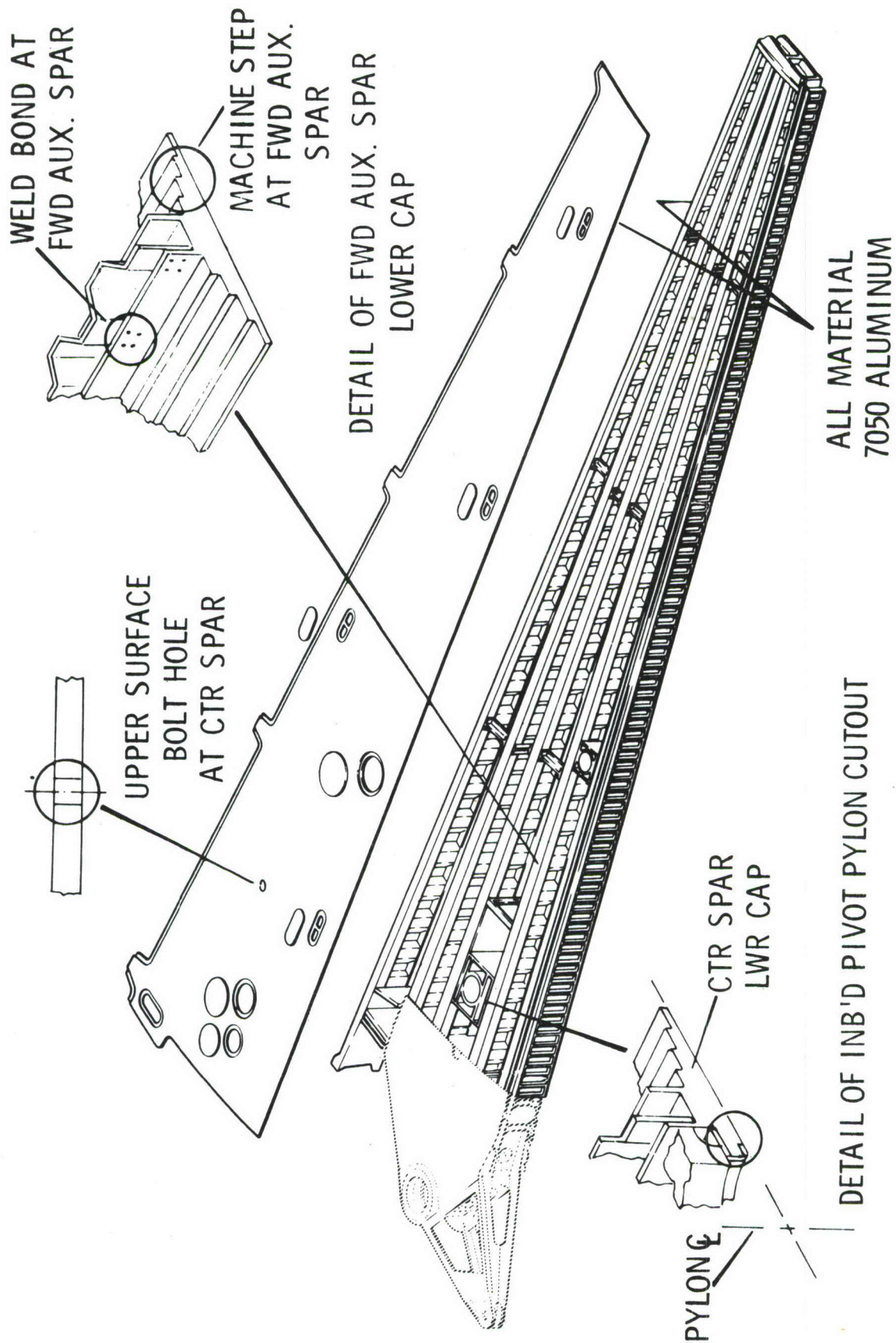


Figure 65 Corrugated Spar - Laminated Al Lower Skin Fatigue Control Points, Configuration 610RW003

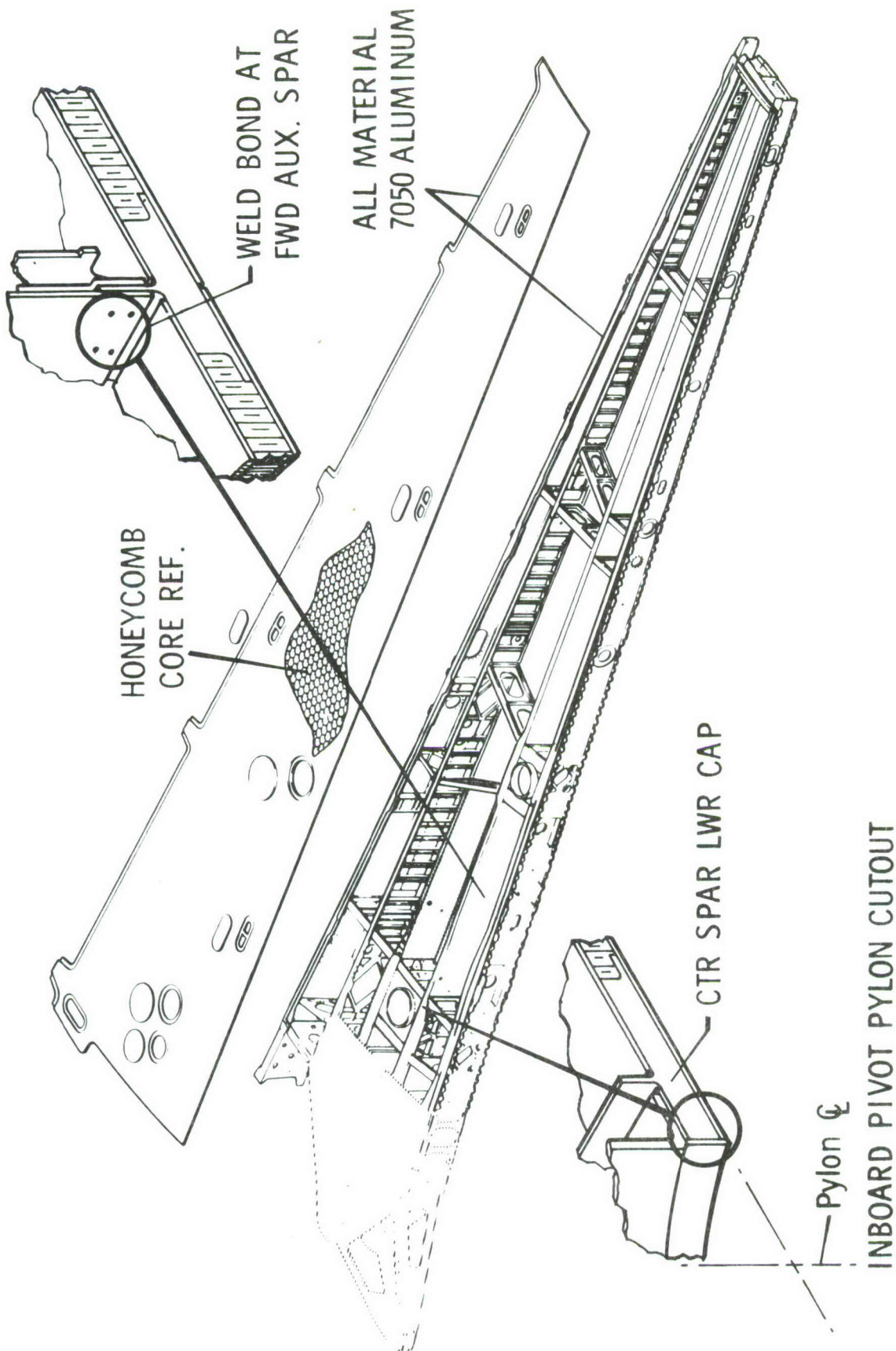


Figure 66 Adhesive Bonded Aluminum Honeycomb Panels
Fatigue Control Points, Configuration 610RW004

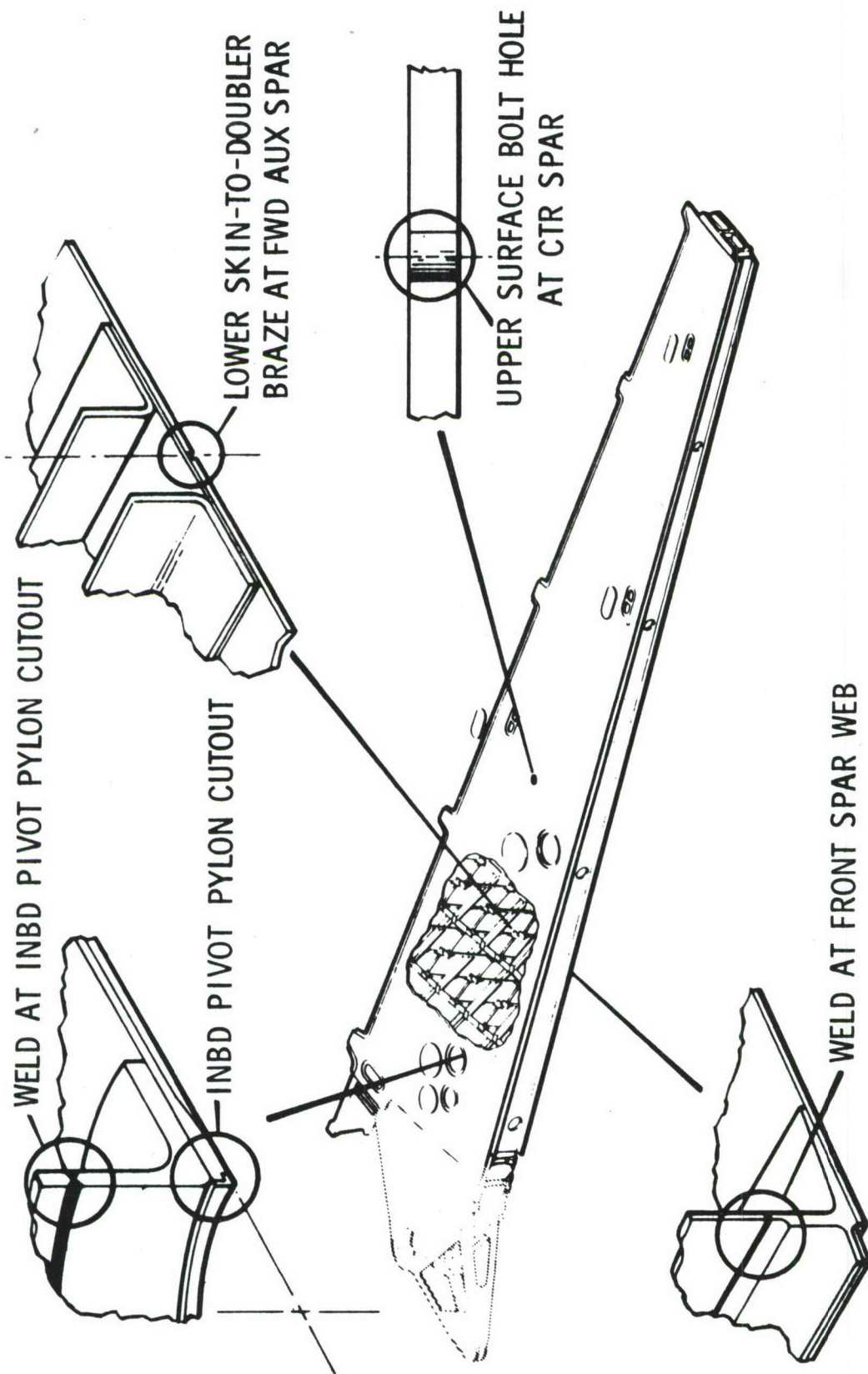


Figure 67 Brazed Titanium Space Truss Fatigue Control Points, Configuration 610RW006

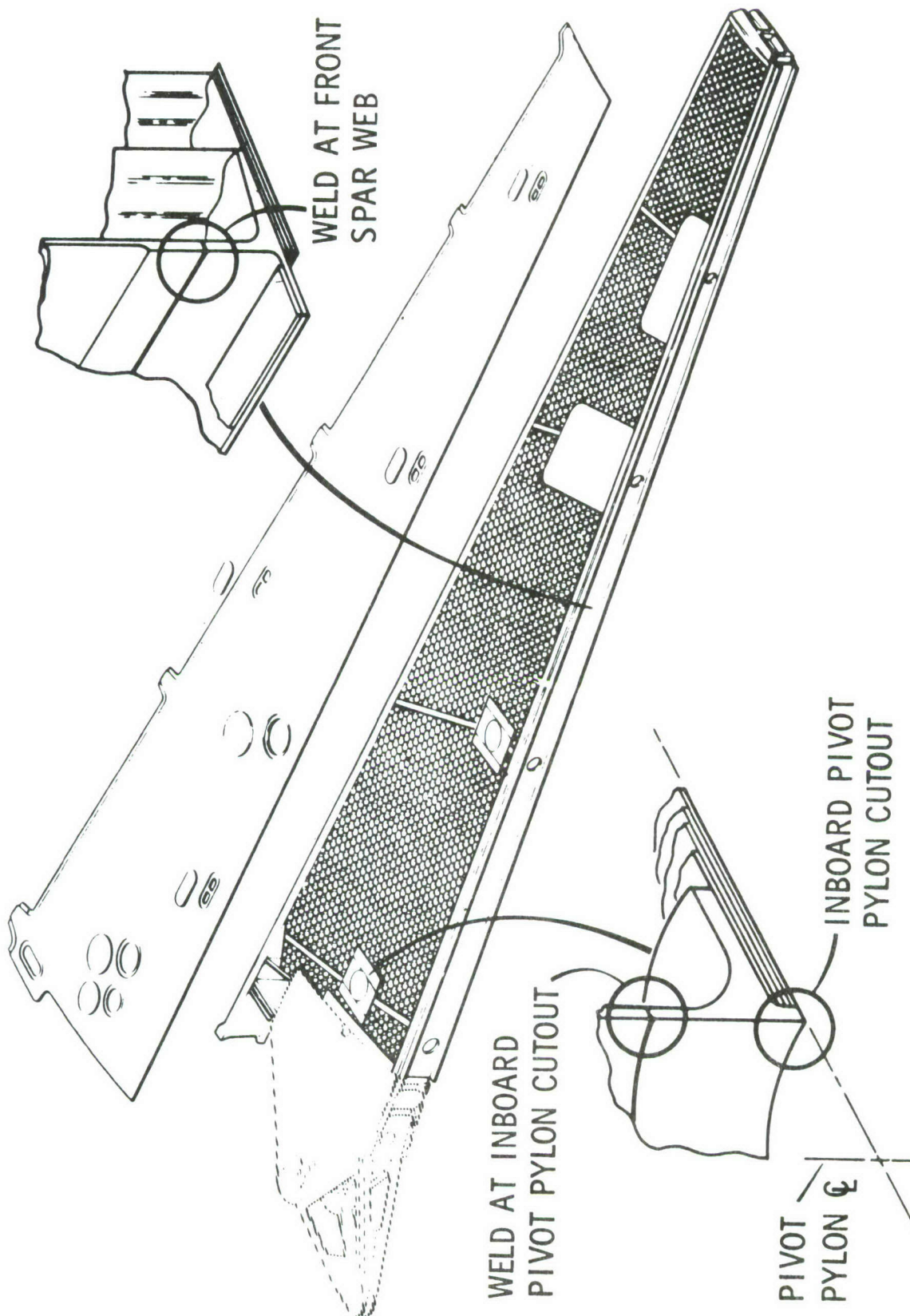


Figure 68 Multi-Wet Cell Construction Fatigue Control Points, Configuration 610RW002

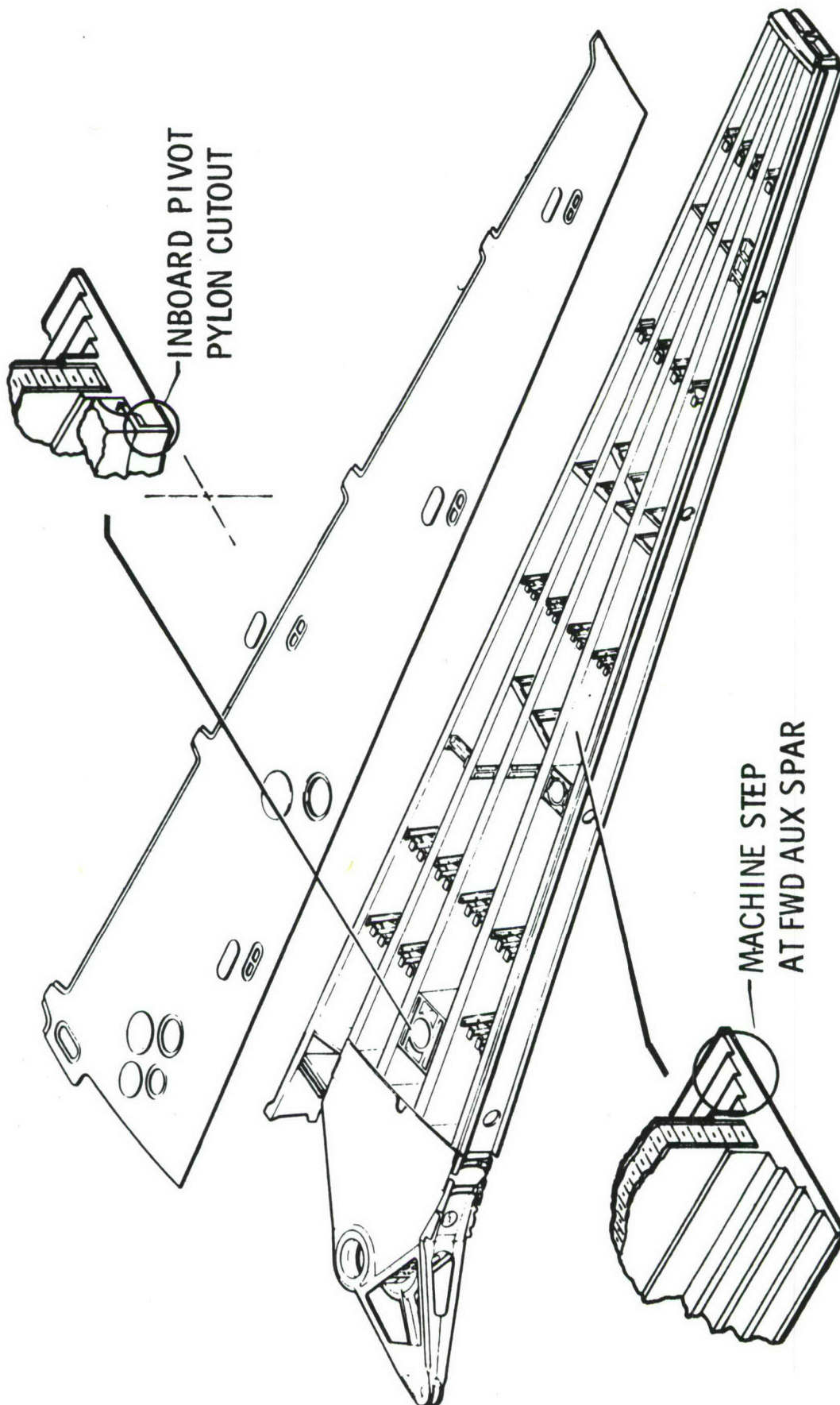


FIGURE 69 Figure 69 Bonded Aluminum Laminated Lower Panel: Hat Stiffener
Upper Panel Fatigue Control Points, Configuration 610RW007

6.4 RELIABILITY ANALYSIS

Scatter factor is a design and test allowance for fatigue variability. However, application of the factor of 4.0 does not bear a fixed relationship to life since material dispersions are unique. Another consideration is that design areas of structure that contribute to possibilities of fatigue failure may in effect have greater than minimum allowable scatter factor by reason of design criticality for fracture mechanics, crippling, etc. Also, with the scatter factor criterion, hazard as affected by fleet size isn't accounted for. Fatigue reliability prediction provides the means to quantitatively estimate probabilities of failure. Prediction analyzes the interaction of material statistical properties and their employment. AFML-TR-69-65 is an approach to such determination. However, in the interests of tangible support to initial design, the techniques are adapted to permit evaluation without the necessity of (but not excluding) after-the-fact full scale product test assessment.

Aircraft and fleet reliabilities are cumulative probability functions of failure frequency distributions of all significant fatigue control points. Predictions, Table XXX, were made for the most critical control points established by fatigue and stress analysis. In accordance with AFML-TR-69-65, GD/CAD, and other investigations, the Weibull probability distribution is accepted as the appropriate description of structural life scatter. The Weibull distribution is characterized by the values of its "a" shaping (dispersion) and "b" scaling (location) parameters. Use of this approach is described below.

1. Weibull shape parameters "a" were derived from material endurance test data generated in this program and from other sources as noted in the following tabulation. Translation between stress levels enhanced the statistical base. Programmed computation by the maximum - likelihood estimation method was used to determine "a".

$$\hat{a} = \frac{n \sum_{i=1}^n t_i^{\hat{a}}}{n \sum_{i=1}^n t_i^{\hat{a}} \ln t_i - \sum_{i=1}^n t_i^{\hat{a}} \sum_{i=1}^n \ln t_i}$$

where n = number of life observations
t_i = individual life observations

Table XXX FATIGUE RELIABILITY PREDICTIONS FOR 506 VEHICLE FLEET

PRELIM DESIGN 610RW-	MOST CRITICAL CONTROL POINT (SEE SEC. 6.3)	PROBABILITY OF NO MORE FAILURES THAN					HR, EVERY VEHICLE, FOR 50% PROBAB OF 1 st FLEET FAILURE
		0	1	2	3	4	
002	Inbd pylon hole lwr skin, 2 pt /hole, 2 wg	.95	1.00	1.00	1.00	1.00	6059.
003	FAS lwr cap step inadvert mach notch, 1 wg, 1 place	.80	.98	1.00	1.00	1.00	5048.
004	Inbd pylon hole lwr skin, 2 pt /hole, 2 wg	.50	.85	.97	.99	1.00	4003.
006	Inbd pylon hole lwr skin dblr, 2 pt/hole, 2 wg	.95	1.00	1.00	1.00	1.00	6059.
007	FAS lwr cap step inadvert mach notch, 1 wg, 1 place	.80	.98	1.00	1.00	1.00	5048.

NOTE: Any failure is the fracture of only an element in multiple load paths, resulting in fractional loss of wing strength.

It was found that scatter apparently becomes greater with decreasing fatigue stress for a material. Smaller "a" values represent greater scatter.

<u>MATERIAL</u>	<u>FATIGUE TEST</u>	<u>"a"</u>
Al 2024-T851 2" plate	R = 0.1; K_t = 3.0; 40 KSI (GD/CAD F-111 Tests)	3.08
Al 2024-T851 2" plate	R = 0.1; K_t = 3.0; 20 KSI (Preceding test)	2.57
Al 7050-T76 .063 sh	R = 0.1; K_t = 3.0; 20 KSI (GD/CAD tests)	4.7
Al 7050-T76 .063 sh	R = 0.0; K_t = 3.0; 25 KSI (Alcoa data)	4.1
Al 7050-T73651 3" plate	R = 0.1; K_t = 3.0; 20 KSI (GD/CAD tests)	4.9
Al 7475-T761 .125 sh	R = 0.1; K_t = 3.0; 20 KSI (GD/CAD tests)	1.69
Al 7475-T761 .125 sh	R = 0.1; K_t = 3.0; 25 KSI (Preceding test)	2.3
Al 7475-T761 .090 sh	R = 0.1; K_t = 3.0, 20 KSI (AFML/U Dayton Tests)	1.42
Al 7475-T761 .090 sh	R = 0.1; K_t = 3.0; 25 KSI (Preceding AFML test)	3.8
Al 7475-T7351 3" plate	R = 0.1; K_t = 3.0; 20 KSI (GD/CAD tests)	6.3
Ti 6-4 STA .125 sh	R = 0.1; K_t = 4.2; 40 KSI (GAEC data)	3.9
Ti 8-8-2-3 .12 sh	R = 0.1; K_t = 3.0; 50 KSI (GD/CAD tests)	6.3
Ti 8-8-2-3 1" plate	R = 0.1; K_t = 2.0; K_t = 3.0 (GD/CAD tests)	Data Insuff

2. Weibull scale parameters "b" were based on analytically estimated operational fatigue damage at the wing box structure critical control points. AFML-TR-69-65 advocates only full scale testing for this purpose, so as to realistically incorporate effects such as size, stress distribution, quality, load response, fretting, environment, etc. However, analysis at this stage as possible, that can be taken in conjunction with particular case limitations, is preferable to foregoing available indications and comparisons. Parameter "b" is calculated from the first moment relationship.

$$t_m = b \int (1/a + 1)$$

where t_m = expected mean life

\int = standard gamma function

Mean design life is 16000 hour (design service life of 4000 hour with 4.0 scatter factor) but, with design generally critical in fracture mechanics instead of fatigue, expected mean life is greater than 16000 hour since Miner cumulative damage is less than 1.0 at design life. Parameter "b" is characteristic mortality with 63.2% of population lives this value or less.

PRELIM DESIGN 610RW-	CONTROL POINT	$\Sigma(n/N)$ DAMAGE 16000 HR	MEAN LIFE $= \frac{16000}{\Sigma(n/N)}$	CHARAC- TERISTIC MORTALITY "b"
002	Same as Table XXX	0.8	20,000	21,501
003		0.9	17,778	19,385
004		0.8	20,000	21,861
006		0.8	20,000	21,501
007		0.9	17,778	19,385

3. Vehicle reliability, R_{veh} , is a series probability, the product of individual control point reliabilities R_{cp} . The Weibull reliability of each control point is

$$R_{cp} = \exp\left(-\left(\frac{t}{b}\right)^a\right), \text{ with } t \text{ design service life of } 4000 \text{ hour}$$

PRELIM DESIGN 610RW-	CONTROL POINT	INDIV CONTR PT RELIAB R_{cp}	VEH RELIAB R_{veh}
002	Same as Table XXX	.999975	.999900 (= R_{cp}^4)
003		.999562	.999562 (= R_{cp})
004		.999659	.998637 (= R_{cp}^4)
006		.999975	.999900 (= R_{cp}^4)
007		.999562	.999562 (= R_{cp})

4. Fleet reliability is expressed as probabilities of no more than 0, 1, 2, etc. vehicle failures. Binomial distribution is applicable. See Table XXX.

$$f(n) = \frac{N!}{n!(N-n)!} (1-R_{veh})^n R_{veh}^{N-n}, \text{ probability of exactly } n$$

in a fleet of N, vehicles failing.

$$\text{Probab of No more than } n \text{ Failures} = \sum_{n=0}^n f(n)$$

5. Time to first fleet failure is another useful index. This is a solution for Weibull t corresponding to the probability of all failures except zero. See Table XXX.

$$t = b \left(\frac{\ln(1 - F_{ff})}{-Nc} \right)^{1/a}, \text{ service time for each and every}$$

vehicle in the fleet, each vehicle having "c" control points of like Weibull "a" and "b" to attain F_{ff} probability of the first failure in the fleet.

S E C T I O N V I I

F R A C T U R E A N A L Y S I S

7.1 FRACTURE CONTROL SUMMARY

The engineering concept of fracture mechanics was utilized throughout Phase IA as primary technology in providing damage tolerant design. Fracture analyses were performed for the purposes of (1) developing fracture design data (allowables) and (2) verifying that the final selected designs meet the damage tolerance criteria.

The detail requirements (Revision D version) proposed by the Air Force for incorporation as a possible revision to MIL-A-8866A were utilized in Phase IA. This constitutes the first time an attempt has been made to meet such detailed requirements on a design program. In addition, extensive criteria sensitivity studies were performed to assess the impact (including cost) of these requirements on the baseline structure.

Structural design support was provided to help reduce potential crack initiation sites (stress concentrations) and ensure damage containment. The result has been elimination of fastener systems in the lower surface through expanded use of bonding, brazing and welding concepts, and the evolvement of multielement crack arrest wing designs. Interpretation of the damage tolerance criteria, including emphasis on increased accessibility for inspection and repair of fail safe structure, has been provided for the design team.

Material selection guidelines have been met with good success for each of the materials utilized in the final Phase IA wing design selections. These guidelines are as follows:

- (1) $K_{IC} \geq \sigma_{ys}(t)^{\frac{1}{2}}$
- (2) $K_{ISCC} \geq K_{IC}/2$
- (3) Comparative surface flaw da/dN screening data tested at 6 cpm and 60 cpm in a corrosive environment.

This data is presented in Section VIII under Materials Engineering.

Additional elements of fracture control, encompassing the efforts of all involved disciplines, have been detailed as a fracture control plan to be utilized in subsequent follow-on phases of this program. The fracture control plan was developed in connection with the baseline damage tolerance assessment and is given in paragraph IX.3.8 of Appendix IX.

7.2 DAMAGE TOLERANCE CRITERIA

The pertinent damage tolerance requirements of MIL-STD-1530, "Aircraft Structural Integrity Program, Airplane Requirements," dated 1 September 1972, and MIL-A-8866A (USAF) were applicable to Phase IA including the detail requirements being proposed by the Air Force as a revision to MIL-A-8866A, dated 18 August 1972. The damage tolerance requirements are summarized in Tables XXXI.

The residual strength requirements for flawed structure have been made somewhat more complicated by the proposed criteria. Residual strength is now specified in terms of P_{xx} and P_{yy} . P_{yy} is simply P_{xx} times a dynamic factor (suggested as 1.15) associated with element failure or crack arrest. P_{xx} is the one occurrence load level associated with degree of inspectability and is determined from a load exceedance curve representing the amount of flight time required as an inspection interval times a factor (10 for fighter type aircraft). Studies were made using this approach on the baseline (see paragraph IX.3.10 of Appendix IX) and results indicated that there was little variation in the one occurrence load level for different degrees of inspectability. This was due to a combination of the well defined nature of the current baseline spectrum, the current operating limits, and the technique used to extrapolate the load exceedance curve down to the one time level. It was therefore decided to use P_{LT} (life-time) or the one time load in (4000×10) hours as the single residual strength requirement for evaluation of preliminary wing designs. This was done whether designing for depot or non-inspectable requirements.

7.2.1 Design Service Loads Spectrum

The design service loads spectrum used in Phase IA was identical to the baseline fatigue spectrum. The spectrum was simplified for use in flaw growth calculations consistent with similar procedures used during the F-111 Recovery Program.

Table XXXI PROPOSED DAMAGE TOLERANCE REQUIREMENTS

SLOW CRACK GROWTH STRUCTURE


DEGREE OF INSPECTABILITY	FREQUENCY OF INSPECTION	MIN. PERIOD OF UNREPAIRED SERVICE USAGE (F _{XX})	MIN. REQ'D RESIDUAL STRENGTH (P _{XX})	MIN. ASSUMED INITIAL DAMAGE SIZES (a)	MIN. ASSUMED IN-SERVICE DAMAGE SIZES (1)	DAMAGE GROWTH LIMITS
IN FLIGHT EVIDENT N/A						
GROUND EVIDENT N/A						
WALK AROUND VISUAL	SPECIFIED IN CONTRACT DOCUMENTS (10 FLTS. TYPICAL)	5 x FREQ (F _{WV})	P _{WV}	$aQ = 0.10$ OR 0.05"  OR SMALLER IF DEMONSTRATED TO .9 P(d) @ 95% C.L.	2" Open thru Crack Unless Detection of Smaller Sizes Demonstrated	1 Shall not grow to critical @ P _{WV} in F _{WV} a Shall not grow to critical @ P _{DM} in F _{DM}
SPECIAL VISUAL	SPECIFIED IN CONTRACT DOCUMENTS (1 YR TYP)	2 x FREQ (F _{SV})	P _{SV}		(aQ) DM On A/P and Off A/P	1 Shall not grow to critical @ P _{SV} in F _{SV} a Shall not grow to critical @ P _{DM} in F _{DM}
DEPOT OR BASE LEVEL	SPECIFIED IN CONTRACT DOCUMENTS (1/4 LIFE-TIME TYP.)	2 x FREQ (F _{DM})	P _{DM}			1 Shall not grow to critical @ P _{DM} in F _{DM} a Shall not grow to critical @ P _{DM} in F _{DM}
NON INSPECTABLE	N/A	² LIFETIMES (F _{LT})	P _{LT}		N/A	a Shall not grow to critical @ P _{LT} in F _{LT}

Table XXXI (Cont'd) PROPOSED DAMAGE TOLERANCE REQUIREMENTS

FAIL SAFE - MULTIPLE LOAD PATH STRUCTURE





DEGREE OF INSPECT-ABILITY	FREQUENCY OF INSPECTION	MIN. PERIOD OF UNREPAIRED SERVICE USAGE (F _{XX})	MIN. REQ'D RESIDUAL STRENGTH (P _{XX})	MIN. ASSUMED INITIAL DAMAGE SIZE			MIN ASSUMED IN-SERVICE DAMAGE SIZE	DAMAGE GROWTH LIMITS
				INTACT NEW STRUCTURE (a ₁)	REMAINING STRUCTURE DEPENDENT LOAD PATH (a ₂)	INDEPENDENT LOAD PATH (a ₃)		
IN FLIGHT EVIDENT	N/A	RETURN TO BASE (F _{FE})	P _{FE}	a/Q = .03 and 	Failed Load Path Plus a ₁ + Δa in Adjacent Load Paths	Failed Load Path Plus a/Q = 0.1 or 		a ₁ Shall not Grow to Critical @ P _{DM} in F _{DM} a ₂ or a ₃ Shall not Grow to Critical @ P _{FE} in F _{FE}
GROUND EVIDENT	EVERY FLIGHT	ONE FLIGHT (F _{GE})	P _{GE}	or Smaller if Demonstrated to .9 P(d) @ 50% C.L.			a ₂ or a ₃	a ₁ Shall not Grow to Critical @ P _{DM} in F _{DM} a ₂ or a ₃ Shall not Grow Critical @ P _{GE} in F _{GE}
WALK AROUND VISUAL	SPECIFIED IN CONTRACT DOCUMENTS (10 FLIGHTS TYPICAL)	5 x FREQ (F _{WV})	P _{WV}		or 2" Crack Plus a ₁ + Δa in Adjacent Load Paths	Δa in Adjacent Load Paths or 2" Crack Plus		a ₁ Shall not Grow to Critical @ P _{DM} in F _{DM} a ₂ or a ₃ Shall not Grow Critical @ P _{WV} in F _{WV}
SPECIAL VISUAL	SPECIFIED IN CONTRACT DOCUMENTS (ONE YEAR TYPICAL)	2 x FREQ (F _{SV})	P _{SV}			2" Crack Plus a/Q = .01 or 		a ₁ Shall not Grow to Critical @ P _{DM} in F _{DM} a ₂ or a ₃ Shall not Grow Critical @ P _{SV} in F _{SV}
DEPOT OR BASE LEVEL	SPECIFIED IN CONTRACT DOCUMENTS (1/4 LIFETIME TYPICAL)	2 x FREQ (F _{DM})	P _{DM}		Adjacent Load Paths	or + Δa in Adjacent Load Paths	(a/Q) DM as Specified in 2.3.5	a ₁ Shall not Grow to Critical @ P _{DM} in F _{DM} a ₂ or a ₃ Shall not Grow Critical @ P _{DM} in F _{DM} (a/Q) DM Shall not Grow to Critical @ P _{DM} in F _{DM}
NON INSPECTABLE	N/A	ONE LIFETIME (F _{LT})	P _{LT}				N/A	a ₁ Shall not Grow to Critical @ P _{LT} in F _{LT} a ₂ or a ₃ Shall not Grow to Critical @ P _{LT} in F _{LT}

Table XXXI (Cont'd) PROPOSED DAMAGE TOLERANCE REQUIREMENTS

FAIL SAFE - CRACK ARREST STRUCTURE

DEGREE OF INSPECT-ABILITY	FREQUENCY OF INSPECTION	MIN. PERIOD OF UNREPAIRED SERVICE USAGE (F _{XX})	MIN. REQUIRED RESIDUAL STRENGTH (P _{XX})	MIN ASSUMED INITIAL DAMAGE SIZE		MIN. ASSUMED IN-SERVICE DAMAGE SIZE (1)	DAMAGE GROWTH LIMITS
				INTACT NEW STRUCTURE a ₁	IN REMAINING STRUCTURE a ₂		
IN FLIGHT EVIDENT	N/A	RETURN TO BASE (F _{FE})	P _{FE}	$a/Q = 0.03$  or Smaller if Demonstrated to .9 P(d) @ 50% C.L.	2 Cracked Skin Panels Plus Failed Central Stringer (or equivalent)	2 Cracked Skin Panels Plus Failed Central Stringer (or Equivalent)	a ₁ Shall not Cause Initial Rapid Propagation @ P _{DM} in F _{DM} 1 Shall not Cause Complete Failure @ P _{FE} in F _{FE}
GROUND EVIDENT	EVERY FLIGHT	ONE FLIGHT (F _{GE})	P _{GE}				a ₁ Shall not Cause Initial Rapid Propagation at P _{DM} in F _{DM} 1 Shall not Cause Complete Failure @ P _{GE} in F _{GE}
WALK AROUND VISUAL	SPECIFIED IN CONTRACT DOCUMENTS (10 FLIGHTS TYPICAL)	5 x FREQ (F _{FW})	P _{WV}				a ₁ Shall not Cause Initial Rapid Propagation @ P _{DM} in F _{DM} 1 Shall not Cause Complete Failure @ P _{WV} in F _{WV}
SPECIAL VISUAL	SPECIFIED IN CONTRACT DOCUMENTS (ONE YEAR TYPICAL)	2 x FREQ (F _{SV})	P _{SV}				a ₁ Shall not Cause Initial Rapid Propagation @ P _{DM} in F _{DM} 1 Shall not Cause Complete Failure @ P _{SV} in F _{SV}
DEPOT OR BASE LEVEL	SPECIFIED IN CONTRACT DOCUMENTS (1/4 LIFETIME TYPICAL)	2 x FREQ (F _{DM})	P _{DM}				a ₁ Shall not Cause Initial Rapid Propagation @ P _{DM} in F _{DM} 1 Shall not Cause Complete Failure @ P _{DM} in F _{DM}

Simplification was attained by reducing the initial 23 maneuver usage blocks to 9 usage blocks. The resulting block type spectrum was considerably shortened while still representing 4000 hours of baseline usage in a conservative manner. The spectra was arranged in 200-hour blocks and then the load levels were randomly ordered. Additional discussion of the rationale for simplifying the baseline spectrum is given in Appendix VI.

A composite flight-by-flight spectrum has been developed in Phase IA for immediate use in the follow-on program. A comparison of the flight-by-flight (F x F) and block spectra has been made regarding the effect on predicted flaw growth. The results are summarized in Figure 70 and show very good agreement with the block spectrum being slightly on the conservative side. To conserve computer time (one of the principal reasons for using a block spectrum), runs equivalent to one 200-hour block were made with the F x F spectrum using four different initial flaw sizes. The delta growth increment was compared with delta growth obtained using the random load level block spectrum at similar initial flaw sizes. The comparative analysis was made for a part through flaw in the baseline lower skin.

7.2.2 Design Environment Definition

The design environment used in Phase IA was also identical to the baseline environment. The thermal environment has been established through an analysis of the design mission profiles for tropical, standard and polar days. Temperature extremes considered in fracture and fatigue analyses include:

- (1) Minimum structural temperature: Standard Day + 10°F
- (2) Maximum temperature: Standard Day + 255°F.

For design purposes, the principal exposures to corrosive environment are as follows:

<u>Flight Exposure</u>	<u>% Flt. Time</u>
Humidity: 75% Relative	45.8
Condensation	3.7
Rain	0.7
Dry Air	49.8
JP-4 Fuel	100.0 (Internal)

FLT X FLT SPECTRUM			BLOCK SPECTRUM		
$2c_0$, IN.	$2c_1$, IN.	$\Delta 2c$	$2c_0$, IN.	$2c_1$, IN.	$\Delta 2c$
0.15000	0.15083	0.00083	0.15000	0.15089	0.00089
0.20067	0.20228	0.00161	0.20053	0.20252	0.00199
0.30000	0.30611	0.00611	0.29971	0.30585	0.00614
0.80000	0.84285	0.04285	0.80222	0.85245	0.05023

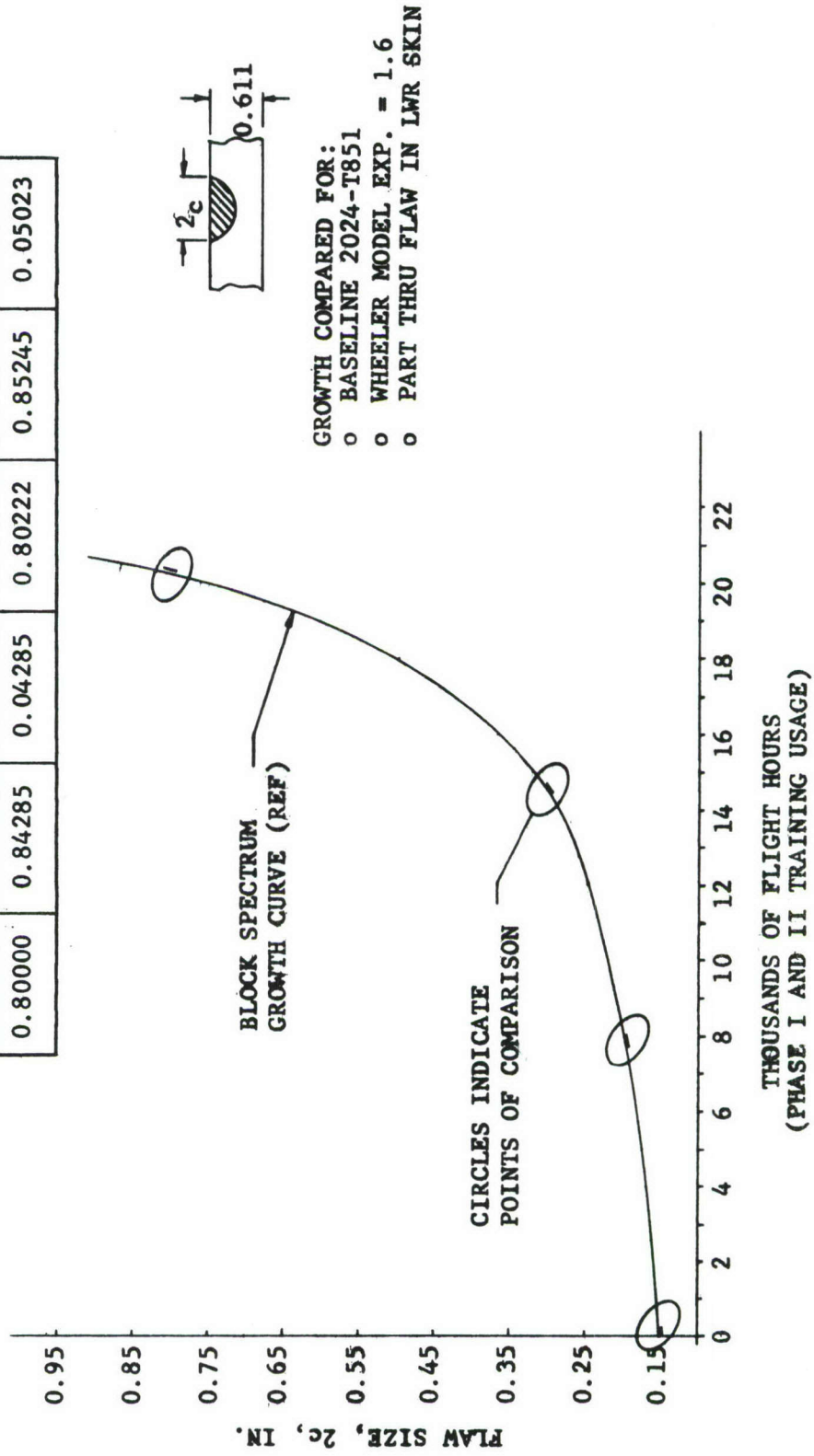


Figure 70 Block Spectrum vs. Flight by Flight Spectrum for Flaw Growth Analysis

<u>Ground Exposure</u>	<u>% Ground Time</u>
Humidity: 50- 75% Relative	35.2
75-100% Relative	34.1
Condensation	19.7
Rain	11.0
JP-4 Fuel	100.0 (Internal)

The above corrosive exposure criteria were established through analysis of planned geographic location and planned mission usage during service. The baseline wing box is a fuel tank so the most significant exposure at the critical lower surface is JP-4 fuel.

The details of the work done to establish both thermal and chemical environment for the baseline are included in paragraph IX.3.5 of Appendix IX.

7.3 CONCEPT ANALYSIS AND EVALUATION

Evaluation of cross section and analytical assembly concepts has been accomplished primarily through development of fracture design data sheets. These data sheets indicate the interaction between stress and initial flaw size for a given period of airplane life. They were generally used by the design team to establish allowable stress levels for the critical lower surface. Preliminary design data was generated for each of the materials selected for evaluation in Phase IA. When the necessary material data (da/dN) was not available, representative data for similar materials was used until test data could be generated. Flaw types initially assessed included both bolt holes and surface flaws. The preliminary allowables required to tolerate bolt hole flaws quickly substantiated the early decision to eliminate fasteners in the lower surface to enable achievement of minimum weight. Design data was not generated for the upper surface for the same reasons given in paragraph 6.2.1 on fatigue design data--very little significant tensile stress is experienced by the upper surface. A fracture analysis for one upper surface bolt hole flaw case was performed on preliminary design 610RW006 to illustrate this (paragraph 7.4).

7.3.1 Fracture Design Data

Fracture design (allowable) data curves were prepared early in Phase IA using preliminary fracture data. The general development procedure is depicted in Figure 71 and specifically involved the following:

- (1) For each anticipated flaw type and thickness, flaw growth analyses were performed to establish a series of growth curves representing a range of factors on stress level.
- (2) From (1) the maximum initial flaw size that permitted one interval of subsequent growth as a function of the maximum stress in the spectrum was determined. The interval selected was a function of the specified period of unrepaired service usage for the applicable degree of inspectability.
- (3) The allowable spectrum stress was plotted as a function of initial flaw size.
- (4) The allowable spectrum stress level was determined from the plot in (3) in accordance with the initial flaw size and period of unrepaired service usage requirements.

Procedures and assumptions used in the Phase IA fracture analysis effort are discussed in paragraph 7.3.2. The basic fracture data utilized for analysis in Phase IA are discussed in paragraph 7.3.3.

Fracture design data curves applicable to the flaw types and materials utilized in the selected preliminary wing designs are shown in Figures 72 through 75. The data shown in Figure 73 for a part through flaw in a relatively thick 7050-T73651 aluminum plate (spar cap) includes, for comparison, a curve representing the 8000-flight-hour requirement associated with noninspectable slow crack growth structure. The advantage, from a minimum weight point of view, of designing fail safe structure is readily apparent.

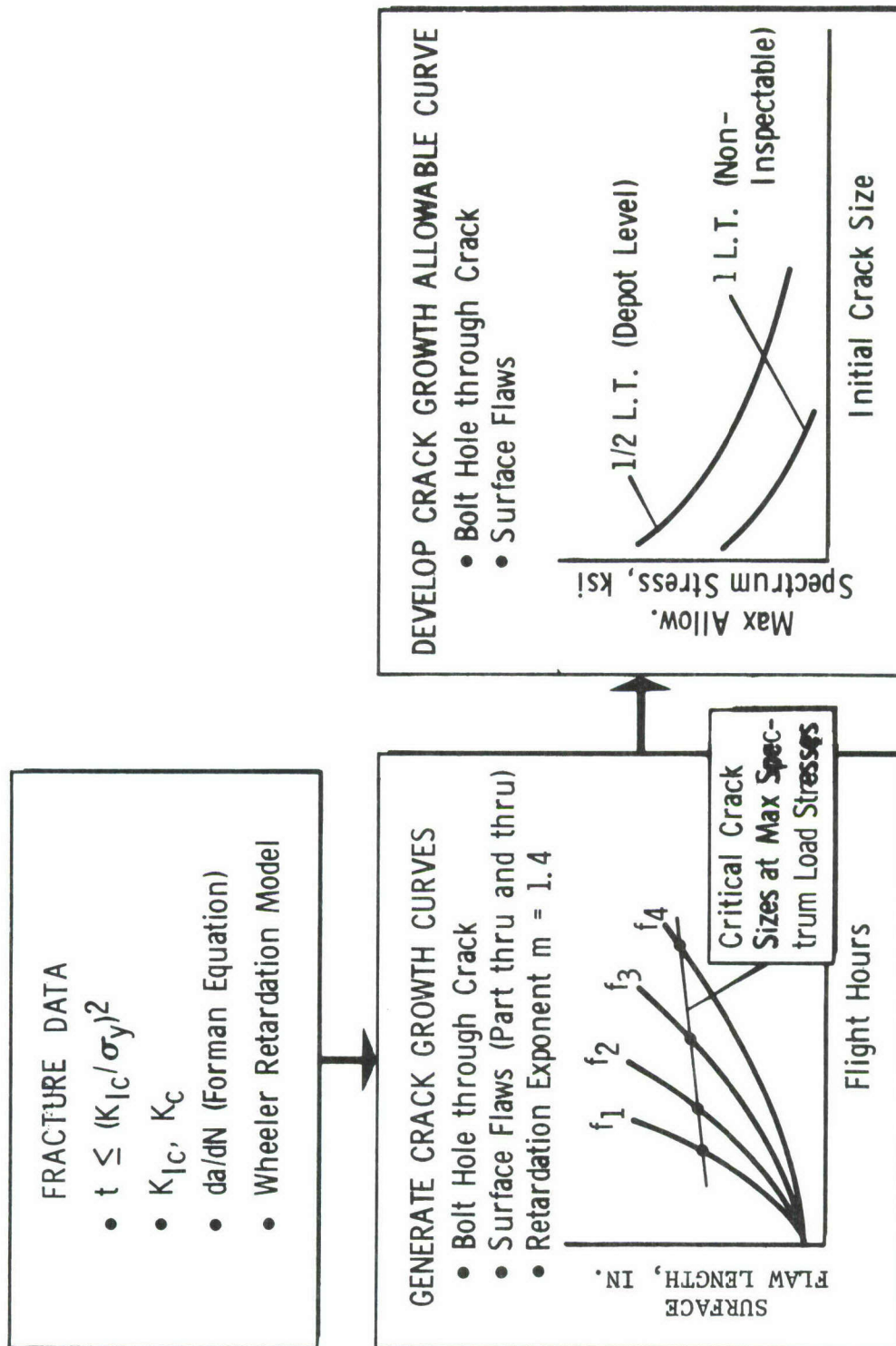


Figure 71 Crack Growth Allowable Approach

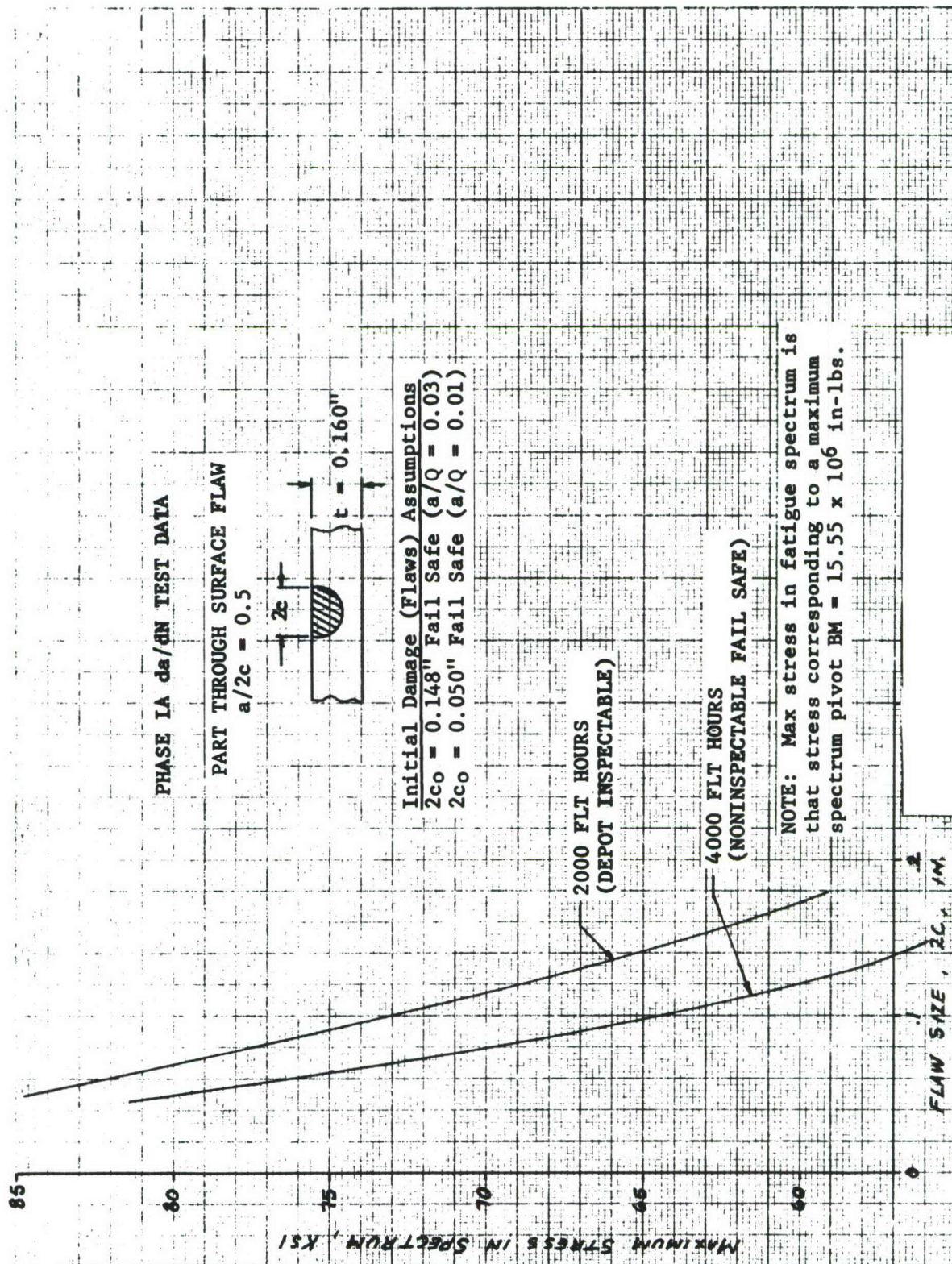


Figure 72 Fracture Desing Data, C.S.S. 140 Lower Surface 8-8-2-3
 Titanium Alloy

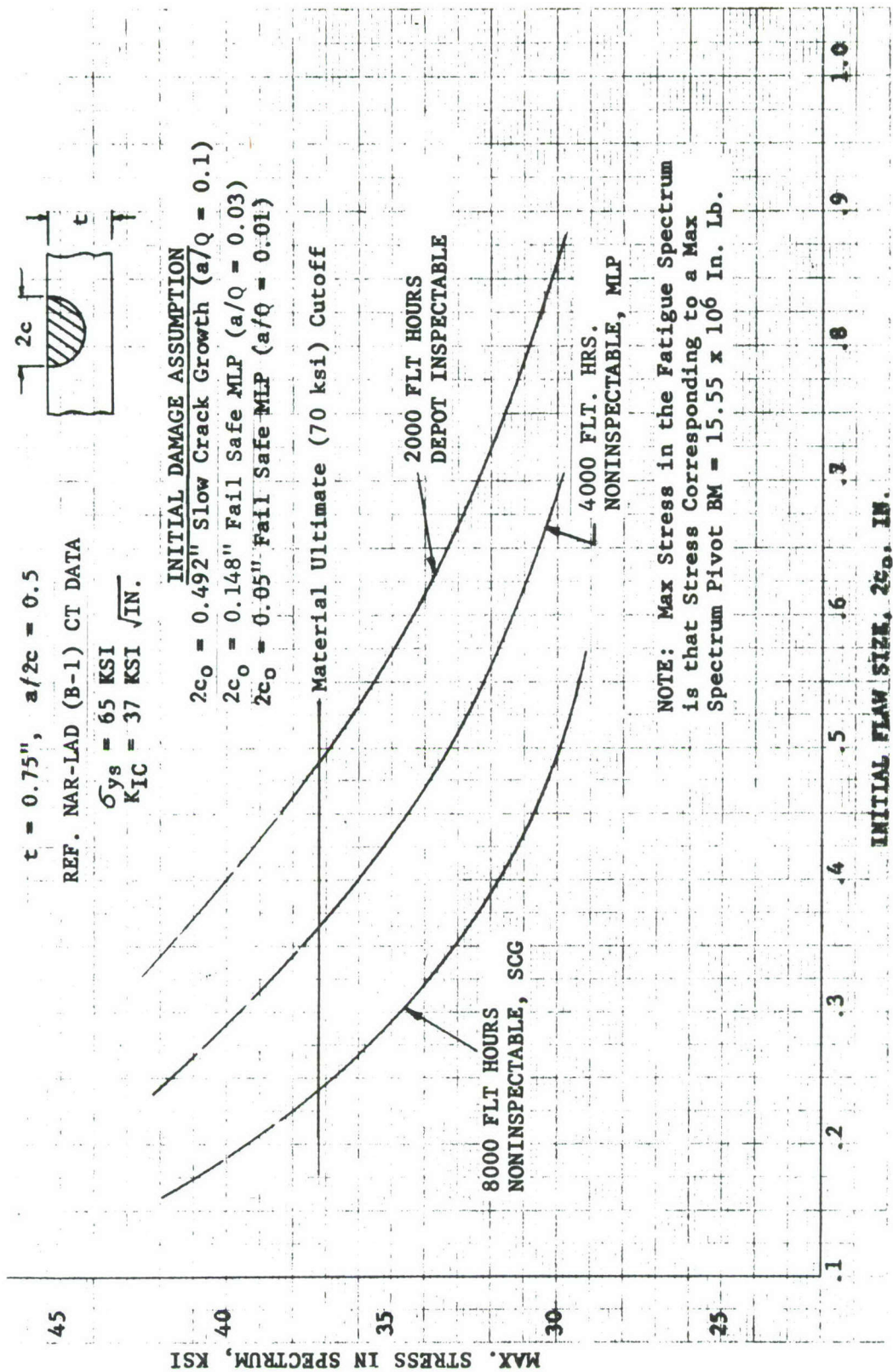


Figure 73 Phase IA Fracture Design Allowables 7050 Aluminum Alloy Plate, Part Through Surface Crack

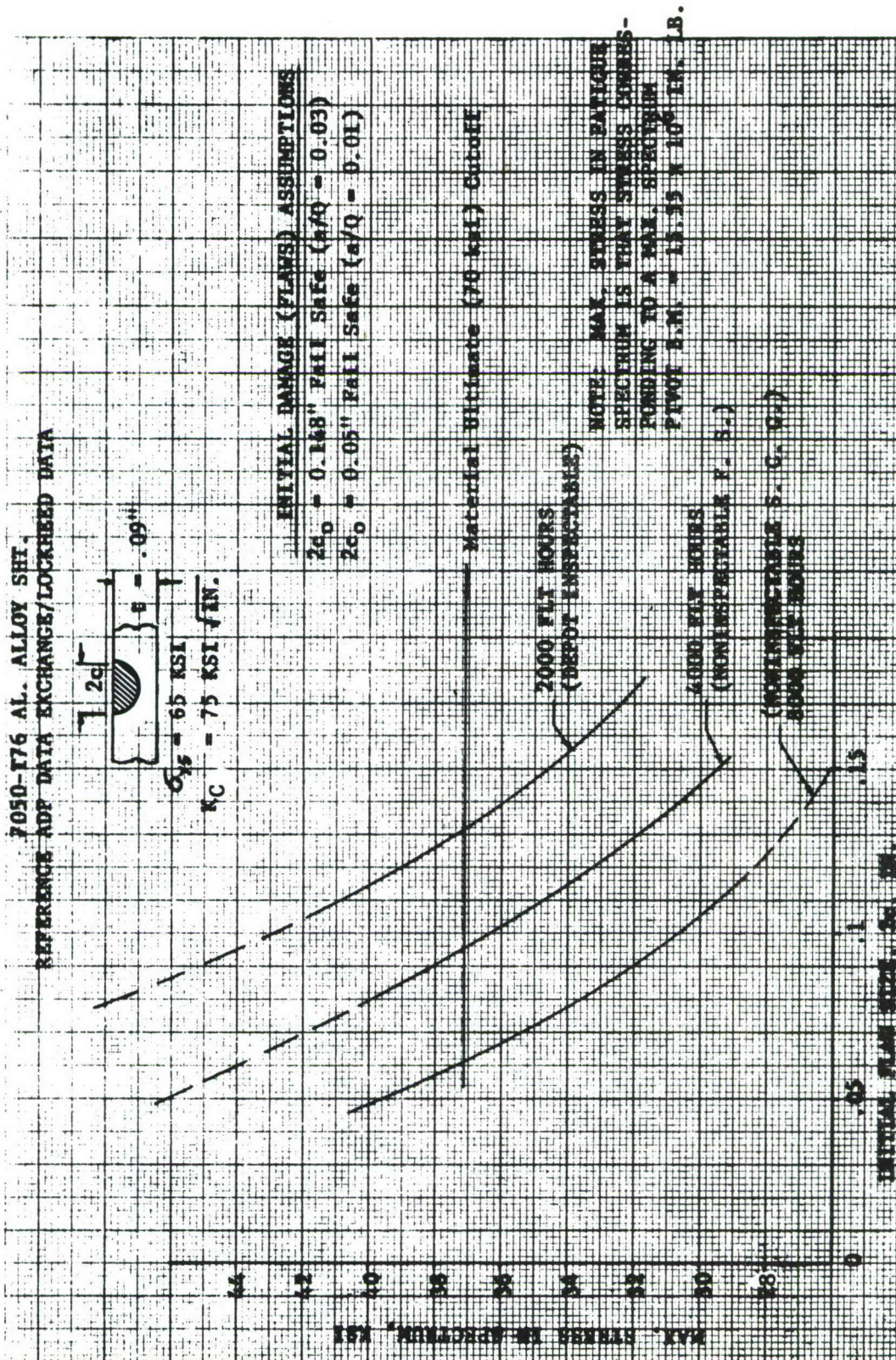
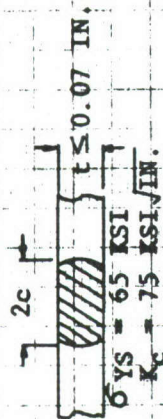


Figure 74 Phase IA Fracture Design Allowables, Part Through Surface Flaw

APPLICABLE TO 7050-T76 AL. SHT.
Reference ADP Data Exchange/Lockheed Data



INITIAL DAMAGE (FLAWS) ASSUMPTIONS

$2c_0 = 0.06$ " Fail Safe ($a/Q = 0.03$)

$2c_0 = 0.02$ " Fail Safe ($a/Q = 0.01$)

2000 FLT. HOURS

(DEPOT INSPECTABLE)

Material Ultimate (70 ksi) Cutoff

4000 FLT. HOURS

(NONINSPECTABLE FAIL SAFE)

NOTE: MAX. STRESS IN SPECTRUM IS THAT
STRESS CORRESPONDING TO A MAX. PIVOT
B.M. = 15.55×10^6 IN. LBS.

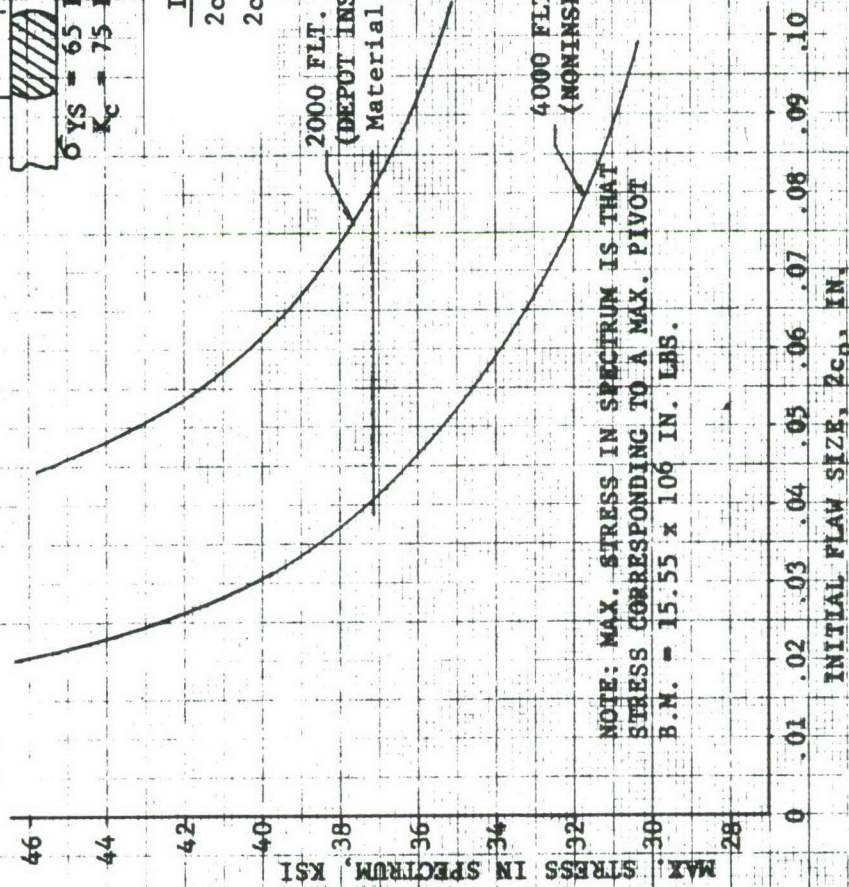


Figure 75 Phase IA Design Allowable Curves Surface Flaw

7.3.2 Analysis Assumptions and Procedures

The fracture analysis process developed at Convair Aerospace for metallic structures is depicted in Figure 76 . In the interest of time and economy, the scope of the process shown in the figure was necessarily limited during Phase IA. The preferred flight-by-flight spectrum approach yielded to a more easily handled block type spectrum in Phase IA. However, the agreement of flaw growth results using the two spectra was very good as previously discussed in paragraph 7.2.1. The flight-by-flight approach will be used exclusively in subsequent phases of this program.

The second Phase IA limitation involved the relatively small amount of testing which was primarily intended for material screening purposes. Sufficient testing to provide a suitable fracture data base and to provide for model correlation, particularly spectrum retardation effects, will be a primary objective of the follow-on program. The data exchange program, conducted by the Air Force for the benefit of all ADP Phase IA contractors, helped to alleviate the fracture data limitation in the case of 7050-T76 aluminum sheet.

The specific assumptions and procedures used to perform fracture analysis are described in the following paragraphs.

7.3.2.1 Flaw Growth Model

The basic flaw growth model used for Phase IA analysis is described as follows:

$$a_n = a_0 + \sum_{n=1}^N (c_p) \left[da/dN = f(\Delta k) \right]$$

where

c_p = Spectrum interaction parameter that reflects retardation of flaw growth.

The spectrum retardation parameter, c_p , is the basis for the Wheeler model, developed for use during the F-111 Recovery Program. See Figure 77 . The Wheeler model is intended to account for spectrum interaction through empirical correlation to establish a retardation exponent "m." The value of "m" is varied repetitively until the analysis produces a crack growth curve which forms a

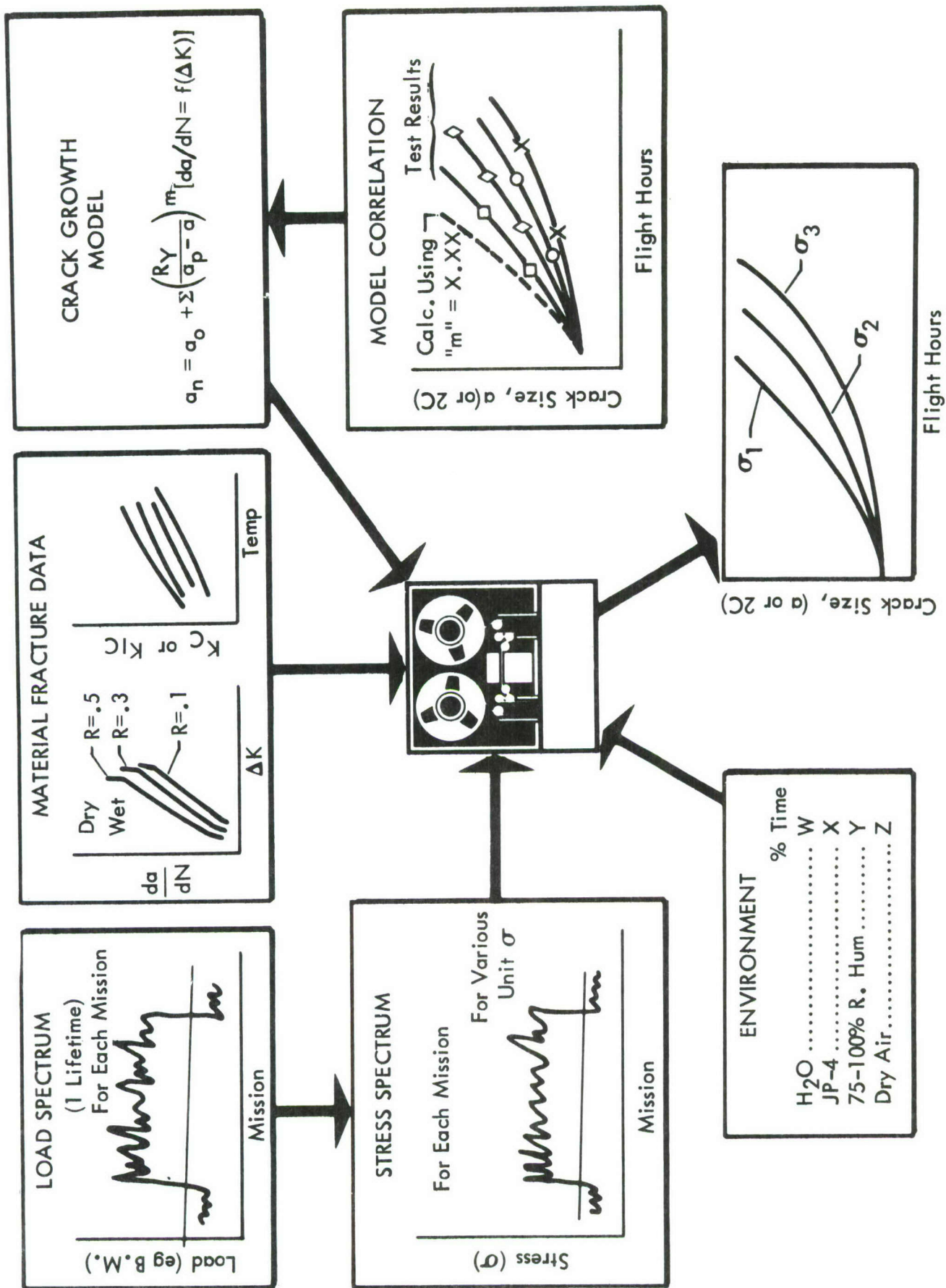


Figure 76 Metals Fracture Analysis Summary

$$a_n = a_{\text{initial}} + \sum_{i=1}^n C_{p_i} [da/dN = f(\Delta K_i)]$$

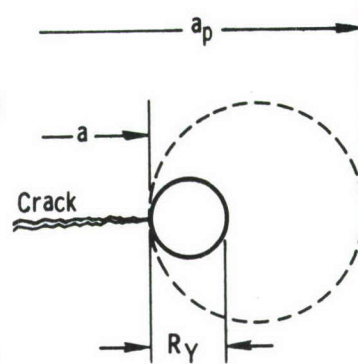
Where $C_{p_i} = \left[\frac{R_Y}{a_p - a} \right]^m$ For $a + R_Y < a_p$

$C_{p_i} = 1$ For $a + R_Y \geq a_p$

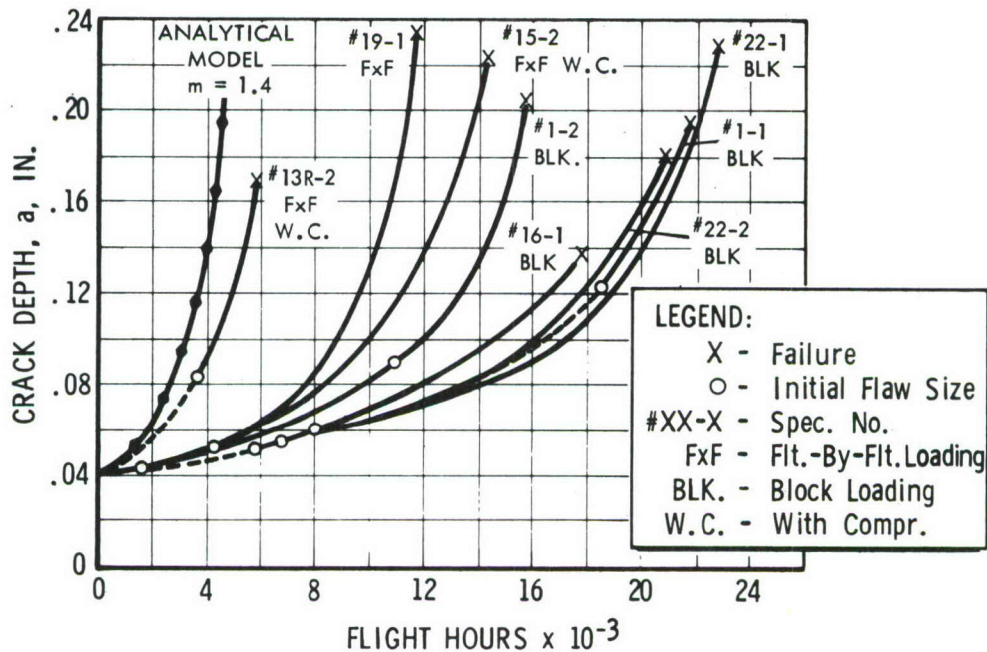
R_Y = Current Yield Zone Size

$a_p - a$ = Distance from Crack Tip to Elastic-Plastic Interface
(These Dimensions are Measured from the Crack Centerline)

m = Shaping Exponent Established Experimentally



WHEELER CRACK GROWTH MODEL



Surface Flaw Growth Test Results for D6ac Steel Under Spectrum Loading in JP-4 Fuel Showing Lower Bound $m = 1.4$

Figure 77 Analytic Flaw Growth Model

lower band of spectrum/environmental test results. Because spectrum/environmental tests were beyond the scope of Phase IA, an "m" factor of 1.4 was used for analysis. This value is based on D6ac steel spectrum tests conducted with the baseline spectrum and is believed to be conservative for aluminum and titanium. In addition, spectrum/environmental tests were run on 2024-T851 aluminum in conjunction with the baseline damage tolerance assessment, and a lower bound value of 1.6 was conservatively established for this material. See paragraph IX.3 of Appendix IX for details of this work.

7.3.2.2 Stress Intensity Models

The stress intensity concept is used in relating stress, flaw size and basic material fracture toughness data to residual strength and flaw growth. Stress intensity expressions used for Phase IA analysis are shown in Figure 78. The secant correction was used to account for finite width when required.

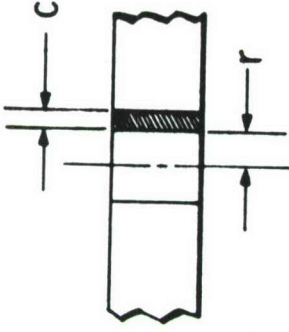
The bolt hole models account for geometric stress concentration at the edge of the hole but do not account for effects of the fastener system. The GKT model was also used for the case of a flaw emanating from the inboard pivot pylon cutout by allowing decay of the stress concentration to occur over a distance equal to the width of the reinforcement fittings. Stress concentration assumed for the cutout was identical to that used for fatigue analysis. However, provision was made to handle the case when stress concentration times the maximum spectrum stress exceeds material yield stress. The maximum value of GKT is then defined as the ratio (σ_{ys}/σ_{max}). This definition is based on the reasoning that peak stresses are limited by plastic flow.

The semicircular shape has been assumed for analyses involving part through surface flaws based on $a/2c$ measurements taken from the postfailure fracture surfaces of baseline 2024-T851 aluminum specimens tested under spectrum loading. These measurements indicated a flaw shape of 0.5 and greater for most of the test history on each specimen. Similar experience with surface flaw D6ac steel specimens tested during the F-111 Recovery Program indicated that flaws having an initial $a/2c = 0.1$ would grow rapidly in the depth direction, tending to form a semicircular shape early in the spectrum loading. An additional study of shape variation (initial $a/2c = 0.1$) was made in support of the Baseline assessment included in Appendix IX. This study also substantiated use of an $a/2c = 0.5$ ratio for flaw growth analysis.

• BOLT HOLES (Bowie Model)

$$K = \sigma \sqrt{\pi c} F(c/r)$$

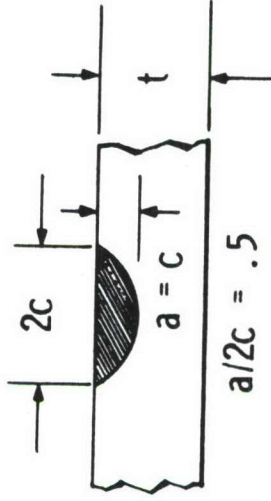
$$C = \frac{K^2}{\pi \sigma^2 [F(c/r)]^2}$$



• SURFACE FLAW (Part through)

$$K = M_K \frac{1.1 \sigma \sqrt{\pi a}}{\sqrt{\phi^2 - 212 (\sigma/\sigma_y)^2}}$$

$$a = \frac{K^2 [2.46 - .212 (\sigma/\sigma_y)^2]}{1.21 \pi \sigma^2 M_K^2}$$



• SURFACE FLAW (through the Thickness)

$$K = \sigma \sqrt{w \tan \left(\frac{\pi a}{w} + \frac{K^2}{2w \sigma_y^2} \right)}$$

DERIVED (FOR $w \geq 6''$)

$$2c = \frac{1}{\pi} \left(2.0 - \frac{\sigma^2}{\sigma_y^2} \right) \left(\frac{K}{\sigma} \right)^2 \quad \text{Plane Stress}$$

$$2c = \frac{1}{\pi} \left(2.0 - \frac{\sigma^2}{3\sigma_y^2} \right) \left(\frac{K}{\sigma} \right)^2 \quad \text{Plane Strain}$$

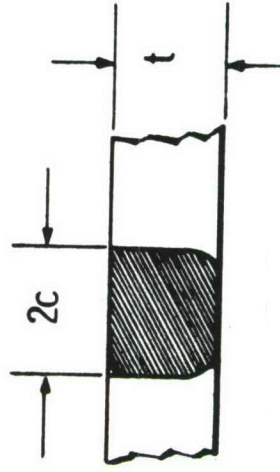


Figure 78 Residual Strength with Cracks

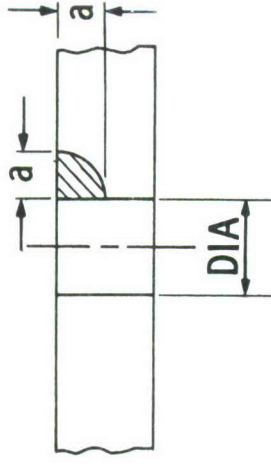
• SEMICIRCULAR CORNER CRACK

$$K = \frac{1.2 \sigma \sqrt{\pi a}}{\phi} (GKT)$$

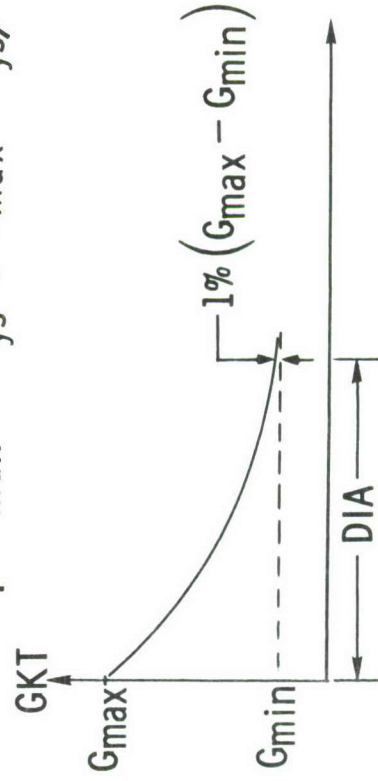
$$a = \frac{K^2 \phi^2}{1.44 \pi \sigma^2} (GKT)^2$$

$$GKT = G_{min} + (G_{max} - G_{min}) \text{Exp} \left[\text{Ln} (.01) \frac{a}{DIA} \right]$$

$$G_{min} = 1.0, \quad G_{max} = K_T$$



For $K_T \times \sigma_{max} \geq \sigma_{ys}$, $G_{max} = \sigma_{ys} / \sigma_{max}$ By Definition



NOTE: Model Applicable to
Pylon Cutout by Making
DIA.= Width of Reinforcement.

Figure 78 (Cont'd) Residual Strength with Cracks

Backface corrections (M_k) for part through flaws were based on curves given in AFFDL-TR-70-107, which describes the flaw growth computer program, "CRACKS." Additional discussion of the M_k effect and comparisons of the AFFDL M_k correction with that used by Convair Aerospace during the F-111 Recovery Program is given in Appendix VI.

When required, transition from part through surface flaw calculations to through the thickness surface flaw calculations was automatic within the flaw growth computer program.

The finite element stress analysis methods described in paragraph 5.2 were used to establish stress distributions remote to the flaw locations. Finite element solutions for stress intensity expressions were not available for use in Phase IA. The development of such solutions is being accomplished on the AMAVS (carry through structure) program at Convair Aerospace. It is hoped that this work will be available for possible use in the follow-on phases of the Advanced Air Superiority wing program.

Flaw growth calculations were made using a Convair Aerospace developed IBM 370 computer program identified as TD9. This program produces results almost identical to those produced by the AFFDL-TR-70-107 CRACKS program. TD9 was used because it involves somewhat less run time for a typical analysis. CRACKS is available at Convair, and a check run was made for one of the baseline flaw cases to verify that TD9 is satisfactory. The details of this comparison are given in Appendix VI.

7.3.2.3 Flaw Growth Spectra

The repeated loads spectra used for flaw growth analysis was representative of baseline unrestricted usage, and simplified as described in paragraph 7.2.1. The wing net pivot bending moment spectrum was used as the basis for analysis in conjunction with unit stress factors (coefficients). Additional discussion of the unit stress concept and use of pivot bending moment spectra for obtaining stress spectra is given in Appendix VI.

7.3.2.4 Initial Flaw Sizes

The damage tolerance criteria specifies initial damage for locations other than bolt holes in terms of a/Q . For intact new fail safe structure, the requirement is $a/Q = 0.03$. For remaining structure at time of and subsequent to load path failure or

crack arrest and intact structure following inservice inspections the requirements are:

- (1) $a/Q = 0.03$ for dependent fail safe structure
- (2) $a/Q = 0.01$ for independent fail safe structure.

Flaw sizes associated with a/Q usually involve part through flaws in relatively thick structure. Application of the a/Q requirements to thin sheet structure was accomplished by using an approach typically described as follows for $a/Q = 0.03$.

Establish the crack size parameter $(K/\sigma)^2$ for a part through flaw, and then calculate the size of a through the thickness flaw which yields an identical value for flaw size parameter.

$a/Q = 0.03$

- . Part through flaw: $K = \sigma \sqrt{\pi a_0/Q}$ where
 a = crack depth. The flaw size parameter becomes:

$$\left(\frac{K}{\sigma}\right)^2 = \pi a_0/Q$$

Ignoring plasticity correction, $Q = \phi^2$ and has a largest value of 2.46 for an $a/2c = 0.5$. For an $a/Q = 0.03$, the value of $a_0 = 0.0738$ inches. The flaw size parameter becomes:

$$\left(\frac{K}{\sigma}\right)^2 = \frac{\pi(0.0738)}{2.46} = 0.03$$

- . Through the thickness flaw: $K = \sigma \sqrt{\pi a_0}$ where
 a = half crack length. The flaw size parameter is:

$$\left(\frac{K}{\sigma}\right)^2 = \pi a_0$$

Substituting the value for flaw size parameter of a part through flaw for that of a through flaw yields the following:

$$0.03\pi = \pi a_0, \text{ or}$$

$$a_0 = 0.03 \text{ inches, and}$$

$$2a_0 = 0.06 \text{ inches through the thickness surface length}$$

Therefore, a through flaw of length $2a_0 = 0.06''$ was assumed for initial damage corresponding to $a/Q = 0.03$ in sheet < 0.074 inches thick. Structure having a thickness greater than 0.074 inches was assumed to have an initial part through semicircular flaw 0.074" deep and 0.148" long.

A similar development for $a/Q = 0.01$ resulted in a through the thickness flaw of length $2a_0 = 0.02''$ for thin sheet structure up to and including 0.03 inches thick. Thicker structure was assumed to have an initial part through flaw 0.025" deep and 0.05" long.

7.3.3 Fracture Data Assumed for Analysis

The basic fracture data necessary for a comprehensive fracture analysis should include complete definition of the following for each material utilized:

- (1) Fracture Toughness, K_{IC} , K_C and K_{ISCC}
- (2) Crack Growth Data, da/dN , da/dt .

The scope of the Phase IA test program was not sufficient to provide a complete data base. Some additional data was obtained from outside sources, but an extensive amount of testing will be required in Phase Ib to support the detail design effort.

Thermal effects on crack growth rates were neglected for Phase IA analysis. This is considered somewhat conservative, and the structural temperature extremes for the F-111F baseline are not particularly severe for aluminum and titanium alloys (+ 10°F min. and + 255°F max.). A survey of available fracture toughness data obtained at temperatures other than room temperature for these alloys indicates virtually no effect due to temperature.

Fracture toughness data used for Phase IA design analyses is summarized below.

Material	K_{IC} , KSI(in.) ^{1/2}	K_C , KSI(in.) ^{1/2}
7050 Al.	37	75
7475 Al.	47	100
8-8-2-3 Ti.	63	80

The values shown in the table are intended to represent values in the L-S direction since their use in the critical wing lower surface was of primary interest in preliminary design analysis.

A K_{IC} of 37 ksi(in.)^{1/2} was expected for 7050 aluminum plate but test data for this material indicated a K_{IC} of only 27 ksi(in.)^{1/2}. However, it is felt that the limited amount of test data generated in Phase IA for a single heat of material is untypically low. ALCOA states that the value of 27 ksi(in.)^{1/2} would represent a definite lower bound value for 7050 plate (See Section VIII for additional discussion of fracture toughness test results). Rather than reflect what seems to be lower bound data in the analyses of Phase IA designs, it was decided to retain the design allowable value of 37 ksi(in.)^{1/2} for analysis purposes. Sufficient testing will be included in the follow-on program to further characterize the fracture toughness of the 7050 aluminum material.

The expected value of K_{IC} for 7475 aluminum plate was 47 ksi(in.)^{1/2} and test specimens were sized in accordance with ASTM requirements for this value. However, test results for this material indicated a greater toughness than anticipated and an average $K_Q = 63$ ksi(in.)^{1/2} is reported in Section VIII. K_Q values were reported because the specimens, designed for $K_{IC} = 47$ ksi(in.)^{1/2}, were of insufficient thickness to yield valid fracture toughness values according to the ASTM requirements. While K_Q values indicate greater fracture toughness, it was decided that the limited amount of testing performed in Phase IA was not conclusive, and the more conservative value of 47 ksi(in.)^{1/2} was retained for analysis purposes. Ultimately, the 7475 material was not used in the three finally selected Phase IA designs since the higher strength (yielding lower weight) 7050 material proved to be sufficient from a fracture standpoint.

The average K_{IC} test value for 8-8-2-3 titanium was 54 ksi(in.)^{1/2}. However, the specified design strength for this material (175 ksi) was exceeded in the sheet material received for the test program. Even after reaging, the tensile strength obtained was 184 ksi. Since the design application of 8-8-2-3 is in sheet form, the higher fracture toughness allowables were retained.

No testing to determine plane stress fracture toughness (K_C) was included in the Phase IA test program. The values shown in the table were based on data from other sources (7050 and 7475 Al.) or engineering judgment (8-8-2-3 Ti). Testing to establish thickness versus K_C curves for 7050 and 8-8-2-3 will be included in Phase Ib.

The surface flaw cyclic crack growth (da/dN) data generated by the Phase IA test program proved to be of limited use for preliminary design analysis because the fail safe design philosophy forced utilization of bonded and braced sheet structure. Crack growth data required to perform detail design must reflect not only sheet forms of the chosen materials but also the decrease in growth rate expected when sheets are bonded and brazed over large areas. The constraint on crack growth, of flaws in thin materials, at the bond or braze lines should be significant. Test data reflecting such arrestment will be emphasized in Phase Ib.

The crack growth data ultimately used for analysis of the Phase IA preliminary wing designs is summarized in Table XXXII. Crack growth plots (da/dN vs. ΔK) are shown in Figures 79 through 83. The forman equation was used to account for spectrum R values when data was available for only one R value, and the equation coefficients are shown on the figures. The data shown in Figure 79 reflects three R values, and line fits of the data are parallel. This allowed use of the Paris equation approach with interpolation accounting for other R values.

The use of the 7050-T73651 compact tension data instead of surface flaw data tested in Phase IA was justified on two accounts. First, the Phase IA test data was completed late in the program while the data in Figure 79 was readily available. Secondly, the compact tension data was better defined, reflecting three R values and higher da/dN rates. However, the Phase IA surface flaw da/dN data was more severe than the selected compact tension data as shown by Figure 126 of Appendix VIII. There has not been sufficient testing to determine whether the differences noted may be due to specimen type and/or the lower ductility experienced with the single heat of 7050 plate material tested in Phase IA. However, to illustrate the effect of the more severe data, the analysis for the lower spar cap of wing design 610RW003 was repeated using the surface flaw dry air data shown in Figure 126. The results are given in paragraph 7.4.1 where the full wing analyses are discussed. Additional da/dN testing for 7050-T73651 plate is scheduled for the follow-on.

The ΔK threshold values assumed for flaw growth analyses are summarized below:

- (1) Aluminums $\Delta K = 3.0 \text{ ksi (in.)}^{\frac{1}{2}}$
- (2) Titaniums $\Delta K = 5.0 \text{ ksi (in.)}^{\frac{1}{2}}$

Table XXXII FLAW GROWTH DATA USED FOR PRELIMINARY DESIGN ANALYSIS

Material	da/dN Data Assumed	Assumed Application of da/dN Data
7050-T73651 Pl.	NAR-LAD B-1 Contract (C.T. Spec.) R = 0.3, 360 cpm, Low Hum. Air	Lower Surface Spar Caps
7050-T76 Sht.	Lockheed, ADP Data Exchange R = 0.1, 2 Hz & 20 Hz, 95% RH	Lower Surface Laminated Skin Planks
8-8-2-3 Ti Pl.	Convair Phase IA (Surf. Flaw) R = 0.3, 360 cpm, Dry Air, R.T.	Lower Surface Skin Planks of 610RW006 which was not included in final 3 selections.
6AL-4V Sta Pl.	NAR-LAD Data in MCIC-HB-01 R = 0.3, 1 Hz, Dry Air, R.T.	Upper Surface Skin
6AL-4V Recrys. Ann. Pl.	NAR-LAD B-1 Contract (C.T. Spec.) Combined Data from Three Specimens R = 0.08, 60 & 360 cpm, Sump Water & Low Hum. Air, R.T. & + 150°F	Lower Surface--Used to Represent 8-8-2-3 Ti Brazed Laminated Wing Skins

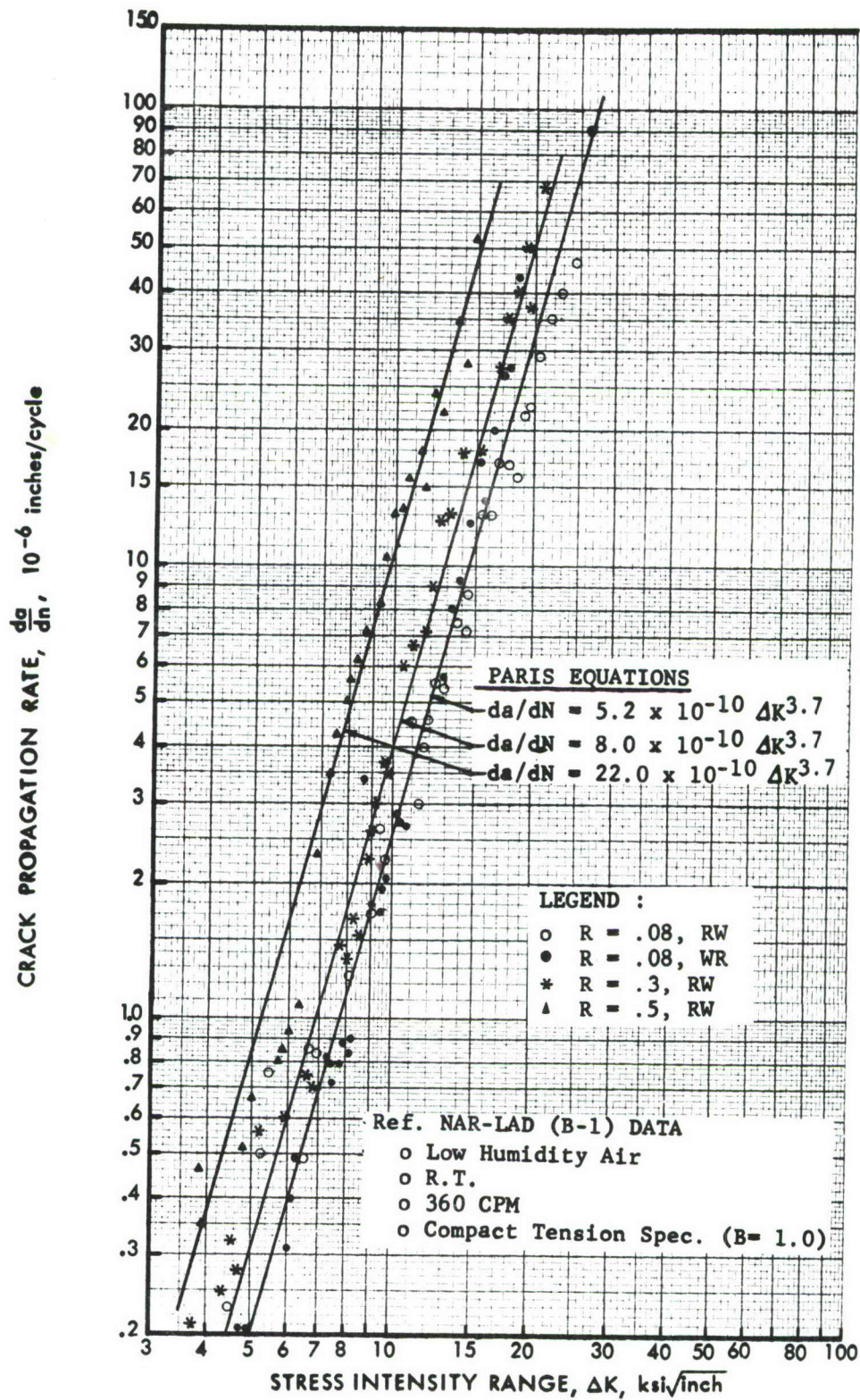
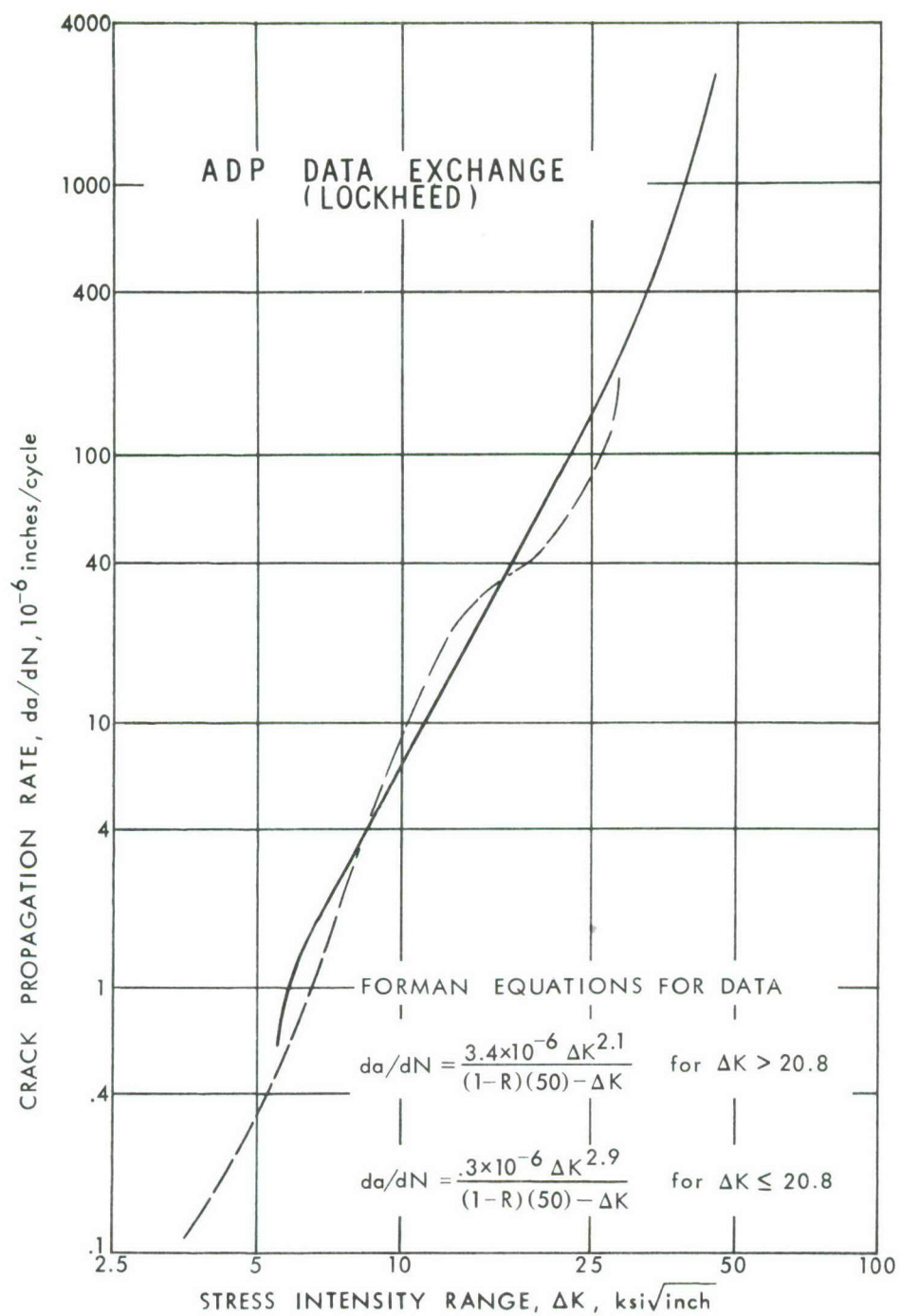


Figure 79 Crack Growth Rate Data for 7050-T3651 Aluminum Plate



7050 - T76 AL. SHEET

95% REL. HUM. AIR

$R = 0.1$

$f = 2 \text{ Hz}$ ———

$f = 20 \text{ Hz}$ ———

$t = 0.148 \text{ in}$

Figure 80 Crack Growth Rate Data for 7050-T76 Aluminum Sheet

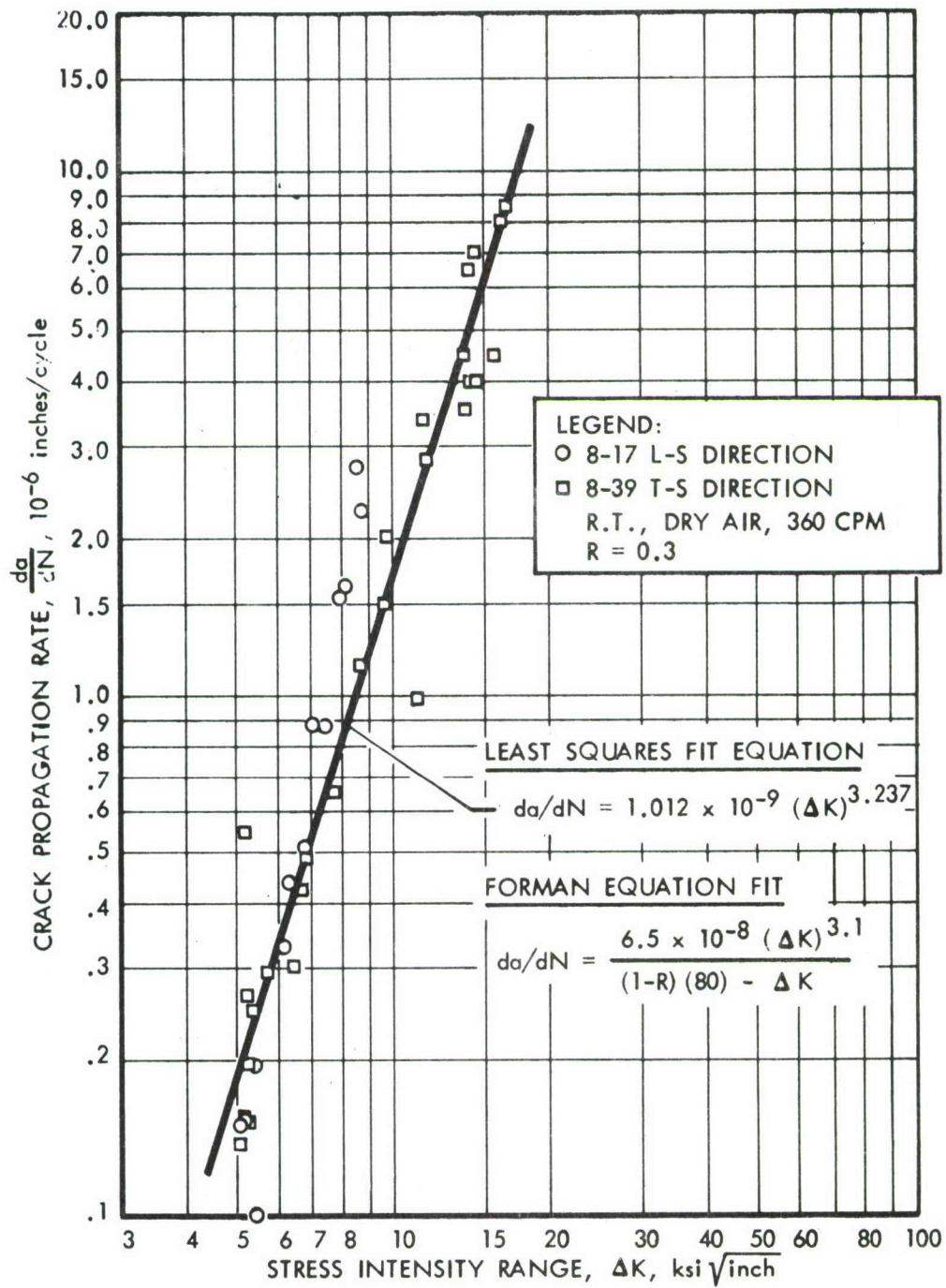
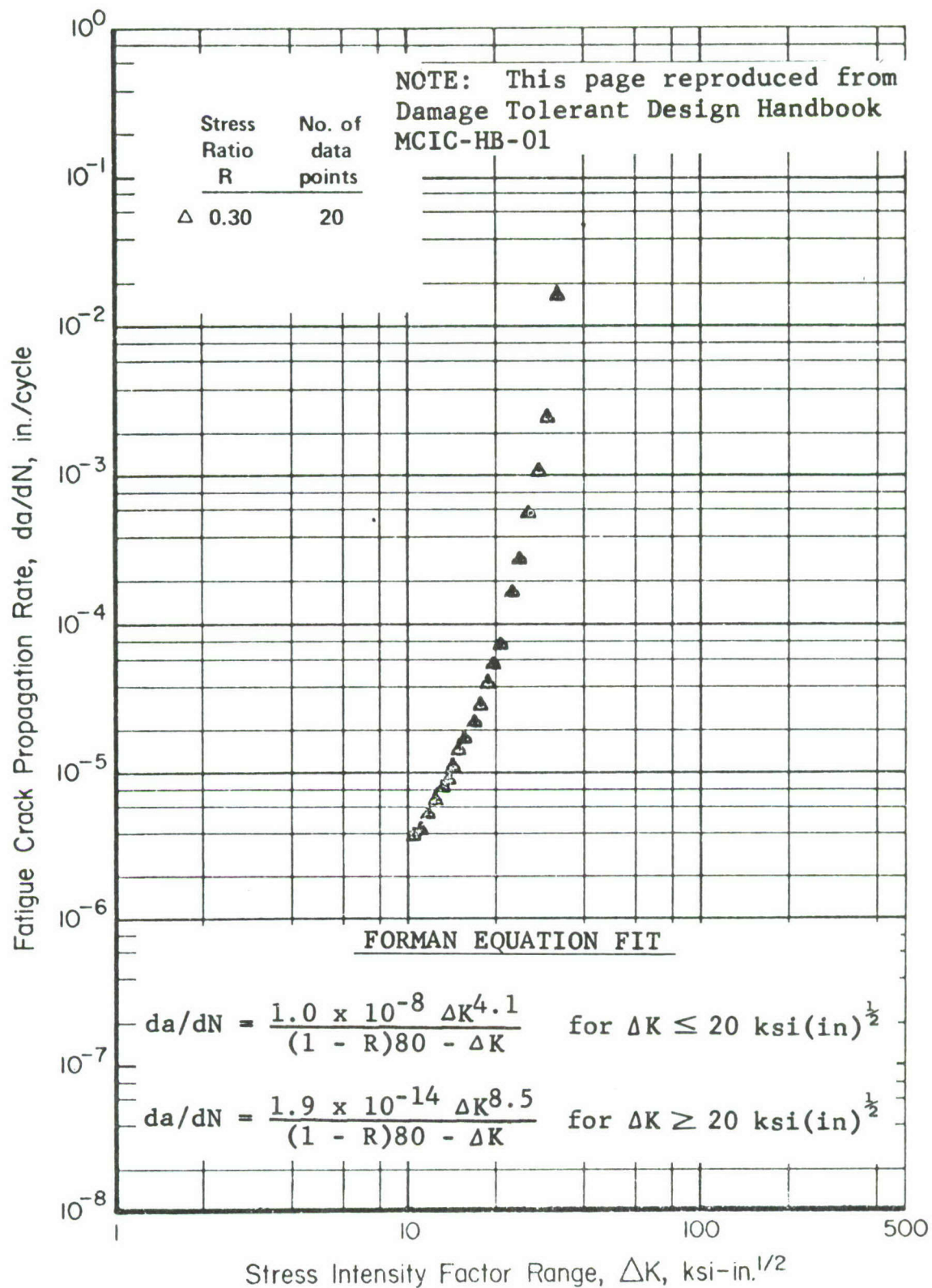


Figure 81 Crack Growth Rate Data for 8-8-2-3Ti Plate



Environment : 70 F, Dry Air; Frequency -- 1.0 Hz
Specimen Thk.: 0.50 in., Width -- 6.00 in.
Reference No. : 84361

Figure 82 Ti-6Al-4V, 0.625 In. Sta Plate, CT Specimens, L-T Direction

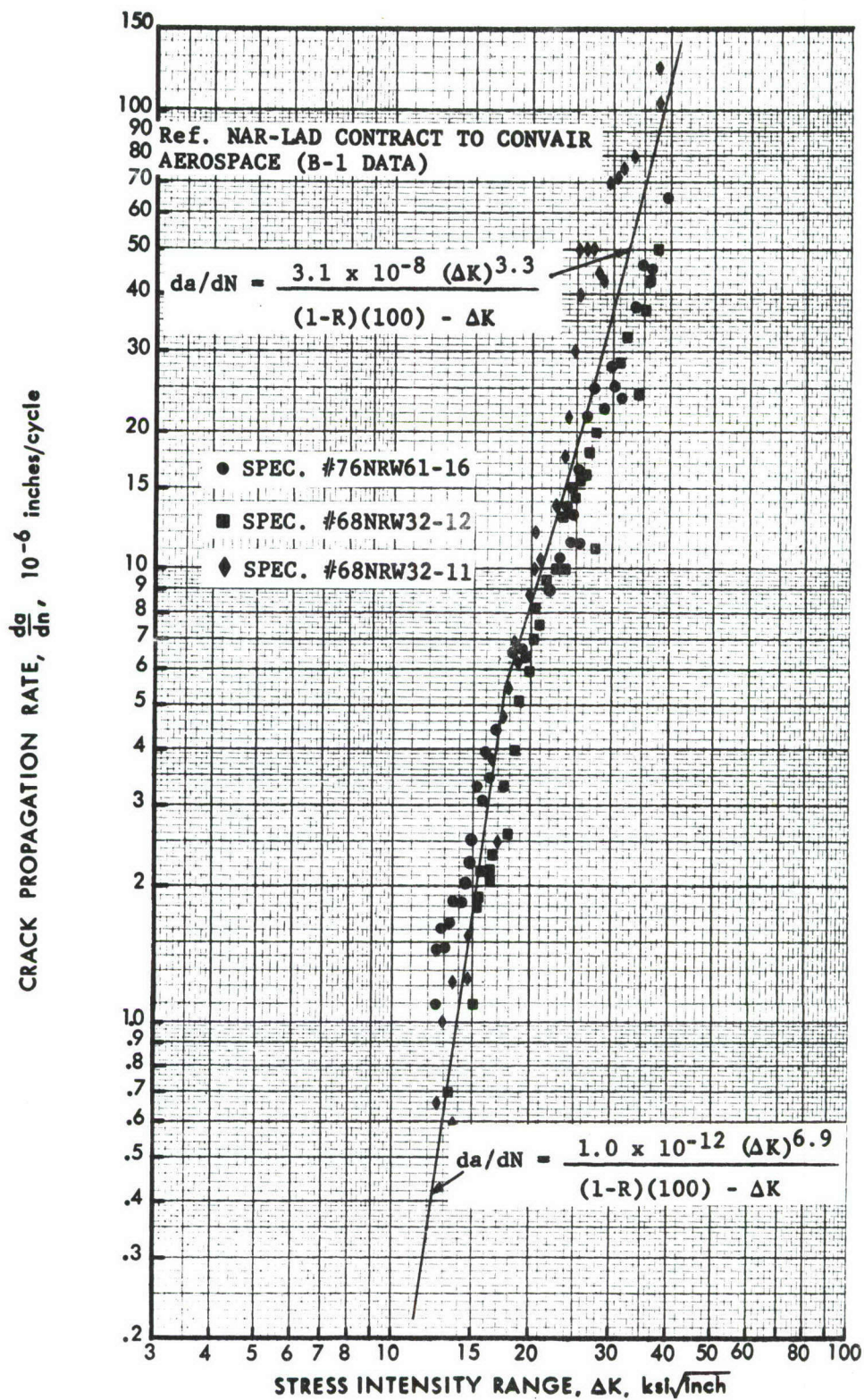


Figure 83 Preliminary da/dN Data, 6Al-4V Titanium Recrystallized Annealed Plate

The limited amount of da/dN data obtained for 8-8-2-3 plate titanium indicates a relatively rapid growth rate compared with the 6Al-4V annealed data in Figure 83 . However, the 8-8-2-3 growth rate is less than that for 6Al-4V STA and 6-2-2-2-2 STA titanium. It is felt that an improvement in growth rate will be obtained for 8-8-2-3 when bonded or brazed thin ply laminates are tested in Phase Ib. This judgment contributed to the decision to assume such an improved growth rate can be approximated by the data available for 6Al-4V Recrys. annealed titanium. This decision and the 6Al-4V data, was utilized to analyze all or portions of the 8-8-2-3 titanium preliminary wing designs in paragraph 7.4. The other important item requiring test data in Phase Ib is the effect of the baseline environment (water saturated JP-4) on the laminated 8-8-2-3 titanium crack growth data.

The results of the material screening eight-load level block spectrum tests also indicate the sensitivity of the high strength 8-8-2-3 titanium plate to the presence of flaws. The results are summarized in Table XXXIII. Additional details of the testing including the eight-load level spectrum are given in Section VIII on Materials Engineering. The specimens utilized for this testing were relatively small in cross section. The initial flaws introduced were relatively large compared with those required to meet the damage tolerance requirements. The 8-8-2-3 specimens failed very early (400 to 800 flight hours) in a dry air environment, and the maximum spectrum stress was 68 ksi compared with the 92.5 ksi currently used in the preliminary designs. Consequently, the use of 8-8-2-3 titanium plate for highly stressed primary structure would seem to be undesirable. Again, the optimism for the Phase IA designs using this material depends on the improvement expected by brazing 8-8-2-3 in thin sheet laminates. In addition to the risk involved with developing a corrosion resistant brazement, the use of 8-8-2-3 titanium itself involves risk until an adequate test program can be conducted. Evaluation of risks such as these is an objective of Advanced Development Programs.

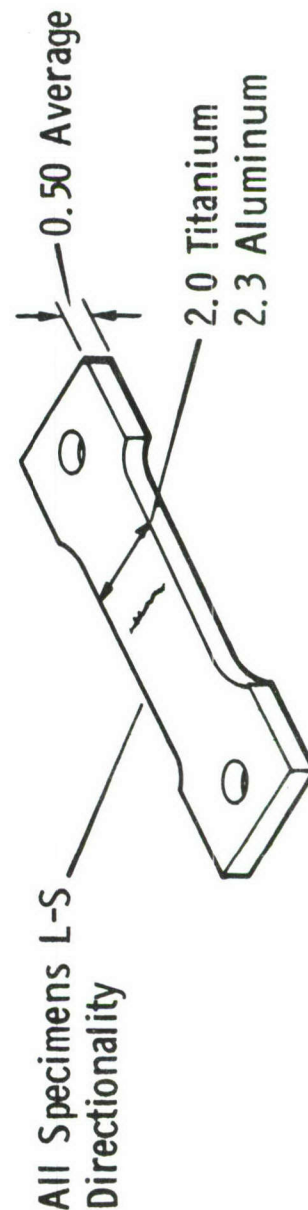
The growth data shown in Figure 83 represents the preliminary results for three compact tension L-T specimens tested at Convair Aerospace under contract from NAR-LAD. Other data available for the T-R direction was not shown but fits within the scatter bands indicated in Figure 83 . The specimens represented on the figure are summarized below:

Table XXXIII SUMMARY OF MATERIAL SCREENING TESTS

8-LOAD LEVEL SURFACE FLAW SPECTRUM TESTS

- DRY AIR ENVIRONMENT, 360 CPM, R.T.
- 200-HOUR BLOCKS

SPECIMEN NO.	MATERIAL	BLOCKS TO FAILURE	CRACK SIZE AT FAILURE, IN.	a/2c INITIAL	a/2c FAILURE
50-48	7050-T73651	84, Layer 7	1.621 Thru Thickness	0.627 .188/.300	--
50-46
75-24	7475-T7351	Early Failure Thru Loading Hole 59, Layer 8	1.520 Thru Thickness	0.614 .190/.310	--
75-26	7475-T7351	48, Layer 6	1.860 Thru Thickness	0.691 .213/.308	--
8-16	8-8-2-3	4, Layer 9	1.273 x 0.443 Part Thru	0.494 .162/.328	0.348
8-18	8-8-2-3	2, Layer 7	1.320 Thru Thickness	-- -- --/.410	--



MATERIAL: Ti-6Al-4V Recrys Ann
 FORM: Unknown TEMP = RT
 SPECIMEN NO.: 76NRW61-16
 FREQUENCY = 360 cpm R = 0.08
 ENVIRONMENT: Low Humidity Air

MATERIAL: Ti-6Al-4V Recrys Ann
 FORM: 2-Inch Plate TEMP = RT
 SPECIMEN NO.: 68NRW32-12
 FREQUENCY = 360 cpm R = 0.08
 ENVIRONMENT: Low Humidity Air

MATERIAL: Ti-6Al-4V Recrys Ann
 FORM: 2-Inch Plate TEMP = + 150°F
 SPECIMEN NO.: 68NRW32-11
 FREQUENCY = 60 cpm R = 0.08
 ENVIRONMENT: Sump Water

Flaw growth analysis due to sustained loading was considered beyond the scope of Phase IA; however, each of the materials ultimately used for preliminary design was rated according to the following criteria:

Sustained load crack growth, da/dt was assumed negligible if the relationship defined below was met.

$$\frac{\text{Max 1-g Sustained Tensile Stress, } f_t \text{ (1-g)}}{\text{Max Service Tensile Stress, } f_t} < \frac{K_{ISCC}}{K_{IC} \text{ (or } K_C)}$$

Typical results are summarized as follows:

Material and Location	$f_t \text{ (1-g)}/f_t$	$K_{ISCC}/K_{IC} \text{ (or } K_C)$
7050-T73651 Lwr Surface	7.7/37.1 = 0.21	35/37 = 0.95 ⁽¹⁾
8-8-2-3 Lwr Surface	19.1/92/5 = 0.21	24.3/54 = 0.45
6Al-4V Ann Lwr Surface	12.1/58.5 = 0.21	60/80 = 0.75

- (1) K_{ISCC} data for the L-S direction was not available. The value of 35 shown in the table was therefore derived based on the relationship between K_{ISCC} and K_{IC} established for this material in the S-L direction, i.e., $K_{ISCC} = 22 \text{ ksi(in.)}^{\frac{1}{2}}$ and $K_{IC} = 23 \text{ ksi(in.)}^{\frac{1}{2}}$.

Sustained stresses were computed for the lower surface based on 1-g inflight loading. The ability of each material to meet the material selection objective of $K_{ISCC}/K_{IC}(\text{or } K_C) = 0.5$ is also indicated by the above table. The sheet forms of 7050 and 8-8-2-3 were assumed to have K_{ISCC} values which are no less than that determined for plate. Stress corrosion testing for sheet will be conducted in Phase Ib.

7.4 PRELIMINARY DESIGN ANALYSIS

Analyses sufficient to assess the conformance of three Phase IA preliminary wing designs with the damage tolerance requirements are presented in this paragraph. The criteria, analysis procedures and fracture data utilized were discussed in paragraphs 7.1, 7.2, and 7.3 respectively.

The three designs included for assessment are the top three among nine reviewed and ranked according to the ranking system described in Section V. The analyses are presented in an order consistent with the rankings. Analyses are primarily directed at the lower surface of each configuration.

An analysis of a bolt hole flaw in the 6Al-4V STA titanium upper skin of design 610RW006 (deleted from the top three selections by the final rankings) was performed to verify that the upper surfaces are not critical. Results of this analysis are shown below:

610RW006 Upper Skin

6Al-4V STA titanium plate da/dN data - reference Figure 82

Assumed bolt hole flaw was a through thickness crack of initial length 0.07 inches. An initial 0.05 inches was attempted but would not grow at all.

The size of the 0.07 crack after 60,000 flight hours was only 0.074 inches.

The lower surface of each configuration was classified as fail safe. Multiple spars provide over-all redundancy. Crack arrest was provided by planking the lower surfaces. Laminated structure was treated as multiple load path structure, i.e., each ply was considered a load path within the laminate, and each ply was made independent fail safe by using bonding and brazing techniques rather than fasteners. Each element or load path was analyzed using safe crack growth procedures. An attempt was made to include the decreased crack growth rate expected in

brazed and laminated titanium structure by using the da/dN data in Figure 83. The da/dN data used for each analysis is given on the figures used to illustrate the discussions in paragraphs 7.4.1 through 7.4.3. See paragraph 7.3.3 for a previous discussion of crack growth data.

The basic approach to satisfying the criteria for fail safe structure was to check a primary and adjacent load path for conformance with applicable criteria requirements. Two of the four preliminary wing box designs have multiple load paths in an overall sense, i.e., multiple spars and planked lower skin panels. In some cases, skin panels were themselves comprised of multiple elements or load paths. Therefore, the assumed analysis procedure was to consider this structure as having a primary load path and one or more adjacent load paths. The calculated time to fail both a primary and an adjacent load path in these cases had to exceed the specified period of unrepaired service usage. Additionally, if the total calculated time to failure for both elements exceeded the required time to failure by a factor of two, it was assumed that further consideration of an adjacent load path for the overall structure (an adjacent panel) was not necessary.

There were several sequences of failure possible in each of the designs. The sequences assumed for analysis are considered conservative. The increased stress in an adjacent load path subsequent to failure of the primary load path was estimated based on the percentage of load carrying area lost. Finite element stress analysis procedures will be used in Phases Ib and II to perform residual strength analysis of the multielement designs. The general area of the lower surface picked for preliminary analysis was the forward auxiliary spar at center spar station 140. Thicknesses and other geometry are representative of this area except in the case of pylon cutouts.

Fastener holes were not a consideration for analysis, but pylon cutouts necessitate having holes through the lower surface. Special attention in these areas resulted in the design of reinforcement fittings to decrease stress levels. An analysis for one inboard pylon cutout (610RW003) is included as a typical case.

The stress intensity, K , was calculated using P_{LT} and the flaw size present in each adjacent load path ($a/Q = 0.01 + \Delta a$). The calculated value is shown on the figures and was a relatively small percentage of critical fracture toughness in each case. The stress intensity corresponding to load path failure or crack arrest ($1.15 P_{LT}$) may be conservatively approximated by increasing

the K for P_{LT} by the ratio of stresses squared. Each adjacent load path (remaining structure) was also able to sustain this increased stress intensity due to dynamic effects. A summary of stresses in the primary and adjacent load paths assumed for each damage tolerance analysis is given in Table XXXIV. Maximum stresses corresponding to P_{LT} and limit load are shown for the primary load path for reference. Stresses at 1.15 P_{LT} and limit load were also calculated for the adjacent load path reflecting both the dynamic factor and the redistribution of stress due to failure of the primary element. Limit load stresses are also shown for reference. In every case, these maximum stresses are less than the yield strength.

Critical crack sizes were calculated using the stress intensity expressions previously defined and P_{LT} (previously defined as 15.6×10^{-6} in-lbs pivot bending moment). The stress state definition was assumed as follows where t = part thickness:

$$\begin{array}{ll} \text{Plane Strain} & t > \left(\frac{K_{IC}}{\sigma_{ys}} \right)^2 \\ \text{Plane Stress} & t < \frac{1}{2.5} \left(\frac{K_{IC}}{\sigma_{ys}} \right)^2 \\ \text{Mixed Mode} & \frac{1}{2.5} \left(\frac{K_{IC}}{\sigma_{ys}} \right)^2 < t < \left(\frac{K_{IC}}{\sigma_{ys}} \right)^2 \end{array}$$

Plane strain fracture toughness (K_{IC}) was used for critical crack size calculations in parts classified as plane strain. Plane stress fracture toughness was directly applicable to parts classed as plane stress. The data required to establish K_C vs t curves was not available to determine fracture toughness for parts classed as mixed mode. A survey of critical part thickness indicated that none of the parts were in mixed mode. See Table XXXV.

7.4.1 Preliminary Design 610RW003 - Laminated Lower Skin, Corrugated Spar Webs, Aluminum

- . Multiple Load Path/Crack Arrest (Ranked No.1)
- . Multiple Spars and Skin Panels
 - . Panels comprised of Sheet Plies Bonded into Laminates

Table XXXIV RESIDUAL STRENGTH SUMMARY FOR LOWER SURFACE OF
PRELIMINARY WING BOX DESIGNS

DESIGN DRAWING AND MATERIAL	ASSUMED PRIMARY LOAD PATH			ASSUMED ADJACENT LOAD PATH (1)			AVERAGE MATERIAL YIELD STRESS
	ELEMENT DESCRIPTION	MAX σ @ P _{LT}	MAX σ @ LIMIT LOAD	ELEMENT DESCRIPTION	MAX σ @ 1.15 P _{LT}	MAX σ @ LIMIT LOAD	
610RW003 7050-T76511 EXTR	① LWR SPAR CAP	37.1	46.5	① ADJ LWR SPAR CAP (10%)	47.1	51.2	65
	② ONE FLY LWR PNL	37.1	46.5	② ADJ FLY LWR PNL (3%)	44.1	48.0	65
	③ LWR SPAR CAP @ PYLON CUTOUT	37.1	46.5	③ ADJ SPAR CAP OPP SIDE CUTOUT (10%)	47.1	51.2	65
610RW002 8-8-2-3 T1 SHT	① LWR SKIN PLANK	92.5	116.0	① ADJ LWR SKIN PLANK (18%)	125.9	137.0	160
610RW004 7050-T73651 PL	① LWR SPAR CAP	37.1	46.5	① ADJ LWR SPAR CAP (19%)	50.9	55.4	65
610RW004 7050-T76 SHT	② LWR PNL OUTER SKIN	37.1	46.5	② LWR PNL INNER SKIN (6%)	45.4	49.4	65

(1) STRESSES SHOWN FOR ADJACENT LOAD PATHS INCLUDE INCREASE DUE TO FAILURE OF PRIMARY LOAD PATH. PERCENT INCREASE SHOWN IN PARENTHESES. ALL STRESSES ARE KSI.

NOTE: P_{LT} DEFINED AS 15.6×10^6 IN. LBS. WING PIVOT BENDING MOMENT. LIMIT LOAD
DEFINED AS 19.52×10^6 IN. LBS. WING PIVOT BENDING MOMENT

Table XXXV PRELIMINARY WING DESIGNS LOWER SURFACE STRUCTURE/
ASSUMED STRESS STATE

Design/Dwg/Material	Part Description	Part Thickness	$(K_{IC}/\sigma_{ys})^2$	Stress State
610RW003--Laminated Lwr Skin, Corrugated Spars, Stepped Spar Caps (7050 AL.)	Lwr Plank Plies Lwr Spar Caps	0.090 0.880	0.325	Plane Stress Plane Strain
610RW004--Sandwich Lwr Skin Planks, Spar Cap Slugs (7050 AL.)	Lwr Panel Skins Lwr Spar Caps	0.90	0.325	Plane Stress
610RW002--Braze Multiwet Cell (8-8-2-3 Ti)	Lwr Skin Planks	0.060	0.155	Plane Stress

Plane Strain	$t > (K_{IC}/\sigma_{ys})^2$
Mixed Mode	$1/2.5(K_{IC}/\sigma_{ys})^2 < t < (K_{IC}/\sigma_{ys})^2$
Plane Stress	$t < 1/2.5(K_{IC}/\sigma_{ys})^2$

. Assumed sequences of failure for analysis:

(1) Part thru crack in lower spar cap (Figure 84)

- . Assumed noninspectable structure
- . Unstable crack propagation failure assumed to omit primary spar cap as tensile load carrying member although arrestment would probably occur at spar cap-to-panel bond lines. Loss of spar cap produces a fuel leak. Initial damage $a/Q = 0.03$ not to grow critical in 4000 hours due to application of P_{LT} .
- . Adjacent load path assumed to be adjacent spar cap. Initial damage $a/Q = 0.01$ plus delta growth that occurs during time to fail primary spar cap; not to grow critical and cause loss of remaining structure in 4000 hours due to application of P_{LT} . Stress increase of 10% due to failure of primary spar cap. Residual strength required in remaining structure at time of prime spar cap failure = $P_{LT} \times 1.15$.
- . Figure 85 presents an identical analysis for the 610RW003 spar caps except the surface flaw da/dN data obtained from the Phase IA test program was utilized. The reduction in growth interval is significant but the requirements are still met.

(2) Part Thru Crack in Laminated Lower Skin Panel (Figure 86)

- . Assumed noninspectable structure.
- . Complete failure of a load path (skin panel) requires failure of all five plies. Therefore, it was assumed for analysis that no more than two plies could fail in a total of 4000 flight hours. The highly stressed outer ply was treated as a primary load path, and the second ply was treated as an adjacent load path with respect to initial damage and residual strength requirements. Arrestment of crack growth due to bond lines was not included in the analysis although definite crack arrest would occur at the skin panel-to-spar cap bonded joints.
- . Initial damage in the primary ply was $a/Q = 0.03$. Residual strength required = P_{LT} . Calculated time to failure was 1700 hours.

① SURFACE FLAW IN SPAR CAP 7050-T76511 AL MACHINED EXTRUSION (7050-T73651 AL PL. da/dN DATA) NONINSPECTABLE--4000 FLIGHT HOURS)

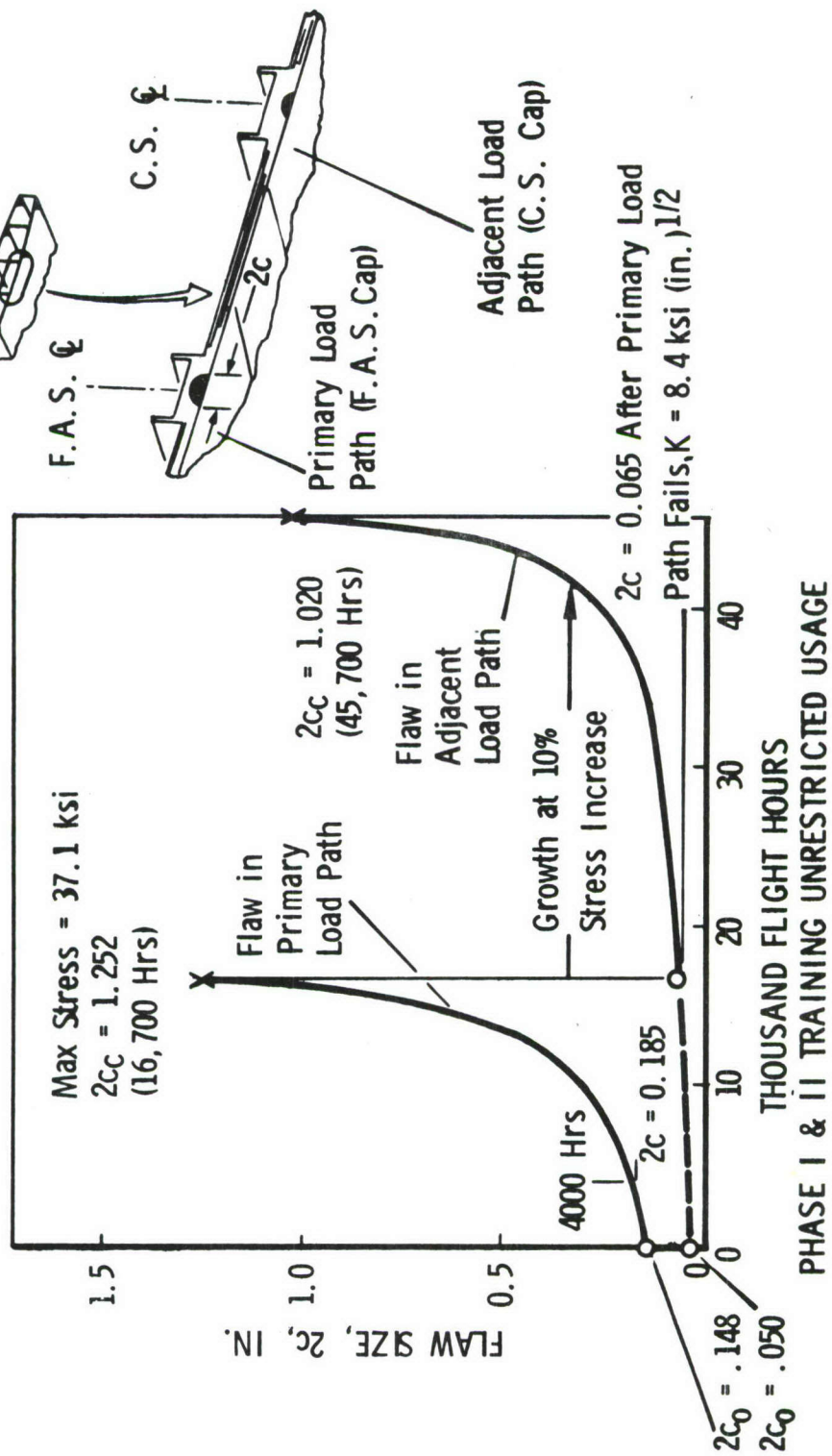


Figure 84 610RW003 Wing Box Laminated Lower Skin, Corrugated Spar Webs, Aluminum Phase IA Fracture Analysis

① SURFACE FLAW IN SPAR CAP
7050-T76511 AL.
MACHINED EXTRUSION
(PHASE Ia TEST DATA--7050-T73651)
NONINSPECTABLE--4000 FLT. HOURS

FIGURE 85

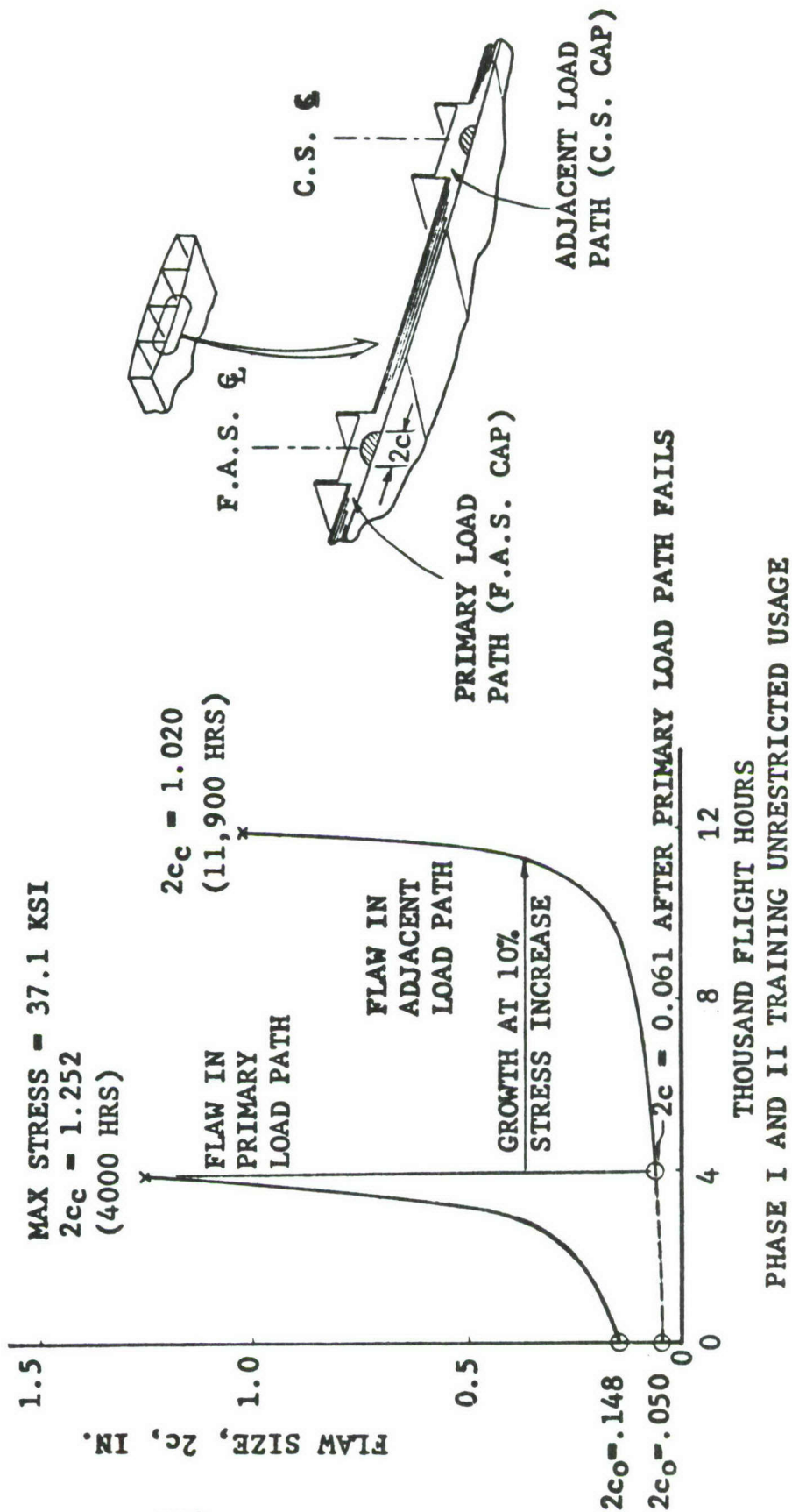


Figure 85 610RW003 Wing Box Laminated Lower Skin, Corrugated Spar Webs, Aluminum Phase Ia Fracture Analysis

② PART THROUGH SURFACE FLAW IN LAMINATED LOWER SKIN PANEL 7050-T76 AI SHEET
(7050-T76 AI SHT. da/dN DATA) NONINSPECTABLE--4000 FLIGHT HOURS

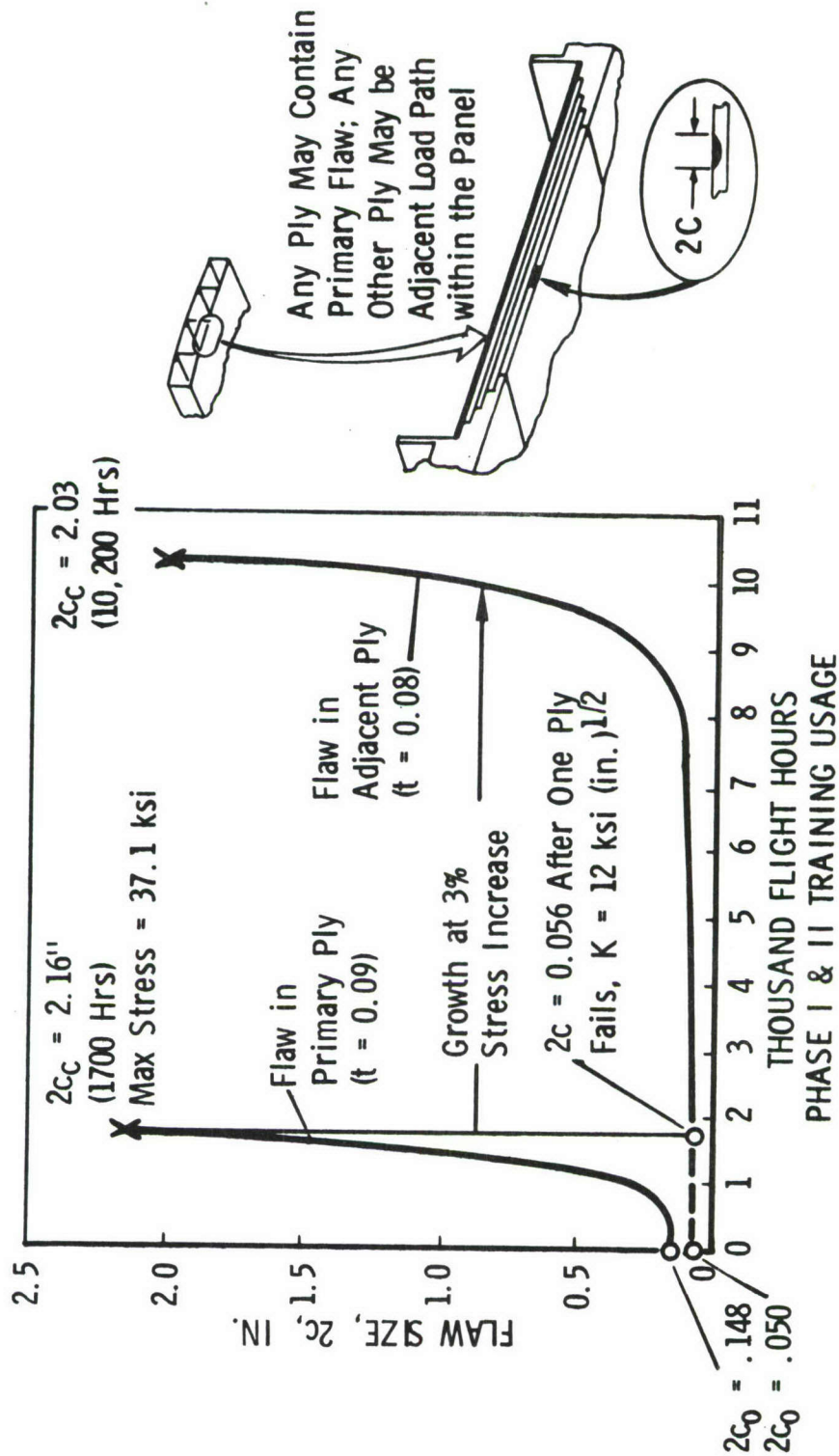


Figure 86 610RW003 Wing Box Laminated Lower Skin, Corrugated Spar Webs, Aluminum Phase IA Fracture Analysis

- Initial damage in the adjacent ply was $a/Q = 0.01$ plus the delta growth that occurred during time to fail the primary ply. The stress increase due to failure of primary ply was 3%. Residual strength required at time of primary ply failure = $1.15 \times P_{LT}$. The initial damage in the adjacent ply could not grow critical in 4000 - 1700 - 2300 hours. Calculated time to failure was 8500 hours.

(3) Semi-circular Corner Crack in Spar Cap Adjacent to Inboard Pivot Pylon Cutout (Figure 87)

- Assumed noninspectable structure.
- Analysis performed identical to case (1) except for flaw type. Stress concentration ($K_T = 2.5$) adjacent to cutout accounted for in analysis. Adjacent load path assumed to be spar cap on the opposite side of cutout.

7.4.2 Preliminary Design 610RW002 -
Multi Wet Cell, Planked Lower
Skin, Titanium

- Crack Arrest/Multiple Load Path (Ranked No. 2)
 - Lower Skin Planks provide Multiple Load Paths and Crack Arrest.
 - Brazed thin-ply laminate assumed to exhibit a decreased crack growth rate compared with that exhibited by the unbrazed titanium. Reduced rate represented by data for 6Al-4V recrys annealed titanium.
- Assumed Sequence of Failure for Analysis

(1) Through the Thickness Crack in Laminated Lower Surface Plank (Figure 88)

- Assumed Depot Inspectable Structure
- The analysis was directed at the thickest ply (0.060") as the worst case.

3 CORNER FLAW IN INBOARD PIVOT PYLON CUTOUT 7050-T76511 AI MACHINED EXTRUSION
(7050-T73651 AI PL. da/dN DATA) NONINSPECTABLE--4000 FLIGHT HOURS

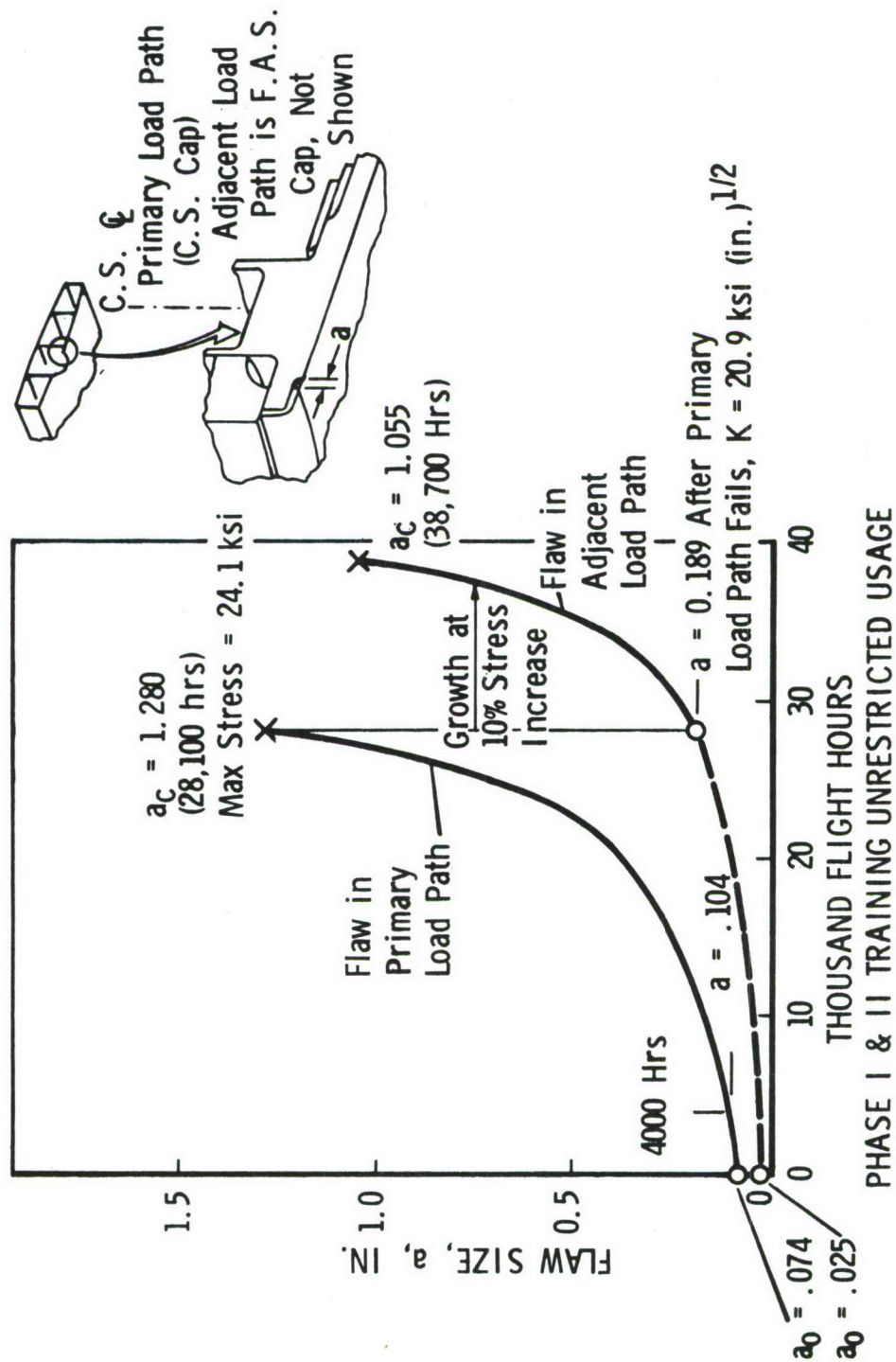


Figure 87 610RW003 Wing Box Laminated Lower Skin, Corrugated Spar Webs, Aluminum Phase IA Fracture Analysis

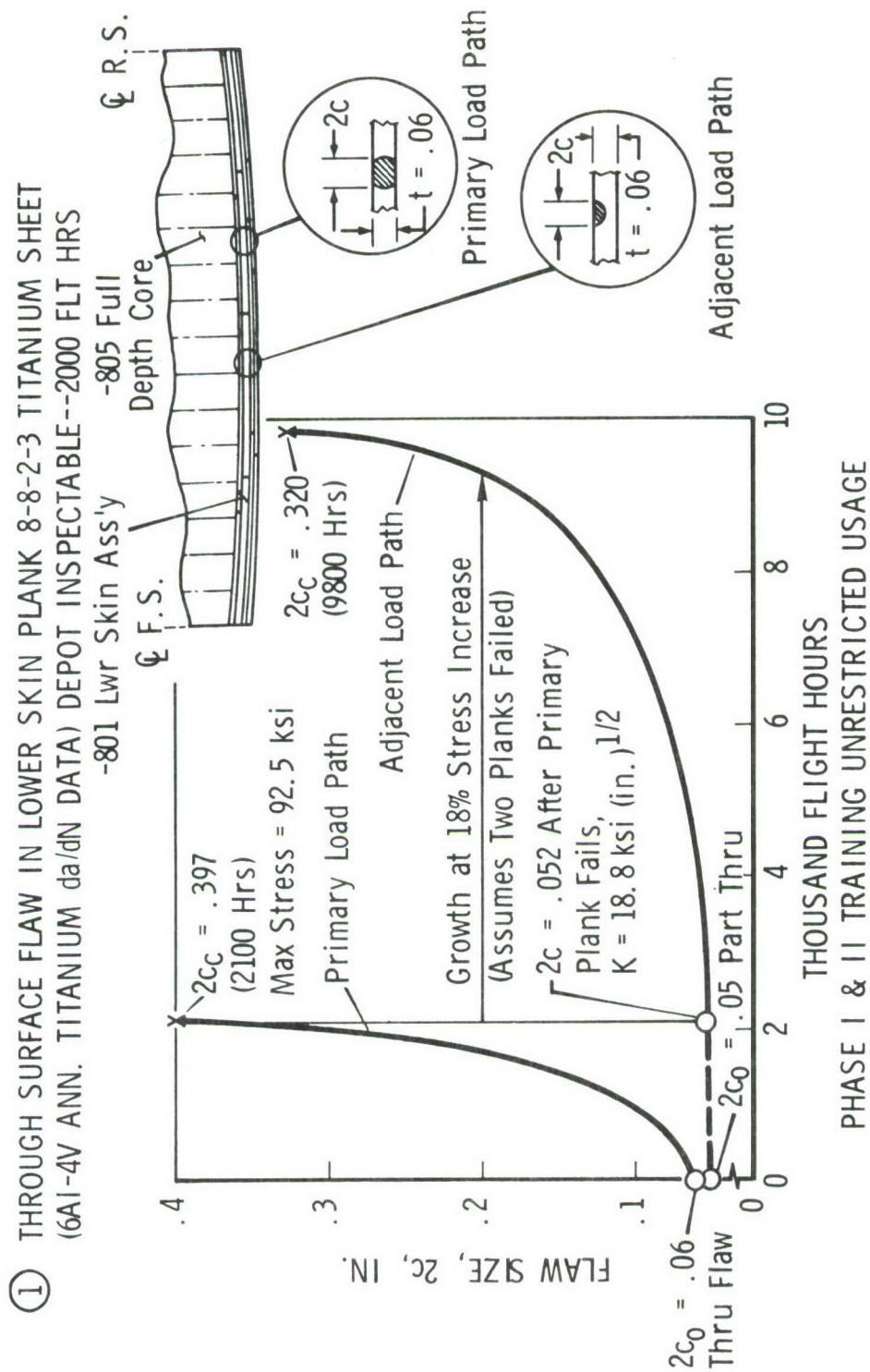


Figure 88 610RW002 Wing Box Multi Wet Cell, Planked Lower Skin
Phase IA Fracture Analysis

- . Unstable crack propagation failure was assumed to omit the primary skin plank as a tensile load carrying member with crack arrestment occurring at the edges of the plank. Initial damage was $a/Q = 0.03$ not to grow critical in 2000 flight hours due to application of P_{LT} . Residual strength required in the remaining structure at time of primary load path failure equals $1.15 \times P_{LT}$.
- . The adjacent load path was assumed to be an adjacent 0.06" plank. Initial damage was $a/Q = 0.01$ plus the delta growth that occurred during time to fail primary plank. In addition, it was arbitrarily assumed that two planks had completely failed making the stress increase in the adjacent load path 18%. The initial damage could not grow critical and cause failure of the remaining structure due to the application of P_{LT} .

7.4.3 Preliminary Wing Design 61ORW004 - Adhesive Bonded Honeycomb Skin Panels, Upper and Lower, Aluminum

- . Multiple Load Path Fail Safe (Ranked No. 3)
 - . Multiple Spars and Honeycomb Skin Panels
 - . Lower Panels comprised of Two Skins
- . Assumed Sequences of Failure for Analysis
 - (1) Part Thru Crack in Spar Cap Slug
(Figure 89)

- . Assumed noninspectable structure.
- . Unstable crack propagation failure assumed to omit primary spar cap as tensile load carrying member. Loss of spar cap will produce a fuel leak. Initial damage $a/Q = 0.03$ not to grow critical in 4000 hours due to application of P_{LT} .
- . Adjacent load path assumed to be adjacent spar cap. Initial damage $a/Q = 0.01$ plus delta growth that occurs during time to fail primary spar cap; not to grow critical and cause loss of remaining structure in 4000 hours due to application of P_{LT} .

① PART THROUGH SURFACE FLAW IN LOWER SPAR CAP 7050-T73651 AI PLATE (7050-T73651 AI PL. da/dN DATA) NONINSPECTABLE--4000 FLIGHT HOURS

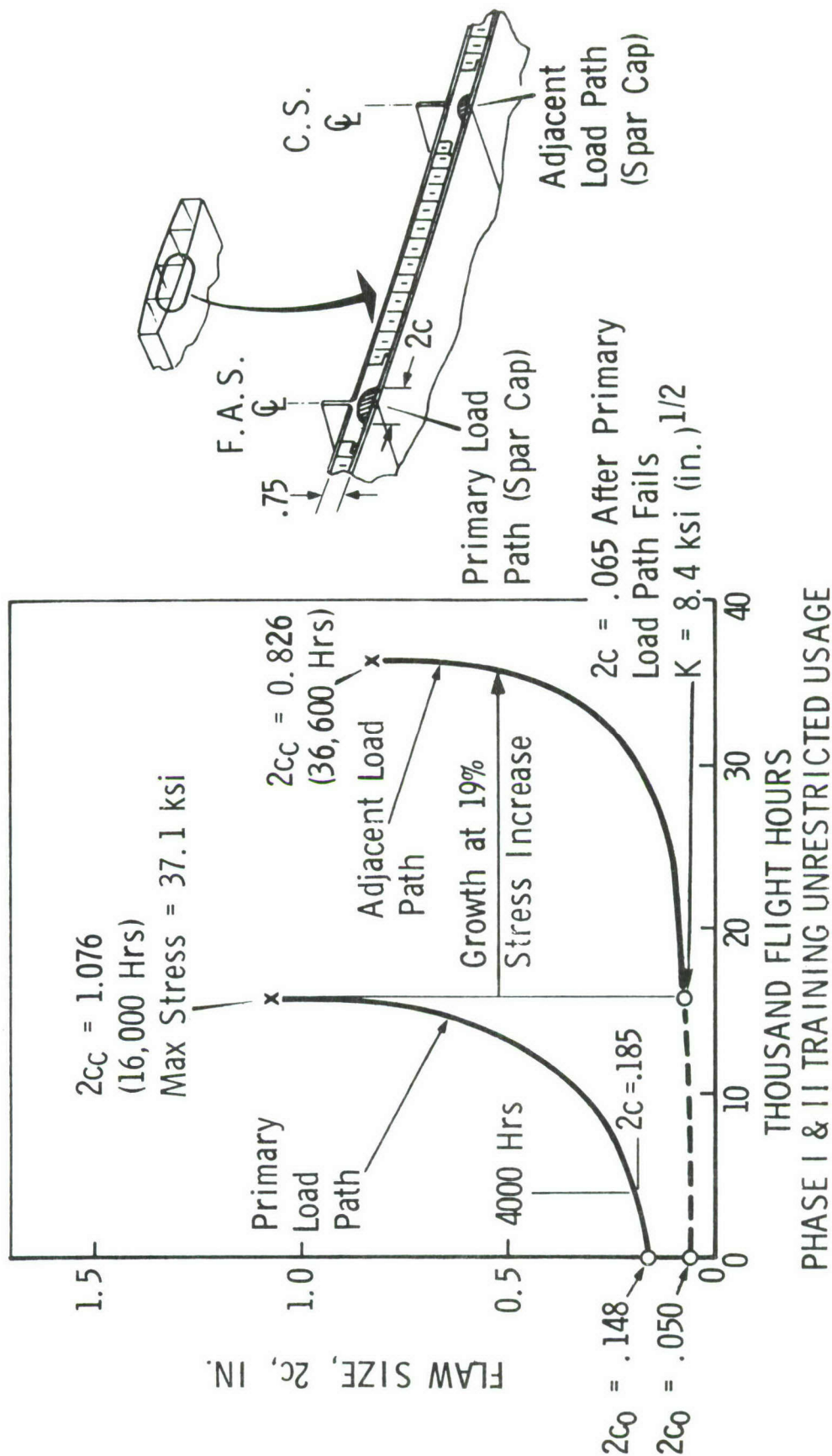


Figure 89 610RW004 Wing Box Adhesive Bonded Honeycomb Panel, Upper and Lower Phase IA Fracture Analysis

Stress increase of 19% due to failure of primary spar cap. Finite width correction included in the analysis. Residual strength required at time of prime spar cap failure = $P_{LT} \times 1.15$.

(2) Part Thru Crack in Outer Skin of Lower Panel (Figure 90)

- . Assumed noninspectable structure.
- . Complete failure of a load path (skin panel) requires failure of both (2) skins. Therefore, it was assumed for analysis that both skins could not fail in a total of 4000 flight hours. The highly stressed outer skin was treated as a primary load path, and the inner skin was treated as an adjacent load path with respect to initial damage and residual strength requirements. Crack arrest would probably occur at the skin-to-spar cap bond lines and definitely occurs at the free edges of the skins.
- . Initial damage in the primary skin was $a/Q = 0.03$. Residual strength required = P_{LT} . Calculated time to failure was 1700 hours.
- . Initial damage in the adjacent skin was $a/Q = 0.01$ plus the delta growth that occurred during the time to fail the primary skin. The stress increase due to failure of primary skin was 6%. Residual strength required at time of primary skin failure = $1.15 \times P_{LT}$. The initial damage in the adjacent skin could not grow critical in $4000 - 1700 = 2300$ hours. Calculated time to failure was 7400 hours. Residual strength required in the remaining structure at time of primary skin failure = $1.15 \times P_{LT}$. A fuel leak would occur when complete panel fails.

② PART THROUGH SURFACE FLAW IN LOWER PANEL OUTER SKIN 7050-T76 AI SHEET
(7050-T76 AI SHEET da/dN DATA) NONINSPECTABLE--4000 FLIGHT HOURS

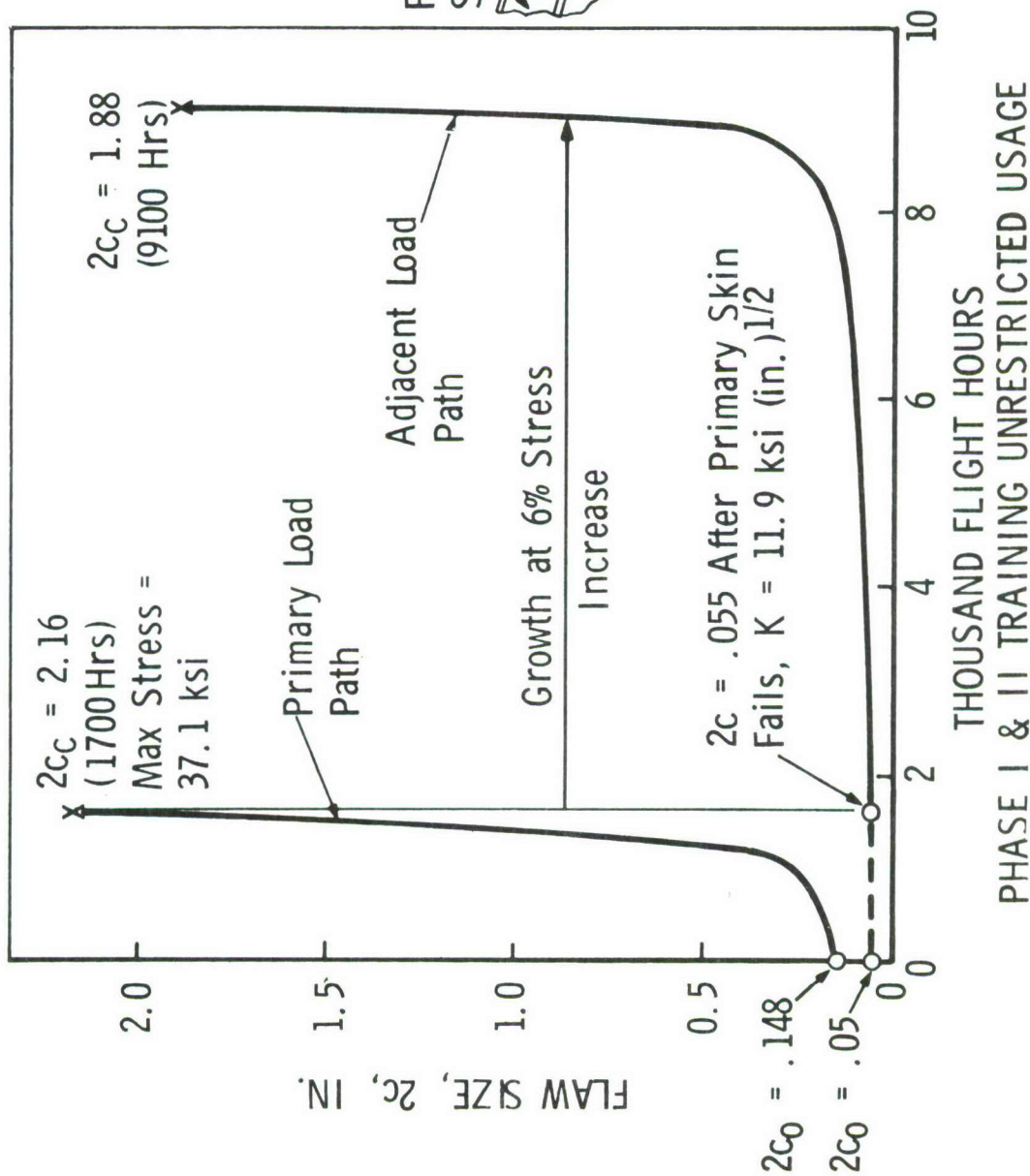


Figure 90 610RW004 Wing Box Adhesive Bonded Honeycomb Panel, Upper and Lower Phase IA Fracture Analysis

7.5 RISK ASSESSMENTS

Risk assessments have been performed to aid in establishing conservative structural inspection intervals for the wing structure of the primary design selection, 610RW003. The assessments can be described as the probabilistic quantifications of the in-flight failure potential of an individual airplane wing structure and of the fleet of wing structures. Failure is defined as the fracture of a structural element which due to multiple load path design of the wing structure results in only fractional loss of wing strength. The risk assessment discussion will present first a summary of the input data and procedures used to derive the risk assessments and secondly the assessment results.

7.5.1 Assessment Method

The major evaluation tool used in the analysis is the risk assessment model developed under the F-111 program. The model, which is programmed into the IBM 360 computer, consists of a set of mathematical equations which describe a close approximation of the probability of no structural failure during aircraft operations in the service environment. The equations are a function of those inputs that influence failure. For this study the following input data were used:

- o Fleet size of 506 airplanes
- o When a wing structure was assumed to have an initial flaw upon delivery to inventory, it was also assumed that the flaw of maximum size (after NDI) was located at the most critical location (fracture control point) and was positioned in the most critical direction. The initial flaw size characterization used (See Figure 91) was derived from best judgment of probability of flaw detection using penetrants by differentiating the probability of flaw detection curve to derive the initial flaw size frequency distribution curve.
- o Flight spectrum - 7.33g.
- o Flaw propagation based on da/dN for the expected environment and a retardation factor of $m = 1.4$. The propagation curves used were those established for 610RW003 in paragraph 7.4.1.

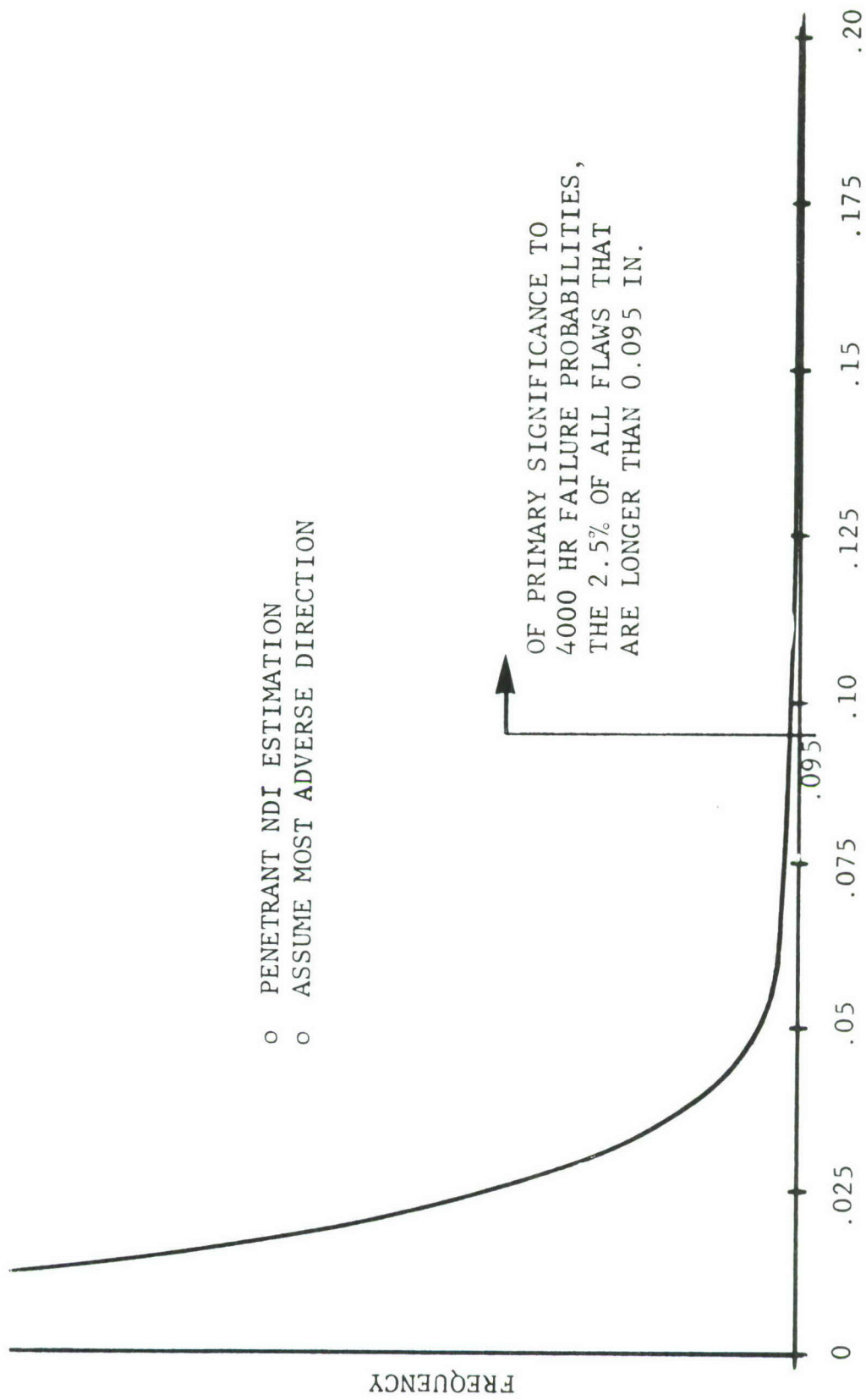


Figure 91 Initial Flaw Length-Inches Flaw Fracture Risk Assessment,
610RW003 Flaw Size Distribution Lower Skin Outer Ply

The method used within the risk assessment model for the determination of control point probability of no structural failure is illustrated in Figure 92 . The assessment is performed by a statistical combination of the initial flaw condition in the part after inspection with the flaw propagation to failure in flight. For example, looking at Figure 92 , assume there is a flaw at the control point under investigation and this flaw is from a population of flaws whose flaw lengths are characterized by some frequency distribution $f(x)$. The probability, ΔP , that the flaw length x lies within the small interval between x_1 and x_2 is the small area under $f(x)$ between x_1 and x_2 . Assuming then that there exists a flaw length x , the probability of survival at some flight time T can be calculated. Let $\phi(T)$ denote the cumulative probability distribution function and $\phi(t)$ denote the associated probability density function of operational life (distribution of flight times for the propagation of a flaw from length x to critical length x_c causing failure in flight.) These probability functions are determined by a scale and shape parameter. The scale parameter is evaluated using fracture mechanics flaw growth prediction techniques which evaluate the median flight hours (M) for a flaw of length x to grow to critical size, x_c , in flight. The shape parameter is derived from variations in load history, K_{Ic} values, flaw growth calculations, etc. The probability that a failure will occur at some flight time T is the integral, $\phi(T)$, of the life distribution from 0 to T as presented in the Figure 92 . The combination of ΔP and $\phi(T)$ then are used as shown to establish the probability of no structural failure in T flight hours.

7.5.2 Assessment Results

A quantification of in-flight failure potential for the airplane wing-structure has been established based upon fracture mechanics techniques for three different cases of flawed wing structure. Risk assessments were performed for an individual wing and for the fleet assuming initial flaws existed in the following locations on the 610RW003 wing when the wing was delivered to inventory:

- . Lower Skin Outer Ply
- . F.A.S. Lower Cap
- . Inboard Pivoting Pylon Cutout

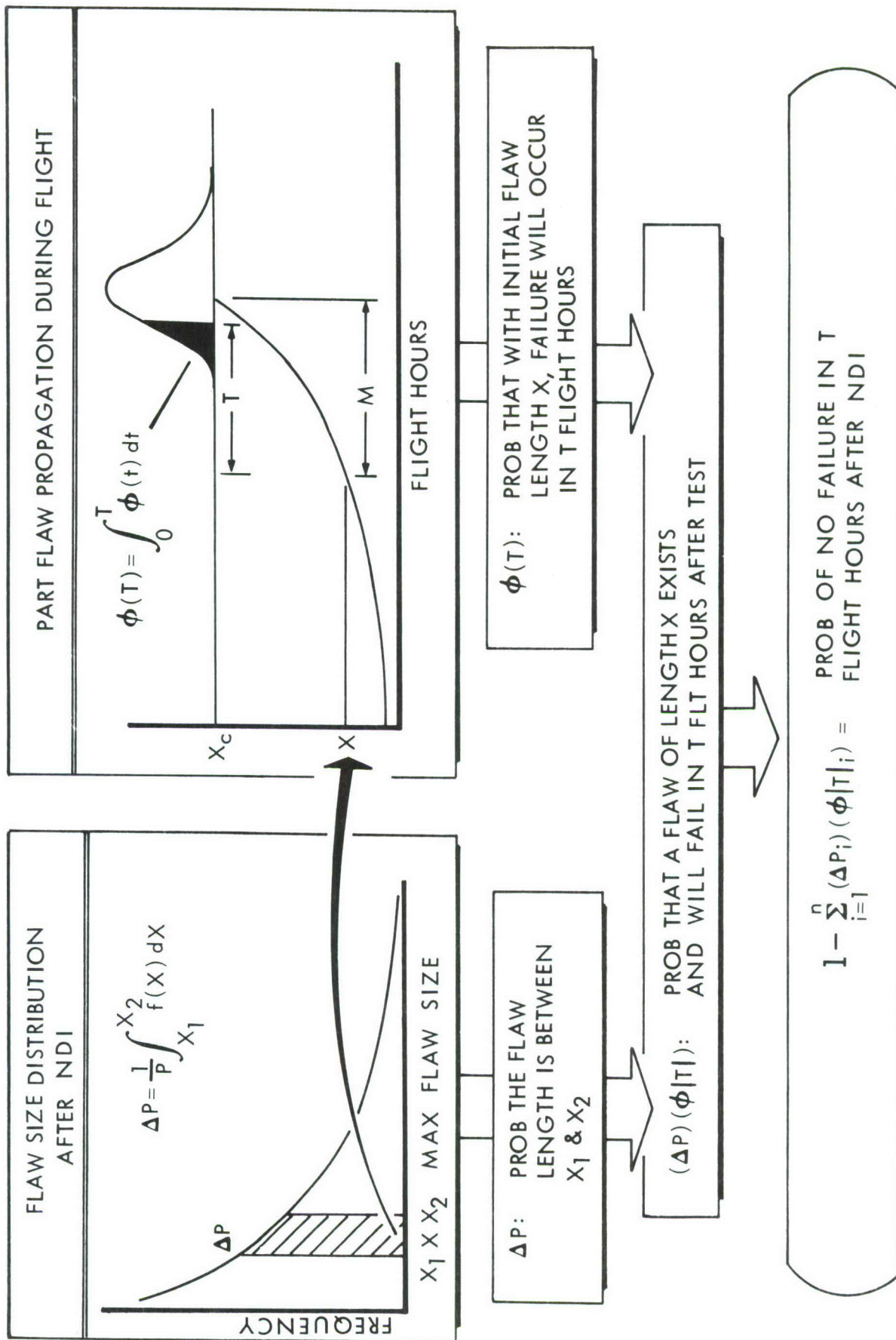


Figure 92 Determination of No Failure Probability

Figure 93 and Table XXXVI present the results for the case of flawed wing structure at the lower skin outer ply critical point. If it is assumed that an individual wing has an initial flaw of the size and location described in paragraph 7.5.1, then there is a 0.975 probability of a failure occurring in the wing during a 4000-flight hour period. Failure is defined as the fracture of a structural element which due to multiple load path design results in only fractional loss of wing strength.

If it is assumed that 10 wings in the fleet of 506 airplanes have an initial flaw located at the lower skin outer ply area, there is a 0.776 probability that the fleet will not encounter any failed lower skin plies due to these flaws during the flight period covering the first 4000 hours of flight on each and every airplane in the fleet.

The risk assessment study indicates that there is essentially no probability of failure for the individual wing or the fleet for a 4000 hour period when it is assumed that flaws exist in the FAS lower cap or the inboard pivoting pylon cutout critical points.

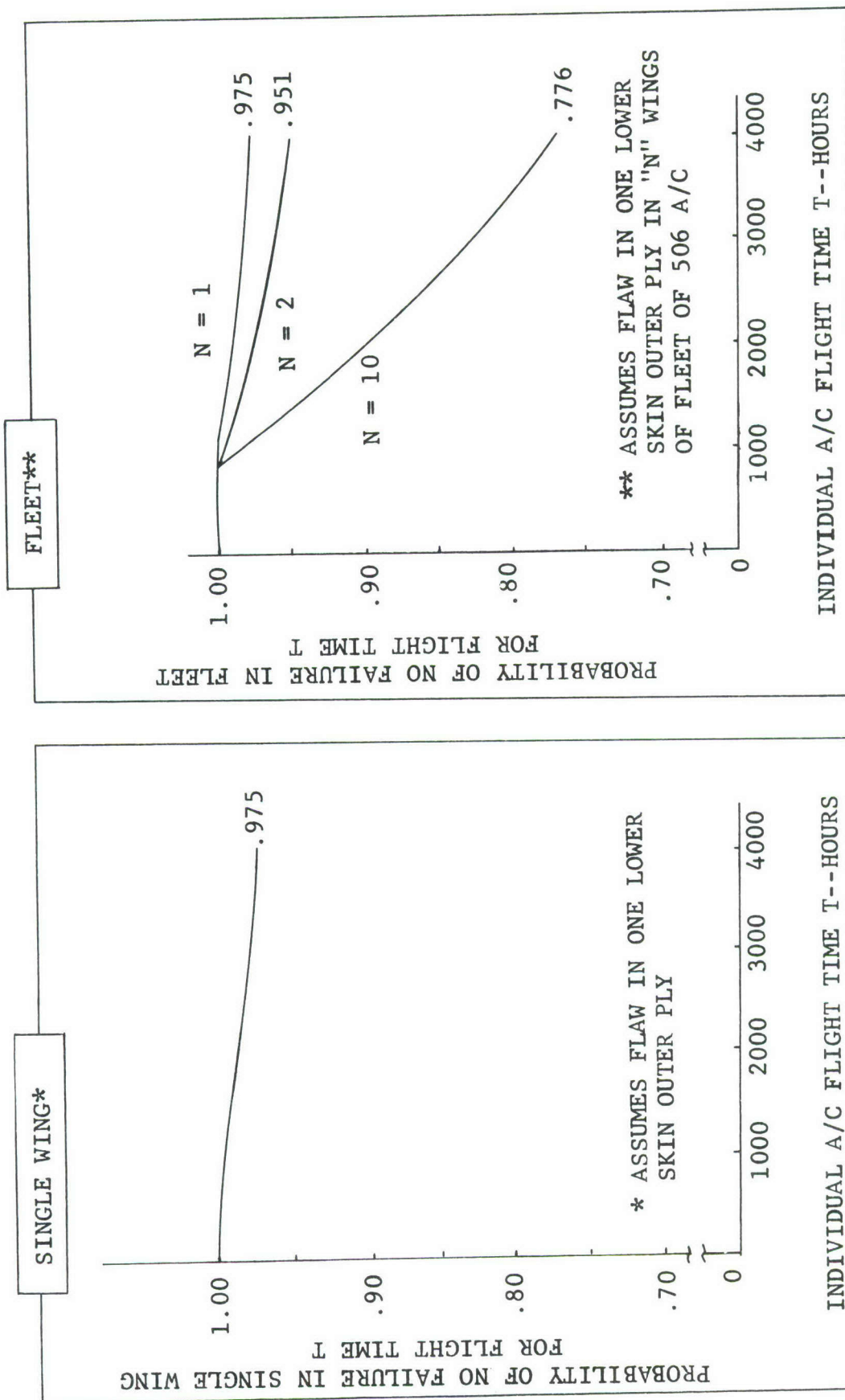


Figure 93 Probability of No Failure Vs. Flight Time

Table XXXVI FLAW FRACTURE RISK ASSESSMENT 610RW003
FAILURE, 506 AIRCRAFT FLEET

FLAW LOCATION	*NO FAIL PROBAB VS NUMBER FLAWED WINGS (4000 HR INDIVIDUAL AIRCRAFT FLIGHT TIME)		
	1 FLAWED	2 FLAWED	10 FLAWED
LOWER SKIN OUTER PLY	0.975	0.951	0.776
FWD AUX SPAR LOWER CAP FACE	~1.0	~1.0	~1.0
FWD AUX SPAR LOWER CAP CORNER INBD PYLON CUTOUT	~1.0	~1.0	~1.0

* FAILURE DEFINED AS FRACTURE OF STRUCTURAL ELEMENT WITH ONLY
FRACTIONAL REDUCTION IN WING STRENGTH DUE TO MULTIPLE LOAD
PATHS.

SECTION VIII MATERIALS ENGINEERING

8.1 MATERIAL SELECTION CRITERIA

The goal in the material selection process has been to obtain a high level of reliability, integrity, and efficiency at minimum cost by considering materials in combination with design and structure.

Primary consideration has been given to the ability of the materials to resist crack growth and corrosion (particularly under conditions of fatigue, stress and environments), as well as strength, toughness, and weight. Also considered has been the interrelated effects of fabricating and manufacturing conditions such as heat treating and temperatures for brazing or bonding. A summary scheme on the materials selection process is shown in Figure 94.

Candidate aluminum, titanium, and steel alloys considered at the beginning of this program are listed in Tables XXXVII, XXXVIII, and XXXIX, respectively, and are discussed in following paragraphs. In addition two new aluminum alloys, X2048 and Alcan GB X3058, are listed in Table XXXVIII even though their initial vendor test data has been obtained since the beginning of this program. Candidate materials were selected for their potential to provide the level of stress corrosion cracking resistance, reliability, integrity, and efficiency required in the proposed wing designs. The materials together with the design concepts considered were intended to supply the required level of fracture resistance to satisfy the damage tolerant requirements of the fracture control plan.

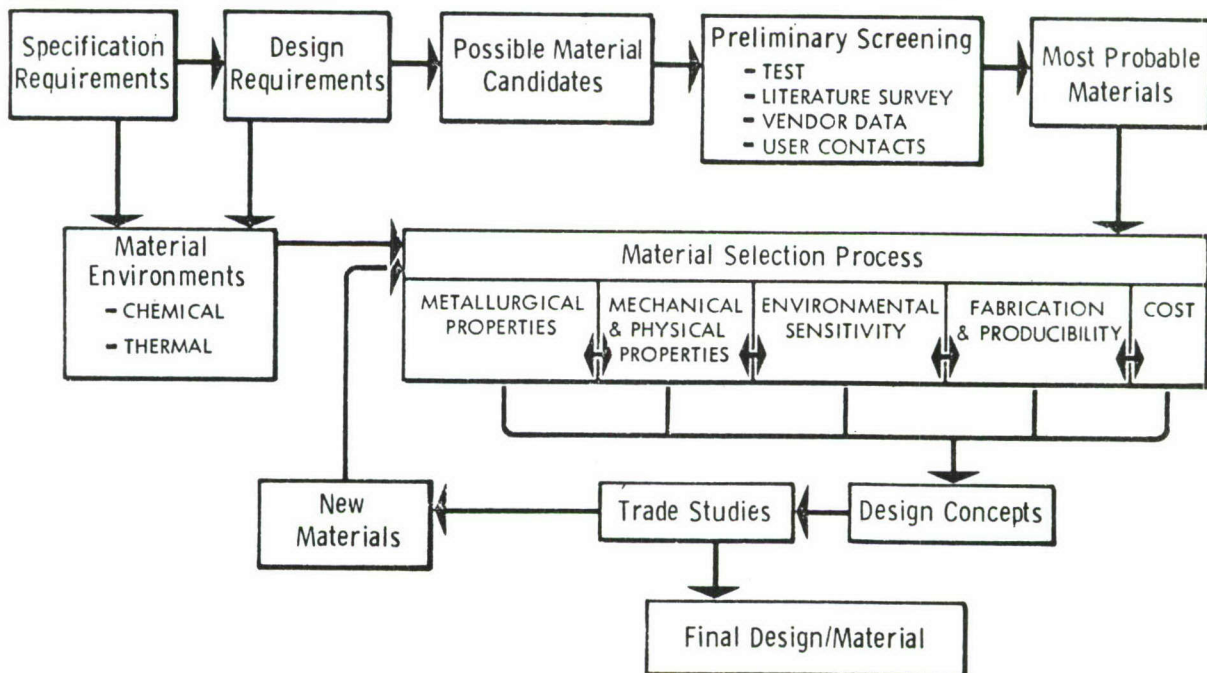


Figure 94 Materials Selection Process

TABLE XXXVII CANDIDATE MATERIALS – ALUMINUM ALLOYS

	SHEET (.100 inch thick)					PLATE (2.0 inches thick)						
	2024-T81	X2048-T81	2618-T6	ALCAN GB X3058-T6	7050-T76	7475-T761	2124-T851	X2048-T851	ALCAN GB X3058-T651	7050-T73651	7475-T7351	2219-T851
TUS (F _{TU}), ksi (L) (LT)	67 67	(Est) 65 (Est) 65	58 58	(Est) 66 (Est) 66	78 78	71 71	65 63(ST)	62(L) Tentative	(Est) 64 (Est) 64	71 68(ST)	67 65(ST)	62 62
CYS(F _{CY}), ksi (MIN)	59	(Est) 55	52	(Est) 54	(Est) 71	60	56	Tentative 55	(Est) 56	(Est) 62	55	47
E _{Mod} of Elast., psi X10 ⁶ (L)	10.5	Tentative 10.2	10.7	(Est) >10.3	(Est) 10.3	10.0	10.7	10.2	(Est) >10.3	(Est) 10.3	10.2	10.5
ρ, Density, lb/in ³	.100	.100	.100	(Est) .102	.102	.101	.100	.100	(Est) .102	.102	.101	.102
(L) TUS/ ρ , X10 ⁶	6.70	6.50	5.80	64.7	7.65	7.03	6.50	6.20	6.2	6.96	6.63	6.08
E/ρ , X10 ⁶	105.	102.	107.	>101.	101.	99.	107.	102.	>101	101	101	103.
K _{IC} , ksi√in (L-T) (TYP)	-	-	-	-	-	-	29 24 22	35 30 25	32 26 22	35 30 26	50 45 33	33 30 20
K _{IC} , ksi√in (TYP) L-T	50	(1 test) 145	Need Data	107	(Est) 75	100	-	-	-	-	-	-
Stress Corrosion Resistance	Good	Good	Need Data	Good	Good	Good	Good	Good	Good	Good	Excellent, Same as 7075-T73	Good
Exfoliation Resistance	Excellent	Excellent	Need Data	Est good Based on SCC	Good	Good	Excellent	Est good Based on SCC	Est good Based on SCC	Excellent	Excellent	Excellent
Industry Experience	Extensive	None	Extensive for Con- corde; in U.S. only in forg- ings	None	None; is being widely tested	None	Extensive as 2024- T851 special test grade	None	None	None; is be- ing widely tested	Limited for present usage but being used on prototype vehicles	Moderate; sheet gages are used in welded applications
Available Sources	Numerous	Experi- mental Reynolds Metals Co alloy	Alcan- Booth in England; Cegedur in France	Experi- mental Alcan- Booth alloy in England	Alcoa now; General avail. eventually	Presently available from Alcoa only	Numerous sources	Est good Based on SCC	Experi- mental Alcan- Booth alloy in England	Alcoa now; generally available eventually	Presently available from Alcoa only	Numerous sources
Remarks	General Airframe use	Possible near 2024 strength at hi temp. but with nearly twice fracture toughness	U.S. pro- ducers would mfg. if there is market	New Al-Cu- Mg-Germanium alloy system; may be weld- able. Strength near 2024 at hi temp; but tougher	Alcoa now; General avail. eventually	Premium quality 7075	Premium quality 2024 used extensively on F-111 in thick plate	Possibly strength at hi temp but with higher frac- ture tough- ness	New Al-Cu- Mg-Germanium alloy system may be weld- able. Strength near 2024 at hi temp but tougher	Good SCC resist- ance with high strength and tough- ness	Premium quality 7075	Weldable

**TABLE XXVIII
CANDIDATE MATERIALS - TITANIUM**

ALLOY CHARACTERISTIC	BETA III 11.5Mo-6Zr-4.5Sn	8-8-2-3 8Mo-8V-2Fe-3Al	BETA C 3Al-8V-6Cr-4Mo-4Zr	6-4 STOA 6Al-4V	6Al-4V BETA ANNEALED	6-4 MILL ANN. 6Al-4V	6-4 STA 6Al-4V
	BETA ALLOYS		ALPHA-BETA ALLOYS				
UTS, Min. Guar., ksi	190 (H900) STA Sheet	Sheet & Plate 175 STA	Sheet & Plate 175 STA	—	130-120 Thickness Dependent	134 Sheet 130, Bar, Billet 140	160 Sheet, < .75" Plate 168
UTS, Typical, ksi	200 ksi STA Sheet 180 ksi (H1000) STOA Sheet	125 ST 196 STA	125 ST 196 STA	150, Forging	143		
E, Mod. of El., PSI	15 x 10 ⁶	15.4 x 10 ⁶	15.4 x 10 ⁶	16.5 x 10 ⁶	16.5 x 10 ⁶	16.5 x 10 ⁶	16.5 x 10 ⁶
Density, ρ	0.183 lbs/cu. in.	0.175	0.174	0.160	0.160	0.160	0.160
UTS/P, Min.: Typ.: x 10 ⁶	1.04 1.09	1.00 1.12	1.01 1.13	— 0.94	— 0.89	0.81 0.88	1.00 1.05
E/P x 10 ⁶	82.0	88.0	88.5	103.0	103.0	103.0	103.0
K _{1C} , ksi √in. (Forging)	58.9-63.4	59.3-67.2	55.7-65.2	60	80-100	50-60	32-46
Stress Corr. Resist.	Very Good, K _{1SCC} ~30	Insufficient Data	Insufficient Data	Good, K _{1SCC} ~30	Very Good	Good; K _{1SCC} ~35-40	Not as Good as Annealed
Creep Strength	Good	Insufficient Data	Insufficient Data	Good	Good, Improved by Beta Forging	Good	Above 500° Affects Aging
Weldability	STA High but Below Base Metal; Good Duct	Insufficient Data	Insufficient Data	Fair, Familiar Process	Fair, Familiar Process	Fair, Familiar Process	Weld in ST + Partial Aged Condition. Further Aging after Welding
Producibility, Cold RH	Excellent; ST + WQ RH = 2	Excellent; ST + AC RH = 2.5	Excellent; ST + AC RH = 2.5	Fair, Hot Dies Req'd	Fair, Hot Dies Req'd	Fair, Hot Dies Req'd	Limited. Effect on Aging Critical
Industry Experience	Limited	Limited	Limited	Limited	Limited, Forging Process Critical	Extensive	Limited
Availability/Sources	All Forms Crucible	New Beta Alloy. Limited Avail. General Use Expected TIMET	New Beta Alloy Limited Avail General Use Expected RMI	Numerous Sources	Numerous Sources	Numerous Sources	Numerous Sources
Remarks	High Strength, Outstanding Fabricability. Handicap is High Density, Low E	Heat Treatable to Higher UTS with Loss in K _{1C} and K _{1SCC} Properties than with 170-175 ksi Selected as Optimum. Competitive with Beta III. Said to Cold Form Better than Beta III. Higher E, Lower Density. Stable Properties to 600°F		Requires Aging by User. Limited Test Data and Experience. Strength & Toughness Improved over Annealed	Limited Test Data and Experience. Fatigue Str. & Ductility Reduced. Toughness, Forgeability and Creep Improved	Most Commonly Used Titanium Alloy and Condition	Limited Formability Prevents General Use

NOTES: 1. Beta Alloys Involve Higher Producer Costs, Lower User Cost. All Beta's shown have Superior Deep Hardenable Properties Compared to Alpha-Beta's

2. Beta Alloys as a Class have Lower Creep Strength and General Thermal Stability than the Alpha-Beta Alloys

TABLE XXXIX
CANDIDATE MATERIALS - STEEL

	9Ni-4Co-20C	PH13-8Mo	Maraging Steel 200 Grade	10Ni-Cr-Mo-Co	D6ac
Strength Level, Ksi	190-210	200-220 (TH-1050)	200-220	190-210	200-220
K _{IC} , ksi√in. (Coupon Tests)	100+	90+	100+	200+	90
Stress Corrosion Resistance	Good	Fair	Good	Excellent	Expected to be Good (K _{ISCC} ≥ 35)
Processing Required by User	Quench plus Temper	Age	Age	Quench and AGE	Quench and Temper
Aerospace Industry Experience	Limited but Increasing	Limited Except for Fasteners	Limited but Increasing	Negligible	Extensive at Convair in the 220-240 ksi Range
Availability	Republic Steel Only	Armco Only	Numerous Sources	U.S. Steel & Others in Dev.	Numerous Sources
Remarks				Alloy still in R&D Stage	Extensive use on F-111 at Higher Strength Level
Possible Application	High Load Airframe Elements	Hot, Corrosive Environ- ment	High Load Airframe Elements	High Load Airframe Elements	High Load Airframe Elements

8.2 CANDIDATE MATERIALS

8.2.1 Baseline Materials

The F-111 wing utilizes 2024-T851 aluminum for upper and lower skins, intermediate spars and ribs in an efficient form, as numerically controlled machined plate with spars spaced to achieve a high buckling strength and a high degree of material utilization. Front and rear spars are machined from higher toughness 2124-T851 plate. A pivoting pylon fitting is machined from a large 2024-F die forging and heat treated to the T6 temper. This is an economically produced and structurally efficient wing with a demonstrated high structural reliability. As a baseline, it presents a major challenge for weight and cost reduction and for increased fatigue life.

8.2.2 Candidate Aluminum Alloys

In the last decade, development of metals has been concentrated on improving material reliability with little increase of ultimate tensile strength. The aluminums have been improved to overcome their serious vulnerability to exfoliation and stress corrosion of the high strength alloys such as 7079 and 7075 in the T6 temper. With the new zinc alloys of aluminum, 7050 and 7475 in the improved tempers, major improvements in exfoliation, stress corrosion resistance and fracture toughness have been achieved while maintaining ultimate tensile strength. Since elevated temperatures cause more strength loss in 7000 series aluminum alloys than in 2000 series alloys, time and temperature combinations are of major importance in aluminum alloy selection. Two new copper alloys of aluminum appear to be competition with 2024/2124 at elevated temperatures but with improved ductility. They are the Reynolds Metals Company X2048 and the British Alcan GB X3058 alloy. The latter is copper-magnesium-germanium alloy of aluminum developed by the Fulmer Research Institute with the laboratory name "Almagen" and now being manufactured by Alcan Booth Sheet, Ltd. Plate of both new 2000 series alloys would have higher strength and possibly equal fracture toughness to 2219-T851 plate. The latter, despite its low yield strength, has been the only elevated temperature aluminum alloy plate tougher than 2124-T851 plate for fracture critical designs.

The F-111 wing skins and the spars under three inches in plate thickness are of conventional 2024-T851. This has proven to be a good material for that program. For plate thicknesses above three inches, the procurement specification required that control of short transverse ductility be achieved. Thus, the heavier spars

have been procured to this requirement. A later specification which required short transverse ductility control from 1.5 to 3.0 inches of plate thickness was released. Suppliers were compelled to provide a higher purity 2024-T851, identified now as 2124-T851, to meet the short transverse requirements in the new specifications. This alloy has excellent exfoliation and stress corrosion resistance, adequate fracture toughness, and remains a competitive candidate, along with the newer 7000 series alloys and tempers, principally because of its superior performance at elevated temperatures. Spars can be improved by the use of 7050-T73651 plate if skin stresses are raised to permit higher spar cap stresses. Fracture toughness of the 7475 is higher than that of the 7050, but the 7050 is substantially tougher than the 2024/2124-T851 alloys. The tensile strength of the 7050 is higher than the 7475.

Designs that shift from the present F-111 machined plate concept to manufacturing from aluminum sheet would have to choose from a number of candidate materials. Both 7475-T761 and 7050-T76 would be stronger than 2000 series alloys unless temperature-time combinations were too high. The 2000 series sheet alloys would be 2024-T81, 2618-T6, X2048-T81, and Alcan GB X3058-T6.

8.2.3 Candidate Titanium Alloys

Candidate titanium alloys include the improved 6Al-4V versions, Beta III, and the newer beta alloys Ti-8Mo-8V-2Fe-3Al and Beta C.

Ti-8-8-2-3 and Beta C alloys have typical properties comparable to Beta III but at the beginning of Phase 1A of this program insufficient test data existed for vendors to show guaranteed properties for these two alloys which are as good as Beta III. Ti-8-8-2-3 and Beta C alloys have excellent fabricability in the ST condition and a lower density and higher stiffness than Beta III. Condition STA target properties of 175 ksi minimum ultimate strength were chosen for design considerations.

The 6Al-4V material in the recrystallized annealed condition, in the Beta processed annealed and in the solution treated and over-aged conditions achieves a high fracture toughness and fatigue strength, but has low tensile strength in all three conditions. Design allowables on 6Al-4V material in various manufactured conditions is available.

8.2.4 Candidate Steel Alloys

As is the case with aluminum, the emphasis in steel development during the last decade has been toward an improvement of fracture toughness and stress corrosion resistance. Consequently, steel with adequate fracture toughness is not competitive with aluminum and titanium on a strength-to-weight ratio for airframe applications except in some areas that are space limited and have a concentration of high loads or where stiffness-to-weight is more important than strength-to-weight.

For this program, it was expected that concentrated load fittings would be of steel or titanium. Steel alloys in the 200 ksi or 220 ksi heat treat range, with ample fracture toughness, could be used to an advantage in the wing root area. Candidate alloys included D6ac, the U. S. Steel 10Ni-Cr-Mo-Co, Republic Steel Corporation 9Ni-4Co-.20C, and maraging 200 grade. D6ac at 200 ksi has a K_{IC} of approximately 90 ksi $\sqrt{\text{in}}$ and 10 Ni (HY180), 9Ni and Maraging 200 are well above 100 ksi $\sqrt{\text{in}}$. All of these alloys are weldable. The 10Ni alloy under development by U. S. Steel, is believed to have better stress corrosion resistance than the other candidates. For strength above 220 ksi, maraging 250 grade is a candidate because of its ease of user processing. However, industry familiarity in aircraft applications of the maraging steels is limited.

8.3 TEST PROGRAM

8.3.1 Test Plan

The basic Phase IA material test program is shown in Table XLIII in Appendix VIII. In addition to the basic program spectrum environmental tests were conducted on surface flawed specimens of the baseline 2024-T851 plate material in support of the baseline damage tolerance analysis. The basic Phase IA material test program represents a minimum dollar expenditure to fill in pre-design material screening gaps. In selecting test materials consideration was given to other test programs in progress. Specific considerations are discussed below.

Aluminum Alloys

Most needed design information on 2024, 2124, and 2219 was available or was being obtained in other programs. The 2618 alloy used in Europe in sheet and plate forms would need more characterization regarding fracture toughness, stress corrosion, and crack growth rates. Since its superiority over 2024-T81 and -T851 in

creep is only for long soak times at temperatures in the range 300°F to 325°F (or shorter times at higher temperature), 2618 alloy test consideration was dropped. All testing was planned to characterize the two new Alcoa developed stress corrosion resistant alloys 7475 and 7050. Particular emphasis was aimed at filling in information gaps on the effect of elevated temperature to permit a choice between them and 2024/2124 for wing exposure near 300°F.

Titanium Alloys

Data on the recrystallized annealed 6Al-4V titanium alloy would be available from the tests being accomplished by Rockwell International for the B-1 aircraft. Data for the beta processed annealed 6Al-4V titanium and Beta C alloy would be evaluated in Convair's Advanced Metallic Air Vehicle Structure (AMAVS) Contract F33615-73-C-3001. Both sheet and plate in Ti-8Mo-8V-2Fe-3Al (Ti-8-8-2-3) alloy in the STA condition were selected for test.

Steel

No steels were selected for tests due to the fact that the most promising high strength ductile alloys were scheduled to be tested either in the B-1 aircraft program or by Convair in its AMAVS program.

8.3.2 Test Specimens

Test specimen configurations are shown in Figures 69 through 72 in Appendix VIII. Standard tensile and compression specimens are shown in Figure 69. Compact tension specimens for K_{Ic} and K_{Isc} tests are shown in Figure 70. The configurations of edge notched fatigue specimens are shown in Figure 71. Figure 72 shows the standard configuration for surface flawed da/dN specimens. Note from the dimension table that the grip end widths were wider for Ti-8-8-2-3 and 2024-T851 specimens. Figure 73 shows the specimen identification system used for the compact tension fracture mechanics specimens. Application of the same system to Figure 72 surface flawed specimens would specify "L-S" for loading specimen in rolling direction with the crack growing in the plate thickness direction.

8.3.3 Materials Tested

One piece of a 7050-T76 aluminum alloy sheet 0.063" x 48" x 48" from Alcoa Lot No. 109-216 was procured for test. The thickness measured .060 inch. Test specimen locations within

this sheet are shown in Figure 74 in Appendix VIII.

One piece 3.0" x 60" (LT) x 50" (L) of X7050-T7E60 was obtained from the Grumman Aerospace Corporation which had been procured from Alcoa Lot No. 729-091. Information from Alcoa indicated that the artificial age cycle used on this lot for "-T7E60" temper has been adopted as the artificial age cycle for future 7050-T73651 plates. Therefore, throughout this report the 7050 plate will be considered to be 7050-T73651 material. Specimen locations are shown in Figures 75 through 77 in Appendix VIII. As noted in Figure 75, a 30 inches wide section from the center of the 60 inches wide plate was selected for test material and was sawed into six pieces labeled A, B, C, D, E, and F. Figures 76 and 77 show the layout of all specimens. Sections A, B, C, and D were milled on each surface prior to layout. Specimens with the letters "A" or "B" were tested from the plate quarter thickness and the remainder tested from the plate center thickness.

One sheet 0.125" x 48" x 144" of 7475-T61 was procured from Alcoa Lot No. 102-145 from master Lot No. 681-036. A piece was cut from each end of the full sheet for test use and these were additionally artificially aged at Convair per Alcoa's recommendation to the -T761 temper. This Convair age was 15 hours at 325°F \pm 5°F. Orientation and location of test specimens in the two pieces of 7475-T761 test material are shown in Figure 78 in Appendix VIII.

One piece of 7475-T7351 aluminum alloy plate 1.5" x 18" (LT) x 48" (L) was procured from Alcoa Lot No. S-416232 and master Lot No. S-395607. Specimen layout for this material is shown in Figure 79. Note that the fatigue specimens were from the plate one quarter thickness while the tensile specimens were from the center thickness to match area tested for crack growth rate.

Three pieces of 0.125 inch thick Ti-8Mo-8V-2Fe-3Al titanium alloy sheet from Titanium Metals Corporation of America (TMCA) Lot No. K4179 were received in the STA condition. Surfaces had been ground and the largest piece was nearly one inch out of flat due to a gentle bow that could be easily flattened by hand pressure. Layout of test specimens on the three pieces is shown in Figure 80. After three tensile specimens and four notched fatigue specimens had been tested, desire for improved ductility necessitated additional aging of remaining specimens. After coordination with TMCA, the remaining fatigue and additional tensile specimens were aged 6 hours at 1050°F in a retort under a dried, purified (hot titanium chips) atmosphere. This reduced the

ultimate tensile strength in the longitudinal direction from 193.2 ksi to 184.1 ksi, still meeting the target of 175 ksi minimum.

One Ti-8Mo-8V-2Fe-3Al titanium alloy plate 1" x 36" (LT) x 48" (L) was received from TMCA Lot No. V4743, TS L8143 in the STA condition. Surfaces had been ground and the plate was extremely wavy. A check of the deviation from flatness was made by using a straight edge contacting high points at center width and four inches in from each edge. The center width had a bow up to .31 inch maximum in 34 inches of length. Plate flatness problems would have to be resolved if this material were used on production parts. Specimens were located in the test plate so that flatness would not be a problem. Specimen layout for the 1 inch thick Ti-8-8-2-3 titanium alloy plate is shown in Figure 81 in Appendix VIII.

Prior to machining of specimens, TMCA's tensile data was completed at their mill. The results indicated the ultimate tensile strength of the 1 inch thick plate to be so far above the target 175 ksi that ductility might be lowered. Based on TMCA lab tests on LT direction plate samples, Convair additionally aged all plate material 6 hours at 1100°F. When L direction specimens were tested, it was noted that resulting tensile values in the longitudinal direction were below the target of 175 ksi even though LT direction properties were near 182 ksi.

Material for the baseline randomized spectrum/environmental fatigue program was from a piece of 1½ inches thick 2024-T851 plate from Alcoa Lot No. 217-921 that met Convair specification FMS-1010. Layout for those fatigue specimens with accompanying tensile and fracture toughness coupons is in Figure 82 of Appendix VIII.

8.2.4 Test Procedures

Testing procedures for tension, compression, fatigue, fracture toughness (K_{Ic}), stress corrosion (K_{Isc}), and crack growth rate specimens are described in the following paragraphs.

Tensile

The 0.505 and 0.357 inch diameter tensile specimens were tested in a 120,000 lb. capacity BLH hydraulic universal test machine. The 0.2% offset yield strength was determined using either a PS-5M or PS-2M extensometer. The 0.5 inch wide sheet specimens were tested in a 20,000 lb. capacity Instron TT-D test machine. A T-1M extensometer was used to determine the yield strength.

Elevated temperature tests at 270, 300, and 350°F for aluminum alloy specimens were conducted in a Missimers environmental chamber. Temperature was monitored by a thermocouple attached directly to the specimen. Temperature was controlled to $\pm 3^\circ\text{F}$. All specimens were soaked $\frac{1}{2}$ hour in the test chamber prior to testing. Long time temperature exposure was accomplished in a Hevi-duty Temprite air-recirculating oven with the temperature monitored directly from a thermocouple attached to a test coupon. All test procedures met the requirements of Federal Test Method Standard 151a, Method 211.1 and ASTM E8-68.

Testing of the short transverse 7050 plate specimens was performed by the Process Control Department using the "tight control" method used in production for measuring low tensile ductility aluminum material.

Compression

The 1.0 inch diameter compression specimens from the 7050-T73651 aluminum alloy plate were tested in a 120,000 lb. capacity BLH hydraulic universal test machine. A spherically-seated lower compression platen and rigid upper platen were used to apply uniform loading to the specimen. A PC-1M averaging compressometer was used to measure the 0.2% offset yield strength.

The 7050 sheet specimens were tested in compression using a specially designed fixture to prevent buckling of the specimen. The fixture employed 1/16 inch diameter ball bearings on 1/8 inch centers to maintain contact with the restraining fixture,

thus preventing buckling while providing minimum friction. A PS5M averaging extensometer was attached to each edge of the specimen by knife edges and extension arms. The microformer was outside the oven. Testing was conducted on the 6,000 lb. range of the BLH test machine. Both the compressometer and extensometer were calibrated prior to testing to improve the accuracy of the modulus determination. Accuracy of strain readings met the requirements of ASTM E83-67 for Class B-2, which would result in some scatter in modulus values obtained. All compression testing met the requirements of ASTM E9-67.

Elevated temperature testing at 270, 300, and 350°F on aluminum alloy specimens was conducted in a Convair constructed, electrically heated, air recirculating oven. Temperature was controlled to $\pm 5^\circ\text{F}$. All specimens were soaked at temperature $\frac{1}{2}$ hour before testing. Long time exposure was conducted identically to the tensile specimens.

Fracture Toughness

Fracture toughness testing of the compact tension specimens was conducted in an Instron TT-D test machine. Fatigue precracking was performed in a Sonntag SF-1-U fatigue machine using a 5:1 multiplying fixture. Two decreasing fatigue loads were used to crack the specimens such that the final stress intensity was $\ll K_{Ic}/2$ as required by the ASTM E399-71 testing specification. The fatigue cracking conditions ($R = 0.1$) were as follows:

7475-T7351 1- $\frac{1}{2}$ Inch Thick Specimens

<u>Max.</u> <u>Lbs.</u>	<u>K_f</u> <u>ksi-$\sqrt{\text{in.}}$</u>	<u>Approx. No.</u> <u>Cycles x 10³</u>	<u>Crack Growth</u> <u>a, Inch</u>	<u>Final Crack</u> <u>Length, Inch</u>
2830	11	45	0.10	1.55
2100	9	40	0.05	1.6

X7050-T73651 1 Inch Thick Specimens

1450	9.4	30	0.05	.97
1000	7	45	0.05	1.02

8-8-2-3 Titanium Cond, STA 1 Inch Thick Specimens

2100	13	25	0.05	.95
1300	9	25	0.05	1.00

A calibrated double cantilever compliance gage was used to obtain the crack opening displacement (COD). Flat bottom fixtures and undersize pins were used to minimize frictional load effects as the crack propagated. All test procedures met the requirements of ASTM E399-71.

Stress Corrosion

Stress corrosion (K_{Isc}) tests in 3.5% NaCl were conducted on the short transverse grain direction of the 7050 aluminum plate using the same type, precracked, compact tension specimens used for K_{Ic} tests. The specimens were sustain-loaded in a Riehle 12,000 lb. deadweight creep machine. The sustained load was calculated in relation to the static K_{Ic} of the material. Testing was conducted to failure or 1000 hours if no crack growth was detected. If failure did not occur, the specimens were statically tested and the residual K_Q strength measured. One specimen (50-59) was progressively step loaded in 100 lb. increments until measurable crack growth occurred.

Stress corrosion specimens were fabricated from the Ti-8-8-2-3 plate in the L-T and T-L directions. The short transverse direction could not be tested because of the plate thickness. The specimens were loaded at a stress intensity level, K_{Ii} , which was below the K_{Isc} of the material. The loads were then progressively increased at approximate 24 hour intervals until crack growth or failure occurred. The highest load attained in the step loading procedure was considered as K_{Isc} .

Crack growth was monitored with a creep extensometer which had been modified to clip into the specimen notch. COD-time curves were recorded from which incubation time and da/dt curves could be obtained.

The 3.5% NaCl corrodent was contained in a plexiglas container adhesively attached to both sides of the specimen with an expandable rubber seal in the notch. Corrosion of the aluminum formed a deposit in the notch which had to be flushed out weekly. Evaporation losses were replaced during the week with distilled water. The corrodent was entirely replaced weekly.

Fatigue

Constant amplitude, axial fatigue testing of the side notched, flat $K_t = 3$ or 5, plate and sheet specimens were conducted in Sonntag SF-1-U, SF-10-U, or MTS fatigue machines. All testing was performed at a stress ratio, $R = 0.1$, and at either 6 or 30 Hz.

Notched aluminum and titanium alloy plate fatigue specimens were machined 0.300 inch thick from plate quarter thickness. Fixturing was properly pre-aligned to provide only true axial loading with no bending. The edges of the notches were carefully deburred by hand using fine emery paper and a 45X stereomicroscope. The notches of the specimens were tested in the "as mill machined" condition for the aluminum and titanium alloy plate specimens and tested in the "as ground" condition for the titanium sheet specimens. The notches of all specimens were measured with an optical comparator for conformity to the drawing tolerances.

The $K_t = 5$ titanium plate specimens were remachined to $K_t = 2$ when it was determined that this stress concentration was more meaningful for design considerations. Because of the larger radius ($R = 0.145$ inch) of the $K_t = 2$, it was possible to polish the notch with fine emery paper to eliminate any transverse machining marks from the notch milling operation.

The small number of twelve specimens tested per condition provided a limited study of the S-N behavior to the materials. Some endurance limits were not adequately defined. The static notch tensile strength was determined by testing the unfailed "run-out" specimens. Fracture surfaces of the statically failed specimens were examined for fatigue origins. Unfortunately, the fracture surfaces of all fatigue failed specimens were obliterated in the failure process and could not be examined.

Fatigue Crack Growth

The da/dN crack growth characteristics of the materials was measured with surface flawed specimens. The surface cracks were prepared by first providing a starter location by arcing a small crater with a mini-thermocouple welder in the center of the specimen. This crater was then subjected to tensile bending fatigue in a SF-1-U fatigue machine. The specimen was precracked by loading it as a cantilever with a $\frac{1}{4}$ inch diameter rod fulcrum located on the opposite surface, directly in line with the crater. Initially, problems were encountered with back side cracking from the bending fatigue. This was circumvented by machining enough material (up to $\frac{1}{8}$ inch) to remove any fatigue cracks. Some of the last specimens were machined with an extra $\frac{1}{8}$ inch to the thickness which was finished to a final thickness of 0.5 inch after precracking. Precracking was in three stages with diminishing loads as the crack grew to 0.1 inch length for the aluminum alloys and 0.2 inch for the titanium alloy.

The specimens were transferred to the special test fixture shown in Figure 95 and the crack was extended to 0.16/.3 inch length in axial tension loading. The loading magnitude was lowered for the final 0.020 inch of surface crack growth so that crack extension was $da/dN \approx 2 \times 10^{-7}$ inch/cycle.

Two types of tensile load application could be applied in the hydraulic, servo controlled fixtures shown in Figure 96 namely:

1. Constant amplitude-constant sinusoidal frequency
or
2. Spectrum loading, computer control of varying amplitude, frequency and number of cycles.

For constant amplitude testing the electronic equipment shown in Figure 96 was used. Two sets of the 38,000 lb. capacity load frames were controlled by two MTS Model 401.03 servo amplifiers and one Model 410.22 function generator. The other two frames were controlled by two Compudyne Model 4196 servo controllers and a Hewlett Packard Model 202A function generator. Each load frame had an individual counter to record applied cycles. Hydraulic pressure was supplied by a 35 gpm pump.

Test frequencies were 360, 60, or 6 cpm. Environments were dry air or 3.5% NaCl. For constant amplitude testing, surface crack growth was measured at approximately 0.05 inch intervals. A Gartner Scientific Model M101A microscope of 10X magnification, equipped with a cross hair was used to measure crack growth. For 6 CPM tests in 3.5% NaCl, greater magnification was required to define the crack tip on the corroding aluminum specimens. A B&L 45X stereomicroscope was used.

A Mylar scale with 0.010 inch divisions was adhesively attached to the specimen. The environmental chamber was made of plexiglas and was clamped to the specimen with an "O" ring providing sealing. While conducting the da/dN tests, marker bands were applied every 0.1 inch by lowering the load 25% and cycling at 360 cpm until 0.05 inch crack growth occurred. From these marker bands it was possible after failure to measure the crack depth progression, da , from the fracture surface and correlate it with the $2c$ surface crack length progression. The titanium marked very poorly and it was extremely difficult to measure crack depth progression. About half of the da/dN specimens were statically tested when the crack progressed through the back surface to an

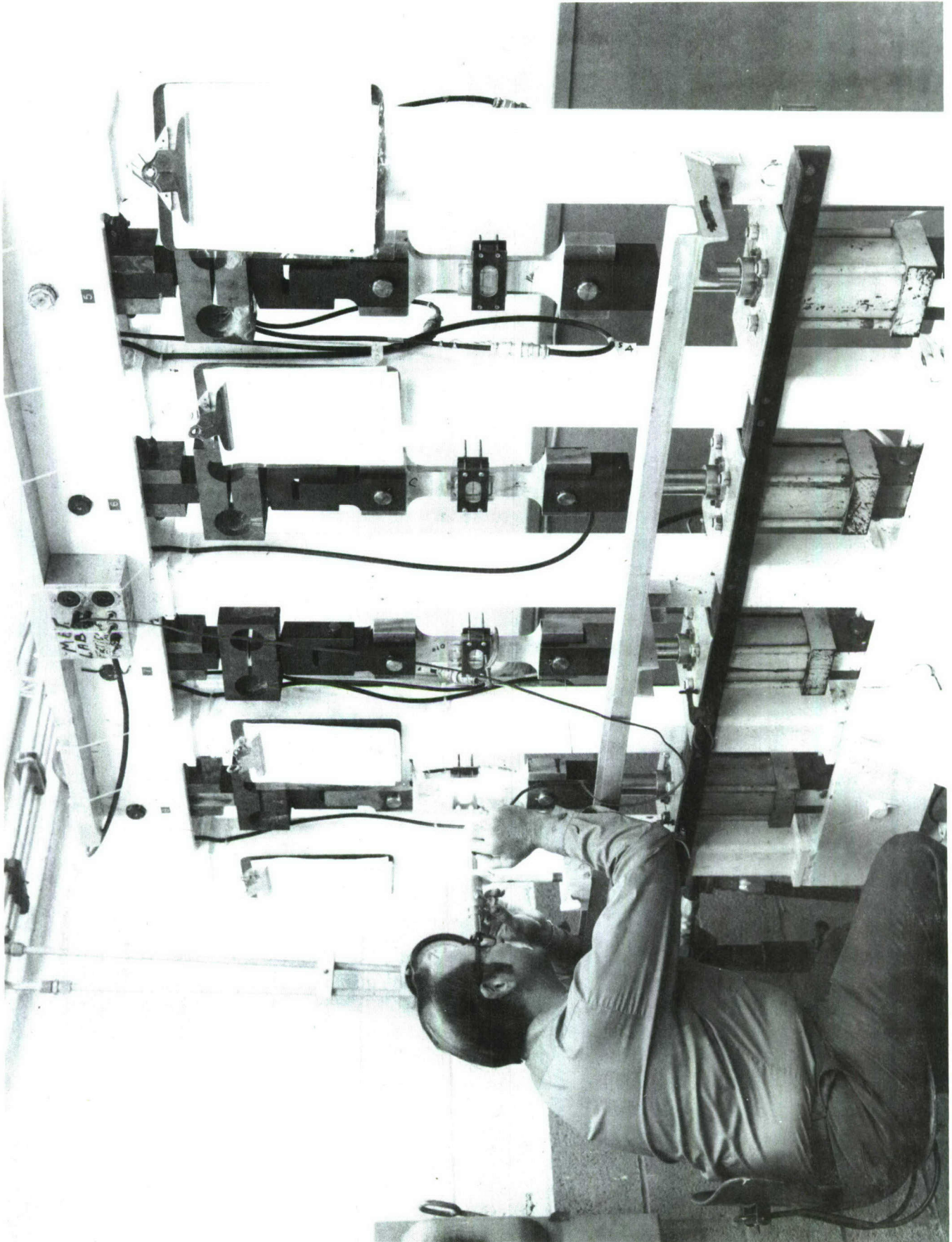


Figure 95 Surface Flawed Crack Growth Rate Specimens in Test

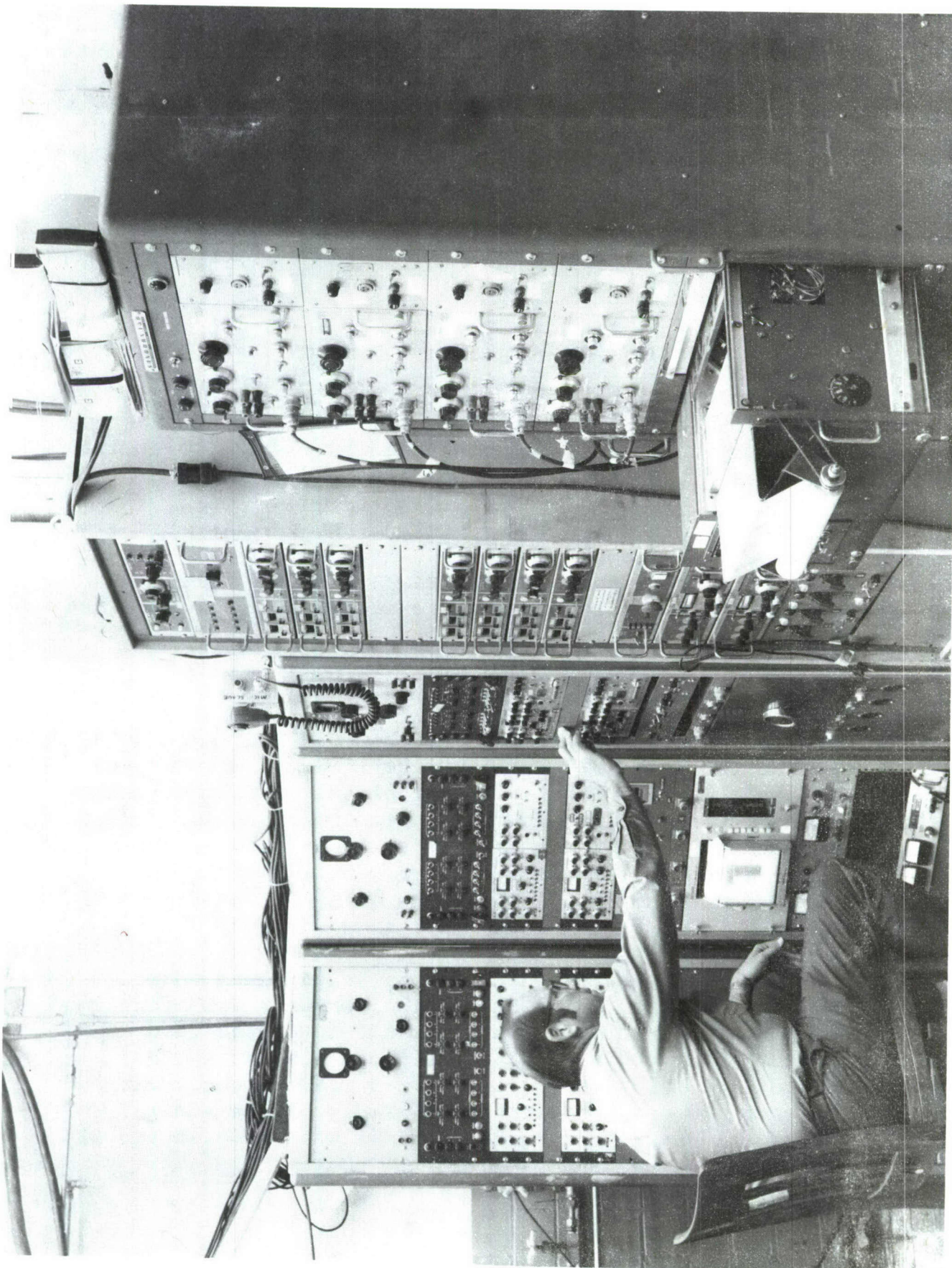


Figure 96 Electronic Control Equipment for Crack Growth Rate Testing

approximately 3/4 inch back surface crack length. About midway through the program it was decided to continue gathering da/dN data for a through crack condition.

The titanium specimens were axially precrack conditioned after initial bending fatigue in a 50,000 lb. MTS electro-hydraulic machine. This was necessary because much higher loads were required to propagate the surface flaws. The 360 cpm specimens were also completely tested in the MTS machine.

Eight Layer Spectrum Program

Testing of aluminum surface flawed specimens with an 8 layer spectrum was accomplished in the four station frame by replacing the signal from the function generators with command signals from a Varian Data Model 620 computer. It was necessary to lower the area by reducing the width so as to attain the maximum stress of 24 ksi. See Table XL for Spectrum.

The titanium specimens having a maximum stress of 68 ksi at the 100% layer were tested in the 100,000 lb. capacity CGS electro-hydraulic fatigue machine shown in Figure 97 . The specimens also had the width reduced to 2 inches to accommodate the required higher load.

Randomized Spectrum Test Program

The spectrum for this program (described previously in this report) selected for four 2024-T851 surface flawed specimens was composed of 20 blocks with 111 layers per block. Spectrum loading was accomplished by replacing the signal from the function generators with command signals from a Varian Data Model 620 computer. This time-share computer was operated at a remote site in the Engineering Test Laboratory with specimens being in the Figure 95 test fixtures.

Each block in the spectrum had 13,756 cycles which took approximately 26 hours for completion. The computer was programmed to stop the test at the end of each block and lower the load to 5% of maximum load. Every 20 blocks, a 100% load was applied at Layer No. 87 automatically by the computer. The frequency varied between 6, 60 and 180 cpm. Environment was dry air or water saturated JP4 fuel. Surface flaw $2c$ readings were made at end of each block. This spectrum is shown in Appendix IX.

Table XL

ADP WING/PHASE IA

8-LOAD LEVEL TEST SPECTRUM

● DRY AIR, R.T.

LOAD LEVEL	SPECTRUM STRESSES FOR 7050 AND 7475 AI		SPECTRUM STRESSES FOR 8-8-2-3 Ti		OCCURRENCES PER 200-HR BLK.	CYCLIC RATE (cpm)
	S _{min} (ksi)	S _{max} (ksi)	S _{min} (ksi)	S _{max} (ksi)		
1	2.5	18.6	6.8	50.3	516	360
2	2.5	7.3	6.8	19.7	17,500	360
3	2.5	15.4	6.8	41.5	2,319	360
4	2.5	4.9	6.8	13.1	18,000	360
5	2.5	9.7	6.8	26.2	5,500	360
6	2.5	12.2	6.8	32.8	3,631	360
7	2.5	21.9	6.8	59.0	34	360
8	2.5	25.2	6.8	68.0	1	360

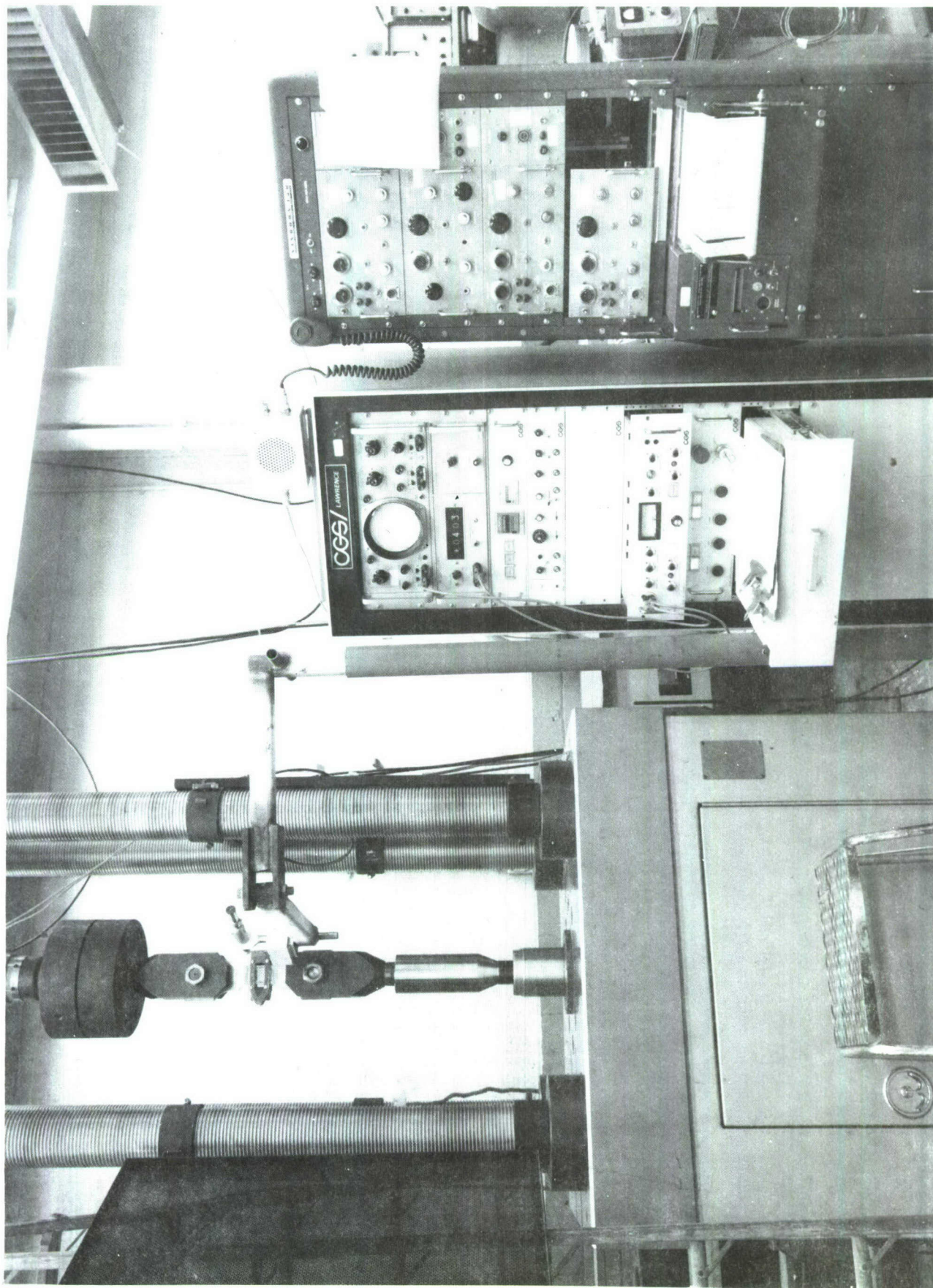


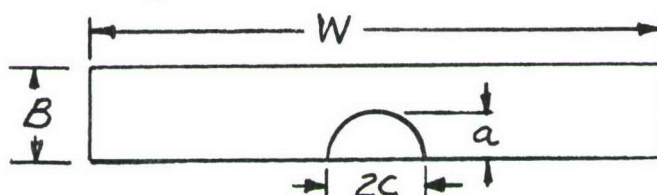
Figure 97 - Titanium Surface Flawed Crack Growth Rate Specimens
in Test in CGS Electrohydraulic Fatigue Machine

Fracture Analysis

Post failure examination of the fracture surfaces involved measuring the crack depth, a , progression and correlating this with the surface, $2c$, progression. These measurements ranged from relative ease for the 7475 to extreme difficulty for the Ti-8-8-2-3. Measurements were made from photographs and directly from the fracture surface. In the case of the titanium, darkfield viewing with a Carl Zeiss metallograph at 150X was necessary to follow and measure crack fronts.

Fracture Mechanics Calculations

Stress intensity factors were determined from the following equations:



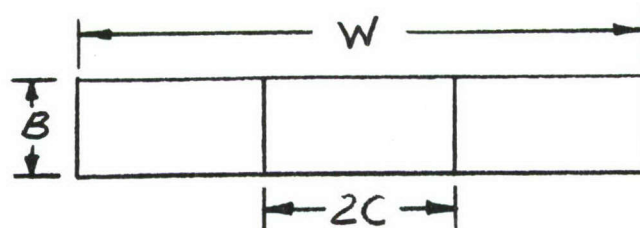
A. Surface Flaw

$$K = 1.1 \Delta \sigma_g \sqrt{\pi a/Q} \quad \text{Eq. 1}$$

$$Q = \phi^2 - .212 \left(\frac{\sigma_g}{F_{ty}} \right)^2 \quad \text{Eq. 2}$$

$$\phi = \int_0^{\pi/2} \sqrt{1 - \left(\frac{c^2 - a^2}{c^2} \right) \sin^2 \theta} d\theta \quad \text{Eq. 3}$$

$$\Delta \sigma_g = \frac{P_{\max} (1-R)}{W B} \quad \text{Eq. 4}$$



B. Center Through Crack

$$K = \Delta \sigma_g \sqrt{\pi a} \sqrt{\sec \frac{\pi}{W}} \quad \text{Eq. 5}$$

where P_{\max} = maximum load

$R = \text{stress factor} = \frac{P_{\min}}{P_{\max}}$

$\sigma_g = \text{gross stress}$

$W = \text{width}$

$B = \text{thickness}$

$F_{ty} = \text{yield stress}$

$\phi = \text{elliptical integral of second order}$

$c = (\text{surface crack length})/2$

$a = \text{crack depth}$

$Q = \text{flaw shape parameter}$

8.3.5 Discussion of Test Results

Tables and figures containing material data are contained in Appendix VIII and summarized in Table XLI. Each specific test is discussed below.

Tensile

Tensile test results are contained in Tables XLIV through L of Appendix VIII. Tensile values from the 1.5 inch thick plate of 2024-T851 used for manufacturing specimens for the spectrum/environmental baseline fatigue program are in Table XLIV and the 0.060 inch thick 7050-T76 sheet tensile data at room and elevated temperature is in Table XLV. The effect of elevated temperature on room temperature properties tested both at elevated temperature and at room temperature after exposure are shown in Figures 83 through 86 of Appendix VIII. The Convair tensile values at room and elevated temperature from the 3.0 inches thick by 60 inches wide 7050-T73651 plate are in Table XLVI. The effect of elevated temperature on room temperature 7050-T73651 plate properties tested both at elevated temperature and at room temperature after exposure are shown in Figures 87 through 90. Table XLVII contains Alcoa test data from the ends of the parent plate of 7050-T73651 from which the 3.0" x 60" wide x 50" long piece of plate used at Convair was cut. The Convair tested material has significantly lower ductility in the short transverse direction than the Alcoa tests. Two

TABLE XLI

SUMMARY OF MECHANICAL PROPERTIES OF ALLOYS

Longitudinal Grain, Room Temperature Tests

Property	7475		7050		Ti-8-8-2-3			2024 T851 1½" Plate
	T761 .125" Sheet	T7351 1½" Plate	T76 .060" Sheet	T73651 3" Plate	STA			
					.125" Sheet	1" Plate		
1. Tensile								
TUS, ksi	74.1	71.5	85.7	77.8	184.1	173.6	71.9	
TYS, ksi	66.8	61.7	81.1	70.2	172.1	169.7	67.5	
Elong., %	13.8	14.5	10.0	9.7	8.3	2.9	6.5	
R.A. %	-	50.7	-	19.6	-	7.8	20.8	
2. Fracture toughness, L-T								
K _{IC} , ksi-√inch	NM	64.0*	NM	27.2	NM	54.0	24.9	
3. Stress Corrosion, 3.5% NaCl								
K _{Isc} , ksi-√inch	NM	NM	NM	~ K _{IC} (S-L)	NM	23 (L-T)	NM	
4.a Axial Fatigue Str. ksi at								
10 ⁷ cycles, R = 0.1								
K _T = 3	17	15	12.2	17.5	25	29	16#	
K _T = 5	11	12	9.5	12	15	NM	10#	
b Notch Ultimate, ksi								
K _T = 3								
K _T = 5	90.8	79.6	80.2	-	192.0	155	95.4#	
	87.5	75.7	78.0	73	149.6	NM	90.6#	
5. Crack Propagation, ΔK								
at da/dN = 10 ⁻⁶ inch/cycle								
for surface flawed specimens Q								
Dry air, 360 CPM								
3.5% NaCl, 60 CPM								
3.5% NaCl, 6 CPM								
	NM	5.7 4.7 (T-S) 5.3	NM	5.4 5.4 4.9 (T-S)	NM	7.4 7.8	NM	

* K_Q , NM = Not measured.

† Ref. 9 on 2 inches thick plate

Q Crack Loading/Propagation Direction L-S Unless Noted Otherwise

reasons for the differences would be location of specimens and exactness of measuring and marking gage marks for elongation determination. It can be noted from Figure 75 of Appendix VIII Convair test specimens were removed from an area between the one-quarter width points. This contains the area of lowest ductility on plates of other aluminum alloys and probably did on the test plate of 7050-T73651. Convair "tight" testing method for elongation involved precision marking and measuring gage marks to nearest 0.002 inch.

Table XLVII contains room temperature tensile test data from 0.125 inch thick 7475-T761 sheet and 1.5 inches thick 7475-T7351 plate.

Table XLIX contains room temperature tensile test data on the 0.125 inch thick Ti-8Mo-8V-2Fe-3Al condition STA sheet both "as received" and after additional aging at Convair. The additional aging was an attempt at raising the ductility and notched fatigue life, and still obtain a target minimum tensile ultimate strength of 175 ksi. Part of the $K_t = 3$ edge notched flat fatigue specimens were tested from both strength levels.

Table L contains room temperature test data on 1.0 inch thick condition STA Ti-8Mo-8V-2Fe-3Al titanium alloy. All material for Ti-8-8-2-3 titanium plate specimens received the additional aging noted in Table L at Convair. Note the directionality effect of cross rolling on the tensile properties of this one inch thick plate. Part of the longitudinal specimens would not meet a target of 175 ksi ultimate tensile strength.

Compression

Tables LI and LII contain room and elevated temperature compression test data on 0.060 inch thick 7050-T76 sheet and 3.0 inches thick 7050-T73651 plate, respectively. Figures 91 and 92 show the effect of elevated temperature on the compression properties of 7050-T76 sheet and 7050-T73651 plate, respectively.

Fracture Toughness

Fracture toughness (K_{Ic}) values for the $1\frac{1}{2}$ inches thick 2024-T851 aluminum alloy, 3.0 inches thick 7050-T73651 aluminum alloy, 1.5 inches thick 7475-T7351 aluminum alloy, and 1.0 inch thick Ti-8Mo-8V-2Fe-3Al titanium alloy plate in this program shown in Tables LIII through LVI. Toughness values on the 3.0 inches thick by 60 inches wide 7050-T73651 plate were below

expectation compared with limited testing by Alcoa in the development stages of the alloy 7050. At least six subsequently manufactured lots of 7050-T73651 plate have shown higher toughness. Alcoa personnel have expressed the opinion that the Table LIV K_{Ic} values are expected to represent the lower limit for 7050-T73651 plate.

The 1.5 inch thick 7475-T7351 plate was the toughest structural aluminum alloy plate material ever tested at Convair. Although the 1.5 inch thick compact tension specimen used was valid for $47 \text{ ksi}\sqrt{\text{in.}}$, K_Q values obtained were 63 to $65 \text{ ksi}\sqrt{\text{in.}}$ for the L-T direction. All validity requirements of ASTM E399-T71 were met except specimen thickness.

There were no directionality effects in the K_{Ic} of the Ti-8Mo-8V-2Fe-3Al plate in the two directions tested, T-L and L-T.

Typical fractures of the fracture toughness specimens are shown in Figure 93.

Stress Corrosion (K_{Isc})

Fatigue cracked compact tension $3\frac{1}{2}\%$ NaCl water environmental sustained load stress corrosion test data are shown in Tables LVII and LVIII for 7050-T73651 aluminum alloy and Ti-8Mo-8V-2Fe-3Al titanium alloy plate.

The 7050-T73651 plate appeared to be resistant to stress corrosion cracking in the S-L direction (normally for aluminum alloys the least resistant direction). Three specimens were tested over 1000 hours at $K_{Ii} = 0.84$ to $0.97 K_{Ic}$ with no crack growth recorded. Because of difficulty encountered with corrosion products clogging the notch in the compact tension stress corrosion specimens tested with a stagnant environment, one specimen, 50-58, was tested with a flowing environment and $K_{Ii} = 0.97 K_{Ic}$. The 3.5% NaCl corrodent was gravity fed at a flow rate of one quart/hour through the notch. No effect on SCC properties was detected in 1000 hours despite keeping the notch front free of stagnant corrodent. One specimen was step-loaded as shown in Figure 94 and no corrosive crack growth was observed at K_{Ii} slightly less than K_{Ic} . Despite the lower ductility and toughness for this plate than had been expected, the 7050 had excellent stress corrosion properties.

The step-loading SCC procedure was very effective in establishing the K_{Isc} of the Ti-8Mo-8V-2Fe-3Al plate. As shown in Figure 95 the K_{Isc} of the plate in either the L-T or T-L direction

was 23 ksi- $\sqrt{\text{in.}}$ or 44% of K_{Ic} . No incubation time or slow sub-critical crack growth was measured. Six of the specimens failed within 5 minutes of being loaded at or above K_{Isc} and only one specimen showed slow crack growth for 0.7 hour.

Fatigue

Notched axial fatigue data for $K_t = 3$ or 5 at $R = 0.1$ are shown in Tables LIX through LXIV for longitudinal edge-notched specimens from each sheet and plate material in this test program. $K_t = 2$ tests were substituted for the $K = 5$ Ti-8-8-2-3 plate specimens. Notched tensile values were obtained on "run-out" specimens after each had been fatigued for the number of cycles shown. These results are shown in Table LXV. The fracture surfaces were examined for fatigue cracks which would have lowered the notch strength because of a higher stress concentration. Plots of the S-N data are summarized in Figures 96 and 97. Individual material plots are shown in Figures 98 through 103.

From Figures 96 and 97, it can be seen that both the 7050 and 7475 plate aluminum alloys had better room temperature notched axial fatigue strength than 2024-T851 plate currently used in the F-111 wing. The improvement at $K_t = 3$ was more significant than at $K_t = 5$. At $K_t = 3$, 7050 plate had better fatigue strength than another high strength Al-Zn-Mg alloy, 7079. Thus, the 7050-T73651 alloy has combined excellent stress corrosion resistance with good fatigue strength. At the higher stress concentration of $K_t = 5$ there was very little difference in fatigue strength at 10^7 cycles for the 7050, 7475, and 7079 alloys in plate form. At $K_t = 3$ the 7050-T73651 plate had a slightly higher endurance limit than the 7475-T7351 plate.

The notched fatigue properties of the 7050 sheet were lower than expected for such a high tensile strength material. Recent data by Alcoa (Ref. 2) is plotted on Figure 98. As can be seen, the Alcoa data was consistently higher with an endurance limit of 15.5 ksi being obtained compared to 12 ksi for the Convair data. The reason for the difference could be either a variation in properties from one sheet to another or a difference in manufacturing techniques in notch preparation. The Convair specimens were tested in the "as milled" condition with no notch polishing other than careful sanding of the edges of the notch to produce about a .005 inch radius.

Good agreement was obtained between Convair and $K_t = 3$ fatigue data from an Alcoa modified Goodman diagram for the 7475

sheet as shown on Figure 100. The scatter in points for the Convair data and the limited definition of the $K_t = 5$ curve indicate the need for further testing to establish more confidence in the fatigue curves. The small number of twelve specimens were intended to screen materials to determine which materials were worthy of establishing complete S/N curves during following study/design phases.

The fatigue data for the Ti-8-8-2-3 sheet was surprisingly low. The $K_t = 3$ endurance limit of 25 ksi was only 14% of the ultimate strength of the material. The $K_t = 5$ endurance limit of 15 ksi was 8% TUS. Because of the difficulty in machining the STA condition titanium, the notches in the sheet had to be ground. Some burning of the side of the notch was noted as shown in Figure 104 but the base of notch did not show any effects of localized heating. Referring to Table LXIII, it can be seen that part of the $K_t = 3$ sheet specimens were reaged for 6 hours at 1050F to reduce the ultimate strength from 193 to 184 ksi. No effect on fatigue properties was observed. Thus, if any resolutioning had occurred from the heat of grinding, the aging treatment should have partially compensated the effect, of course, the effect of hydrogen contaminate pick up would not be eliminated.

A comparison of the $K_t = 3$ fatigue data for Ti-8-8-2-3 sheet and plate shows the plate having a 4 ksi higher endurance limit than the sheet. Machining techniques had been improved by the time the plate arrived so that the $K_t = 3$ specimen notches were milled rather than ground. It is possible, therefore, that higher results could have been obtained for the sheet if the notch had been milled instead of ground. The $K_t = 2$ notch of the plate was sufficiently large to permit hand polishing.

In comparison to other reported data on Beta titanium alloys, in the STA condition, Ti-8-8-2-3 appears to have inferior notched fatigue strength as shown below:

<u>Alloy</u>	<u>Form</u>	$K_t = 3, R = 0.1$ <u>Life at 10^7 Cycles</u>	<u>Ref.</u>
Beta III	Sheet	56	3
Beta C	Billet	40	3
Ti-13V-11Cr-3Al	Sheet	30	4
Ti-8-8-2-3	Plate	29	

However, comparison to data generated in the AMAVS program at Convair on Beta C shown in Figure 105 indicates the results fall within the range of the Ti-8-8-2-3 plate curves. For designs that eliminate holes in Condition STA Ti-8-8-2-3, such as in brazed structure, fatigue life would be considerably raised as shown for $K_t = 2.0$ data.

Fatigue Crack Growth Rate

The results of the da/dN tests on the 7050, 7475 and Ti-8-8-2-3 plates are presented in the computer printout of Tables LXVI through LXXXII. The computer plots of the da/dN data are contained in Figures 106 thru 125 (App. VIII). Besides the basic da/dN vs ΔK data, points are also plotted of the change in one half the surface flaw crack length, dc/dN , and the change in the flaw shaped parameter, $d(a/Q)/dN$. For through-crack conditions, plots of dc/dN are also provided. The slopes M , and intercepts C , of the da/dN were determined by a least squares regression analysis of individual data points. The Paris-Erdogan relation for crack growth was applied,

$$da/dN = C \Delta K^m,$$

to establish the straight line function. A compilation of these slopes and intercepts for the materials, crack growth directions, cyclic rates and environments studied is presented in Table LXXXIII. A composite of da/dN curves for the individual materials is given in Figures 126 through 128

Two of the da/dN curves have very limited data because of premature failures resulting from secondary cracks starting from the back surface or a corner. The back surface crack originated during the bending precrack operation. This problem was eliminated by finish machining the back surface after precracking the surface flaw. The corner failure originated from a sharp edge which had not been properly deburred. Three other specimens failed from hole failures despite the installation of a 1/8" thick bronze bushing press-fitted into all holes to eliminate fretting. These failures were traced to improper hole machining and deburring.

Six of the specimens have both surface flaw and center through-crack da/dN curves. This reflects an added effort to obtain more crack growth data in the faster da/dN ranges. The specimen width and thickness limited the amount of data which could be obtained before back surface penetration occurred. It should be noted that the crack propagation direction translates from the "S" to the "T" or "L" direction as the crack becomes a

through crack.

As seen in Figures 126 through 129 the crack shape transition from a surface flaw to a through crack is accompanied by a decrease in the rate of crack growth. This is partially explained by the 90° switch in the direction of crack growth measurement. Also plotted on Figure 126 are some comparative compact tension data on 7050-T73651 (Ref. 7) from Rockwell International's B-1 program run under identical conditions to the dry air -360 CPM- $R = 0.3$ data. As can be seen from the data, the crack growth rate of the compact tension specimen is slower than for the surface flaw specimen. Also included on the same figure is data on 1-3/8" thick 2024-T851 plate. It was tested (Ref. 5) as a center crack tension specimen under nearly identical circumstances except that the environment was lab air, 20-60% relative humidity. The results indicate that 7050 would have superior dry air crack growth resistance particularly at slow crack rates $<10^{-6}$ inch/cycle.

The effects of crack growth direction, cyclic rates and environment are difficult to differentiate because of the scatter in data. First, consider the 7050 plate results in Figure VIII-58. At slow cyclic crack growth rates of 10^{-7} inch/cycle, there is no significant difference in the range of stress intensity factor, ΔK for the L-S or T-S specimens. In the range 10^{-6} to 10^{-5} inch/cycle the L-S direction fatigue cracked slower than the T-S direction. In a surface flaw configuration, no significant effects were observed from the 3.5% NaCl environment or changing the cyclic rate from 6 to 60 CPM. In a through crack condition the crack growth in the T-L direction was greater at 6 CPM than at 60 CPM.

For the 7475 plate, da/dN results shown in Figure 127, the L-S direction had slower crack growth in dry air than the T-S direction. The effect of 3.5% NaCl environment at 60 CPM was to increase the crack growth in the T-S direction compared to the dry air results. For example at $\Delta K = 5 \text{ ksi-}\sqrt{\text{in.}}$ the da/dN would double to 1.5×10^{-6} inch/cycle. This same effect was observed in the L-S direction for the 6 CPM results. However, as the crack growth rate increased above 10^{-7} inch/cycle, the effect was less pronounced. Comparison to compact tension 7075-T7351 plate results (Ref. 8) shows that the 7475-T7351 surface flaw configuration provides a more severe crack growth condition.

The effects of crack growth direction on the da/dN results were not well defined for the Ti-8-8-2-3 plate, as shown in Figure 128. The dry air-surface flaw curves and the 60 CPM, 3.5%

NaCl through crack curves cross each other showing faster crack growth rates for the L-S or L-T directions than the T-S or T-L directions. Such differences were not observed in the aluminum alloys. Considering the K_{Iscc} results, such anisotropy was not demonstrated. There was very little difference in the longitudinal and transverse directions. The tensile results for the Ti-8-8-2-3 plate did show higher TUS (182 vs 174 ksi) in the long transverse direction.

A comparison of the 60 CPM -3.5% NaCl results shows the expected slower crack growth rates in the L-S direction. The dry air T-S results more closely parallels the 60 CPM 3.5% NaCl results than do the L-S dry results. Consider the method in which the tests were conducted as observed in Tables LXVI through LXXXI. It can be seen that the loads were increased as the crack grew for all specimens except the L-S dry air specimen. Possibly some stress level effects as proposed by Tiffany caused the variation in results. The effect of 3.5% NaCl was to double the crack growth rate of the surface flawed T-S specimens at rates above 10^{-6} inch/cycle. The effect of 3.5% NaCl on the crack growth rate was much greater in the 10^{-4} inch/cycle range where a through crack existed. In this range the crack growth rate increased by a factor of four in going from dry air to 3.5% NaCl environment. Unfortunately, the 6 CPM test was not completed in time to be reported.

A comparison of the overall results of each material is plotted in Figure 129 showing the relative position of the envelope of results, regardless of test conditions. As can be seen, the aluminum alloys more or less coincide with each other. The crack growth rates for the Ti-8-8-2-3 STA plate are lower.

Photographs of the constant amplitude da/dN fracture surfaces are given for each specimen tested in Figures 130, 131, and 132. It is evident that the flaw shape for the 7475 could be established very easily by the marking bands established by lowering the ΔK by 25%. The 7050 crack shapes were somewhat more difficult to ascertain. The Ti-8-8-2-3 fracture surfaces were extremely difficult to analyse for crack shape progression. Spectrum fatigue crack progression was more easily defined as is evident in the fracture surfaces shown in Figure 133. A summary of the spectrum fatigue tests are given in Section 7 Fracture Analysis of this report.

8.4 SELECTED MATERIALS

Since the selected designs for Phase Ib are mainly of sheet construction, more testing emphasis in Phase Ib will have to be placed on sheet properties. In the aluminum choices from a sheet product, 7050-T76 won over 7475-T761 even though the 7475 alloy has higher toughness. In consideration of thin sheet $<.125$ inch thick, plane stress or mixed mode failure considerations plus the higher strength of 7050-T76 indicate it to be adequate from a fracture mechanics standpoint and the strongest of the two.

Time-temperature combinations for elevated temperature exposure are critical in aluminum alloy selection. Because high maneuver loads on the F-111 come at points during flight where the temperature is less than 200°F , 7050-T76 is slightly superior in strength to 2024-T81 and should prove tougher than 2024-T81. However, if the performance of a vehicle were raised so that maneuvers occurred at higher temperatures than 270°F , a shift to one of the 2000 series alloys shown in Table XXXVII, would be necessary. The high K_C values obtained during the small amount of testing to date on both the Alcan GB X3058 and the Reynolds X2048 sheet products are very attractive. The small amount of testing indicates that both alloys have strength at elevated temperatures near that of 2024-T81. For Phase Ib program 7050 products have been selected since the design data is more nearly complete and indicated temperature effects are not damaging enough to warrant the large testing program needed for the two newer alloys.

Even though the STA condition of Ti-8-8-2-3 titanium alloy sheet appears to have some notched fatigue problems at a high K_t , the designs selected have low K_t and the high strength can be used to advantage. At the start of Phase Ib, if it has been determined from the in house AMAVS test program that Beta C has an advantage at low K_t , a change could be made to the Beta C alloy. Vendor production capabilities should be more clearly defined on both Ti-8-8-2-3 and Beta C at that time.

In Phase Ib extensive bonding studies will need to be conducted on 7050-T76 sheet. For adhesives to operate in the $250\text{-}300^{\circ}\text{F}$ range presently used adhesive system are cured at 350°F . Since the 350°F cure would be detrimental to a 7000 series alloy's strength, the adhesive used will be one of the epoxy-novalac adhesives recently available that cure at 270°F and can be used at higher temperatures. Also in Phase Ib, joint allowables and the effect of the brazing temperatures on the STA condition of

both Ti-6Al-4V and Ti-8-8-2-3 titanium alloys will be determined. The brazing alloy to be used is presently being developed under a corporate funded IRAD program.

SECTION IX

VALUE ENGINEERING

Accurate cost data has been computed for design concepts at each phase of the program identifiable by element within the concept. These costs were then used to identify to the designer the areas within a concept that contribute the most to the total cost and need further trade study effort. The final concept costs have then been used to arrive at a weighted cost score as a part of the overall evaluation and ranking for each phase of the Phase IA effort.

9.1 COST ESTIMATING PROCEDURES

The ground rules for Phase IA were established at the beginning of the program and the baseline costs were defined. This was reported in FZM-5990 entitled "Advanced Air Superiority Fighter Wing Structures Baseline Definition Cost Description" and these details are described in Volume III Appendix VII of this report.

9.1.1 Detail Estimates

The detail estimates were developed in consonance with Industrial Engineering, Tooling, and Material Department estimators. A "grass roots" type estimating system was used which utilized vendor material quotes and data from recent purchase orders in conjunction with manufacturing and tooling time standards. Experience curves were then used to project these standards to the appropriate baseline unit and in accord with the program groundrules. The aforementioned departments provided the designers with detail costs to the level of fasteners, adhesives, etc., that resulted in highlighting areas of excessive cost concepts and/or manufacturing techniques so that cost effective final wing configurations are achieved. The detail cost estimates were developed for all concepts, including the baseline, at each of the following phases of the Phase IA effort:

- (a) Cross Section Concepts
- (b) Analytical Assembly Concepts
- (c) Optimized Full Wing Box Concepts

9.1.2 Example of Detail Estimating Procedures

Analytical Assembly 610RA006 (reference Figure 98) will be used to provide an explanation of the detail estimating procedure used in this program. This particular analytical assembly is traceable to element concepts 610-132, 610-127, 610R-013B and 610R029 (reference Appendix I, Volume II) one-inch cross section concepts No. 610R013B, 610R029 (reference Appendix II, Volume II) and full wing drawing No. 610RW003 (reference Appendix IV, Volume II) the number one ranked full wing concept.

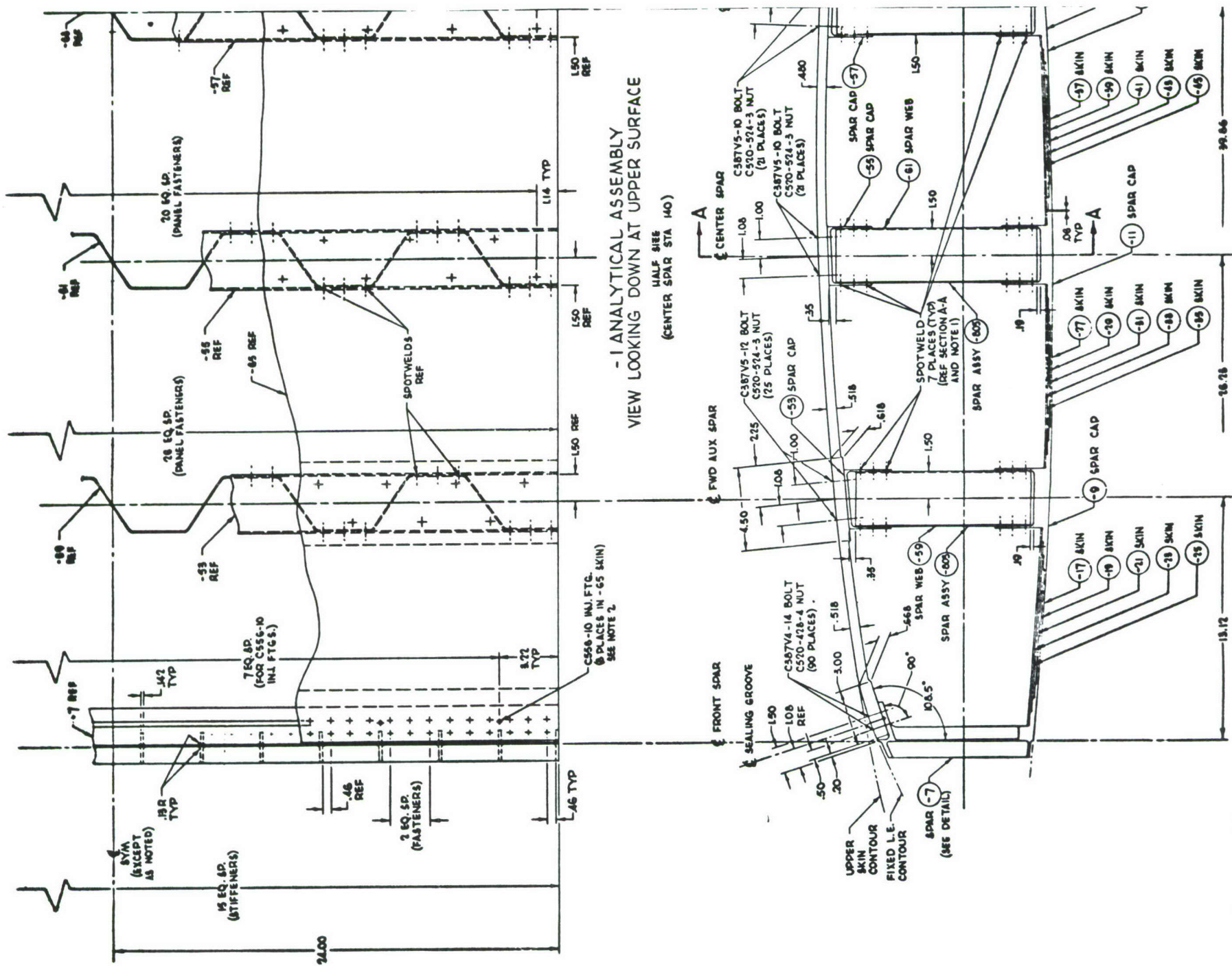
References to Tables which are in this particular section will be to the Tables on Figure 98. The explanation will start with Table II since Table I details are contained therein. The particular portion of this Table pertinent to this discussion is as follows:

Table II - -801 Lower Surface Assembly

<u>Detail Part No. & Name</u>	<u>No. Req'd</u>	<u>Raw Stock Weight</u>	<u>Finished Weight</u>
-7 Front Spar	1	233.52	15.79
-9 Fwd. Aux. Spar Cap	1	67.52	21.46
-11 Center Spar Cap	1	61.12	18.54
-13 Aft Aux Spar Cap	1	55.06	14.91
-15 Rear Spar	1	206.01	10.75
All Lower Surface Skin (See Table I)		-	54.55
Adhesive 63.25 ft. ²		-	6.33

Factory Estimates

There are a number of different Industrial Engineering techniques for use in arriving at the anticipated cost of a machined part. For instance: use of feed and speed data in conjunction with square inches and depth of material to be removed, similarity of parts and use of historical data, pounds of material removed, etc., The particular method, which is used by an Industrial Engineer in arriving at the most accurate projected cost of machining, is a matter of part configuration and



and engineering judgement. In each instance Industrial Engineering used the technique which they determined would give them the greatest degree of accuracy in their estimate. In providing the detail estimates for the -7, -9, -11, -13 and -15 spars, the manufacturing man-hour task was developed through application of a manufacturing estimating standard involving use of an aluminum material removal rate factor. There are two of these factors: one for machining the other for hand finishing after machining. For example, on the -7 front spar the following calculations and formulas were used in arriving at a labor cost:

- . Raw Stock weight less finished weight equals pounds of material removed (233.52 - 15.79 equals 217.73#).
- . (Pounds of material removed) X (Material removal rate time standard for machining aluminum) equals machine hours.
- . (Pounds of material removed) X (Time standard for material removal rate for hand finishing) equals hand finish hours.
- . (Machine hours + hand finish hours) X (Processing factor 5%) equals #1 Manufacturing hours for the -7 detail.
- . (#1 Manufacturing hours) X (Learning curve factor at Unit No. 506) equals Manufacturing hours for -7 front spar (20.57 hrs.).
- . A composite rate was established for factory operation such as direct labor costs, quality control, overhead, etc. The composite rate was then applied to the detail manufacturing hour costs to provide a dollar cost for manufacturing. The -7 front spar factory cost was for example established at \$276.46.

The same factory man-hour development and composite rate application procedure was used in arriving at costs for each of the other spars in Table II. It was also used in arriving at the \$132.68 manufacturing cost for the -65 upper skin which is called out in the -1 analytical assembly concept summary Table.

The eighteen lower surface skins were costed in a detail manner using manufacturing estimating time standard data for shearing each skin to size, deburring, and processing. Both set-up and operational costs were considered. The set-up costs were prorated over an assumed 50 unit production lot. The #1 production unit cost was ascertained and projected on a learning curve to unit #506.

Factory man-hour costs for bonding of the Table II details were developed through use of bonding standard factory hour historical data. Again, there are a number of methods for gathering bonding standard hour data. Convair standard data used in developing the cost for bonding the -801 Lower Surface Assembly involved use of bonding hours based on the number of square foot of surface. After developing the square feet of surface area in this particular assembly, the following formulas were applied in arriving at a manufacturing cost:

- o Number one unit bonding cost per square foot times the number of square feet equals unit number one factory cost for the assembly.
- o Number one unit costs for the factory man-hours were then projected on a learning curve to production unit #506 manhour cost of 35.7 labor hour.
- o A composite factory rate was then applied to arrive at a cost of \$479.81 for bonding the -801 Lower Surface Assembly.

Tables III, IV and V of Figure 98 contain the detail information on the forward auxiliary, center, and aft auxiliary spars, respectively. Information from Table III will be used to illustrate the methods used in arriving at a factory man-hour cost for one of the inner spar assemblies. The remaining two assemblies used exactly the same approach.

Table III identifies the details in the -803 Forward Auxiliary Spar Assembly, specifically the -53 Forward Auxiliary Cap, the -59 spar web and .04 pounds of adhesive.

The -53 forward auxiliary spar is finish machined from an extrusion. In calculating the machining cost, a factory time standard was used involving the numbers of finish machine passes, the length of the part and the number of surfaces to be finished.

The calculated inches of machining was multiplied times the standard hours per inch of machining to arrive at a machining hour estimate. Costs for the other operations, such as sawing the extrusion to size, part numbering, processing, etc., were factored from historical standard data and Industrial Engineering judgement at two and one-half times the cost of the machine operation. Total cost for the cap was established at .69 manhours. A composite labor rate was applied to the labor hours

to arrive at a factory cost of \$9.27 for the -53 forward auxiliary spar cap.

The -59 corrugated spar web costs were developed considering that the bends would be accomplished on the brake machine. The bend form operations were calculated by counting the number of bends that would be necessary in a 48" section predicated on one bend for each 2 1/2" span. A standard set-up time for the brake machine was prorated over an assumed fifty unit production lot. The estimating standard for the brake machine run time was then used to develop costs for the forming operation using a formula of (48" wing span ÷ 2.5" spacing/bend) X (Manufacturing standard hour per bend). Cost of the forming operations was then added to the proportionate share of set-up costs and the total multiplied by 120% to account for added processing costs.

Trimming the corrugated spar web to size was calculated using saw set-up, part handling and layout, sawing, and burring standards. For the sawing and de-burring costs the number of inches of trim were calculated and multiplied times the manufacturing standard estimating factor for sawing and de-burring. This factor is calculated on a per inch basis. Parts handling and layout cost are a standard factor in the sawing operation and were included along with the prorata share of saw set-up costs based on a groundruled 50 unit production lot. After the trimming, deburring, set-up, parts handling and other costs were accumulated a 20% processing cost was added. The #1 unit cost of all the forming and sawing operations was then extended on a learning curve to unit #506 and a composite labor rate applied to arrive at a manufacturing cost of \$3.01 per web.

Manufacturing costs were then developed for weld bonding of the -59, -61 and -63 corrugated spar webs to the upper and lower spar caps. This process combines spot welding and adhesive bonding. Manufacturing labor hours for application of the adhesive, and performance of the spot weld operations, were determined after the number of spots on the upper and lower caps was ascertained. The quantity of spots (173) was multiplied by the standard hour per spot weld. Learning curves were again applied and a total cost of 3.2 labor hours for the -59, 61 and -63 corrugated spars was projected. A composite labor rate was applied and a manufacturing cost per spar of \$14.34 for these operations was determined.

Sub-assembly, assembly and other operations were also detail estimated as above. Costs for installation of the various details into the assembly fixture were also projected using an analysis of fixture preparation time required, part handling time, hole drilling cost, de-burring, bolt installation, etc. These costs were projected to be \$64.26 per Analytical Assembly at Unit #506.

The costs of all the various operations, such as parts fabrication, adhesive bonding, weld bonding, assembly, etc., were finally accumulated to a total manufacturing cost of 112.95 hours per 48" assembly.

Material Cost

Material costs for each of the details were projected on an appropriate dollars per pound basis for raw material. Material cost estimating accuracy requires that factors other than base price be considered. For example, the base cost of 8Al-1Mo-1V Titanium is quoted at \$7 per pound. Thickness and width costs are considered "extras" and in some dimensions add \$40 per pound "extra" cost to the base cost of the material. Other extras that were considered besides material size were such factors as cut length, heat treating and material form. For example, the -7 front spar in Table II was machined from Raw 7050 aluminum material (4.7" x 9.3" x 54") costed at \$1.045/pound. Material cost for the -7 was calculated by multiplying 233.52 pounds times \$1.045/pound for a total material cost of \$244.03. The next item in Table II, the -9 forward auxiliary spar is machined from a 7050 aluminum extrusion. The cost, per pound of raw material was adjusted for material form. Material cost of the -9 spar was determined through the following calculation: 67.52 pounds of raw extruded material times \$2.79 per pound equals \$188.38.

Adhesives were calculated on the basis of weight. For example, adhesives for the -803 forward auxiliary spar assembly in Table III were calculated as follows: .04 pounds times \$5.00/pound equals \$.20.

Hardware was calculated on a per item basis. For example, the -1 Analytical Assembly Concept Data Summary Table calls for (96) C387V4-9 bolts. These bolts were priced at \$.44 each for a total of \$42.24. Hardware cost call outs on the 610RA006 Analytical Assembly totaled \$251.51.

Tooling Cost

Tool Manufacturing manhours provide a base from which other tooling costs, such as tool engineering, tool maintenance, tool material, etc., can be projected or to which they can be related. Tool Manufacturing man-hours were calculated by Tooling Department estimators using a comprehensive set of tool manufacturing time standards. These standards were derived from historical tool manufacturing data and experience. Each of the details in the analytical assemblies were evaluated for tool manufacturing manhour requirements and a composite rate was applied to arrive at a tooling cost for each concept. Rate tooling was also a major consideration since a twenty unit per month production rate was specified in the program costing groundrules. The basic and rate tooling for the -7 front spar, for example, consisted of four mill fixtures at a tool manufacturing cost of forty hours each. The composite rate was applied to arrive at a non-recurring tooling cost for the -7 spar of \$3,347.20. This cost could then be prorated over 506 units at \$6.62 per unit. Prorating the cost over 800 units would further have reduced it to \$4.18. However, since the manufacturing and material costs were evaluated at unit #506, a like number of production units were assumed for consistency purposes.

Another factor to be considered in the tooling cost is tool maintenance. The maintenance rate was established at 1% per month based on total tool manufacturing hours. This factor is determined from historical standards and can be applied to the -7 spar for example as follows:
$$\text{(160 Tool Manufacturing Hours)} \times \text{(Tool Maintenance Rate)} \times \text{(1\% per month)} \times \text{(25 production months)}$$
 is divided by 506 production units. The tool maintenance cost for each unit of the -7 spar then is calculated to be \$1.06 over the life of the program.

While this particular configuration tends to lend itself to assignment of tooling cost on a detail level, several of the other configurations do not. The question of how to properly allocate the cost of assembly tools, braze tools, etc., to a detail level was left unresolved in favor of providing expeditious recurring type costs to the design team. Tool Manufacturing hours were detail estimated and the total cost for these hours determined, however, the information was left available to the design team in the form of tool manufacturing hours and is included in the cost column as a prorata share of a bulk figure.

For example, Figure 98 shows a -1 assembly cost of \$784.95. Of that amount \$198.42 represents the prorata share of the Analytical Assembly tooling cost determined as follows: The sum of (4138 tool manufacturing hours x Tooling composite rate) plus (4138 TMH x Tool Maintenance rate x 1% x 25 months) is \$100,398.23. When this amount is prorated over 506 units, each unit is assigned \$198.42 of cost.

Summary

Finally, the detail factory, material, and prorata share of tooling costs were accumulated and a total analytical assembly cost derived. A material and labor cost breakdown for the 610RA006 drawing is illustrated below:

<u>Table No. from Figure 98</u>	<u>Material</u>	<u>Labor</u>	<u>Total</u>
Table I	\$(64.87)	\$(19.24*)	\$ (84.11*)
Table II	1,036.70	762.11	1,798.81
Table III	34.02	12.26	46.28
Table IV	35.16	12.26	47.42
Table V	33.51	12.26	45.77
Upper Skin	236.32	132.68	369.00
Hardware	251.51	-	251.51
Assembly Costs	-	-	586.53
Prorata Share of Tooling Cost	-	-	198.42
			<u>\$ 3,343.74</u>

* Included in Table II.

9.2 BASELINE COSTS

The first cost task was that of defining the baseline. This was developed and reported as noted above (reference Appendix VII Volume III). This document defined the costs associated with producing the F-111 wing box at production unit #506. From this cost point, learning curve and rate projections were applied to achieve recurring costs for units numbered 1, 2, 50, 200 and 800

at a production rate of twenty aircraft per month. Baseline component costs were also established for skins, ribs, pylon, etc., at aircraft no. 506. This information later served to initially highlight the areas for greatest potential cost savings. The report also included a description of the manufacturing sequence of the F-111 wing and illustrated the basic cost structure used by Convair Aerospace Division, Fort Worth Operation of the General Dynamics Corporation.

9.3 CROSS SECTION CONCEPTS

Following design innovation and compilation of the element concepts; fifty(50) one-inch cross section concepts, some with multiple iterations, were selected and costed in detail against the baseline.

9.3.1 Early Cost Estimating Problems

The novel nature of some of the designs; difficulty in applying existing cost standards and learning curves to unconventional designs, plus the use of non-standard material shapes and gauges, presented problems during the early cost estimating effort. The first two problems caused manpower estimates to be made in great detail rather than by using ready made standards and procedures. The third problem, non-standard material shapes and gauges required special coordination with metal producers and design personnel.

9.3.2 Cross Section Data

For comparison, evaluation, prediction, and ranking purposes, a one-inch baseline cross section was identified and completely costed. A summary may be found in Volume II Appendix II. A considerable amount of the cost data generated in this phase was found to be useful in other Air Force and NASA programs. These programs involve use of computer developed estimates. Such information was forwarded to those programs, as applicable.

9.4 ANALYTICAL ASSEMBLY CONCEPTS

The next phase of the program involved development of detail cost estimates for twenty-five, constant cross section, forty-eight inch span, analytical assemblies. This phase permitted additional refinement of the cost estimates due to the larger sections. Again, detail costs and support were provided to the designer for use in achieving, or exceeding, program goals. During this phase, brazing was highlighted as a significant cost

factor in the concepts. This is largely attributable to the recurring cost nature of the braze tooling. As such, it becomes assignable to each unit of production in lieu of a one-time cost which can be amortized over a large production run.

Again, for comparison purposes and to eliminate deviations attributable to "actual costs versus standards applications," two baseline analytical assemblies were designed and detail estimated. These estimates used the same standards criteria as was used in the other analytical assemblies. This effort proved to be an invaluable aid in providing a "pre-look" at complete wing concept costs during the fourth step of this program. A summary of the Analytical Assembly costs may be found in Volume II Appendix III.

9.5 FULL WING BOX PRELIMINARY DESIGN CONCEPTS

The 48" analytical assembly costs were used to project complete wing costs based on the relationship of the baseline analytical assembly recurring costs to the baseline full wing recurring costs. The projections were accomplished on nine different concepts using the following rationale.

Loads path curves indicated the logical location for a splice would be CSS280. Therefore, the analytical assembly at CSS140 would be 180" long, while the analytical assembly at CSS340 would be 89" long.

For a preliminary screening tool the non-recurring costs were removed from the estimates and only the recurring costs were compared to the baseline. (These non-recurring costs had been provided as a separate line item along with the recurring costs for the analytical assemblies in order to provide a total comparison of all occurring cost factors). The following relationship was then developed: $[(\text{Recurring cost of CSS140 Analytical Assembly}) \div (48'')] \times (180)$ plus $[(\text{Recurring cost of CSS340 Analytical Assembly}) \div (48'')] \times (89'')$ relates to the unknown cost of a full wing as the $[(\text{Recurring cost of baseline analytical assembly at CSS140}) \div (48'')] \times (180'')$ plus $[(\text{Recurring cost of baseline analytical assembly at CSS340}) \div (49'')] \times (89'')$ relates to the recurring cost of the full baseline wing as outlined in FZM-5990, the baseline document.

9.5.1 Splices

Since it is possible to reduce weight and/or cost by splicing two different wing concepts together, four different wing splice concepts were defined and costed. Full wing costs

involving splices were then projected using the relationship discussed in the preceding paragraph. Costs for manufacturing and installing each splice were established and added as a separate input to the projection to arrive at a full spliced wing cost. Utilizing these projections in conjunction with the other performance ratings, the four full wing box configurations receiving the highest overall evaluation in the total merit rating system were chosen for additional optimization in the next phase of the Phase IA program. A summary of the nine full wing box costs may be found in Volume II Appendix IV.

9.6 OPTIMIZED FULL WING BOX CONCEPTS

Costs on four full wing drawings were developed using a "grass roots" bid exercise as outlined in paragraph 9.1.1 and as further defined in Appendix VII of Volume IV. Factors such as material attrition rates, over-head rates, etc., were applied against the basic estimate and are exactly the same as those applied to the baseline costs. This provides for a direct comparison of the costs for the four full wing boxes against the F-111 wing box baseline cost.

9.6.1 Final Cost Comparisons

Table XLII is included to provide a comparison of the costs for the full wing drawings as compared to the costs in the baseline document. The table highlights an item which merits additional explanation in this text, namely item #C1 "Purchased Parts and Outside Production."

The baseline document (FZM-5990) reflects actual cost experiences on the F-111-F wing box as projected to a twenty per month production rate. As such, a portion of the costs are vendor, or supplier generated in payment for machining, fabrication, etc. Since obtaining numerous vendor quotes was prohibitive because of schedule and the task involved, a ground rule was established by Value Engineering that all machining and other fabrication costs were to be considered as an in-house task. Therefore, costs that would normally have been accumulated under the terminology "Purchased Parts and Outside Production" are now included in Raw Material, factory, Quality Assurance, etc. Differences in the proportionate amount of costs that are attributable to materials and labor among the various concepts are also clearly discernable in Figure 99.

Table XLII

ADVANCED AIR SUPERIORITY FIGHTER

FULL WING BOX COSTS - UNIT #506 - 20 A/C PER MONTH

BASELINE		610RW002		610RW003		610RW004		610RW006	
Hrs.	\$	Hrs	\$	Hrs	\$	Hrs	\$	Hrs	\$
A. DIRECT LABOR									
1. Engr. Liaison	70	527	692	70	526	73	549	89	669
2. Prod. Assur.	2.5	19	23	3	23	3	23	3	23
3. Conf. Mgmt.	1.5	9	12	2	12	2	12	2	12
4. Total Engr. Pool	74	555	727	75	561	78	584	94	704
5. Tool Maint. (Eng.)	140	810	697	95	552	105	610	658	3823
6. Tool Maint. (Mfg.)	122	630	544	90	466	92	477	573	2968
7. Total Tool Maint.	262	1440	1241	185	1018	197	1087	1231	6791
8. Factory	1684	7946	14254	2286	10790	2401	11333	2947	13910
9. Quality Assurance	355	1927	3459	482	2617	506	2748	622	3378
10. Total Mfg. Pool	2301	11313	18954	2953	14425	3104	15168	4800	24079
11. Total Direct Labor		11868	19681		14986		15752		24783
B. OTHER DIRECT CHARGES									
1. Engineering		28	28		28		28		28
2. Product Assur.		2	2		2		2		2
3. Tooling		5	5		12		5		5
4. Manufacturing		116	116		116		116		116
5. Total Other Dir. Chgs.		151	151		158		151		151
C. PROCUREMENT/SUBCONTRACT									
1. Purc. Parts & Outside Prod.		17254	*		*		*		*
2. Raw Material		11758	28415		14047		11284		50515
3. Production Aid		88	159		103		135		289
4. Total Proc/Sub-cont.		29100	28574		14150		11419		50804
TOTAL FABRICATION COSTS		41119	48406		29294		27322		75738
D. OVERHEAD-DIVISION									
1. Engineering	74	530	696	75	538	78	559	94	674
2. Manufacturing	2301	15982	26980	2953	20523	3104	21572	4800	33360
3. Material		1891	1847		920		742		3302
4. Total Div. Oh'd		18403	29523		21981		22873		37336
E. TOTAL A-D		59522	77929		51275		50195		113074
F. GEN. & ADM.		4761	6234		4102		4016		9046
G. TOTAL COST		64283	84163		55377		54211		122120

* NOTE: This category of purchased parts and outside vendor production was eliminated. Providing timely estimates required ground ruling that all brazing, welding, machining, etc., was to be considered and bid as an in-house task. Therefore, these costs were included in raw materials, factory, and tooling as applicable.

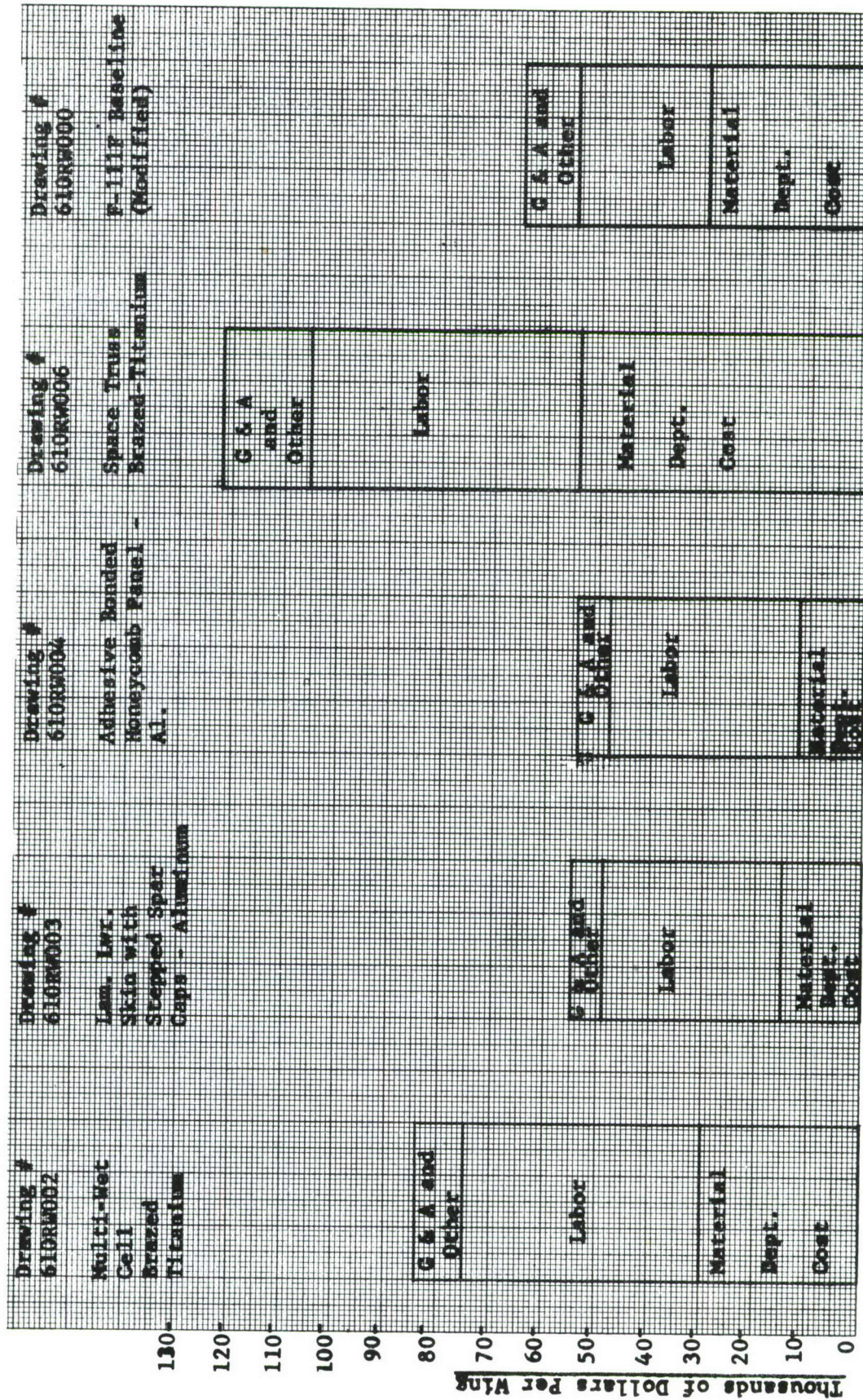


Figure 99 - Rating System for the Analytical Assembly Drawings**
Advanced Air Superiority Fighter Wing Structures Program

9.6.2 Comparison of Estimating Techniques

Throughout this program, the grass roots estimating methodology has been used in developing costs. This technique was again used in arriving at full wing cost estimates. However, for comparison purposes, a cost estimate was developed on full wing drawing number 610 RW 004 "A" utilizing the AFFDL cost estimating technique for Aerodynamic surfaces.

This technique involves use of a computer program which retains and utilizes various cost estimating relationships to predict the cost of flight vehicle structure. The principal author and project leader on this program is Mr. R. E. Kenyon of the Convair, San Diego Operation.

Information provided to Mr. Kenyon for use in AFFDL computer program included: Certain weight and other information on various wing components such as skins, types of fasteners, skin thickness, type of material, etc; learning curves for use in projecting the number one cost value to the appropriate production unit; a copy of the 610 RW 004 "A" full wing drawing; and a copy of the F-111F baseline cost document FZM-5990.

Results of these two estimating methods are as follows: The AFFDL computer estimating method reflected a total manufacturing cost at unit number 506 of 2875 hours. Of this amount 2430 hours are assignable to the manufacturing and assembly tasks and 445 hours are assignable to quality control. Cost of material on a 95% learning curve at unit #506 is \$10,400.

The grass roots estimating method which has been used in developing all of the costs for the various phases of this program reflected a total manufacturing cost at unit #506 of 2907 hours. Of this amount 2401 hours are assignable to factory. Cost of material at unit #506 is \$11,284.

A comparison of material and manufacturing costs in terms of dollars and including overhead and general administrative expenses is reflected in Table XLIII.

Table XLIII

ESTIMATING METHODOLOGIES COMPARISONS FOR 610RWOOD "A"

ELEMENT	AFFDL Methodology		Grass Roots Methodology	
	Hours	\$	Hours	\$
Factory	2430	11,470	2401	11,332
Quality Control	445	2,416	506	2,748
Manufacturing Overhead	2875	19,981	2907	20,204
Materials		10,400		11,284
Materials Overhead		676		734
Sub Total		44,943		46,302
General and Administrative		3,595		3,704
Total Material, Factory Overhead, and Proportionate General and Administrative		48,538		50,006
*Note: The following additional costs (totaling \$4,205) were not ascertained for the AFFDL methodology but are included for traceability to Table 9.1 Items #A1 through A7 (\$1671); B1 through B5 (\$151); C3 (\$135); D1 (\$559); \$1368 of item D2; \$8 of Item D3; 2nd \$313 of Item F	not ascertained			\$4,205
				54,211

9.7 DESIGN SUPPORT ACTIVITIES

Value Engineering, in consonance with estimating personnel, have continuously provided cost evaluations and support to the design personnel as they developed the one-inch cross section concepts; and analytical assembly concepts, and the full wing box drawings. This cost information has been developed on multiple concepts of the various details within the assemblies, such as spars, spar caps, fastener costs, installation variables, machining variables, etc. Intent of these exercises was to highlight cost savings opportunities while still in the Analytical Assembly stage. With this information the designer could in some cases replace an element within an Assembly with a less costly element from another Assembly to optimize a new Analytical Assembly for cost. These efforts could then be transcribed into hardware and design cost savings for the entire wing box concept stage and subsequently, the follow-on program.

9.7.1 Support Benefits

As stated previously, costs were provided on a detailed level to the designers on the program. One of the distinct advantages gained from this type cost approach was traceability. Inasmuch as detail manufacturing, material, and tooling costs were incorporated on a drawing and left open and available in the design area, the reason for high cost was only a step away from any of the design boards. Additionally, since in essence the Air Force Materials Lab had established a "design to cost" approach, and, since the estimated costs were provided to the designer in a timely and valid manner, the designer had at hand a target and performance rating.

Results of the costing activities are reflected in the final wing box configurations with savings in the following areas:

- a. A savings of raw material and metal removal through utilization of sheet stock in lieu of plate stock.
- b. Use of extrusions and castings in lieu of metal removal on heavy plate and billets.
- c. Elimination of Taper lock fasteners from the lower surface.
- d. Reduced finished weight through special design configurations which consequently reduced raw stock requirements.

- e. Replaced bolts and Davis pressnuts in upper surface with blind fasteners thus reducing both labor and material cost.

In addition to the design support outlined in the preceding paragraphs, cost information has also been supplied at various times to personnel at the Air Force Materials Lab. This information has included such items: Cost of certain Titanium materials and production and life cycle cost savings per 1,000# of weight savings based on a "rubber airplane concept". Additionally support has been provided to an Air Force Flight Dynamics Laboratory structure estimating program in being at Convair Aerospace Division, San Diego Operation, of General Dynamics Corporation.

SECTION X

MANUFACTURING

Tool engineers and manufacturing research and development engineers have provided on-board design support to this program from the original "brainstorming" sessions to the completion of wing box structural designs. Preliminary concepts were reviewed by manufacturing specialists to determine potential applications of new manufacturing methods and to assess their risk and cost impact.

10.1 INFLUENCE OF MANUFACTURING ON DESIGN

As a minimum, the new manufacturing methods as shown in Figures 100 and 101 were proposed candidates in the pre-concept design phase of the program. Numbers under "APPLICATIONS" indicate the numbers of concept drawings which considered use of the method.

The prime goal of the manufacturing engineer for this program was to assist the design engineer in utilizing advanced manufacturing technology to improve weight, cost and structural integrity.

To properly assess the potential of new and emerging manufacturing processes, it has been necessary to review in-house independent research and development (IRAD) programs, vendors' equipment and process developments, and Government funded contractor research and development (CRAD) programs. A summary of the most recent and applicable programs reviewed follows.

10.1.1 Basic Metal Processing Programs

Evaluation of advanced manufacturing processes applicable to candidate materials and basic design concepts was influenced by the following development programs:

a. Convair IRAD programs

Elevated Temperature Creep Forming Titanium, Report
No. FMR 72-2213

Hot Stretch Forming, Program No. C003756

Diffusion Molding Titanium Alloy Fittings, R. K.
Malik, Convair Aerospace Division of General Dynamics,
San Diego, California

b. Government-funded programs (CRAD)

Isothermal Forging of Titanium Alloy Main Landing Gear Wheels and Nose Wheels, Technical Report AFML-TR-72-270

Isothermal Forging of Titanium Alloy Bulkheads, IIT Research Institute, Chicago, Illinois Contract F33615-71-C-1167

Isothermal Forging of Titanium Alloys Using Large Precision-Cast Dies, IIT Research Institute, Chicago, Illinois, Contract F33615-67-C-1722

High-Integrity Forgings of Aluminum and Titanium Alloys, Boeing Aircraft Corporation, Seattle, Washington, Contract No. F33615-71-C-1693

Titanium Casting Development, TRW, Inc., Cleveland Ohio, Contract No. F33615-70-C-1409

Titanium Casting Development, REM Metals Corporation, Albany, Oregon, Contract No. F33615-70-C-1410

Development of Design and Manufacturing Technology for Integrally Formed Structures, LTV Aerospace Corporation, Dallas, Texas, Contract No. 33(615)3756

Titanium Panel Extrusion Production Program, Lockheed Aircraft Corporation, Marietta, Georgia, Contract AF33(615)3839

Manufacturing Process for the Production of Tapered Titanium Alloy Plate and Sheet, TMC, Toronto, Ohio, Contract F33615-71-C-1513

Development of a High Temperature Multi-Stage Section Rolling Machine, Boeing Aircraft Corporation, Seattle, Washington, Contract No. F33615-67-C-1164.

c. Other information sources

Extruded shapes, H. M. Harper Company, Morton Grove, Illinois, Technical Bulletin No. 201-B

Titanium Extrusion, H. M. Harper Company, Morton Grove, Illinois, Technical Bulletin No. 207

<u>WHAT TECHNOLOGY?</u>		<u>USE HOW?</u>					
BASIC MANUFACTURING		APPLICATIONS	REDUCE COST	REDUCE WEIGHT	IMPROVE FATIGUE	RETARD CRACK	LOAD PATH
PRES. Ti EXTRUSION		34	X				
PRES. ALUM. FORGING		12	X				
INTEGRAL PANEL EXT.		10	X				
INTEGRAL FORMED PANEL		9	X	X	X	X	
ISOTHERMAL FORGING		6	X				
DIFFUSION MOLDING		4	X				
TAPERED ROLLED SHAPE		3	X				
PRES. Ti CASTING		2	X				

FIGURE 100 ADVANCED BASIC MANUFACTURING TECHNIQUES

WHAT TECHNOLOGY?	APPLICATIONS	USE HOW?				
		REDUCE COST	REDUCE WEIGHT	IMPROVE FATIGUE	RETARD CRACK	LOAD PATH
SECONDARY MANUFACTURING						
LOW TEMP BRAZING	54				X	X
T-BURN WELDING	49		X	X		
GTA PULSED WELDING	43		X			
WELD BONDING	43	X		X		
RIVET BONDING	38			X	X	
D. B. RIVETING	31			X	X	
ADH. BOND LAMINATE	29				X	X
C. S. DIFF. BOND	19	X	X			

FIGURE 101 ADVANCED SECONDARY MANUFACTURING TECHNIQUES

10.1.2 Secondary Metal Processing

Development of element concepts and cross section designs utilized information on advanced metal joining processes reported in part under the following programs.

a. Convair IRAD programs

Electron Beam Welding of Complex Structures

Report No. FMS 72-2200

Plasma Arc Welding Developments, Report No. FMR 72-2201

Weldbonding for Multi-Temperature Applications,

Report No. FMR 72-2205

Diffusion Bond Riveting, Report No. C003753

b. Government funded programs (CRAD)

Weldbond Flight Component Design/Manufacture

Program, Lockheed Aircraft Corporation

Marietta, Georgia Contract F33615-71-C-1716

Adhesively Bonded Multi-Layer F-104 Aft Fuselage

Ring Fitting, LTV Aerospace Corporation, Dallas, Texas

Contract F33615-72-C-1618

High Frequency Resistance Welded Structures

(Titanium), Battelle Memorial Institute,

Columbus, Ohio, Contract F33615-68-C-1289

Brazing Alloy Development (Titanium Honeycomb)

Rohr Aircraft, San Diego, California, Contract

F33615-71-C-1888

The Roll Diffusion Bonding of Structural Shapes

and Panels, Battelle Memorial Institute, Columbus,

Ohio, Contract F33615-68-C-1325

Low Temperature Brazing of Titanium Sandwich

Structures, Aeronca, Inc., Middletown, Ohio,

Paper presented to the 1970 WESTEC Conference,

American Society of Metals, author: Byron L. Reynolds

Advanced Lightweight Fighter Structural Concept Study,

Northrop Corporation, Aircraft Division,

Contract F33615-72-C-1451

Advanced Metallic Air Vehicle Structures Program
(AMAVS), General Dynamics, Convair Aerospace
Division, Fort Worth, Texas, Contract AF33615-73-C-3001.
(Brazing and adhesive bonding of titanium laminates)

c. Other information sources

Test data on CSDB (Continuous Seam Diffusion Bonding)
Solar Division of International Harvester Company,
San Diego, California, Report RDR 1639

10.2 NEW MANUFACTURING METHODS AND THEIR APPLICATIONS TO DESIGN CONCEPTS

The application of new manufacturing methods was stressed from the beginning of the Element Concept Phase, and many were introduced somewhat incorrectly. No effort was made to back-track and clean up these early concept drawings, but each succeeding phase attempted to correct the misuse and effect reliability of the process in the reiterated designs. The basic approach was to develop a design concept which met all the requirements of the improved structure including weight and cost and at that point evaluate proposed manufacturing methods of fabricating the concept.

In Tables numbered XLI through LXI individual drawings are identified with advanced manufacturing processes. Each advanced method lists the drawing numbers where the process is shown or was considered applicable by manufacturing engineers. Drawings referenced under manufacturing processes are in the appendices to this report. These appendices are:

Appendix I	Element Concepts
Appendix II	Cross Section Drawings
Appendix III	Analytical Assembly Drawings
Appendix IV	Preliminary Design Drawings

Many drawings do not call out the process related to them in the tables. Processes other than those indicated on the drawing were proposed in manufacturing studies of finished drawings. These are alternate approaches and candidates for trade studies in final design evaluation.

10.2.1 Basic Metal Processing Applications

The applications for advanced methods in basic metal processing of individual details are shown in Tables XLIV through XLXI.

Table XLIV TITANIUM CASTINGS

<u>Appendix No.</u>	<u>Drawing No.</u>	<u>Application</u>
I	610-500	Ribs/Bulkheads
I	610-502	Ribs/Bulkheads

Applications of titanium castings are most desirable where complex shapes are required. Most rib and bulkhead designs were of simple configuration and other methods appeared less costly.

Table XLV DIFFUSION MOLDING

<u>Appendix No.</u>	<u>Drawing No.</u>	<u>Application</u>
I	610-500	Ribs/Bulkheads
I	610-502	Ribs/Bulkheads
I	610-308	Spars
II	610R009	Spars

In house IRAD developments of diffusion molding are directed to producing reliable structure at low cost. Very favorable results have been obtained. Continued developments are needed.

Table XLVI PRECISION FORGING

<u>Appendix No.</u>	<u>Drawing No.</u>	<u>Application</u>
I	610-105	Lower skin planks
I	610-114	Lower skin planks
I	610-131	Lower skin planks
I	610-500	Ribs/Bulkheads
I	610-502	Ribs/Bulkheads
IV	610RW001	Ribs/Bulkheads
IV	610RW003	Ribs/Bulkheads
IV	610RW004	Pylon fitting Ribs/Bulkheads
IV	610RW005	Ribs/Bulkheads
IV	610RW007	Ribs/Bulkheads
IV	610RW008	Ribs/Bulkheads

Skin planks made from aluminum precision forging were considered only for the outboard sections of the wing. Equipment size and scale-up restrictions prevent use of a full size wing forging. Most aluminum ribs and bulkheads will have a size of less than 400 square inches in plan view area (PVA) which is the current goal of CRAD programs for development of precision forgings.

Table XLVII ISOTHERMAL FORGINGS

<u>Appendix No.</u>	<u>Drawing No.</u>	<u>Application</u>
I	610-105	Lower skin planks
I	610-114	Lower skin planks
I	610-131	Lower skin planks
I	610-500	Ribs/Bulkheads
I	610-502	Ribs/Bulkheads
IV	610RW006	Pylon fitting

Isothermal forgings of titanium have the same restrictions on size as the aluminum precision forgings. Detail designs in the follow-on phase of a final wing box are expected to find additional applications in ribs, bulkheads and fittings.

Table XLVIII INTEGRAL PANEL EXTRUSIONS

<u>Appendix No.</u>	<u>Drawing No.</u>	<u>Application</u>
I	610-101	Lower skin planks
I	610-104	Lower skin planks
I	610-114	Lower skin planks
I	610-116	Lower skin planks
I	610-121	Lower skin planks
I	610-131	Lower skin planks
I	610-202	Spar/Skin planks
I	610-207	Spars
II	610R113"A"	Upper and lower skin planks
II	610R115	Upper and lower skin planks

Integral panel extrusion has greatest cost saving potential with titanium material. It can be best utilized with parallel auxiliary spar designs. The basic panel must be extruded with excess material to be machined away for final size.

Table XLIX PRECISION TITANIUM EXTRUSIONS

Appendix No.	Drawing No. and Application		
	Upper Skin	Lower Skin	Spars
I	610-006	610-101	610-205
I	610-007	610-104	610-206
I	610-008	610-112	610-216
I	610-036	610-113	610-220
I			610-304
II	610R015C	610R015C	610R019
II	610R018C	610R018C	610R012
II	610R021	610R021	610R021
II		610R024	610R023
II	610R110	610R110	
II	610R111	610R111	
II	610R114	610R114	
III			610RA002
III			610RA008
III			610RA102
III			610RA105

Precision titanium extrusions have found a wide area of usage. The process is quite attractive yet difficult in thin gage shapes. Process control is a major factor in producing reliable extrusions to tolerance.

Table L INTEGRAL FORMED PANEL

<u>Appendix No.</u>	<u>Drawing No.</u>	<u>Application</u>
I	610-118	Lower skin panel
I	610-124	Lower skin panel
I	610-210	Spar panel
II	610R002	Lower skin panel
II	610R009	Upper skin panel
II	610R019A	Upper and lower skin panels
II	610R120	Upper and lower skin panels
III	610RA011	Upper and lower skin panels
III	610RA104	Upper and lower skin panels

This process requires high cost start-up tooling, especially for titanium alloys. The 8-8-2-3 titanium alloy appears to be one of the better titanium materials for this process. Aluminum and titanium alloys have been proposed in these concepts. The formed panels are used with subsequent operations such as brazing or adhesive bonding. They provide good buckling resistance to compressive skin loads on the upper wing surface and good stiffness to resist internal wing box fuel pressures on both upper and lower wing surfaces.

Table LI TAPERED ROLLED SHAPES

<u>Appendix No.</u>	<u>Drawing No.</u>	<u>Application</u>
I	610-101	Lower wing skin stiffeners
I	610-121	Lower wing skin laminates
I	610-124	Lower skin panel

Tapered rolled sections were not good members for wing skin stiffeners due to the high fuel pressures which existed at the outboard stations of the wing box. Constant sections were more attractive to the structures engineer.

10.2.2 Secondary Metal Processing

Advanced methods considered for joining assemblies and their drawing applications are listed in Tables LII thru LXIV.

Table LII DIFFUSION BONDING

<u>Appendix No.</u>	<u>Drawing No.</u>	<u>Application</u>
I	610-103	Lower wing skin and spar
I	610-114	Lower wing skin panels
I	610-206	Spar web panel
I	610-500	Ribs/Bulkheads
I	610-502	Ribs/Bulkheads
II	610R021	Upper and lower skin panels

Diffusion bonding was dropped as a method of bonding skin panels due to high cost and failure of the process to prevent crack propagation. The process is best suited for plate material in applications for fittings, bulkheads, etc. High tooling cost is associated with the process.

Table LIII CONTINUOUS SEAM DIFFUSION BONDING (CSDB)

<u>Appendix No.</u>	<u>Drawing No.</u>	<u>Application</u>
I	610-005	Skin stiffener attachment
I	610-008	Skin stiffener attachment
I	610-012	Skin panel trussed
I	610-015	Upper skin panel
I	610-016	Upper skin panel
I	610-021	Upper skin panel
I	610-034	Upper skin panel
I	610-101	Lower skin panel
I	610-102	Lower skin and spar joint
I	610-104	Lower skin panel
I	610-109	Lower skin and spar cap joint
I	610-110	Lower skin and spar cap joint
I	610-205	Spar cap
I	610-206	Spar cap
I	610-502	Ribs/Bulkheads
II	610R021	Upper and lower skin stiffeners
II	610R107A	Lower spar web-to-cap joint
II	610R113A	Upper and lower skin panels
II	610R115A	Upper and lower skin panels

This process is an attractive method of fabricating T-stiffener details. It is also proposed for making T-stiffened and trussed skins. Major equipment modifications may be required in the process of scale-up to a wing or spar panel size.

Table LIV ROLL DIFFUSION BONDING

<u>Appendix No.</u>	<u>Drawing No.</u>	<u>Application</u>
I	610-002	Upper skin panel
I	610-012	Upper skin truss panel
I	610-015	Upper skin truss panel
I	610-016	Upper skin truss panel
I	610-018	Upper skin panel
I	610-021	Upper skin panel
I	610-024	Upper skin panel
I	610-029	Upper skin panel
I	610-101	Lower skin stiffened panel
I	610-104	Lower skin stiffened panel
II	610-020A	Upper and lower skin trussed panel

The basic application of roll diffusion bonding is in fabrication of skin panels. It was dropped from consideration because of high cost, inspectability, contour forming problems, and other design requirements.

Table LV DIFFUSION BOND RIVETING

<u>Appendix No.</u>	<u>Drawing No.</u>	<u>Application</u>
I	610-005	Skin stiffener attachment
I	610-008	Skin stiffener attachment
I	610-032	Skin stiffener fasteners
I	610-105	Lower skin and spar attachment
I	610-106	Lower skin and spar attachment
I	610-107	Lower skin and spar attachment
I	610-108	Lower skin and spar attachment
I	610-114	Lower skin and spar attachment
I	610-120	Spar web/Cap/Skin assembly
I	610-122	Lower skin and spar attachment
I	610-131	Lower skin plank and spar attachment
I	610-208	Lower spar web and cap attachment
I	610-221	Lower spar-to-skin attachment
I	610-304	Spar-to-skins attachment
I	610-400	Skin, spar splice joints
I	610-500	Rib/Bulkhead installation
I	610-600	Stud head-to-skin attachment
I	610-601	Nut plate-to-skin attachment
I	610-705	Fitting installing
II	610R006	Lower skin stiffener attachment
		Spar and lower skin attachment
II	610R012	Spar and lower skin attachment
II	610R017	Spar and lower skin attachment
II	610R020A	Spar and lower skin attachment
II	610R021	Spar and lower skin attachment
II	610R024A	Spar and lower skin attachment
II	610R110	Spar and lower skin attachment
II	610R111	Spar and lower skin attachment
II	610R113A	Spar and lower skin plank assy
II	610R114	Spar and lower skin attachment
II	610R115	Spar and lower skin attachment

Diffusion bond riveting has many applications where titanium material is used. It is an improved method of fastener application which promises to reduce the threat of cracking around holes. Additional development is required in equipment and more test data needs to be developed.

Table LVI T-BURN THROUGH WELDING

<u>Appendix No.</u>	<u>Drawing No. and Application</u>			
	<u>Upper Skin</u>	<u>Lower Skin</u>	<u>Spars</u>	<u>Pylon Fittings</u>
I	610-021	610-101	610-205	
I	610-034	610-129	610-208	
I	610-036		610-213	
I			610-219	
I			610-302	
II	610R008		610R009	
II			610R012	
II	610R017A	610R017A	610R017A	
II	610R018	610R018	610R018	
II	610R020A	610R020A	610R020A	
II	610R021	610R021	610R021	
II	610R023	610R023		
II		610R031	610R024	
II	610R109	610R109		
II	610R110	610R110		
II	610R113A	610R113A		
II	610R115	610R115		
III			610R002	
III		610RA004A	610RA004A	
III		610RA013	610RA007	
III			610RA012A	
III	610RA108A	610RA108A	610RA108A	
III	610RA109	610RA109		
IV				

The T-burn through process has received much IRAD support in the Convair Aerospace Division of General Dynamics. The basic application has been established. Above average tooling costs are associated with the process. Additional testing is required for engineering data.

Table LVII GAS TUNGSTEN ARC WELDING (PULSED)

<u>Appendix No.</u>	<u>Drawing No. and Application</u>		
	<u>Upper Skin</u>	<u>Lower Skin</u>	<u>Spars and Ribs</u>
I	610-004	610-103	610-201
I	610-005	610-109	610-206
I	610-008	610-111	610-216
I	610-014	610-112	610-218
I	610-036	610-113	610-220
I		610-131	610-301
I			610-302
I			610-305
I			610-502
II			610R001
II	610R008		610R012
II			610R014
II	610R018		610R015
II			610R019A
II	610R023	610R023	610R023
II	610R110	610R110	
II	610R111	610R111	
II	610R114	610R114	
III			610RA001
III			610RA002
III			610RA011
III			610RA105
III			610RA109
IV	610RW002	Front and rear spar web to cap	
IV	610RW006	Front and rear spar web to cap	

The GTA pulsed welding process has been utilized in welding D6ac steel for the F-111 airplane wing carry-through structure and the wing pivot fitting structure. Much additional work has been done by Convair Aerospace Division in welding titanium alloys under subcontract and IRAD programs. Development and testing work would be needed to support some applications presented in proposed concepts.

Table LVIII ELECTRON BEAM WELDING

<u>Appendix No.</u>	<u>Drawing No.</u>	<u>Application</u>
I	610-023	Upper skin panel
I	610-025	Upper skin panel
I	610-026	Upper skin panel
I	610-214	Spar web to cap
I	610-219	Spar web panel
I	610-502	Rib truss member
II	610R005	Spar web panel
II	610R005	Upper skin panel
IV	610RW002	Front and rear spar web-to-caps Pylon fittings
IV	610RW006	Truss members

Industry has developed many applications for electron beam welding. It is well adapted for titanium in the material gages being considered. A prime concern is the requirements for large vacuum chambers to accommodate major components. Testing is required to support some concepts presented.

Table LIX HIGH FREQUENCY RESISTANCE WELDING

<u>Appendix No.</u>	<u>Drawing No.</u>	<u>Application</u>
I	610-021	Upper skin panel
I	610-034	Upper skin panel
I	610-036	Upper skin panel stiffener
I	610-101	Lower wing stiffener
I	610-205	Spar web and cap joint
I	610-219	Spar web panel
III	610RA008	Truss tube members
IV	610RW006	Truss tube members

This process is considered as a candidate where T-burn through welding or CSDB is proposed. It is considered best suited for high production quantities such as would be required in the truss tube members as shown in drawing No. 610RW006.

Table LX - LOW TEMPERATURE BRAZING

<u>Appendix No.</u>	<u>Drawing No. and Application</u>			
	<u>Upper Skin</u>	<u>Lower Skin</u>	<u>Spar</u>	<u>Splice and Fittings</u>
I	610-005	610-103	610-200	610-401
I	610-008	610-112	610-202	610-700
I	610-010	610-113	610-211	610-701
I	610-013	610-114	610-214	
I	610-015	610-115	610-218	
I	610-016	610-122	610-303	
I	610-018	610-123		
I	610-019	610-133		
I	610-033			
I	610-034			
I	610-035			
II		610R006	610R006	
II	610R007	610R007		
II		610R009		
II		610R012		
II	610R014	610R014		
II	610R015	610R015		
II	610R024	610R024		
II		610R031		
II	610R101B	610R101B		
II		610R103A	610R103A	
II		610R106		
II		610R107		
II	610R108	610R108	610R111	
II	610R114	610R114		
IV	610RW002	Braze core assembly		
IV	610RW006	Truss assy and lower skins		
		Front and rear spars		

Low temperature brazing developments are needed for two major reasons. The new all beta titanium alloys need to be brazed in the 950 to 1050° range to utilize the high strength advantage of the material. Another need is for a braze alloy to braze in the 1200°F range. This alloy would perform secondary brazing operations where the first brazing operation was at 1575°F which is the temperature being used on the current AMAVS program referenced in paragraph 10.1.2.b.

Convair Aerospace Division is currently evaluating low temperature brazing alloys developed under IRAD programs. Preliminary results indicate good quality braze joints are obtained. Stress corrosion and other aspects are being evaluated.

Table LXI ADHESIVE BONDED LAMINATES

<u>Appendix No.</u>	<u>Drawing No.</u>	<u>Application</u>
I	610-100	Lower skin
I	610-114	Lower skin planks
I	610-119	Lower skin and spar cap
I	610-120	Lower skin
I	610-121	Lower skin
I	610-124	Lower skin panel
I	610-132	Lower skin and spar cap
I	610-200	Lower spar and skin planks
I	610-211	Spar web
I	610-700	Fitting
I	610-705	Fitting
II	610R001	Lower skin and spar caps
II	610R002A	Lower skin and spar planks
II	610R004	Lower skin
II	610R013B	Lower skin and spar caps
II	610R029	Lower skin and spar caps
II	610R102	Upper and lower skin planks
III	610R003	Lower skins and spar caps
III	610R005	Lower skin and spar caps
III	610R006	Lower skin and spar caps
III	610R007	Lower skin and spar caps
III	610R009	Lower skin and spar caps
III	610R011	Upper and lower skin panels
III	610R104	Spar concepts
IV	610RW001	Lower skin planks
IV	610RW003	Lower skin planks
IV	610RW007	Lower skin planks
IV	610RW008	Upper and lower skins

Basic application of adhesive bonded laminates is for lower skin panel. It provides excellent fail safe characteristics for multiple load path design and stopper. Development is needed in the process of coordinating contoured surfaces during bonding cycle.

Size of the wing skin makes the tooling task quite difficult and this is compounded where full depth spars are designed as bonded components to the lower skin panel. Other process developments for handling large thin laminates through prefit and cleaning operations are needed. These requirements have become evident from the work performed on the current AMAVS program (reference paragraph 10.1.2.b of this report). The AMAVS program is dealing with as many as 10 plies of flat sheets in the .090 to .125 inch thickness range.

Table LXII RIVET BONDING

<u>Appendix No.</u>	<u>Drawing No.</u>	<u>Application</u>
I	610-005	Upper skin stiffener attachment
I	610-032	Upper skin stiffener attachment
I	610-120	Spar web and cap joint
I	610-122	Lower spar web-to-cap attachment
I	610-208	Lower spar web-to-cap attachment
I	610-210	Spar web stiffener attachment
I	610-214	Spar web-to-cap attachment
I	610-221	Spar web-to-cap attachment
I	610-400	Splice joint
I	610-601	Nut plate inst.
I	610-705	Splice joint
II	610R002A	Upper skin stiffener attachment
II	610R006	Lower skin stiffener attachment
		Lower skin and spar attachment
II	610R012	Lower skin panel and spar attachment
II	610R017A	Lower skin panel and spar attachment
II	610R020A	Lower skin panel and spar attachment

Table LXII- RIVET BONDING (Cont'd)

II	61OR021	Lower skin panel and spar attachment
II	61OR024A	Lower skin panel and spar attachment
II	61OR026A	Lower skin panel
II	61OR029	Spar web to caps
II	61OR100	Lower skin panel and spar cap attachment
II	61OR105	Lower skin stiffener attachment
II	61OR109	Spar web straps and skins
II	61OR110	Lower skin panel and spar assy
III	61ORA006	Corrugated spar web and spar caps
III	61ORA010	Spar web stiffener attachment
III	61ORA011	Upper and lower skin and rib attachment
III	61ORA013	Lower skin and rib attachment
III	61ORA101	Rib assy, lower surface and spar attachment
III	61ORA102	Lower skin panel and spar attachment
III	61ORA104	Lower skin to spar and ribs
IV	61ORW003	Corrugated spars
IV	61ORW004	Lower skin-to-spar attachment
IV	61ORW005	Lower skin-to-spar attachment
IV	61ORW007	Lower skin-to-spar attachment
IV	61ORW008	Splice
		Upper skin stringer attachment

Rivet bonding is not a complex process. It requires controlled procedures in cleaning and handling.

<u>Appendix No.</u>	<u>Drawing No.</u>	<u>Application</u>
I	610-005	Upper skin stiffener attachment
I	610-007	Formed bulb tee
I	610-011	Upper skin panel trussed
I	610-012	Upper skin panel stiffener
I	610-013	Upper skin panel - trussed core
I	610-028	Elongated core fabrication
I	610-030	Ribbon core fabrication
I	610-032	Upper skin stiffener fabrication
I	610-120	Spar web and cap joint
I	610-122	Lower spar web-to-cap attachment
I	610-208	Lower spar web-to-cap attachment
I	610-210	Spar web stiffener attachment
I	610-214	Spar web-to-cap attachment
I	610-221	Spar web-to-cap attachment
I	610-400	Splice attachment
I	610-601	Nutplate installation
I	610-705	Splice joints
II	610R002	Upper skin stiffener attachment
II	610R006	Lower skin stiffener attachment
		Lower skin panel and spar attachment
II	610R012	Lower skin panel and spar attachment
II	610R017A	Lower skin panel and spar attachment
II	610R020A	Lower skin panel and spar attachment
II	610R021	Lower skin panel and spar attachment
II	610R024A	Lower skin panel and spar attachment
II	610R026A	Lower skin panel and spar attachment

Table LXIII - WELDBONDING (Cont'd)

II	61OR029	Spar web to caps
II	61OR109	Spar web straps and skins
II	61OR110	Lower skin panel and spars
III	61ORA005	Upper skin stiffener attachments
III	61ORA006	Corrugated spar web and caps
III	61ORA010	Spar web stiffener attachment
III	61ORA011	Upper and lower skin and rib attachment
III	61ORA013	Lower skin and rib attachment
III	61ORA101	Rib stiffener attachment
III	61ORA102	Lower skin-to-spar attachment
III	61ORA104	Lower skin-to-spar and ribs
IV	61ORW003	Corrugated spar
		Fitting installations
IV	61ORW004	Lower skin-to-spar attachment
IV	61ORW005	Lower skin-to-spar attachment
IV	61ORW008	Splice
		Upper skin stiffeners attachment

Weldbonding is a very attractive process which is considered to be low risk with high payoff. The Air Force funded program as referenced in paragraph 10.1.2.b has been the basis for Convair's in-house evaluation. It reports that certain parameters for the process have been established. Additional development and engineering data are needed in the area of multi-layer laminated joints as proposed in may of the design concepts.

Application to major assembly fabrication will require special accessory fixturing to make the process adaptable to the condition. Successful development of the process would include a reliable inspection method.

Table LXIV COMPOSITE REINFORCED STRUCTURE
(Boron or Graphite)

<u>Appendix No.</u>	<u>Drawing No.</u>	<u>Application</u>
I	610-115	Lower skin panel
I	610-116	Lower skin panel
I	610-117	Lower skin panel
I	610-121	Lower skin panel
I	610-125	Panel insert
I	610-129	Lower skin panel
I	610-207	Spar web
I	610-300	Spar cap and stiffeners
I	610-702	Fitting
I	610-703	Fitting
II	610R010	Lower skin slug

Composite reinforced structure has been applied to the current F-111 production airplanes in the form of a boron doubler adhesively bonded to the lower surface of the wing pivot fitting. The application may still be considered for components where size does not provide the problem resulting from a difference in coefficient in expansion between dissimilar materials.

10.3 CONCEPT EVALUATION AND RATING

It has been necessary to evaluate and rate each concept in a design phase before proceeding to the next progressive design phase. Ratings for the manufacturing methods proposed were established per the merit rating system inaugurated at the beginning of the program. Results of the ratings for manufacturing were integrated in the combined ratings for all disciplines considered.

10.3.1 Merit Rating System for Manufacturing

The weighing factors for manufacturing can be best shown by looking at their relation to other factors of the total as shown in Table LXV.

Table LXV MERIT RATING SYSTEM FOR CONCEPT DESIGNS

Structural Efficiency (0.3)	Technology Advancement (0.3)	Integrity and Reliability (0.3)	Abilities (0.1)
Cost = .5	Concepts = .3	Static = .1	Inspectability = .5
Weight = .5	Manufacturing = .3	Fatigue = .3	Manufacturability = .2
	Material = .3	Safe crack = .3	Maintainability = .1
	Fracture = .1	Fail safe = .3	Repairability = .1
			Predictability = .1

The rationale for evaluating and rating design concepts and the final scores for manufacturing were determined by engineers of the Manufacturing Engineering Department of Convair Aerospace Division, Fort Worth, Texas. Ratings were made on a judgment basis since the contract for this program specified that no manufacturing development was authorized

10.3.1.1 Manufacturing Technology Advancement

A prime goal of this total program was technology advancement; however, it could be utilized only if it enhanced the status of other disciplines such as weight, cost, fatigue, material, etc.

The basic advantage of advanced manufacturing methods proposed for detail part fabrication is to reduce cost based on a production application.

Advanced manufacturing methods of joining are costly as compared to present fabrication methods. Their basic advantage is in the ability to reduce component or assembly weight through the use of newer high strength-to-weight materials and reduction of conventional fasteners. Another important consideration is that they improve the integrity of a structure by providing fail-safe design configurations and reducing the risk of crack propagation.

Only a few of the new processes being considered have been used on major production programs. It follows that unless production applications can be found these will remain undeveloped and costly to use. For this reason the assumption has been made that adequate time and budget will be allowed to develop required

technology and that a normal learning curve will follow in production. Evaluation of these advanced processes is based on a production quantity of 800 airplanes or 1600 wing units since the process would be the same for left and right hand parts. Learning curves for this quantity of units should have a significant impact on manufacturing reliability and cost.

In rating an advanced manufacturing method it was first determined that it met the basic requirements of the program. Other factors pertaining to direct evaluation of the process are:

1. Adaptation of the method to the concept design.
2. Current state of reliability of the method and related equipment and scale-up requirements.
3. Development risks and potential back-up manufacturing methods.
4. Economical advantages of the method.
5. Use of advanced materials with improved properties.

Rating schedules were made based on manufacturing methods and materials. A maximum percent of the total weighting factor was established for each method and for the utilization of advanced material. The schedule for titanium alloys and related manufacturing methods is shown in Figure 102.

A separate schedule for aluminum alloys is shown in Figure 103. The percent factors are much lower because less overall technology advancement is obtained when the application is to aluminum alloys. Another way of expressing the reason is that much more is known about manufacturing of aluminum alloys.

10.3.1.2 Manufacturability

Evaluating and rating this category were based on ease and reliability of the proposed fabrication method. Some designs were based on well-developed processes but required difficult coordination and fixturing. A typical example is an adhesive bonded wing skin panel with full depth spars included in the bonding operation. Independently, spars or skins present no major fabrication problems. Together the fixturing task is difficult. Typical of this concept is drawing No. 610R027 in Appendix No. II. For this type situation a complexity factor was imposed on the rating.

MANUFACTURING METHOD	(80% MAX)	MATERIAL	(20% MAX)
	(% MAX)		(% MAX)
LOW TEMP BRAZING	80	6-4 Ti	10
DIFFUSION MOLDING	80	8-8-2-3 Ti	20
PRECISION CASTING	80	BETA III Ti	20
ISOTHERMAL FORGING	80		
PRECISION EXTRUSION	80		
ROLL TAPERED SHAPE	80		
INTEGRAL PANEL, FORMED	80		
INTEGRAL PANEL, EXTRUDE	80		
ADH. BOND LAMINATE	50		
T-BURN WELDING	40		
PLASMA ARC WELDING	30		
E. B. WELDING	30		
WELD BONDING	30		
D. R. RIVETING	30		
RIVET BONDING	20		

Figure 102 Advanced Manufacturing Technology
Concept Rating Schedule,
Titanium Alloys

MANUFACTURING METHOD	(80% MAX)	MATERIAL	(20% MAX)
	(<u>%</u> MAX)		(<u>%</u> MAX)
PRECISION FORGING	50	7050 ALUM.	10
INTEGRAL PANEL, FORMED	40	7475 ALUM.	10
INTEGRAL PANEL, EXTRUDE - MACHINE	30		
ADHESIVE BONDING LAMINATES	25		
RIVET BONDING	15		

Figure 103 Advanced Manufacturing Technology
Concept Rating Schedule,
Aluminum Alloys

To properly assess this category, it was divided into three manufacturing conditions:

1. Basic metal processing or detail part fabrication.
2. Secondary metal processing or subassembly joining, i.e., bonding, welding or riveting.
3. Final assembly of major components such as spars, ribs, bulkheads and skins.

For the purpose of evaluation a maximum percent value was assigned to each as shown:

50% for basic manufacturing

30% for secondary manufacturing

20% for final assembly

The method or methods of fabrication were the major factors in the manufacturing ratings. It was also concluded that a desirable method for aluminum such as machining a spar is not so desirable for fabricating a titanium spar. For this reason aluminum and titanium alloys have individual rating schedules as shown in Figure 104 (for titanium alloys) and Figure 105 (for aluminum alloys).

10.3.1.3 Scoring Methodology for Design Concepts

In arriving at the rating score for a design concept, consideration was given to the percent of the concept to be manufactured by each method, i.e., what percent of the total fabrication of details is done by machining, extruding, forming, etc.

Ease and reliability of the manufacturing methods were the major factors in evaluating a design concept. Basic costs for tooling and facilities were ignored except where those costs appeared excessive or where high maintenance is forecase, i.e., pack diffusion roll bonding of titanium integrally stiffened panels is quite expensive with high tooling costs. For these conditions a complexity factor based on judgment was applied.

Manufacturability scores for individual concepts were obtained through a rough formula as follows.

BASIC MANUFACTURING	SECONDARY MANUFACTURING	FINAL ASSEMBLY
(50% MAX)	(30% MAX)	(20% MAX)
(% MAX)	(% MAX)	(% MAX)
MACHINING 25	RIVET BOND 25	TAPER-LOK BOLT 10
EXTRUDING 30	WELD BOND 25	RIVET BOND 10
FORMING 40	ADHESIVE BOND LAMINATES 30	WELD BOND 10
SHEAR & ROUT 50	ADHESIVE BOND SANDWICH 30	BOLTS, STD. 15
PRECISION FORGE 50		RIVETED 20

Figure 105 Manufacturability
Concept Rating Schedule,
Aluminum Alloys

LET:

Method 1 = % of concept x schedule % x weighing factor

Method 2 = % of concept x schedule % x weighing factor

NOTE: $\%(\text{method 1}) + \%(\text{method 2}) = 100\%$ of concept

AND: $(\text{method 1 score}) = (\text{method 2 score}) = \text{total score}$

Individual scores for cross section drawing concepts and analytical assembly drawing concepts were calculated. Resulting scores were posted to Preliminary Manufacturing Analysis and Concept Rating sheets for the concepts as shown in Figure 106.

Preliminary Manufacturing Analysis and Concept Rating sheets for cross section drawings are shown in Appendix II. Those for analytical assembly drawings are shown in Appendix III.

10.3.2 Rating of Element Concept Drawings

Ratings of element concept drawings concentrated on the compression skin concepts for the upper wing surface and tension skin concepts for the lower wing surface. All concepts were considered to have met the requirement for advanced technology to some degree and the prime objective in this design phase was to rate those concepts for effective use of manufacturing methods.

Results of the Element Concept Phase evaluation was recorded as shown in Figure 107 for compression skins and Figure 108 for tension skins. The highest numbered ranking indicated the most desirable manufacturing method and approach.

Other elements of this phase were evaluated by verbal comments as to their applications in the subsequent design phase concepts.

10.3.3 Rating of Cross Section Drawings

Cross section drawings were evaluated by the Merit Rating System for manufacturing as shown in Table LXII of paragraph 10.3.1. Included in these concept ratings were ratings for drawings of the F-111 baseline structure.

TITLE WING SECTION - LAMINATED LOWER DWG. NO. 610R-006
SKINS WITH STEPPED SPAR CAPS: C S S 140
PLATE UPPER SKIN: CORRUGATED SPAR
WEBS

<u>MATERIAL</u>	<u>COMPONENT</u>	<u>ADV. MATL.</u>
7050-T761 (Plate)	U. Skin & F/R Spars	Yes
7050-T76 (Sheet)	L. Skin & Corr. Spars	Yes
7050-T761 (Bar)	Spar Caps	Yes

<u>MFG. PROCESS</u>	<u>COMPONENT</u>	<u>ADV. METH.</u>
Brake Form & Machine	U. Skin	No
Machine	U. Spar Caps	No
Machine	F & R Spar	No
Form -	Corr. Spar Webs	No
Adh. Bond	L. Skin Laminate	Yes
Weld Bond	Corr. Spar to L.S.Caps	Yes

COMMENTS:

Laminated bonded lower skin and spar caps will require development.

Weld bonding of 7050 alum will need development. Suggest rivet bonding of upper and lower spar caps to webs be evaluated in trade study.

CONCEPT RATING

ADVANCED TECHNOLOGY			MANUFACTURING				COST FACTOR
MFG.	MATL.	TOTAL	BASIC	SECOND	FINAL	TOTAL	TOOL: 125
.027	.010	.0375	.007	.003	.003	.013	MFG:

Figure 106 Wing Section - Laminated Lower Skins
 With Stepped Spar Caps: Plate Upper
 Skin: Corrugated Spar Webs

MANUFACTURING AND ASSEMBLY

DWG. NO.	CONCEPT	MATL.	100-75	75-50	50-25	25-0
610-000	AB-HC PANEL	A	▼			▼
-001	DB-EXP CORE	T				
-002	BEADED PANEL	AT				▼
-003	AB-HC PANEL		▼			
-004	AB-HC (WELD) PAN	T			▼	
-005	SS PANEL (MULTI)	AT	▼			
-006	SS PANEL (Z)	AT	▼			
-007	SS PANEL	AT		▼(A)	(T)▼	
-008	SS PANEL	AT	▼			
-009	AB-HC + SLUG PAN	AT		▼		
-010	AB-HC-NO SLUG-PAN	AT		▼		
-011	TRUSS-LATTICE-PAN	TS			▼(T) (S)▼	
-012	TRUSS-CORR-PAN	AT			▼	
-013	PYM CORE	ATS				▼
-014	STRESSKIN (WELD) PAN	TS		▼(T)		▼(S)
-015	EXP TRUSS CORE-BZ	TS				
-016	ROLL DB-TRUSS PAN	T				
	AB-TRUSS PAN	A		▼		
-017	AB-HC-PLANK PAN	A	▼			
-018	STAMPED CORE-PAN	AT		(A)▼	(T)▼	
-019	BZ PAN-SW CORE	TS			(T) (S)▼	
-020	AB-BULB STIFF	AT				(A) (T)
-021	T-BURN THRU PAN (TIG)	T			▼	
-022	AB-HC PANEL	A	▼			
-023	T-BURN THRU PAN (EB)	T				
-024	AB-SQ TUBE PANEL	T				
-025	T-BURN THRU PAN (EB)	T				▼
-026	O-TUBE PAN-EB	AT			▼	
-027	AB-SQ TUBE + 1 + SKINS	T				▼
-028	AB-HC-ELG CORE	AT		▼		
-029	TRI-TRUSS-AB PAN	AT			(A)▼	▼(T)
-030	RIBBON CORE	AT			▼	
-031	WAFFLE GRID	AT	▼(A) ▼(T)			
-032	Y-STRINGER-PAN	T		▼		
-033	CORR-PANEL	AT			▼	
-034	45° TRUSS T-BURN	ATS		▼		
-035	AB-HC CONST. TAPER	ATS		▼		
-036	T-BURN Y STIFR	TS			▼	

CODE: AB- ADHESIVE BOND A - ALUMINUM
 DB - DIFFUSION BOND T - TITANIUM
 SS - SKIN STRINGER S - STEEL
 HC - HONEYCOMB

Figure 107 Compression Skins Concept Rating

DWG. NO.	CONCEPT	MATL	100-75	75-50	50-25	25-0
610-100	AB-BEADED-LAMIN	AT		(A)▼	▼(T)	
-101	CSDB-T STIFFENER	T			▼	
-102	CSDB-BD STIF + SPAR	T				▼
-103	STRESS SKIN-DB+EB	T				▼
-104	RDB-T STIFFENER	T			▼	
-105	FORGE/MACH-PLANKS	AT		▼(A)	▼(T)	
-106	PLANK-LAMINATE	AT	▼			
-107	PLANK-MACHINED	AT	▼			
-108	PLANK-SPLICED	AT	▼			
-109	AB-HC+DB STIF	T				▼
-110	AB-HC+DB SLUG	T			▼	
-111	AB-HC+SP CP-LAM SKIN	AT		▼		
-112	BZ-HC+SPAR CAP	TS			▼	
610-113	BZ-SLUG + SPAR CAP	TS			▼	
-114	INT. STIF PAN-AB/BZ/DB	TS	▼(AB)	(Bz)▼	▼(DB)	
-115	BZ SP CP + HC/COMP	T B/G			▼	
-116	AB INT STIF-B-LAM	AT B/G		▼		
-117	TI-B/G COMPOSITE	T B/G		▼		
-118	AB-INT STIF-BULB	ATS	(A)▼		▼(T-S)	
-119	AB-HC PAN-SKIN-SPR	AT			▼	
-120	AB-LAM + WB	AT	▼			
-121	AB-LAM-IS-TAPER	AT		(A)▼(T)▼		
-122	BZ HC + SPAR CAP	T			▼	
-123	BZ/AB LAM (T & S)	TS				▼
610-124	AB-HAT-SPAR LAM	AT	▼			
-125	AB-HC + COMP SLUG	TG		▼		
-126	AB-HC-RIBBONS	ATS			▼	
-127	AB-HC + HC SPAR	T			▼	
-128	AB-HC + LAM SPAR	T		▼		
-129	SPAR SKIN-T BURN + COMP	TS				▼
-130	AB/BZ-HC + TI SLUG	TS	(AB)▼		▼(Bz)	
-131	EX-PLANK + SPAR	AT		▼(A)▼(T)		
-132	AB-LAM + SPAR	AT	▼			
-133	BZ-FULL DEPTH DIAG.	TS				▼

AB-ADHESIVE BOND A-ALUMINUM
 DB-DIFFUSION BOND T-TITANIUM
 SS-SKIN STRINGER S-STEEL
 HC-HONEYCOMB

FIGURE 108 TENSION SKINS CONCEPT RATINGS

Ratings for the concepts at center spar station 140 are shown in Figure 109 and those for the outboard station 340 are shown in Figure 110. As previously stated these drawings are shown in Appendix II of this report. Included with the drawings are Preliminary Manufacturing Analysis and Concept Rating sheets as shown in Figure 106 of paragraph 10.3.1. These sheets indicate the desired manufacturing methods and contain details of the scoring.

10.3.4 Rating of Analytical Assembly Drawings

Rating of analytical assembly drawings followed the same procedure as that for rating of cross section drawings. The analytical assembly drawings and the respective Preliminary Manufacturing Analysis and Concept Rating sheets are shown in Appendix III of this report. Evaluation of analytical assembly drawings led to the selection of candidate design concepts for the final full wing design in the Preliminary Design Drawing Phase.

10.3.5 Rating of Preliminary Design Drawings

Those ratings made for analytical assembly drawings were also applied to rating of these final design concepts in the selection of the three top configurations. No major deviations were made in manufacturing methods from the analytical assembly drawings which represented the final concept.

MANUFACTURING

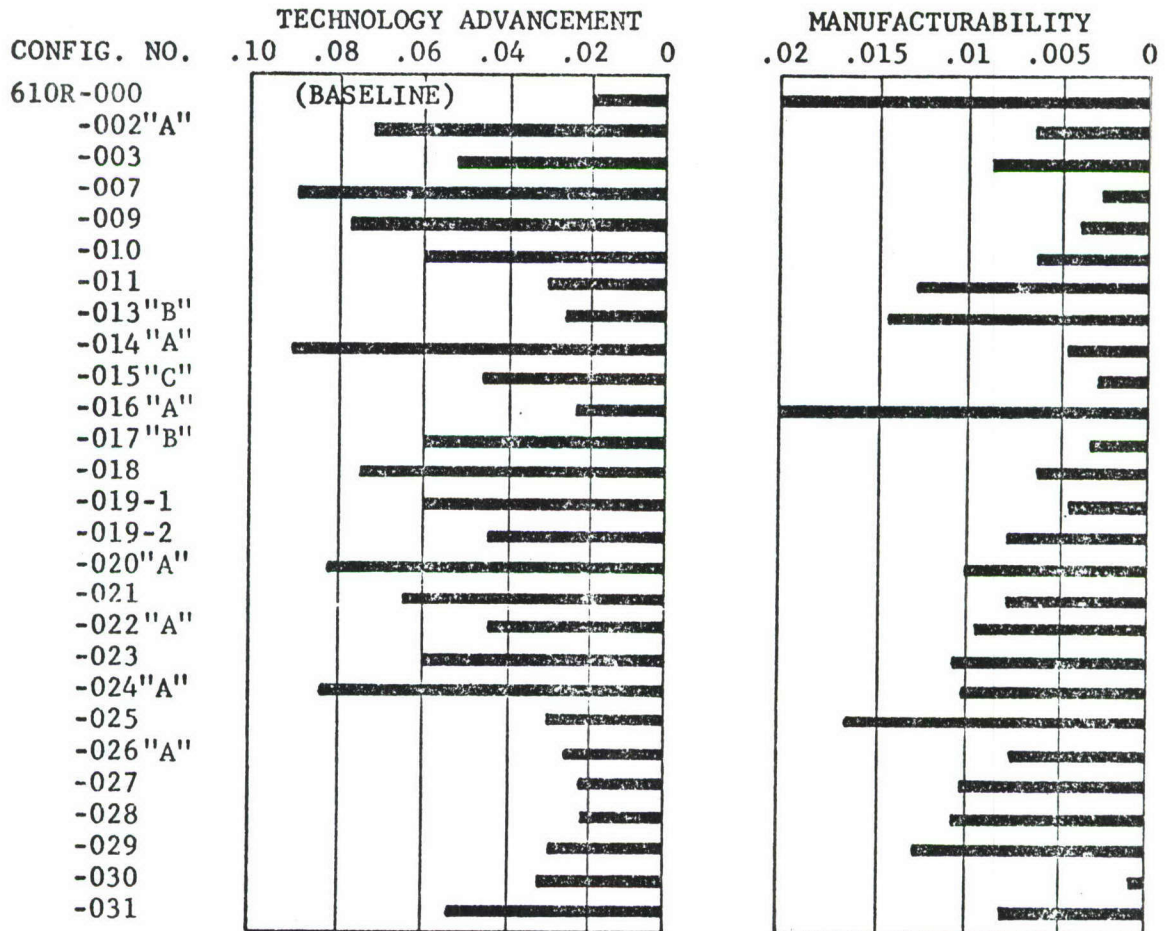


Figure 109 Concept Rating Cross-Section Concepts at C.S.S. 140

MANUFACTURING

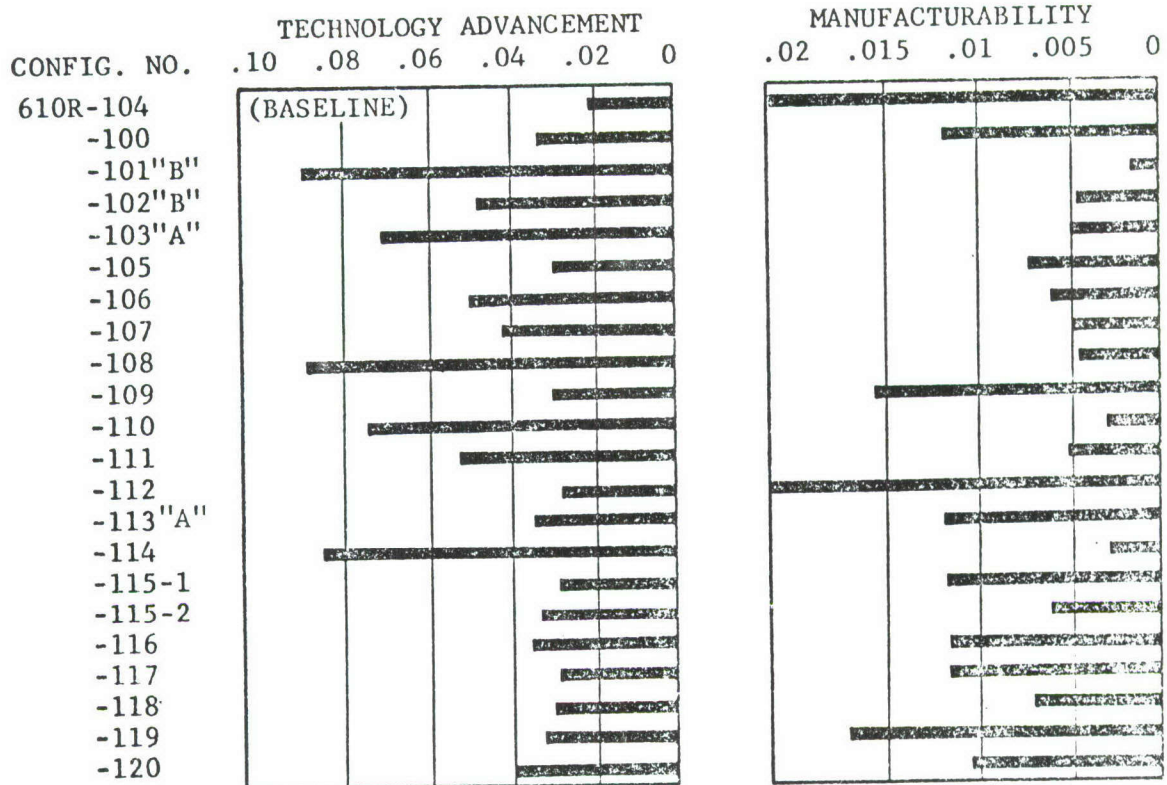


Figure 110 Concept Rating Cross-Section Concepts at C.S.S. 340

10.4 PRELIMINARY MANUFACTURING PLANNING

Preliminary manufacturing plans were prepared to assist in the evaluation of the design configurations. The plans for the three top designs are discussed in this section.

10.4.1 Preliminary Manufacturing Plan for 610RW003

The manufacturing approach for the number one ranked design is discussed below. The process is also shown schematically in Figures 111 through 120.

10.4.1.1 Front Spar Fabrication

The front spar is a one piece, integrally machined structure made from 7050-T73651 aluminum alloy plate stock. Numerically controlled milling machines are used to pocket and contour the spar (Reference Figure 111).

10.4.1.2 Corrugated Spar Fabrication

The upper and lower spar caps are tapered and stepped channel type structural pieces machined from 7050-T76511 al. alloy extrusions.

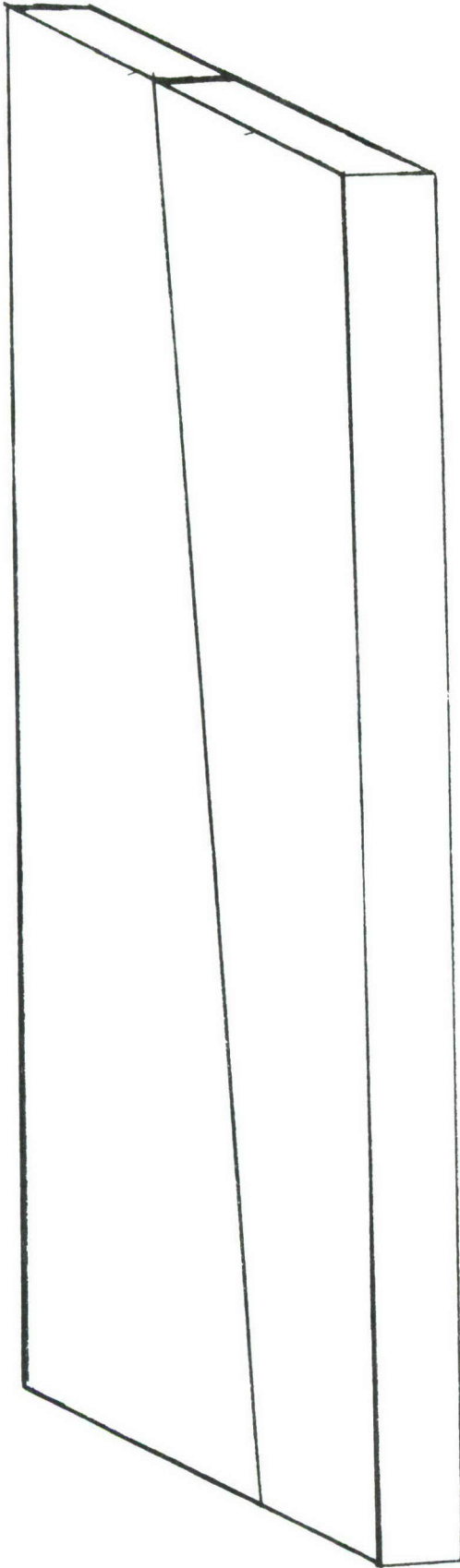
Upper caps are contour machined to the inner surface of upper skin, while lower caps will maintain the outer contour of lower wing surface as well as supporting lower surface skin panel laminates.

Numerical control machining techniques will be used for fabrication of all upper and lower spar caps to generate maximum effective metal removal and ultimate dimensional control. These details will be machined to net dimensions for installation in lower wing skin assembly.

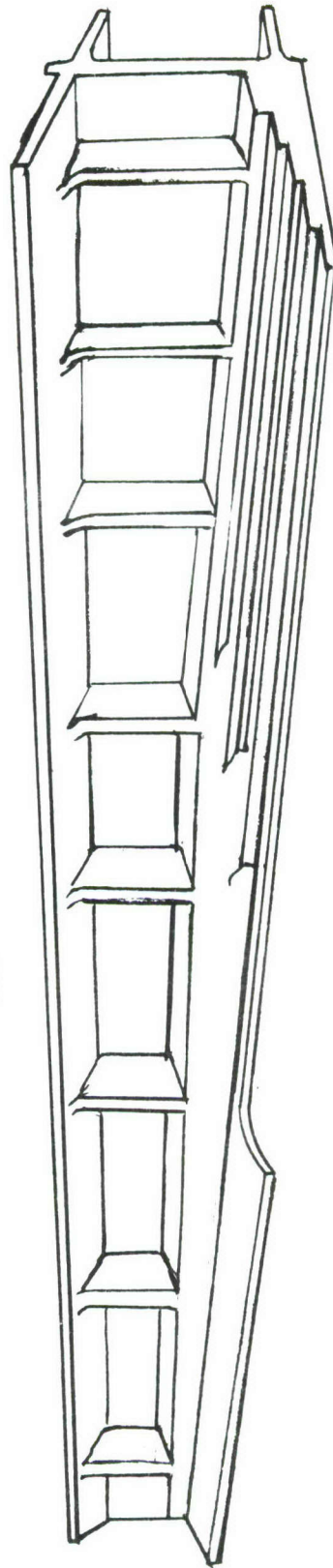
The corrugated spar webs will be formed from .071, .063, and .040 inch thick 7050-T76 aluminum alloy sheet stock.

Spar webs are to be sheared to rough width, brake formed on developed draw dies and routed to finish profile. (It has not been determined at this time if parts can be formed full depth, if not they will require intermediate thermal conditioning.)

The important manufacturing steps are shown in Figure 112.



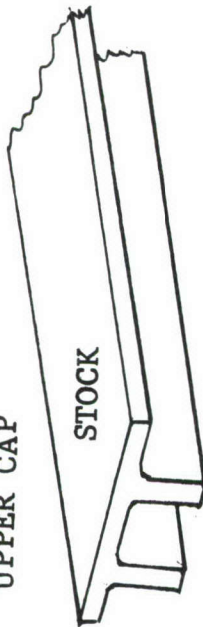
1. MAKE FROM ALUM. PLATE
SAW CUT - MAKES 1L & 1R



2. MACHINE COMPLETE BY N/C

Figure 111 Basic Manufacturing - Front Spar

UPPER CAP

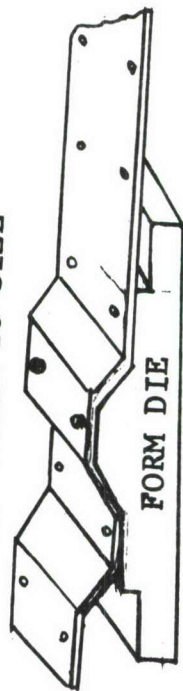


MAKE FROM ALUM. EXTRUSION
OR BAR STOCK

SPAR WEB

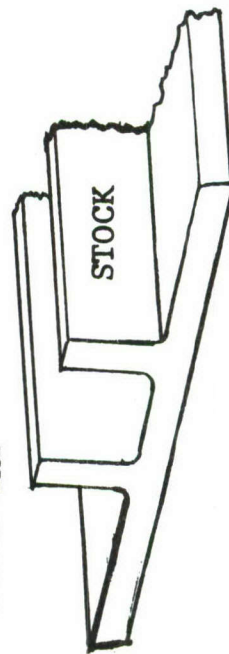


1. SHEAR TO SIZE

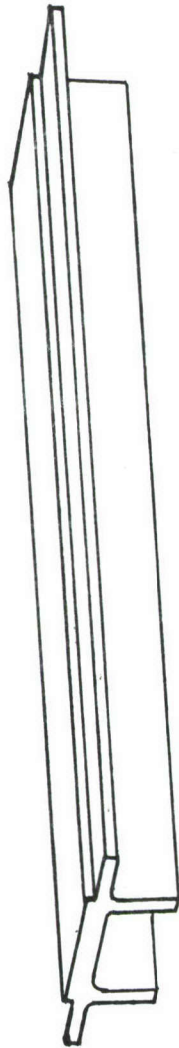


3. FORM CORRUGATIONS

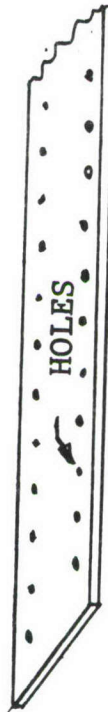
LOWER CAP



MAKE FROM ALUM EXTRUSION

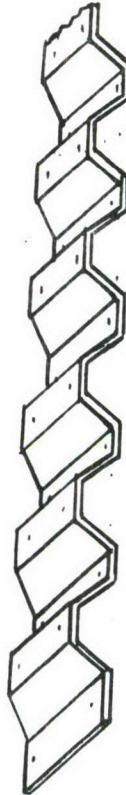


1. N/C MACHINE TO CONTOUR
2. HAND ROUTE FLANGES

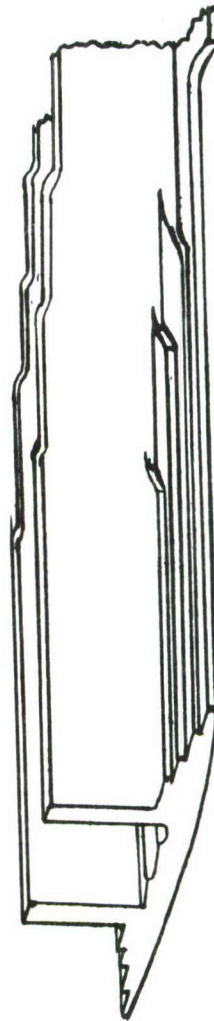


HOLES

2. DRILL INDEXING HOLES



4. HAND ROUTE TO SIZE



1. MACHINE STEPS & CONTOUR
2. HAND ROUTE FLANGES

Figure 112 Basic Manufacturing Corrugated Spar Details

10.4.1.3 Lower Skin Laminates

Each bay of the lower skin will be prepared separately. The bay laminates will be formed from various thickness of 7050-T76 aluminum alloy sheet stock, ranging from .070 to .125 inch thickness.

Laminates are to be sheared, rolled to contour, taper etched, routed, and deburred in preparation for bonding operation (Reference Figure 113).

10.4.1.4 Upper Skin Fabrication

The upper skin is a one piece sculptured plate similar in type to the present F-111. It contains the entire upper surface contour.

Basic tapers on the inside skin will be machined on numerical control skin mill. Contour will be formed on 1000 ton numerical control brake. The skin will then be etched and routed to finish dimensions (Reference Figure 114).

10.4.1.5 Fabrication of Bulkheads, Ribs, and Pylon Fittings

Major fittings may be fabricated by machining from plate or by precision forging. Production quantity and rate will determine the most economical method. Figure 115 depicts the two methods.

10.4.1.6 Rear Spar Fabrication

The rear spar webs will be made from .040 inch thick 7050-T76 aluminum sheet stock.

Rear spar webs will be sheared to rough width and routed to net profile in preparation for weld bonding operation.

Spar caps will be fabricated using methods shown in Figure 112.

Assembly of the cap and web components is classified as a secondary manufacturing process as shown in Figure 116.

10.4.1.7 Assembly of Lower Surface

This assembly consists of aluminum skin sheets laminated and joined to the lower spar caps which were step machined in detail to provide overlap of each individual skin laminate with

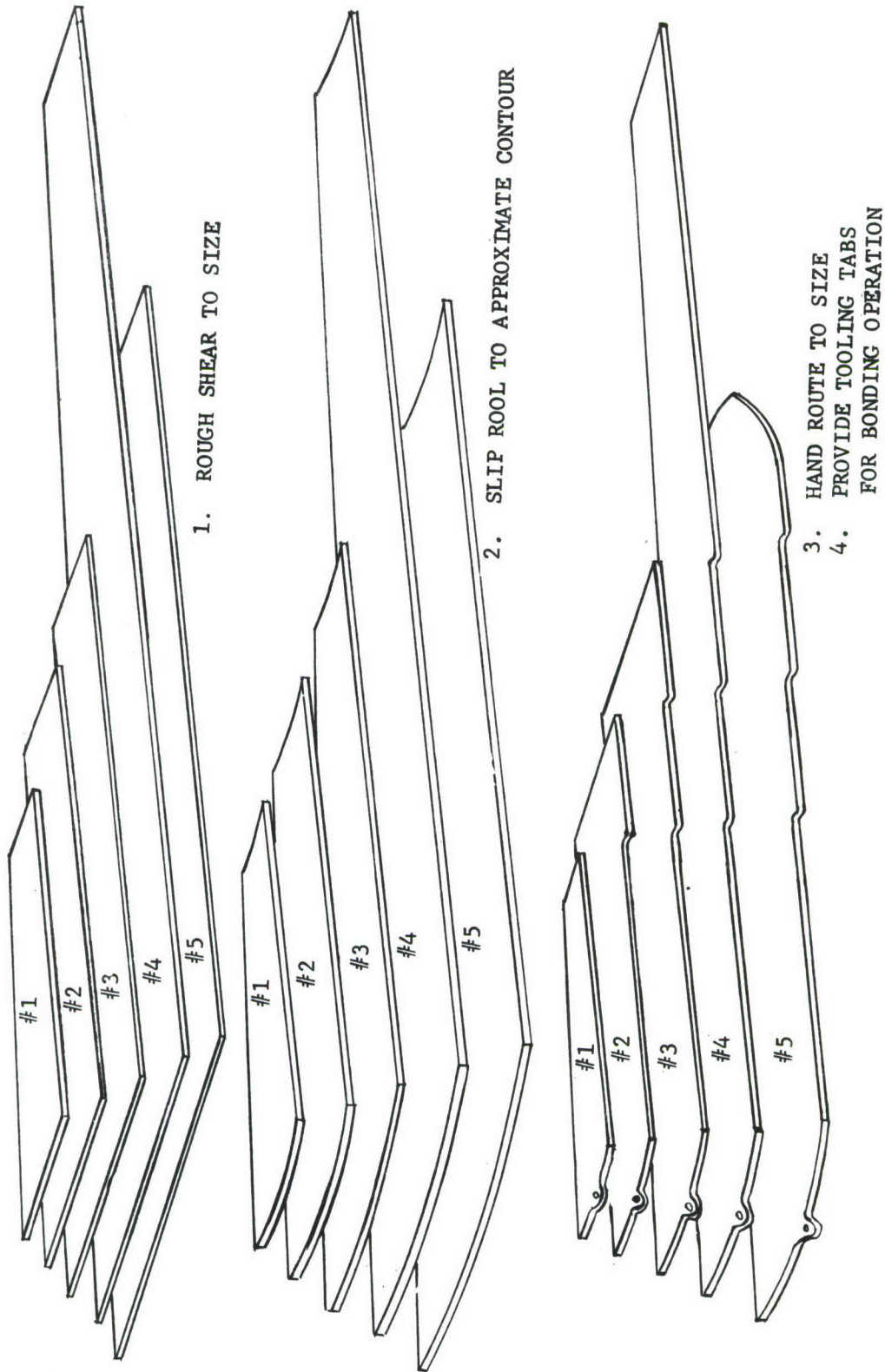


Figure 113 Basic Manufacturing Lower Skin Laminates

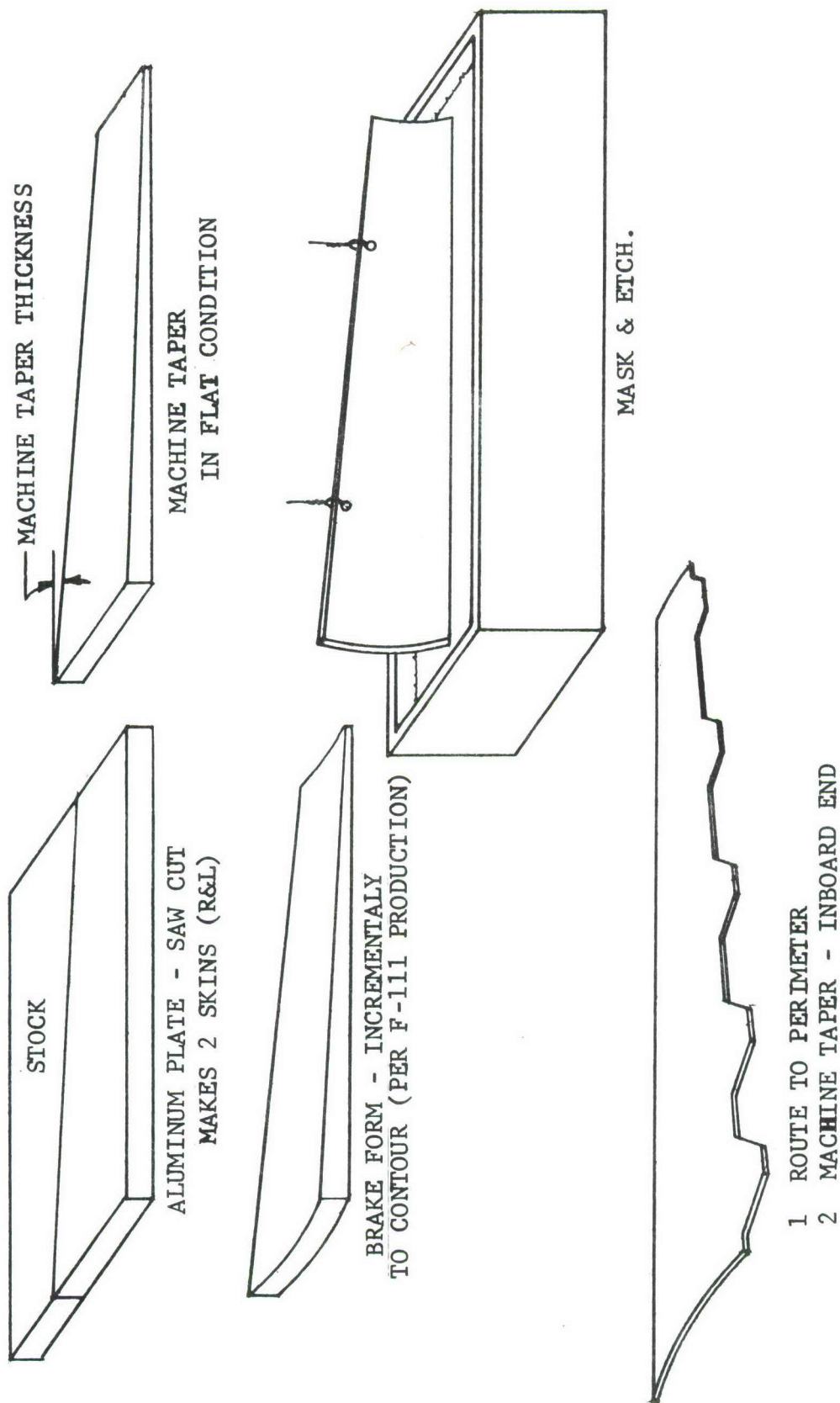


Figure 114 Basic Manufacturing Upper Skin

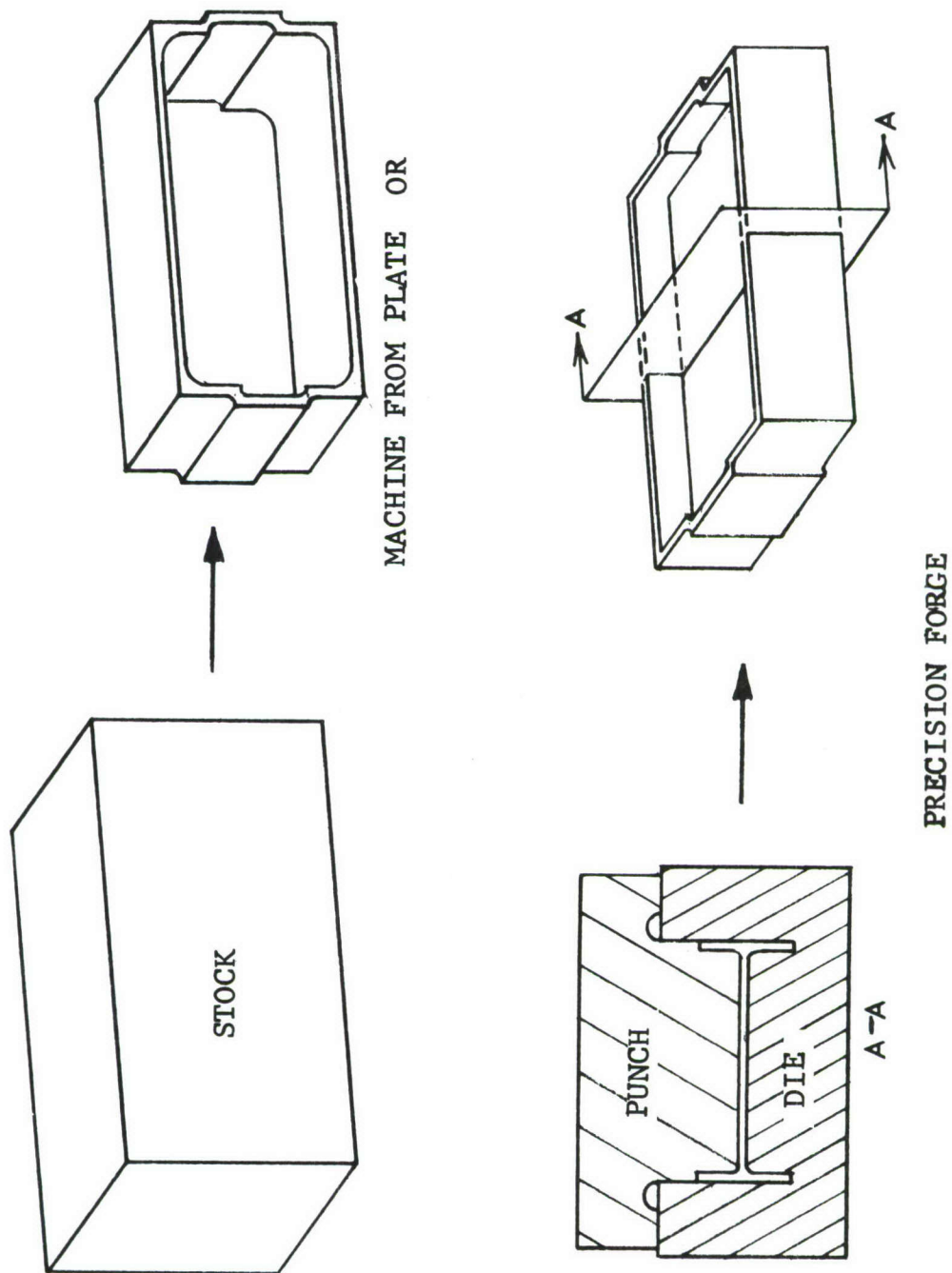
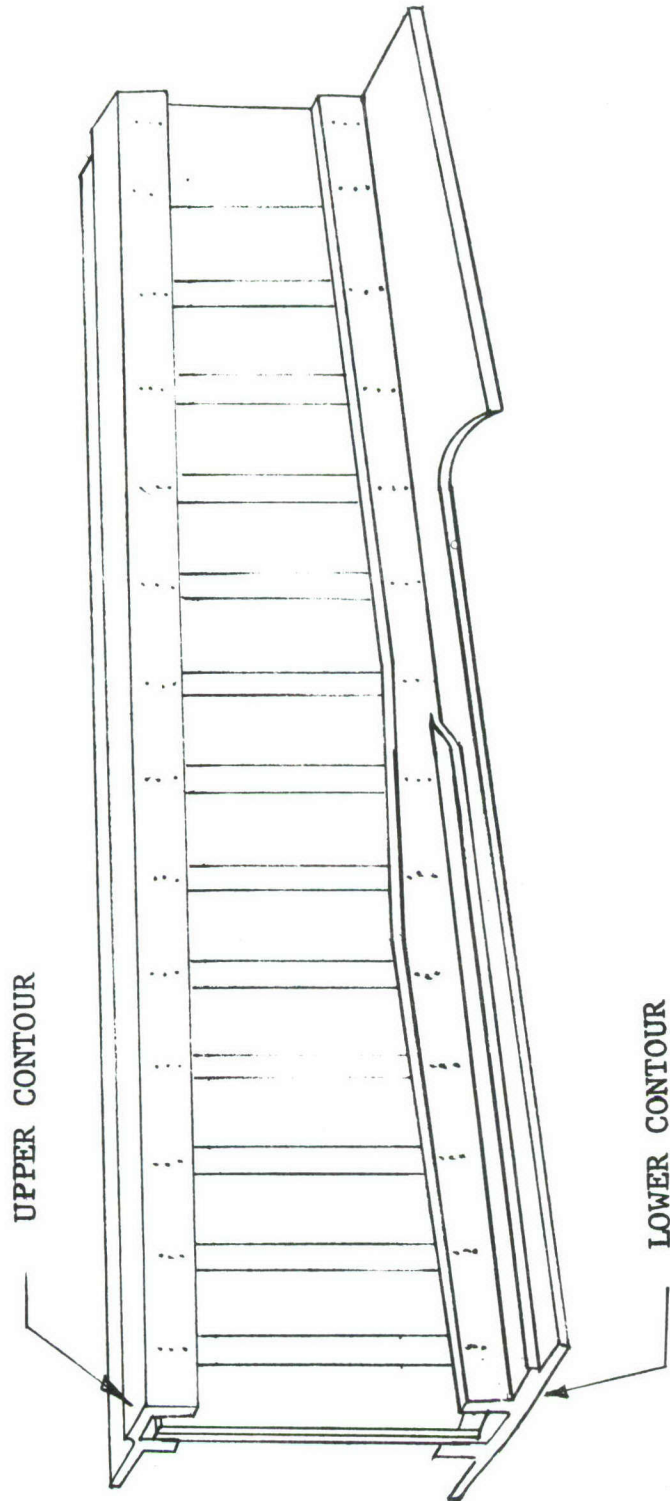


Figure 115 Basic Manufacturing Bulkheads, Ribs, and Pylon Fittings



1. POSITION SPAR CAPS IN FIXTURE HOLDING UPPER AND LOWER CONTOUR
2. LOCATE WEBS IN RELATION TO SPAR CAPS AND APPLY ADHESIVE BONDING TAPE
3. SPOTWELD IN HOLDING FIXTURE
4. TRANSFER ASSEMBLY TO BONDING TOOL FOR ADHESIVE CURE AND BONDING

Figure 116 Secondary Manufacturing Rear Spar Assembly Weldbond Spar Webs And Caps

the spar cap flange. Design of the one piece front spar requires that bonding tooling be able to support the full depth spar during the bonding cycle. Also, the full depth pylon fittings will be positioned and held during bonding (Reference Figure 117).

10.4.1.8 Lower Wing Box Adhesive Bonded Assembly

The first step in assembly of this structure is to prefit spar webs, upper spar caps, ribs, and bulkheads to the previously bonded lower skin assembly. This operation will require unusual type assembly and prefit fixturing necessary to accomplish either weld bonding or rivet bonding, as selected from manufacturing testing. Following prefit and cleaning the details will be prepared and assembled for weld bonding or rivet bonding (Reference Figure 118). After completion of these operations the assembly will go to the oven or autoclave for cure of adhesives used in the layup of the assembly. Fixturing for this operation will be a combination wing assembly fixture and adhesive bonding tool having provisions for locating the rear spar assembly during bonding (Reference Figure 119).

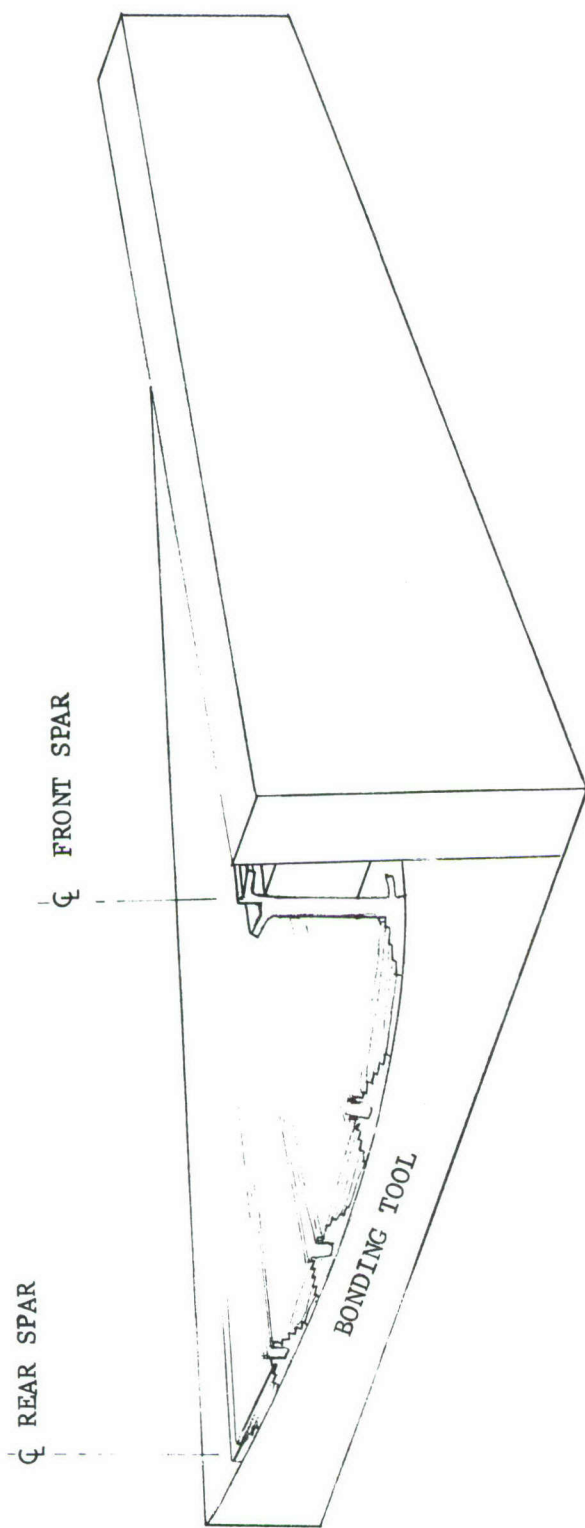
10.4.1.9 Final Assembly of Wing Box

A major assembly and drill fixture commonly known as a "wing buck" will be required to perform final assembly operations of the box. The fixture will receive the basic lower box assembly and provide a method of positioning, holding, and locating hole drilling tooling for drilling holes common to the one piece upper skin and understructure. Following the hole drilling operations the skin is removed and self locking nuts will be installed in the attach surfaces of the lower box upper surface. With the skin removed all attachments to the front and rear spar will be made. At this point all faving surfaces formed by the upper skin will have fuel sealing applications and the upper skin will be permanently attached with bolts.

No reference is made to attaching the inboard end of the box to a test fixture. It is assumed that provisions for attachment of necessary fittings or bulkheads associated with testing will be accomplished in the final assembly fixture prior to final attachment of the upper wing skin to the lower box assembly.

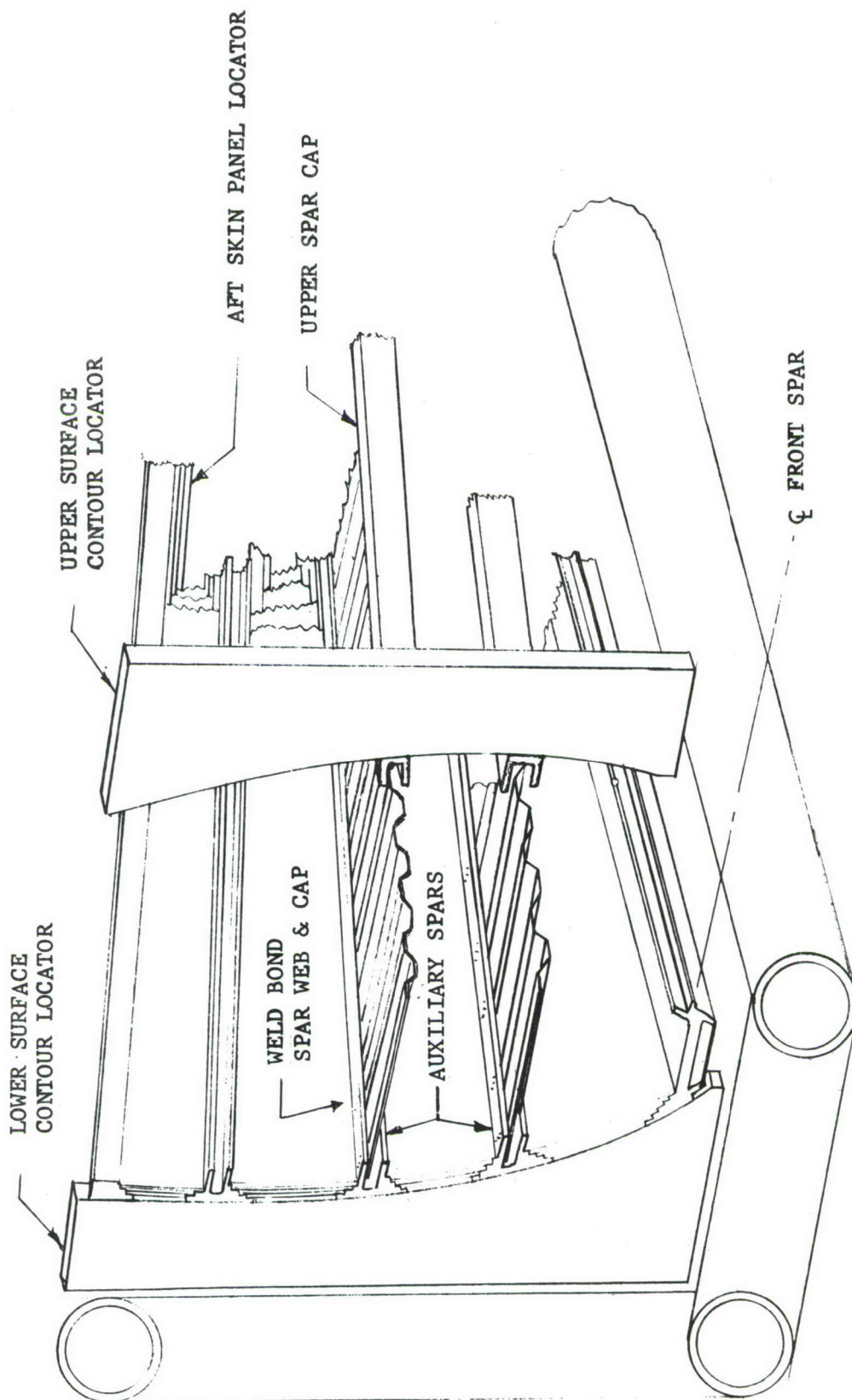
10.4.2 Preliminary Manufacturing Plan for 610RW004

The manufacturing approach for the number two ranked design configuration is described below. Figures 121 through 128 show the process schematically.



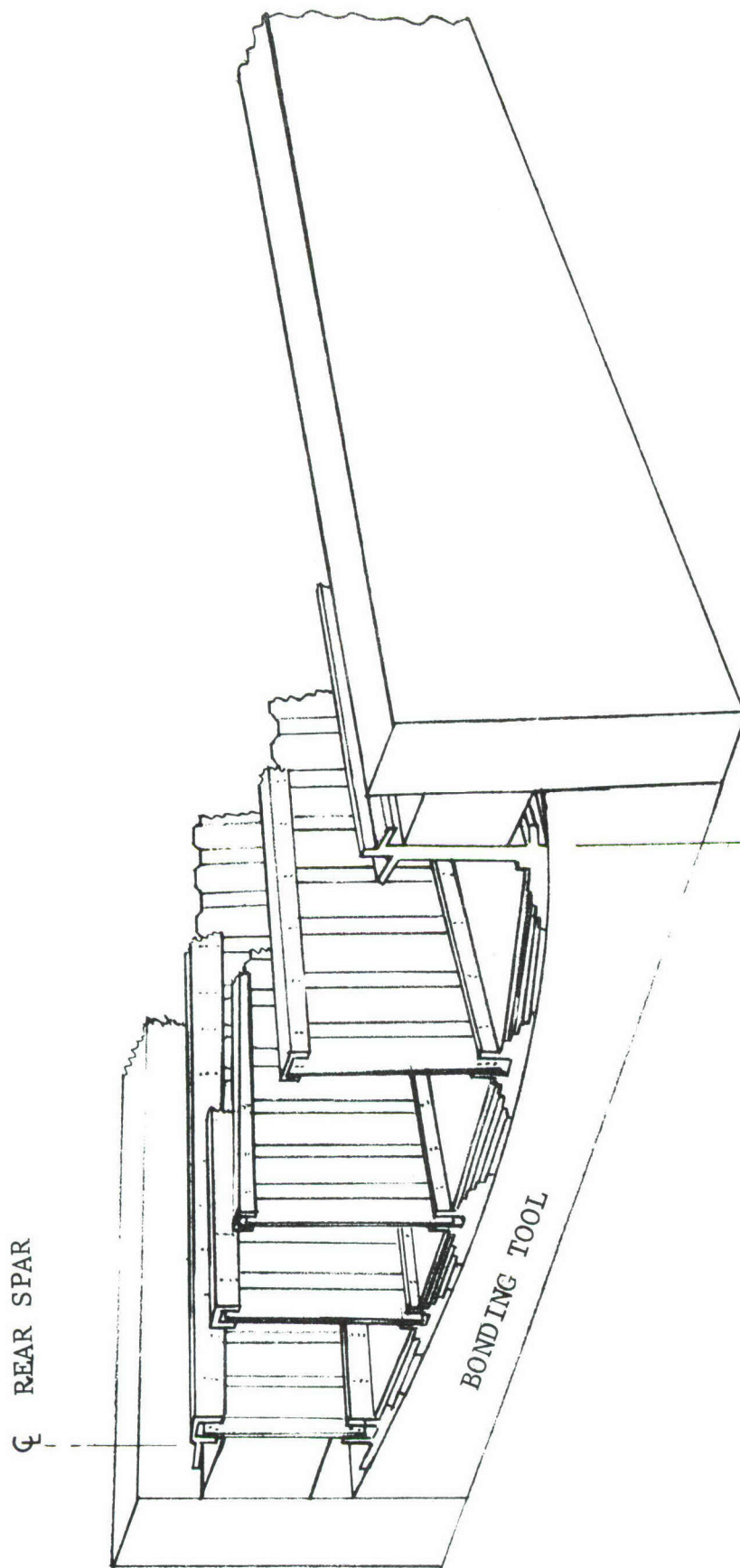
1. LOCATE FRONT SPAR AND AUXILIARY SPAR CAPS FROM LOCATORS ON FIXTURE
2. LOCATE LAMINATES FROM TOOLING HOLES AT INBOARD ENDS OF DETAILS

Figure 117 Secondary Manufacturing Lower Surface Laminated Skin Panel Adhesive Bonded Assembly



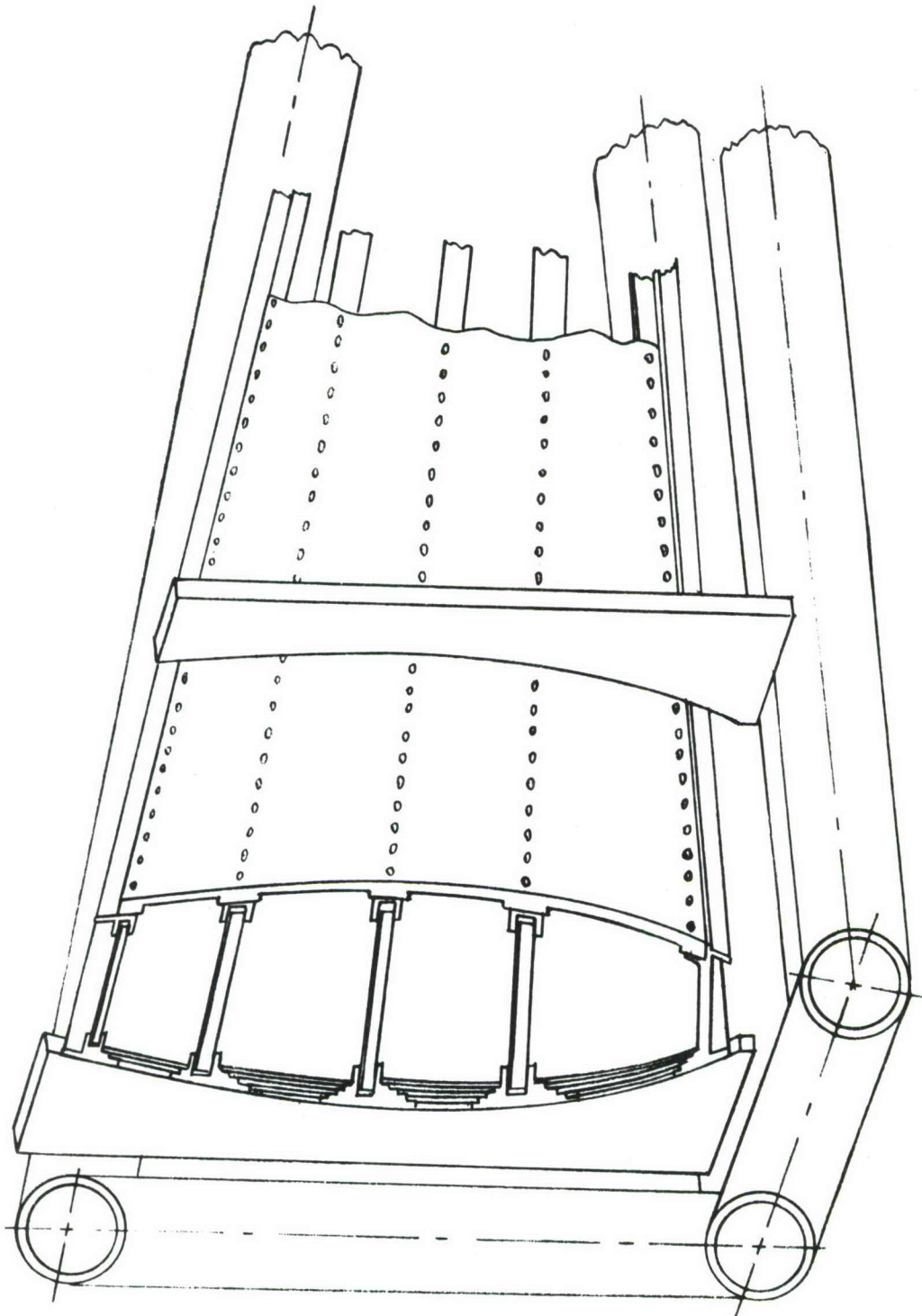
1. POSITION LOWER SKIN PANEL IN HOLDING FIXTURE
2. LOCATE SPAR WEBS AND UPPER SPAR CAPS
3. APPLY ADHESIVE AND SPOTWELD

Figure 118 Secondary Manufacturing Weldbond Spar Webs & Caps



1. LOCATE REAR SPAR ASSEMBLY FROM FIXTURE LOCATORS
2. LOCATE LOWER SKIN LAMINATE FROM TOOLING HOLE TABS ON INBOARD END OF SKIN PANEL
3. BOND REAR SPAR TO LOWER SKIN PANEL AND CURE ADHESIVE IN WELDBOND AREA

Figure 119 Secondary Manufacturing Final Bond Assembly and Weldbond Cure
Lower Surface Laminated Skins and Corrugated Spars



1. INSTALL BULKHEADS AND FITTINGS
2. LOCATE UPPER SKIN TO UNDERSTRUCTURE
3. DRILL ATTACH HOLES FROM TEMPLATES
4. REMOVE UPPER SKIN AND INSTALL PRESS NUTS
5. REASSEMBLE SKIN AND INSTALL FASTENERS

Figure 120 Secondary Manufacturing Final Assembly Upper Skin and Understructure

10.4.2.1 Front and Rear Spar Fabrication

As shown in Figure 121, the spar caps are machined from 7050-T736511 aluminum extrusions. Spar webs are honeycomb sandwich panels.

10.4.2.2 Auxiliary Spar Fabrication

Upper and lower spar caps are machined from aluminum extrusions. Spar webs are aluminum sheet stiffened by weld-bonded angles. The basic steps are shown in Figure 122.

10.4.2.3 Fabrication of Skin Panel Details

Slugs of solid aluminum plate (7050-T73651) are bonded between aluminum sheet skins (7050-T76) to form the basic skin panels. Fabrication of the details is shown in Figure 123.

10.4.2.4 Front and Rear Spar Assembly

Assembly of the front and rear spar details is classified as a secondary manufacturing operation. The process is shown in Figure 124.

10.4.2.5 Lower Skin Panel Assembly

The front and rear spars, lower spar caps for auxiliary spars, and the lower skin panel details are bonded together in one bond cycle. A sketch showing these components in the bond form is shown in Figure 125.

10.4.2.6 Assembly of Lower Skin Panel and Auxiliary Spars

Using a fixture to control both upper and lower surface contour, the upper caps and webs for auxiliary spars are weld-bonded into place. The sequence is described in Figure 126.

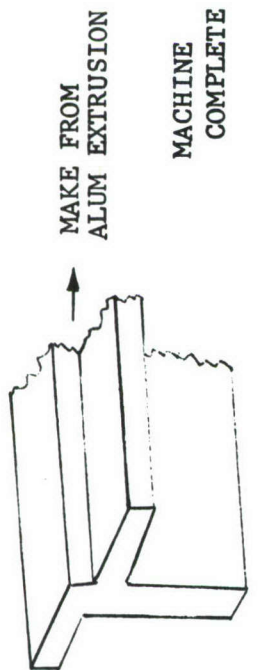
10.4.2.7 Upper Skin Panel Assembly

The upper skin panel is adhesive bonded as shown in Figure 127. It is a more conventional bonding operation since all surfaces are smooth contours.

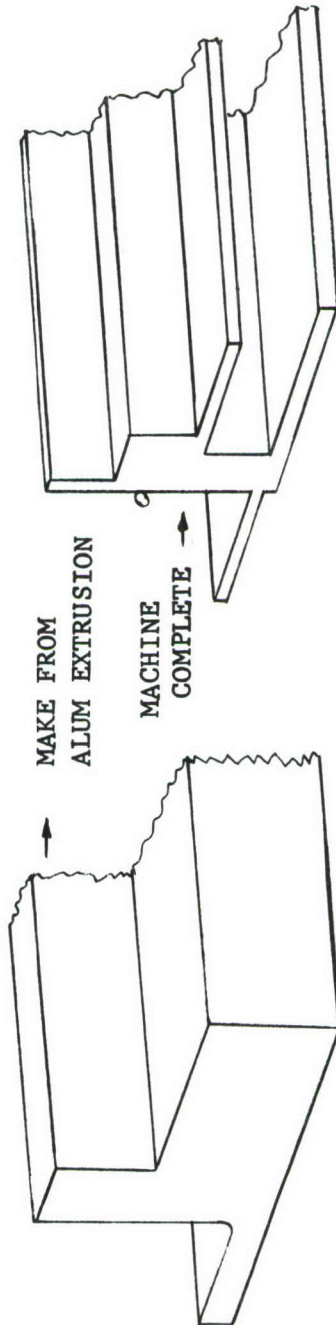
10.4.2.8 Final Assembly of Wing Box

Installation of the upper skin panel completes the wing box. This operation is shown in Figure 128.

UPPER CAPS



LOWER CAPS



WEBS



CORE

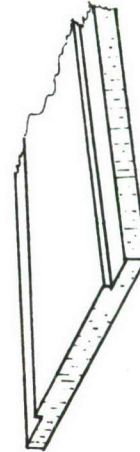
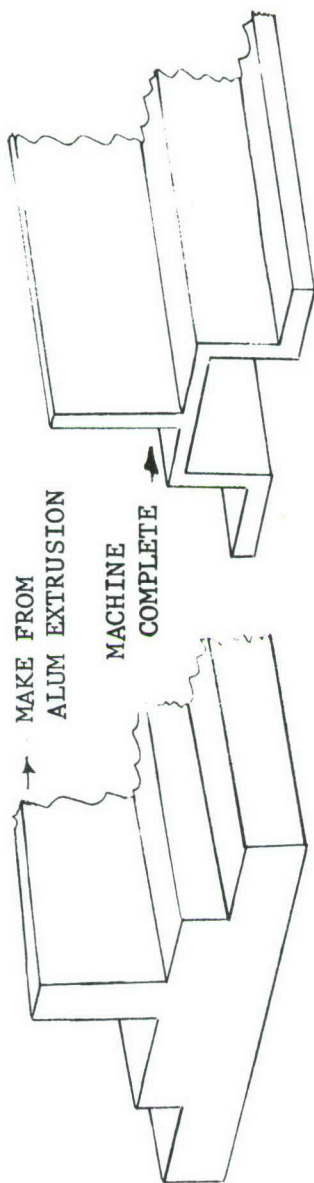
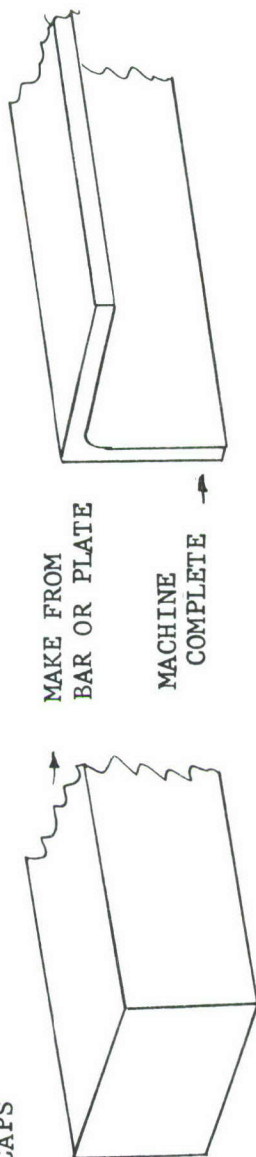


Figure 121 Basic Manufacturing Spar Details Front and Rear Spars

LOWER CAPS



UPPER CAPS



WEBS

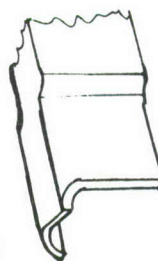


SHEAR TO SIZE
DRILL TOOLING HOLES
USE FLAT TEMPLATE

STIFFENER ANGLES



SHEAR TO SIZE
USE FLAT TEMPLATE



BRAKE FORM
AND JOGGLE

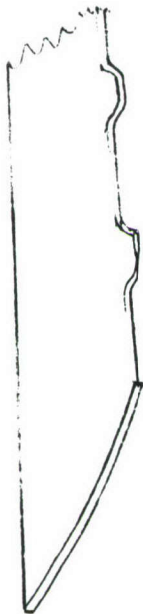
Figure 122 Basic Manufacturing Spar Details Auxiliary Spars

SKINS



1. SHEAR TO ROUGH SIZE

2. ROLL TO CONTOUR
3. ROUTE TO SHAPE



SLUGS-ALUMINUM



1. SAW TO ROUGH SIZE



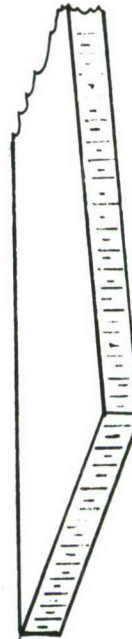
2. MACHINE COMPLETE TO CONTOUR

SLUGS - FIBERGLASS



MOLD TO SHAPE

CORE DETAILS - ALUMINUM



SAW TO SHAPE - HAND FORM

Figure 123 Basic Manufacturing Skin Panel Details

1. PREFIT AND LOCATE DETAILS IN BOND FORM
2. APPLY ADHESIVE AND CURE IN BONDING PRESS

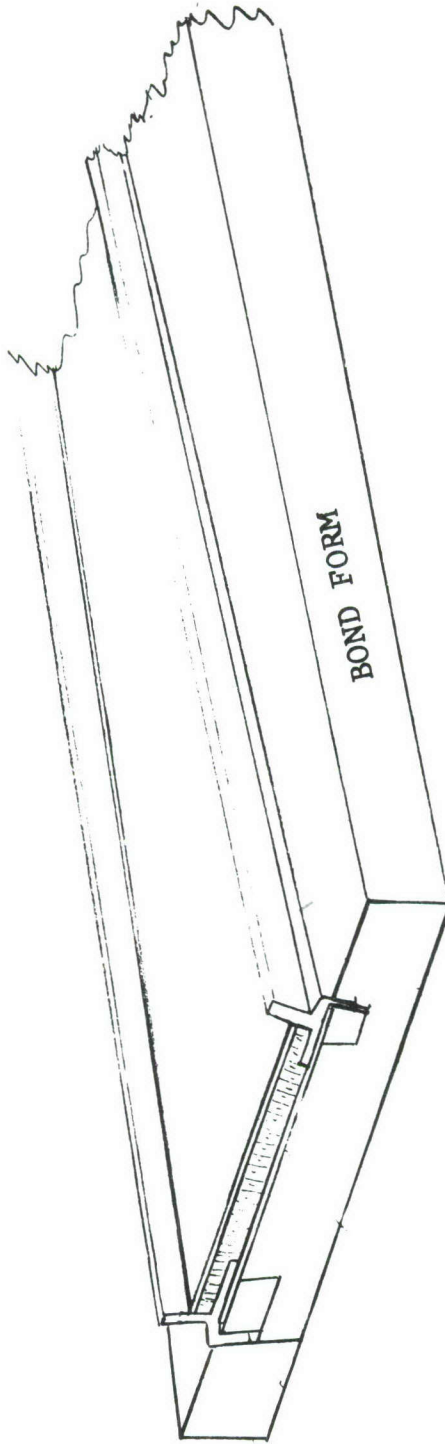


Figure 124 , Secondary Manufacturing Front & Rear Spars Adhesive Bonded Assembly

1. LOCATE SPARS AND PREFIT DETAILS IN BOND FORM
2. APPLY ADHESIVE AND BOND IN AUTOCLAVE

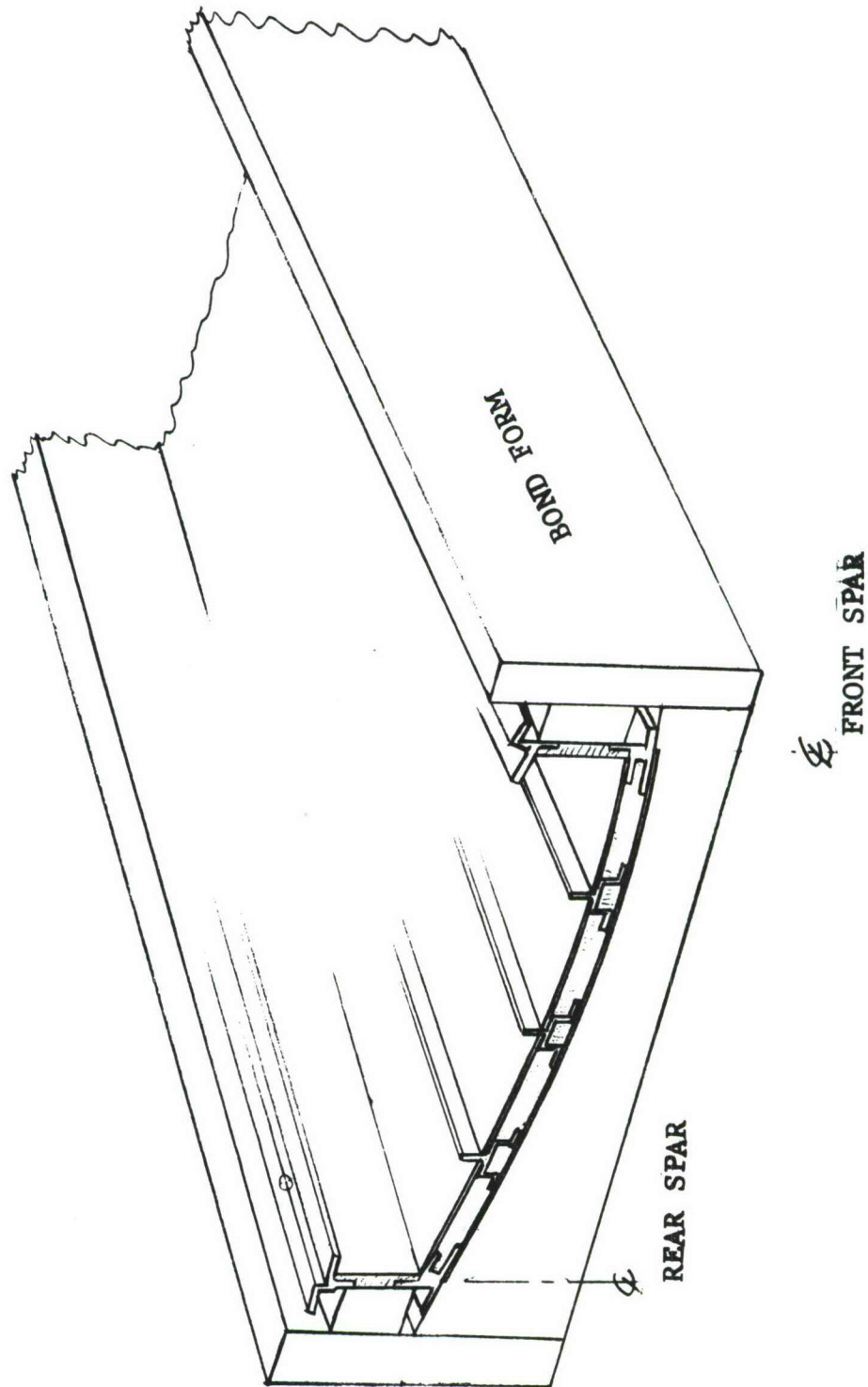
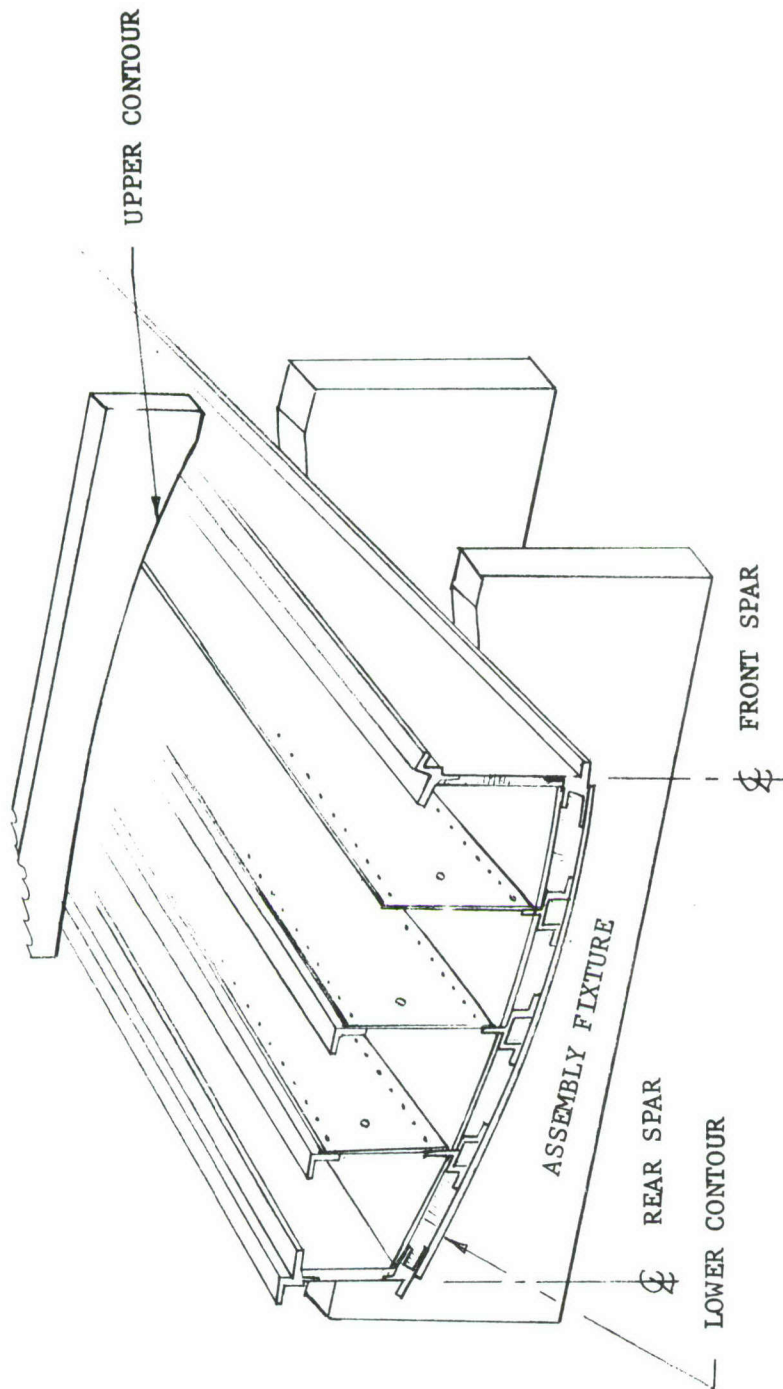
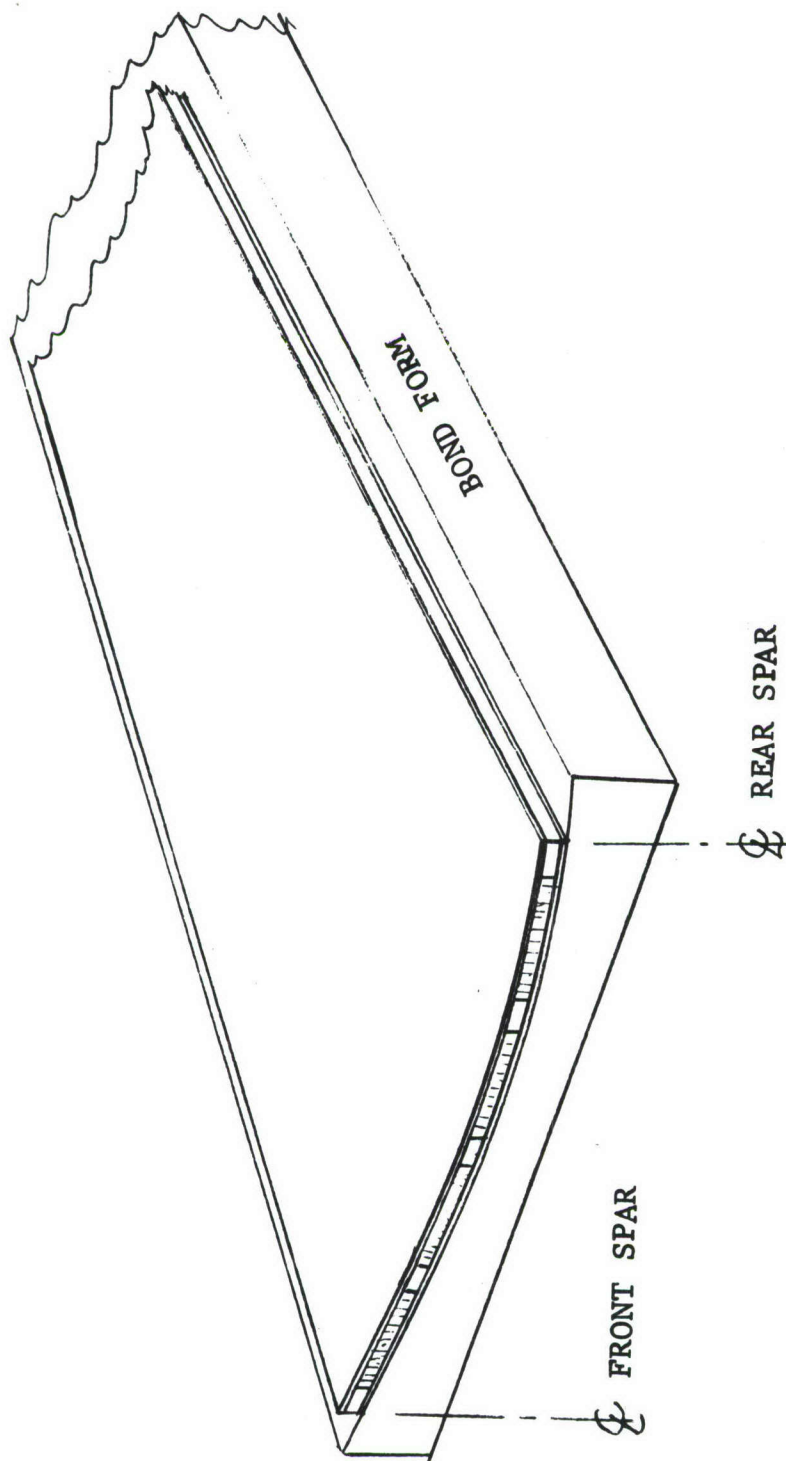


Figure 125 Secondary Manufacturing Lower Skin Panel Assembly



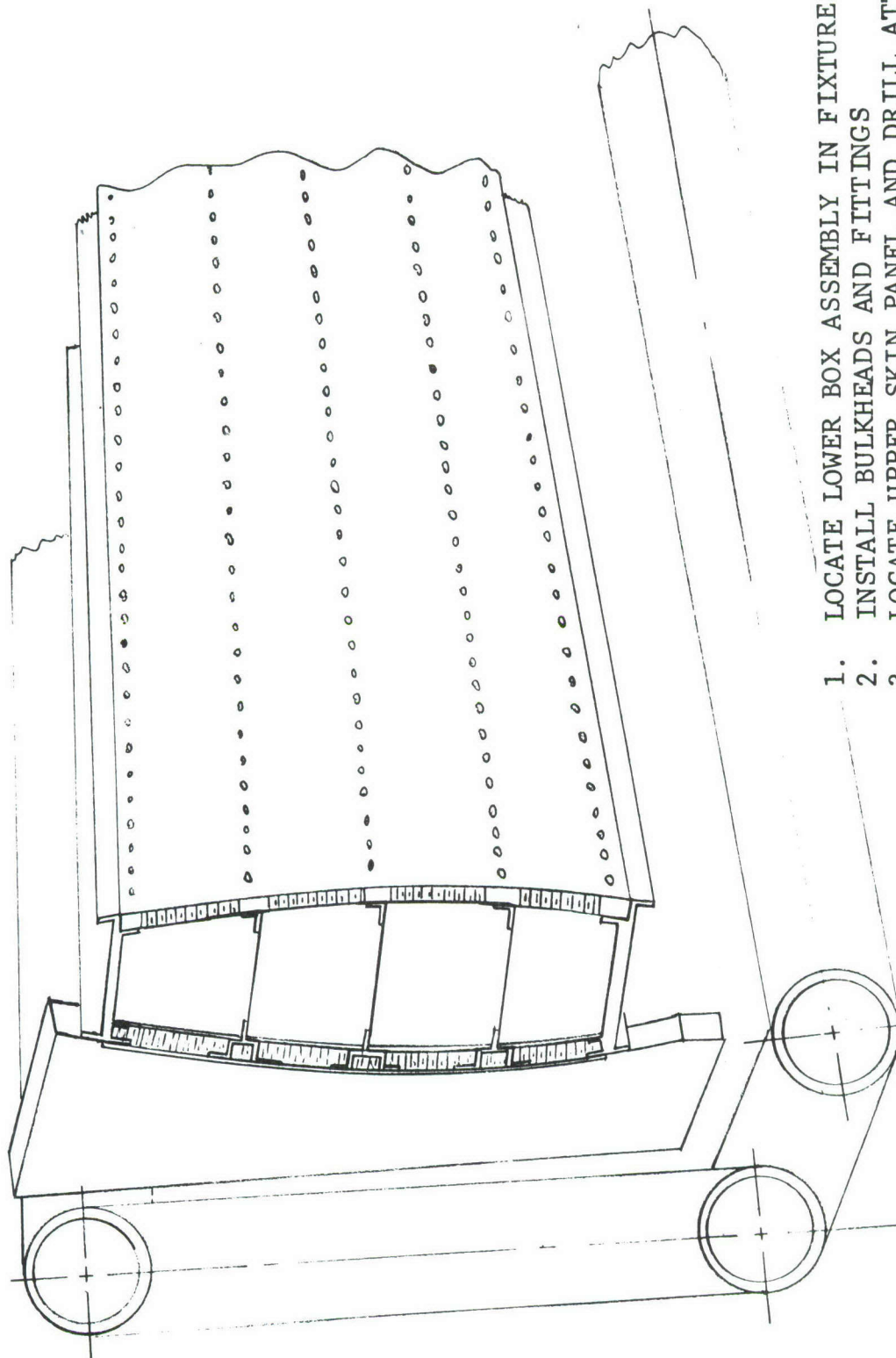
1. LOCATE LOWER PANEL IN ASSEMBLY FIXTURE
2. APPLY ADHESIVE TO AUXILIARY SPAR WEB AND LOCATE IN FIXTURE
3. SPOTWELD SPAR WEBS TO LOWER SPAR CAP FLANGES
4. LOCATE UPPER SPAR CAPS AND SPOTWELD TO SPARE WEBS
5. LOCATE STIFFENER ANGLES AND SPOTWELD TO WEB & CAPS
6. RETURN ASSEMBLY TO BOND FORM AND CURE IN AUTOCLAVE

Figure 126 Secondary Manufacturing Assembly of Lower Skin Panel and Auxiliary Spars



1. PREFIT AND LOCATE DETAILS IN BOND FORM
2. APPLY ADHESIVE AND BOND IN AUTOCLAVE

Figure 127 Secondary Manufacturing Upper Skin Panel Assembly



1. LOCATE LOWER BOX ASSEMBLY IN FIXTURE
2. INSTALL BULKHEADS AND FITTINGS
3. LOCATE UPPER SKIN PANEL AND DRILL ATTACH HOLES
4. REMOVE UPPER SKIN PANEL AND INSTALL PRESS NUTS
5. REASSEMBLE SKIN PANEL AND INSTALL FASTENERS

Figure 128 Secondary Manufacture Final Assembly of Wing Box Structure

10.4.3 Preliminary Manufacturing Plan for 61ORW002

The manufacturing approach for the number three ranked design is discussed below. The process is also shown schematically in Figures 129 through 142.

10.4.3.1 Front and Rear Spar Detail Fabrication

The front and rear spars details consist of upper and lower spar caps which are butt welded to a spar web. All details are made from 6al4V titanium alloy material. The spar caps are extruded to rough tee shapes and machined complete. The spar webs are sheared from sheet stock and machine routed to size for welding. (Reference Figure 129.) The steps in welding are explained in paragraph 10.4.3.7.

10.4.3.2 Upper and Lower Skin Details

Each section of skin will be rough sheared from 6al4V titanium alloy sheet stock. Conventional tooling tabs will be machine routed and drilled for coordination to station and contour location. Ceramic hotform dies will be used to creep form each detail prior to prefit in the final brazing fixture (Reference Figure 130).

10.4.3.3 Inboard and Outboard Pylon Fittings

Pylon fittings will originate as rough machined 6al4V titanium alloy plate and bar material. The rough machined shapes will be electron beam welded to a configuration which can be machined to produce the desired part for the assembly welding (Reference Figure 131).

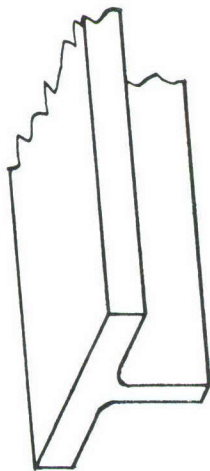
10.4.3.4 Core Cell Details

The core cell details will originate from commercially pure titanium sheet stocked in rolled coils. The material will be fed from the coil into a punch die or a combination punch and form die which cold forms the cell wall shape and punches a series of holes predetermined to size and location. These holes may be used for dual purpose as fuel flow holes and coordination holes in fabricating welded core blocks and later in prefitting, machining, and joining core segments (Reference Figure 132).

10.4.3.5 Core Cell Fabrication

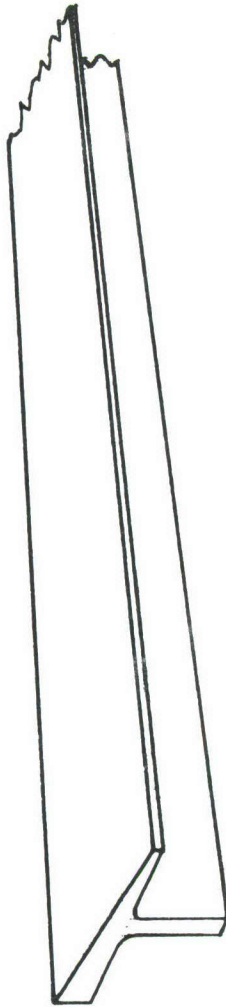
The performed core cell ribbons are located in a seam welding fixture using the prepunched coordinating holes to establish shape

SPAR CAPS

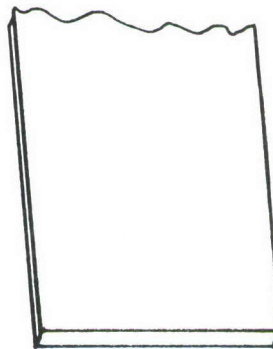


MAKE FROM ROUGH
TITANIUM EXTRUSION

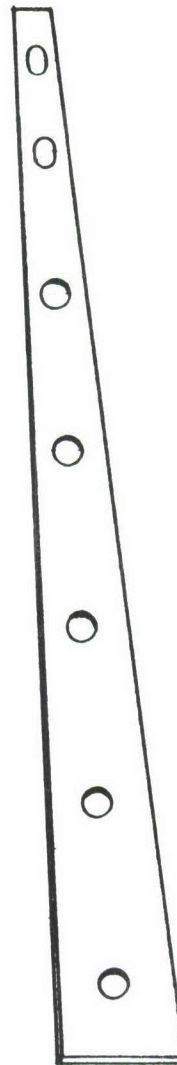
MACHINE COMPLETE



SPAR WEBS



SHEAR TO ROUGH SIZE



MACHINE ROUTE PERIMETER AND CUTOUTS

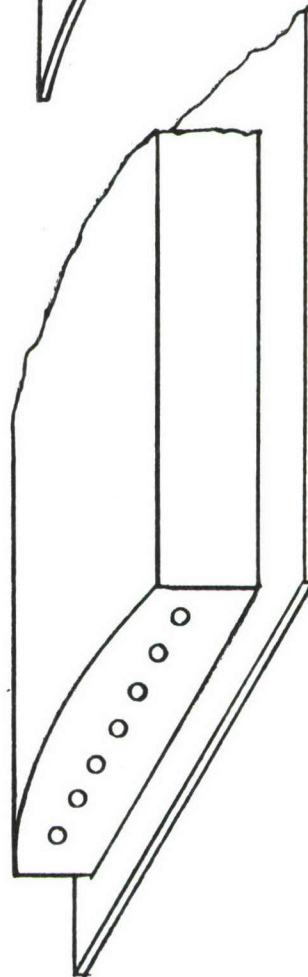
Figure 129 Basic Manufacture Spar Details Front and Rear Spars



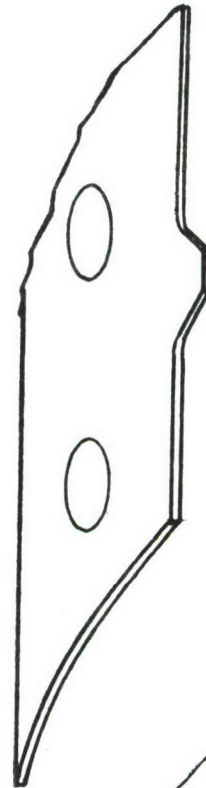
MACHINE TOOLING TABS AND DRILL TOOLING HOLES



ROUGH SHEAR TO STOCK SIZE



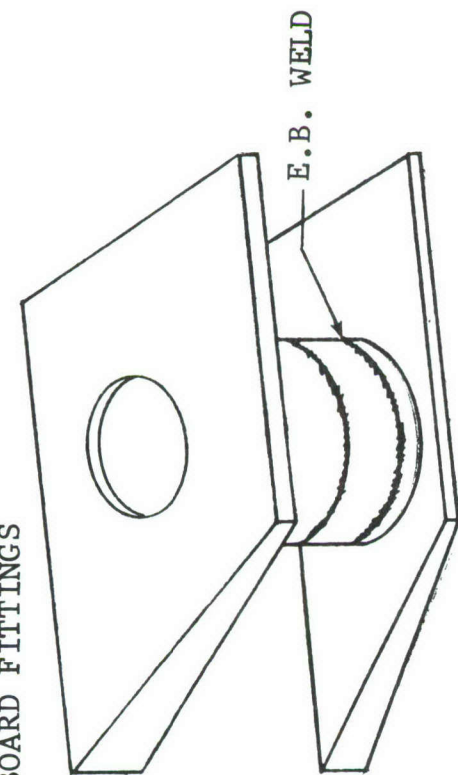
HOT FORM SKINS TO CONTOUR



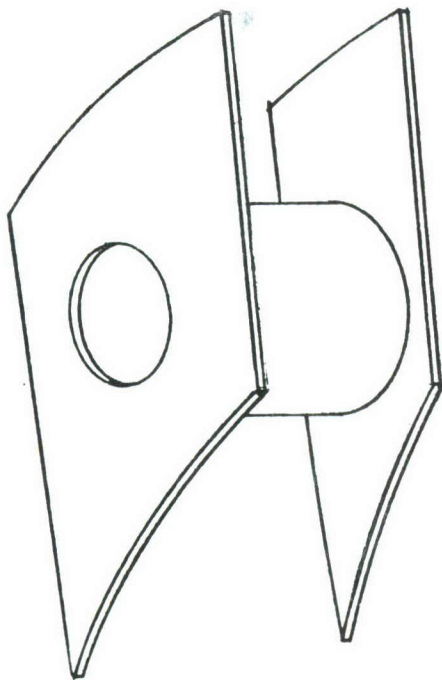
MACHINE PERIMETER AND CUTOUTS (FLAP TRACK TABS)

Figure 130 Basic Manufacturing Wing Skin Details

INBOARD FITTINGS

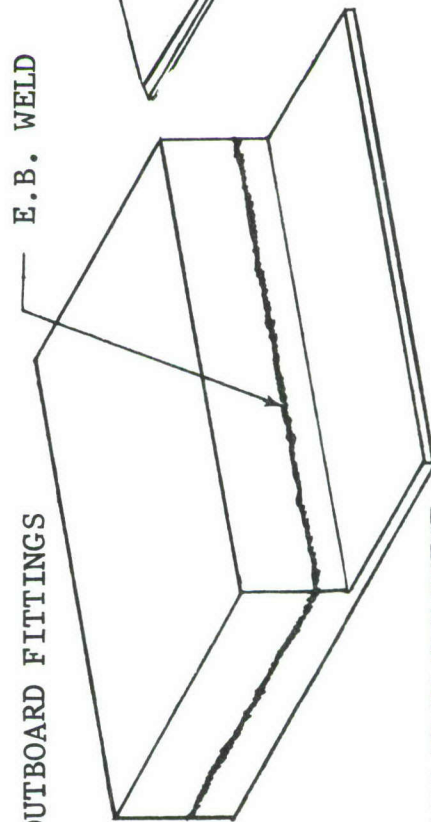


MAKE FROM WELDMENT

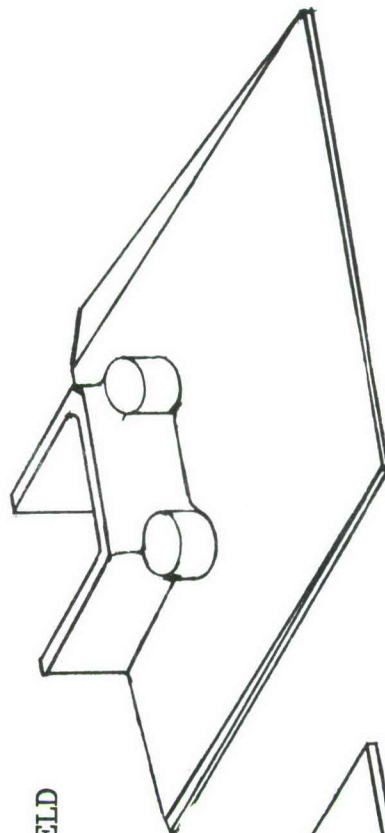


MACHINE TO SIZE

OUTBOARD FITTINGS

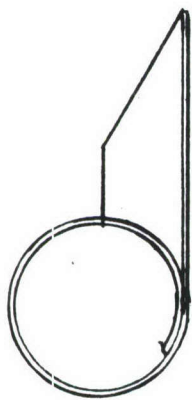


MAKE FROM WELDMENT



MACHINE COMPLETE

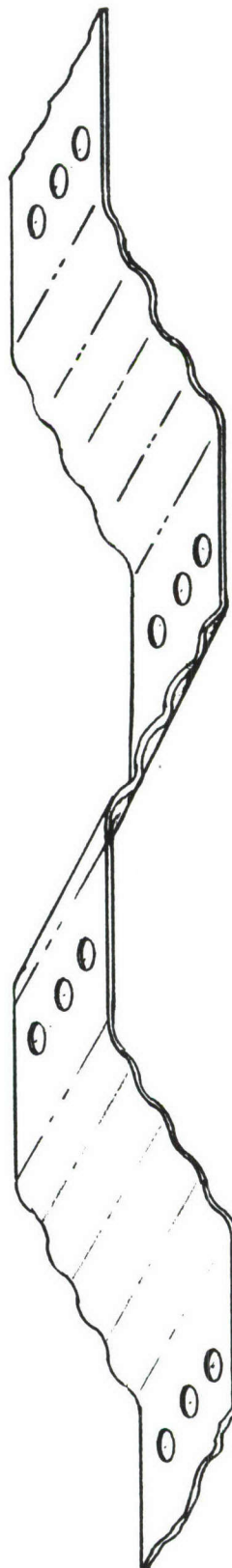
Figure 131 Basic Manufacturing Pylon Fittings



MAKE FROM COIL STOCK



PUNCH TOOLING INDEXING HOLES
AND FUEL FLOW HOLES



FORM CELL SHAPE IN PROGRESSIVE DIE
STOCK IN RANDOM LENGTHS

Figure 132 Basic Manufacturing Fabrication of Core Cell Details

and alignment. Rectangular block of core will be sized to allow for cutting to final shape at prefit operations (Reference Figure 133).

10.4.3.6 Pylon Fitting Assemblies

Details of the pylon fitting assemblies will be jig located for contour and station location and GTA welded as butt welds and burn through welds (Reference Figure 134).

10.4.3.7 Rear Spar and Front Spar Weld Assembly

The front and rear spars become an integral spar and pylon fitting weld assembly as the first steps in approaching the wing box assembly. Steps in fabricating this weld assembly are:

(1) Weld pylon assembly fittings to rear spar web using GTA burn thru welding (Reference Figure 134). Locate pylon fitting assembly from pylon attach points in a major positioning and welding fixture which also positions the spar web for welding.

(2) Locate upper and lower spar caps and GTA butt weld in the rear spar pylon fitting welding fixture (Reference Figure 135).

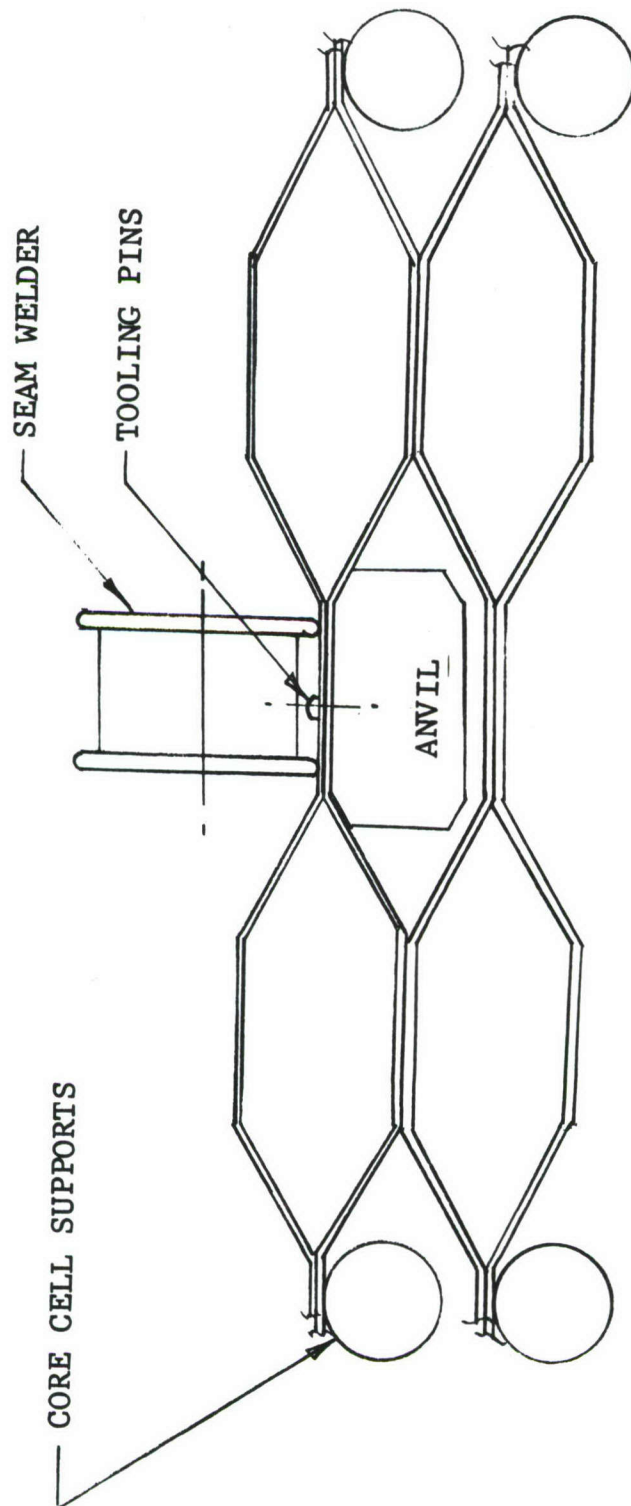
(3) Move the rear spar pylon weld assembly to a weld fixture for joining the front spar details to the existing assembly. GTA burn through the pylon fittings and front spar web as the first operation and follow by GTA butt welding the spar caps to the spar web (Reference Figure 136).

10.4.3.8 Wing Box Structure Assembly

The spar pylon fitting welded assembly is located in an assembly fixture where end bulkheads, slat track housings, and other special details are assembled prior to receiving the multi-wet cell core panels (Reference Figure 137).

10.4.3.9 Machining of Finish Stage Multi-Wet Cell Core

The welded core blocks fabricated for areas of the pylon fittings are installed in a prefit fixture which contains the perimeter of the second stage core for mating. The tooling for this core perimeter employs the tooling hole coordination to insure a second stage match fit. Only the perimeter of the first stage core is prefit. The upper and lower surfaces remain flat.



1. LOCATE CORE RIBBON FROM PRE PUNCHED TOOLING HOLES
2. SEAM WELL FULL WIDTH OF CORE RIBBON
3. STOCK WELDED CORE IN PRE DETERMINED BLOCK SIZES

Figure 133 Secondary Manufacturing Core Cell Fabrication

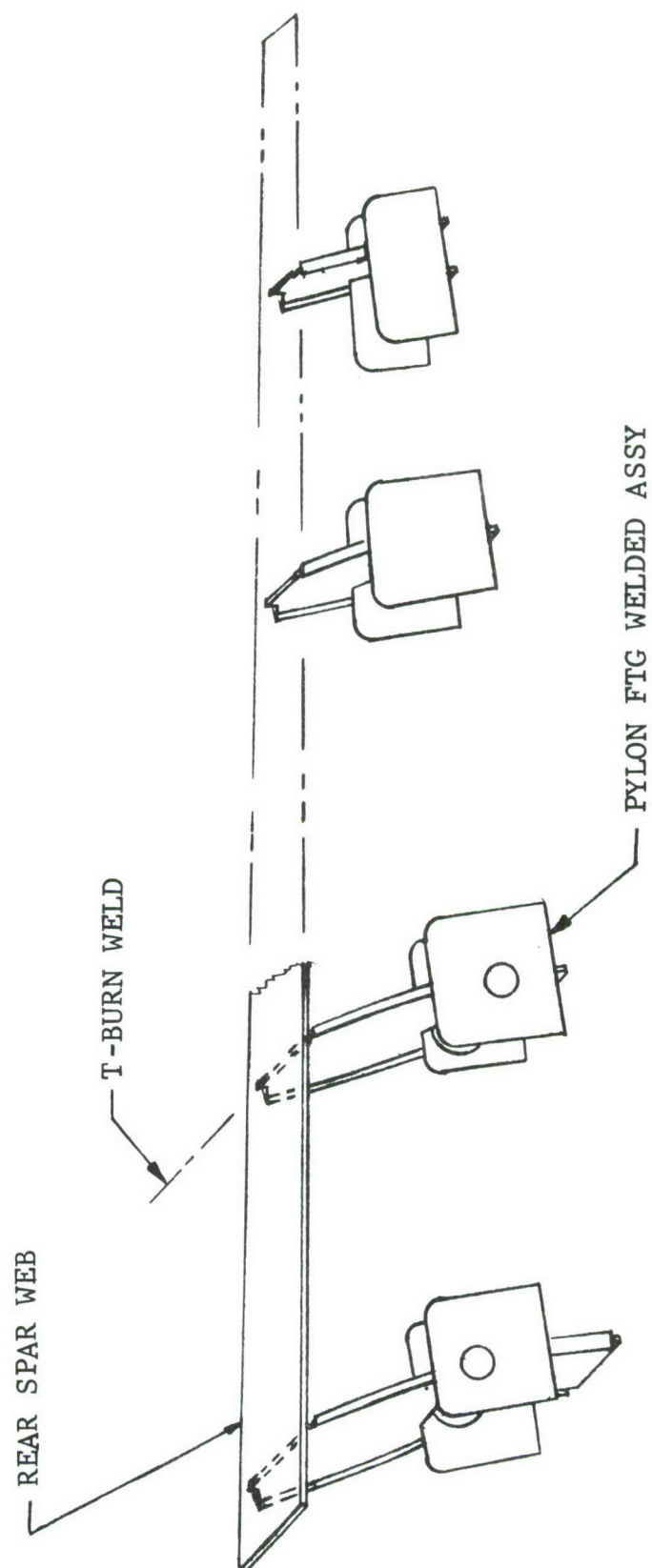


Figure 134 Rear Spar and Pylon Fitting Joining

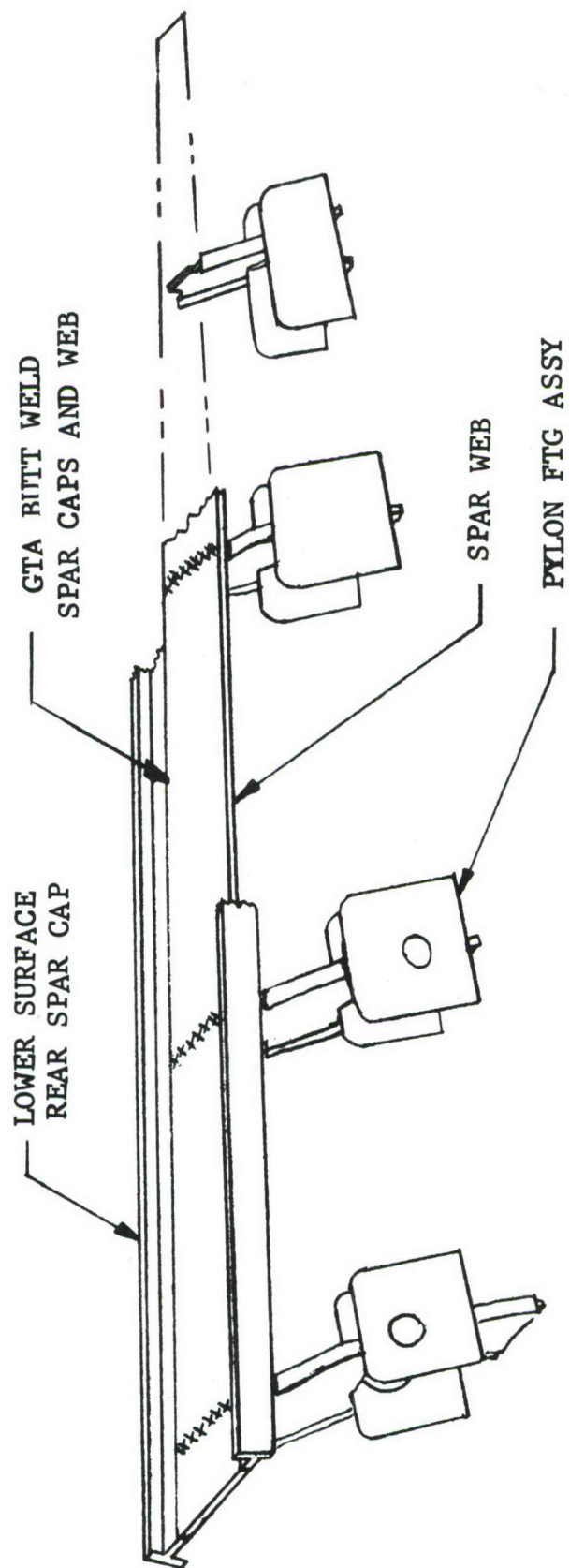


Figure 135 Welding of Rear Spar Web and Caps

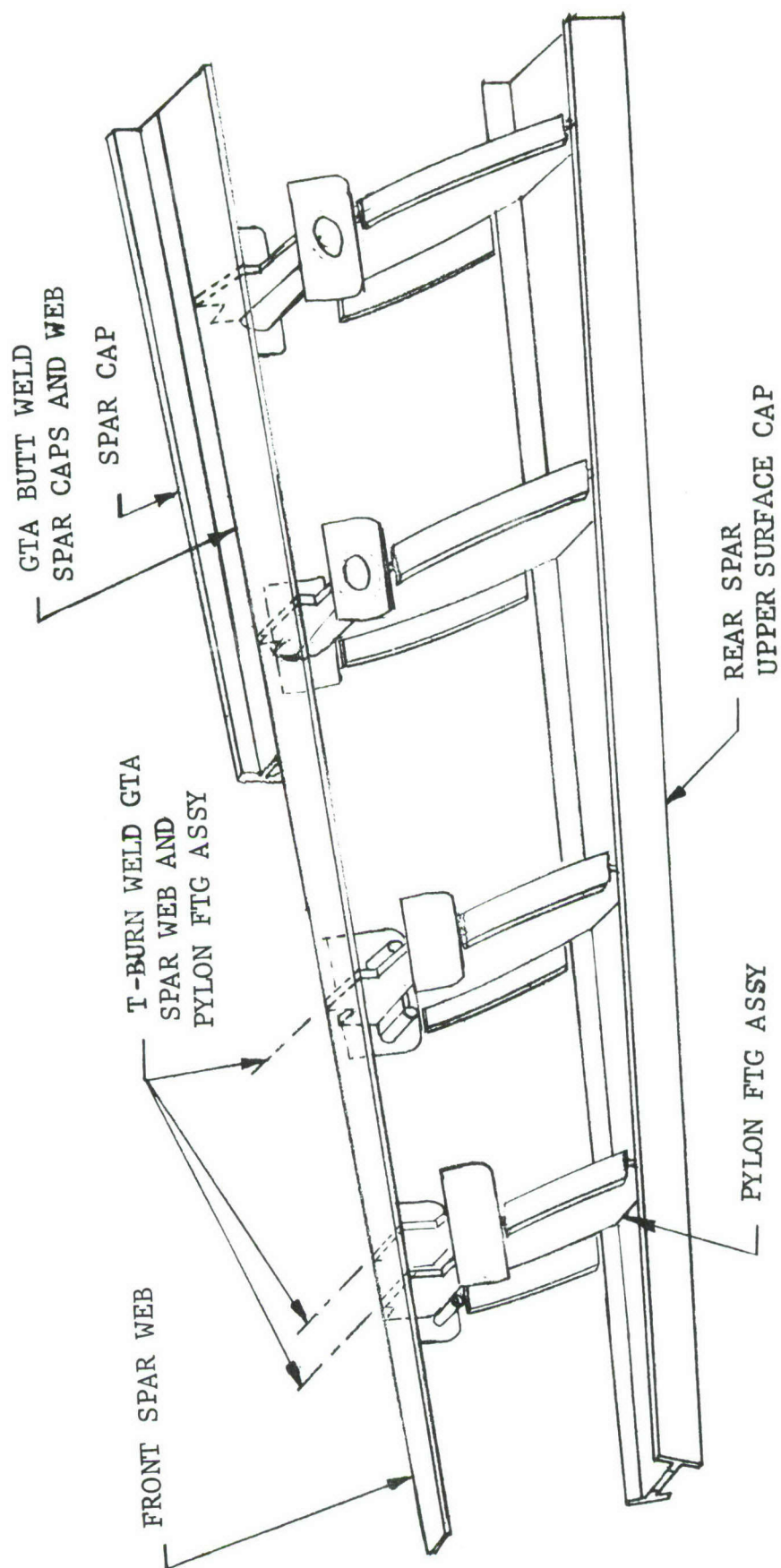


Figure 136 Welding of Front Spar Assembly

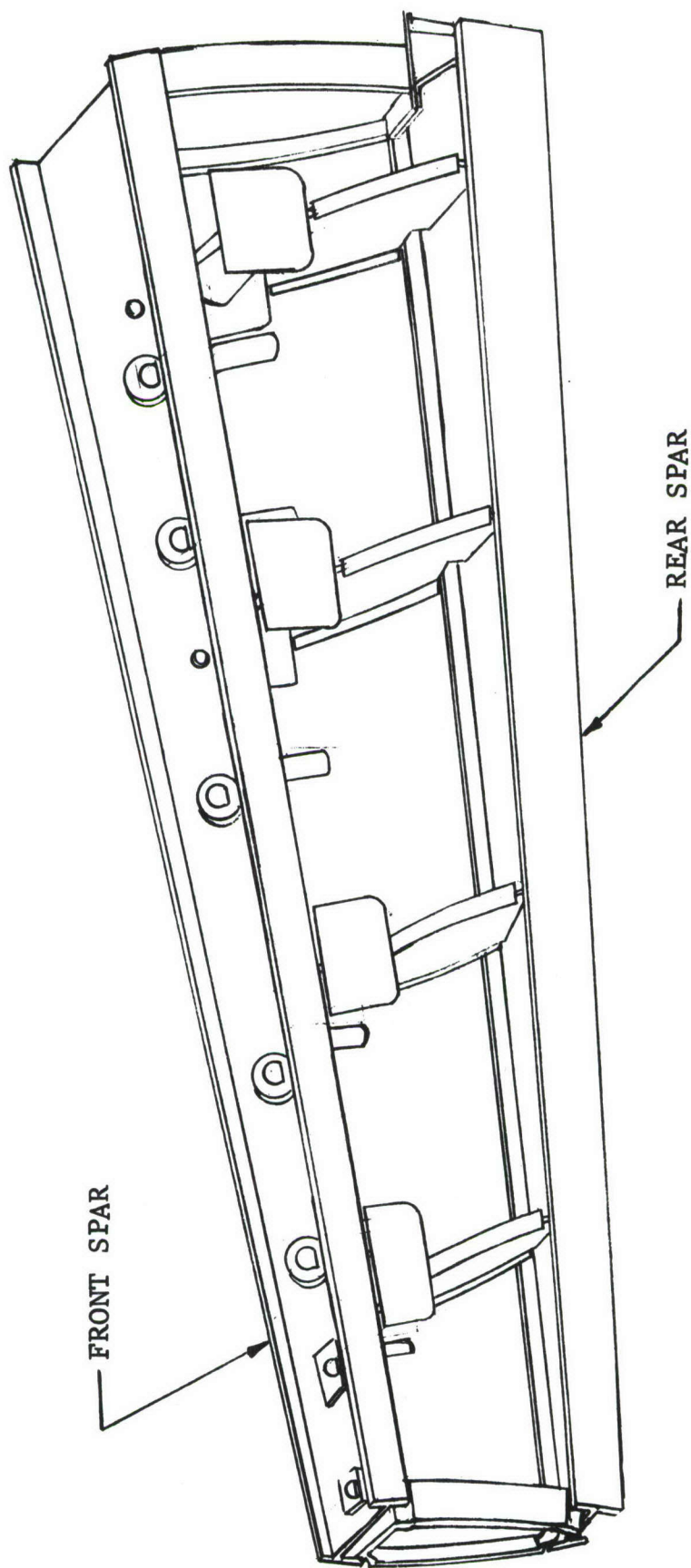


Figure 137 Installation of End Bulkheads and Fittings

A special filler is poured in the core cells and allowed to set. This filler supports the cell wall during subsequent contour machining operations in the prefit fixture (Reference Figure 138). Following machining of the lower contour surface by the N.C. core mill the filler is removed by heating and the core is transferred to a second prefit fixture which coordinates the machining of the upper surface contour.

10.4.3.10 Machining of Second Stage Multi-Wet Cell Core

The second stage core follows the basic procedure and tooling concept as described for the first stage core. The same tooling coordination for the splice joints is employed (Reference Figure 139).

10.4.3.11 Installation of Multi-Wet Cell Core

The first stage core is installed with the aid of a fixture which simulates the second stage core for coordination. Final phase of the core installation includes hand sanding the slightly oversize core near fittings and spar caps. The core is attached to the joining structure by spot welding or poke welding. At this time a braze alloy foil is inserted between the spot welded joint for capillary flow brazing during the final braze assembly operation (Reference Figure 140).

The second stage core is installed much in the same manner as described for the first stage. The pre punched holes in the core are used for coordination with the first stage core. The splice joint is deflected only slightly in this joining process but due to the flexibility of the core cell no problem is expected in this operation (Reference Figure 141).

10.4.3.12 Final Braze Assembly

The final brazing of the assembly is accomplished in a vacuum retort type fixture which contains a ceramic platen with embedded heating elements for the lower surface and a flexible blanket heating element over the upper surface. A flexible diaphragm transmits atmospheric pressure on the wing box assembly during brazing.

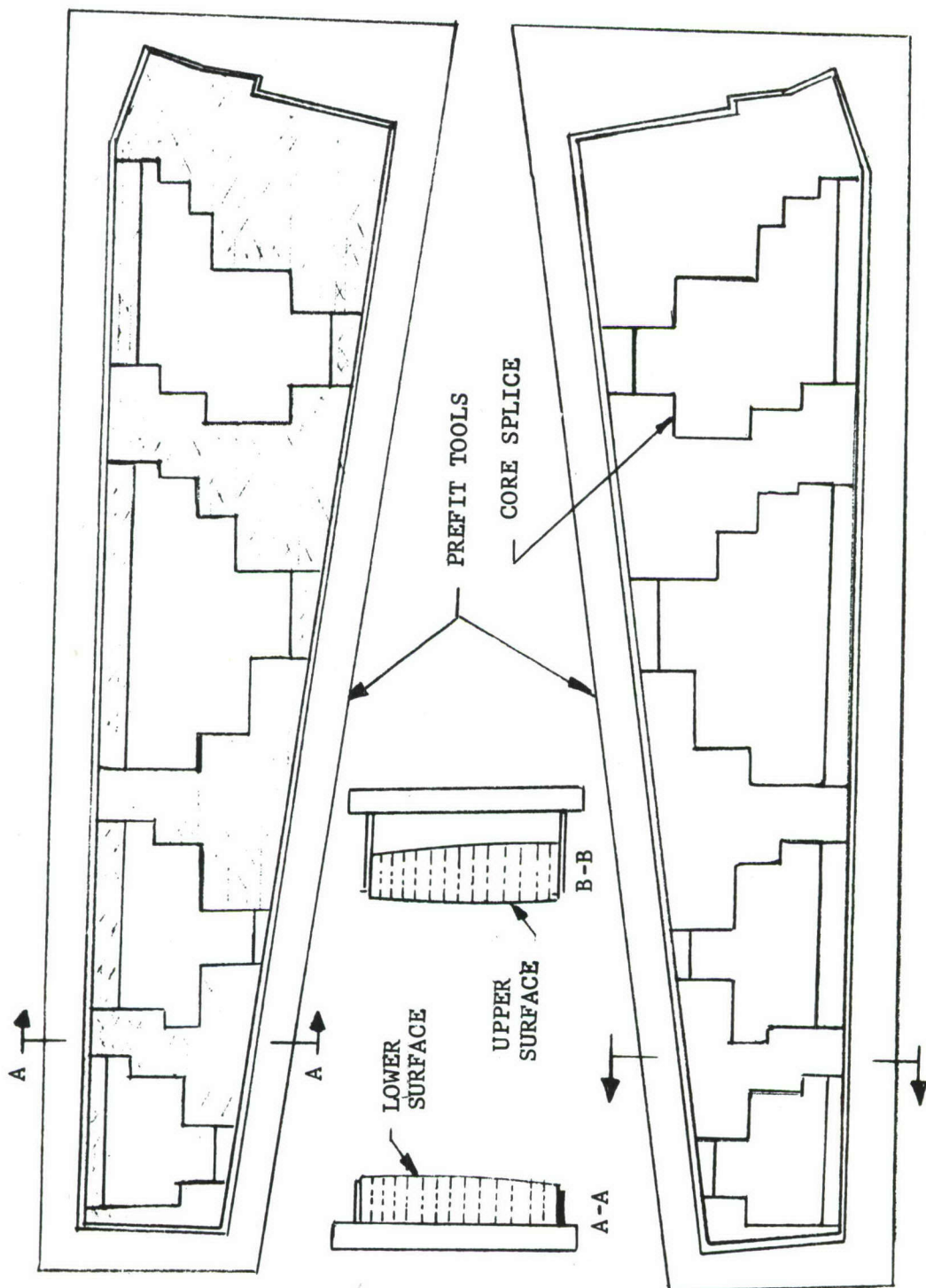


Figure 138 Machining of First Stage Multi Wet Cell Core

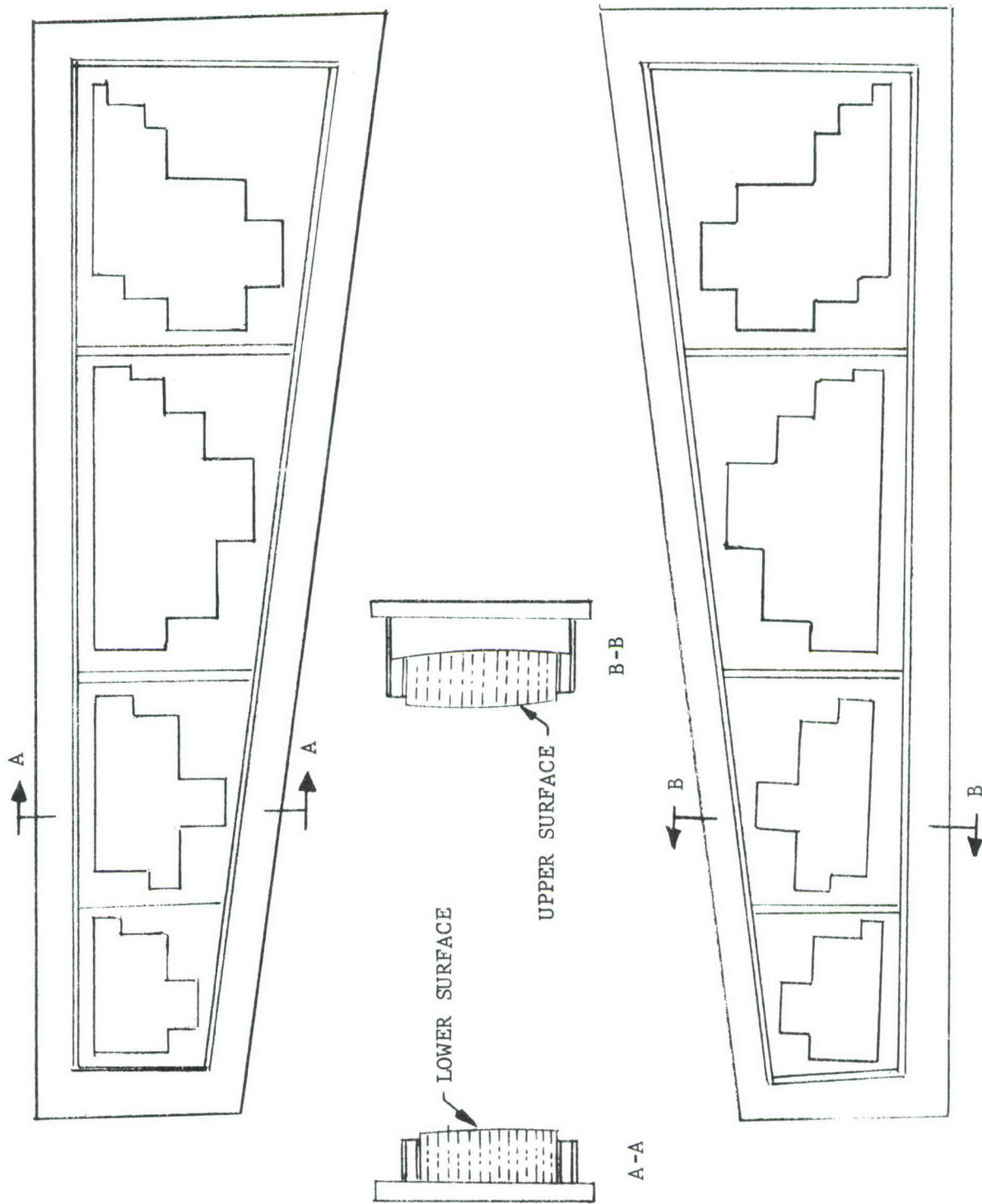


Figure 139 Machining of Second Stage Multi Wet Cell Core

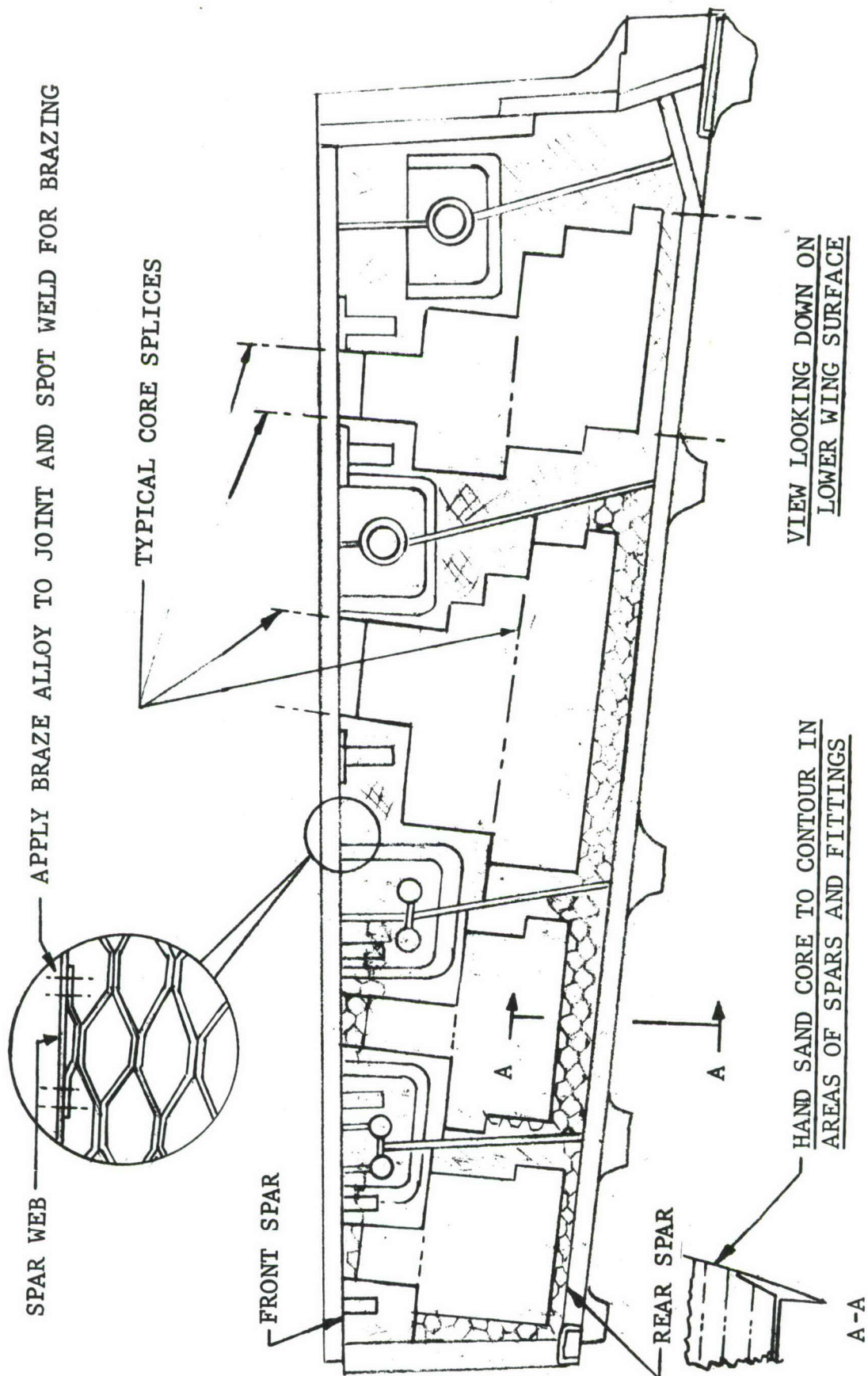


Figure 140 Installation of First Stage Multi Wet Cell Core

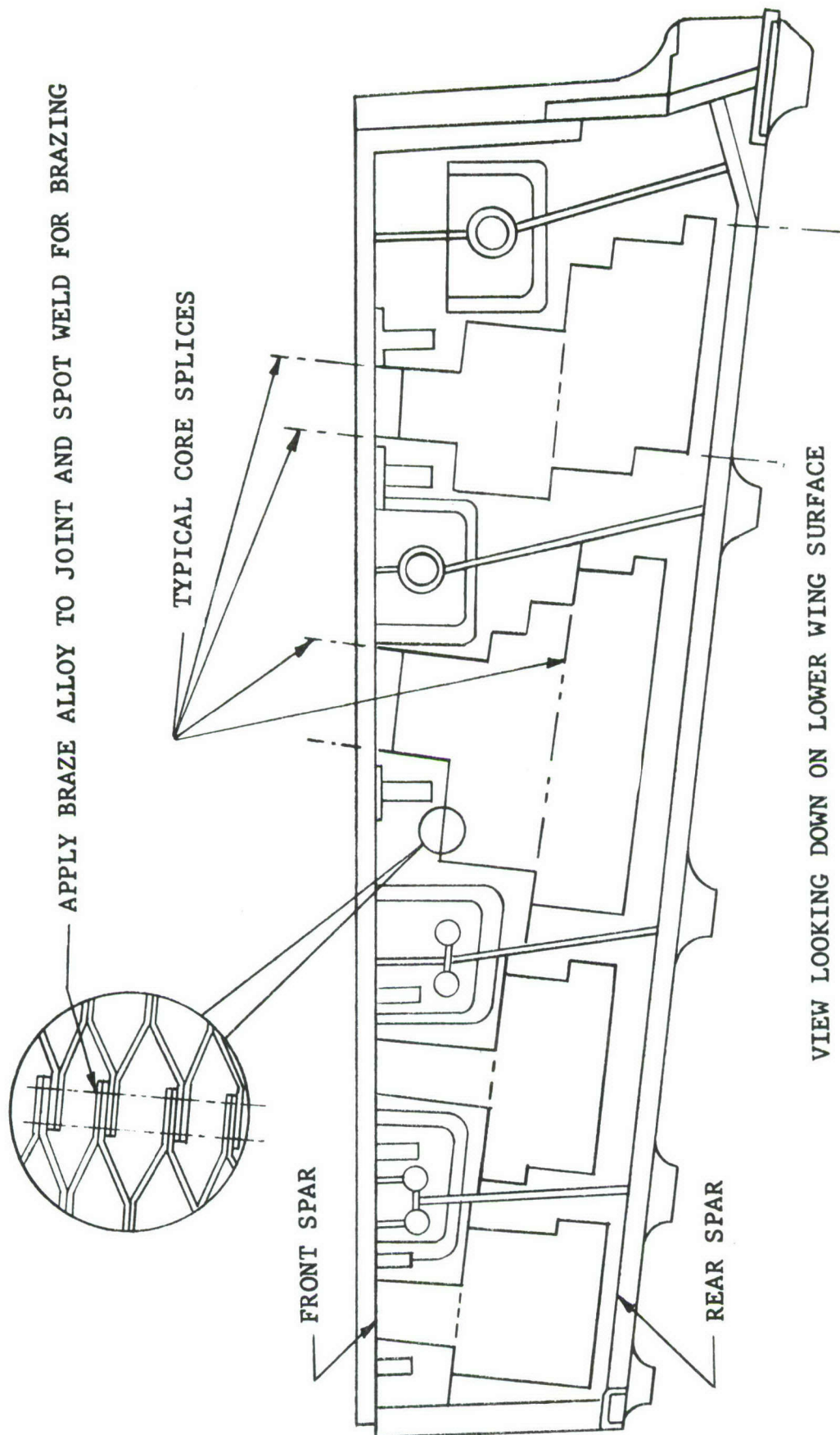


Figure 141 Installation of Second Stage Multi-Wet Cell Core

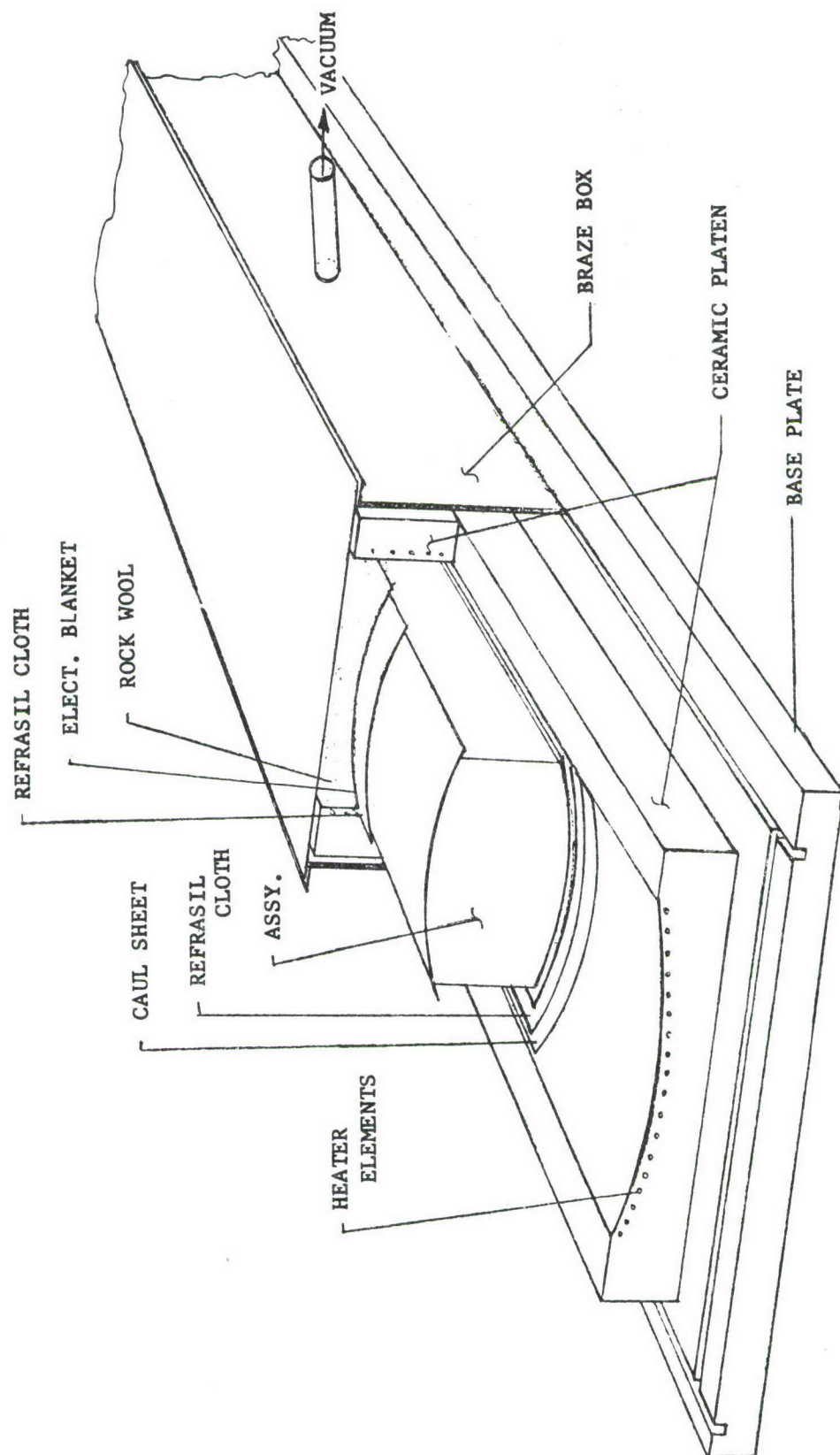


Figure 142 Final Braze Operation Large Area Brazing

S E C T I O N X I

Q U A L I T Y A S S U R A N C E A N D N D I

Most existing quality assurance and nondestructive inspection (NDI) processes evolved from increasing requirements to monitor and verify the design and fabrication of high performance aircraft structures. These processes were developed to respond to specific needs and were not generated as part of the overall quality assurance plan established for major subassemblies.

In the Advanced Air Superiority Fighter Wing Structures program this concept was extended. The Quality Assurance organization was charged with the responsibility for monitoring preliminary design concepts and advising engineers of design changes to provide more reliable, cost effective inspection systems. To aid in design support, the following objectives were proposed:

1. Obtain the theoretical parameters of the new materials that affect the sensitivity of NDI techniques.
2. Determine the adequacy of existing quality control and NDI equipment and procedures.
3. Estimate the lower limit of flaw detection on a production line basis.
4. Determine the accessibility/inspectability of each structural concept from engineering design drawings.
5. Prepare preliminary quality assurance plans for each selected preliminary design.

11.1 INSPECTION CAPABILITIES

In recent years extensive experience has been obtained in inspecting aircraft structures of increasingly complex design and fabrication process. New and improved NDI techniques and capabilities were developed and applied for the detection or measurement of the significant properties and performance capabilities of materials, parts and assemblies. However, most existing NDI procedures are oriented toward specific applications and cannot be directly transferred to new concepts. For these concepts

new inspection capabilities had to be estimated from existing experience and technology. Every effort was made to insure that only the most advanced NDI techniques were considered for this program. Consideration was given the availability of only limited information about the inspection of the new materials and manufacturing processes.

The various facets that provided a basis for estimating the inspection capabilities are given in Figure 143. During Phase IA of the Advanced Metallics Air Vehicle Structure program, literature and industrial surveys were conducted to define the most current NDI methods and techniques. Over 75 publications were reviewed, and NDI engineers from most of the major aircraft companies were contacted for possible applications. This activity was continued into the AASFWS program. Specific attention was given to those reports that were directed toward improvement of inspection capabilities for titanium materials. Other areas of interest were new techniques for inspecting the following materials and processes.

Titanium (All Alloys)	New High Strength Steels (Ni, PH alloys)
Weldments (GTA, EB, Plasma)	
Brazed Joints	Diffusion Bonds
Adhesive Bonds	Weld Bonds
Rivet Bonds	Fastener Holes

This information aided in estimating capabilities of existing techniques as applied to the new structures, but no new applicable techniques were discovered.

Each raw material supplier was contacted to obtain the basic material properties that affect nondestructive inspection systems. The average elasticity, density, permeability, and quality level for each material were requested. Since no testing was done, these characteristics provided an indication of the relative inspectability of the candidate materials as compared with production materials that have similar properties. Table 143 gives the resulting comparisons.

Early in the program it was proposed that six of the compact tension specimens and two surface flaw specimens be examined with existing NDI techniques. The purpose of these tests was to identify very preliminary NDI parameters for estimating capabilities and planning the follow-on program. However, due to the tight fabrication and testing schedules for the engineering test specimens, the NDI tests were not conducted. The necessary data is

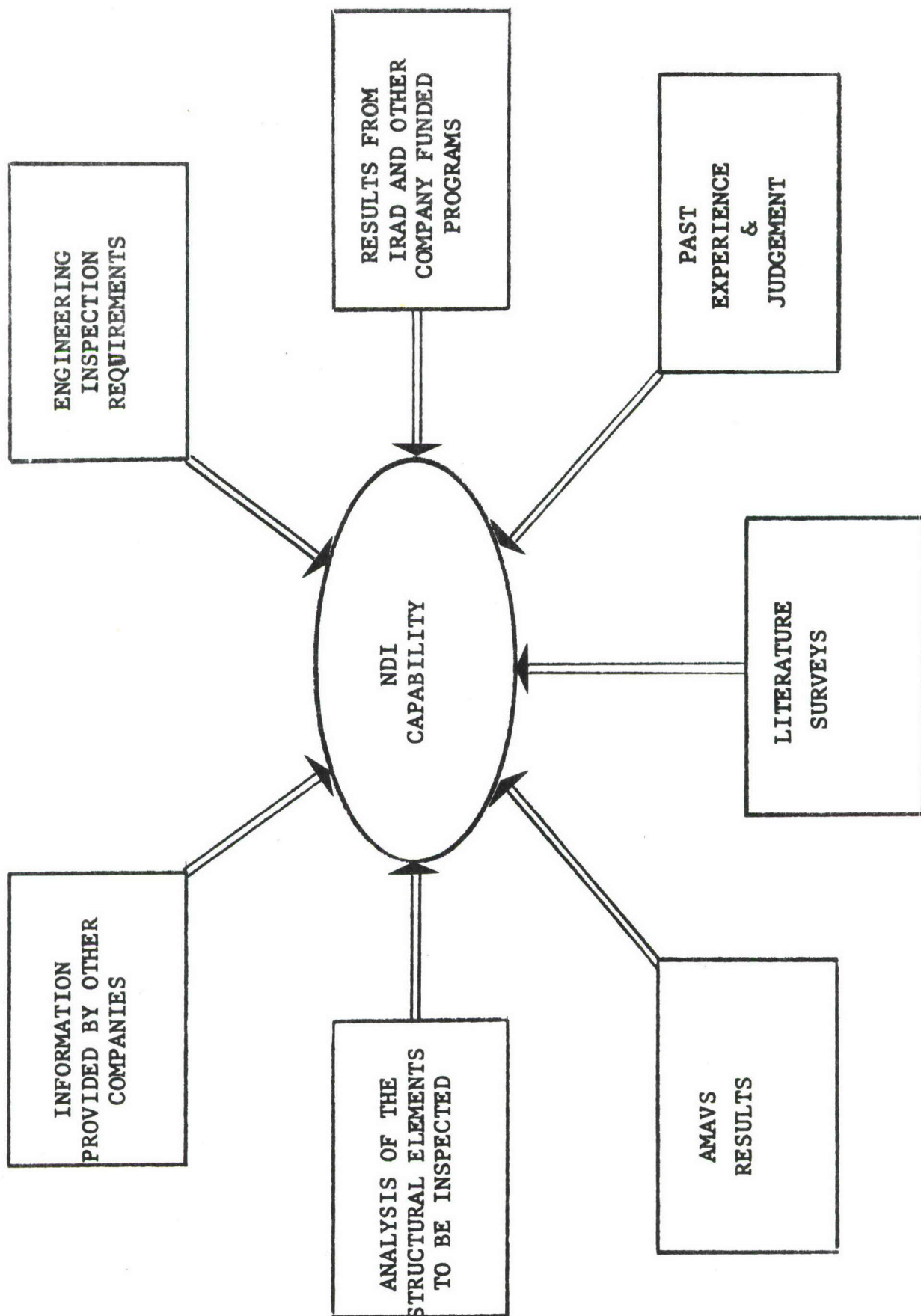


Figure 143 - Logic For Estimating Inspection Capabilities

Table LXVI
MATERIAL PARAMETERS THAT AFFECT NDI SENSITIVITIES

	Material	Modulus of Elasticity PSI x 10 ⁶	Density Lb/In ³	Magnetic	Ultrasonic Quality Level
Steel	9Ni-4Co-C	28.5	.28	Yes	AA
	PH 13-8 Mo	29.4	.279	Yes	A
	10Ni-Cr-Mo-Co	28.0	.287	Yes	AA
	D6ac	30.0	.283	Yes	AA
Aluminum	7475	10.3	.101	No	A
	2219	10.5	.102	No	A
	2124	10.7	.100	No	A
	7050	10.3	.102	No	A
Titanium	Beta III	16.5	.183	No	A
	8-8-2-3	16.7	.175	No	A
	6-6-2	16.5	.164	No	A
	6-4	15.0	.160	No	A

Table LXVII
ESTIMATED NDI CAPABILITIES

TECHNIQUE	POSSIBLE APPLICATIONS	ESTIMATED DETECTION CAPABILITY	LIMITATIONS	DEVELOPMENT POTENTIAL
Visual	All details, subassemblies and assemblies	Only relatively large flaws Depends on inspector's skill	Surface flaws only	Limited
Penetrant	Aluminum and titanium details subassemblies and assemblies	.030L x .003D	Open surface flaws only	Limited
Magnetic Particle	Steel details, subassemblies and assemblies	.030L x .0002W	Open surface and slightly subsurface flaws	Limited
Magnetic Casting	Steel parts, holes and other difficult magnetic inspection applications	.015L x .0002W	Surface and slightly sub-surface	Moderate
Radiography	Welded joints	2% of material thickness (50% for tight crack)	Orientation sensitive	Moderate
Eddy Current	Holes, cracks under platings and coatings	.030L x .005D	Surface and near surface flaws	High
Cellulose Replica	Holes, all material surfaces	Capability limits unknown	Open surface flaws only	Limited
Thermal	Bonded-Brazed structures	3/8 dia. under .20 skin, capability proportional to skin thickness	Upper skin must be less than .100" thick	Moderate

Table LXVII (Cont'd)
ESTIMATED NDI CAPABILITIES

TECHNIQUE	POSSIBLE APPLICATIONS	ESTIMATED DETECTION CAPABILITY	LIMITATIONS	DEVELOPMENT POTENTIAL
<u>ULTRASONIC</u> Thru Transmission	Bonded-brazed structures	.5 diameter for 1" thick Proportional to thickness	Surface conditions and geometry restrict capability	Limited
Pulse-Echo	Raw Material	3/64 dia. - steel 5/64 dia. - Tit., Alum.	Orientation sensitive	High
Pulse-Echo	Bonded-brazed structures	.5 diameter under .062 skin, proportional to skin thickness	Difficult to interpret	High
Shear Wave	Welded or Brazed structures, assemblies and subassemblies	.060L x .030D	Orientation sensitive	High
Surface Wave	Welded structures, subassemblies and assemblies	.030L x .020D	Orientation sensitive, surface smoothness critical	Moderate
Resonant	Bonded structures	3/8" dia under .03" skin proportional to skin thickness	Upper skins must be less than .080	Limited
Delta Scan	Welded or Brazed Structures, subassemblies and assemblies	.060 L x .030D	Less Orientation sensitive	High

being generated in the Advanced Metallics Air Vehicle Structures Program.

The estimated NDI capabilities are listed in Table LXVII. Note that the values given are only estimates for idealized structures. An NDI development program would be required to establish absolute configuration oriented capabilities. Also, because of the configurational differences between the various design concepts, it would be difficult to establish one inspection technique that would satisfy all conditions. In fabrication of the 610RW003 design, it is anticipated that the primary NDI will be penetrant for the details machined from plate and extrusions, penetrant for formed sheet details, ultrasonic for the adhesive bond lines, and ultrasonic plus X-ray for the weld bond joints.

11.2 CONCEPT EVALUATIONS

Each concept was reviewed periodically to identify the inspection methods required and to evaluate the designs for relative inspectability. The design variations such as types of materials, geometries, manufacturing processes, joining methods, and structural arrangements were noted. These variations along with the applicability and efficiency of the associated non-destructive inspection methods provided a basis for rating each design. All quality assurance functions were considered in the evaluations but the NDI requirements carried the most weight (about 90%).

In evaluating each structure, it was assumed that all types of defects must be considered. There are some types of defects that cannot be readily detected by current state-of-the-art NDI methods. For example, a void or air pocket in an adhesive bond line is easily detected, but current NDI methods cannot detect a "slick" bond where the adhesive is in very close contact with the skin but not stuck. Similarly, a "non-wetted" surface in a brazed laminate cannot be detected. Obviously, these inspection problems multiply as the number of lamina increase.

11.2.1 Element Concepts

The element concepts were basic design ideas that were later used in cross-section concepts and preliminary designs. With this in mind, it was preferable to comment on the inspectability of the concepts and establish a very generalized rating system. This approach proved to be economical yet the requirements of the program were satisfied.

The inspectability comments informed design engineers that specific concepts would generate unusually high inspection costs or a reduced inspection capability. These comments were considered in selecting element concepts to be used in cross-sections. Examples of these comments are:

<u>Drawing</u>	<u>Comment</u>
610-132	Some inspection difficulty. Stepped configuration increases inspection costs.
610-217	Some inspection difficulty. Costly to inspect weld bonds. Cannot field inspect corrugations for small cracks.

In addition, each concept was given a letter rating. The letter ratings are explained as follows:

A	Easy to inspect
B	Normal inspection difficulty
C	Difficult to inspect
D	Hard to inspect
E	Noninspectable.

The rating for each concept was reported in FZM-6057.

11.2.2 Cross Sections and Analytical Assemblies

One rating system was established to be applied to both the cross-section concepts and the analytical assemblies. Each configuration was given three ratings--a manufacturing inspectability, a field inspectability and an overall inspectability. The manufacturing inspectability rating defines the relative inspectability of each concept in the factory during fabrication. The field inspectability rating is a measure of the efficiency of inspecting the assemblies after installation in the aircraft. The overall rating is a weighted average of the other two. The three ratings were necessary to explain the difference in inspectability at each stage in the fabrication and life of the assembly.

The major difference in each design stage was the amount of detail evaluation required. The cross-section concepts were given total rating for each element in the rating system as shown in Table LXVIII. The analytical assemblies were given a separate series of ratings for each major subassembly (Table LXIX). The inspectability ratings for all of the cross-section concepts and the analytical assemblies are documented in FZM-6058 and FZM-6086.

The inspectability comments were continued and expanded for the cross-section concepts and analytical assemblies. The comments were directed toward specific design areas that would cause inspection problems. In addition, advisory reports were prepared to address geometries and designs that applied to several concepts.

11.2.3 PRELIMINARY DESIGNS

The preliminary designs were full wing drawings of selected analytical assemblies or combinations of analytical assemblies. Therefore, the same inspectability rating system was applied. Each preliminary design was rechecked to assure that all of the structural elements were considered. As with the other design iterations, the inspectability ratings addressed the relative inspection difficulties throughout the fabrication and service

Table LXVIII

EXAMPLES OF CROSS SECTION INSPECTABILITY RATINGS

DRAWING NO.	MANUFACTURING INSPECTABILITY	FIELD INSPECTABILITY	OVERALL INSPECTABILITY
610R013B	75	85	77
610R029	70	80	75
610R107	50	60	55
610R108	35	5	10
610R109	85	85	85
610R110	55	80	70
610R111	70	75	72
610R112	95	95	95
610R113	70	75	73
610R114	60	70	65

Table LXIX

EXAMPLE OF ANALYTICAL INSPECTABILITY RATING SHEET

Drawing 610RA006

Baseline = 100%

PART NAME AND DASH NO.	MFG INSPECT (%)		FLD INSPECT (%)		OVERALL AVG (%)		Min A/DI Detect	SCORE (.05)
	Rate	Max	Rate	Max	Rate	Max	Meth	
1.-65 Upper Skin	30	30	30	30	30	30	.05 PEN	.015
2.-3 Spar Skin Assembly	32	70	60	70	45	70	450 UT X-RAY	.0225
					75			..0375

- Comments: 1. Can only detect gross damage in corrugations after assembly.
2. -3 minimum crack length determined by the difficulty of detecting cracks in inter lamina of lower skin.

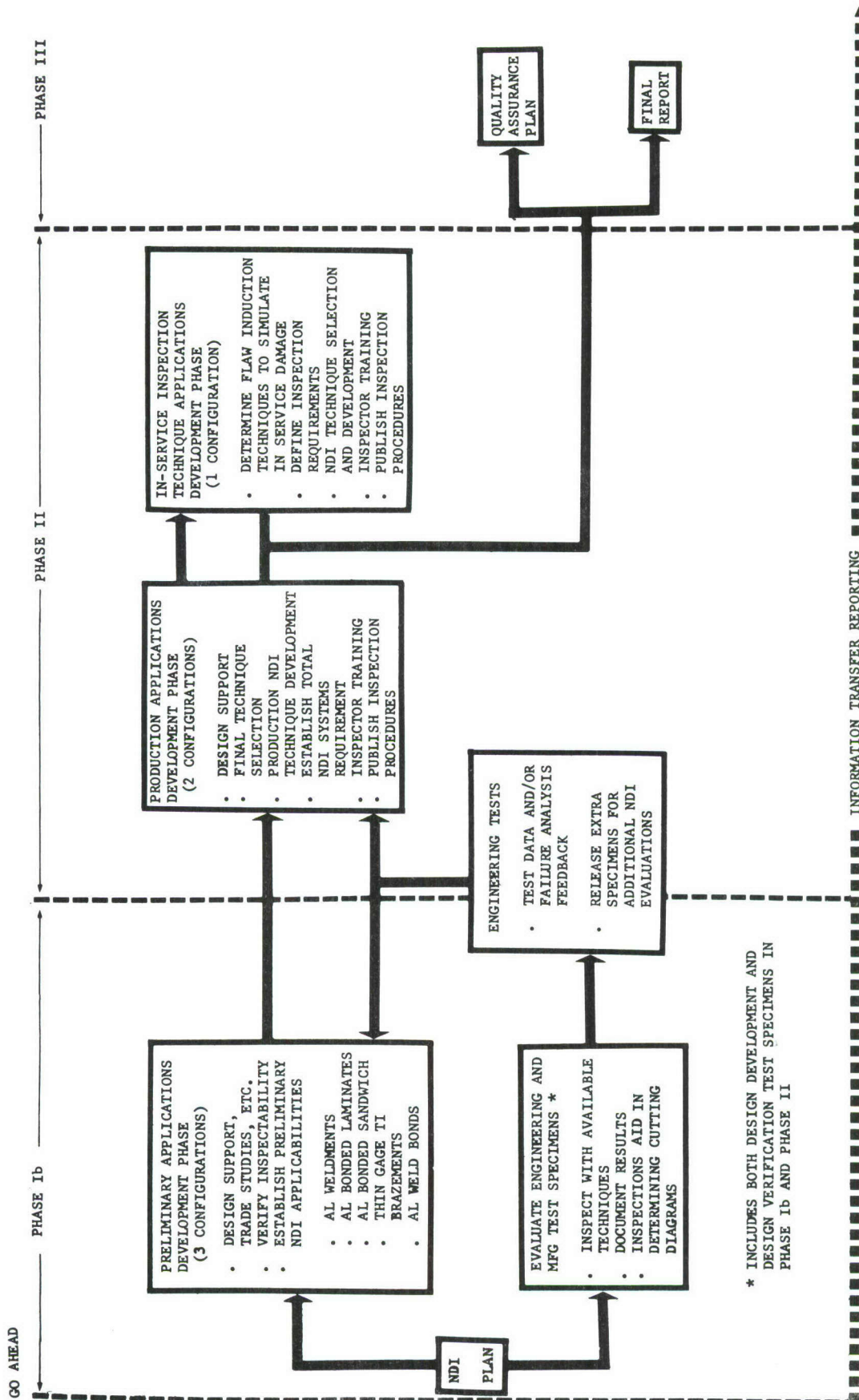


Figure 144 NDI Engineering Task Flow Diagram for the Follow-on Program

life of each element. The relative weight given to each fabrication stage is as follows:

	Approximate weight
Raw Material	0 - 1
Joining Process	0 - 2
Detail Parts	0 - 1
Subassembly Configuration	0 - 3
NDI Techniques	0 - 3
Total	10

The overall inspectability rating system was consistent throughout all design stages of the program. A comparison of the inspectability ratings for the various design configurations ultimately incorporated into the preliminary design 610RW003 is depicted in Table LXX . Note that the element concept used letter designations while the other concepts used finite number expressions. This was attributed to design configuration; as the designs became more complicated the rating system became more complex. Variations in the ratings were not extensive. In general, for the cross section, analytical assembly, and preliminary design concepts, the inspection ability rating on a percentage basis ranged from 60 to 75%. The NDI rating in Table LXVII was obtained by multiplying the applicable percentage scores by the appropriate weighing factor, 0.5 in the cases herein.

11.3 QUALITY ASSURANCE PLANNING

To meet the objectives of the overall AASFWS program, a NDT and Quality Assurance plan was necessary to aid in the support of design and fabrication requirements. For NDI, the requirements for an applications development program were established. The preliminary NDI plan involves support of design, evaluation of test specimens and components, and NDI techniques development. Figure 144 depicts a flow diagram of the anticipated NDI engineering tasks for the follow-on program.

Table LXX

INSPECTABILITY RATING TRACEABILITY FOR PRELIMINARY DESIGN 610RW003

Configuration	Inspectability Rating	Remarks
Element Concept (FZM-6057) Number -132 and -217 ➡	C B	NDI Rating based on letter rating as discussed, where B = Normal inspection difficulty, and C = difficult to inspect.
Cross-Section (FZM-6058) Concept No. 610R029 610R013 ➡	.038 .039	Total NDI rating equals .05
Analytical Assembly (FZM 6086) Concept No. 610 RA006 ➡	.0375	Same as above
Preliminary Design 610RW003	.0375	Same rating as Analytical assembly but more detailed analysis

The preliminary design drawings for the various configurations were reviewed in detail to identify materials, inspection steps, and process controls for preliminary Quality Assurance planning. Figures 145 and 146 and depict examples of the Quality Assurance plan for the 610RW003 design.

Figure 145 shows the inspection plan for 610RW003 prior to fabrication. At this stage, Receiving Inspection and Process Control work closely together in performing those functions listed. For the 610RW003 configuration, aluminum alloy 7050 will be purchased as sheet, plate, and extrusions in the heat treated condition (stress corrosion cracking resistant tempers). Upon receipt, plate material will be ultrasonic inspected and extrusions will be penetrant inspected. Sheet, plate, and extrusions will be sampled for tensile properties and results compared with vendor's data. Fracture toughness properties will also be verified as required. A convenient method of monitoring aluminum alloys for heat treat condition (to check for possible overheating from processes which could degrade strength) is by electrical conductivity. In association with the above tensile tests, conductivity measurements will be made.

An outline of the Quality Assurance plan to be utilized during fabrication as well as in-service inspection is presented in Figures 146. In fabrication of 610RW003, primary NDI will be penetrant for the details machined from plate and extrusions, penetrant for formed sheet details, ultrasonic for the adhesive bond lines, and ultrasonic plus X-ray for the weld bond joints. It is anticipated that in-service inspection will consist of penetrant, X-ray and ultrasonic techniques.

Certain standards are shown in the Quality Assurance plan (Figure 146). However, it must be noted that these are only preliminary at this point. By following the program closely through the development phases, QA personnel will be in a position to recognize the need for specific operation instructions covering other processes, tests, or inspections. This information will then be incorporated in the plan of Figures 146.

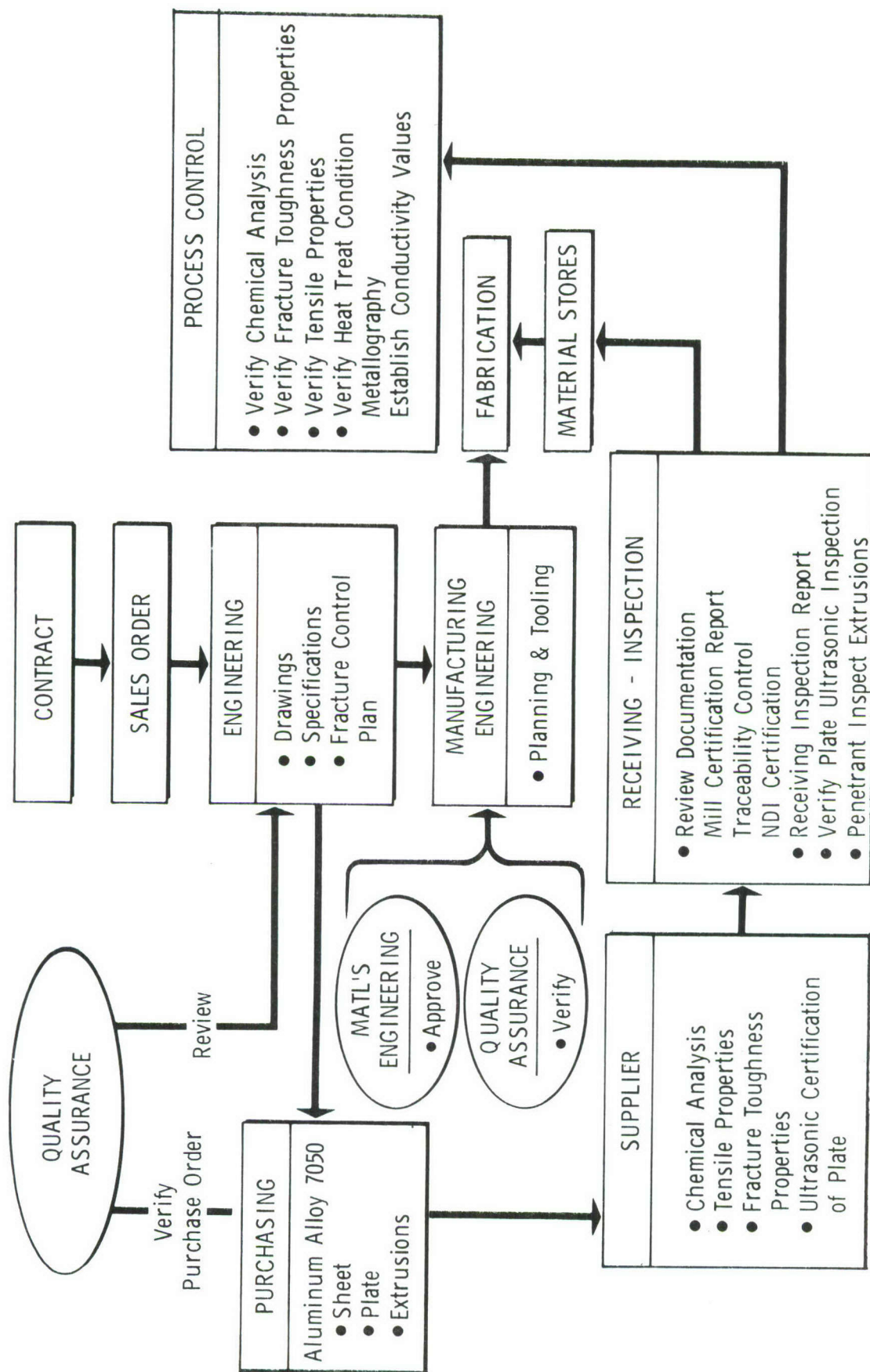
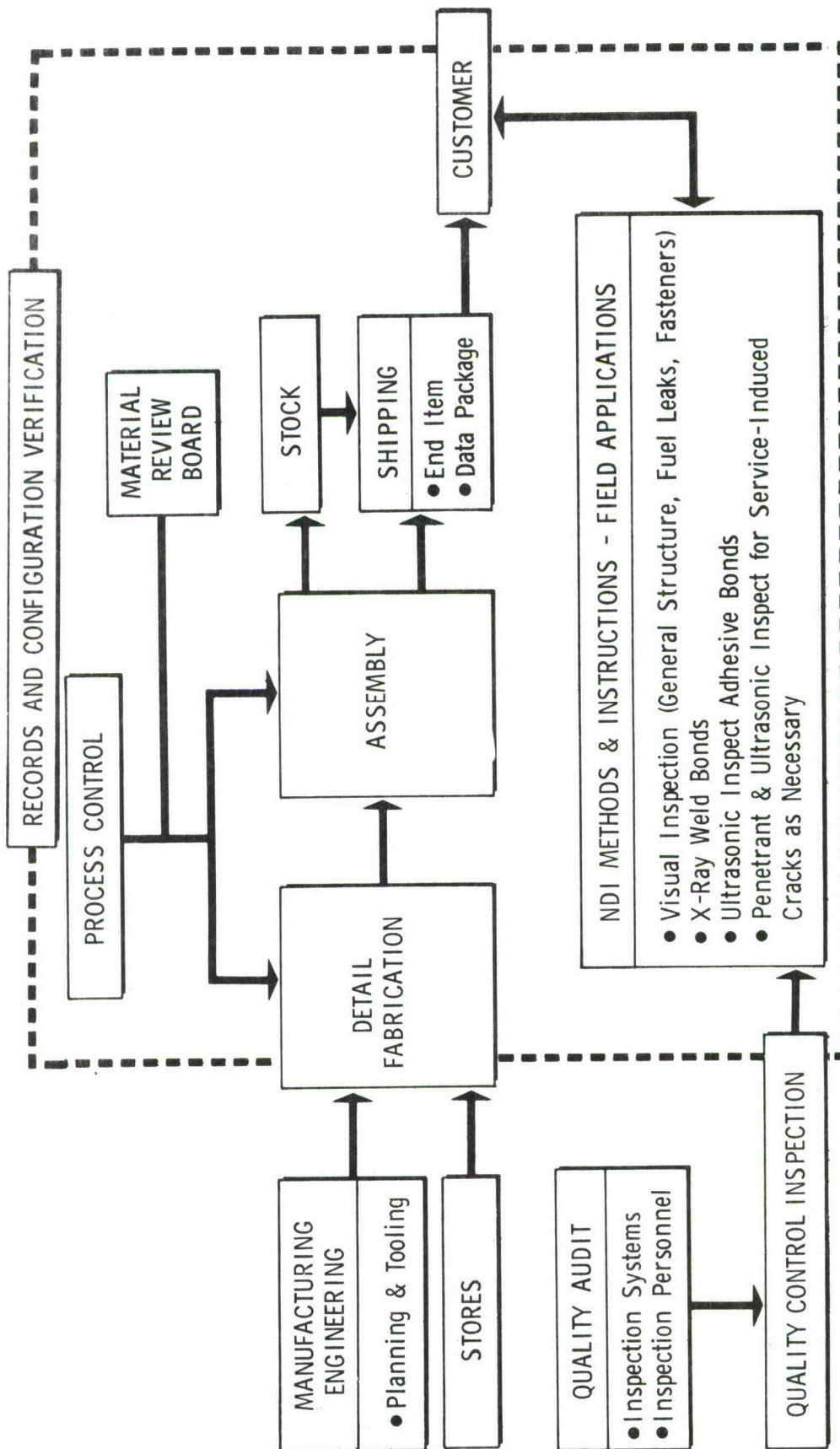


Figure 145 Example of Quality Assurance Plan Prior to Fabrication



NOTE: If Titanium, Clean with MEK QUALITY CONTROL INSPECTION

Figure 146 Example of Fabrication Inspection Outline

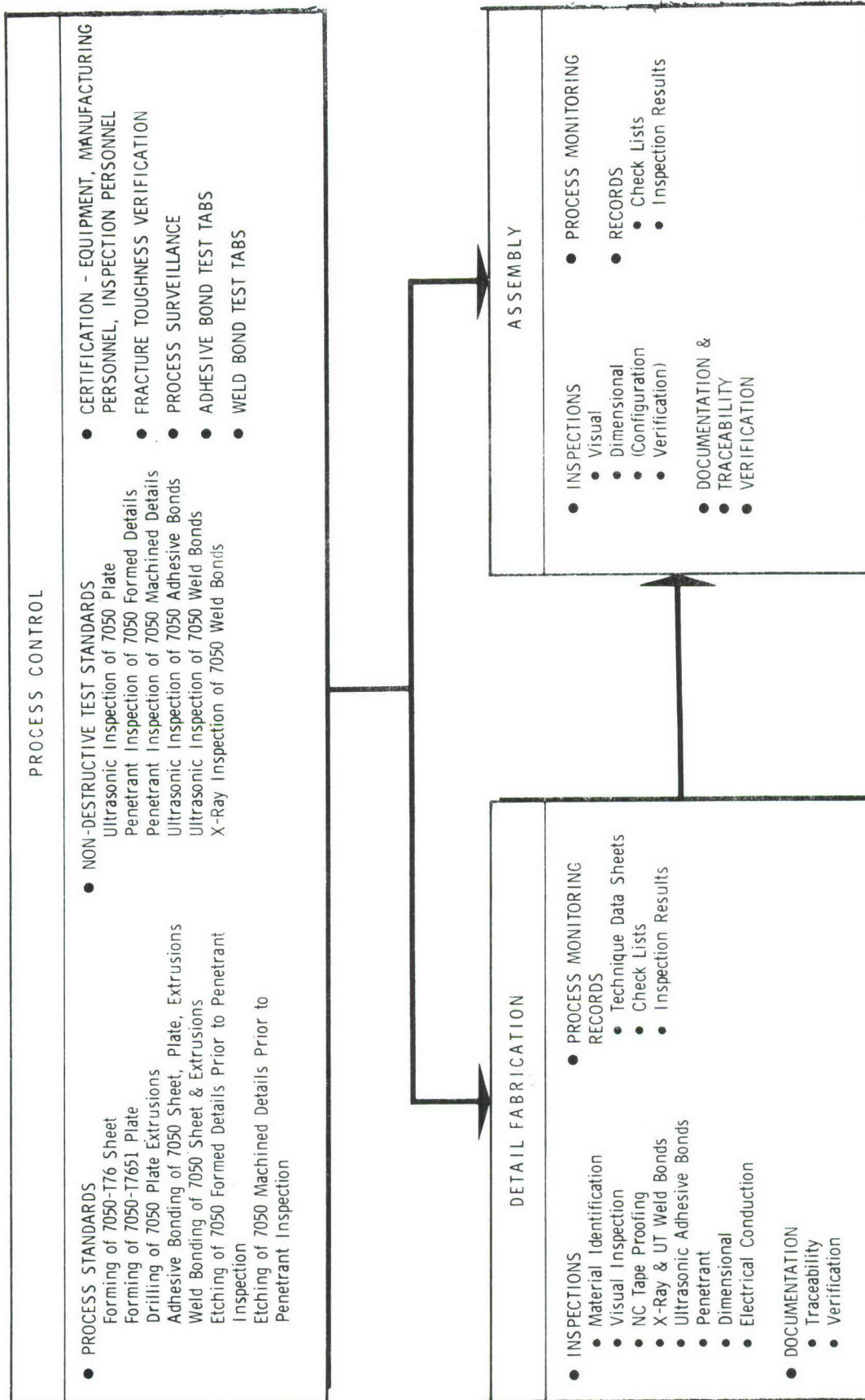


Figure 146 (Cont'd) - Example of Fabrication Inspection Outline

SECTION XII
POTENTIAL TECHNOLOGY
ADVANCEMENT

Several concepts have been defined during Phase IA which embody features that when fully developed will represent significant aircraft structures technology advancements. These are discussed in the following paragraphs.

12.1 ELIMINATION OF FASTENERS THRU TENSION MEMBERS

The elimination of fasteners through tension members such as lower wing skins and spar lower caps promises to be a means of greatly reducing wing box weight on future aircraft. Eliminating lower skin fasteners by utilizing bonding or brazing as a joining method, results in the panels stress concentration factor K_T being reduced to a value of less than 2.0. The existence of K_T being less than 2.0, safely permits increasing the operating stress in wing box tension members by 60% to 110% (depending on material) over the safe operating stress where fastener holes are present. Higher operating stress levels equate to reduced cross-sectional area in tension members; hence, weight savings.

12.2 THIN SKIN LAMINATES IN TENSION MEMBERS

Configuring tension members of thin aluminum or titanium laminates by bonding or brazing will increase fatigue life, retard crack growth rates and achieve fail safe structure. Configuring structures with laminates in conjunction with eliminating fasteners permits safe operation of tension members to operating stresses in the load spectrum to 2/3 of the ultimate stress capability of the material. The crack growth rate decrease effect in brazed and bonded laminates permits the safe use of high strength but less tough alloys. Convair Aerospace is confident that follow-on testing will show that 3 laminates of 8-8-2-3 Ti (175,000 F_{ty}) joined by low temperature brazing will demonstrate a lower crack growth rate than 6Al-4V Ann Ti (134,000 F_{tu}) used as a single plate member. The safe use of 8-8-2-3 titanium versus the safe use of 6Al-4V Ann Ti equates to a weights savings

of approximately 19% in bending material members considering 6Al-4V Ann as the baseline material.

12.3 LOW TEMPERATURE BRAZING OF HIGH HEAT TREAT TITANIUM ALLOYS

Brazing of titanium to date has been accomplished by using braze alloys with melting points above 1600°F. Temperatures in the range of 1600°F are high enough to anneal titanium alloys as we know them today. In order to take advantage of the weight savings offered by a Ti alloy such as 8-8-2-3 (175,000 Ftu) or 6Al-4V STA (160,000 Ftu) in a brazed assembly, brazing must be accomplished at the material aging temperature of 1000 to 1150°F. Initial investigations were conducted under a General Dynamics funded program that show feasibility of developing workable low temperature braze alloys.

SECTION XIII

SUMMARY OF FOLLOW-ON PLAN

The follow-on program is structured to evaluate the potential of the three design configurations selected from the analytical studies of Phase IA, to provide a reliable, advanced fighter wing that will achieve the program objectives as outlined in Section I, Introduction.

A five phase program is planned for this effort as follows:

Phase Ib - Preliminary Design and Analysis

Preliminary design and analysis of three configurations selected from the current Phase IA program will be performed during this phase. Trade studies, material testing, and design verification testing will also be accomplished. Parameters for manufacturing processes and NDI methods will be developed for use later in the program. After careful evaluation, two configurations will be chosen for the next phase of the program.

Phase II - Detail Design and Analysis

Detail design and analysis of these two configurations will be performed during this phase. Both configurations will undergo several iterations of study and analysis to arrive at an optimum design. Additional material testing and pre-production validation testing of selected components will also be accomplished in this phase. A final design will be chosen for fabrication and testing.

Phase III - Fabrication

Two identical left hand full scale wing box structural articles will be built to the engineering drawings developed in Phase II. Test plans, including instrumentation requirements, will be finalized. Cost and weight records will be maintained during fabrication to verify earlier estimates.

Phase IV - Test and Evaluation

A static test, fatigue test, and optional damage tolerance verification testing will be accomplished on the assemblies fabricated in Phase III. The testing will be compatible with the test program already conducted on the basic F-111 wing.

Phase V - Information Transfer

The purpose of this portion of the program is to insure proper documentation of program results and the reporting of significant accomplishments in such a manner that they are useful to future Air Force systems programs. Documentation will include monthly progress reports, semi-annual technical reports, phase reports, test reports, industry seminars, and a final report. Movies, slides, and viewgraphs will be used to insure clear concise reporting.

This plan includes those items which General Dynamics Corporation feels are necessary to evaluate the design methodology.

13.1 PROGRAM DISCUSSION

The Follow-On Program Plan (FZM-6134) is included in Section IX.7 of Appendix IX. The following elements are contained in the plan.

1. Material testing will be conducted to establish a statistically significant data base for design allowables. Testing of aluminum and titanium alloys is planned.
2. Structural element tests will be conducted during Phase Ib to provide qualitative and quantitative data for configuration selection prior to beginning the Phase II effort. A series of confidence tests are planned to assist in the evaluation of each configuration. Static, fatigue, and damage tolerance tests will be conducted of critical components. Manufacturing and inspection techniques will be verified as part of this Phase Ib effort.
3. Design iteration will be accomplished to optimize the structure using the statistical allowables data base.
4. Analysis techniques will be used to demonstrate the compliance of the structure with static, fatigue and damage tolerance criteria.
5. Detail design drawings will be prepared to allow production of hardware.

6. Manufacturing and Quality Assurance plans will be formulated to establish fabrication and inspection criteria.
7. Design development and validation tests will be planned to generate design information and to demonstrate the feasibility of the configurations selected in Phase IA.
8. Design verification tests of a complete wing box will provide proof of compliance in meeting the static, fatigue, and damage tolerance criteria.
9. Information transfer will insure dissemination of all advanced technology developed during the program.

Completion of the follow-on effort will provide a data bank readily available to every designer of wing structure.

While the program utilizes a specific baseline, the catalog of design concepts, design methodology, analysis techniques, and manufacturing and inspection procedures generated as part of this effort will be applicable to any wing design program.

Realistic criteria for fatigue and fracture will evolve from the follow-on program that includes the ground rules for a cost effective fracture control plan.

It is estimated that all future programs (ATF, AMST, RPV's, and growth versions of the LWF) will benefit from these activities.

REFERENCES

1. John A. Dickson, "Alcoa 467 Process X7475 Alloy", Alcoa Green Letter 216 (Rev. 10-71).
2. Private Communication between T. E. Coyle and D. J. Hendrickson of Alcoa, 5 March 1973.
3. Deel, O. L., and Mindlin, H., "Engineering Data on New and Emerging Structural Materials", Technical Report AFML-TR-70-252, October, 1970.
4. "Aircraft Designers' Handbook for Titanium and Titanium Alloys", AFML-TR-67-142, March, 1967.
5. Nordmark, G. E. and J. G. Kaufman, "Fatigue-Crack Propagation Characteristics of Aluminum Alloys in Thick Sections", Engineering Fracture Mechanics, Vol. 4, No.2, June 1972, p. 201.
6. Sprowls, D. O. and Kaufman, J. G., "Discussion on Fracture Toughness and Stress Corrosion Properties of Aluminum Alloy Hand Forgings", Jr. of Materials, 1972, pp. 263-265.
7. To be published, data generated at Convair/Fort Worth for Rockwell International/B-1 Division, Contract 1000Q,F33657-700-0800.
8. Bunting, P. M. and Little, C. D., "Crack Propagation Rate Data For Metallic Materials - Interim Report", Convair/Ft. Worth Report ERR-FW-1412, 31 December 1972.
9. Z. R. Wolanski, "Material 2024-T851 Aluminum Alloy Plate Fatigue and Tensile Properties Of", Convair Report FGT-3153, dtd 15 December 1964, p. 37.
10. H. I. McHenry, "Fatigue Strength of 7079-T651 Plate", Convair Report FTDM-3523, dtd 17 August 1965, pp 8 and 9.

Unclassified
Security Classification

DOCUMENT CONTROL DATA - R & D		
(Security classification of title, body of abstract and indexing annotation must be entered when the overall report is classified)		
1. ORIGINATING ACTIVITY (Corporate author) Air Force Flight Dynamics Laboratory (FBA) Wright-Patterson Air Force Base, Ohio 45433		2a. REPORT SECURITY CLASSIFICATION Unclassified
		2b. GROUP
3. REPORT TITLE Advanced Metallic Structures: Air Superiority Fighter Wing Design for Improved Cost, Weight and Integrity		
4. DESCRIPTIVE NOTES (Type of report and inclusive dates) Final Report Covering the Period 15 June 1972 through 15 June 1973		
5. AUTHOR(S) (First name, middle initial, last name) D. F. Davis, et al.		
6. REPORT DATE July 1973	7a. TOTAL NO. OF PAGES 394	7b. NO. OF REFS 10
8a. CONTRACT OR GRANT NO.	9a. ORIGINATOR'S REPORT NUMBER(S) AFFDL-TR-73-50, Vol. I	
b. PROJECT NO.		
c.	9b. OTHER REPORT NO(S) (Any other numbers that may be assigned this report)	
d.		
10. DISTRIBUTION STATEMENT Approved for public release; distribution unlimited.		
11. SUPPLEMENTARY NOTES		12. SPONSORING MILITARY ACTIVITY Air Force Flight Dynamics Laboratory Wright-Patterson AFB, Ohio 45433
13. ABSTRACT <p>This report describes the preliminary design and analysis for an Advanced Air Superiority Fighter Stores Loaded, Wet Wing Structure. The wing box of the F-111F airplane designed by the Convair Aerospace Division of General Dynamics was used as the baseline vehicle.</p> <p>A unique design methodology was followed to arrive at three configurations which offer an optimum balance between structural efficiency and technological advancement. This methodology consists of compiling element concepts; integrating them into cross-section drawings; optimizing them in analytical assemblies; and finally preparing full wing box designs. Each step was followed with a detailed evaluation and ranking step which utilized a formal merit rating system. This system permitted the evaluation of numerous concepts and insured that each technical discipline participated in the design selection.</p> <p>A subsequent program is proposed to evaluate the capability of the selected design to meet the overall program goals of advancing technology without significantly affecting costs. The subsequent program involves additional preliminary design, a development test program, detail design, manufacture, and tests; including static, fatigue, and damage tolerance testing. Information generated during this effort will be disseminated to the Air Force and industry in general through an intensive information transfer effort.</p>		

14. KEY WORDS	LINK A		LINK B		LINK C	
	ROLE	WT	ROLE	WT	ROLE	WT
Structural Design Stress Analysis Fatigue Fracture Analysis Materials Mass Properties Value Engineering Manufacturing Engineering Nondestructive Inspection Quality Assurance						